ISSN 1007-9327 (print)
ISSN 2219-2840 (online)

World Journal of *Gastroenterology*

World J Gastroenterol 2023 June 21; 29(23): 3574-3747

Published by Baishideng Publishing Group Inc

World Journal of Gastroenterology

Contents

Weekly Volume 29 Number 23 June 21, 2023

EDITORIAL

MINIREVIEWS

ORIGINAL ARTICLE

Basic Study

Retrospective Study

Observational Study

World Journal of Gastroenterology

Weekly Volume 29 Number 23 June 21, 2023

Contents

ABOUT COVER

Editorial Board Member of *World Journal of Gastroenterology*, Kamran Rostami, FRACP, MD, PhD, Department of Gastroenterology, MidCentral District Health Board Palmerston Hospital, Palmerston North 4472, New Zealand. kamran.rostami@midcentraldhb.govt.nz

AIMS AND SCOPE

The primary aim of *World Journal of Gastroenterology* (*WJG*, *World J Gastroenterol*) is to provide scholars and readers from various fields of gastroenterology and hepatology with a platform to publish high-quality basic and clinical research articles and communicate their research findings online. *WJG* mainly publishes articles reporting research results and findings obtained in the field of gastroenterology and hepatology and covering a wide range of topics including gastroenterology, hepatology, gastrointestinal endoscopy, gastrointestinal surgery, gastrointestinal oncology, and pediatric gastroenterology.

INDEXING/ABSTRACTING

The *WJG* is now abstracted and indexed in Science Citation Index Expanded (SCIE, also known as SciSearch®), Current Contents/Clinical Medicine, Journal Citation Reports, Index Medicus, MEDLINE, PubMed, PubMed Central, Scopus, Reference Citation Analysis, China National Knowledge Infrastructure, China Science and Technology Journal Database, and Superstar Journals Database. The 2023 edition of Journal Citation Reports® cites the 2022 impact factor (IF) for *WJG* as 4.3; IF without journal self cites: 4.1; 5-year IF: 5.3; Journal Citation Indicator: 0.82; Ranking: 32 among 93 journals in gastroenterology and hepatology; and Quartile category: Q2. The *WJG*'s CiteScore for 2021 is 8.3 and Scopus CiteScore rank 2022: Gastroenterology is 22/149.

RESPONSIBLE EDITORS FOR THIS ISSUE

Production Editor: *Yi-Xuan Cai*; **Production Department Director:** *Xiang Li*; **Editorial Office Director:** *Jia-Ru Fan*.

NAME OF JOURNAL
World Journal of Gastroenterology

ISSN
ISSN 1007-9327 (print) ISSN 2219-2840 (online)

LAUNCH DATE
October 1, 1995

FREQUENCY
Weekly

EDITORS-IN-CHIEF
Andrzej S Tarnawski

EDITORIAL BOARD MEMBERS
http://www.wjgnet.com/1007-9327/editorialboard.htm

PUBLICATION DATE
June 21, 2023

INSTRUCTIONS TO AUTHORS
https://www.wjgnet.com/bpg/gerinfo/204

GUIDELINES FOR ETHICS DOCUMENTS
https://www.wjgnet.com/bpg/GerInfo/287

GUIDELINES FOR NON-NATIVE SPEAKERS OF ENGLISH
https://www.wjgnet.com/bpg/gerinfo/240

PUBLICATION ETHICS
https://www.wjgnet.com/bpg/GerInfo/288

PUBLICATION MISCONDUCT
https://www.wjgnet.com/bpg/gerinfo/208

ARTICLE PROCESSING CHARGE
https://www.wjgnet.com/bpg/gerinfo/242

STEPS FOR SUBMITTING MANUSCRIPTS
https://www.wjgnet.com/bpg/GerInfo/239

ONLINE SUBMISSION
https://www.f6publishing.com

World Journal of Gastroenterology

Submit a Manuscript: https://www.f6publishing.com

World J Gastroenterol 2023 June 21; 29(23): 3574-3594

DOI: 10.3748/wjg.v29.i23.3574

ISSN 1007-9327 (print) ISSN 2219-2840 (online)

EDITORIAL

Recent advances in treatment of nodal and gastrointestinal follicular lymphoma

Takuya Watanabe

Specialty type: Gastroenterology and hepatology

Provenance and peer review: Invited article; Externally peer reviewed.

Peer-review model: Single blind

Peer-review report's scientific quality classification

Grade A (Excellent): 0
Grade B (Very good): 0
Grade C (Good): C, C
Grade D (Fair): 0
Grade E (Poor): 0

P-Reviewer: Long X, China; Seledtsov V, United States

Received: April 13, 2023
Peer-review started: April 13, 2023
First decision: May 12, 2023
Revised: May 14, 2023
Accepted: May 22, 2023
Article in press: May 22, 2023
Published online: June 21, 2023

Takuya Watanabe, Department of Internal Medicine and Gastroenterology, Watanabe Internal Medicine Aoyama Clinic, Niigata-city 9502002, Japan

Corresponding author: Takuya Watanabe, MD, PhD, Director, Doctor, Department of Internal Medicine and Gastroenterology, Watanabe Internal Medicine Aoyama Clinic, 1-2-21 Aoyama, Nishi-ku, Niigata-city 9502002, Japan. nabetaku@dia-net.ne.jp

Abstract

Follicular lymphoma (FL) is the most common low-grade lymphoma, and although nodal FL is highly responsive to treatment, the majority of patients relapse repeatedly, and the disease has been incurable with a poor prognosis. However, primary FL of the gastrointestinal tract has been increasingly detected in Japan, especially due to recent advances in small bowel endoscopy and increased opportunities for endoscopic examinations and endoscopic diagnosis. However, many cases are detected at an early stage, and the prognosis is good in many cases. In contrast, in Europe and the United States, gastrointestinal FL has long been considered to be present in 12%-24% of Stage-IV patients, and the number of advanced gastrointestinal cases is expected to increase. This editorial provides an overview of the recent therapeutic advances in nodal FL, including antibody-targeted therapy, bispecific antibody therapy, epigenetic modulation, and chimeric antigen receptor T-cell therapy, and reviews the latest therapeutic manuscripts published in the past year. Based on an understanding of the therapeutic advances in nodal FL, we also discuss future possibilities for gastroenterologists to treat gastrointestinal FL, especially in advanced cases.

Key Words: Nodal and gastrointestinal follicular lymphoma; Antibody-based therapy; Bispecific antibody therapy; Phosphatidylinositol-3 kinase inhibitor; Epigenetic modulator; Chimeric antigen receptor-T cell therapy

Core Tip: Primary gastrointestinal follicular lymphomas (FLs) have been increasingly detected in Japan, especially due to recent advances in small bowel endoscopy and increased opportunities for endoscopic examination and endoscopic diagnosis. Previously, many gastrolienal FL cases are detected at an early stage, however, the number of advanced cases is expected to increase in the future. This editorial provides an overview of the recent therapeutic advances in nodal FL, including antibody-targeted therapy, bispecific antibody therapy, epigenetic mutations, and chimeric antigen receptor T-cell therapy, and we also discuss future possibilities for gastroenterologists to treat gastrointestinal FL, especially in advanced cases.

Citation: Watanabe T. Recent advances in treatment of nodal and gastrointestinal follicular lymphoma. *World J Gastroenterol* 2023; 29(23): 3574-3594
URL: https://www.wjgnet.com/1007-9327/full/v29/i23/3574.htm
DOI: https://dx.doi.org/10.3748/wjg.v29.i23.3574

INTRODUCTION

Follicular lymphoma (FL) is a typical indolent B-cell lymphoma that accounts for 10%-20% of all non-Hodgkin lymphomas (NHLs)[1]. Its incidence is increasing rapidly in Western and Asian countries[2]. In particular, the number of FL cases in Japan has recently increased[3]. FL is histopathologically classified as grades 1, 2, 3a, or 3b, with grade 3b usually treated as aggressive (intermediate/high-grade) lymphoma. Most patients present with enlarged lymph nodes, and 70%-85% of patients have advanced clinical stage III or IV disease at diagnosis, with a high rate of bone marrow involvement. The gastrointestinal tract is the most common site of extranodal NHL, accounting for 30-40% of primary extranodal NHL cases[4,5]; however, gastrointestinal FL (GI-FL) is rare, with a frequency of approximately 2% of GI-NHL[6-8]. However, in recent years, the number of patients with primary GI-FL has increased because capsule and double-balloon endoscopies of the small intestine have become common in Japan. Most GI-FL cases are stage I, but there are 3.4%-40.0% with metastasis or invasion to intra-abdominal lymph nodes (stage II), extensive extranodal organ (stage IV) to extensive extranodal organs or beyond the diaphragm (12%-24%) have been reported[9], and the number of advanced cases of GI-FL (stage III, IV) is expected to increase in the future. Hiddemann *et al*[10] reported the efficacy and prolonged overall survival (OS) of rituximab, an anti-CD20 monoclonal antibody, in combination with cyclophosphamide, doxorubicin, vincristine, and prednisolone (CHOP) in patients with advanced FL. Prior to the introduction of rituximab, the 50% survival period for FL patients was 7-10 years, recent reports have indicated that the 50% survival period exceeds 20 years for patients under 40 years of age at diagnosis[11]. Furthermore, progress has been made in the studies and clinical trials of combination therapies using other monoclonal antibodies and conventional chemotherapy combinations. In the last decade, new therapeutic agents for nodal FL have been developed, including antibody-targeted therapy, bispecific antibody therapy, epigenetic mutation, and chimeric antigen receptor (CAR)-T cell therapy, and many clinical trials of monotherapy and various combinations of two or three of these agents have been conducted, showing high response rates, progression-free survival (PFS). Many clinical trials have been conducted to evaluate the efficacy of single agents and combinations of two or three of these drugs, and have shown high response rates, PFS, and OS. However, the large number of new drugs has led to the creation of many combinations of these drugs, so there is still no definitive conclusion as to which combination is the best in terms of efficacy and safety, and what the optimal order of these therapies should be. We reviewed and summarized the recently reported therapeutic advances in nodal FL, especially the most recent therapeutic publications during the past year. We then discuss the possibilities and directions in which gastroenterologists should utilize and reflect on recent advances in the treatment of nodal FL in primary GI-FL.

Recent advances in the treatment of nodal FL

Radiation therapy used to be the first choice for the treatment of nodal FL when the lesions were localized or multiple but few in number, however, the choice of radiation therapy has been greatly reduced in recent years due to its strong adverse reactions, and chemotherapy, which has advanced significantly in the past 20 years, immunotherapy, which has fewer side effects, or their combination therapies have emerged.

This editorial describes recent advances in the treatment of advanced FL, primarily stage III or IV, with reference to tables summarizing them.

ANTIBODY-BASED THERAPY

Monoclonal antibody-based therapy

Immunotherapy with rituximab and other anti-CD antibodies is highly effective in the treatment of FL and is superior and still central to current FL therapy. The objective response rate (ORR) with single-agent rituximab was 67% in untreated FL patients and 46% in previously treated relapsed FL patients [12].

A German Low-Grade Lymphoma Study Group conducted a randomized trial of CHOP alone *vs* rituximab plus CHOP (R-CHOP) in untreated advanced FLs. In a randomized comparison of CHOP monotherapy and R-CHOP combination therapy, the R-CHOP group significantly outperformed the CHOP group not only in time to failure but also in OS[13]. This evidence is important because it heralds the subsequent progress of combination therapy using anti-CD monoclonal antibody immunotherapy and other novel agents, in addition to conventional chemotherapy. Following rituximab administration, new antibody-based agents have been developed, including tafasitamab, an anti-CD19 antibody; polatuzumab vedotin, an anti-CD79b antibody-drug conjugate (ADC); loncastyximab tesirine, an ADC composed of a humanized antibody targeting the protein CD19; magrolimab, an anti-CD47 antibody; and obinutumab, a humanized anti-CD20 monoclonal antibody. Obinutumab, a humanized anti-CD20 monoclonal antibody, has been developed (Table 1).

Tafasitamab plus lenalidomide, which enhances NK cell activity and antibody-dependent cytotoxicity (ADCC), has been shown to be superior to the monotherapy[14].

Polatuzumab vedotin is a CD79b-directed ADC. In the phase II ROMULUS trial of relapsed and refractory (r/r) FL and diffuse large B-cell lymphoma (DLBCL), patients with FL were treated with rituximab plus polatuzumab (CD79-directed ADC) or rituximab plus pinatuzumab (CD22-directed ADC), and their efficacy was compared[15].

Loncastuximab tesirineis (ADCT-402) is a noble antibody-drug conjugated to a cytotoxic dimer. After bindig to the tumor cells the antibody is internalized, the cytotoxic drug is released, and the cancer cells are killed. The ORR in patients with FL in a phase I study was 78.6%; phase II findings (LOTIS-2 study) of loncastaximab tecilin in r/r DLBCL patients showed a good and sustained antitumor effect with an ORR of 48.3% and complete response rate (CRR) of 24.2%[16]. Clinical trials are currently underway for other carcinomas; a phase II study in combination with rituximab for r/r FL patients is ongoing in Florida, United States.

Magrolimab is a CD47-directed antibody, and a phase I study of its combination with rituximab in r/r lymphoma has been reported[17].

Obinutumab is a humanized anti-CD20 monoclonal antibody with low fucose content in the Fc region through glycosylation technology and the unique properties of a type-2 antibody. Phase 3 trials have shown improved efficacy in indolent non-NHL (iNHL) and chronic lymphocytic leukemia (CLL), and phase 2 trials of these therapeutic regimens have shown promising results in CLL, FL, and mantle cell lymphoma (MCL)[18].

Results of a phase I study of the combination of venetoclax plus obinutumab in previously untreated FL patients ORR and CRR were 87.5% and 25.0%, respectively, by CT evaluation; 84.2% and 68.4%, respectively, by PET/CT evaluation; 1-year PFS was 77.8% and 79%, respectively; 30-mo PFS was 73.2% and 79.0%, respectively and showed efficacy of the combination of venetoclax plus obinutumab[19]. However, in the GALLIUM trial, obinutuzumab had a better PFS than rituximab when combined with conventional chemotherapy as frontline therapy in previously untreated advanced FL patients[20]. Furthermore, transformed-FL (t-FL) patients with more aggressively transformed, more malignant potential had worse survival than r/r FL patients (2-year rate: 55.9% *vs* 83.1%). t-FL relapsed earlier than FL (median observation time: 0.8 years *vs* 2.3 years)[21].

Finally, we discuss the key points regarding recent rituximab biosimilars. In recent years, four rituximab biosimilars have been approved to date in Europe and the United States. CT-P10 is the first Rituximab biosimilar approved CT-P10 is as effective and safe as Rituximab in untreated FL with small tumor volume[22]. They also reported no statistically significant differences in efficacy and serious adverse events between the Rituximab biosimilar group and the reference drug, Mabusera[23]. The Japanese government's policy for 2022 also states that biosimilar will be steadily promoted with a target value set by the end of 2022 based on the effect of medical cost optimization. It is expected that the use of rituximb biosimulators will be recommended and increased worldwide from the viewpoint of cost benefit in reducing the enormous medical costs in the future.

Antibody therapies against novel targets, such as CD19, CD79b, and CD47, as well as rituximab, an anti-CD20 monoclonal antibody and obinutumab, a humanized anti-CD20 monoclonal antibody, have been developed and have demonstrated efficacy in FL. Antibody targeted therapies to FL are innovative immunotherapy medication that offers great efficacy and safety for FL treatment. We have high expectations for improved outcomes in the near future.

Bispecific T cell binding antibody = bispecific antibody therapy

Bispecific T-cell binding antibodies (BTEs) = bispecific antibodies are molecules designed to bind to two or more different antigens, a powerful therapy that allows T cells to more precisely target specific tissues and cells. Summary of clinical trials of BTE treatment for FL is shown in Table 2.

Table 1 Summary of clinical trial results of monoclonal antibody-based therapies

Study	Target disease	No. of patients	Objective response rate	Complete response rate	Median progression-free survival	Overall survival	Adverse events or other subjects	Ref.
Tafasitamab plus lenalidomide phase-II L-MID	r/r DLBCL (no FL) > 35 mo follow up	*n* = 80	57.5% (*n* = 46/80)	40.0% (*n* = 32/80)	11.6 mo	33.5 mo	No unexpected toxicity	[14]
Phase-II ROMULUS, rituximab-polatuzumab *vs* rituximab-pinatuzumab	r/r FL	*n* = 42, *n* = 20, *n* = 21	70% (*n* = 14/20); 62% (*n* = 13/21)	45% (*n* = 9/20); 5% (*n* = 1/21)	Unknown	Unknown		[15]
Loncastuximab tesirine (ADTC-402) frontline therapy	Untreated FL	Total, DLBCL, MZL, FL	45.6%, 42.3%, 46.7%, 78.6%	26.7%	Unknown	Unknown	Median duration response: 5.4 mo	[16]
Magrolimab plus rituximab phase-Ib	r/r DLBCL; r/r FL	*n* = 22; DLBCL:15; FL: 7	50% (CR or PR); 40%, 71% (*n* = 5/7)	33%, 43% (*n* = 3/7)	Unknown	Unknown	90% response were on going, a median follow-up of 6.2 (DLBCL)/8.1 (FL) mo	[17]
Venetoclax plus obinutumab phase-I	Untreated FL	CT, PET/CT	87.5%, 84.2%	25.0%, 68.4%	77.8% (at one yr); 79.0% (at one yr); 73.2% (at 30 mo); 79.0% (at 30 mo)	Unknown; unknown		[19]
GALLIUM trial obinutuzumab + CTx rituximab + CTx	Untreated FL	*n* = 1202, *n* = 601, *n* = 601	88.5%, 86.9%	Unknown, unknown	80.0% (at 3 yr); 73.3% (at 3 yr)	Unknown, unknown	Obinutuzumab is better	[20, 21]

"Unknown" means data not shown, unknown information or not reached. r/r: Refractory and relapsed; FL: Follicular lymphoma; DLBCL: Diffuse large B-cell lymphoma; MZL: Marginal zone lymphoma; (R-)CHOP: (Rituximab plus) cyclophosphamide, doxorubicin, vincristine, and prednisolone; CT: Computed tomography; PET/CT: Positron emission tomography/computed tomography; CTx: Traditional chemotherapy.

The BTEs most commonly used for FL treatment are CD3 and CD20, with Mosunetuzumab and Glofitamab being pioneering representative novel BTEs.

A phase I trial of single-agent mosunetuzumab in patients with r/r iNHL (including FL and t-FL) showed an ORR of 66% and a CRR of 49%, with grade 3 or higher adverse events in 71% of patients with low-grade lymphoma (r/r and t-FL, 96%)[24]. Mosnetuzumab, a CD20 × CD3 bispecific monoclonal antibody, showed a significantly higher CRR of 60% than that of the control group with copanlisib of 14%, when administered to patients with r/r FL, indicating high efficacy[25]. Mosunetuzumab was also studied in combination with lenaridomide; a phase I study of combination therapy in r/r FL patients showed an ORR of 92%, CR of 77%, and grade 3 or higher adverse events in 30% of patients in the abstruct.

Glofitamab was observed to have a better response rate at higher dose levels in the r/r B-NHL (including indolent lymphoma of 25.7%) phase I trial, with an ORR of 65.7% and a CRR of 57.1%. CRS occurred in 50.3% of cases[26]. The results of a study comparing glofitamab with or without obinutuzumab in r/r FL showed an ORR of 81% and a CRR of 70% for glofitamab alone and 100% and 74% for the combination group in the Abstruct.

The results of a phase I/II trial of epcoritamab, an anti-CD3 and anti-CD20 BTE, in r/r NHL patients showed an ORR of 90% and a CRR of 50% in FL patients[27]. The results of a phase I/II study of epcoritamab in combination with lenaridomide and rituximab in patients with r/r FL showed high efficacy, with an ORR of 100% and a CRR of 93%[28].

Odronextamab is a hinge-stabilized fully human IgG4-based CD20 × CD3 bispecificity antibody that binds to CD3 on T cells and CD20 on B cells. In the Odronextamab ELM-1 phase I study, patients with r/r FL who received 5 mg or more of odronextamab had an ORR of 91% and a CRR of 72%; Odronextamab monotherapy showed promising preliminary activity, especially in patients with long-standing previously treated BCL with sustained response[29,30].

BTE is a novel immunotherapy agent that shows high efficacy and safety for FL treatment. We would like to greatly anticipate further improvements in outcomes through future clinical trials.

Anti-programmed death ligand 1 antibody

Programmed death ligand 1 (PD-1) blockade enhances anti-tumor T cell function and ADCC in NK cells. Recntly, the efficacy of the anti-PD-1 ligand (PD-L1) antibodies, atezolitumab and pembrolizumab, in FL has also attracted attention (Table 3).

Table 2 Summary of clinical trial results of bispecific T cell binding antibody therapies

Study	Target disease	No.of patients	Objective response rate	Complete response rate	Median progression-free survival	Overall survival	Adverse events or other subjects	Ref.
Mosunetuzumab alone, phase-I	r/r NHL (including FL and t-FL)	*n* = 157	66.2% (i B-NHL)	48.5% (i B-NHL)	Median duration of response 20.4 mo (i B-NHL	Unknown	G3 and higher in 71% of iNHL patients	[24]
Mosunetuzumab alone, phase-II	r/r FL (Grade 1-3a)	*n* = 90 (median follow-up was 18.3 mo)	Unknown	60% (*n* = 54/90) (14% higher than CRR with copanlisib), high efficacy	Unknown	Unknown	High efficacy	[25]
Mosunetuzumab with lenaridomide, phase-I	r/r FL	Unknown	92%	77%	Unknown	Unknown	G3 and higher in 30% of patients	In abstruct
Glofitamab alone, phase-I	r/r B-NHL (including r/r FL)	*n* = 155	65.7% (at the recommended phase-II dose)	57.1% (at the recommended phase-II dose)	Unknown	Unknown	CRS occurred in 50.3% of patients	[26]
Glofitamab alone *vs* glofitamab with obinutuzumab	r/r FL	Unknown	81%, 100%	70%, 74%	Unknown	Unknown	Combination has a better response rate	In Abstruct
Epcoritamab, phase-I/II	r/r B-NHL	*n* = 68	90% (full dose)	50% (full dose)	Unknown	Unknown	Pyrexia 69%, CRS 59%	[27]
Epcoritamab with lenaridomide and rituximab	r/r FL	Unknown	100%	93%	Unknown	Unknown	High efficacy is revealed	[28]
Odronextamab alone phase-I ELM-1 trial	r/r B-NHL (including r/r FL)	*n* = 145	91% (r/r FL)	72% (r/r FL)	Unknown	Unknown	CRS 28%	[29]

"Unknown" means data not shown, unknown information or not reached. r/r: Refractory and relapsed; (i)NHL: (Indolent) non-Hodgkin lymphoma; i B-NHL: Indolent B-cell non-Hodgkin lymphoma; FL: Follicular lymphoma; t-FL: Transformed follicular lymphoma; G: Grade; CRS: Cytokine release syndrome.

Table 3 Summary of clinical trial results of anti-programmed death ligand 1 antibody-based therapies

Study	Target disease	No. of patients	Objective response rate	Complete response rate	Median progression-free survival	Overall survival	Adverse events or other subjects	Ref.
Atezolitumab (anti-PD-1 antibody) plus obinutumab	Total	*n* = 49				Unknown		[31]
phase-I	r/r FL	*n* = 26	54%	23%	9 mo			
	r/r DLBCL	*n* = 23	17%	4%	3 mo			
Pembrolizumab(anti-PD-1antibody) plus rituximab	r/r FL (one or more prior therapy)	*n* = 30	67%	50%	12.6 mo	97% (at 3 yr)	23% in remission at medianfollow-up of 35 mo	[32]

"Unknown" means data not shown, unknown information or not reached. r/r: Refractory and relapsed; FL: Follicular lymphoma; DLBCL: Diffuse large B-cell lymphoma; PD-1: Programmed death ligand 1.

The results of a phase I study of the combination of atezolizumab, an anti-PD-L1 antibody, and obinutumab showed an ORR of 54% (CRR: 23%) for r/r FL and r/r DLBCL and 17% (CRR: 4%) for DLBCL; PFS was 9 mo in the FL group and 3 mo in the DLBCL group[31]. In addition, a clinical trial of pembrolizumab, an anti-PD-1 monoclonal antibody, in combination with rituximab, an anti-CD20 monoclonal antibody, in r/r FL patients showed an ORR of 67% and CRR of 50%; median PFS was 12.6 mo, 3-year OS was 97%, and at a median follow-up of 35 mo 23% of patients were in remission[32]. Pembrolizumab in combination with rituximab as a novel therapeutic agent for r/r FL showed high efficacy and remission maintenance.

PD-1 blockade enhances anti-tumor T cell function and ADCC in NK cells, and its mechanism of action is more fundamental and makes more sense. We expect further improvement of the therapeutic effect of anti-PD-1 antibody therapy for FL patients.

IMMUNOMODULATORS

Lenaridomide is a typical oral immunomodulatory drug (IMiD) used to treat FL. Lenaridomide is a derivative of thalidomide with a similar structure. Lenaridomide is a derivative of thalidomide with a similar structure. It has both a "tumor-killing" effect by inhibiting the growth of hematological malignancies and inducing apoptosis, and an "immunomodulatory" effect by acting on immune cells and activating their immunity[33]. The combination of lenaridomide and CD20 antibody was initially tested as a salvage therapy for r/r FL in combination with an anti-CD20 antibody; however, owing to its high efficacy, it was recently tested as a frontline therapy for patients with advanced, untreated FL, with good results. Table 4 lists clinical trials in which lenaridomide was administered.

A phase II study comparing lenaridomide alone with R2 (lenaridomide plus rituximab) in patients with r/r FL showed an ORR favoring the R2 group (35% *vs* 24%), with a median follow-up of 2.5 years. The time to progression (median) was also superior in the R2 group (2.0 years *vs* 1.1 years), but there was no significant difference in OS[34].

The results of the phase III AUGMENT study evaluating R2 (lenaridomide plus rituximab) in r/r FL and marginal zone lymphoma (MZL) showed a median PFS of 39 mo in the R2 group compared to 14 mo in the rituximab group, with no difference in OS[35].

The phase IIIb MAGNIFY trial investigated extended R2 treatment in patients with r/r FL and MZL. After 12 cycles of R2 treatment, patients were randomized to receive an additional 18 mo of R2 treatment or rituximab maintenance therapy. The R2 cohort had ORR of 69% and CRR of 40%. The median PFS was 40 mo, similar to that observed in the AUGMENT trial[36].

In a single-arm phase II GALEN trial of patients with r/r FL, Obinutuzumab and lenaridomide were studied[37]. The patients received lenaridomide and obinutuzumab for 18 mo, followed by 1 year of obinutuzumab maintenance therapy[37]. After a median follow-up of 2.6 years, the ORR was 95%, 2-year PFS was 65%, and OS was 87%. No clinical trials have directly compared rituximab and obinutuzumab in combination with lenaridomide, and it is unclear which combination is superior in efficacy.

The phase III RELEVANCE trial of R2 as frontline therapy for advanced FL was conducted[38]. Patients were randomized to receive 18 cycles of R2 therapy plus 6 cycles of rituximab maintenance therapy or a chemoimmunotherapy regimen including rituximab [R-CHOP, bendamustine plus rituximab (BR), or rituximab plus cyclophosphamide, vincristine, and prednisone (R-CVP)]. The primary endpoints of the CR rate (48%-53%) and 3-year PFS (77%-78%) at 120 wk were similar; no superiority of R2 over chemoimmunotherapy in the front-line treatment of FL has been demonstrated [38].

The phase II E2408 trial randomized untreated FL patients into BR induction and R2 maintenance, BR induction and rituximab maintenance, or BR and the proteasome inhibitor boltezomib plus rituximab maintenance, and compared the efficacy among the three groups[39]. The three groups had similar (approximately 90%) and high CRRs, and the 1-year disease-free survival was higher in the rituximab maintenance group (85%) than in the R2 group (67%), possibly due to a higher discontinuation rate due to adverse events in the R2 group.

A clinical trial of lenaridomide plus obinutuzumab as frontline therapy for patients with advanced untreated FL showed very good results, with an ORR of 98%, CR of 92%, and 2-year PFS of 96% after a median follow-up of 22 mo[40]. In the future, the combination of lenalidomide and CD20 antibodies is expected to be the mainstay of front-line therapy for FL.

With the introduction of bendamustine, obinutuzumab, and lenalidomide, which have shown high efficacy in maintenance therapy, front-line treatment of FL has improved and developed. However, how they can be combined to provide the best treatment has recently been studied by network meta-analysis of randomized controlled trials to compare treatment efficacy[41].

With lenaridomide, a further improvement in the therapeutic effect in FL patients was obtained when used in combination with other main agents. As one of the important combination drugs, it is expected to improve treatment outcomes in the future.

MOLECULAR TARGETED THERAPIES (SMALL MOLECULE CONPOUNDS)

Bruton's tyrosine kinase inhibitor

Bruton's tyrosine kinase (BTK) is a type of protein kinase that exists in immune cells and regulates B cell differentiation and activation upon stimulation from the B cell receptor (BCR). Since BCR signaling plays an important role in blood cancers such as B-cell NHL and CLL, BTK inhibitors have been expected to have therapeutic effects in these blood cancers including FL. The results of the clinical trials

Table 4 Summary of clinical trial results of immunomodulator-based therapies

Study	Target disease	No.of patients	Objective response rate	Complete response rate	Progression-free survival	Overall survival	Adverse events or other subjects	Ref.
Randomized phase-II; lenaridomide alone (L) lenaridomide + rituximab (LR)	r/r FL	*n* = 91, *n* = 45 (L); *n* = 46 (LR)	53%, 76%	20%, 39%	Median time to progression: 1.1 yr (at 2.5 yr); 2.0 yr (at 2.5 yr)	Unknown		[34]
Phase-III AUGMENT lenaridomide + R (R2) *vs* lenaridomide + placebo	r/r FL; r/r MZL	*n* = 358; *n* = 180; *n* = 178	Unknown	Unknown	Median duration: 39.4 mo; 14.1 mo	Unknown	Grade 3 neutropenia of R2 is higher than L	[35]
Phase-IIIb MAGNIFY trial; R maintain after R2 additional lenarimide + rituximab (R2) 18 mo after R2	r/r FL; r/r MZL	*n* = 393	69% (R2)	40% (R2)	40 mo (similar to AUGMENT trial)	Unknown		[36]
Phase-II GALEN study; lenarimide + obinutuzumab (R2) 18 mo followed by obinutuzumab alone maintenance therapy 1 year	r/r FL	*n* = 68; evaluable	95% (at 2.6 yr)	38% (*n* = 33/86)	65% (at 2 yr)	87% (at 2 yr); 81% (*n* = 70/86); 84% (*n* = 72/86)		[37]
Phase-III RELEVANCE study, lenaridomide + rituximab (R2) + Rituximab maintenance therapy *vs* CTx (R-CHOP, BR, or R-CVP)	Untreated advanced FL	*n* = 1030; R-maintenance, *n* = 513; CTx, *n* = 517	Unknown	48%-53%, about the same	3 years-PFS 77%-78%, almost equal to superiority of R2 in F2 frontline not proven	Unknown		[38]
	Untreated advanced FL		Unknown	All 3 groups approximately 90%, about the same	3 yr PFS (5 yr median follow-up); -R 77%, BVR-R 82%, BR-LR 76% (higher in the R-maintenance group than in the R2 group) because of more discontinuations in the R2 group)	3 yr PFS (5 yr median follow-up), BR-R 87%, BVR-R 90%, BR-LR 84%		[39]
Single center phase-II frontline therapy; lenaridomide plus obinutuzumab	Untreated advanced FL	*n* = 90	98% (after a median follow-up of 22 mo)	92% (after a median follow-up of 22 mo)	2 yr-PFS 96 (after a median follow-up of 22 mo)	Unknown		[40]

"Unknown" means data not shown, unknown information or not reached. r/r: Refractory and relapsed; FL: Follicular lymphoma; MZL: Marginal zone lymphoma; L: Lenaridomide; R: Rituximab; LR: Lenaridomide plus rituximab; R2: Lenaridomide plus rituximab; (R-)CHOP: (Rituximab plus) cyclophosphamide, doxorubicin, vincristine, and prednisolone; BR: Bendamustine plus rituximab; (R-)CVP: (Rituximab plus) cyclophosphamide, vincristine and prednisolone; BR-R: BR induction followed by 2-year rituximab maintenance; BVR-R: BR with bortezomib and rituximab maintenance; BB-LR: BR followed by lenalidomide (1 year) with rituximab maintenance; CTx: Traditional chemotherapy.

of BTKi treatments for FL are listed in Table 5.

Representative BTKi include, in order of oldest to youngest, first-generation ibrutinib, second-generation acalabrutinib and zanubrutinib, and third-generation piltobrutinib. These BTKi have shown high efficacy in B-cell NHL and CLL[42-46].

The efficacy of zanurutinib monotherapy in patients with r/r FL was sluggish, with an ORR of 36.4% and CR of 18.2%. After a median follow-up of 33.9 mo, the median PFS was 10.4 mo[42]. On the other hand, a phase II study in r/r MCL showed that after a median follow-up of 35.3 mo, the ORR was 83.7%, the CRR was 79.9%, and the median PFS was 33.0 mo[43]. Zanurutinib alone was highly effective in r/r MCL, however, limited in r/r FL.

The phase II DAWN trial evaluated the therapeutic efficacy of single-agent ibrutinib in patients with r/r FL; the ORR was 21% and did not meet the primary endpoint[47]. Frontline therapy was administered to investigate a combination of Ibrutinib and Rituximab. This phase II trial included two arms, both with ibrutinib 560 mg/d, with Rituximab in arm-1 starting at week 1 for four cycles per

Table 5 Summary of Clinical Trial Results of Bruton's Tyrosine Kinase inhibitors

Study	Target disease	No. of patients	Objective response rate	Complete response rate	Progression-free survival	Overall survival	Adverse events or others	Ref.
Zanubrutinib (other BTKi) alone	r/r FL		36.4%	18.2%	Median PFS 10.4 mo (median follow-up 33.9 mo)	Unknown		[42]
Zanubrutinib phase-II	r/r MCL	83.7%	77.9%	Unknown	33.0 mo	Unknown		[43]
	r/r FL	n = 100	21.0% (poor)	Unknown	Unknown	Unknown		[47]
Ibrutinib with rituximab phase-II trial	Untreated FL, r/r FL	n = 13, n = 27	85% (arm-1), 75% (arm-2)	Unknown	62% of untreated FL, 26% of r/r FL, continued treatment	Unknown		[48]

"Unknown" means data not shown, unknown information or not reached. r/r: Refractory and relapsed; FL: Follicular lymphoma; MCL: Mantle cell lymphoma; PFS: Progression-free survival.

week, and Rituximab in arm-2 starting at week 9. The ORR was 85% in arm-1 and 75% in arm-2[48].

Acalabrutinib is an effective BTKi for r/r MCL Results of a phase I trial comparing acalabrutinib with or without rituximab as frontline therapy for untreated FL and salvage therapy for r/r FL, after a median follow-up of 22 mo, 62% of untreated FL patients and 26% of r/r FL patients remained on therapy and showed high tolerability[49].

Results of the randomized phase II ROSEWOOD trial in patients with r/r FL showed that combination therapy with zanubrutinib had better PFS than obinutuzumab alone. Zanubrutinib suggested to be more effective against r/r FL when used in combination with Obinutuzumab[50].

Although the single-agent activity of BTKis in FL is modest, their activity may be demonstrated when used in combination, and there is hope for their efficacy. We will keep a close eye on the future improvements in combination therapy with various combinations of new BTKs and other drugs in patients with FL.

Pro-apoptotic pathway inhibitors (BCL2 inhibitor)

Venetoclax selectively binds with strong affinity to BCL2, an anti-apoptotic protein involved in many blood cancers, and liberates apoptosis-promoting proteins, thus rapidly and irreversibly promoting apoptosis of blood cancer cells because BCL2 is overexpressed in FL, Venetoclax, a BCL2 inhibitor, has shown great promise. A phase I trial of venetoclax monotherapy was conducted in patients with FL, with an ORR of 38% and a median PFS of 11 mo[51]. The phase II CONTRALTO trial compared three groups of patients with r/r FL: Venetoclax plus rituximab, venetoclax plus BR, and BR in combination with venetoclax[52]. The CRR were 17%, 75%, and 69%, respectively; grade 3 or higher adverse events were extremely common in the venetoclax plus BR group (94%). r/r FL was included. In addition, combination therapy with ibrutinib was tested in a phase I/II study of venetolax plus ibrutinib with an ORR of 69% and a CRR of 25%[53].

Since BCL2 is overexpressed in FL, BCL2 inhibitors are expected to have a fundamental antitumor effect on FL tumor cells in terms of their mechanism of action. We look forward to improving the therapeutic outcome of BCL2 inhibitors for FL patients in the near future.

Epigenetic regulator

Progress has been made in drug development that is active against blood cancers through the epigenetic regulation of gene expression, such as DNA methylation. The results of clinical trials of EZH2 treatments in patients with FL are listed in Table 6.

Tazemetostat is a small molecule that inhibits the activity of enhancer of zeste homolog 2 (EZH2), a methyltransferase of histones, *etc.* Tazemetostat inhibits the methylation activity of mutant EZH2, thereby inhibiting the methylation of lysine residue 27 of histone H3 and other methyltransferases. A phase II study of tazemetostat in EZH2-mutant and wild-type r/r FL patients showed a higher ORR in the EZH2-mutant cohort (69% *vs* 35%)[54]. It is important to note that higher activity was observed in patients with FL with high-risk characteristics. Currently, combination therapy for r/r FL with tazemetostat is under investigation in the phase II SYMPHONY-2 trial in combination with rituximab and in the phase Ib/III trial in combination with R2. Tazemetostat as a third, fourth, and subsequent treatment for FL and DLBCL patients, especially r/r FL, has a reduced risk of adverse events compared to the PI3K inhibitors ideralisib, duvelisib, copanlisib, and umbralisib, while the therapeutic efficacy and benefit were comparable[55-57].

More than 10 EZH2 inhibitors have recently entered clinical trials, including tazemetostat[56], and we look forward to improved outcomes in the future.

Table 6 Summary of clinical trial results of epigenetic regulators

Study	Targeted disease	No. of patients	Objective response rate	Complete response rate	Progression-free survival	Overall survival	Adverse events or others	Ref.
Tazemetostat alone, phase-II	r/r FL, EZH2-mut; FL, EZH2-wt. FL	*n* = 99, mut FL *n* = 45; wt FL *n* = 54	69% (EZH2 mut); 35% (EZH2 wt)	Unknown; unknown	Median PFS: 13.8 mo (EZH2 mut); 13.1 mo (EZH2 wt)	Unknown	G3 or higher 27%+, treatment discontinued at 8%	[54]
Tazemetostat (first EZH2 inhibitor) *vs* inderalisib, duvelisib, copanlishib, umbralisib	r/r FL, systematic literature review		Tazemetostat *vs* inderalisib 43% *vs* 56; duvelisib 48% *vs* 47; Kopanlisib 49% *vs* 61; umbralisib 57% *vs* 47; no significant difference in either case	Unknown	Unknown	Unknown	Predominantly reduced risk of adverse events compared to PI3Ki	[57]
Vorinostat (HDACi), phase-II	r/r Inhl + MCL, median with one or more prior treatment	*n* = 39 (r/r FL)	49%	Unknown	Median PFS, 20 mo	Unknown	G3 or higher 8%	[58]
Vorinostat + rituximab, phase-II	Untreated and r/r FL (4 or less prior treatment)	*n* = 22	46% (all patients); 67% (untreated pts); 41% (r/r FL)	Unknown	Median PFS, 29.2 mo (all patients); not reached (untreated pts); 18.8 mo (r/r FL)	Unknown		[59]
Mocetinostat, phase-II	r/r DLBCL, r/r FL	*n* = 41, *n* = 31	18.9% (r/r DLBCL), 11.5% (r/r FL)	Unknown	1.8-22.8 mo (DLBCL); 11.8-26.3 mo (FL)	Unknown	Fatigue (75.0%); nausea (69.4%); diarrhea (61.1%)	[60]

"Unknown" means data not shown, unknown information or not reached. r/r: Refractory and relapsed; FL: Follicular lymphoma; EZH2: Enhancer of zeste homolog 2; mt: Mutant; wt: Wild type; (i)NHL: (Indolent) non-Hodgkin lymphoma; DLBCL: Diffuse large B-cell lymphoma; MZL: Marginal zone lymphoma; MCL: Mantle cell lymphoma; G: Grade; PI3Ki: Phosphoinositide 3 kinase inhibitor.

Vorinostat is a histone deacetylase inhibitor (HDACi). A phase II study of vorinostat in patients with r/r FL reported an ORR of 49%, with a median PFS of 20 mo. Grade 3 or greater adverse events were observed in 80% of the patients, mostly cytopenia[58]. Vorinostat was also evaluated in combination with rituximab, with an ORR of 50% and a CR of 41% in a phase II study of 22 untreated and r/r FL patients[59]. Another HDACi, mocetinostat, has shown poor efficacy, with an ORR of only 12% in patients with FL (*n* = 31) evaluated in a phase II trial of patients with r/r FL[60].

EZH2 inhibitors demonstrate effectiveness as an epigenetic regulator by the mechanism that inhibits the activity of methyltransferase of histones, *etc*. These agents are expected to further improve their therapeutic outcomes in the future, especially as a treatment for t-FL.

Phosphatidylinositol-3 kinase inhibitor

The BCR-mediated signaling pathway has been found to be permanently activated in B cell tumor cells, and inhibitors targeting molecules in the BCR signaling pathway are being developed.

Phosphatidylinositol-3 kinaseb (PI3K) is a lipid kinase that mediates the phosphorylation of the inositol ring 3 of inositol phospholipids, a membrane component[61]. Class I PI3Ks are heterologous. Class I PI3Ks are heterodimers that play important roles in signal transduction. Class 1 kinases are further divided into α, β, ϒ, and δ isoforms. For example, p110α and β are expressed in all cells, their knock out mouse is embryonic lethal[62]. p110γ is involved in neutrophil and macrophage migration [63] and mast cell degranulation[64]. This pathway is important in cancer, including B cell malignancies, and several small-molecule PI3K inhibitors (PI3Ki) have been developed for its treatment. The results of clinical trials of PI3K inhibitors in patients with r/r FL are listed in Table 7.

Idelalisib, a selective inhibitor of the delta isoform, was the first PI3Ki developed for the treatment of FL. In the European phase II DELTA study, idelalisib demonstrated the highest efficacy to date in r/r/ FL patients, with a median treatment duration of 10 mo (range 1-43) and an overall response rate of 73% [65].

In addition, a phase II open-label study of idelalisib in r/r iNHL, including FL, in the United.States. confirmed a response rate of 57% and a median PFS of 11 mo[66]. While idelalisib showed high efficacy against r/r FL, grade 3 or higher adverse events were observed in most participants (54%). Higher rates of adverse events have been observed in relatively young patients with less severe prior therapy, fewer complications, and stronger immune responses[67,68]. Fatal adverse events complicate the use of PI3K inhibitors.

Table 7 Summary of Clinical Trial Results of phosphoinositide 3 kinase inhibitors

Study	Target disease	No. of patients	Objective response rate	Complete response rate	Progression-free survival	Overall survival	Adverse events or others	Ref.
Indelalisib, phase-II DELTA trial	r/r FL	*n* = 55	73% (highest ever reported)	Unknown	72% disease-free after 12 mo	80% alive after 12 months	54% of G3 or higher	[65]
Indelalisib phase-II open-labeled trial	r/r NHL (including FL), median of 4 lines prior therapy	iNHL, *n* = 72; FL, *n* = 42)	57%	Unknown	11 mo	Unknown	54% of G3 or higher	[66]
Duvelisib	iNHL (including FL)	*n* = 187	70% good	Unknown	Unknown	Unknown	63% of G3 or higher	[63, 69]
Conpalisib, phase-II CHRONOS-1 trial	r/r FL, median 3-lines of prior therapy	*n* = 142	59%	12%	11 mo (median)	43 mo (median)	G3 84%, 6 cases of G5 events	[70, 71]
Umbralisib, phase-II trial	iNHL (including FL) median 3-lines or more of prior therapy	*n* = 208 (FL = 117)	47.1% of (after a median follow-up of 27.7 mo)	Unknown	10.6 mo (median PFS)	Unknown		[74]
Parsaclisib, phase-Ib, CITADEL-111 trial	Japanease: r/r FL; r/r MZL; r/r DLBCL	*n* = 9; *n* = 2; *n* = 6	9 cases (= 100%); 2 cases (= 100%); 1 case (= 16.7%)	22.2% (*n* = 2/9); 100% (*n* = 2/2); 16.7% (*n* = 1/6)	Unknown	High incidence of adverse events-need to carefully select target patients	Neutropenia above G3 interrupted in 58.8% and reduced in 29.4%	[75]
Parsaclisib, phase-I/II (phase-II trial is ongoing)	r/r B-NHL	*n* = 72	71% (r/r FL); 78% (r/r MZL); 67% (r/r MCL); 30% (r/r DLBCL)	Unknown	Unknown	Unknown	G3/4 neutropenia occurred in 19%	[76]
Zandelisib (ME-401), phase-I trial	Japanese, r/r iNHL	*n* = 9	100% (*n* = 9/9)	22% (*n* = 2/9), median duration of response 7.9 mo; median time to response 1.9 mo		Unknown	G3 or higher neutropenia 6/9 (55.6%) diarrhea 3/9 (33.3%) and many events	[77]
Zandelisib alone *vs* zandelisib + rituximab	r/r FL	*n* = 12	92% (*n* = 11/12) in the 60 mg group; 83% (*n* = 5/6) in the 180 mg group	Unknown	Unknown	Unknown		[78]
	r/r iNHL, median 3-lines of prior therapy	*n* = 30 + BR (*n* = 19) *vs* + R-CHOP (*n* = 11)	90% (+ BR) *vs* 100% (+ R-CHOP)	Unknown	Unknown	Unknown	G3 or higher, high rate of 70% (BR), 91% (R-CHOP)	[79]

"Unknown" means data not shown, unknown information or not reached. r/r: Refractory and relapsed; FL: Follicular Lymphoma; B-NHL: B-cell non-Hodgkin lymphoma; (i)NHL: (Indolent) non-Hodgkin lymphoma; DLBCL: Diffuse large B-cell lymphoma; MZL: Marginal zone lymphoma; MCL: Mantle cell lymphoma.

Duvelisib is the first FDA-approved oral dual inhibitor of PI3K-δ and PI3K-γ. Wang *et al*[69] reported on the safety and efficacy of duvelisib, a dual PI3K-δ and γ inhibitor, in patients with relapsed and refractory lymphoid neoplasms in a systematic prospective clinical trial reviews and meta-analyses have been reported[63,69]. Although the ORR of 187 patients with iNHL including FL showed a good efficacy of 70%, the relatively high rate of grade 3 or higher adverse events (63%) is still a safety concern[63,69].

The high rate of adverse events associated with these two drugs has made it difficult to gain general acceptance for FL treatment. In such a situation, only conpalisib has been approved for r/r FL after more than two lines of therapy. The phase II CHRONOS-1 study[70,71] of copanlisib in patients with r/r iNHL showed an ORR of 59%, CR of 12%, median PFS of 11 mo, and median OS of 43 mo. There was no increase in serious adverse events during the long-term follow-up period, although the rate of grade 3 or higher adverse events was as high as 84%, including 6 grade 5 events[70,71].

Umbralisib (TGR-1202) is an orally available, effective, potent and selective PI3-K δ and casein kinase-1-ε (CK1ε) inhibitor[72]. Umbralisib is a fourth-generation, late-stage PI3Ki that may play an important role in therapeutic algorithms[73]. The results of a phase II trial of r/r iNHL showed an ORR of 45% and

median PFS of 10.6 mo in a cohort of patients with FL after a median follow-up period of 27 mo[74]. Most recently, a phase II trial of Frontline with umbralisib and ubrituximab in untreated advanced FL patients was completed in Florida, the United States.

Parsaclisib is a potent δ isoform of the PI3Ki. The results of CITADEL-111, a phase Ib study in Japanese patients with relapsed/refractory B-cell lymphoma, showed an ORR of 100% in r/r FL and CR in two patients (22.2%), indicating efficacy. The results for MZL and DLBCL are shown in Table 7. Although potent, adverse events were frequent, requiring careful patient selection and implementation [75]. The Phase I/II trial of parsaclisib in patients with r/r FL showed an ORR of 71%. Grade 3 or higher adverse events were observed in 19% of all participants, and phase II trial is ongoing[76].

Zandelisib (ME-401) is a novel PI3-Kδ inhibitor, and phase I trials have recently been reported in Japanese patients with r/r iNHL. ORR was 100% and CR was 22% in 9 Japanese patients with r/r iNHL, and the median duration of response, progression-free survival, and time to response were 7.9 mo, 11.1 mo, and 1.9 mo, respectively. Neutropenia was the most common adverse event, with 55.6% (6/9) of the patients having neutropenia, and thrombocytopenia was the most common adverse event. In Japanese patients with r/r iNHL, zandelisib showed good antitumor efficacy[77]. The results of a study comparing zandelisib monotherapy with zandelisib plus rituximab combination therapy for r/r FL showed an ORR of 92% in the 60 mg group and 83% in the 180 mg group. Serious adverse events occurred in 21% and 8% of patients in the continuous- and intermittent-dose groups, respectively. There were no treatment-related deaths. The 60 mg once-daily intermittent dose was safe, with a low incidence of grade 3 or higher adverse events[78].

PI3Ki has also been considered in combination with conventional chemotherapy, immunotherapy, and other targeted therapies to achieve more potent therapeutic effects. Results of the phase III CHRONOS-4 trial comparing the efficacy and safety of Conpalisib in combination with BR or R-CHOP in patients with r/riNHL showed an ORR of 90% in the BR group and 100% in the R-CHOP group, with grade 3 or higher adverse events occurring in 70% of the BR group and 91% of the R-CHOP group[79]. Early clinical trials of PI3Ki in combination with other immune checkpoint inhibitors and IMiDs are currently underway.

Inderalisib-induced acute liver injury has also been reported and has been noted to be severe and potentially fatal[80]. In a phase I trial in patients with FL or MCL, the triple combination of inderalisib with lenaridomide and rituximab was discontinued early because of the excessive toxicity of all three drugs[81]. Combination therapy with other drugs, including inderalisib, is complicated for future treatment because of significant safety concerns owing to overtoxicity.

PI3K inhibitors were initially expected to have therapeutic effects, and various types of agents were developed, but due to the large number of adverse reactions, only zandelisib remains in Japan, for example, and clinical trials are continuing. We hope that the treatment effect for FL patients will improve in the future.

PI3K/mechanistic target of rapamycin inhibitor

Numerous studies have shown that somatic mutations in PI3K/Akt/mechanistic target of rapamycin (mTOR)-related genes may induce homeostatic activation of various types of cancer pathways, leading to dysregulation of tumor cell growth, growth, differentiation, metabolism, apoptosis, and other functions supporting tumor cell survival It has been shown[82].

Recently, dual inhibitors targeting two targets of the PI3K/PKB/mTOR signaling pathway have been developed and investigated for their therapeutic effects; PI3K/mTOR inhibitors not only inhibit cell proliferation but also promote cell apoptosis. They are also expected to be promising anticancer agents because of their high efficacy at low doses and low drug resistance[83].

The TOR inhibitors, temisirolimusm (TEM) and lenaridomide (LEN) combination therapy, overlapped within the PAM axis and were expected to have synergistic effects. the FL cohort was discontinued early due to low case numbers. the ORR and CRR of the DLBCL and exploratory cohorts were 26% and 13%, 64% and 18%, respectively. The ORR and CRR of the exploratory cohort for classical Hodgkin lymphoma (CHL) patients were 80% and 35%, respectively. Forty percent of CHL patients could be transferred to allogeneic transplant after TEM/LEN therapy. Grade 3 or higher hematologic adverse events were common, and three grade 5 adverse events occurred; TEM/LEN combination therapy was highly effective in advanced untreated lymphomas and especially in r/r CHL[84].

We look forward to the further development of new PI3K/Akt/mTOR dual inhibitors, and to the improvement of therapeutic results and progress as FL treatment agents through the accumulation of clinical trials.

CELL THERAPY

CAR-T cell therapy uses autologous T cells genetically engineered to attack cancer and other cells by introducing CARs.

CAR-T cell therapy is a highly effective, innovative, and revolutionary treatment for patients with r/r hematologic malignancies and shows great promise. When reinjected into the same patient, these CAR-

T cells trigger a T-cell-mediated immune response against the antigen-expressing malignancy and induce cell death. CAR-T cell therapy has recently been used in the treatment of iNHL such as FL and MCL. However, CAR T-cell therapy has a unique hematological toxicity, and post-treatment cytopenia is a major side effect[85,86].

Recent clinical trials have compared the efficacy and safety of three cell therapy modalities (autologous transplantation, allogeneic transplantation, and CAR-T with respect to their validity and rationale as therapeutic modalities[87]. In addition, there are various issues and barriers to the realization of CAR-T therapy, including complex logistics, manufacturing limitations, toxicity concerns, and economic burdens, which must be addressed and remedy[88]. The results of clinical trials on CAR-T cell therapy are summarized in Table 8.

Clinical trials of the autologous anti-CD19 CART agents axicabtagene ciloleucel (Axi-cell), tisagenlecleucel (Tisa-cell), and lisocabtagene maraleucel (Liso-cell) for r/r DLBCL containing approximately 20% transformed FL (Liso-cell) have shown high efficacy, with ORRs ranging from 52% to 82%[89-91]. Long-term follow-up has shown sustained remission in approximately 40% of the patients and high remission maintenance against t-FL[92]. The results of the Phase II ZUMA-5 trial showed that Axi-cells in r/r FL had a median follow-up of 18 mo, with an ORR of 94%, a CRR of 79%, and an estimated PFS of 66% at 18 mo, although the median PFS and OS were not reached. Grade 3 or higher adverse events were observed in 86%, with Grade-5 adverse events in 3%[93,94].

The results of the phase II ELARA trial showed an ORR of 86% and a CR of 69% after a median follow-up of 17 mo for Tisa-cell r/r FL. The results of the Phase II ELARA trial of Tisa-cell therapy for r/r FL showed an ORR of 86% and CR of 69% at a median follow-up of 17 mo[95-97]. It is important to note that the results of these trials showed that Tisa-cells had a higher sustained response in higher-risk patients with refractory, relapsed, and heavily pretreated FL[98].

Liso-cells are autologous anti-CD19 CAR-T cells. The results of a clinical trial as a second-line therapy for patients with r/r DLBCL not scheduled for hematopoietic stem cell transplantation showed high efficacy, with a median follow-up of 12.3 mo and an ORR of 80%. Grade 3 or higher adverse events ranged from 20%-48% for thrombocytopenia and 21% for serious adverse events[99]. Based on these results, Liso cells have the potential for future use in patients with r/r FL.

The TRANSFORM and PILOT trials demonstrated the high efficacy of Liso-cell in the second-line treatment of r/r large B-cell lymphoma. As a result, Liso-cell was approved as a third-line agent for aggresive B-cell lymphoma[100].

Expectations are high for the future development of CAR-T cell therapy as a fundamental therapeutic tool for FL.

MOLECULAR RESPONSE ADAPTIVE THERAPY RESPONSE-ADOPTED POST-INDUCTION STRATEGY

The FOLL12 study compared a standard 2-year rituximab maintain therapy arm with an experimental post-remission induction arm in patients with FL who responded to induction immunochemotherapy. In the experimental arm, post-induction treatment consisted of observation for patients with complete metabolic response (CMR) and minimal residual disease (MRD)-negative disease, four doses of rituximab for patients with CMR and MRD-positive disease until MRD-negative, and one dose of ibritumomab tixetan for non-CMR patients, followed by three standard treatments with RM. Results showed that After a median follow-up of 53 mo, patients in the standard arm had significantly better PFS than those in the experimental arm (3-year PFS, 86% *vs* 72%; $P < 0.001$). All subgroups except non-CMR patients confirmed the superior PFS of the standard group *vs* the experimental group, with 3-year OS rates of 98% and 97% (95%CI, 95-99) in the reference and experimental groups, respectively[101]. In FL patients who benefited from induction therapy, standard 2-year rituximab maintenance therapy prolonged PFS after the induction of remission.

Future prospects for nodal FL treatment

Although FL progresses slowly and can be effective if treated, it is prone to recurrence and has been considered an incurable disease. Recently, however, research and progress in various new treatment modalities have been remarkable, and improvements in treatment outcomes have been confirmed. In addition, the direction of research is beginning to turn toward how to combine two or more of these anticancer agents, immune agents, immunomodulators, and CAR-T cell therapy, which have different mechanisms of action, and how to arrange the order of treatment in such combinations to obtain the best results. After discussing this important topic, I will conclude this section with the hope that the era of complete cure of FL will arrive in the future.

Prospects for GI-FL treatment

Based on an understanding of the recent advances in the treatment of nodal FL that have been discussed, the current status and future of GI-FL treatment and how gastroenterologists should treat

Table 8 Summary of clinical trials results of chimeric antigen receptor T-cell therapies

Study	Target disease	No. of patients	Objective response rate	Complete response rate	Progression-free survival	Overall survival	Adverse events and others	Ref.
Axicabtagene ciloleucel (Axi-cell), phase-II	r/r DLBCL, t-FL	*n* = 101	82%	40%	Unknown	52% (overall survival rate at 18.8 mo)	Neutropenia 78%; anemia 43%; thrombocytopenia 38%	[90]
Tisagenlecleucel (Tisa-cell), phase-II JULIET trial	r/r DLBCL	*n* = 93	52%	40%	65% (relapse-free survival rate)	Unknown	CRS 22%; neurologic events 12%; infections 20%	[91]
Axicabtagene ciloleucel (Axi-cell), phase-II	r/r iNHL (FL and MZL) after 2 or more treatment	*n* = 148, *n* = 124 (FL), *n* = 24 (MZL)	92%	74%	Unknown	Unknown	Serious adverse events (any grade) occurred in 50% of all	[93]
Tisagenlecleucel (Tisa-cell), phase-II ELARA trial	r/r FL (with 2 and more prior treatments)	*n* = 97	86.2%	69.1%	Unknown	Unknown	CRS 48.5% (> G3) neurological events 37.1% (> G3)	[96]
Lisocabtagene maraleucel (Liso-cell), phase-II	r/r large BCL	*n* = 61	80% (median follow-up 12.3 mo)	Unknown	Unknown	Unknown	Neutropenia 48%, thrombocytopenia 20%, CRS 38%	[99]

"Unknown" means data not shown, unknown information or not reached. r/r: Refractory and relapsed; FL: Follicular lymphoma; t-FL: Transformed follicular lymphoma; (i)NHL: (Indolent) non-Hodgkin lymphoma; DLBCL: Diffuse large B-cell lymphoma; BCL: B-cell lymphoma; MZL: Marginal zone lymphoma; CRS: Cytokine release syndrome.

gastrointestinal FL in the future will be discussed.

FL is the most common low-grade lymphoma, and although nodal FL is highly responsive to treatment, the majority of patients relapse repeatedly, and the disease has been said to be incurable with a poor prognosis. In contrast, primary GI-FL has been detected and treated in a larger number of cases in Japan, especially due to recent advances in small bowel endoscopy and increased opportunities for endoscopic examinations, such as health checkups, diagnostic imaging equipment, endoscopist examination techniques, and endoscopic diagnostic procedures. However, many cases are detected at an early stage, and many of them are at a later stage than those detected at an early stage, owing to the bias of reported cases, and the prognosis is excellent. Therefore, there is still a mainstream view that "watch and wait" is preferable, taking into account the adverse effects of treatment and the decline in patient quality of life. Schmatz *et al*[102] compared the progression of 63 stage I GI-FLs in the treatment, watch, and wait groups and reported no significant difference in PFS or OS. Tari *et al*[103] also reported no difference in prognosis in a study of GI-FL patients with low tumor volume divided between the "watch and wait" groups and the rituximab combination chemotherapy group. GI-FL is considered a potential candidate for "watch and wait" in many cases because of its pathological characteristics: The lesions are widely distributed and not amenable to local therapy, many patients are asymptomatic in the localized stage, and the degree of tumor extension and invasion is lower than that of nodal FL. The number of patients with nodal FL was high, and the degree of tumor progression and invasiveness was low. Yamamoto *et al*[104] have reported that 128 (66.3%) of 193 cases of GI-FL in Japan were stage I and 52 (26.9%) were stage II. The authors attribute this to the higher frequency of grade 1 lymphoma. However, we think that the reported cases may not necessarily represent the overall picture of GI-FL cases in Japan due to a large bias arising when they selected. In a Japanese multicenter study by Takata *et al*[105] in 125 patients with localized GI-FL, CR was observed in 61 (49%) out of 125 patients treated with Watch and Wait (33 patients), combination chemotherapy including rituximab (42 patients), rituximab alone (29 patients), surgical resection (4 patients), radiation therapy (1 patient), and *Helicobacter pylori (H. pylori)* eradication therapy (3 patients). pylori eradication therapy in three cases, 61 cases (49%) achieved CR, and by treatment method, 39/42 cases (93%) were treated with multi-agent chemotherapy including rituximab, 20/29 (69%) with rituximab alone, 1/4 (25%) with surgical resection, 0/1 case (0%) with radiation therapy, *H. pylori* eradication in 1/3 (33%), and Watch and Wait 1/33 (3%). The median follow-up was 40 mo (6-148 mo), with no primary deaths, a 5-year survival rate of 100%, a progression-free survival rate of 93 %, and very good results[105]. It should be noted that the Watch and Wait group had a CR rate of 3%, which was lower than the CR rate in the treatment group, excluding radiotherapy. Damaj *et al*[9] reported that most GI-FL are Stage I, but metastasis or invasion of intra-abdominal lymph nodes (Stage II) is 3.4%-40.0%, and extensive extranodal dissemination or transdiaphragmatic invasion (Stage IV) is reported in 12%-24% of GI-FL cases. The number of reports of advanced GI-FL cases (stages III and IV) is expected to increase further in the future. To understand the recent advances in the treatment of nodal FL, how should gastroenterologists treat gastrointestinal FL in the future? In early stage I cases, endoscopic resection of the gastrointestinal tract or surgical resection plus R-CHOP is the

standard of care. The prognosis was good and the PFS and OS were excellent. The number of refractory and advanced GI-FL cases, grade 3b or higher at the cellular level, and stage II or higher are expected to increase in the future. These cases will likely be treated with the same advanced and recent therapeutic modalities for nodal FL, such as antibody-targeted therapy, bispecific antibody therapy, epigenetic mutation, and CAR T-cell therapy, as described previously. The importance of nodal and Gastrointestinal-FL treatments is expected to increase. The difference is that when GI-FL is treated, the risk of perforation of the gastrointestinal tract must always be considered because if perforation develops due to a decrease in tumor volume, subsequent peritonitis may develop, making the disease more severe, and subsequent treatment impossible to continue. After careful consideration of the risk of gastrointestinal perforation, surgical resection of the gastrointestinal lesion should be performed first, followed by adjuvant therapy. For postoperative recurrence, lymph node metastases outside the gastrointestinal tract, and other distant metastases, it is necessary to collaborate with hematology and gastrointestinal surgery departments to predict possible complications and changes in disease status due to treatment, such as in the treatment of nodal and r/r-FL, and to discuss a royal policy in collaboration with these departments. We look forward to the future development and progress of GI-FL treatment.

Differences in treatment strategies between nodal FL and GI-FL

Staging of nodal FL is determined using the Ann-Arbor clinical staging classification, while GI-FL is classified according to the Lugano staging classification[106], a modified version of the Ann-Arbor staging classification. Basically, the Lugano staging classification[106] should be followed to determine a treatment strategy similar to that for nodal FL. However, due to the characteristics of the gastrointestinal tract, a treatment strategy specific to gastrointestinal FL may be considered in the following cases, which differ from nodal FL.

First, and most importantly, one must be very mindful of gastrointestinal perforation due to the loss of tumor tissue associated with the mass reduction effect of treatment. Careful consideration should be given to the risk of gastrointestinal tract perforation before initiating any type of treatment.

In GI-FL cases, whether the distribution of lesions is unifocal or multifocal is important in the choice of treatment; Yamamoto *et al*[104] reported that in more than 70% of GI-FL patients with lesions in the gastrointestinal tract other than the small bowel, new secondary lesions were found in the small bowel. If the disease is found to be multifocal, immunochemotherapy may be the treatment of choice.

Primary FL in the gastrointestinal tract should be treated with surgical resection first, followed by postoperative chemotherapy (or combination chemotherapy and immunotherapy), depending on the extent of extension and invasion, if the lesions arise from deep submucosal layers and are localized within the wall, lumen, or regional lymph nodes. However, if the disease has invaded or spread beyond the gastrointestinal tract or has distant metastasis beyond the diaphragm, it is stage-4 according to the Lugano classification, and if there is no or little deterioration in quality of life due to gastrointestinal obstruction, local surgical resection is of course not indicated, and combination chemotherapy plus immunotherapy or immunomodulators is the chemotherapy plus immunotherapy or immunomodulators is the first choice.

In cases of extra-gastrointestinal primary disease with gastrointestinal involvement, surgical resection or radiotherapy should be considered if the disease is localized. If there are metastases in multiple organs or bone marrow, the disease is basically stage-4, and chemotherapy (plus immunotherapy) is the first choice.

In addition, other factors such as age, gender, site of disease, and extent of spread should determine the best overall treatment for each case of gastrointestinal FL that is most appropriate for the patient and that offers a better prognosis, especially longer treatment-free period and improved patient quality of life. Because gastrointestinal FL is an organ with "gastrointestinal" characteristics, the treatment strategy is often more controversial than that for nodal FL, and in a sense, the range of treatment options is wider.

In addition, the underlying nature of FL itself, which as a tumor is indolent in its extension, growth, and invasion, responds well to chemotherapy, but is prone to relapse and is currently incurable, further complicates and complicates the treatment options for gastrointestinal FL. The differences in treatment strategy between nodal FL and gastrointestinal FL are described in the author's previous review[107], which should also be consulted.

In the future, the number of advanced-stage, multifocal GI-FL cases will increase more and more, and the treatment strategy should be carefully determined by cooperating multiple physicians in each department, including gastroenterology, surgery, hematology, and radiology.

CONCLUSION

Treatment with Nodal-FL improved the ORR, CRR, PFS, and OS with the addition of rituximab, an anti-CD20 monoclonal antibody, to CHOP therapy, which was the standard chemotherapy regimen for malignant lymphomas 20 years ago. Maintenance therapy with an anti-CD20 antibody prolongs

remission. The last decade has seen remarkable progress with the addition of new therapeutic modalities such as antibody-targeted therapy, bispecific antibody therapy, epigenetic modulator therapy, CAR-T cell therapy, and conventional chemotherapy. The combination of lenaridomide and anti-CD20 antibodies was effective in r/r FL treatment. In contrast, lenaridomide shows good results as frontline therapy for untreated patients with advanced FL and may become a mainstay treatment modality. Antibody therapies against novel targets, such as CD19, CD79b, and CD47, as well as obinutumab, a humanized anti-CD20 monoclonal antibody, have been developed and have demonstrated efficacy in FL. More recently, anti-PD-L1 antibodies such as atezolitumab and pembrolizumab have also demonstrated efficacy in relapsed FL. PI3Kinase inhibitors are effective for treating FL and multiple relapsed lesions. However, the high number of adverse events associated with its toxicity complicates its future use as a combination therapy. As an epigenetic modulator treatment, tazemetostat showed more activity in r/r FL patients with higher risk characteristics. Vorinostat, a histone deacetylase inhibitor HDACi, is also a potential treatment for r/r FL patients. CAR-T cell therapy for FL and T-cell immune attack with bispecific antibodies have shown remarkable efficacy and are expected to become a fundamental therapy, as evidenced by the current approval of CAR-T cell therapy for relapsed and refractory FL in the United States. In Europe and the United States, Damaj *et al*[9] have reported that most GI-FL cases are stage I, but metastasis or invasion of intra-abdominal lymph nodes (stage-II) is present in 3.4%-40.0% and extensive extranodal organ dissemination or involvement beyond the diaphragm (stage-IV) in 12%-24%. The number of advanced GI-FL cases (stages III and IV) is expected to increase further in the future. The number of refractory and advanced GI-FL cases, grade 3b or higher at the cellular level, and stage II or higher are expected to increase in the future. For these cases, recent advances in nodal FL, such as antibody-targeted therapy, bispecific antibody therapy, epigenetic mutation, and CAR-T cell therapy, as described above, should be considered as treatment options, but with careful attention to gastrointestinal perforation and cooperation among the departments of gastroenterology, hematology, and gastroenterological surgery need to work together.

FOOTNOTES

Author contributions: Takuya Watanabe solely contributes to this manuscript.

Conflict-of-interest statement: The authors declare that they have no conflict of interest.

Country/Territory of origin: Japan

ORCID number: Takuya Watanabe 0000-0003-3820-0262.

S-Editor: Chen YL
L-Editor: A
P-Editor: Cai YX

REFERENCES

1 The world health organization classification of malignant lymphomas in japan: incidence of recently recognized entities. Lymphoma Study Group of Japanese Pathologists. *Pathol Int* 2000; **50**: 696-702 [PMID: 11012982 DOI: 10.1046/j.1440-1827.2000.01108.x]

2 **Jaffe ES**, Harris NL, Stein H, Vardiman J. World Health Organization Classification of Tumors: Tumors of the Hematopoietic and Lymphoid Tissues. 2001. [cited 20 April 2023]. Avaliable from: https://tumourclassification.iarc.who.int/welcome/

3 **Chihara D**, Ito H, Matsuda T, Shibata A, Katsumi A, Nakamura S, Tomotaka S, Morton LM, Weisenburger DD, Matsuo K. Differences in incidence and trends of haematological malignancies in Japan and the United States. *Br J Haematol* 2014; **164**: 536-545 [PMID: 24245986 DOI: 10.1111/bjh.12659]

4 **d'Amore F**, Christensen BE, Brincker H, Pedersen NT, Thorling K, Hastrup J, Pedersen M, Jensen MK, Johansen P, Andersen E. Clinicopathological features and prognostic factors in extranodal non-Hodgkin lymphomas. Danish LYFO Study Group. *Eur J Cancer* 1991; **27**: 1201-1208 [PMID: 1835586 DOI: 10.1016/0277-5379(91)90081-n]

5 **Cirillo M**, Federico M, Curci G, Tamborrino E, Piccinini L, Silingardi V. Primary gastrointestinal lymphoma: a clinicopathological study of 58 cases. *Haematologica* 1992; **77**: 156-161 [PMID: 1398301]

6 **Yoshino T**, Miyake K, Ichimura K, Mannami T, Ohara N, Hamazaki S, Akagi T. Increased incidence of follicular lymphoma in the duodenum. *Am J Surg Pathol* 2000; **24**: 688-693 [PMID: 10800987 DOI:

10.1097/00000478-200005000-00007]
7 **Lewin KJ**, Ranchod M, Dorfman RF. Lymphomas of the gastrointestinal tract: a study of 117 cases presenting with gastrointestinal disease. *Cancer* 1978; **42**: 693-707 [PMID: 354774 DOI: 10.1002/1097-0142(197808)42:2<693::aid-cncr2820420241>3.0.co;2-j]
8 **Filippa DA**, Lieberman PH, Weingrad DN, Decosse JJ, Bretsky SS. Primary lymphomas of the gastrointestinal tract. Analysis of prognostic factors with emphasis on histological type. *Am J Surg Pathol* 1983; **7**: 363-372 [PMID: 6869665 DOI: 10.1097/00000478-198306000-00008]
9 **Damaj G**, Verkarre V, Delmer A, Solal-Celigny P, Yakoub-Agha I, Cellier C, Maurschhauser F, Bouabdallah R, Leblond V, Lefrère F, Bouscary D, Audouin J, Coiffier B, Varet B, Molina T, Brousse N, Hermine O. Primary follicular lymphoma of the gastrointestinal tract: a study of 25 cases and a literature review. *Ann Oncol* 2003; **14**: 623-629 [PMID: 12649111 DOI: 10.1093/annonc/mdg168]
10 **Hiddemann W**, Buske C, Dreyling M, Weigert O, Lenz G, Forstpointner R, Nickenig C, Unterhalt M. Treatment strategies in follicular lymphomas: current status and future perspectives. *J Clin Oncol* 2005; **23**: 6394-6399 [PMID: 16155025 DOI: 10.1200/JCO.2005.07.019]
11 **Conconi A**, Lobetti-Bodoni C, Montoto S, Lopez-Guillermo A, Coutinho R, Matthews J, Franceschetti S, Bertoni F, Moccia A, Rancoita PM, Gribben J, Cavalli F, Gaidano G, Lister TA, Montserrat E, Ghielmini M, Zucca E. Life expectancy of young adults with follicular lymphoma. *Ann Oncol* 2015; **26**: 2317-2322 [PMID: 26362567 DOI: 10.1093/annonc/mdv376]
12 **Ghielmini M**, Schmitz SF, Cogliatti SB, Pichert G, Hummerjohann J, Waltzer U, Fey MF, Betticher DC, Martinelli G, Peccatori F, Hess U, Zucca E, Stupp R, Kovacsovics T, Helg C, Lohri A, Bargetzi M, Vorobiof D, Cerny T. Prolonged treatment with rituximab in patients with follicular lymphoma significantly increases event-free survival and response duration compared with the standard weekly x 4 schedule. *Blood* 2004; **103**: 4416-4423 [PMID: 14976046 DOI: 10.1182/blood-2003-10-3411]
13 **Hiddemann W**, Kneba M, Dreyling M, Schmitz N, Lengfelder E, Schmits R, Reiser M, Metzner B, Harder H, Hegewisch-Becker S, Fischer T, Kropff M, Reis HE, Freund M, Wörmann B, Fuchs R, Planker M, Schimke J, Eimermacher H, Trümper L, Aldaoud A, Parwaresch R, Unterhalt M. Frontline therapy with rituximab added to the combination of cyclophosphamide, doxorubicin, vincristine, and prednisone (CHOP) significantly improves the outcome for patients with advanced-stage follicular lymphoma compared with therapy with CHOP alone: results of a prospective randomized study of the German Low-Grade Lymphoma Study Group. *Blood* 2005; **106**: 3725-3732 [PMID: 16123223 DOI: 10.1182/blood-2005-01-0016]
14 **Duell J**, Maddocks KJ, González-Barca E, Jurczak W, Liberati AM, De Vos S, Nagy Z, Obr A, Gaidano G, Abrisqueta P, Kalakonda N, André M, Dreyling M, Menne T, Tournilhac O, Augustin M, Rosenwald A, Dirnberger-Hertweck M, Weirather J, Ambarkhane S, Salles G. Long-term outcomes from the Phase II L-MIND study of tafasitamab (MOR208) plus lenalidomide in patients with relapsed or refractory diffuse large B-cell lymphoma. *Haematologica* 2021; **106**: 2417-2426 [PMID: 34196165 DOI: 10.3324/haematol.2020.275958]
15 **Morschhauser F**, Flinn IW, Advani R, Sehn LH, Diefenbach C, Kolibaba K, Press OW, Salles G, Tilly H, Chen AI, Assouline S, Cheson BD, Dreyling M, Hagenbeek A, Zinzani PL, Jones S, Cheng J, Lu D, Penuel E, Hirata J, Wenger M, Chu YW, Sharman J. Polatuzumab vedotin or pinatuzumab vedotin plus rituximab in patients with relapsed or refractory non-Hodgkin lymphoma: final results from a phase 2 randomised study (ROMULUS). *Lancet Haematol* 2019; **6**: e254-e265 [PMID: 30935953 DOI: 10.1016/S2352-3026(19)30026-2]
16 **Hamadani M**, Radford J, Carlo-Stella C, Caimi PF, Reid E, O'Connor OA, Feingold JM, Ardeshna KM, Townsend W, Solh M, Heffner LT, Ungar D, Wang L, Boni J, Havenith K, Qin Y, Kahl BS. Final results of a phase 1 study of loncastuximab tesirine in relapsed/refractory B-cell non-Hodgkin lymphoma. *Blood* 2021; **137**: 2634-2645 [PMID: 33211842 DOI: 10.1182/blood.2020007512]
17 **Advani R**, Flinn I, Popplewell L, Forero A, Bartlett NL, Ghosh N, Kline J, Roschewski M, LaCasce A, Collins GP, Tran T, Lynn J, Chen JY, Volkmer JP, Agoram B, Huang J, Majeti R, Weissman IL, Takimoto CH, Chao MP, Smith SM. CD47 Blockade by Hu5F9-G4 and Rituximab in Non-Hodgkin's Lymphoma. *N Engl J Med* 2018; **379**: 1711-1721 [PMID: 30380386 DOI: 10.1056/NEJMoa1807315]
18 **Davies A**, Kater AP, Sharman JP, Stilgenbauer S, Vitolo U, Klein C, Parreira J, Salles G. Obinutuzumab in the treatment of B-cell malignancies: a comprehensive review. *Future Oncol* 2022; **18**: 2943-2966 [PMID: 35856239 DOI: 10.2217/fon-2022-0112]
19 **Stathis A**, Mey U, Schär S, Hitz F, Pott C, Mach N, Krasniqi F, Novak U, Schmidt C, Hohloch K, Kienle DL, Hess D, Moccia AA, Unterhalt M, Eckhardt K, Hayoz S, Forestieri G, Rossi D, Dirnhofer S, Ceriani L, Sartori G, Bertoni F, Buske C, Zucca E, Hiddemann W. SAKK 35/15: a phase 1 trial of obinutuzumab in combination with venetoclax in patients with previously untreated follicular lymphoma. *Blood Adv* 2022; **6**: 3911-3920 [PMID: 35537101 DOI: 10.1182/bloodadvances.2021006520]
20 **Marcus R**, Davies A, Ando K, Klapper W, Opat S, Owen C, Phillips E, Sangha R, Schlag R, Seymour JF, Townsend W, Trněný M, Wenger M, Fingerle-Rowson G, Rufibach K, Moore T, Herold M, Hiddemann W. Obinutuzumab for the First-Line Treatment of Follicular Lymphoma. *N Engl J Med* 2017; **377**: 1331-1344 [PMID: 28976863 DOI: 10.1056/NEJMoa1614598]
21 **Casulo C**, Herold M, Hiddemann W, Iyengar S, Marcus RE, Seymour JF, Launonen A, Knapp A, Nielsen TG, Mir F. Risk Factors for and Outcomes of Follicular Lymphoma Histological Transformation at First Progression in the GALLIUM Study. *Clin Lymphoma Myeloma Leuk* 2023; **23**: 40-48 [PMID: 36379880 DOI: 10.1016/j.clml.2022.09.003]
22 **Gmoshinskiĭ IV**, Mazo VK, Shaternikov VA. [Breakdown of the soluble soybean antigen in the digestive tract of adult rats]. *Vopr Pitan* 1986; 43-46 [PMID: 3532538]
23 **Yang L**, Zheng Z, Li N, Zheng B, Liu M, Cai H. Efficacy and safety of rituximab biosimilars or reference product as first-line treatment in patients with low-tumour-burden follicular lymphoma: A systematic review and meta-analysis. *J Clin Pharm Ther* 2022; **47**: 1923-1931 [PMID: 36345167 DOI: 10.1111/jcpt.13799]
24 **Budde LE**, Assouline S, Sehn LH, Schuster SJ, Yoon SS, Yoon DH, Matasar MJ, Bosch F, Kim WS, Nastoupil LJ, Flinn

IW, Shadman M, Diefenbach C, O'Hear C, Huang H, Kwan A, Li CC, Piccione EC, Wei MC, Yin S, Bartlett NL. Single-Agent Mosunetuzumab Shows Durable Complete Responses in Patients With Relapsed or Refractory B-Cell Lymphomas: Phase I Dose-Escalation Study. *J Clin Oncol* 2022; **40**: 481-491 [PMID: 34914545 DOI: 10.1200/JCO.21.00931]

25 **Budde LE**, Sehn LH, Matasar M, Schuster SJ, Assouline S, Giri P, Kuruvilla J, Canales M, Dietrich S, Fay K, Ku M, Nastoupil L, Cheah CY, Wei MC, Yin S, Li CC, Huang H, Kwan A, Penuel E, Bartlett NL. Safety and efficacy of mosunetuzumab, a bispecific antibody, in patients with relapsed or refractory follicular lymphoma: a single-arm, multicentre, phase 2 study. *Lancet Oncol* 2022; **23**: 1055-1065 [PMID: 35803286 DOI: 10.1016/S1470-2045(22)00335-7]

26 **Hutchings M**, Morschhauser F, Iacoboni G, Carlo-Stella C, Offner FC, Sureda A, Salles G, Martínez-Lopez J, Crump M, Thomas DN, Morcos PN, Ferlini C, Bröske AE, Belousov A, Bacac M, Dimier N, Carlile DJ, Lundberg L, Perez-Callejo D, Umaña P, Moore T, Weisser M, Dickinson MJ. Glofitamab, a Novel, Bivalent CD20-Targeting T-Cell-Engaging Bispecific Antibody, Induces Durable Complete Remissions in Relapsed or Refractory B-Cell Lymphoma: A Phase I Trial. *J Clin Oncol* 2021; **39**: 1959-1970 [PMID: 33739857 DOI: 10.1200/JCO.20.03175]

27 **Hutchings M**, Mous R, Clausen MR, Johnson P, Linton KM, Chamuleau MED, Lewis DJ, Sureda Balari A, Cunningham D, Oliveri RS, Elliott B, DeMarco D, Azaryan A, Chiu C, Li T, Chen KM, Ahmadi T, Lugtenburg PJ. Dose escalation of subcutaneous epcoritamab in patients with relapsed or refractory B-cell non-Hodgkin lymphoma: an open-label, phase 1/2 study. *Lancet* 2021; **398**: 1157-1169 [PMID: 34508654 DOI: 10.1016/S0140-6736(21)00889-8]

28 **Falchi L**, Lepp¨ AS, Wahlin BE, Nijland M, Christensen JH, De Vos S, Holte H, Linton KM, Abbas A, Wang LW, Dinh M, Elliott B, Belada D. Subcutaneous epcoritamab with rituximab + lenalidomide (R2) in patients (pts) with relapsed or refractory (R/R) follicular lymphoma (FL): Update from a phase 1/2 trial. *J Clin Oncol* 2022; **40** Suppl 16: 7524 [DOI: 10.1200/jco.2022.40.16_suppl.7524]

29 **Bannerji R**, Arnason JE, Advani RH, Brown JR, Allan JN, Ansell SM, Barnes JA, O'Brien SM, Chávez JC, Duell J, Rosenwald A, Crombie JL, Ufkin M, Li J, Zhu M, Ambati SR, Chaudhry A, Lowy I, Topp MS. Odronextamab, a human CD20×CD3 bispecific antibody in patients with CD20-positive B-cell malignancies (ELM-1): results from the relapsed or refractory non-Hodgkin lymphoma cohort in a single-arm, multicentre, phase 1 trial. *Lancet Haematol* 2022; **9**: e327-e339 [PMID: 35366963 DOI: 10.1016/S2352-3026(22)00072-2]

30 **Dickinson M**. Challenges in the development of bispecific antibodies for non-Hodgkin lymphoma. *Lancet Haematol* 2022; **9**: e314-e315 [PMID: 35366964 DOI: 10.1016/S2352-3026(22)00104-1]

31 **Palomba ML**, Till BG, Park SI, Morschhauser F, Cartron G, Marks R, Shivhare M, Hong WJ, Raval A, Chang AC, Penuel E, Popplewell LL. Combination of Atezolizumab and Obinutuzumab in Patients with Relapsed/Refractory Follicular Lymphoma and Diffuse Large B-Cell Lymphoma: Results from a Phase 1b Study. *Clin Lymphoma Myeloma Leuk* 2022; **22**: e443-e451 [PMID: 35031227 DOI: 10.1016/j.clml.2021.12.010]

32 **Nastoupil LJ**, Chin CK, Westin JR, Fowler NH, Samaniego F, Cheng X, Ma MCJ, Wang Z, Chu F, Dsouza L, Obi C, Mims J, Feng L, Zhou S, Green M, Davis RE, Neelapu SS. Safety and activity of pembrolizumab in combination with rituximab in relapsed or refractory follicular lymphoma. *Blood Adv* 2022; **6**: 1143-1151 [PMID: 35015819 DOI: 10.1182/bloodadvances.2021006240]

33 **Gandhi AK**, Kang J, Havens CG, Conklin T, Ning Y, Wu L, Ito T, Ando H, Waldman MF, Thakurta A, Klippel A, Handa H, Daniel TO, Schafer PH, Chopra R. Immunomodulatory agents lenalidomide and pomalidomide co-stimulate T cells by inducing degradation of T cell repressors Ikaros and Aiolos *via* modulation of the E3 ubiquitin ligase complex CRL4(CRBN.). *Br J Haematol* 2014; **164**: 811-821 [PMID: 24328678 DOI: 10.1111/bjh.12708]

34 **Leonard JP**, Jung SH, Johnson J, Pitcher BN, Bartlett NL, Blum KA, Czuczman M, Giguere JK, Cheson BD. Randomized Trial of Lenalidomide Alone Versus Lenalidomide Plus Rituximab in Patients With Recurrent Follicular Lymphoma: CALGB 50401 (Alliance). *J Clin Oncol* 2015; **33**: 3635-3640 [PMID: 26304886 DOI: 10.1200/JCO.2014.59.9258]

35 **Leonard JP**, Trneny M, Izutsu K, Fowler NH, Hong X, Zhu J, Zhang H, Offner F, Scheliga A, Nowakowski GS, Pinto A, Re F, Fogliatto LM, Scheinberg P, Flinn IW, Moreira C, Cabeçadas J, Liu D, Kalambakas S, Fustier P, Wu C, Gribben JG; AUGMENT Trial Investigators. AUGMENT: A Phase III Study of Lenalidomide Plus Rituximab Versus Placebo Plus Rituximab in Relapsed or Refractory Indolent Lymphoma. *J Clin Oncol* 2019; **37**: 1188-1199 [PMID: 30897038 DOI: 10.1200/JCO.19.00010]

36 **Coleman M**, Andorsky DJ, Yacoub A, Melear JM, Fanning SR, Kolibaba KS, Jason M, Lansigan F, Reynolds CM, Nowakowski GS, Gharibo M, Ahn E, Li J, Rummel MJ, Sharman JP. Patients with relapsed/refractory marginal zone lymphoma in the MAGNIFY phase IIIb interim analysis of induction R2 followed by maintenance. *Blood* 2020; **136** Suppl 1: 24-25 [DOI: 10.1016/j.htct.2021.10.167]

37 **Morschhauser F**, Le Gouill S, Feugier P, Bailly S, Nicolas-Virelizier E, Bijou F, Salles GA, Tilly H, Fruchart C, Van Eygen K, Snauwaert S, Bonnet C, Haioun C, Thieblemont C, Bouabdallah R, Wu KL, Canioni D, Meignin V, Cartron G, Houot R. Obinutuzumab combined with lenalidomide for relapsed or refractory follicular B-cell lymphoma (GALEN): a multicentre, single-arm, phase 2 study. *Lancet Haematol* 2019; **6**: e429-e437 [PMID: 31296423 DOI: 10.1016/S2352-3026(19)30089-4]

38 **Morschhauser F**, Fowler NH, Feugier P, Bouabdallah R, Tilly H, Palomba ML, Fruchart C, Libby EN, Casasnovas RO, Flinn IW, Haioun C, Maisonneuve H, Ysebaert L, Bartlett NL, Bouabdallah K, Brice P, Ribrag V, Daguindau N, Le Gouill S, Pica GM, Martin Garcia-Sancho A, López-Guillermo A, Larouche JF, Ando K, Gomes da Silva M, André M, Zachée P, Sehn LH, Tobinai K, Cartron G, Liu D, Wang J, Xerri L, Salles GA; RELEVANCE Trial Investigators. Rituximab plus Lenalidomide in Advanced Untreated Follicular Lymphoma. *N Engl J Med* 2018; **379**: 934-947 [PMID: 30184451 DOI: 10.1056/NEJMoa1805104]

39 **Evens AM**, Hong F, Habermann TM, Advani RH, Gascoyne RD, Witzig TE, Quon A, Ranheim EA, Ansell SM, Cheema PS, Dy PA, O'Brien TE, Winter JN, Cescon TP, Chang JE, Kahl BS. A Three-Arm Randomized Phase II Study of Bendamustine/Rituximab with Bortezomib Induction or Lenalidomide Continuation in Untreated Follicular Lymphoma: ECOG-ACRIN E2408. *Clin Cancer Res* 2020; **26**: 4468-4477 [PMID: 32532790 DOI: 10.1158/1078-0432.CCR-20-1345]

40 **Nastoupil LJ**, Westin JR, Hagemeister FB, Lee HJ, Fayad L, Samaniego F, Ahmed S, Claret L, Steiner RE, Nair R, Parmar S, Rodriguez MA, Wang ML, Green MR, Neelapu SS, Fowler NH. Results of a Phase II study of obinutuzumab in

combination with lenalidomide in previously untreated, high tumor burden follicular lymphoma (FL). *Blood* 2019; **134** Suppl 1: 125 [DOI: 10.1182/blood-2019-129422]

41 **Wang Y**, Zhou S, Qi X, Yang F, Maurer MJ, Habermann TM, Witzig TE, Wang ML, Nowakowski GS. Efficacy of front-line immunochemotherapy for follicular lymphoma: a network meta-analysis of randomized controlled trials. *Blood Cancer J* 2022; **12**: 1 [PMID: 34987165 DOI: 10.1038/s41408-021-00598-x]

42 **Phillips T**, Chan H, Tam CS, Tedeschi A, Johnston P, Oh SY, Opat S, Eom HS, Allewelt H, Stern JC, Tan Z, Novotny W, Huang J, Trotman J. Zanubrutinib monotherapy in relapsed/refractory indolent non-Hodgkin lymphoma. *Blood Adv* 2022; **6**: 3472-3479 [PMID: 35390135 DOI: 10.1182/bloodadvances.2021006083]

43 **Song Y**, Zhou K, Zou D, Zhou J, Hu J, Yang H, Zhang H, Ji J, Xu W, Jin J, Lv F, Feng R, Gao S, Guo H, Zhou L, Huang J, Novotny W, Kim P, Yu Y, Wu B, Zhu J. Zanubrutinib in relapsed/refractory mantle cell lymphoma: long-term efficacy and safety results from a phase 2 study. *Blood* 2022; **139**: 3148-3158 [PMID: 35303070 DOI: 10.1182/blood.2021014162]

44 **Byrd JC**, Brown JR, O'Brien S, Barrientos JC, Kay NE, Reddy NM, Coutre S, Tam CS, Mulligan SP, Jaeger U, Devereux S, Barr PM, Furman RR, Kipps TJ, Cymbalista F, Pocock C, Thornton P, Caligaris-Cappio F, Robak T, Delgado J, Schuster SJ, Montillo M, Schuh A, de Vos S, Gill D, Bloor A, Dearden C, Moreno C, Jones JJ, Chu AD, Fardis M, McGreivy J, Clow F, James DF, Hillmen P; RESONATE Investigators. Ibrutinib versus ofatumumab in previously treated chronic lymphoid leukemia. *N Engl J Med* 2014; **371**: 213-223 [PMID: 24881631 DOI: 10.1056/NEJMoa1400376]

45 **Sharman JP**, Egyed M, Jurczak W, Skarbnik A, Pagel JM, Flinn IW, Kamdar M, Munir T, Walewska R, Corbett G, Fogliatto LM, Herishanu Y, Banerji V, Coutre S, Follows G, Walker P, Karlsson K, Ghia P, Janssens A, Cymbalista F, Woyach JA, Salles G, Wierda WG, Izumi R, Munugalavadla V, Patel P, Wang MH, Wong S, Byrd JC. Acalabrutinib with or without obinutuzumab versus chlorambucil and obinutuzmab for treatment-naive chronic lymphocytic leukaemia (ELEVATE TN): a randomised, controlled, phase 3 trial. *Lancet* 2020; **395**: 1278-1291 [PMID: 32305093 DOI: 10.1016/S0140-6736(20)30262-2]

46 **Mato AR**, Shah NN, Jurczak W, Cheah CY, Pagel JM, Woyach JA, Fakhri B, Eyre TA, Lamanna N, Patel MR, Alencar A, Lech-Maranda E, Wierda WG, Coombs CC, Gerson JN, Ghia P, Le Gouill S, Lewis DJ, Sundaram S, Cohen JB, Flinn IW, Tam CS, Barve MA, Kuss B, Taylor J, Abdel-Wahab O, Schuster SJ, Palomba ML, Lewis KL, Roeker LE, Davids MS, Tan XN, Fenske TS, Wallin J, Tsai DE, Ku NC, Zhu E, Chen J, Yin M, Nair B, Ebata K, Marella N, Brown JR, Wang M. Pirtobrutinib in relapsed or refractory B-cell malignancies (BRUIN): a phase 1/2 study. *Lancet* 2021; **397**: 892-901 [PMID: 33676628 DOI: 10.1016/S0140-6736(21)00224-5]

47 **Gopal AK**, Schuster SJ, Fowler NH, Trotman J, Hess G, Hou JZ, Yacoub A, Lill M, Martin P, Vitolo U, Spencer A, Radford J, Jurczak W, Morton J, Caballero D, Deshpande S, Gartenberg GJ, Wang SS, Damle RN, Schaffer M, Balasubramanian S, Vermeulen J, Cheson BD, Salles G. Ibrutinib as Treatment for Patients With Relapsed/Refractory Follicular Lymphoma: Results From the Open-Label, Multicenter, Phase II DAWN Study. *J Clin Oncol* 2018; **36**: 2405-2412 [PMID: 29851546 DOI: 10.1200/JCO.2017.76.8853]

48 **Fowler NH**, Nastoupil L, De Vos S, Knapp M, Flinn IW, Chen R, Advani RH, Bhatia S, Martin P, Mena R, Davis RE, Neelapu SS, Eckert K, Ping J, Co M, Beaupre DM, Neuenburg JK, Palomba ML. The combination of ibrutinib and rituximab demonstrates activity in first-line follicular lymphoma. *Br J Haematol* 2020; **189**: 650-660 [PMID: 32180219 DOI: 10.1111/bjh.16424]

49 **Fowler NH**, Coleman M, Stevens DA, Smith SM, Venugopal P, Martin P, Phillips TJ, Agajanian R, Stephens DM, Izumi R, Cheung J, Slatter JG, Yin M, Hiremath M, Hunder NNH. Acalabrutinib alone or in combination with rituximab (R) in follicular lymphoma (FL). *J Clin Oncol* 2018; **36** Suppl 15: 7549

50 **Zinzani PL**, Mayer J, Auer R, Bijou F, de Oliverira AC, Flowers C, Merli M, Bouabdallah K, Ganly PS, Johnson R, Yuen S, Kingsley E, Tumyan G, Assouline SE, Ivanova E, Kim P, Huang J, Delarue R, Trotman J. Zanubrutinib plus Obinutuzumab (ZO) vs Obinutuzumab (O) monotherapy in patients (pts) with relapsed or refractory (R/R) follicular ltmphoma (FL): Primary analysis of the phase 2 randomized ROSEWOOD trial. *J Clin Oncol* 2022; **40** Suppl 16: 7510 [DOI: 10.1200/jco.2022.40.16_suppl.7510]

51 **Parikh A**, Gopalakrishnan S, Freise KJ, Verdugo ME, Menon RM, Mensing S, Salem AH. Exposure-response evaluations of venetoclax efficacy and safety in patients with non-Hodgkin lymphoma. *Leuk Lymphoma* 2018; **59**: 871-879 [PMID: 28797193 DOI: 10.1080/10428194.2017.1361024]

52 **Zinzani PL**, Flinn IW, Yuen SLS, Topp MS, Rusconi C, Fleury I, Le Dû K, Arthur C, Pro B, Gritti G, Crump M, Petrich A, Samineni D, Sinha A, Punnoose EA, Szafer-Glusman E, Spielewoy N, Mobasher M, Humphrey K, Kornacker M, Hiddemann W. Venetoclax-rituximab with or without bendamustine vs bendamustine-rituximab in relapsed/refractory follicular lymphoma. *Blood* 2020; **136**: 2628-2637 [PMID: 32785666 DOI: 10.1182/blood.2020005588]

53 **Ujjani CS**, Lai C, Leslie LA, Ramzi P, Tan M, Wang S, Wang HK, Shim E, Swanson N, Broome CM, Gopal AK, Smith SD, Warren EH, Blue K, Kdiry S, Till BG, Lynch RC, Shadman M, Johnson M, Coye H, Shelby M, Tseng YD, Shustov A, Maloney DG, Cheson BD. Ibrutinib and venetoclax in relapsed and refractory follicular lymphoma. *Blood* 2020; **136** Suppl 1: 46-47 [DOI: 10.1182/blood-2020-136219]

54 **Morschhauser F**, Tilly H, Chaidos A, McKay P, Phillips T, Assouline S, Batlevi CL, Campbell P, Ribrag V, Damaj GL, Dickinson M, Jurczak W, Kazmierczak M, Opat S, Radford J, Schmitt A, Yang J, Whalen J, Agarwal S, Adib D, Salles G. Tazemetostat for patients with relapsed or refractory follicular lymphoma: an open-label, single-arm, multicentre, phase 2 trial. *Lancet Oncol* 2020; **21**: 1433-1442 [PMID: 33035457 DOI: 10.1016/S1470-2045(20)30441-1]

55 **Chung C**. A Promising Future for Precision Epigenetic Therapy for Follicular and Diffuse Large B-Cell Lymphoma? *Blood Lymphat Cancer* 2022; **12**: 99-106 [PMID: 35959380 DOI: 10.2147/BLCTT.S282247]

56 **Barghout SH**, Machado RAC, Barsyte-Lovejoy D. Chemical biology and pharmacology of histone lysine methylation inhibitors. *Biochim Biophys Acta Gene Regul Mech* 2022; **1865**: 194840 [PMID: 35753676 DOI: 10.1016/j.bbagrm.2022.194840]

57 **Proudman D**, Nellesen D, Gupta D, Adib D, Yang J, Mamlouk K. A Matching-Adjusted Indirect Comparison of Single-Arm Trials in Patients with Relapsed or Refractory Follicular Lymphoma Who Received at Least Two Prior Systemic Treatments: Tazemetostat was Associated with a Lower Risk for Safety Outcomes Versus the PI3-Kinase Inhibitors Idelalisib, Duvelisib, Copanlisib, and Umbralisib. *Adv Ther* 2022; **39**: 1678-1696 [PMID: 35157216 DOI:

10.1007/s12325-022-02054-z]
58 **Ogura M**, Ando K, Suzuki T, Ishizawa K, Oh SY, Itoh K, Yamamoto K, Au WY, Tien HF, Matsuno Y, Terauchi T, Mori M, Tanaka Y, Shimamoto T, Tobinai K, Kim WS. A multicentre phase II study of vorinostat in patients with relapsed or refractory indolent B-cell non-Hodgkin lymphoma and mantle cell lymphoma. *Br J Haematol* 2014; **165**: 768-776 [PMID: 24617454 DOI: 10.1111/bjh.12819]
59 **Chen R**, Frankel P, Popplewell L, Siddiqi T, Ruel N, Rotter A, Thomas SH, Mott M, Nathwani N, Htut M, Nademanee A, Forman SJ, Kirschbaum M. A phase II study of vorinostat and rituximab for treatment of newly diagnosed and relapsed/refractory indolent non-Hodgkin lymphoma. *Haematologica* 2015; **100**: 357-362 [PMID: 25596263 DOI: 10.3324/haematol.2014.117473]
60 **Batlevi CL**, Crump M, Andreadis C, Rizzieri D, Assouline SE, Fox S, van der Jagt RHC, Copeland A, Potvin D, Chao R, Younes A. A phase 2 study of mocetinostat, a histone deacetylase inhibitor, in relapsed or refractory lymphoma. *Br J Haematol* 2017; **178**: 434-441 [PMID: 28440559 DOI: 10.1111/bjh.14698]
61 **Vanhaesebroeck B**, Leevers SJ, Ahmadi K, Timms J, Katso R, Driscoll PC, Woscholski R, Parker PJ, Waterfield MD. Synthesis and function of 3-phosphorylated inositol lipids. *Annu Rev Biochem* 2001; **70**: 535-602 [PMID: 11395417 DOI: 10.1146/annurev.biochem.70.1.535]
62 **Bi L**, Okabe I, Bernard DJ, Nussbaum RL. Early embryonic lethality in mice deficient in the p110beta catalytic subunit of PI 3-kinase. *Mamm Genome* 2002; **13**: 169-172 [PMID: 11919689 DOI: 10.1007/BF02684023]
63 **Sasaki T**, Irie-Sasaki J, Jones RG, Oliveira-dos-Santos AJ, Stanford WL, Bolon B, Wakeham A, Itie A, Bouchard D, Kozieradzki I, Joza N, Mak TW, Ohashi PS, Suzuki A, Penninger JM. Function of PI3Kgamma in thymocyte development, T cell activation, and neutrophil migration. *Science* 2000; **287**: 1040-1046 [PMID: 10669416 DOI: 10.1126/science.287.5455.1040]
64 **Laffargue M**, Calvez R, Finan P, Trifilieff A, Barbier M, Altruda F, Hirsch E, Wymann MP. Phosphoinositide 3-kinase gamma is an essential amplifier of mast cell function. *Immunity* 2002; **16**: 441-451 [PMID: 11911828 DOI: 10.1016/s1074-7613(02)00282-0]
65 **Isidori A**, Loscocco F, Visani G, Paolasini S, Scalzulli P, Musto P, Perrone T, Guarini A, Pastore D, Mazza P, Tonialini L, Pavone V, De Santis G, Tarantini G. Real-life efficacy and safety of idelalisib in 55 double-refractory follicular lymphoma patients. *Br J Haematol* 2022; **199**: 339-343 [PMID: 36002151 DOI: 10.1111/bjh.18426]
66 **Gopal AK**, Kahl BS, de Vos S, Wagner-Johnston ND, Schuster SJ, Jurczak WJ, Flinn IW, Flowers CR, Martin P, Viardot A, Blum KA, Goy AH, Davies AJ, Zinzani PL, Dreyling M, Johnson D, Miller LL, Holes L, Li D, Dansey RD, Godfrey WR, Salles GA. PI3Kδ inhibition by idelalisib in patients with relapsed indolent lymphoma. *N Engl J Med* 2014; **370**: 1008-1018 [PMID: 24450858 DOI: 10.1056/NEJMoa1314583]
67 **Gordon MJ**, Huang J, Chan RJ, Bhargava P, Danilov AV. Medical comorbidities in patients with chronic lymphocytic leukaemia treated with idelalisib: analysis of two large randomised clinical trials. *Br J Haematol* 2021; **192**: 720-728 [PMID: 32599655 DOI: 10.1111/bjh.16879]
68 **Coutré SE**, Barrientos JC, Brown JR, de Vos S, Furman RR, Keating MJ, Li D, O'Brien SM, Pagel JM, Poleski MH, Sharman JP, Yao NS, Zelenetz AD. Management of adverse events associated with idelalisib treatment: expert panel opinion. *Leuk Lymphoma* 2015; **56**: 2779-2786 [PMID: 25726955 DOI: 10.3109/10428194.2015.1022770]
69 **Wang Z**, Zhou H, Xu J, Wang J, Niu T. Safety and efficacy of dual PI3K-δ, γ inhibitor, duvelisib in patients with relapsed or refractory lymphoid neoplasms: A systematic review and meta-analysis of prospective clinical trials. *Front Immunol* 2022; **13**: 1070660 [PMID: 36685572 DOI: 10.3389/fimmu.2022.1070660]
70 **Dreyling M**, Santoro A, Mollica L, Leppä S, Follows G, Lenz G, Kim WS, Nagler A, Dimou M, Demeter J, Özcan M, Kosinova M, Bouabdallah K, Morschhauser F, Stevens DA, Trevarthen D, Munoz J, Rodrigues L, Hiemeyer F, Miriyala A, Garcia-Vargas J, Childs BH, Zinzani PL. Long-term safety and efficacy of the PI3K inhibitor copanlisib in patients with relapsed or refractory indolent lymphoma: 2-year follow-up of the CHRONOS-1 study. *Am J Hematol* 2020; **95**: 362-371 [PMID: 31868245 DOI: 10.1002/ajh.25711]
71 **Dreyling M**, Santoro A, Mollica L, Leppä S, Follows GA, Lenz G, Kim WS, Nagler A, Panayiotidis P, Demeter J, Özcan M, Kosinova M, Bouabdallah K, Morschhauser F, Stevens DA, Trevarthen D, Giurescu M, Cupit L, Liu L, Köchert K, Seidel H, Peña C, Yin S, Hiemeyer F, Garcia-Vargas J, Childs BH, Zinzani PL. Phosphatidylinositol 3-Kinase Inhibition by Copanlisib in Relapsed or Refractory Indolent Lymphoma. *J Clin Oncol* 2017; **35**: 3898-3905 [PMID: 28976790 DOI: 10.1200/JCO.2017.75.4648]
72 **Maharaj K**, Powers JJ, Achille A, Mediavilla-Varela M, Gamal W, Burger KL, Fonseca R, Jiang K, Miskin HP, Maryanski D, Monastyrskyi A, Duckett DR, Roush WR, Cleveland JL, Sahakian E, Pinilla-Ibarz J. The dual PI3Kδ/CK1ε inhibitor umbralisib exhibits unique immunomodulatory effects on CLL T cells. *Blood Adv* 2020; **4**: 3072-3084 [PMID: 32634240 DOI: 10.1182/bloodadvances.2020001800]
73 **Schweitzer J**, Hoffman M, Graf SA. The evidence to date on umbralisib for the treatment of refractory marginal zone lymphoma and follicular lymphoma. *Expert Opin Pharmacother* 2022; **23**: 535-541 [PMID: 35209784 DOI: 10.1080/14656566.2022.2043273]
74 **Fowler NH**, Samaniego F, Jurczak W, Ghosh N, Derenzini E, Reeves JA, Knopińska-Posłuszny W, Cheah CY, Phillips T, Lech-Maranda E, Cheson BD, Caimi PF, Grosicki S, Leslie LA, Chavez JC, Fonseca G, Babu S, Hodson DJ, Shao SH, Burke JM, Sharman JP, Law JY, Pagel JM, Miskin HP, Sportelli P, O'Connor OA, Weiss MS, Zinzani PL. Umbralisib, a Dual PI3Kδ/CK1ε Inhibitor in Patients With Relapsed or Refractory Indolent Lymphoma. *J Clin Oncol* 2021; **39**: 1609-1618 [PMID: 33683917 DOI: 10.1200/JCO.20.03433]
75 **Fukuhara N**, Suehiro Y, Kato H, Kusumoto S, Coronado C, Rappold E, Zhao W, Li J, Gilmartin A, Izutsu K. Parsaclisib in Japanese patients with relapsed or refractory B-cell lymphoma (CITADEL-111): A phase Ib study. *Cancer Sci* 2022; **113**: 1702-1711 [PMID: 35201656 DOI: 10.1111/cas.15308]
76 **Forero-Torres A**, Ramchandren R, Yacoub A, Wertheim MS, Edenfield WJ, Caimi P, Gutierrez M, Akard L, Escobar C, Call J, Persky D, Iyer S, DeMarini DJ, Zhou L, Chen X, Dawkins F, Phillips TJ. Parsaclisib, a potent and highly selective PI3Kδ inhibitor, in patients with relapsed or refractory B-cell malignancies. *Blood* 2019; **133**: 1742-1752 [PMID: 30803990 DOI: 10.1182/blood-2018-08-867499]

77 **Goto H**, Izutsu K, Ennishi D, Mishima Y, Makita S, Kato K, Hanaya M, Hirano S, Narushima K, Teshima T, Nagai H, Ishizawa K. Zandelisib (ME-401) in Japanese patients with relapsed or refractory indolent non-Hodgkin's lymphoma: an open-label, multicenter, dose-escalation phase 1 study. *Int J Hematol* 2022; **116**: 911-921 [PMID: 36107394 DOI: 10.1007/s12185-022-03450-5]

78 **Pagel JM**, Soumerai JD, Reddy N, Jagadeesh D, Stathis A, Asch A, Salman H, Kenkre VP, Iasonos A, Llorin-Sangalang J, Li J, Zelenetz AD. Zandelisib with continuous or intermittent dosing as monotherapy or in combination with rituximab in patients with relapsed or refractory B-cell malignancy: a multicentre, first-in-patient, dose-escalation and dose-expansion, phase 1b trial. *Lancet Oncol* 2022; **23**: 1021-1030 [PMID: 35835137 DOI: 10.1016/S1470-2045(22)00333-3]

79 **Matasar MJ**, Dreyling M, Leppä S, Santoro A, Pedersen M, Buvaylo V, Fletcher M, Childs BH, Zinzani PL. Feasibility of Combining the Phosphatidylinositol 3-Kinase Inhibitor Copanlisib With Rituximab-Based Immunochemotherapy in Patients With Relapsed Indolent B-cell Lymphoma. *Clin Lymphoma Myeloma Leuk* 2021; **21**: e886-e894 [PMID: 34389273 DOI: 10.1016/j.clml.2021.06.021]

80 LiverTox: Clinical and Research Information on Drug-Induced Liver Injury [Internet]. Bethesda (MD): National Institute of Diabetes and Digestive and Kidney Diseases; 2012- [PMID: 31643176]

81 **Smith SM**, Pitcher BN, Jung SH, Bartlett NL, Wagner-Johnston N, Park SI, Richards KL, Cashen AF, Jaslowski A, Smith SE, Cheson BD, Hsi E, Leonard JP. Safety and tolerability of idelalisib, lenalidomide, and rituximab in relapsed and refractory lymphoma: the Alliance for Clinical Trials in Oncology A051201 and A051202 phase 1 trials. *Lancet Haematol* 2017; **4**: e176-e182 [PMID: 28314699 DOI: 10.1016/S2352-3026(17)30028-5]

82 **Wu X**, Xu Y, Liang Q, Yang X, Huang J, Wang J, Zhang H, Shi J. Recent Advances in Dual PI3K/mTOR Inhibitors for Tumour Treatment. *Front Pharmacol* 2022; **13**: 875372 [PMID: 35614940 DOI: 10.3389/fphar.2022.875372]

83 **McCurdy A**, Visram A. The Role of Belantamab Mafodotin, Selinexor, and Melflufen in Multiple Myeloma. *Curr Hematol Malig Rep* 2022; **17**: 306-318 [PMID: 36417082 DOI: 10.1007/s11899-022-00682-4]

84 **Major A**, Kline J, Karrison TG, Fishkin PAS, Kimball AS, Petrich AM, Nattam S, Rao K, Sleckman BG, Cohen K, Besien KV, Rapoport AP, Smith SM. Phase I/II clinical trial of temsirolimus and lenalidomide in patients with relapsed and refractory lymphomas. *Haematologica* 2022; **107**: 1608-1618 [PMID: 34320785 DOI: 10.3324/haematol.2021.278853]

85 **Sharma N**, Reagan PM, Liesveld JL. Cytopenia after CAR-T Cell Therapy-A Brief Review of a Complex Problem. *Cancers (Basel)* 2022; **14** [PMID: 35326654 DOI: 10.3390/cancers14061501]

86 **Yassine F**, Murthy H, Ghabashi E, Kharfan-Dabaja MA, Iqbal M. Understanding the Etiology of Pancytopenias in the CAR T-Cell Therapy Setting: What We Know and What We Don't? *Hematol Oncol Stem Cell Ther* 2022; **15**: 122-130 [PMID: 36633964 DOI: 10.56875/2589-0646.1047]

87 **Goldsmith SR**, Ghobadi A, Dipersio JF, Hill B, Shadman M, Jain T. Chimeric Antigen Receptor T Cell Therapy versus Hematopoietic Stem Cell Transplantation: An Evolving Perspective. *Transplant Cell Ther* 2022; **28**: 727-736 [PMID: 35878743 DOI: 10.1016/j.jtct.2022.07.015]

88 **Gajra A**, Zalenski A, Sannareddy A, Jeune-Smith Y, Kapinos K, Kansagra A. Barriers to Chimeric Antigen Receptor T-Cell (CAR-T) Therapies in Clinical Practice. *Pharmaceut Med* 2022; **36**: 163-171 [PMID: 35672571 DOI: 10.1007/s40290-022-00428-w]

89 **Abramson JS**, Palomba ML, Gordon LI, Lunning MA, Wang M, Arnason J, Mehta A, Purev E, Maloney DG, Andreadis C, Sehgal A, Solomon SR, Ghosh N, Albertson TM, Garcia J, Kostic A, Mallaney M, Ogasawara K, Newhall K, Kim Y, Li D, Siddiqi T. Lisocabtagene maraleucel for patients with relapsed or refractory large B-cell lymphomas (TRANSCEND NHL 001): a multicentre seamless design study. *Lancet* 2020; **396**: 839-852 [PMID: 32888407 DOI: 10.1016/S0140-6736(20)31366-0]

90 **Neelapu SS**, Locke FL, Bartlett NL, Lekakis LJ, Miklos DB, Jacobson CA, Braunschweig I, Oluwole OO, Siddiqi T, Lin Y, Timmerman JM, Stiff PJ, Friedberg JW, Flinn IW, Goy A, Hill BT, Smith MR, Deol A, Farooq U, McSweeney P, Munoz J, Avivi I, Castro JE, Westin JR, Chavez JC, Ghobadi A, Komanduri KV, Levy R, Jacobsen ED, Witzig TE, Reagan P, Bot A, Rossi J, Navale L, Jiang Y, Aycock J, Elias M, Chang D, Wiezorek J, Go WY. Axicabtagene Ciloleucel CAR T-Cell Therapy in Refractory Large B-Cell Lymphoma. *N Engl J Med* 2017; **377**: 2531-2544 [PMID: 29226797 DOI: 10.1056/NEJMoa1707447]

91 **Schuster SJ**, Bishop MR, Tam CS, Waller EK, Borchmann P, McGuirk JP, Jäger U, Jaglowski S, Andreadis C, Westin JR, Fleury I, Bachanova V, Foley SR, Ho PJ, Mielke S, Magenau JM, Holte H, Pantano S, Pacaud LB, Awasthi R, Chu J, Anak Ö, Salles G, Maziarz RT; JULIET Investigators. Tisagenlecleucel in Adult Relapsed or Refractory Diffuse Large B-Cell Lymphoma. *N Engl J Med* 2019; **380**: 45-56 [PMID: 30501490 DOI: 10.1056/NEJMoa1804980]

92 **Chong EA**, Ruella M, Schuster SJ; Lymphoma Program Investigators at the University of Pennsylvania. Five-Year Outcomes for Refractory B-Cell Lymphomas with CAR T-Cell Therapy. *N Engl J Med* 2021; **384**: 673-674 [PMID: 33596362 DOI: 10.1056/NEJMc2030164]

93 **Jacobson CA**, Chavez JC, Sehgal AR, William BM, Munoz J, Salles G, Munshi PN, Casulo C, Maloney DG, de Vos S, Reshef R, Leslie LA, Yakoub-Agha I, Oluwole OO, Fung HCH, Rosenblatt J, Rossi JM, Goyal L, Plaks V, Yang Y, Vezan R, Avanzi MP, Neelapu SS. Axicabtagene ciloleucel in relapsed or refractory indolent non-Hodgkin lymphoma (ZUMA-5): a single-arm, multicentre, phase 2 trial. *Lancet Oncol* 2022; **23**: 91-103 [PMID: 34895487 DOI: 10.1016/S1470-2045(21)00591-X]

94 **Mohty R**, Kharfan-Dabaja MA. CAR T-cell therapy for follicular lymphoma and mantle cell lymphoma. *Ther Adv Hematol* 2022; **13**: 20406207221142133 [PMID: 36544864 DOI: 10.1177/20406207221142133]

95 **Jacobson CA**, Chavez JC, Sehgal A, William BM, Munoz J, Salles GA. Outcomes in ZUMA-5 with axicabtagene ciloleucel (axi-cel) in patients (pts) Outcomes in ZUMA-5 with axicabtagene ciloleucel (axi-cel) in patients (pts) with relapsed/refractory (R/R) indolent non-Hodgkin lymphoma (iNHL) who had the high-risk feature of progression within 24 mo from initiation of first anti-CD20-containing chemoimmunotherapy (POD24). *J Clin Oncol* 2021; **39** Suppl 15: 7515 [DOI: 10.1200/jco.2021.39.15_suppl.7515]

96 **Fowler NH**, Dickinson M, Dreyling M, Martinez-Lopez J, Kolstad A, Butler J, Ghosh M, Popplewell L, Chavez JC, Bachy E, Kato K, Harigae H, Kersten MJ, Andreadis C, Riedell PA, Ho PJ, Pérez-Simón JA, Chen AI, Nastoupil LJ, von

Tresckow B, Ferreri AJM, Teshima T, Patten PEM, McGuirk JP, Petzer AL, Offner F, Viardot A, Zinzani PL, Malladi R, Zia A, Awasthi R, Masood A, Anak O, Schuster SJ, Thieblemont C. Tisagenlecleucel in adult relapsed or refractory follicular lymphoma: the phase 2 ELARA trial. *Nat Med* 2022; **28**: 325-332 [PMID: 34921238 DOI: 10.1038/s41591-021-01622-0]

97 **Salles G**, Schuster SJ, Dreyling M, Fischer L, Kuruvilla J, Patten PEM, von Tresckow B, Smith SM, Jiménez-Ubieto A, Davis KL, Anjos C, Chu J, Zhang J, Lobetti Bodoni C, Thieblemont C, Fowler NH, Dickinson M, Martínez-López J, Wang Y, Link BK. Efficacy comparison of tisagenlecleucel vs usual care in patients with relapsed or refractory follicular lymphoma. *Blood Adv* 2022; **6**: 5835-5843 [PMID: 35973192 DOI: 10.1182/bloodadvances.2022008150]

98 **Sarkozy C**, Maurer MJ, Link BK, Ghesquieres H, Nicolas E, Thompson CA, Traverse-Glehen A, Feldman AL, Allmer C, Slager SL, Ansell SM, Habermann TM, Bachy E, Cerhan JR, Salles G. Cause of Death in Follicular Lymphoma in the First Decade of the Rituximab Era: A Pooled Analysis of French and US Cohorts. *J Clin Oncol* 2019; **37**: 144-152 [PMID: 30481079 DOI: 10.1200/JCO.18.00400]

99 **Sehgal A**, Hoda D, Riedell PA, Ghosh N, Hamadani M, Hildebrandt GC, Godwin JE, Reagan PM, Wagner-Johnston N, Essell J, Nath R, Solomon SR, Champion R, Licitra E, Fanning S, Gupta N, Dubowy R, D'Andrea A, Wang L, Ogasawara K, Thorpe J, Gordon LI. Lisocabtagene maraleucel as second-line therapy in adults with relapsed or refractory large B-cell lymphoma who were not intended for haematopoietic stem cell transplantation (PILOT): an open-label, phase 2 study. *Lancet Oncol* 2022; **23**: 1066-1077 [PMID: 35839786 DOI: 10.1016/S1470-2045(22)00339-4]

100 **St-Pierre F**, Gordon LI. Lisocabtagene maraleucel in the treatment of relapsed/refractory large B-cell lymphoma. *Future Oncol* 2023; **19**: 19-28 [PMID: 36651471 DOI: 10.2217/fon-2022-0774]

101 **Luminari S**, Manni M, Galimberti S, Versari A, Tucci A, Boccomini C, Farina L, Olivieri J, Marcheselli L, Guerra L, Ferrero S, Arcaini L, Cavallo F, Kovalchuk S, Skrypets T, Del Giudice I, Chauvie S, Patti C, Stelitano C, Ricci F, Pinto A, Margiotta Casaluci G, Zilioli VR, Merli A, Ladetto M, Bolis S, Pavone V, Chiarenza A, Arcari A, Anastasia A, Dondi A, Mannina D, Federico M; Fondazione Italiana Linfomi. Response-Adapted Postinduction Strategy in Patients With Advanced-Stage Follicular Lymphoma: The FOLL12 Study. *J Clin Oncol* 2022; **40**: 729-739 [PMID: 34709880 DOI: 10.1200/JCO.21.01234]

102 **Schmatz AI**, Streubel B, Kretschmer-Chott E, Püspök A, Jäger U, Mannhalter C, Tiemann M, Ott G, Fischbach W, Herzog P, Seitz G, Stolte M, Raderer M, Chott A. Primary follicular lymphoma of the duodenum is a distinct mucosal/submucosal variant of follicular lymphoma: a retrospective study of 63 cases. *J Clin Oncol* 2011; **29**: 1445-1451 [PMID: 21383289 DOI: 10.1200/JCO.2010.32.9193]

103 **Tari A**, Kitadai Y, Mouri R, Takigawa H, Asaoku H, Mihara K, Takata K, Fujihara M, Yoshino T, Koga T, Fujimori S, Tanaka S, Chayama K. Watch-and-wait policy versus rituximab-combined chemotherapy in Japanese patients with intestinal follicular lymphoma. *J Gastroenterol Hepatol* 2018; **33**: 1461-1468 [PMID: 29377265 DOI: 10.1111/jgh.14100]

104 **Yamamoto S**, Nakase H, Yamashita K, Matsuura M, Takada M, Kawanami C, Chiba T. Gastrointestinal follicular lymphoma: review of the literature. *J Gastroenterol* 2010; **45**: 370-388 [PMID: 20084529 DOI: 10.1007/s00535-009-0182-z]

105 **Takata K**, Okada H, Ohmiya N, Nakamura S, Kitadai Y, Tari A, Akamatsu T, Kawai H, Tanaka S, Araki H, Yoshida T, Okumura H, Nishisaki H, Sagawa T, Watanabe N, Arima N, Takatsu N, Nakamura M, Yanai S, Kaya H, Morito T, Sato Y, Moriwaki H, Sakamoto C, Niwa Y, Goto H, Chiba T, Matsumoto T, Ennishi D, Kinoshita T, Yoshino T. Primary gastrointestinal follicular lymphoma involving the duodenal second portion is a distinct entity: a multicenter, retrospective analysis in Japan. *Cancer Sci* 2011; **102**: 1532-1536 [PMID: 21561531 DOI: 10.1111/j.1349-7006.2011.01980.x]

106 **Rohatiner A**, d'Amore F, Coiffier B, Crowther D, Gospodarowicz M, Isaacson P, Lister TA, Norton A, Salem P, Shipp M. Report on a workshop convened to discuss the pathological and staging classifications of gastrointestinal tract lymphoma. *Ann Oncol* 1994; **5**: 397-400 [PMID: 8075046 DOI: 10.1093/oxfordjournals.annonc.a058869]

107 **Watanabe T**. Treatment strategies for nodal and gastrointestinal follicular lymphoma: current status and future development. *World J Gastroenterol* 2010; **16**: 5543-5554 [PMID: 21105187 DOI: 10.3748/wjg.v16.i44.5543]

World Journal of Gastroenterology

Submit a Manuscript: https://www.f6publishing.com

World J Gastroenterol 2023 June 21; 29(23): 3595-3605

DOI: 10.3748/wjg.v29.i23.3595

ISSN 1007-9327 (print) ISSN 2219-2840 (online)

MINIREVIEWS

Prognostic role of intestinal ultrasound in Crohn's disease

Cristina Manzotti, Francesco Colombo, Tommaso Zurleni, Piergiorgio Danelli, Giovanni Maconi

Specialty type: Gastroenterology and hepatology

Provenance and peer review: Invited article; Externally peer reviewed.

Peer-review model: Single blind

Peer-review report's scientific quality classification

Grade A (Excellent): 0
Grade B (Very good): 0
Grade C (Good): C, C
Grade D (Fair): 0
Grade E (Poor): 0

P-Reviewer: Iizuka M, Japan; Miyoshi E, Japan

Received: March 9, 2023
Peer-review started: March 9, 2023
First decision: March 20, 2023
Revised: April 5, 2023
Accepted: May 23, 2023
Article in press: May 23, 2023
Published online: June 21, 2023

Cristina Manzotti, Giovanni Maconi, Gastroenterology Unit, Department of Biomedical and Clinical Sciences, University of Milan, L.Sacco University Hospital, Milano 20157, Italy

Francesco Colombo, Tommaso Zurleni, Piergiorgio Danelli, Division of General Surgery, Department of Biomedical and Clinical Sciences, University of Milan, L.Sacco University Hospital, Milano 20157, Italy

Corresponding author: Francesco Colombo, MD, Assistant Professor, Division of General Surgery, Department of Biomedical and Clinical Sciences, University of Milan, L.Sacco University Hospital, Via Giovanni Battista Grassi 74, Milano 20157, Italy.
colombo.francesco@asst-fbf-sacco.it

Abstract

The majority of patients affected by Crohn's disease (CD) develop a chronic condition with persistent inflammation and relapses that may cause progressive and irreversible damage to the bowel, resulting in stricturing or penetrating complications in around 50% of patients during the natural history of the disease. Surgery is frequently needed to treat complicated disease when pharmacological therapy failes, with a high risk of repeated operations in time. Intestinal ultrasound (IUS), a non-invasive, cost-effective, radiation free and reproducible method for the diagnosis and follow-up of CD, in expert hands, allow a precise assessment of all the disease manifestations: Bowel characteristics, retrodilation, wrapping fat, fistulas and abscesses. Moreover, IUS is able to assess bowel wall thickness, bowel wall stratification (echo-pattern), vascularization and elasticity, as well as mesenteric hypertrophy, lymph-nodes and mesenteric blood flow. Its role in the disease evaluation and behaviour description is well assessed in literature, but less is known about the potential space of IUS as predictor of prognostic factors suggesting response to a medical treatment or postoperative recurrence. The availability of a low cost exam as IUS, able to recognize which patients are more likely to respond to a specific therapy and which patients are at high risk of surgery or complications, could be a very useful instrument in the hands of IBD physician. The aim of this review is to present current evidence about the prognostic role that IUS can show in predicting response to treatment, disease progression, risk of surgery and risk of post-surgical recurrence in CD.

Key Words: Intestinal ultrasound; Crohn's disease; Postoperative recurrence; Bowel wall thickness; Remission; Intestinal surgery

Core Tip: Intestinal ultrasound (IUS) and magnetic resonance enterography are better tolerated and safer than endoscopy, with IUS more easily available and less expensive than magnetic resonance imaging. Moreover, IUS allows complete visualization of the small-bowel even in patients with stenoses and/or severe inflammation, and can assess for extraintestinal disease. In addition, IUS may predict outcomes better than endoscopic mucosal assessment, possibly identifying more relevant therapeutic targets. This review discusses the role of IUS in Crohn's disease not only as first line investigation but as an extremely useful instrument in predicting response to medical treatment, disease evolution and risk of recurrence before and after surgery.

Citation: Manzotti C, Colombo F, Zurleni T, Danelli P, Maconi G. Prognostic role of intestinal ultrasound in Crohn's disease. *World J Gastroenterol* 2023; 29(23): 3595-3605
URL: https://www.wjgnet.com/1007-9327/full/v29/i23/3595.htm
DOI: https://dx.doi.org/10.3748/wjg.v29.i23.3595

INTRODUCTION

Crohn's disease (CD) is a chronic inflammatory condition that can affect the whole gastrointestinal tract, more frequently involving the ileum and colon, usually presenting in its active phases with abdominal pain, diarrhoea (bloody or non-bloody), urgency, fatigue and weight loss[1]. The majority of patients affected by CD show chronic relapsing disease with potential chronic continuous abdominal symptoms after diagnosis[2].

The available treatments often fail to achieve disease remission or lose their efficacy over time. Moreover, in CD, chronic inflammation and relapses may cause progressive and irreversible damage to the bowel[3], which results in stricturing or penetrating complications in approximately 50% of patients during the natural history of the disease, with a high risk of surgery or repeated surgery[4].

It has been realized that patients' symptoms in CD do not necessarily reflect the underlying inflammatory burden of the disease and that, independent of clinical symptoms, patients can have different rates of disease progression and outcomes[2]. Most CD patients at the time of diagnosis have a disease with inflammatory features, but in some patients, it can evolve to a stenosing or penetrating pattern during follow-up[5]. Therefore, the possibility of identifying which patients are nonresponsive to medical treatment and prone to develop stricturing and penetrating CD would be very important to properly address the treatment. Prognostic factors for favourable or unfavourable outcomes of CD have been extensively researched and assessed with both invasive and noninvasive methods.

Intestinal ultrasound (IUS) is a non-invasive, cost-effective, radiation free and reproducible method for the diagnosis and follow-up of CD, with an accuracy comparable to magnetic resonance imaging and computed tomography[6,7]. IUS can assess several features of the bowel wall and surrounding tissue: Bowel wall thickness (BWT) (Figure 1A), bowel wall stratification (echo-pattern) (Figure 1B), vascularization (Figure 1C) and elasticity, as well as mesenteric hypertrophy (Figure 1D), lymph-nodes (Figure 1E) and mesenteric blood flow. IUS is also able to assess complications such as stenosis, dilations, fistulas and abscesses[8]. During the follow-up of CD patients undergoing biological therapy, IUS features have been correlated with clinical activity, endoscopic activity, laboratory markers (faecal calprotectin and C-reactive protein) and drug serum levels[9-13]. However, IUS specific features have also been suggested as predictive factors for evaluating the response to medical treatment, the risk of clinical relapse or surgery, and the risk of postoperative recurrence[14-17]. We present the current evidence on the prognostic value of IUS and especially the IUS features of the bowel wall in predicting response to treatment and risk of relapse in CD.

LITERATURE REVIEW

Search strategy and selection criteria

Two authors (Manzotti C and Maconi G) searched the literature using the PubMed database from January 2000 to January 2022. The search used the following terms in different combinations: "intestinal ultrasound", "bowel ultrasound", "transabdominal ultrasound", "IUS", "bowel wall thickness", "Doppler", "CEUS", "transmural healing", "Crohn", "Crohn's disease", "IBD", "inflammatory bowel disease", "surgery", "clinical remission", "remission", "predictive value", "outcome", and "post-surgical recurrence". In particular, the following string was used: [(ultrasound OR sonography) AND (bowel OR intestinal) AND (Crohn's disease OR IBD) AND (remission OR response OR transmural OR outcome OR predictive)].

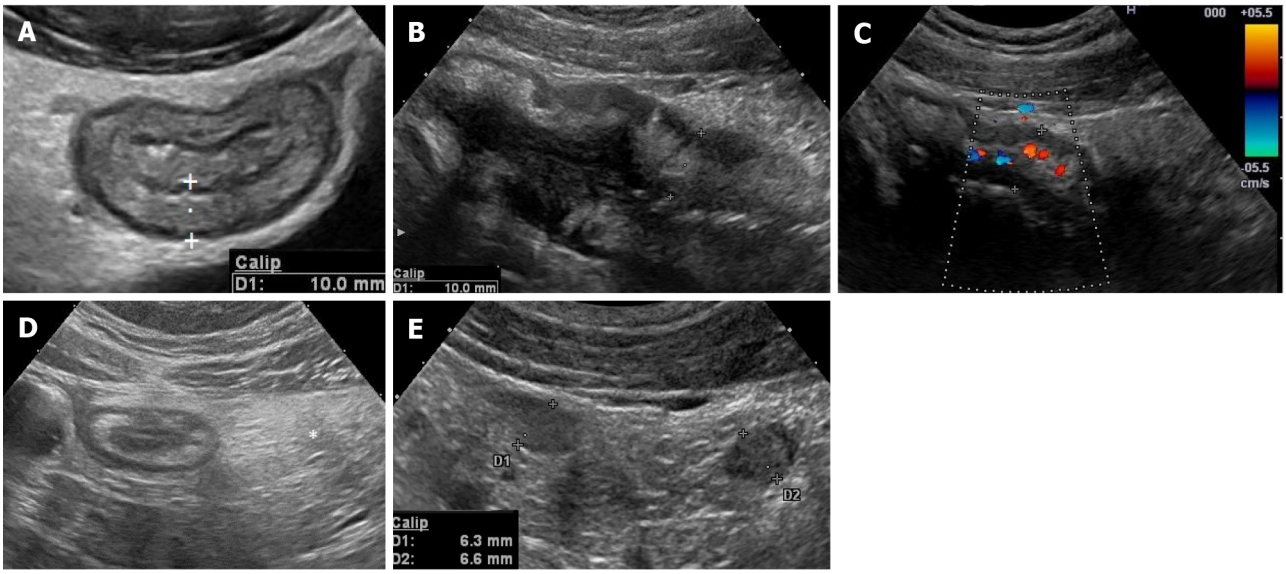

DOI: 10.3748/wjg.v29.i23.3595

Figure 1 Intestinal ultrasound assess several features of the bowel wall and surrounding tissue. A: Bowel wall thickness should be measured perpendicular to the anterior wall of the bowel (or where it is better visible) avoiding haustrations and mucosal folds. The cursor/calipers should be placed at the end of the interface echo between the serosa and the proper muscle to the start of the interface echo between the lumen and the mucosa; B: Bowel wall stratification. The wall layers in case of active disease may appear focally or extensively disrupted (disrupted or hypoechoic echo pattern); C: Bowel wall vascularity. Bowel wall vascularity can be determined both by colour Doppler or power Doppler signal at the level of the most thickened segments, using special presets optimized for slow flow detection; D: Mesenteric hypertrophy. Mesenteric hypertrophy also called fat wrapping or creeping fat appears on ultrasound (US) as hyperechoic tissue or "mass effect" encircling the diseased bowel; E: Lymphnodes. Enlarged inflammatory mesenteric lymph nodes related to Crohn's disease are usually described at US as oval or elongated with lesser diameter > 5 mm and seem to be correlated with young age, early disease, or disease with shorter duration, and with the presence of fistulae and abscesses.

Additional potentially eligible articles were manually searched through the bibliography of relevant articles. Eligible articles were randomized controlled trials, prospective or retrospective cohort studies, reviews, and systematic reviews with a meta-analysis; duplications and studies in languages other than English were excluded. In each eligible paper, we searched for information on the predictive value of IUS for patients affected by active or quiescent CD in terms of response to treatment, disease course, transmural healing, risk of surgery, and risk of postsurgical recurrence. Two authors (Manzotti C and Maconi G) screened the title and abstract of potentially eligible papers, followed by a full-text analysis of relevant articles. Starting from a total of 1040 articles, 49 were considered suitable and were included in this review.

DISCUSSION

Active disease

Intestinal US, before and early after the start of biologic treatment, showed high accuracy in predicting long-term clinical and endoscopic remission and response[17,18]. Although few data have shown that pretreatment IUS features may predict the outcome and somewhat drive the choice of treatment, much more data have shown that sonographic improvement of BWT, echopattern and vascularization as early as weeks 2-4 of biologic treatment may predict a better long-term response compared to those of patients without an early treatment response[19]. Studies considering predictive value of IUS parameters for response to treatment and course of CD are shown in Table 1.

Intestinal US to predict response to treatment and disease course

Increased BWT and bowel wall vascularity assessed by colour Doppler or IV contrast-enhanced ultrasound (CEUS), variably powered in bowel US scores, was identified as an independent predictor of a negative disease course, namely, the need for steroids, change of therapy, treatment intensification, hospitalization, or need for surgery through 6-12 mo[20,14]. In addition, increased echopatterns coupled with disrupted echopatterns of the bowel wall or lack of bowel wall stratification were independent predictors for the need for subsequent therapeutic optimization[20].

Sonographic response and clinical response

It seems that sonographic response after 12 or 14 wk of therapy with anti-tumor necrosis factor (TNF)

Table 1 Predictive value of intestinal ultrasound parameters for response to treatment and course of Crohn's disease

Ref.	Treatment	Timing of IUS after start of treatment	IUS parameter	Predictive value for
Albshesh *et al*[18], 2020	Anti-TNF	> 14 wk	BWT > 4 mm	Treatment failure
			BWT < 4 mm	Duration of failure-free response
Calabrese *et al*[52], 2022	Anti-TNF, vedolizumab, ustekinumab	Baseline	"Higher BWT"	Low risk of TR
			Colonic localization	High risk of TR
Chen *et al* [19], 2022	Anti-TNF	Baseline-2 wk	Reduction in BWT, vascularization, SWE	Response to treatment
De Voogd *et al*[17], 2022	Anti-TNF	Baseline-4/8 wk	BWT reduction > 18%	Endoscopic response and remission at 12-34 wk
Helwig *et al* [32], 2022	All available biological therapies	Baseline-12 wk	BWT reduction > 25%	Clinical remission and no therapy change at 52 wk
Les *et al*[20], 2021	5-ASA, budesonide, AZA, anti TNF		Worsened BWT, echopattern, vascularization	Need for treatment escalation, negative disease course
Orlando *et al* [29], 2018	Anti-TNF	Baseline	SWE strain ratio > 2	Surgery
Paredes *et al* [53], 2019	Anti-TNF	12 wk	BWT ≤ 3 mm	"Good outcome" (no treatment intensification, no surgery) at 1 yr
Ripollés *et al* [21], 2016	Anti-TNF	Baseline-12 wk	Sonographic response (BWT decrease > 2 mm, diminution of one grade of ECD, decrease > 20% of mural enhancement, disappearance of transmural complications or stenosi	1-yr sonographic response and further 1-yr clinical response and treatment efficacy
Smith *et al* [22], 2022	All available biological therapies and thiopurines	Baseline-14 wk	Sonographic response (BWT decreasing > 0.5 mm and vascularity improvement by ≥ one grade)	Treatment response at 46 wk
Zorzi *et al* [23], 2020	Anti-TNF, budesonide, thiopurines	Baseline-18 mo	Normalization of SICUS (BWT, disease extension, complications)	Long term lower cumulative probability of need for surgery, hospitalization, and need for steroids
Laterza *et al* [54], 2021	Anti-TNF	12 wk	CEUS increased PI and Pw	Clinical relapse within 6 mo
Ungar *et al* [55], 2020	Adalimumab	NA	Terminal ileum BWT < 4 mm	Therapy retention
Quaia *et al* [56], 2019	Anti-TNF	Baseline-6 wk	CEUS pretreatment values and % variations of peak enhancement, AUC, AUC during wash-in, AUC during wash-out	Long term response to therapy

IUS: Intestinal ultrasound; BWT: Bowel wall thickness; ECD: Eco-color-doppler; SWE: Shear wave elastography; UEI: Ultrasound elastography imaging; TR: Transmural remission; CEUS: Contrast enhanced ultrasound; AUC: Area under the curve; TNF: Tumor necrosis factor; NA: Not available; 5-ASA: 5-aminosalicylic acid; AZA: Azacitidine.

drugs predicts the 1-year sonographic response, which in turn correlates with the 1-year clinical response, predicts efficacy of further treatment and inversely correlated with the need for surgery. Stricturing behaviour, namely, the detection of strictures with prestenotic dilatation, seems to be the only sonographic feature associated with a long-term negative predictive value of clinical response[21, 22].

Similar results were demonstrated by using small intestinal contrast US (SICUS), which is used to monitor patients undergoing anti-TNF therapy. An improvement in BWT, a reduction of disease extension, or the absence of intestinal complications as detected by SICUS predicted a better response after 1 year of therapy, as well as a reduction in steroid therapy and hospital admissions[23].

Monitoring BWT with IUS also showed predictive value for patients starting therapy with ustekinumab. A decrease in BWT > 1 mm at week 8 after the start of therapy was a helpful parameter for selecting patients with an early response to ustekinumab and for providing assistance in terms of further treatment intervals[24]. The thickening of each single layer of the bowel wall and its clinical significance in CD have been poorly investigated thusfar. It seems that the thickening of the proper muscle layer in active CD patients is correlated with poor clinical and sonographic responses to vedolizumab treatment[25]. In this regard, smooth muscle hyperplasia has been underlined as a central

contributor to the stricturing phenotype, whereas fibrosis is less significant, and the 'inflammation-smooth muscle hyperplasia axis' seems to be the most important step in the pathogenesis of Crohn's strictures[26].

Additionally, the assessment of bowel wall vascularity by CEUS seems to provide relevant prognostic information regarding treatment efficacy in patients with CD. The improvement of several perfusion parameters, such as peak contrast enhancement, rate of wash-in and wash-out and the area under the time intensity curve of the intestinal wall 4-6 wk after starting anti-inflammatory treatment (anti-TNF-alpha), were correlated with a favourable response[25,27,28]. Finally, the evaluation of ultrasound elasticity of the bowel wall may have a predictive role as well, correlating with therapeutic outcomes for CD patients treated with anti-TNF[29].

With regard to extra bowel findings, especially mesenteric lymphadenopathy and mesenteric fat hypertrophy, their prognostic role in response to treatment remains controversial. Regional mesenteric lymphadenopathy detected by IUS is a common but nonspecific sonographic finding in early CD and could be linked to young age, early disease, and the presence of abscesses or fistulae[30]. However, its prognostic significance remains poorly investigated. Mesenteric fat hypertrophy is associated with clinical and biochemical disease activity, and it may disappear or improve in patients who have responded to medical treatment[31]. However, its prognostic value in predicting response to therapy and risk of relapse is debatable[16,31].

IUS to predict transmural remission

Transmural remission (TR) or transmural healing with different definitions in literature, is now considered as an objective and relevant target in CD. It may be assessed by IUS taking into account BWT normalization (≤ 3 mm) with or without normalization of Doppler vascular signs and peri-intestinal inflammatory signs[32]. It is correlated with improved clinical outcome, such as a reduced demand of medication escalation, corticosteroid use, hospitalization and CD-related surgery.

The rate of TR, with more or less extensive definitions, in patients undergoing biological therapy was obtained from 12% to 46.2% of patients after 12 wk to 2 years of therapy (see Table 2). TR was strictly correlated with time, being higher at later assessments compared with early assessments. Moreover, it is more prevalent in colic CD than in ileal CD and it is associated with lower BWT and lower shear wave elastography strain ratio at baseline (see Table 2). However, a few studies have evaluated baseline or early IUS factors predictive of TR. Further prospective trials are needed to reach more consistent evidence on IUS predictive value, to help in properly selecting the right treatment for the right CD patient and plain maintenance therapy.

IUS to predict the risk of surgery

The ileal localization and stricturing and perforating behaviour of CD are well-known risk factors for surgery both in children and in adults. Children with ileal CD requiring surgical resection may have more severe IUS manifestations (such as loss of mural stratification and severe fibrofatty proliferation) associated with both active inflammation and chronic fibrosis than those managed medically[33].

Even in adults, the routine use of IUS in CD patients may identify a subgroup at high risk of surgery, taking into account that nearly half of patients with CD may require surgery within 10 years of diagnosis[1]. Irrespective of the treatment performed, BWT > 7 mm at IUS, altered bowel wall echopattern, and the presence of complications such as fistulas or stenosis are risk factors for intestinal resection over a short period of time[34-36]. In particular, the presence of strictures, fistulae, and abscesses at baseline bowel US seems to predict the need for surgery through 12 mo[14].

The assessment of fibrosis by means of strain elastography may identify patients who are nonresponsive to anti-TNF and need surgery. Orlando *et al*[29] in a small series of patients, showed that the strain ratio of the thickened bowel wall may predict surgery much better than the degree of its thickening and vascularization and that a strain ratio ≥ 2 before starting anti-TNF was the cut-off value correlated with poor lack of improvement, surgery and worst outcome. Likewise, the lack of improvement or the increase in BWT after the start of treatment is correlated with a high risk of surgery[21,34]. It is debatable whether in selected populations at high risk of surgery, such as CD patients with well-known strictures and fistulas, the features of BWT may suggest the response to treatment and ultimately surgery. In the STRIDENT study, 77 CD patients with a *de novo* or postoperative anastomotic intestinal stricture with symptoms consistent with chronic or subacute intestinal obstruction were randomly assigned to receive adalimumab alone or combined with thiopurines. IUS at 12 mo showed improvement (> 25%) in BWT in 45% of patients, with no significant difference between the two groups of patients and an overall low risk of surgery, but no predictors of improvement were given[10].

IUS to predict post-surgical recurrence

Several studies and systematic reviews have assessed the role of IUS in postoperative follow-up, showing that a BWT > 3 mm of the anastomosis or neoterminal ileum is an accurate indicator for recurrence[11]. In this regard, prospective studies have shown that the use of PEG solution (SICUS)[37] and colour Doppler or CEUS[38] can increase the sensitivity, albeit with a decrease in specificity in detecting postoperative recurrence at 1 year after surgery. Moreover, both IUS and SICUS, adopting

Table 2 Rate of transmural remission and intestinal ultrasound parameters predictive of transmural remission in Crohn's disease patients treated with biologics

Ref.	Patients, *n*	TR definition	Study drug	Treatment duration	Rate of TR	IUS parameters predictive of TR
Calabrese *et al*[52], 2022	188	Normalization of BWT, no ECD, no extra bowel signs of inflammation	Adalimumab, infliximab, vedolizumab, ustekinumab	52 wk	27.5% (26.8% adalimumab; 37% infliximab; 27.2% vedolizumab; 20% ustekinumab	Colonic localization, lower BWT at baseline
Castiglione *et al*[57], 2013	66	NA	Anti-TNF	2 yr	25%	
	67		Thiopurines		4%	
Castiglione *et al*[58], 2017	40	BWT ≤ 3 mm	Anti-TNF	2 yr	25%	
Castiglione *et al*[59], 2019	218	BWT ≤ 3 mm	Anti-TNF	12 wk	31.2%	
Helwig *et al* [32], 2022	180	BWT ≤ 2 mm terminal ileum or ≤ 3 mm colon; BWT ≤ 2 mm terminal ileum or ≤ 3 mm colon + two factors among no ECD, no fibrofatty proliferation, normal stratification; normalization of all parameters	All available biologics	12 wk	33.3%; 38.5%; 24.4% (18.4% I; 29% C)	
	78			46 wk	46.2%; NA; NA	
Kucharzik *et al*[60], 2023	77	Normalization of all IUS parameters	Ustekinumab	48 wk	24.1% (13.2% I; 50.0% C)	
Miranda *et al* [61], 2021	35	BWT ≤ 3 mm	Ustekinumab	52 wk	31.4%	
Orlando *et al* [29], 2018	30	BWT ≤ 3 mm	Anti-TNF	14 wk	29%	UEI strain ratio
				52 wk	30%	
Paredes *et al* [53], 2019	36	BWT ≤ 3 mm	Anti-TNF	52 wk	39%	
Ripollés *et al* [21], 2016	51	BWT ≤ 3 mm, no ECD, absence of complications	Anti-TNF	12 wk	14%	
				52 wk	29.5%	
Civitelli *et al* [62], 2016	32	BWT < 3 mm, no ECD, normal stratification, absence of strictures and dilatation	Anti-TNF	9-12 mo	14%	
Paredes *et al* [63], 2010	24	BWT < 3 mm, no increased ECD	Anti-TNF	2 wk	20.8%	
Vaughan *et al*[64], 2022	79	BWT ≤ 3 mm, no increased ECD	Infliximab	12 wk	41%	
Han *et al* [65], 2022	92	BWT ≤ 3 mm, no increased ECD	Anti-TNF	14 wk	12%	
				52 wk (only 22 patients)	22.7%	
Dolinger *et al* [66], 2021	13	BWT ≤ 3 mm	Infliximab	14 wk	23%	
Zorzi *et al* [23], 2020	80	SICUS normal value for BWT, absence of any length of disease, and absence of perienteric inflammation, fistulas, phlegmon, or abscess)	Anti-TNF, budesonide, thiopurines	18 mo	41%	

TR: Transmural remission; BWT: Bowel wall thickness; ECD: Eco-color-doppler vascular signal; I: Ileal Crohn's disease; C: Colonic Crohn's disease; UEI: Ultrasound elastography imaging; SICUS: Small intestine contrast ultrasonography; IUS: Intestinal ultrasound; TNF: Tumor necrosis factor; NA: Not available.

different cut-off levels for bowel thickness (> 5 mm for conventional sonography and > 4 mm for SICUS), can suggest severe endoscopic postoperative recurrence and could accordingly replace endoscopy in postsurgical follow-up[37] (for detection of recurrence).

IUS is accurate not only in detecting postoperative clinical recurrence but also in predicting endoscopic and surgical recurrence. IUS assessment 3 mo after surgery showed high sensitivity in predicting postoperative recurrence at 12 mo, with lower sensitivity[38] but higher specificity than calprotectin[39]. A retrospective study showed that in postoperative CD patients, independent of the

time elapsed from earlier surgery, patients with BWT > 3 mm had a doubled risk of surgical recurrence compared with patients with BWT < 3 mm, and that the absolute incidence of new surgical interventions positively correlated with increased BWT[40]. In this respect, the prognostic value of increased BWT, as assessed by IUS several years after surgery, needs further confirmation, and in particular, the usefulness of therapy escalation for these patients remains unconfirmed[12].

Additionally, in CD patients treated with conservative surgery (*e.g.*, strictureplasty or minimal bowel resections), IUS is useful for monitoring the postoperative behaviour of BWT and can provide prognostic information: US detection of unchanged or worsened wall thickness 6 mo after surgery or the postoperative persistence of wall thickness > 6 mm is predictive of a high risk of recurrence[41].

In this subset of patients, the estimated 5-year survival probability of symptomatic CD recurrence was 90% and 33%, respectively, for unchanged/worsened BWT *vs* improved BWT at 12 mo after surgery. A BWT > 6.0 mm at 12 mo after surgery was directly associated with the risk of CD recurrence. Hence, systematic IUS follow-up of diseased bowel walls after conservative surgery seems to allow the early identification of patients at high risk of clinical/surgical recurrence[42].

Clinical remission

In CD patients, bowel wall changes such as increased BWT and vascularization may persist after therapy and despite clinical remission. The meaning and prognostic significance of these IUS findings have been widely investigated. In quiescent CD, increased vascularity, detected either by colour Doppler or CEUS, after treatment may suggest an increased risk of relapse[21,43,44].

Vascularization and BWT currently represent the main features of sonographic activity scores, and the investigation on prognostic significance of these scores in clinical studies is still ongoing. However, it is clear that normalization of the bowel wall (the so-called TR), namely, a BWT < 3 mm[45] or a more stringent definition such as the combination of BWT < 3 mm, normalization of vascularity and wall stratification, absence of mesenteric fat hypertrophy, node enlargement, or disease complications (*i.e.*, strictures, fistulas)[46,47], is associated with favourable prognostic long-term outcomes[40,43,46,48,49].

Indeed, it has been demonstrated that sonographic remission evaluated after one year of anti-TNF therapy is associated with a longer remission without the need for a therapy change and a reduced need for surgery[21]. In patients with CD in clinical remission, achieving TR is associated with reduced clinical complications, including medication escalation, corticosteroid use, hospitalization, and surgery. When examining clinical complications occurring more than 90 d following IUS, sonographic inflammation remains associated with an increased risk of clinical complications such asmedication escalation, hospitalization, and surgery[46,50,51].

CONCLUSION

IUS is a useful imaging method to assess CD disease activity and can have a prognostic role in predicting response to treatment, disease progression, risk of surgery and risk of postsurgical recurrence. Response to treatment may be predicted by increased BWT and vascularization, reduced elasticity and absence of CD complications. Disease progression or risk of surgery may be predicted by increased BWT, loss of bowel stratification and the presence of CD complications. Postoperative clinical and surgical relapse may be predicted by increased BWT. As more biological therapies become available in the coming years, further prospective trials will be needed to reach definite evidence on IUS predictive value at baseline, to recognize which patients are more likely to respond to a specific therapy and which patients are at high risk of surgery or complications, needing early intensive treatment.

FOOTNOTES

Author contributions: Manzotti C and Maconi G gave substantial contributions to conception and design of the review, and literature review; Manzotti C drafted and edited the article; Colombo F and Maconi G revised the manuscript critically for important intellectual content; Colombo F, Zurleni T, and Danelli P worked together for the final approval of the version to be published.

Conflict-of-interest statement: All the authors report no relevant conflicts of interest for this article.

Country/Territory of origin: Italy

ORCID number: Cristina Manzotti 0000-0003-2836-3068; Francesco Colombo 0000-0002-6478-7055; Tommaso Zurleni 0000-0002-3971-2297; Piergiorgio Danelli 0000-0003-1461-9835; Giovanni Maconi 0000-0003-0810-4026.

S-Editor: Wang JJ
L-Editor: A
P-Editor: Wang JJ

REFERENCES

1 **Torres J**, Mehandru S, Colombel JF, Peyrin-Biroulet L. Crohn's disease. *Lancet* 2017; **389**: 1741-1755 [PMID: 27914655 DOI: 10.1016/S0140-6736(16)31711-1]
2 **Peyrin-Biroulet L**, Reinisch W, Colombel JF, Mantzaris GJ, Kornbluth A, Diamond R, Rutgeerts P, Tang LK, Cornillie FJ, Sandborn WJ. Clinical disease activity, C-reactive protein normalisation and mucosal healing in Crohn's disease in the SONIC trial. *Gut* 2014; **63**: 88-95 [PMID: 23974954 DOI: 10.1136/gutjnl-2013-304984]
3 **Pariente B**, Cosnes J, Danese S, Sandborn WJ, Lewin M, Fletcher JG, Chowers Y, D'Haens G, Feagan BG, Hibi T, Hommes DW, Irvine EJ, Kamm MA, Loftus EV Jr, Louis E, Michetti P, Munkholm P, Oresland T, Panés J, Peyrin-Biroulet L, Reinisch W, Sands BE, Schoelmerich J, Schreiber S, Tilg H, Travis S, van Assche G, Vecchi M, Mary JY, Colombel JF, Lémann M. Development of the Crohn's disease digestive damage score, the Lémann score. *Inflamm Bowel Dis* 2011; **17**: 1415-1422 [PMID: 21560202 DOI: 10.1002/ibd.21506]
4 **Farmer RG**, Whelan G, Fazio VW. Long-term follow-up of patients with Crohn's disease. Relationship between the clinical pattern and prognosis. *Gastroenterology* 1985; **88**: 1818-1825 [PMID: 3922845 DOI: 10.1016/0016-5085(85)90006-x]
5 **Solberg IC**, Vatn MH, Høie O, Stray N, Sauar J, Jahnsen J, Moum B, Lygren I; IBSEN Study Group. Clinical course in Crohn's disease: results of a Norwegian population-based ten-year follow-up study. *Clin Gastroenterol Hepatol* 2007; **5**: 1430-1438 [PMID: 18054751 DOI: 10.1016/j.cgh.2007.09.002]
6 **Gonzalez-Montpetit E**, Ripollés T, Martinez-Pérez MJ, Vizuete J, Martín G, Blanc E. Ultrasound findings of Crohn's disease: correlation with MR enterography. *Abdom Radiol (NY)* 2021; **46**: 156-167 [PMID: 32607648 DOI: 10.1007/s00261-020-02622-3]
7 **Rimola J**, Torres J, Kumar S, Taylor SA, Kucharzik T. Recent advances in clinical practice: advances in cross-sectional imaging in inflammatory bowel disease. *Gut* 2022; **71**: 2587-2597 [PMID: 35927032 DOI: 10.1136/gutjnl-2021-326562]
8 **Maconi G**, Nylund K, Ripolles T, Calabrese E, Dirks K, Dietrich CF, Hollerweger A, Sporea I, Saftoiu A, Maaser C, Hausken T, Higginson AP, Nürnberg D, Pallotta N, Romanini L, Serra C, Gilja OH. EFSUMB Recommendations and Clinical Guidelines for Intestinal Ultrasound (GIUS) in Inflammatory Bowel Diseases. *Ultraschall Med* 2018; **39**: 304-317 [PMID: 29566419 DOI: 10.1055/s-0043-125329]
9 **Dillman JR**, Dehkordy SF, Smith EA, DiPietro MA, Sanchez R, DeMatos-Maillard V, Adler J, Zhang B, Trout AT. Defining the ultrasound longitudinal natural history of newly diagnosed pediatric small bowel Crohn disease treated with infliximab and infliximab-azathioprine combination therapy. *Pediatr Radiol* 2017; **47**: 924-934 [PMID: 28421251 DOI: 10.1007/s00247-017-3848-3]
10 **Schulberg JD**, Wright EK, Holt BA, Hamilton AL, Sutherland TR, Ross AL, Vogrin S, Miller AM, Connell WC, Lust M, Ding NS, Moore GT, Bell SJ, Shelton E, Christensen B, De Cruz P, Rong YJ, Kamm MA. Intensive drug therapy versus standard drug therapy for symptomatic intestinal Crohn's disease strictures (STRIDENT): an open-label, single-centre, randomised controlled trial. *Lancet Gastroenterol Hepatol* 2022; **7**: 318-331 [PMID: 34890567 DOI: 10.1016/S2468-1253(21)00393-9]
11 **Calabrese E**, Maaser C, Zorzi F, Kannengiesser K, Hanauer SB, Bruining DH, Iacucci M, Maconi G, Novak KL, Panaccione R, Strobel D, Wilson SR, Watanabe M, Pallone F, Ghosh S. Bowel Ultrasonography in the Management of Crohn's Disease. A Review with Recommendations of an International Panel of Experts. *Inflamm Bowel Dis* 2016; **22**: 1168-1183 [PMID: 26958988 DOI: 10.1097/MIB.0000000000000706]
12 **Fraquelli M**, Castiglione F, Calabrese E, Maconi G. Impact of intestinal ultrasound on the management of patients with inflammatory bowel disease: how to apply scientific evidence to clinical practice. *Dig Liver Dis* 2020; **52**: 9-18 [PMID: 31732443 DOI: 10.1016/j.dld.2019.10.004]
13 **Puca P**, Del Vecchio LE, Ainora ME, Gasbarrini A, Scaldaferri F, Zocco MA. Role of Multiparametric Intestinal Ultrasound in the Evaluation of Response to Biologic Therapy in Adults with Crohn's Disease. *Diagnostics (Basel)* 2022; **12** [PMID: 36010341 DOI: 10.3390/diagnostics12081991]
14 **Allocca M**, Craviotto V, Bonovas S, Furfaro F, Zilli A, Peyrin-Biroulet L, Fiorino G, Danese S. Predictive Value of Bowel Ultrasound in Crohn's Disease: A 12-Month Prospective Study. *Clin Gastroenterol Hepatol* 2022; **20**: e723-e740 [PMID: 33895360 DOI: 10.1016/j.cgh.2021.04.029]
15 **Huang X**, Li X. Predictive Value of Bowel Ultrasound in Crohn's Disease. *Clin Gastroenterol Hepatol* 2022; **20**: e345-e346 [PMID: 33940228 DOI: 10.1016/j.cgh.2021.04.040]
16 **Maconi G**, Sampietro GM, Sartani A, Bianchi Porro G. Bowel ultrasound in Crohn's disease: surgical perspective. *Int J Colorectal Dis* 2008; **23**: 339-347 [PMID: 18188575 DOI: 10.1007/s00384-007-0418-4]
17 **de Voogd F**, Bots S, Gecse K, Gilja OH, D'Haens G, Nylund K. Intestinal Ultrasound Early on in Treatment Follow-up Predicts Endoscopic Response to Anti-TNFα Treatment in Crohn's Disease. *J Crohns Colitis* 2022; **16**: 1598-1608 [PMID: 35639823 DOI: 10.1093/ecco-jcc/jjac072]
18 **Albshesh A**, Ungar B, Ben-Horin S, Eliakim R, Kopylov U, Carter D. Terminal Ileum Thickness During Maintenance Therapy Is a Predictive Marker of the Outcome of Infliximab Therapy in Crohn Disease. *Inflamm Bowel Dis* 2020; **26**: 1619-1625 [PMID: 32860057 DOI: 10.1093/ibd/izaa219]

19 **Chen YJ**, Chen BL, Liang MJ, Chen SL, Li XH, Qiu Y, Pang LL, Xia QQ, He Y, Zeng ZR, Chen MH, Mao R, Xie XY. Longitudinal Bowel Behavior Assessed by Bowel Ultrasound to Predict Early Response to Anti-TNF Therapy in Patients With Crohn's Disease: A Pilot Study. *Inflamm Bowel Dis* 2022; **28**: S67-S75 [PMID: 34984455 DOI: 10.1093/ibd/izab353]

20 **Les A**, Iacob R, Saizu R, Cotruta B, Saizu AI, Iacob S, Gheorghe L, Gheorghe C. Bowel Ultrasound: a Non-invasive, Easy to Use Method to Predict the Need to Intensify Therapy in Inflammatory Bowel Disease Patients. *J Gastrointestin Liver Dis* 2021; **30**: 462-469 [PMID: 34752586 DOI: 10.15403/jgld-3726]

21 **Ripollés T**, Paredes JM, Martínez-Pérez MJ, Rimola J, Jauregui-Amezaga A, Bouzas R, Martin G, Moreno-Osset E. Ultrasonographic Changes at 12 Weeks of Anti-TNF Drugs Predict 1-year Sonographic Response and Clinical Outcome in Crohn's Disease: A Multicenter Study. *Inflamm Bowel Dis* 2016; **22**: 2465-2473 [PMID: 27580385 DOI: 10.1097/MIB.0000000000000882]

22 **Smith RL**, Taylor KM, Friedman AB, Gibson DJ, Con D, Gibson PR. Early sonographic response to a new medical therapy is associated with future treatment response or failure in patients with inflammatory bowel disease. *Eur J Gastroenterol Hepatol* 2022; **34**: 613-621 [PMID: 35352696 DOI: 10.1097/MEG.0000000000002367]

23 **Zorzi F**, Ghosh S, Chiaramonte C, Lolli E, Ventura M, Onali S, De Cristofaro E, Fantini MC, Biancone L, Monteleone G, Calabrese E. Response Assessed by Ultrasonography as Target of Biological Treatment for Crohn's Disease. *Clin Gastroenterol Hepatol* 2020; **18**: 2030-2037 [PMID: 31866561 DOI: 10.1016/j.cgh.2019.10.042]

24 **Hoffmann T**, Fusco S, Blumenstock G, Sadik S, Malek NP, Froehlich E. Evaluation of bowel wall thickness by ultrasound as early diagnostic tool for therapeutic response in Crohn's disease patients treated with ustekinumab. *Z Gastroenterol* 2022; **60**: 1212-1220 [PMID: 33233006 DOI: 10.1055/a-1283-6550]

25 **Saevik F**, Nylund K, Hausken T, Ødegaard S, Gilja OH. Bowel perfusion measured with dynamic contrast-enhanced ultrasound predicts treatment outcome in patients with Crohn's disease. *Inflamm Bowel Dis* 2014; **20**: 2029-2037 [PMID: 25185684 DOI: 10.1097/MIB.0000000000000159]

26 **Chen W**, Lu C, Hirota C, Iacucci M, Ghosh S, Gui X. Smooth Muscle Hyperplasia/Hypertrophy is the Most Prominent Histological Change in Crohn's Fibrostenosing Bowel Strictures: A Semiquantitative Analysis by Using a Novel Histological Grading Scheme. *J Crohns Colitis* 2017; **11**: 92-104 [PMID: 27364949 DOI: 10.1093/ecco-jcc/jjw126]

27 **Quaia E**, Sozzi M, Angileri R, Gennari AG, Cova MA. Time-Intensity Curves Obtained after Microbubble Injection Can Be Used to Differentiate Responders from Nonresponders among Patients with Clinically Active Crohn Disease after 6 Weeks of Pharmacologic Treatment. *Radiology* 2016; **281**: 606-616 [PMID: 27192460 DOI: 10.1148/radiol.2016152461]

28 **Pecere S**, Holleran G, Ainora ME, Garcovich M, Scaldaferri F, Gasbarrini A, Zocco MA. Usefulness of contrast-enhanced ultrasound (CEUS) in Inflammatory Bowel Disease (IBD). *Dig Liver Dis* 2018; **50**: 761-767 [PMID: 29705029 DOI: 10.1016/j.dld.2018.03.023]

29 **Orlando S**, Fraquelli M, Coletta M, Branchi F, Magarotto A, Conti CB, Mazza S, Conte D, Basilisco G, Caprioli F. Ultrasound Elasticity Imaging Predicts Therapeutic Outcomes of Patients With Crohn's Disease Treated With Anti-Tumour Necrosis Factor Antibodies. *J Crohns Colitis* 2018; **12**: 63-70 [PMID: 28961950 DOI: 10.1093/ecco-jcc/jjx116]

30 **Maconi G**, Di Sabatino A, Ardizzone S, Greco S, Colombo E, Russo A, Cassinotti A, Casini V, Corazza GR, Bianchi Porro G. Prevalence and clinical significance of sonographic detection of enlarged regional lymph nodes in Crohn's disease. *Scand J Gastroenterol* 2005; **40**: 1328-1333 [PMID: 16243717 DOI: 10.1080/00365510510025746]

31 **Kucharzik T**, Wittig BM, Helwig U, Börner N, Rössler A, Rath S, Maaser C; TRUST study group. Use of Intestinal Ultrasound to Monitor Crohn's Disease Activity. *Clin Gastroenterol Hepatol* 2017; **15**: 535-542.e2 [PMID: 27856365 DOI: 10.1016/j.cgh.2016.10.040]

32 **Helwig U**, Fischer I, Hammer L, Kolterer S, Rath S, Maaser C, Kucharzik T. Transmural Response and Transmural Healing Defined by Intestinal Ultrasound: New Potential Therapeutic Targets? *J Crohns Colitis* 2022; **16**: 57-67 [PMID: 34185843 DOI: 10.1093/ecco-jcc/jjab106]

33 **Rosenbaum DG**, Conrad MA, Biko DM, Ruchelli ED, Kelsen JR, Anupindi SA. Ultrasound and MRI predictors of surgical bowel resection in pediatric Crohn disease. *Pediatr Radiol* 2017; **47**: 55-64 [PMID: 27687769 DOI: 10.1007/s00247-016-3704-x]

34 **Castiglione F**, de Sio I, Cozzolino A, Rispo A, Manguso F, Del Vecchio Blanco G, Di Girolamo E, Castellano L, Ciacci C, Mazzacca G. Bowel wall thickness at abdominal ultrasound and the one-year-risk of surgery in patients with Crohn's disease. *Am J Gastroenterol* 2004; **99**: 1977-1983 [PMID: 15447760 DOI: 10.1111/j.1572-0241.2004.40267.x]

35 **Rigazio C**, Ercole E, Laudi C, Daperno M, Lavagna A, Crocella L, Bertolino F, Viganò L, Sostegni R, Pera A, Rocca R. Abdominal bowel ultrasound can predict the risk of surgery in Crohn's disease: proposal of an ultrasonographic score. *Scand J Gastroenterol* 2009; **44**: 585-593 [PMID: 19148846 DOI: 10.1080/00365520802705992]

36 **Kunihiro K**, Hata J, Manabe N, Mitsuoka Y, Tanaka S, Haruma K, Chayama K. Predicting the need for surgery in Crohn's disease with contrast harmonic ultrasound. *Scand J Gastroenterol* 2007; **42**: 577-585 [PMID: 17454878 DOI: 10.1080/00365520601002716]

37 **Castiglione F**, Bucci L, Pesce G, De Palma GD, Camera L, Cipolletta F, Testa A, Diaferia M, Rispo A. Oral contrast-enhanced sonography for the diagnosis and grading of postsurgical recurrence of Crohn's disease. *Inflamm Bowel Dis* 2008; **14**: 1240-1245 [PMID: 18398896 DOI: 10.1002/ibd.20469]

38 **Paredes JM**, Ripollés T, Cortés X, Moreno N, Martínez MJ, Bustamante-Balén M, Delgado F, Moreno-Osset E. Contrast-enhanced ultrasonography: usefulness in the assessment of postoperative recurrence of Crohn's disease. *J Crohns Colitis* 2013; **7**: 192-201 [PMID: 22542055 DOI: 10.1016/j.crohns.2012.03.017]

39 **Orlando A**, Modesto I, Castiglione F, Scala L, Scimeca D, Rispo A, Teresi S, Mocciaro F, Criscuoli V, Marrone C, Platania P, De Falco T, Maisano S, Nicoli N, Cottone M. The role of calprotectin in predicting endoscopic post-surgical recurrence in asymptomatic Crohn's disease: a comparison with ultrasound. *Eur Rev Med Pharmacol Sci* 2006; **10**: 17-22 [PMID: 16494106]

40 **Cammarota T**, Sarno A, Robotti D, Bonenti G, Debani P, Versace K, Astegiano M, Pera A. US evaluation of patients affected by IBD: how to do it, methods and findings. *Eur J Radiol* 2009; **69**: 429-437 [PMID: 19121906 DOI: 10.1016/j.ejrad.2008.11.008]

41 **Maconi G**, Sampietro GM, Cristaldi M, Danelli PG, Russo A, Bianchi Porro G, Taschieri AM. Preoperative characteristics and postoperative behavior of bowel wall on risk of recurrence after conservative surgery in Crohn's disease: a prospective study. *Ann Surg* 2001; **233**: 345-352 [PMID: 11224621 DOI: 10.1097/00000658-200103000-00007]

42 **Parente F**, Sampietro GM, Molteni M, Greco S, Anderloni A, Sposito C, Danelli PG, Taschieri AM, Gallus S, Bianchi Porro G. Behaviour of the bowel wall during the first year after surgery is a strong predictor of symptomatic recurrence of Crohn's disease: a prospective study. *Aliment Pharmacol Ther* 2004; **20**: 959-968 [PMID: 15521843 DOI: 10.1111/j.1365-2036.2004.02245.x]

43 **Ripollés T**, Martínez MJ, Barrachina MM. Crohn's disease and color Doppler sonography: response to treatment and its relationship with long-term prognosis. *J Clin Ultrasound* 2008; **36**: 267-272 [PMID: 18067121 DOI: 10.1002/jcu.20423]

44 **Di Sabatino A**, Fulle I, Ciccocioppo R, Ricevuti L, Tinozzi FP, Tinozzi S, Campani R, Corazza GR. Doppler enhancement after intravenous levovist injection in Crohn's disease. *Inflamm Bowel Dis* 2002; **8**: 251-257 [PMID: 12131608 DOI: 10.1097/00054725-200207000-00003]

45 **Zacharopoulou E**, Craviotto V, Fiorino G, Furfaro F, Zilli A, Gilardi D, Peyrin-Biroulet L, Danese S, Allocca M. Targeting the gut layers in Crohn's disease: mucosal or transmural healing? *Expert Rev Gastroenterol Hepatol* 2020; **14**: 775-787 [PMID: 32515627 DOI: 10.1080/17474124.2020.1780914]

46 **Nardone OM**, Calabrese G, Testa A, Caiazzo A, Fierro G, Rispo A, Castiglione F. The Impact of Intestinal Ultrasound on the Management of Inflammatory Bowel Disease: From Established Facts Toward New Horizons. *Front Med (Lausanne)* 2022; **9**: 898092 [PMID: 35677820 DOI: 10.3389/fmed.2022.898092]

47 **Kucharzik T**, Tielbeek J, Carter D, Taylor SA, Tolan D, Wilkens R, Bryant RV, Hoeffel C, De Kock I, Maaser C, Maconi G, Novak K, Rafaelsen SR, Scharitzer M, Spinelli A, Rimola J. ECCO-ESGAR Topical Review on Optimizing Reporting for Cross-Sectional Imaging in Inflammatory Bowel Disease. *J Crohns Colitis* 2022; **16**: 523-543 [PMID: 34628504 DOI: 10.1093/ecco-jcc/jjab180]

48 **Ma L**, Li W, Zhuang N, Yang H, Liu W, Zhou W, Jiang Y, Li J, Zhu Q, Qian J. Comparison of transmural healing and mucosal healing as predictors of positive long-term outcomes in Crohn's disease. *Therap Adv Gastroenterol* 2021; **14**: 17562848211016259 [PMID: 34178114 DOI: 10.1177/17562848211016259]

49 **Geyl S**, Guillo L, Laurent V, D'Amico F, Danese S, Peyrin-Biroulet L. Transmural healing as a therapeutic goal in Crohn's disease: a systematic review. *Lancet Gastroenterol Hepatol* 2021; **6**: 659-667 [PMID: 34090579 DOI: 10.1016/S2468-1253(21)00096-0]

50 **Vaughan R**, Tjandra D, Patwardhan A, Mingos N, Gibson R, Boussioutas A, Ardalan Z, Al-Ani A, Gibson PR, Christensen B. Toward transmural healing: Sonographic healing is associated with improved long-term outcomes in patients with Crohn's disease. *Aliment Pharmacol Ther* 2022; **56**: 84-94 [PMID: 35343603 DOI: 10.1111/apt.16892]

51 **Wilkens R**, Novak KL, Maaser C, Panaccione R, Kucharzik T. Relevance of monitoring transmural disease activity in patients with Crohn's disease: current status and future perspectives. *Therap Adv Gastroenterol* 2021; **14**: 17562848211006672 [PMID: 33948115 DOI: 10.1177/17562848211006672]

52 **Calabrese E**, Rispo A, Zorzi F, De Cristofaro E, Testa A, Costantino G, Viola A, Bezzio C, Ricci C, Prencipe S, Racchini C, Stefanelli G, Allocca M, Scotto di Santolo S, D'Auria MV, Balestrieri P, Ricchiuti A, Cappello M, Cavallaro F, Guarino AD, Maconi G, Spagnoli A, Monteleone G, Castiglione F. Ultrasonography Tight Control and Monitoring in Crohn's Disease During Different Biological Therapies: A Multicenter Study. *Clin Gastroenterol Hepatol* 2022; **20**: e711-e722 [PMID: 33775896 DOI: 10.1016/j.cgh.2021.03.030]

53 **Paredes JM**, Moreno N, Latorre P, Ripollés T, Martinez MJ, Vizuete J, Moreno-Osset E. Clinical Impact of Sonographic Transmural Healing After Anti-TNF Antibody Treatment in Patients with Crohn's Disease. *Dig Dis Sci* 2019; **64**: 2600-2606 [PMID: 30874986 DOI: 10.1007/s10620-019-05567-w]

54 **Laterza L**, Ainora ME, Garcovich M, Galasso L, Poscia A, Di Stasio E, Lupascu A, Riccardi L, Scaldaferri F, Armuzzi A, Rapaccini GL, Gasbarrini A, Pompili M, Zocco MA. Bowel contrast-enhanced ultrasound perfusion imaging in the evaluation of Crohn's disease patients undergoing anti-TNFα therapy. *Dig Liver Dis* 2021; **53**: 729-737 [PMID: 32900648 DOI: 10.1016/j.dld.2020.08.005]

55 **Ungar B**, Ben-Shatach Z, Selinger L, Malik A, Albshesh A, Ben-Horin S, Eliakim R, Kopylov U, Carter D. Lower adalimumab trough levels are associated with higher bowel wall thickness in Crohn's disease. *United European Gastroenterol J* 2020; **8**: 167-174 [PMID: 32213067 DOI: 10.1177/2050640619878974]

56 **Quaia E**, Gennari AG, Cova MA. Early Predictors of the Long-term Response to Therapy in Patients With Crohn Disease Derived From a Time-Intensity Curve Analysis After Microbubble Contrast Agent Injection. *J Ultrasound Med* 2019; **38**: 947-958 [PMID: 30208230 DOI: 10.1002/jum.14778]

57 **Castiglione F**, Testa A, Rea M, De Palma GD, Diaferia M, Musto D, Sasso F, Caporaso N, Rispo A. Transmural healing evaluated by bowel sonography in patients with Crohn's disease on maintenance treatment with biologics. *Inflamm Bowel Dis* 2013; **19**: 1928-1934 [PMID: 23835441 DOI: 10.1097/MIB.0b013e31829053ce]

58 **Castiglione F**, Mainenti P, Testa A, Imperatore N, De Palma GD, Maurea S, Rea M, Nardone OM, Sanges M, Caporaso N, Rispo A. Cross-sectional evaluation of transmural healing in patients with Crohn's disease on maintenance treatment with anti-TNF alpha agents. *Dig Liver Dis* 2017; **49**: 484-489 [PMID: 28292640 DOI: 10.1016/j.dld.2017.02.014]

59 **Castiglione F**, Imperatore N, Testa A, De Palma GD, Nardone OM, Pellegrini L, Caporaso N, Rispo A. One-year clinical outcomes with biologics in Crohn's disease: transmural healing compared with mucosal or no healing. *Aliment Pharmacol Ther* 2019; **49**: 1026-1039 [PMID: 30854708 DOI: 10.1111/apt.15190]

60 **Kucharzik T**, Wilkens R, D'Agostino MA, Maconi G, Le Bars M, Lahaye M, Bravatà I, Nazar M, Ni L, Ercole E, Allocca M, Machková N, de Voogd FAE, Palmela C, Vaughan R, Maaser C; STARDUST Intestinal Ultrasound study group. Early Ultrasound Response and Progressive Transmural Remission After Treatment With Ustekinumab in Crohn's Disease. *Clin Gastroenterol Hepatol* 2023; **21**: 153-163.e12 [PMID: 35842121 DOI: 10.1016/j.cgh.2022.05.055]

61 **Miranda A**, Gravina AG, Cuomo A, Mucherino C, Sgambato D, Facchiano A, Granata L, Priadko K, Pellegrino R, de Filippo FR, Camera S, Cuomo R, Melina R, D'Onofrio V, Manguso F, Ciacci C, Romano M. Efficacy of ustekinumab in the treatment of patients with Crohn's disease with failure to previous conventional or biologic therapy: a prospective observational real-life study. *J Physiol Pharmacol* 2021; **72** [PMID: 34987127 DOI: 10.26402/jpp.2021.4.05]

62 **Civitelli F**, Nuti F, Oliva S, Messina L, La Torre G, Viola F, Cucchiara S, Aloi M. Looking Beyond Mucosal Healing: Effect of Biologic Therapy on Transmural Healing in Pediatric Crohn's Disease. *Inflamm Bowel Dis* 2016; **22**: 2418-2424 [PMID: 27598739 DOI: 10.1097/MIB.0000000000000897]

63 **Paredes JM**, Ripollés T, Cortés X, Martínez MJ, Barrachina M, Gómez F, Moreno-Osset E. Abdominal sonographic changes after antibody to tumor necrosis factor (anti-TNF) alpha therapy in Crohn's Disease. *Dig Dis Sci* 2010; **55**: 404-410 [PMID: 19267199 DOI: 10.1007/s10620-009-0759-7]

64 **Vaughan R**, Murphy E, Nalder M, Gibson RN, Ardalan Z, Boussioutas A, Christensen B. Infliximab Trough Levels Are Associated With Transmural Sonographic Healing in Inflammatory Bowel Disease. *Inflamm Bowel Dis* 2022 [PMID: 36094156 DOI: 10.1093/ibd/izac186]

65 **Han ZM**, Elodie WH, Yan LH, Xu PC, Zhao XM, Zhi FC. Correlation Between Ultrasonographic Response and Anti-Tumor Necrosis Factor Drug Levels in Crohn's disease. *Ther Drug Monit* 2022; **44**: 659-664 [PMID: 35427284 DOI: 10.1097/FTD.0000000000000988]

66 **Dolinger MT**, Choi JJ, Phan BL, Rosenberg HK, Rowland J, Dubinsky MC. Use of Small Bowel Ultrasound to Predict Response to Infliximab Induction in Pediatric Crohn's Disease. *J Clin Gastroenterol* 2021; **55**: 429-432 [PMID: 32453126 DOI: 10.1097/MCG.0000000000001367]

World Journal of Gastroenterology

Submit a Manuscript: https://www.f6publishing.com

World J Gastroenterol 2023 June 21; 29(23): 3606-3621

DOI: 10.3748/wjg.v29.i23.3606

ISSN 1007-9327 (print) ISSN 2219-2840 (online)

ORIGINAL ARTICLE

Basic Study

BMI-1 activates hepatic stellate cells to promote the epithelial-mesenchymal transition of colorectal cancer cells

Zhong-Yang Jiang, Xi-Mei Ma, Xiao-Hui Luan, Zhen-Yu Liuyang, Yi-Yang Hong, Yuan Dai, Qing-Hua Dong, Guan-Yu Wang

Specialty type: Gastroenterology and hepatology

Provenance and peer review: Unsolicited article; Externally peer reviewed.

Peer-review model: Single blind

Peer-review report's scientific quality classification
Grade A (Excellent): 0
Grade B (Very good): B
Grade C (Good): C, C
Grade D (Fair): 0
Grade E (Poor): 0

P-Reviewer: Emran TB, Bangladesh; Wu C, China

Received: February 1, 2023
Peer-review started: February 1, 2023
First decision: February 12, 2023
Revised: February 25, 2023
Accepted: May 4, 2023
Article in press: May 4, 2023
Published online: June 21, 2023

Zhong-Yang Jiang, Xiao-Hui Luan, Zhen-Yu Liuyang, Guan-Yu Wang, Department of General Surgery, Sir Run Run Shaw Hospital, School of Medicine, Zhejiang University, Hangzhou 310016, Zhejiang Province, China

Xi-Mei Ma, Department of Emergency, The Second Affiliated Hospital of Zhejing University, Hangzhou 310016, Zhejiang Province, China

Yi-Yang Hong, Yuan Dai, Qing-Hua Dong, Biomedical Research Center, Sir Run Run Shaw Hospital, School of Medicine, Zhejiang University, Hangzhou 310016, Zhejiang Province, China

Qing-Hua Dong, Key Laboratory of Cancer Prevention and Intervention, China National Ministry of Education, Hangzhou 310009, Zhejiang Province, China

Corresponding author: Guan-Yu Wang, MD, PhD, Surgeon, Department of General Surgery, Sir Run Run Shaw Hospital, School of Medicine, Zhejiang University, No. 3 East Qingchun Road, Hangzhou 310016, Zhejiang Province, China. wangguanyu@zju.edu.cn

Abstract

BACKGROUND

Activated hepatic stellate cells (aHSCs) are the major source of cancer-associated fibroblasts in the liver. Although the crosstalk between aHSCs and colorectal cancer (CRC) cells supports liver metastasis (LM), the mechanisms are largely unknown.

AIM

To explore the role of BMI-1, a polycomb group protein family member, which is highly expressed in LM, and the interaction between aHSCs and CRC cells in promoting CRC liver metastasis (CRLM).

METHODS

Immunohistochemistry was carried out to examine BMI-1 expression in LM and matched liver specimens of CRC. The expression levels of BMI-1 in mouse liver during CRLM (0, 7, 14, 21, and 28 d) were detected by Western blotting (WB) and the quantitative polymerase chain reaction (qPCR) assay. We overexpressed BMI-1 in HSCs (LX2) by lentivirus infection and tested the molecular markers of aHSCs by WB, qPCR, and the immunofluorescence assay. CRC cells (HCT116 and DLD1)

were cultured in HSC-conditioned medium (LX2 NC CM or LX2 BMI-1 CM). CM-induced CRC cell proliferation, migration, epithelial-mesenchymal transition (EMT) phenotype, and transforming growth factor beta (TGF-β)/SMAD pathway changes were investigated *in vitro*. A mouse subcutaneous xenotransplantation tumor model was established by co-implantation of HSCs (LX2 NC or LX2 BMI-1) and CRC cells to investigate the effects of HSCs on tumor growth and the EMT phenotype *in vivo*.

RESULTS

Positive of BMI-1 expression in the liver of CRLM patients was 77.8%. The expression level of BMI-1 continued to increase during CRLM in mouse liver cells. LX2 overexpressed BMI-1 was activated, accompanied by increased expression level of alpha smooth muscle actin, fibronectin, TGF-β1, matrix metalloproteinases, and interleukin 6. CRC cells cultured in BMI-1 CM exhibited enhanced proliferation and migration ability, EMT phenotype and activation of the TGF-β/SMAD pathway. In addition, the TGF-βR inhibitor SB-505124 diminished the effect of BMI-1 CM on SMAD2/3 phosphorylation in CRC cells. Furthermore, BMI-1 overexpressed LX2 HSCs promoted tumor growth and the EMT phenotype *in vivo*.

CONCLUSION

High expression of BMI-1 in liver cells is associated with CRLM progression. BMI-1 activates HSCs to secrete factors to form a prometastatic environment in the liver, and aHSCs promote proliferation, migration, and the EMT in CRC cells partially through the TGF-β/SMAD pathway.

Key Words: BMI-1; Hepatic stellate cells; Colorectal cancer; Liver metastasis; Epithelial-mesenchymal transition

Core Tip: This study revealed that BMI-1 was upregulated in liver cells during colorectal cancer (CRC) liver metastasis. BMI-1-activated LX2 hepatic stellate cells (HSCs) promoted CRC cell proliferation, migration, and the epithelial-mesenchymal transition both *in vitro* and *in vivo*. Mechanistically, transforming growth factor beta 1 was increased in BMI-1 overexpressed LX2 HSCs, and triggered the phosphorylation of downstream SMAD2/3 in CRC cells and the interaction of activated HSCs and CRC cells, thereby further promoting CRC progression.

Citation: Jiang ZY, Ma XM, Luan XH, Liuyang ZY, Hong YY, Dai Y, Dong QH, Wang GY. BMI-1 activates hepatic stellate cells to promote the epithelial-mesenchymal transition of colorectal cancer cells. *World J Gastroenterol* 2023; 29(23): 3606-3621
URL: https://www.wjgnet.com/1007-9327/full/v29/i23/3606.htm
DOI: https://dx.doi.org/10.3748/wjg.v29.i23.3606

INTRODUCTION

Colorectal cancer (CRC) is the third most common cancer and ranks second in terms of cancer mortality worldwide[1,2]. Liver metastasis (LM) is the primary cause of death in CRC patients, and the liver plays a major role in survival as it is often the only site of metastasis. In CRC patients, approximately 14%-35% have LM at diagnosis, and about 70% have LM in the late stage of the disease[3]. In colorectal cancer (CRC) liver metastasis (CRLM) patients, liver resection is the primary curative treatment option, with a 5-year survival rate of 20%-50%[4]. Although treatments have advanced in recent years, the rate of intrahepatic recurrence is still high.

During CRLM, CRC cells can orchestrate a premetastatic niche by changing the tumor microenvironment[5,6]. For example, tumor cells secrete cytokines and extracellular vesicles containing microRNAs (miRNAs), integrins, and cytokines, which can modulate distant niches[7]. Zhao *et al*[8] found that CRC-derived miRNA-181a-5p-rich extracellular vesicles induced the activation of hepatic stellate cells (HSCs)[8]. The hepatic microenvironment has numerous signaling factors in liver cells, which consist of parenchymal and nonparenchymal cells, and the interaction between cancer cells and stromal cells facilitates the development of LM[9,10]. Cancer-associated fibroblasts (CAFs), comprising the major stromal cell type, are fibroblast populations found in primary and metastatic cancers and are related to tumor initiation, progression, and metastasis by regulating extracellular matrix (ECM) remodeling and the immune response[11-13]. HSCs are the major nonparenchymal liver cells, which store retinol and

play a role in liver repair, liver fibrosis, and hepatocellular carcinoma (HCC)[14-17]. HSCs contribute 85%–95% of fibroblasts in the liver[18]. HSCs are activated to CAFs by cancer cells to support tumor growth and metastasis[8,19]. Hepatic CAFs are thought to come primarily from HSCs and to a lesser extent from bone marrow-derived precursors, portal fibroblasts, and endothelial cells[20]. In intrahepatic cholangiocarcinoma, HSC-derived CAFs are the main tumor-interacting population[21]. Although CRC is the most common primary cancer that metastasizes to the liver, the mechanisms by which HSCs interact with CRC cells to promote LM are largely unclear.

BMI-1, one of the polycomb group protein family members, plays a critical role in negatively regulating the Ink4a/Arf locus which encodes $p16^{INK4a}$ and $p19^{ARF}$[22]. BMI-1 regulates self-renewal of stem cells and participates in the carcinogenesis of human cancers including CRC[23-25]. We previously reported that BMI-1 was overexpressed in CRLM and contributes to LM by regulating the epithelial-mesenchymal transition (EMT) of CRC cells *in vitro* and *in vivo*[26]. Interestingly, we observed BMI-1-positive staining in liver cells both in human and mouse specimens of CRLM. Studies have shown that quiescent HSCs can be activated by cancer cells and transformed into CAFs, and in turn activated HSCs (aHSCs) promote cancer cell invasion and the EMT[8,19]. Thus, we speculated that BMI-1 plays a role in the crosstalk between HSCs and CRC cells during LM.

In this study, both CRLM patients and mice showed increased BMI-1 expression in liver cells. BMI-1 overexpressed HSCs were activated and transformed into CAFs. CRC cells cultured in conditioned medium (CM) from BMI-1 overexpressed HSCs showed enhanced proliferation, migration, and EMT ability. The experimental *in vivo* subcutaneous xenotransplantation tumor model also showed increased tumor proliferation and EMT of CRC cells cocultured with BMI-1 overexpressed HSCs. These findings may provide a potential new target for the treatment of CRLM.

MATERIALS AND METHODS

Immunohistochemistry analysis of CRLM patients

LM and adjacent normal liver tissues from 18 clinically diagnosed patients with CRLM were collected from the Pathology Department (from 2013 to 2020), Sir Run Run Shaw Hospital, Hangzhou, China. The expression of BMI-1 was investigated by immunohistochemistry (IHC) staining. Anti-BMI-1 (1:100; Cell Signaling Technology, Danvers, MA, United States) was used as the primary antibody before secondary antibody incubation.

Cell culture and treatment

The high metastatic human CRC cell line (HCT116), low metastatic human CRC cell line (DLD1), mouse CRC cell line (CT26), and human HSC line (LX2) were purchased from the American Type Culture Collection (Manassas, VA, United States). Cells were cultured in Dulbecco's Modified Eagle's Medium (Gibco, Waltham, MA, United States) with 10% fetal bovine serum and 1% penicillin/streptomycin in a 5% carbon dioxide humidified incubator at 37 °C. The BMI-1 overexpressed lentiviral construct (pGC-FU-GFP-*BMI-1*) and negative control (pGC-FU-GFP) were obtained from Genechem (Shanghai, China). The control (LX2 NC) and stable BMI-1 overexpressed LX2 (LX2 BMI-1) cells were established by lentivirus transfection following the manufacturer's instructions. In addition, to prepare the CM, we first cultured transfected LX2 cells in a 10 cm plate at a density of 1×10^6 cells. We then used 6 mL serum-free DMEM to culture the cells for 24 h. The supernatants were collected, centrifuged at 1000 × *g* for 10 min, and filtered through a 0.22 mm filter unit (Millex, Duluth, GA, United States). CM from NC LX2 (NC CM) and BMI-1 LX2 (BMI-1 CM) was prepared by mixing the different supernatant with complete medium (1:1). Then the CRC cells were cultured in CM for 24 h. All CM was used within 2 d. CRC cells were pretreated with SB-505124 (0.05 μM) for 1 h to inhibit SMAD2 phosphorylation, and then the cells were incubated with BMI-1 CM for 24 h.

Western blotting

Whole proteins from the tissue and cell samples were extracted using RIPA buffer with a 1% protease/phosphatase inhibitor. After centrifugation of the extraction solutions, the BCA Protein Concentration Assay Kit (Solarbio, Beijing, China) was used to quantify the proteins. Following sodium dodecyl sulfate-polyacrylamide gel electrophoresis, the proteins were electrotransferred to polyvinylidene fluoride membranes. Antibodies against BMI-1, glyceraldehyde-3-phosphate dehydrogenase, β-actin, vimentin, SMAD2/3, phosphorylated SMAD3 (1:1000; Cell Signaling Technology), alpha smooth muscle actin (α-SMA), transforming growth factor beta 1 (TGF-β1), phosphorylated SMAD2 (1:1000; Abcam, Cambridge, MA, United States), fibronectin (1:1000; BD Biosciences, San Jose, CA, United States), E-cadherin, zinc finger E-box-binding homeobox 1 (ZEB-1), Twist-1 (1:1000; Novus Biologicals, Centennial, CO, United States), and Snail (1:1000; Proteintech Group, Rosemont, IL, United States) were used as primary antibodies. After washing with Tris-buffered saline with 0.1% Tween 20 three times every 10 min, goat anti-rabbit/mouse immunoglobulin G (Abcam) was used as the secondary antibody. The Bio-Rad CD Touch Detection System (Hercules, CA, United States) with enhanced chemiluminescence detection reagents was used to detect protein bands.

Quantitative polymerase chain reaction

Whole RNAs from the tissue and cell samples were extracted using Trizol reagent (Cwbio, Dalian, China). HiScript II Q RT SuperMix (Vazyme Biotech, Nanjing, China) was subsequently used for reverse transcription. ChamQ Universal SYBR quantitative polymerase chain reaction (qPCR) Master Mix (Vazyme Biotech) was used for qPCR. The Bio-Rad CFX-96 Real-Time PCR System was utilized to analyze the results. The sequences of all primers are listed in Supplementary Table 1.

Immunofluorescence staining

Immunofluorescence staining was performed in 96-well plates. Cells were fixed in paraformaldehyde and permeabilized with Triton X-100. Before incubation with secondary antibody, antibodies against vimentin (1:100; Cell Signaling Technology) and Snail (1:100; Proteintech Group) were used as primary antibodies. The Zeiss AXIO Observer A1 inverted fluorescence microscope system (Jena, Germany) was used to obtain images.

Cell viability assay

Cells were cultured in CM separately for 24, 48, 72, and 96 h. After treatment, Cell Counting Kit-8 (CCK-8) reagent (Yeasen Biotechnology, Shanghai, China) was added and incubated for 2 h. A spectrophotometer (Thermo Fisher Scientific, Waltham, MA, United States) was used to detect the optical density value (450 nm).

Colony formation assay

CRC cells were cultured in CM for 2 wk. Cells were fixed in paraformaldehyde and stained with crystal violet. Colonies were viewed with the Olympus CKK53 microscope (Tokyo, Japan), and photos were taken. ImageJ software was utilized to measure the number of colonies.

Wound healing assay

CRC cells were cultured until they reached 90% confluence. Following the creation of a linear wound, cells were cultured in CM for 48 h. Wounds were viewed with the Olympus CKK53 microscope, and photos were taken at 0, 24, and 48 h. ImageJ software was used to measure the migration rate.

Transwell migration assay

Transwell chambers were purchased from Corning Inc. (Corning, NY, United States). CRC cells were plated in the upper chambers with serum-free DMEM, while CM was placed in the lower chambers. After 48 h, cells in the upper chambers were removed, and cells on the lower membrane surface were fixed and stained. The migrated cells were viewed with the Olympus CKK53 microscope, and photos were taken. ImageJ software was used to measure the number of cells.

IHC

Tissue samples were fixed, dehydrated, paraffin-embedded, and sectioned. After deparaffinization, the sections were blocked in goat serum and incubated with primary antibodies for 24 h. The sections were incubated with secondary antibody for 30 min, followed by counterstaining with Mayer's hematoxylin. The Olympus CKK53 microscope was used to view and photograph the stained sections.

Animal experiments

All animal experimental procedures were approved by the Committee on the Ethics of Animal Experiments of Zhejiang University (No. ZJU20220447; Hangzhou, China).

Treatment protocol 1

Five-week-old male BALB/c mice (19-20 g) were randomly divided into five groups (n = 3). Isoflurane (inhalation) was utilized to anesthetize the mice. The spleen was then exteriorized through a left flank incision. CT26 cells (2×10^6) were injected intrasplenically to establish the tumor, and then the injection site was pressed for 5 min. Surgical thread was used to close the peritoneum and skin. The mice were sacrificed at 0, 7, 14, 21, and 28 d after inoculation of CT26 cells. Resected liver tissues were collected for qPCR, Western blotting (WB), and the IHC assay.

Treatment protocol 2

Five-week-old male BALB/c nude mice (17-18 g) were randomly divided into four groups (n = 5): (1) HCT116 cells (5×10^6) were mixed with LX2 NC cells (1×10^6); (2) HCT116 cells (5×10^6) were mixed with LX2 BMI-1 cells (1×10^6); (3) DLD1 cells (5×10^6) were mixed with LX2 NC cells (1×10^6); and (4) DLD1 cells (5×10^6) were mixed with LX2 BMI-1 cells (1×10^6). The mixed cells were subcutaneously injected into mouse flanks to establish the tumors. When measurable, tumor sizes were estimated every 2 d. The mice were killed 28 d after cell inoculation. Resected tumor tissues were collected for qPCR, WB, and the IHC assay. Total tumor volume (mm^3) = $L \times W^2/2$ (L = length and W = width).

Table 1 Correlation between clinicopathological characteristics of colorectal cancer patients and *BMI-1* expression in the liver

Characteristics	Cases, *n* = 18	*BMI-1* expression		*P* value
		Negative, *n* = 4	Positive, *n* = 14	
Age in yr				0.051
< 60	12	4	8	
≥ 60	6	0	6	
Sex				0.509
Male	11	3	8	
Female	7	1	6	
Primary tumor site				0.018[a]
Colon	10	4	6	
Rectum	8	0	8	
Tumor size in the liver in mm				0.278
< 30	8	3	5	
30-50	3	0	3	
≥ 50	5	1	5	
Tumor numbers in the liver				0.432
1-2	12	2	10	
≥ 3	6	2	4	
Differentiation degree				0.881
Low	4	1	3	
Middle-high	14	3	11	
T stage				1
III	18	4	14	
N stage				0.248
N0	9	3	6	
N1 + N2	7	1	8	

[a]$P < 0.05$.

Statistical analyses

In all experiments, the data are shown as the mean ± standard deviation based on three independent experiments. The difference between the groups was analyzed by the χ^2 test, Fisher's exact probability, Student's *t*-test, or one-way analysis of variance using GraphPad Prism 8 software or SPSS 25.0. $P < 0.05$ was considered statistically significant.

RESULTS

BMI-1 expression is upregulated in liver cells during CRLM

In our previous research, it was found that BMI-1 was overexpressed in LM of human CRC[26]. Interestingly, although normal liver cells were BMI-1-negative, 77.8% of liver cells from CRLM patients (14 of 18 samples; Figure 1A) were BMI-1-positive. The positive expression of BMI-1 was not strongly related to the clinical pathological characteristics (including tumor size and tumor number in the liver, differentiation degree, T stage, N stage) except the tumor site (Table 1). Positive BMI-1 expression in the liver cells of patients with rectal cancer LM was significantly higher (100%) than in patients with CRLM (60%). To investigate BMI-1 expression level in liver cells during CRLM, we measured BMI-1 expression at 0, 7, 14, 21, and 28 d following intrasplenic injection of CT26 cells in mice (Figure 1B). As shown in Figure 1C, small LM had formed by day 7. Compared with healthy control mice, the protein expression level of BMI-1 did not significantly change at 7 and 14 d, but markedly increased 4.58-fold at 21 d and

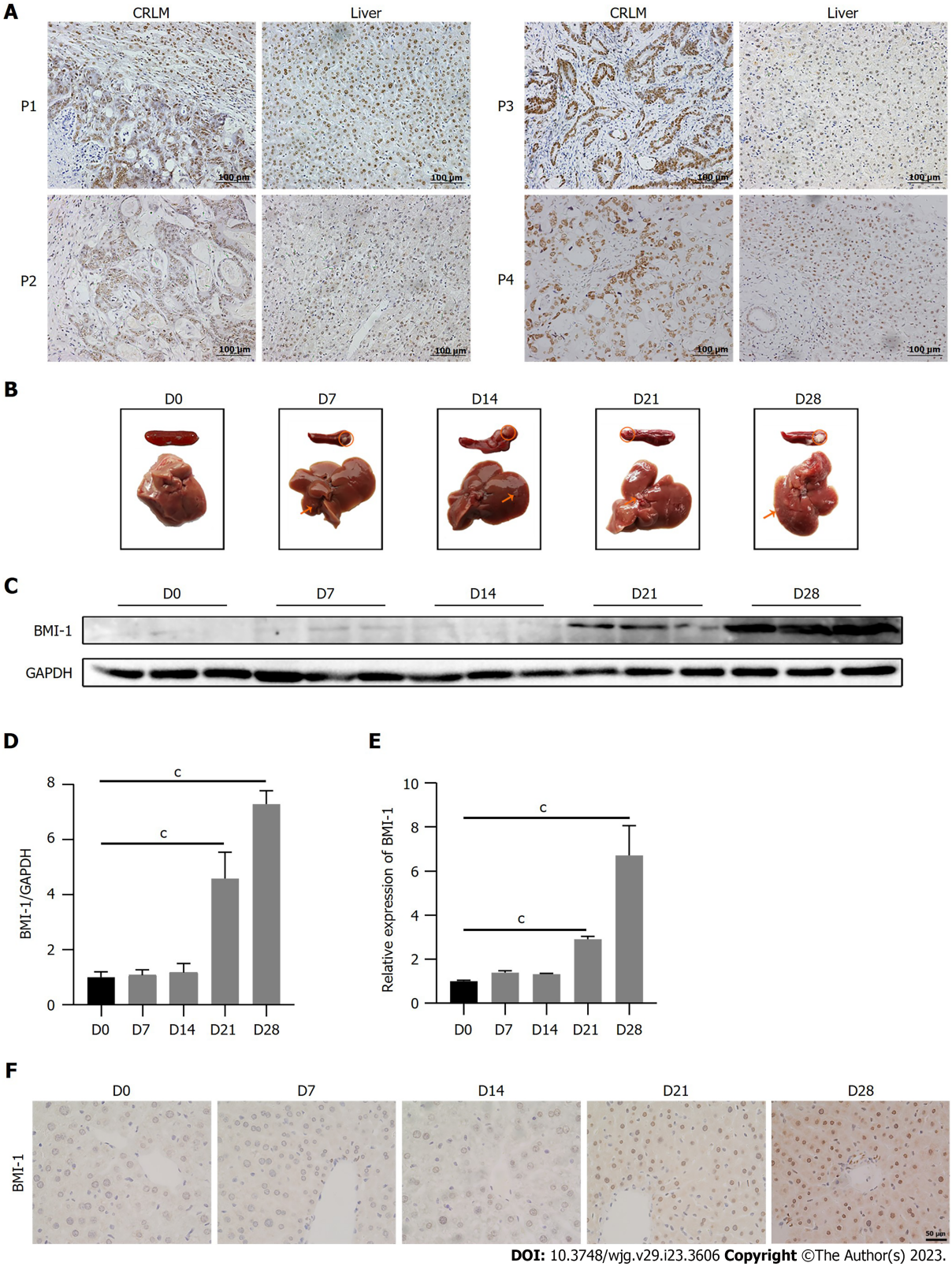

DOI: 10.3748/wjg.v29.i23.3606

Figure 1 BMI-1 expression increases in liver cells during colorectal cancer liver metastasis. A: Immunohistochemistry analysis of BMI-1 in liver metastasis and paired liver tissues of colorectal cancer liver metastasis (CRLM) patients; B: Spleens and livers of mice were photographed after intrasplenic injection of CT26 cells at the indicated times; C: Western blot analysis of BMI-1 expression in mouse livers (n = 3); D: Quantitative protein expression of BMI-1 normalized to glyceraldehyde-3-phosphate dehydrogenase (GAPDH) in mouse livers (n = 3); E: Quantitative polymerase chain reaction detection of BMI-1 expression in mouse livers (n = 3); $^cP < 0.001$ *vs* D0; F: Immunohistochemistry confirmed that BMI-1 expression was increased in mouse livers during CRLM.

continued increasing up to 7.29-fold at 28 d (Figure 1D). The mRNA expression level of BMI-1 accordingly increased 2.92-fold at 21 d and 6.71-fold at 28 d (Figure 1E). The IHC results also showed that few nuclei in liver cells were BMI-1-positive in CRLM mice from 14 d, but the BMI-1-positive rate and intensity increased markedly at 21 and 28 d (Figure 1F). These results suggest that BMI-1 was

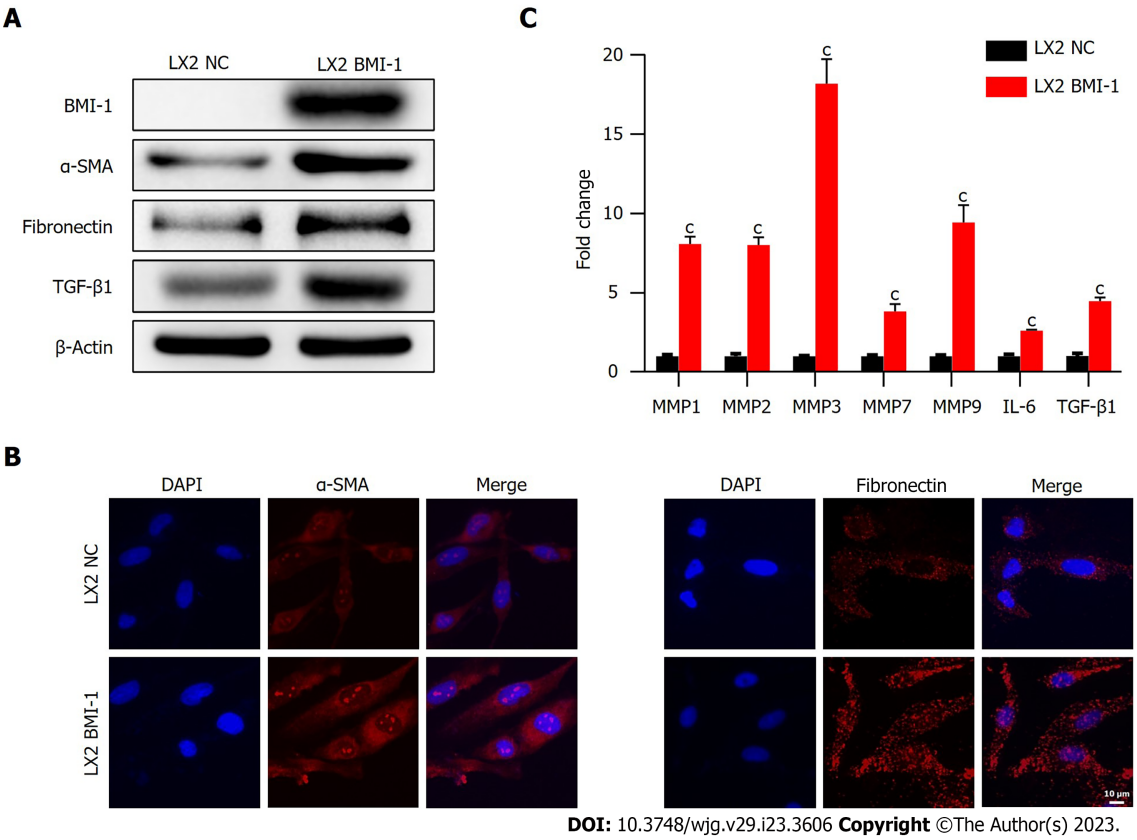

DOI: 10.3748/wjg.v29.i23.3606

Figure 2 BMI-1 activates LX2 hepatic stellate cells. A: Western blot analysis of BMI-1 and activated hepatic stellate cell (aHSC)-related markers (alpha smooth muscle actin [α-SMA], fibronectin and transforming growth factor beta 1) in control (LX2 NC) and LX2 BMI-1 HSCs; B: Quantitative polymerase chain reaction detection of matrix metalloproteinases (MMPs) and cytokines in LX2 HSCs, $^{c}P < 0.001$; C: Immunofluorescence analysis showed that α-SMA and fibronectin expression levels were increased in LX2 BMI-1 HSCs. DAPI: 4',6-diamidino-2-phenylindole; IL: Interleukin; NC: Negative control.

upregulated in liver cells after CRC cells metastasized to the liver, and may play a role in CRLM.

BMI-1 activates HSCs

To investigate the effects of BMI-1 on liver cells, we overexpressed BMI-1 in LX2 HSCs and confirmed the overexpression by WB (Figure 2A). High expression of α-SMA, a myofibroblast marker, is a key marker of aHSCs. aHSCs highly secrete the key cytokine TGF-β1 and promote hepatic fibrosis with fibronectin expression[27]. Compared with control quiescent HSCs, BMI-1 overexpressed LX2 HSCs showed a significant increase in α-SMA expression. Fibronectin and TGF-β1 expression were also markedly increased in BMI-1 overexpressed LX2 HSCs. Immunofluorescence staining also confirmed that the expression of α-SMA and fibronectin was significantly increased in LX2 cells overexpressing BMI-1 (Figure 2B). It was also observed that the transcript levels of matrix metalloproteinases (MMP1, MMP2, MMP3, MMP7, MMP9) and inflammatory cytokines (TGF-β1 and interleukin 6 [IL-6]) were markedly increased (Figure 2C). Thus, LX2 HSCs were activated by the overexpression of BMI-1.

BMI-1 overexpressed HSC CM enhances CRC cell proliferation and migration

To examine the effect of BMI-1 on the interaction between HSCs and CRC cells, CRC cells (HCT116 and DLD1) were cultured in control LX2 CM (NC CM) or BMI-1 overexpressed LX2 CM (BMI-1 CM). We first measured cell proliferation using the CCK-8 assay. Compared with cells cultured in NC CM, the proliferation of CRC cells cultured in BMI-1 CM was markedly enhanced on day 4 (Figure 3A), and the colony formation ability of CRC cells cultured in BMI-1 CM also significantly increased (Figure 3B). In addition, CRC cells cultured in BMI-1 CM showed higher wound healing rates (Figure 3C). Transwell migration assays showed the same results (Figure 3D). Then we investigated EMT-related molecular changes. Consistent with the above results, the mRNA and protein expression levels of ZEB-1, Twist-1, vimentin, and Snail in CRC cells cultured in BMI-1 CM were significantly increased while E-cadherin was decreased (Figure 3E and F). Immunofluorescence staining further demonstrated that Snail and vimentin expression was obviously increased in CRC cells cultured in BMI-1 CM (Figure 3G). Therefore, BMI-1 may be an important regulator in aHSCs, which promoted the malignant phenotype of CRC cells.

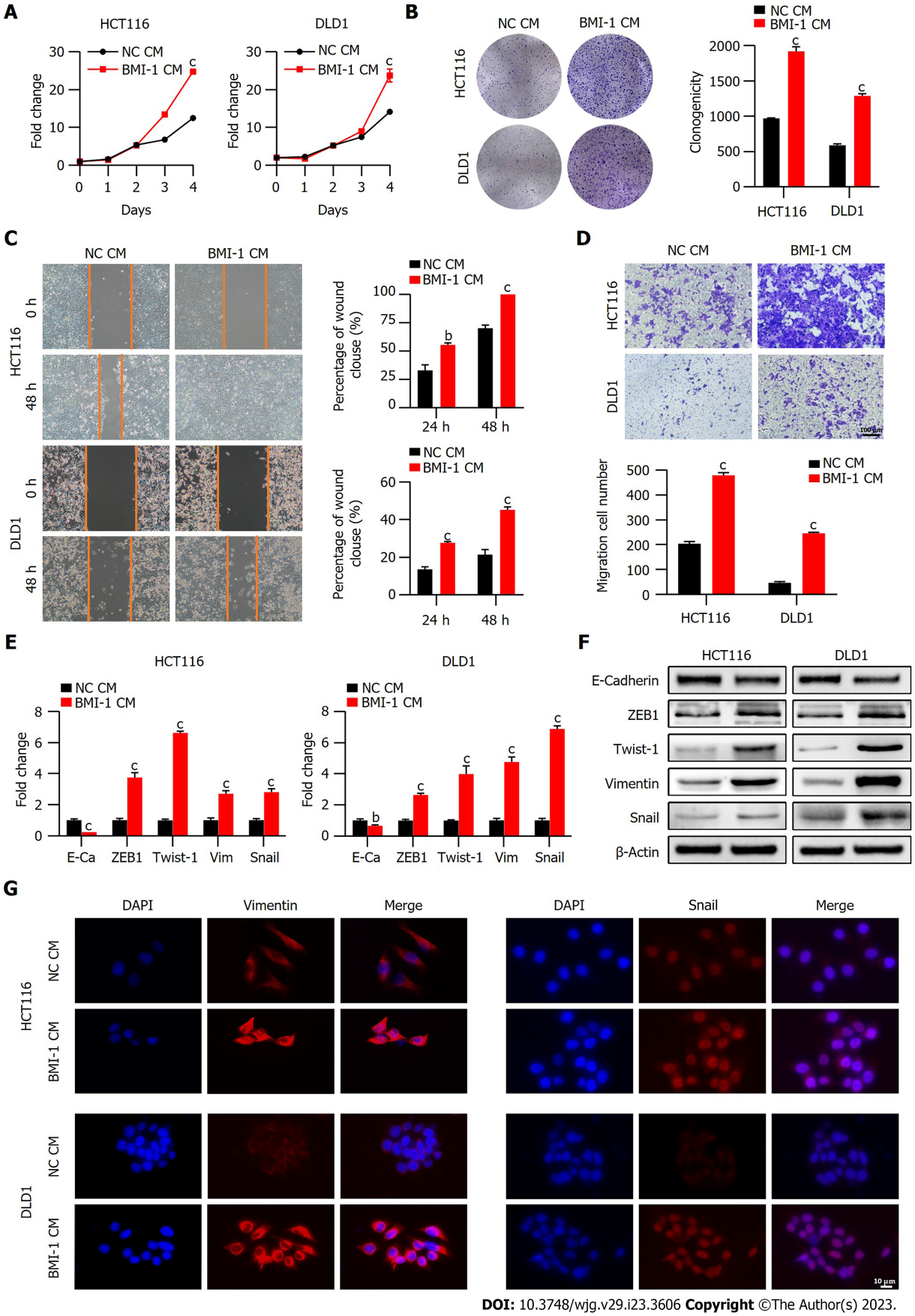

DOI: 10.3748/wjg.v29.i23.3606

Figure 3 Effects of BMI-1 overexpressed hepatic stellate cell conditioned medium on cell proliferation and migration of colorectal cancer cells. A: Viability of HCT116 and DLD-1 cells cultured in conditioned medium (CM) from negative control (NC) LX2 (NC CM) or CM from BMI-1 overexpressed LX2 (BMI-1 CM) was confirmed by the Cell Counting Kit-8 assay; B: Colony formation assay of colorectal cancer (CRC) cells cultured in NC CM or BMI-1 CM; C: Wound healing assay of CRC cells cultured in NC CM or BMI-1 CM, the healing percentages were calculated at 24 h and 48 h; D: Transwell migration assay of CRC cells

cultured in NC CM or BMI-1 CM, the numbers of cells which migrated were counted; E: Quantitative polymerase chain reaction assay of the expression of epithelial-mesenchymal transition (EMT)-related markers in CRC cells cultured in NC CM or BMI-1 CM; F: Western blot assays of the expression of EMT-related markers in CRC cells cultured in NC CM or BMI-1 CM; G: Immunofluorescence analysis showed that vimentin and Snail expression levels were increased in CRC cells cultured in BMI-1 CM. $^{b}P < 0.01$, $^{c}P < 0.001$ *vs* NC CM. DAPI: 4',6-diamidino-2-phenylindole.

BMI-1 overexpressed HSC CM promotes CRC cell EMT by activating the Smad2/3 pathway

As previously mentioned, TGF-β1 was upregulated in BMI-1 overexpressed LX2 HSCs (Figure 2A). The TGF-β/SMAD signal pathway plays an important role in metastasis by modulating the EMT process[28,29]; therefore, we hypothesized that BMI-1 CM induces EMT in CRC cells by activating SMADs. We first determined the expression levels of SMAD2/3. As shown in Figure 4A and B, although the mRNA and protein expression levels of SMAD2 and SMAD3 showed no changes in CRC cells cultured in BMI-1 CM, SMAD2 and SMAD3 phosphorylation was significantly increased compared with CRC cells cultured in NC CM. We then used SB-505124 (a TGF-β receptor [TGF-βR] inhibitor, which inhibits SMAD2 phosphorylation) to further confirm the involvement of SMADs in the pro-EMT effects of BMI-1 CM. SB-505124 markedly decreased BMI-1 CM-induced SMAD2 and SMAD3 phosphorylation in CRC cells (Figure 4C and D). In addition, the downstream target proteins (Snail and vimentin) of the TGF-β/SMAD pathway accordingly decreased in SB-505124-treated CRC cells cultured in BMI-1 CM (Figure 4C and D). These results confirmed that BMI-1 CM induces EMT in CRC cells partially by activating SMAD2/3.

BMI-1 overexpressed HSCs promotes tumor growth in vivo

We further evaluated the effects of BMI-1 overexpressed LX2 HSCs on CRC cell growth *in vivo*. A subcutaneous xenotransplantation tumor model was established by co-implantation of HSCs (LX2 NC or LX2 BMI-1) and CRC cells (Figure 5A). Compared with mice co-implanted with LX2 NC, tumors grew faster and larger in mice co-implanted with LX2 BMI-1 HSCs and CRC cells as shown by increased tumor volume and weight (Figure 5B and C). Moreover, consistent with the *in vitro* results, we found that Snail and vimentin were upregulated in mice co-implanted with LX2 BMI-1 HSCs and CRC cells as shown by the qPCR and WB results (Figure 5D and E). Furthermore, the increased expression of Snail and vimentin in mouse liver co-implanted with LX2 BMI-1 HSCs and CRC cells was confirmed by IHC (Figure 5F). These results showed that LX2 BMI-1 HSCs promoted CRC tumor growth and EMT in the mouse model.

DISCUSSION

The liver is the most common target organ in terms of CRC metastases. Accumulating evidence suggests that the interactions between cancer cells and the liver microenvironment promote the progression of LM. In the liver microenvironment, HSC-derived CAFs are the main tumor-interacting population and play a vital role in cancer cell metastasis[8,30]. During the development of CRLM, HSC activation was found to be the most common biological process. Tumor-derived factors such as TGF-β and platelet-derived growth factor can activate HSCs[31]. BMI-1 has been proved to promote tumorigenesis and tumor progression in different types of cancers including CRC and HCC[24,26,32-34]. We previously reported that BMI-1 was abnormally highly expressed in CRLM and inhibition of BMI-1 in CRC cells dramatically reduced LM *in vivo*[26]. Normal liver cells were BMI-1-negative, and we observed that BMI-1-positive liver cells were common in CRLM samples from humans and mice. In particular, the mRNA and protein expression levels of BMI-1 in liver cells gradually increased during the development of CRLM in mice, suggesting that BMI-1 also participates in regulating liver cells during the course of CRLM. In this study, we found that BMI-1 had a novel function as a regulator in activating HSCs and plays an important role in the crosstalk between HSCs and CRC cells.

Quiescent HSCs normally resident in the space of Disse become activated with a myofibroblast-like phenotype (α-SMA^{+}) in response to inflammatory stimuli and liver damage[27]. Studies have shown that cancer cells can also activate HSCs to release cytokines and chemokines to promote LM[8,35]. aHSCs reportedly orchestrate a premetastatic and prometastatic niche, which accelerate CRLM[5,6,36]. In this study, we found that BMI-1-positive liver cells appeared on day 14 and increased on days 21 and 28 after injection of CT26 cells, while small LM had formed on day 7. We further confirmed that BMI-1 overexpressed HSCs were activated to α-SMA^{+} myofibroblasts with increased expression of fibronectin, TGF-β1, MMPs, and IL-6. These secreted components can maintain the activated status of HSCs by enhancing the autocrine signaling loop[37]. aHSCs are the major source of ECM, and aHSC-secreted factors play a pivotal role in remodeling the ECM during tumor invasion and metastasis[38]. TGF-β1 is the most potent fibrogenic cytokine and is a fibrotic marker[39,40]. Fibronectin and MMPs are important ECM regulators in the liver fibrosis process[41]. ECM deposition by aHSCs provides a prometastatic environment. Thus, BMI-1 activates HSCs to secrete factors to form a prometastatic environment in the liver.

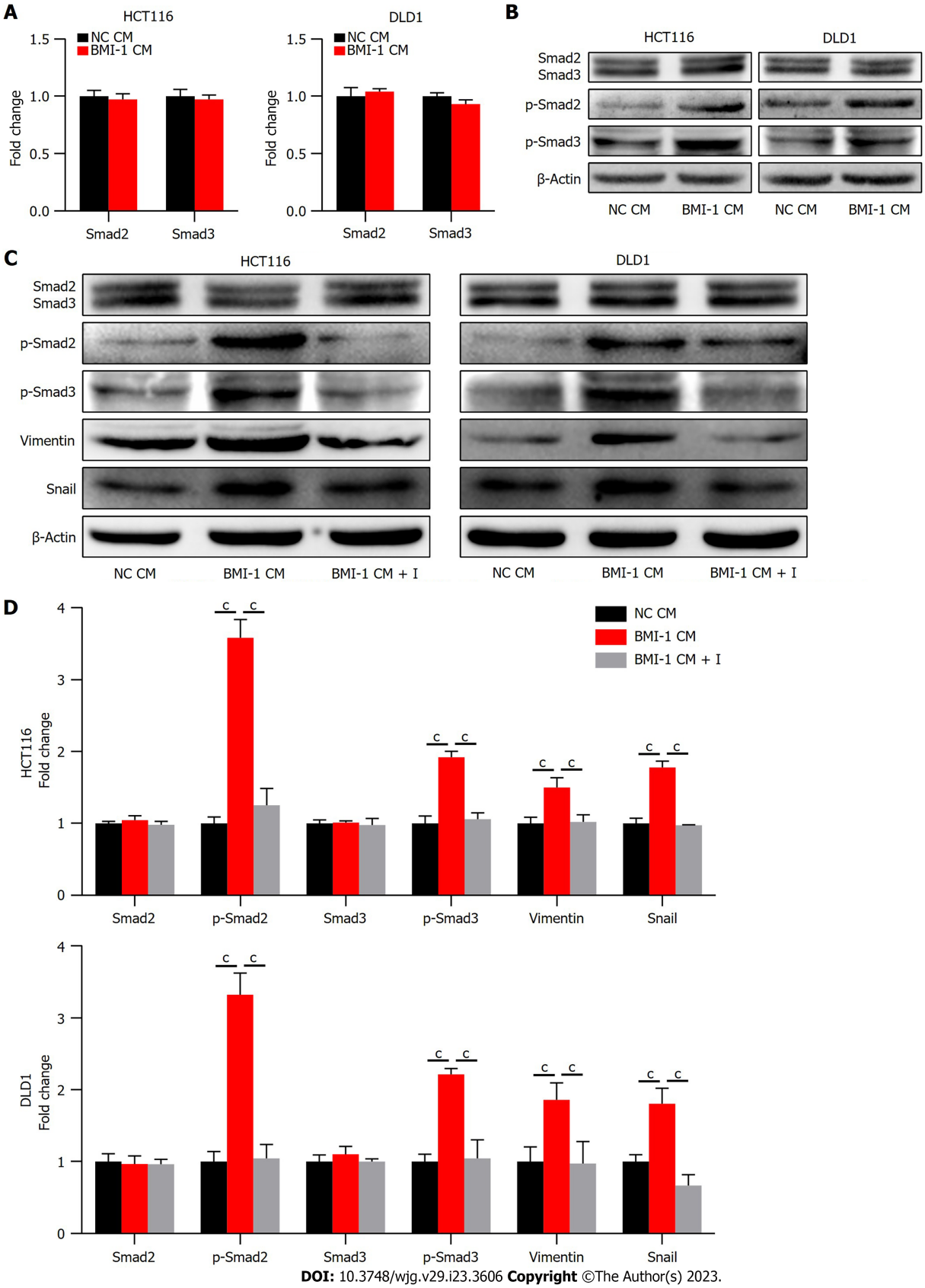

DOI: 10.3748/wjg.v29.i23.3606

Figure 4 BMI-1 conditioned medium induces activation of the transforming growth factor beta/SMAD pathway in colorectal cancer cells. A: Quantitative polymerase chain reaction analysis showed no difference in the expression of SMAD2 and SMAD3 in colorectal cancer (CRC) cells cultured in conditioned medium (CM) from negative control NC) (NC CM) or CM from BMI-1 overexpressed LX2 (BMI-1 CM); B: Western blot assays of SMAD2, SMAD3, phosphorylated (p)-SMAD2, and p-SMAD3 expression levels in CRC cells cultured in NC CM or BMI-1 CM; C and D: Western blot analysis of the expression of SMAD pathway members and epithelial-mesenchymal transition-related proteins (Snail and vimentin) in CRC cells cultured in NC CM or BMI-1 CM with/without 0.5 μM SB-505124 treatment, the relative expression levels of the proteins were calculated and are shown in D. °$P < 0.001$.

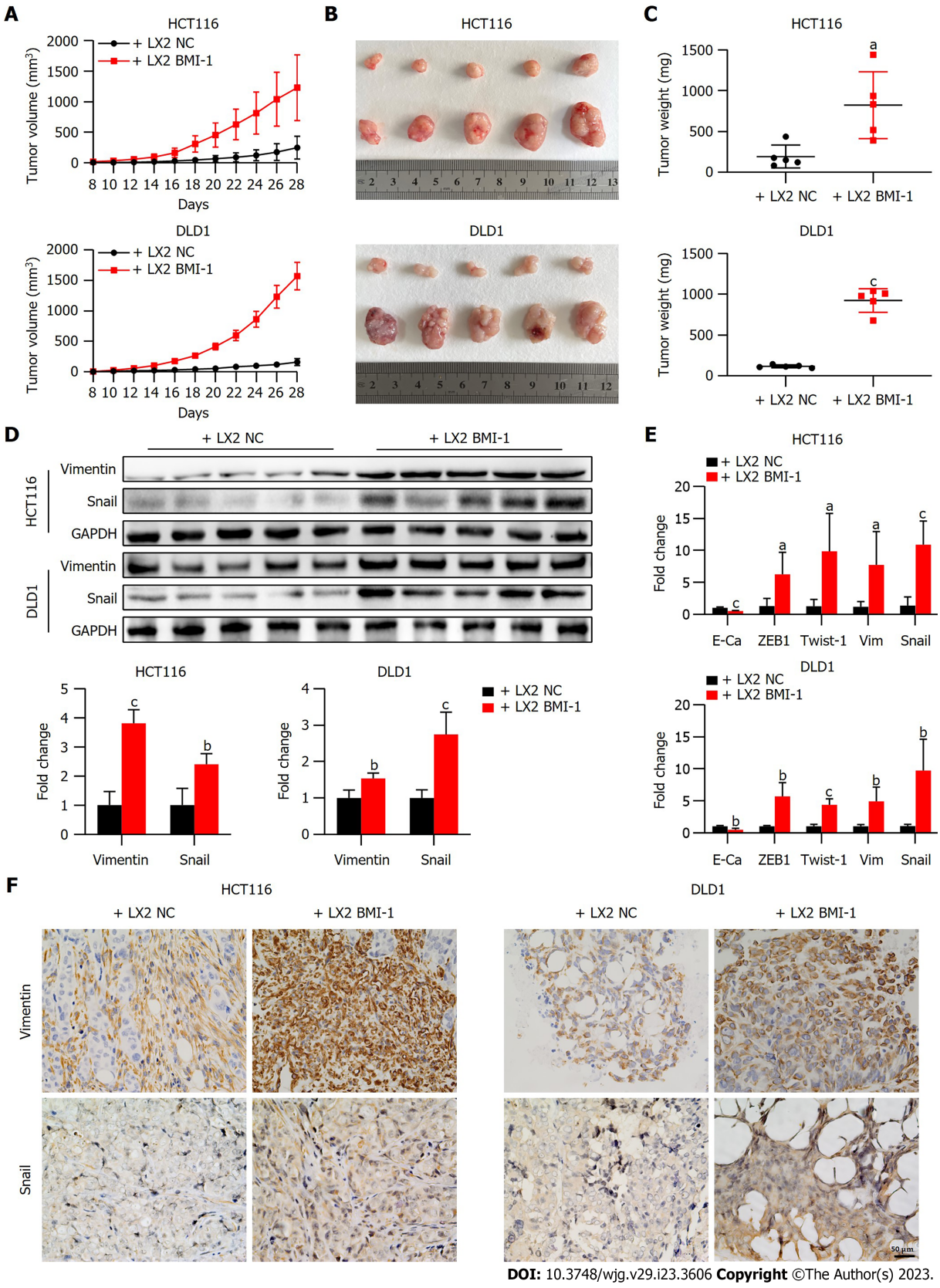

DOI: 10.3748/wjg.v29.i23.3606

Figure 5 BMI-1 overexpressed LX2 promotes tumor growth of colorectal cancer *in vivo*. A: Colorectal cancer cells (HCT116 or DLD-1) and LX2 cells (negative control [NC] or BMI-1 overexpressed) were co-implanted subcutaneously into the flanks of nude mice. After 7 d, tumor volume was measured every 2 d from 8 d to 28 d; B: Tumors were photographed at 28 d; C: Tumors were weighed (n = 5); D: Western blot assay of vimentin and Snail expression in mouse tumors in the different groups, and the fold changes were calculated; E: Quantitative polymerase chain reaction assay of the expression of epithelial-mesenchymal transition-related markers in mouse tumors in the different groups; F: Immunohistochemistry analysis of vimentin and Snail expression in mouse tumors. $^{a}P < 0.05$, $^{b}P < 0.01$, $^{c}P < 0.001$ *vs* LX2 NC. GAPDH: Glyceraldehyde-3-phosphate dehydrogenase.

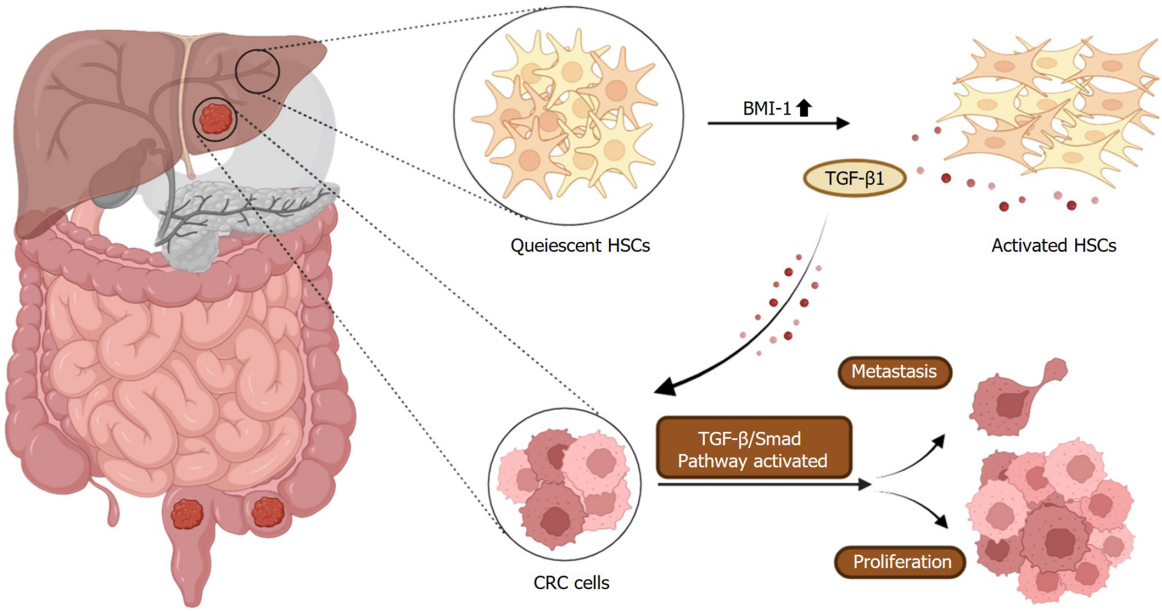

DOI: 10.3748/wjg.v29.i23.3606

Figure 6 Schematic summary of BMI-1-activated hepatic stellate cells, which promote colorectal cancer cell epithelial-mesenchymal transition and liver metastasis. CRC: Colorectal cancer; HSC: Hepatic stellate cell; TGF-β1: Transforming growth factor beta 1.

The interactions between cancer cells and aHSCs promote tumor growth and metastasis. CRC cells can stimulate aHSCs to release cytokines and chemokines, which in turn promote CRC growth and invasion[8,35]. In addition, aHSCs can secrete ECM components, induce angiogenesis, and modulate immunity to facilitate tumor growth and metastasis[31]. We found that high-metastatic HCT116 and low-metastatic DLD1 CRC cells cultured in CM from BMI-1 overexpressed HSCs showed the same enhanced proliferation and migration ability, and both HCT116 and DLD1 cells co-implanted with BMI-1 overexpressed HSCs showed increased tumor growth *in vivo*. These results demonstrated that BMI-1 aHSCs promote CRC cell proliferation and migration regardless of their ability to metastasize.

TGF-β signaling is important in tumor-stroma crosstalk. The TGF-β/SMAD pathway can act as both a tumor suppressor and promoter in CRLM[42,43]. The effect of the TGF-β/SMAD pathway in most malignant tumors is toward migration, the EMT or stemness, thereby promoting LM[44-46]. CRC cells are able to recruit and activate HSCs into CAFs by secreting TGF-β, and aHSCs lead to secretion of TGF-β which influences CRC cells[7]. LM has been found to be dependent on TGF-β signaling in liver stroma [47-50]. TGF-β1 is a key inducer of EMT transcription factors, which can promote EMT through the TGF-β/SMAD pathway[28,29]. The markers of EMT, including vimentin, Snail, ZEB-1, and Twist-1, were upregulated in CRC cells cultured in CM from BMI-1 overexpressed HSCs. The TGF-β/SMAD signaling pathway was activated and the phosphorylation of SMAD2/3 was induced in CRC cells cultured in CM from BMI-1 overexpressed HSCs, and treatment with the TGF-βR inhibitor SB-505124 attenuated the effect of BMI-1. Moreover, CRC cells co-implanted with BMI-1 overexpressed HSCs showed increased expression of EMT markers *in vivo*. Taken together, these findings indicate that BMI-1 overexpressed HSCs promote CRC cell growth and migration partly by activating the TGF-β/SMAD pathway and enhancing the EMT.

CONCLUSION

We propose a novel mechanism for BMI-1 involvement in promoting CRLM. BMI-1 was upregulated in liver cells during CRLM. BMI-1 aHSCs released cytokines and chemokines (fibronectin, TGF-β, MMPs, *etc*) to form a prometastatic environment in the liver, and promoted CRC cell proliferation, migration, and the EMT partially by activating the TGF-β/SMAD pathway (Figure 6). These findings provide a potential target for the treatment of CRLM.

ARTICLE HIGHLIGHTS

Research background

Hepatic stellate cells (HSCs) are an important component of liver tissue and are a major source of

cancer-associated fibroblasts. Cancer cells can activate HSCs, and in turn activated HSCs (aHSCs) promote tumor growth and metastasis. However, the mechanisms by which HSCs interact with colorectal cancer (CRC) cells to promote liver metastases (LM) are largely unknown.

Research motivation

We previously discovered that the expression of BMI-1 was abnormally high in LM of CRC. We speculated that BMI-1 plays an important role in the interaction between HSCs and CRC cells.

Research objectives

To examine the role of BMI-1 in HSC activation, and investigate the potential mechanisms of BMI-1 in the interaction between HSCs and CRC cells.

Research methods

The expression of BMI-1 in liver tissue of patients with CRC liver metastasis (CRLM) was determined by immunohistochemistry analysis. We established a mouse LM model to assess the expression of BMI-1 during CRLM. We used lentiviral vectors to overexpress BMI-1 in LX2 HSCs (LX2 BMI-1) and evaluated the molecular markers of aHSCs. The proliferation and mobility of CRC cells in LX2 BMI-1 conditioned medium (CM) was detected. The epithelial-mesenchymal transition (EMT) and transforming growth factor beta (TGF-β)/SMAD pathway in CRC cells treated with LX2 BMI-1 CM were investigated by Western blot analysis and quantitative polymerase chain reaction. A mouse xenograft model was established to investigate the effects of co-implantation of LX2 BMI-1 and CRC cells on tumor growth, and the EMT phenotype of CRC.

Research results

BMI-1 expression was upregulated in liver cells during CRLM. Overexpression of BMI-1 induced the activation of LX2 HSCs. CRC cells cultured in LX2 BMI-1 CM showed higher proliferation, migration, and EMT ability compared with cells cultured in NC CM. LX2 BMI-1 CM induced activation of the TGF-β/SMAD pathway in CRC cells, and the TGF-βR inhibitor SB-505124 diminished the effect of BMI-1 CM. In addition, LX2 BMI-1 HSCs promoted CRC tumor growth and EMT in the mouse model.

Research conclusions

BMI-1 aHSCs promoted the proliferation and migration of CRC partly *via* the TGF-β/SMAD pathway.

Research perspectives

Targeting BMI-1 in liver tissues may have potential therapeutic implications for the treatment of CRLM.

ACKNOWLEDGEMENTS

We thank Xiao-Li Hong and Chao Bi from the Core Facilities of Zhejiang University School of Medicine for their technical support.

FOOTNOTES

Author contributions: Jiang ZY, Dong QH, and Wang GY conceived and designed the study; Jiang ZY, Ma XM, Luan XH, Liuyang ZY, Hong YY, and Dai Y performed the research, and collected and analyzed the data; Jiang ZY, Dong QH, and Wang GY wrote the manuscript; All authors read and approved the final manuscript.

Supported by National Natural Science Foundation of China, No. 81472213; the Health Commission of Zhejiang Province, No. 2019ZD010 and No. 2019ZD029; the Science Technology Department of Zhejiang Province, No. LGF20H220001; and the Zhejiang Provincial Administration of Traditional Chinese Medicine, No. 2021ZA088.

Institutional review board statement: This study was reviewed and approved by the Ethics Committee of Sir Run Run Shaw Hospital affiliated with the Zhejiang University School of Medicine, No. 2023-404-01.

Institutional animal care and use committee statement: All animal experiments were performed in accordance with the guidelines of the Committee on the Ethics of Animal Experiments of Zhejiang University, No. ZJU20220447.

Informed consent statement: All study participants or their legal guardian provided informed written consent about personal and medical data collection prior to study enrolment.

Conflict-of-interest statement: All the authors report no relevant conflicts of interest for this article.

Data sharing statement: No additional data are available.

ARRIVE guidelines statement: The authors have read the ARRIVE guidelines, and the manuscript was prepared and revised according to the ARRIVE guidelines.

Country/Territory of origin: China

ORCID number: Qing-Hua Dong 0000-0002-7543-7528; Guan-Yu Wang 0000-0003-0849-7114.

S-Editor: Fan JR
L-Editor: Filipodia
P-Editor: Chen YX

REFERENCES

1 **Bray F**, Ferlay J, Soerjomataram I, Siegel RL, Torre LA, Jemal A. Global cancer statistics 2018: GLOBOCAN estimates of incidence and mortality worldwide for 36 cancers in 185 countries. *CA Cancer J Clin* 2018; **68**: 394-424 [PMID: 30207593 DOI: 10.3322/caac.21492]
2 **Siegel RL**, Miller KD, Goding Sauer A, Fedewa SA, Butterly LF, Anderson JC, Cercek A, Smith RA, Jemal A. Colorectal cancer statistics, 2020. *CA Cancer J Clin* 2020; **70**: 145-164 [PMID: 32133645 DOI: 10.3322/caac.21601]
3 **Valderrama-Treviño AI**, Barrera-Mera B, Ceballos-Villalva JC, Montalvo-Javé EE. Hepatic Metastasis from Colorectal Cancer. *Euroasian J Hepatogastroenterol* 2017; **7**: 166-175 [PMID: 29201802 DOI: 10.5005/jp-journals-10018-1241]
4 **Tsilimigras DI**, Brodt P, Clavien PA, Muschel RJ, D'Angelica MI, Endo I, Parks RW, Doyle M, de Santibañes E, Pawlik TM. Liver metastases. *Nat Rev Dis Primers* 2021; **7**: 27 [PMID: 33859205 DOI: 10.1038/s41572-021-00261-6]
5 **Illemann M**, Eefsen RH, Bird NC, Majeed A, Osterlind K, Laerum OD, Alpízar-Alpízar W, Lund IK, Høyer-Hansen G. Tissue inhibitor of matrix metalloproteinase-1 expression in colorectal cancer liver metastases is associated with vascular structures. *Mol Carcinog* 2016; **55**: 193-208 [PMID: 25594187 DOI: 10.1002/mc.22269]
6 **Schütte M**, Risch T, Abdavi-Azar N, Boehnke K, Schumacher D, Keil M, Yildiriman R, Jandrasits C, Borodina T, Amstislavskiy V, Worth CL, Schweiger C, Liebs S, Lange M, Warnatz HJ, Butcher LM, Barrett JE, Sultan M, Wierling C, Golob-Schwarzl N, Lax S, Uranitsch S, Becker M, Welte Y, Regan JL, Silvestrov M, Kehler I, Fusi A, Kessler T, Herwig R, Landegren U, Wienke D, Nilsson M, Velasco JA, Garin-Chesa P, Reinhard C, Beck S, Schäfer R, Regenbrecht CR, Henderson D, Lange B, Haybaeck J, Keilholz U, Hoffmann J, Lehrach H, Yaspo ML. Molecular dissection of colorectal cancer in pre-clinical models identifies biomarkers predicting sensitivity to EGFR inhibitors. *Nat Commun* 2017; **8**: 14262 [PMID: 28186126 DOI: 10.1038/ncomms14262]
7 **Marvin DL**, Heijboer R, Ten Dijke P, Ritsma L. TGF-β signaling in liver metastasis. *Clin Transl Med* 2020; **10**: e160 [PMID: 33252863 DOI: 10.1002/ctm2.160]
8 **Zhao S**, Mi Y, Zheng B, Wei P, Gu Y, Zhang Z, Xu Y, Cai S, Li X, Li D. Highly-metastatic colorectal cancer cell released miR-181a-5p-rich extracellular vesicles promote liver metastasis by activating hepatic stellate cells and remodelling the tumour microenvironment. *J Extracell Vesicles* 2022; **11**: e12186 [PMID: 35041299 DOI: 10.1002/jev2.12186]
9 **Milette S**, Sicklick JK, Lowy AM, Brodt P. Molecular Pathways: Targeting the Microenvironment of Liver Metastases. *Clin Cancer Res* 2017; **23**: 6390-6399 [PMID: 28615370 DOI: 10.1158/1078-0432.CCR-15-1636]
10 **Brodt P**. Role of the Microenvironment in Liver Metastasis: From Pre- to Prometastatic Niches. *Clin Cancer Res* 2016; **22**: 5971-5982 [PMID: 27797969]
11 **Mao X**, Xu J, Wang W, Liang C, Hua J, Liu J, Zhang B, Meng Q, Yu X, Shi S. Crosstalk between cancer-associated fibroblasts and immune cells in the tumor microenvironment: new findings and future perspectives. *Mol Cancer* 2021; **20**: 131 [PMID: 34635121 DOI: 10.1186/s12943-021-01428-1]
12 **Kalluri R**. The biology and function of fibroblasts in cancer. *Nat Rev Cancer* 2016; **16**: 582-598 [PMID: 27550820 DOI: 10.1038/nrc.2016.73]
13 **Sahai E**, Astsaturov I, Cukierman E, DeNardo DG, Egeblad M, Evans RM, Fearon D, Greten FR, Hingorani SR, Hunter T, Hynes RO, Jain RK, Janowitz T, Jorgensen C, Kimmelman AC, Kolonin MG, Maki RG, Powers RS, Puré E, Ramirez DC, Scherz-Shouval R, Sherman MH, Stewart S, Tlsty TD, Tuveson DA, Watt FM, Weaver V, Weeraratna AT, Werb Z. A framework for advancing our understanding of cancer-associated fibroblasts. *Nat Rev Cancer* 2020; **20**: 174-186 [PMID: 31980749 DOI: 10.1038/s41568-019-0238-1]
14 **Higashi T**, Friedman SL, Hoshida Y. Hepatic stellate cells as key target in liver fibrosis. *Adv Drug Deliv Rev* 2017; **121**: 27-42 [PMID: 28506744 DOI: 10.1016/j.addr.2017.05.007]
15 **Friedman SL**. Hepatic stellate cells: protean, multifunctional, and enigmatic cells of the liver. *Physiol Rev* 2008; **88**: 125-172 [PMID: 18195085 DOI: 10.1152/physrev.00013.2007]
16 **Barry AE**, Baldeosingh R, Lamm R, Patel K, Zhang K, Dominguez DA, Kirton KJ, Shah AP, Dang H. Hepatic Stellate Cells and Hepatocarcinogenesis. *Front Cell Dev Biol* 2020; **8**: 709 [PMID: 32850829 DOI: 10.3389/fcell.2020.00709]

17 **Shiraha H**, Iwamuro M, Okada H. Hepatic Stellate Cells in Liver Tumor. *Adv Exp Med Biol* 2020; **1234**: 43-56 [PMID: 32040854 DOI: 10.1007/978-3-030-37184-5_4]

18 **Mederacke I**, Hsu CC, Troeger JS, Huebener P, Mu X, Dapito DH, Pradere JP, Schwabe RF. Fate tracing reveals hepatic stellate cells as dominant contributors to liver fibrosis independent of its aetiology. *Nat Commun* 2013; **4**: 2823 [PMID: 24264436 DOI: 10.1038/ncomms3823]

19 **Makino Y**, Hikita H, Kodama T, Shigekawa M, Yamada R, Sakamori R, Eguchi H, Morii E, Yokoi H, Mukoyama M, Hiroshi S, Tatsumi T, Takehara T. CTGF Mediates Tumor-Stroma Interactions between Hepatoma Cells and Hepatic Stellate Cells to Accelerate HCC Progression. *Cancer Res* 2018; **78**: 4902-4914 [PMID: 29967264 DOI: 10.1158/0008-5472.CAN-17-3844]

20 **Biffi G**, Tuveson DA. Diversity and Biology of Cancer-Associated Fibroblasts. *Physiol Rev* 2021; **101**: 147-176 [PMID: 32466724 DOI: 10.1152/physrev.00048.2019]

21 **Affo S**, Nair A, Brundu F, Ravichandra A, Bhattacharjee S, Matsuda M, Chin L, Filliol A, Wen W, Song X, Decker A, Worley J, Caviglia JM, Yu L, Yin D, Saito Y, Savage T, Wells RG, Mack M, Zender L, Arpaia N, Remotti HE, Rabadan R, Sims P, Leblond AL, Weber A, Riener MO, Stockwell BR, Gaublomme J, Llovet JM, Kalluri R, Michalopoulos GK, Seki E, Sia D, Chen X, Califano A, Schwabe RF. Promotion of cholangiocarcinoma growth by diverse cancer-associated fibroblast subpopulations. *Cancer Cell* 2021; **39**: 866-882.e11 [PMID: 33930309 DOI: 10.1016/j.ccell.2021.03.012]

22 **Jacobs JJ**, Kieboom K, Marino S, DePinho RA, van Lohuizen M. The oncogene and Polycomb-group gene bmi-1 regulates cell proliferation and senescence through the ink4a locus. *Nature* 1999; **397**: 164-168 [PMID: 9923679]

23 **Jiang L**, Li J, Song L. Bmi-1, stem cells and cancer. *Acta Biochim Biophys Sin (Shanghai)* 2009; **41**: 527-534 [PMID: 19578716]

24 **Tateishi K**, Ohta M, Kanai F, Guleng B, Tanaka Y, Asaoka Y, Tada M, Seto M, Jazag A, Lianjie L, Okamoto M, Isayama H, Yoshida H, Kawabe T, Omata M. Dysregulated expression of stem cell factor Bmi1 in precancerous lesions of the gastrointestinal tract. *Clin Cancer Res* 2006; **12**: 6960-6966 [PMID: 17145814]

25 **Gil J**, Bernard D, Peters G. Role of polycomb group proteins in stem cell self-renewal and cancer. *DNA Cell Biol* 2005; **24**: 117-125 [PMID: 15699631]

26 **Xu Z**, Zhou Z, Zhang J, Xuan F, Fan M, Zhou D, Liuyang Z, Ma X, Hong Y, Wang Y, Sharma S, Dong Q, Wang G. Targeting BMI-1-mediated epithelial-mesenchymal transition to inhibit colorectal cancer liver metastasis. *Acta Pharm Sin B* 2021; **11**: 1274-1285 [PMID: 34094833 DOI: 10.1016/j.apsb.2020.11.018]

27 **Tsuchida T**, Friedman SL. Mechanisms of hepatic stellate cell activation. *Nat Rev Gastroenterol Hepatol* 2017; **14**: 397-411 [PMID: 28487545 DOI: 10.1038/nrgastro.2017.38]

28 **Xu J**, Lamouille S, Derynck R. TGF-beta-induced epithelial to mesenchymal transition. *Cell Res* 2009; **19**: 156-172 [PMID: 19153598 DOI: 10.1038/cr.2009.5]

29 **Hao Y**, Baker D, Ten Dijke P. TGF-β-Mediated Epithelial-Mesenchymal Transition and Cancer Metastasis. *Int J Mol Sci* 2019; **20** [PMID: 31195692 DOI: 10.3390/ijms20112767]

30 **Kubo N**, Araki K, Kuwano H, Shirabe K. Cancer-associated fibroblasts in hepatocellular carcinoma. *World J Gastroenterol* 2016; **22**: 6841-6850 [PMID: 27570421 DOI: 10.3748/wjg.v22.i30.6841]

31 **Kang N**, Gores GJ, Shah VH. Hepatic stellate cells: partners in crime for liver metastases? *Hepatology* 2011; **54**: 707-713 [PMID: 21520207 DOI: 10.1002/hep.24384]

32 **Effendi K**, Mori T, Komuta M, Masugi Y, Du W, Sakamoto M. Bmi-1 gene is upregulated in early-stage hepatocellular carcinoma and correlates with ATP-binding cassette transporter B1 expression. *Cancer Sci* 2010; **101**: 666-672 [PMID: 20085590 DOI: 10.1111/j.1349-7006.2009.01431.x]

33 **Li X**, Yang Z, Song W, Zhou L, Li Q, Tao K, Zhou J, Wang X, Zheng Z, You N, Dou K, Li H. Overexpression of Bmi-1 contributes to the invasion and metastasis of hepatocellular carcinoma by increasing the expression of matrix metalloproteinase (MMP)2, MMP-9 and vascular endothelial growth factor *via* the PTEN/PI3K/Akt pathway. *Int J Oncol* 2013; **43**: 793-802 [PMID: 23807724 DOI: 10.3892/ijo.2013.1992]

34 **Xu Z**, Tao J, Chen P, Chen L, Sharma S, Wang G, Dong Q. Sodium Butyrate Inhibits Colorectal Cancer Cell Migration by Downregulating Bmi-1 Through Enhanced miR-200c Expression. *Mol Nutr Food Res* 2018; **62**: e1700844 [PMID: 29418071 DOI: 10.1002/mnfr.201700844]

35 **Huang WH**, Zhou MW, Zhu YF, Xiang JB, Li ZY, Wang ZH, Zhou YM, Yang Y, Chen ZY, Gu XD. The Role Of Hepatic Stellate Cells In Promoting Liver Metastasis Of Colorectal Carcinoma. *Onco Targets Ther* 2019; **12**: 7573-7580 [PMID: 31571908 DOI: 10.2147/OTT.S214409]

36 **Eveno C**, Hainaud P, Rampanou A, Bonnin P, Bakhouche S, Dupuy E, Contreres JO, Pocard M. Proof of prometastatic niche induction by hepatic stellate cells. *J Surg Res* 2015; **194**: 496-504 [PMID: 25528682 DOI: 10.1016/j.jss.2014.11.005]

37 **Watanabe T**, Tajima H, Hironori H, Nakagawara H, Ohnishi I, Takamura H, Ninomiya I, Kitagawa H, Fushida S, Tani T, Fujimura T, Ota T, Wakayama T, Iseki S, Harada S. Sodium valproate blocks the transforming growth factor (TGF)-β1 autocrine loop and attenuates the TGF-β1-induced collagen synthesis in a human hepatic stellate cell line. *Int J Mol Med* 2011; **28**: 919-925 [PMID: 21822535 DOI: 10.3892/ijmm.2011.768]

38 **Ahmad SA**, Berman RS, Ellis LM. Biology of colorectal liver metastases. *Surg Oncol Clin N Am* 2003; **12**: 135-150 [PMID: 12735135]

39 **Xu F**, Liu C, Zhou D, Zhang L. TGF-β/SMAD Pathway and Its Regulation in Hepatic Fibrosis. *J Histochem Cytochem* 2016; **64**: 157-167 [PMID: 26747705 DOI: 10.1369/0022155415627681]

40 **Hellerbrand C**, Stefanovic B, Giordano F, Burchardt ER, Brenner DA. The role of TGFbeta1 in initiating hepatic stellate cell activation in vivo. *J Hepatol* 1999; **30**: 77-87 [PMID: 9927153]

41 **Klingberg F**, Hinz B, White ES. The myofibroblast matrix: implications for tissue repair and fibrosis. *J Pathol* 2013; **229**: 298-309 [PMID: 22996908 DOI: 10.1002/path.4104]

42 **Are C**, Simms N, Rajput A, Brattain M. The role of transforming growth factor-beta in suppression of hepatic metastasis from colon cancer. *HPB (Oxford)* 2010; **12**: 498-506 [PMID: 20815859 DOI: 10.1111/j.1477-2574.2010.00219.x]

43 **Korkut A**, Zaidi S, Kanchi RS, Rao S, Gough NR, Schultz A, Li X, Lorenzi PL, Berger AC, Robertson G, Kwong LN, Datto M, Roszik J, Ling S, Ravikumar V, Manyam G, Rao A, Shelley S, Liu Y, Ju Z, Hansel D, de Velasco G, Pennathur A, Andersen JB, O'Rourke CJ, Ohshiro K, Jogunoori W, Nguyen BN, Li S, Osmanbeyoglu HU, Ajani JA, Mani SA, Houseman A, Wiznerowicz M, Chen J, Gu S, Ma W, Zhang J, Tong P, Cherniack AD, Deng C, Resar L; Cancer Genome Atlas Research Network, Weinstein JN, Mishra L, Akbani R. A Pan-Cancer Analysis Reveals High-Frequency Genetic Alterations in Mediators of Signaling by the TGF-β Superfamily. *Cell Syst* 2018; **7**: 422-437.e7 [PMID: 30268436 DOI: 10.1016/j.cels.2018.08.010]

44 **Zhang B**, Halder SK, Kashikar ND, Cho YJ, Datta A, Gorden DL, Datta PK. Antimetastatic role of Smad4 signaling in colorectal cancer. *Gastroenterology* 2010; **138**: 969-80.e1 [PMID: 19909744 DOI: 10.1053/j.gastro.2009.11.004]

45 **Tsushima H**, Ito N, Tamura S, Matsuda Y, Inada M, Yabuuchi I, Imai Y, Nagashima R, Misawa H, Takeda H, Matsuzawa Y, Kawata S. Circulating transforming growth factor beta 1 as a predictor of liver metastasis after resection in colorectal cancer. *Clin Cancer Res* 2001; **7**: 1258-1262 [PMID: 11350892]

46 **Zhang C**, Gao H, Li C, Tu J, Chen Z, Su W, Geng X, Chen X, Wang J, Pan W. TGFβ1 Promotes Breast Cancer Local Invasion and Liver Metastasis by Increasing the CD44(high)/CD24(-) Subpopulation. *Technol Cancer Res Treat* 2018; **17**: 1533033818764497 [PMID: 29658391 DOI: 10.1177/1533033818764497]

47 **Calon A**, Espinet E, Palomo-Ponce S, Tauriello DV, Iglesias M, Céspedes MV, Sevillano M, Nadal C, Jung P, Zhang XH, Byrom D, Riera A, Rossell D, Mangues R, Massagué J, Sancho E, Batlle E. Dependency of colorectal cancer on a TGF-β-driven program in stromal cells for metastasis initiation. *Cancer Cell* 2012; **22**: 571-584 [PMID: 23153532 DOI: 10.1016/j.ccr.2012.08.013]

48 **Tauriello DVF**, Palomo-Ponce S, Stork D, Berenguer-Llergo A, Badia-Ramentol J, Iglesias M, Sevillano M, Ibiza S, Cañellas A, Hernando-Momblona X, Byrom D, Matarin JA, Calon A, Rivas EI, Nebreda AR, Riera A, Attolini CS, Batlle E. TGFβ drives immune evasion in genetically reconstituted colon cancer metastasis. *Nature* 2018; **554**: 538-543 [PMID: 29443964 DOI: 10.1038/nature25492]

49 **Zubeldia IG**, Bleau AM, Redrado M, Serrano D, Agliano A, Gil-Puig C, Vidal-Vanaclocha F, Lecanda J, Calvo A. Epithelial to mesenchymal transition and cancer stem cell phenotypes leading to liver metastasis are abrogated by the novel TGFβ1-targeting peptides P17 and P144. *Exp Cell Res* 2013; **319**: 12-22 [PMID: 23153552 DOI: 10.1016/j.yexcr.2012.11.004]

50 **Zhang B**, Halder SK, Zhang S, Datta PK. Targeting transforming growth factor-beta signaling in liver metastasis of colon cancer. *Cancer Lett* 2009; **277**: 114-120 [PMID: 19147275 DOI: 10.1016/j.canlet.2008.11.035]

World Journal of Gastroenterology

Submit a Manuscript: https://www.f6publishing.com

World J Gastroenterol 2023 June 21; 29(23): 3622-3644

DOI: 10.3748/wjg.v29.i23.3622

ISSN 1007-9327 (print) ISSN 2219-2840 (online)

ORIGINAL ARTICLE

Basic Study

18β-glycyrrhetinic acid inhibits proliferation of gastric cancer cells through regulating the miR-345-5p/TGM2 signaling pathway

Xia Li, Xiao-Ling Ma, Yi Nan, Yu-Hua Du, Yi Yang, Dou-Dou Lu, Jun-Fei Zhang, Yan Chen, Lei Zhang, Yang Niu, Ling Yuan

Specialty type: Gastroenterology and hepatology

Provenance and peer review: Unsolicited article; Externally peer reviewed.

Peer-review model: Single blind

Peer-review report's scientific quality classification

Grade A (Excellent): 0
Grade B (Very good): B, B
Grade C (Good): 0
Grade D (Fair): 0
Grade E (Poor): 0

P-Reviewer: Kotelevets SM, Russia; Liu YQ, United States

Received: March 20, 2023
Peer-review started: March 20, 2023
First decision: April 10, 2023
Revised: April 24, 2023
Accepted: May 17, 2023
Article in press: May 17, 2023
Published online: June 21, 2023

Xia Li, Yu-Hua Du, Ling Yuan, College of Pharmacy, Ningxia Medical University, Yinchuan 750004, Ningxia Hui Autonomous Region, China

Xiao-Ling Ma, Yi Nan, Yan Chen, Yang Niu, Traditional Chinese Medicine College, Ningxia Medical University, Yinchuan 750004, Ningxia Hui Autonomous Region, China

Yi Nan, Lei Zhang, Yang Niu, Key Laboratory of Hui Ethnic Medicine Modernization of Ministry of Education, Ningxia Medical University, Yinchuan 750004, Ningxia Hui Autonomous Region, China

Yi Yang, College of Basic Medicine, Ningxia Medical University, Yinchuan 750004, Ningxia Hui Autonomous Region, China

Dou-Dou Lu, Jun-Fei Zhang, College of Clinical Medicine, Ningxia Medical University, Yinchuan 750004, Ningxia Hui Autonomous Region, China

Corresponding author: Ling Yuan, MD, PhD, Assistant Professor, College of Pharmacy, Ningxia Medical University, No. 1160 Shengli Street, Yinchuan 750004, Ningxia Hui Autonomous Region, China. 20080017@nxmu.edu.cn

Abstract

BACKGROUND

Gastric cancer (GC) is a common gastrointestinal malignancy worldwide. Based on cancer-related mortality, the current prevention and treatment strategies for GC still show poor clinical results. Therefore, it is important to find effective drug treatment targets.

AIM

To explore the molecular mechanism of 18β-glycyrrhetinic acid (18β-GRA) regulating the miR-345-5p/TGM2 signaling pathway to inhibit the proliferation of GC cells.

METHODS

CCK-8 assay was used to determine the effect of 18β-GRA on the survival rate of GES-1 cells and AGS and HGC-27 cells. Cell cycle and apoptosis were detected by flow cytometry, cell migration was detected by a wound healing assay, the effect of 18β-GRA on subcutaneous tumor growth in BALB/c nude mice was inves-

tigated, and the cell autophagy level was determined by MDC staining. TMT proteomic analysis was used to detect the differentially expressed autophagy-related proteins in GC cells after 18β-GRA intervention, and then the protein-protein interaction was predicted using STRING (https://string-db.org/). MicroRNAs (miRNAs) transcriptome analysis was used to detect the miRNA differential expression profile, and use miRBase (https://www.mirbase/) and TargetScan (https://www.targetscan.org/) to predict the miRNA and complementary binding sites. Quantitative real-time polymerase chain reaction was used to detect the expression level of miRNA in 18β-GRA treated cells, and western blot was used to detect the expression of autophagy related proteins. Finally, the effect of miR-345-5p on GC cells was verified by mir-345-5p overexpression.

RESULTS

18β-GRA could inhibit GC cells viability, promote cell apoptosis, block cell cycle, reduce cell wound healing ability, and inhibit the GC cells growth *in vivo*. MDC staining results showed that 18β-GRA could promote autophagy in GC cells. By TMT proteomic analysis and miRNAs transcriptome analysis, it was concluded that 18β-GRA could down-regulate TGM2 expression and up-regulate miR-345-5p expression in GC cells. Subsequently, we verified that TGM2 is the target of miR-345-5p, and that overexpression of miR-345-5p significantly inhibited the protein expression level of TGM2. Western blot showed that the expression of autophagy-related proteins of TGM2 and p62 was significantly reduced, and LC3II, ULK1 and AMPK expression was significantly increased in GC cells treated with 18β-GRA. Overexpression of miR-345-5p not only inhibited the expression of TGM2, but also inhibited the proliferation of GC cells by promoting cell apoptosis and arresting cell cycle.

CONCLUSION

18β-GRA inhibits the proliferation of GC cells and promotes autophagy by regulating the miR-345-5p/TGM2 signaling pathway.

Key Words: 18β-glycyrrhetinic acid; Gastric cancer; MiR-345-5p; TGM2; Proliferation; Autophagy

Core Tip: Gastric cancer (GC) is a global health problem that seriously endangers human life, so it is urgent to find drugs to treat it. 18β-glycyrrhetinic acid (18β-GRA), as one of the main components of glycyrrhiza, has a strong antitumor effect. In this paper, the inhibitory effect of 18β-GRA on GC was verified by *in vitro* and *in vivo* experiments. In addition, it was found that 18β-GRA promoted autophagy and inhibited the proliferation of GC cells through the miR-345-5p/TGM2 signaling pathway. These findings provide the theoretical basis for the GC clinical treatment of 18β-GRA.

Citation: Li X, Ma XL, Nan Y, Du YH, Yang Y, Lu DD, Zhang JF, Chen Y, Zhang L, Niu Y, Yuan L. 18β-glycyrrhetinic acid inhibits proliferation of gastric cancer cells through regulating the miR-345-5p/TGM2 signaling pathway. *World J Gastroenterol* 2023; 29(23): 3622-3644
URL: https://www.wjgnet.com/1007-9327/full/v29/i23/3622.htm
DOI: https://dx.doi.org/10.3748/wjg.v29.i23.3622

INTRODUCTION

The fourth most common cause of cancer-related death worldwide is gastric cancer (GC)[1]. Environment, diet, genetic factors, and *Helicobacter pylori* infection are the main causes of GC. Because there are no specific diagnostic indicators, the majority of patients ignore their early symptoms because they are inconspicuous. By the time the body shows obvious discomfort, the disease has progressed to intermediate or advanced cancer, and the disease has worsened significantly, allowing the best opportunity for treatment to pass. The existing treatment methods for GC are mainly drug therapy, chemotherapy and surgery[2,3]. But the drug resistance and toxic side effects of anticancer drugs, the low compliance of patients during chemotherapy and the low survival rate after surgery all suggest that we can find a natural, effective and low-toxic active ingredient to treat GC.

18β-glycyrrhetinic acid (18β-GRA) is a compound extracted from licorice[4]. Studies have revealed that 18β-GRA has multiple pharmacological effects, like anti-inflammatory, anti-viral, anti-tumor, liver protection and so on[5-9]. In recent years, the therapeutic effect of 18β-GRA on lung cancer[7], breast

cancer[10], ovarian cancer[11], prostate cancer[12] and other cancers has been confirmed. Cao *et al*[13] revealed that 18β-GRA inhibited GC cells proliferation, energy metabolism and carcinogenesis by down-regulating toll-like receptor 2. Through reactive oxygen species/protein kinase C-α/extracellular signal-regulated kinase pathway, as well as matrix metalloproteinase MMP2 and MMP9 activity, 18β-GRA inhibited GC cells migration and invasion[14]. And our previous study found that 18β-GRA inhibited GC cells proliferation by regulating MRPL35[15]. These results indicated that 18β-GRA may be a useful drug for the prevention and treatment of GC.

MicroRNAs (miRNAs) are highly conserved non-coding RNA molecules, that take part in the occurrence and development of cancer[16]. Many sequences of human miRNAs associated with cancer mechanisms have been identified. They regulate protein expression levels by their target mRNA, and participate in vital cellular processes and pathways[17]. There is growing evidence that the difference in miRNAs expression exists not only between normal and cancer tissues and between different cancer types and subtypes, but also between early and advanced cancers[18,19]. Komatsu *et al*[20] found that up-regulation of miR-148a inhibited the GC cells proliferation, invasion and EMT. The researchers revealed that *Helicobacter pylori* infection reduced miR-1298-5p expression in GC cells, while low-expressed miR-1298-5p could promote GC cells proliferation, migration and invasion[21].

Autophagy is a biological process that occurs in cells[22]. A lot of research has found that it plays a key role in physiological processes and disease occurrences, including development, metabolism, inflammation and cancer[23]. Dysfunctional autophagy results in incorrect organelles and protein breakdown, which kill autophagic cells and affect tumor cell survival. Wei *et al*[24] revealed that miR-183 induced GC cells autophagy and inhibited proliferation *via* targeted inhibition of mechanistic target of rapamycin (mTOR) expression.

In our study, we revealed 18β-GRA's effect on GC cells phenotype and tumor formation in nude mice, and 18β-GRA's effect on GC cells autophagy. We used TMT proteomic analysis and the STRING database to predict the differentially expressed autophagy-related proteins and their interactions. The differentially expressed miRNAs were analyzed using miRNAs transcriptome analysis, and the corresponding miRNAs and complementary binding sites of autophagy-related proteins were predicted using the miRBase and TargetScan databases. Later, we verified the link between miR-345-5p and TGM2 using a dual-luciferase reporter assay. Quantitative real-time polymerase chain reaction (qRT-PCR) was used to detect expression of miR-345-5p, western blot was used to detect autophagy-related proteins, and lentivirus transfection technique verified the effect of miR-345-5p on TGM2. We concluded that 18β-GRA can inhibit GC cells proliferation and promote autophagy *via* regulating the miR-345-5p/TGM2 signaling pathway, which may afford a theoretical basis for GC treatment with 18β-GRA. The research idea is shown in Figure 1.

MATERIALS AND METHODS

Experimental materials

Human gastric epithelial cell GES-1 was purchased from BNCC (Cat. No. BNCC353464, Beijing, China). Human GC cell lines AGS, HGC-27 and MKN-45 were purchased from Procell (Cat. No. CL-0022/CL-0107/CL-0292, Wuhan, China). Fetal bovine serum (FBS) was purchased from Corning (Cat. No. 35-076-CV, United States). DMEM, DMEM/F-12 and RPIM-1640 mediums were purchased from Gibco. The dual-luciferase reporter assay system was purchased from Promega (United States). Shanghai Gene Biotechnology Co., Ltd. (China) provided the plasmid and lentiviral expression vector. The MDC kit, cell apoptosis kit and cell cycle kit (Cat. No. KGATG001/KGA1026/KGA512, Jiangsu, China) were purchased from Jiangsu KeyGEN Bio TECH Corp., Ltd. TaKaRa provided the PrimeScript™ RT reagent kit and TB Green Premix Ex Taq II (Cat. No. RR047A/RR82LR, Japan). Thermofisher provided Trizol. MedChemExpress provided cisplatin (DDP) and 18β-GRA (Cat. No. HY17394/HY-N0180, United States). Immunoway provided TGM2, AMPK, p62, ULK1, LC3I/II, GAPDH and β-actin antibodies, while CST provided anti-mouse/rabbit immunoglobulin G antibodies.

BABL/c nude mice (male, 18-22g, SPF) were provided by the Animal Laboratory Center of Ningxia Medical University. All animals were fed standard laboratory feed and water in 12 h light/dark cycle environment. The animal protocols (IACUC-NYLAC-2022-108) were approved by the Institutional Animal Care and Use Committee of Ningxia Medical University. All animals were euthanized by CO_2.

Cell culture and cell transfection

GES-1 cells were cultured in DMEM medium, HGC-27 cells were cultured in RPIM-1640 medium, and AGS and MKN-45 cells were cultured in DMEM/F-12 medium, and 10% FBS and 1% penicillin-streptomycin liquid were added into all mediums to. The cell culture flask was placed in an incubator with a constant temperature of 37 °C and 5% CO_2. The GFP-labeled miR-345-5p overexpression lentiviral vector (LV-miR-345-5p) and empty lentiviral vector (LV-NC) were then transfected into HGC-27 and AGS cells using the tool virus user manual as a guide.

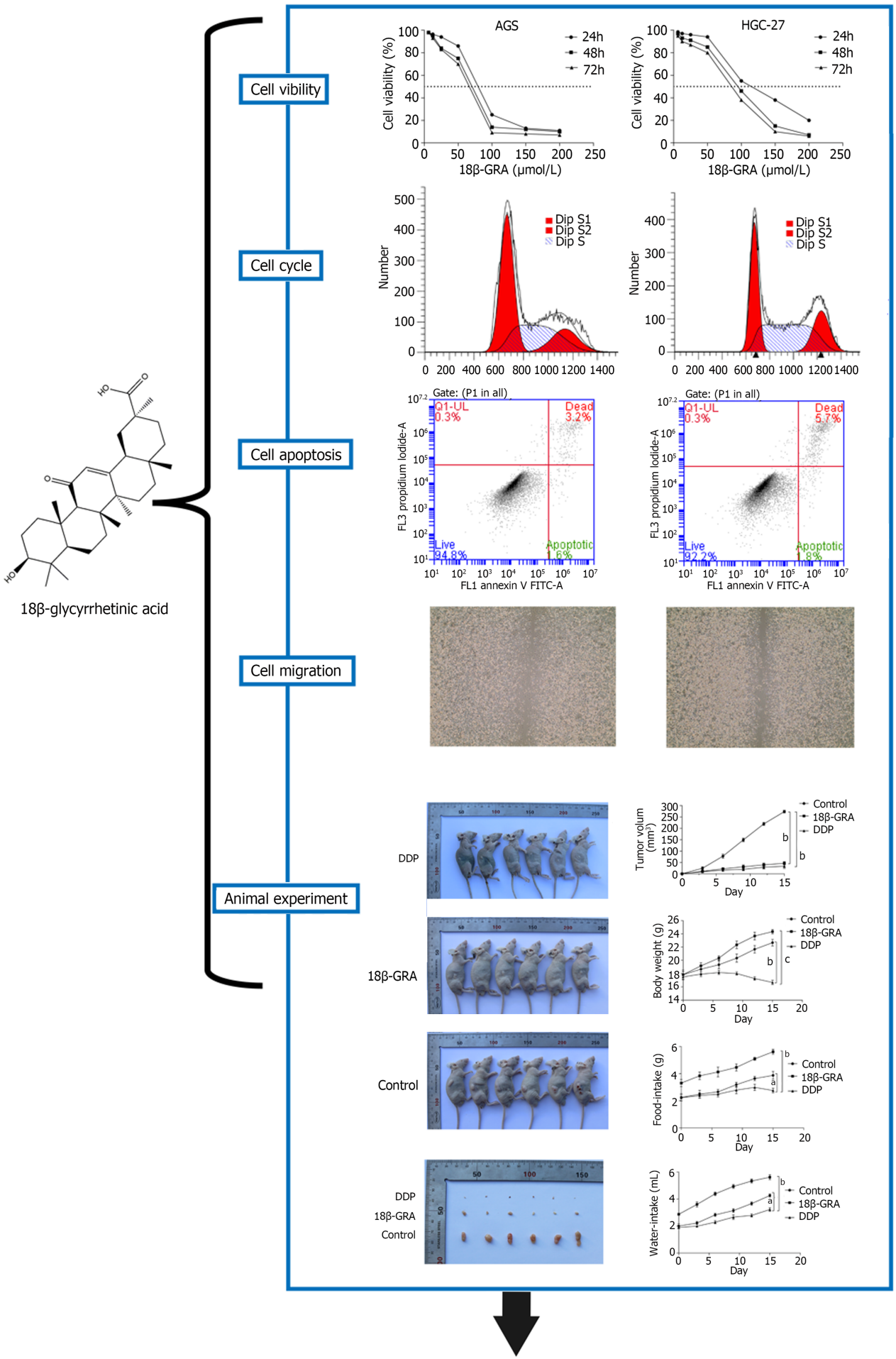
18β-glycyrrhetinic acid
Cell vibility
Cell cycle
Cell apoptosis
Cell migration
Animal experiment
AGS
HGC-27
Cell viability (%)
18β-GRA (μmol/L)
24h
48h
72h
Dip S1
Dip S2
Dip S
Number
Gate: (P1 in all)
Q1-UL 0.3%
Dead 3.2%
Dead 5.7%
Live 94.8%
Live 92.2%
Apoptotic 1.6%
Apoptotic 1.8%
FL3 propidium Iodide-A
FL1 annexin V FITC-A
DDP
18β-GRA
Control
Tumor volum (mm³)
Body weight (g)
Food-intake (g)
Water-intake (mL)
Day

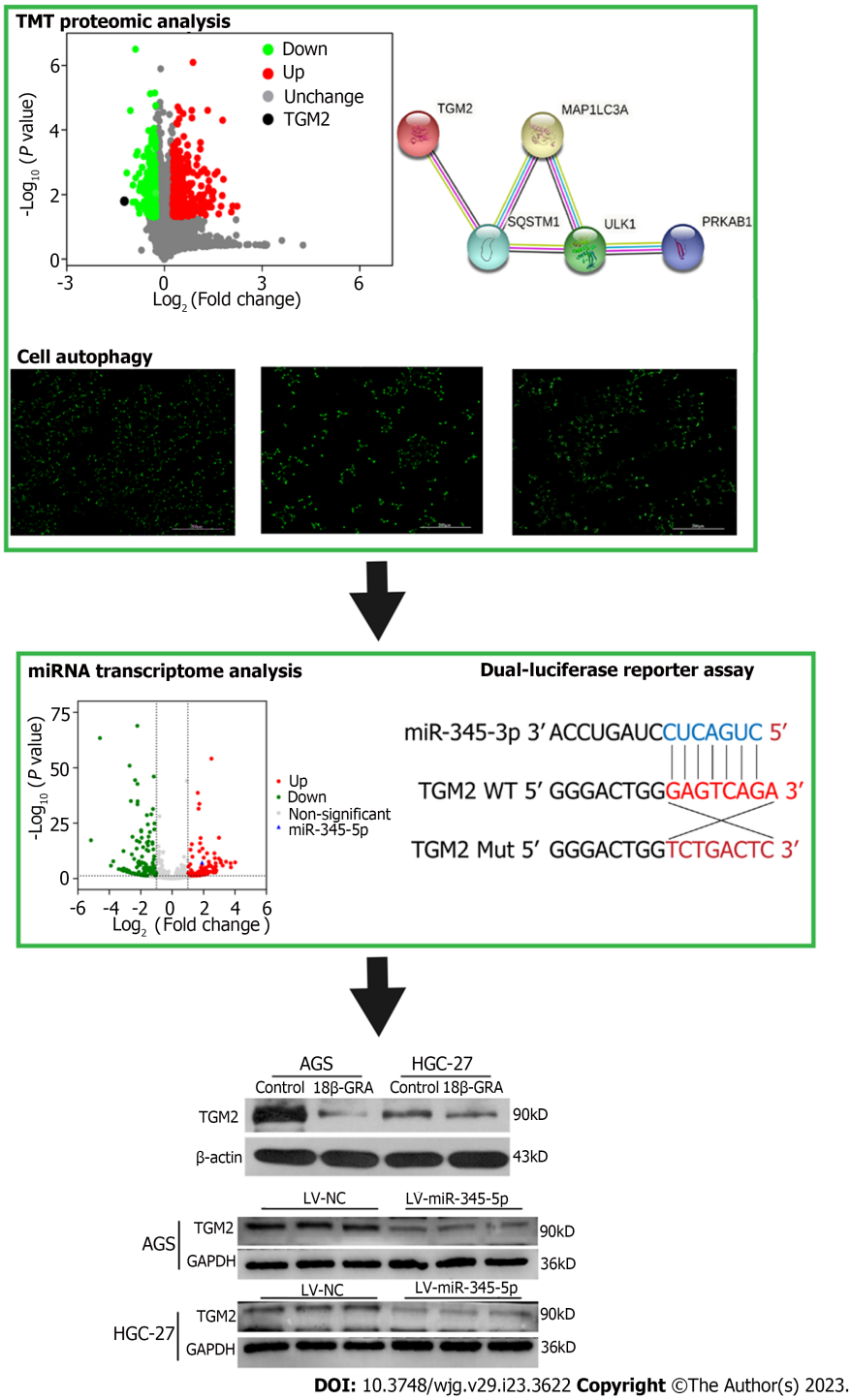

DOI: 10.3748/wjg.v29.i23.3622

Figure 1 Flow chart. In this study, we revealed 18β-glycyrrhetinic acid (18β-GRA)'s effect on gastric cancer (GC) cells phenotype and tumor formation in nude mice, and 18β-GRA's effect on GC cells autophagy. We used TMT proteomic analysis and the STRING database to predict the differentially expressed autophagy-related proteins and their interactions. Later, we verified the link between miR-345-5p and TGM2 using a dual-luciferase reporter assay. Quantitative real-time polymerase chain reaction was used to detect expression of miR-345-5p, western blot was used to detect autophagy-related proteins, and lentivirus transfection technique verified the effect of miR-345-5p on TGM2. LV-NC: Empty lentiviral vector.

Cell viability assay

The cells were inoculated into 96-well plates at 4000 cells per well and treated with 18β-GRA (12.5 μmol/L-200 μmol/L) for 24 h, 48 h and 72 h. Next, 10 μL CCK-8 was added to each well, and the absorbance was detected at 450 nm.

Cell cycle and cell apoptosis assay

The cells were treated with 18β-GRA at concentrations of 30, 60 and 120 μmol/L or 45, 90 and 135 μmol/L for 48 h, respectively. Next, the cells were collected and fixed with 70% pre-cooled ethanol. The fixative solution was washed off with PBS. 500 μL pre-configured working solution (RNase A:PI = 1:9)

was added. The percentage of cell cycle was determined by flow cytometry after 30 min. The cells in each group were collected, 500 μL binding buffer, 5 μL Annexin V-FITC and 5 μL PI or 500 μL binding buffer, 5 μL Annexin V-APC and 5 μL 7-AAD were added and mixed. Cell apoptosis was determined after 15 min using flow cytometry.

Wound healing assay

The cells were inoculated into the 6-well plates at the appropriate concentration and cultured for 24 h. Next, we made a scratch in the central part of each hole, and 18β-GRA at concentrations of 30, 60, 120 μmol/L or 45, 90, 135 μmol/L was added for 48 h. Finally, the cells were washed and photographed with a microscope. Cell migration area was calculated by Image J.

MDC staining assay

The cells were treated with 18β-GRA at concentrations of 30, 60 and 120 μmol/L or 45, 90 and 135 μmol/L for 48 h, respectively. Next, the cells were gently washed twice with a wash buffer, stained with MDC and incubated away from light for 15-45 min. Photographs were taken under a fluorescence microscope after washing twice with 1 × wash buffer.

Tumor formation experiment in BALB/c nude mice

The BALB/c nude mice were fed for 1 wk, then 200 μL MKN-45 cells suspension containing 4×10^6 cells were inoculated subcutaneously into nude mice using a microsyringe. The experiment was divided into three groups: Control, cisplatin group (DDP) and 18β-GRA groups. After 5 d of subcutaneous inoculation, the 18β-GRA group was intraperitoneally injected with 50 mg/kg[13,25], the DDP group with 2 mg/kg[26], and the control group was given normal saline. $V = (L \times W^2)/2$ was used to calculate tumor volumes (V, volume; W, width; L, length). After 14 d of continuous administration, all nude mice were killed by CO_2 inhalation and photographed.

TMT proteomic analysis

GC cells were treated with 18β-GRA, and differentially expressed proteins were detected and analyzed by China Gene Biotechnology Co., Ltd. All the obtained original data files were processed by Proteome Discoverer 2.2 (Thermo Fisher, United States) software. Proteins with expression ratio > 1.2 and $P < 0.05$ were considered as differentially expressed proteins.

Cellular processes, biological processes, and molecular functions of differentially expressed proteins were analyzed using Metascape (https://metascape.org/gp/index.html#/main/step1). Gene Ontology annotation, Kyoto Encyclopedia of Genes and Genomes pathway, and InterPro domain enrichment analysis were performed using Fisher accuracy test. WoLFPSOR was used to locate and predict the differentially expressed proteins. The protein expression levels are classified by Matplotlib to form hierarchical clustering heatmaps.

miRNAs transcriptome analysis

GC cells were treated with 18β-GRA at concentrations of 60 μmol/L and total RNA was extracted from it. Agarose gel electrophoresis, Nanodrop, Qubit 2.0, and Agilent 2100 were used to ensure that the quality of the collected RNA met the requirements of subsequent experiments. A small RNA Sample Pre kit was used to construct the library, and specific enzymes were used to connect the PCR primer connectors at the 3′ and 5′ ends. Then the cDNA synthesis can be completed efficiently and rapidly by reverse transcription. The single strand of DNA is combined with the primer and the PCR amplification stage begins. After PAGE electrophoresis, a cDNA library (effective concentration > 2 nM) was obtained. Qubit 2.0 and Agilent 2100 were combined with qPCR to ensure the quality of the library. The optical signal was transformed into a sequence by computer analysis. The original sequencing data was further assessed for quality with $P < 0.05$ and $|\text{Log}_2 \text{(fold change)}| > 1$ as a filter condition, with a certain number of differential expressions of miRNAs eventually selected.

Target prediction analysis

We predicted protein-protein interaction (PPI) networks from the STRING database (https://string-db.org/). The miRBase website (http://www.mirbase.org/) was used to predict the corresponding miRNAs of autophagy-related proteins and the TargetScan database (https://www.targetscan.org/) was used to predict the binding sites of miRNA and mRNA.

Dual-luciferase reporter assay

TargetScan predicted the binding sites for miR-345-5p and TGM2. The fragments, including the wild 3′UTR regions or mutant 3′UTR regions of TGM2, were inserted into GV716 with a firefly and renilla luciferase reporter gene. The overexpressed miR-345-5p plasmid was then individually transfected into AGS cells. After 48 h of transfection, the relative luciferase activity was detected using a dual-luciferase reporter assay system.

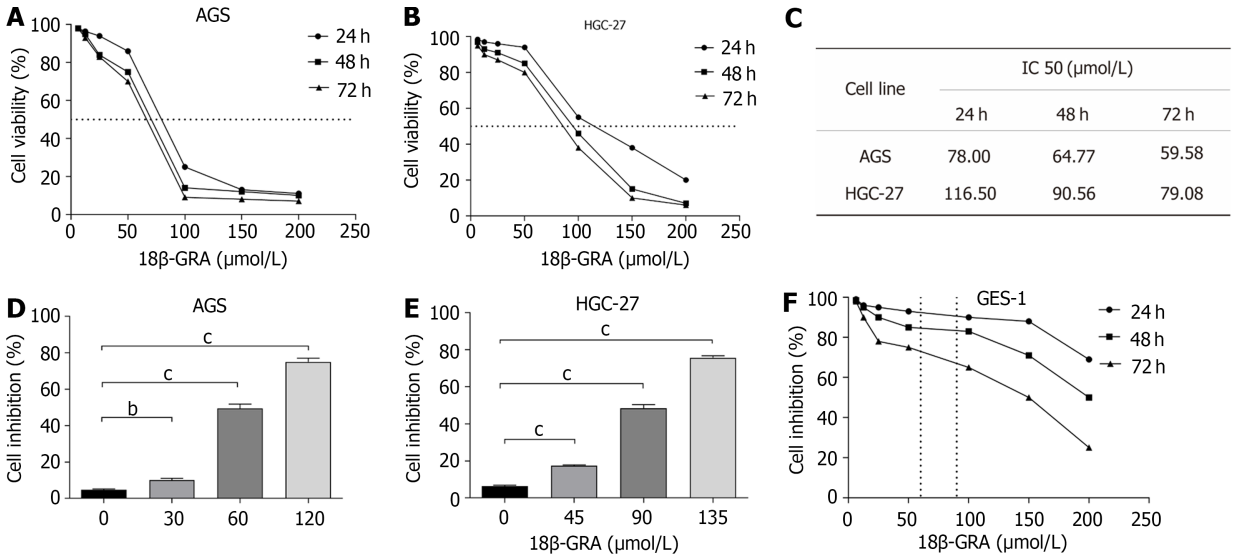

DOI: 10.3748/wjg.v29.i23.3622

Figure 2 Effect of 18β-glycyrrhetinic acid on cell viability of GES-1, AGS and HGC-27 cells were detected by CCK-8 assay. A: Effect of 18β-glycyrrhetinic acid (18β-GRA) on cell viability of AGS cells; B: Effect of 18β-GRA on cell viability of HGC-27 cells; C: IC_{50} value of AGS and HGC-27 cells were treated with 18β-GRA for 24, 48 and 72 h; D: Effect of low, medium and high doses of 18β-GRA on cell viability of AGS cells; E: Effect of low, medium and high doses of 18β-GRA on cell viability of HGC-27 cells; F: Effect of 18β-GRA on cell viability of GES-1 cells. All data are from three independent samples. The data is represented as the mean ± SD. $^{a}P < 0.05$, $^{b}P < 0.01$, $^{c}P < 0.001$. 18β-GRA: 18β-glycyrrhetinic acid.

qRT-PCR

The cells were cultured and treated 18β-GRA at concentrations of 30, 60 and 120 μmol/L or 45, 90 and 135 μmol/L for 48 h, respectively. Total RNA was extracted using Trizol, and cDNA was synthesized using PrimeScript™ RT reagent kit. The expression level was detected with TB Green Premix Ex Taq II. The primer sequences are as follows: miR-345-5p, forward, 5′-GCTGACTCCTAGTCCAGGGCTC-3′ and reverse, 5′-GGCCAACCGCGAGAAGATG-3′; U6, forward, 5′-CTGCGCAAGGATGACACGCAAATT-3′ and reverse, 5′-GGCCAACCGCGAGAAGATG-3′. U6 as a housekeeping gene. The relative expression was calculated by the $2^{-\Delta\Delta Ct}$ method.

Western blot

The cells were cultured and treated 18β-GRA at concentrations of 60 μmol/L or 90 μmol/L for 48 h, respectively. The cells were collected and the total protein was extracted, the protein content was detected with BCA method. The protein was isolated and transferred onto a PVDF membrane, which is then sealed with 5% skim milk powder, soaked in primary antibodies and incubated overnight. The next day, the PVDF membrane was cleaned with TBST and soaked in secondary antibodies for 2 h. The protein was detected using an ECL solution, and ultimately the grey values were measured using ImageJ.

Statistical analysis

The statistical methods of this study were reviewed by Li-Qun Wang, Department of Epidemiology and Medical Statistics, Institute of Public Health and Management, Ningxia Medical University. All data were statistically analyzed using GraphPad Prism 7. All data were shown as mean ± SD, and the differences between different groups were analyzed using a one-way ANOVA or *t*-test. The significance level was set at $P < 0.05$.

RESULTS

18β-GRA reduced the GC cells viability

The results demonstrated that when the 18β-GRA concentration was 12.5 μmol/L-200 μmol/L, the inhibitory effect of 18β-GRA on AGS and HGC-27 cells viability was enhanced as the 18β-GRA dose was increased (Figures 2A and B). Next, 18β-GRA treated AGS and HGC-27 cells for 24 h, 48 h and 72 h, IC_{50} value was shown in Figure 2C. Therefore, we determined that the low, medium and high concentrations of 18β-GRA treated AGS cells for 48 h were 30, 60 and 120 μmol /L, and the low, medium and high concentrations of 18β-GRA treated HGC-27 cells for 48 h were 45, 90 and 135 μmol/L. AGS and HGC-27 cells viability was inhibited at low, medium and high doses of 18β-GRA when compared with the

control group (0 μmol/L) ($P < 0.01$) (Figures 2D and E).

18β-GRA had slight effect on normal gastric epithelial GES-1 cells

Subsequently, we investigated 18β-GRA's effect on GES-1 cells viability. The results demonstrated that GES-1 cells viability was slightly affected when 18β-GRA concentration was 12.5 μmol/L-100 μmol/L (Figure 2F). When the 18β-GRA concentration was less than 150 μmol/L, the GES-1 cells viability remained above 71% at 48 h.

18β-GRA arrested GC cells cycle

18β-GRA's effect on GC cells cycle results demonstrated that the percentage of G0/G1 phase (49.15%, 56.23% and 73.07%) in AGS cells treated with low, medium and high doses of 18β-GRA was higher than the control group (33.71%) (Figures 3A and B). The percentage of G0/G1 phase (46.58%, 51.69% and 77.11%) in HGC-27 cells treated with low, medium and high doses of 18β-GRA was higher than the control group (41.67%) (Figures 3C and D).

18β-GRA promoted GC cells apoptosis

18β-GRA's effect on GC cells apoptosis results demonstrated that the apoptosis rates of AGS cells treated with low, medium and high doses of 18β-GRA were 7.50%, 19.80% and 72. 00%, which were obviously higher than the control group (4. 80%) ($P < 0.01$) (Figures 3E and F). The apoptosis rates of HGC-27 cells treated with low, medium and high doses of 18β-GRA were 6.50%, 8.10% and 15.40%, which were obviously higher than the control group (6.40%) ($P < 0.05$) (Figures 3G-H).

18β-GRA inhibited the GC cells wound healing

The wound healing assay revealed that both high and medium doses of 18β-GRA can inhibit AGS and HGC-27 cells' wound healing abilities ($P < 0.001$) (Figures 4A-D). The inhibitory effect of 18β-GRA on wound healing ability was gradually enhanced as the 18β-GRA dose was increased in AGS and HGC-27 cells.

18β-GRA inhibited subcutaneous tumor growth in BALB/c nude mice

Through the subcutaneous tumor formation experiment in BALB/c nude mice, we observed that the back tumors in the control group were larger than those in the DDP and 18β-GRA groups ($P < 0.01$) (Figures 5A and B). The tumor volume was measured every 3 d and the tumor growth curve was plotted. In comparison to the control group, tumor size and growth rate were slower in the 18β-GRA and DDP groups ($P < 0.001$) (Figure 5C). Additionally, the body weight of DDP group was lower than the control and 18β-GRA groups. Diet and water intake were lower in the 18β-GRA and DDP groups when compared with the control group ($P < 0.05$) (Figures 5D-F).

Identification of autophagy-related proteins by TMT proteomic analysis and MDC staining assay

Part of the data of TMT proteomics analysis comes from the previous research of our team (Figures 6A-F)[15]. Cluster analysis was performed for differential proteins and heat map was drawn (Figure 6G), and the expression of TGM2 was down-regulated ($P = 0.01593178$). We used the STRING database to construct the PPI network, and the interaction diagram between the differentially expressed autophagy-related protein TGM2 and the autophagy marker proteins ULK1, p62 (SQSTM1), LC3I/II (MAPILC3) and AMPK (PRKAB1) was shown in Figure 6H, which indicated TGM2 was closely related to autophagy marker proteins. The results of MDC staining showed that AGS and HGC-27 cells displayed various degrees of autophagy after 18β-GRA intervention, and the number of autophagy cells increased as the dose of 18β-GRA was increased ($P < 0.05$) (Figures 6I-L).

Effect of 18β-GRA on the expression of autophagy-related proteins

Western blot analysis was used to determine 18β-GRA's influence on autophagy-related proteins in the AGS and HGC-27 cells. The findings demonstrated that, in contrast to the control group, the 18β-GRA group's protein expressions of TGM2 and p62 were lowered, whereas LC3II, ULK1 and AMPK were elevated ($P < 0.01$) (Figures 7A-E).

MiR-345-5p is a drug target of 18β-GRA

283 miRNAs were identified as differentially expressed by miRNAs transcriptome analysis, of which 163 miRNAs were down-regulated and 120 miRNAs were up-regulated, and the selection criteria for $|\text{Log}_2(\text{fold change})| > 1$, $P < 0.05$. Among them, the expression of miR-345-5p was up-regulated ($P =$ 5.68E-08) (Figure 8A). The miRBase website was used to predict the corresponding miRNAs of autophagy-related proteins, and then we intersected the miRNAs corresponding to autophagy-related proteins with the differentially expressed miRNAs screened by miRNA transcriptome. Among the obtained miRNAs, miR-345-5p was expressed most significantly.

We used qRT-PCR to determine the expression changes of miR-345-5p in AGS and HGC-27 cells treated with 18β-GRA. The outcomes demonstrated that miR-345-5p was highly up-regulated in AGS

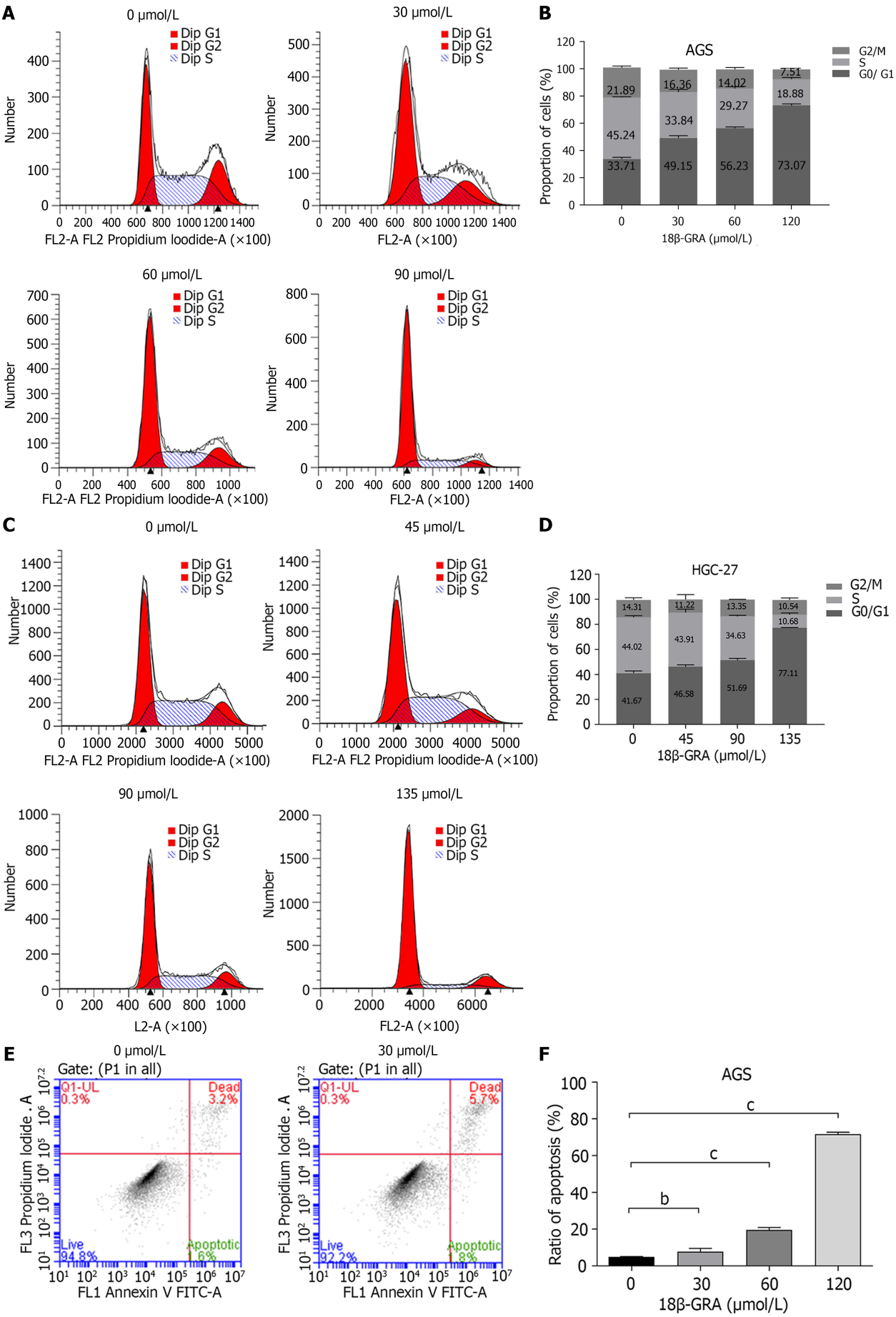
A
0 μmol/L
30 μmol/L
60 μmol/L
90 μmol/L
Dip G1
Dip G2
Dip S
Number
FL2-A FL2 Propidium loodide-A (×100)
FL2-A (×100)
B
AGS
G2/M
S
G0/ G1
Proportion of cells (%)
18β-GRA (μmol/L)
21.89
45.24
33.71
16.36
33.84
49.15
14.02
29.27
56.23
7.51
18.88
73.07
C
0 μmol/L
45 μmol/L
90 μmol/L
135 μmol/L
L2-A (×100)
D
HGC-27
G2/M
S
G0/G1
14.31
44.02
41.67
11.22
43.91
46.58
13.35
34.63
51.69
10.54
10.68
77.11
E
0 μmol/L
30 μmol/L
Gate: (P1 in all)
Q1-UL
0.3%
Dead
3.2%
5.7%
Live
94.8%
92.2%
Apoptotic
4.6%
8%
FL3 Propidium Iodide . A
FL1 Annexin V FITC-A
F
AGS
Ratio of apoptosis (%)
18β-GRA (μmol/L)
b
c
c

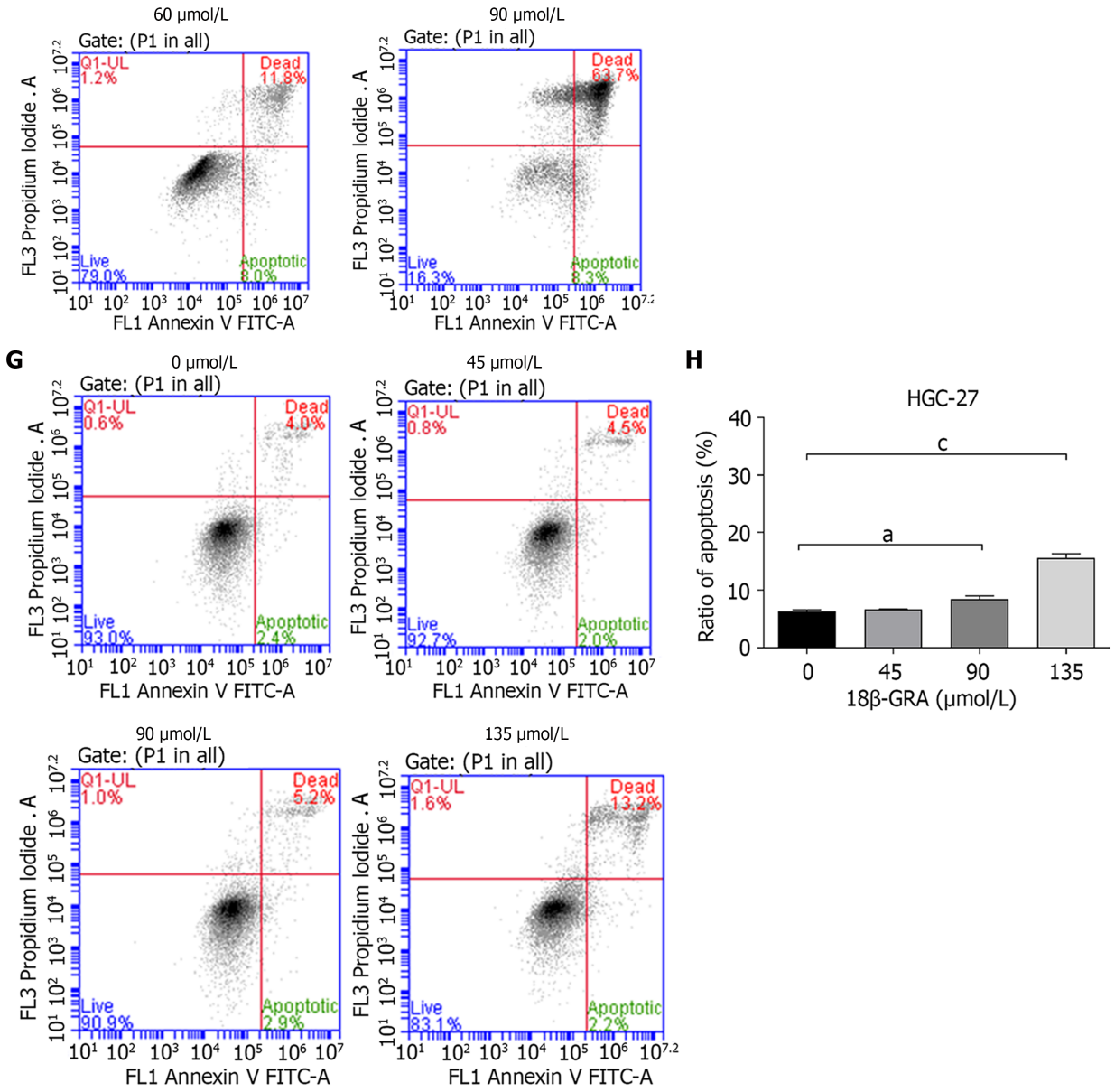

DOI: 10.3748/wjg.v29.i23.3622

Figure 3 Effect of 18β-glycyrrhetinic acid on cell cycle and cell apoptosis of AGS and HGC-27 cells. A: Effect of 18β-glycyrrhetinic acid (18β-GRA) on AGS cells cycle; B: Statistical results of AGS cell cycle; C: Effect of 18β-GRA on HGC-27 cells cycle; D: Statistical results of HGC-27 cells cycle; E: Effect of 18β-GRA on AGS cells apoptosis; F: Statistical results of AGS cells apoptosis; G: Effect of 18β-GRA on HGC-27 cells apoptosis; H: Statistical results of HGC-27 cells apoptosis. All data are from three independent samples. The data is represented as the mean ± SD. $^{a}P < 0.05$, $^{b}P < 0.01$, $^{c}P < 0.001$. 18β-GRA: 18β-glycyrrhetinic acid.

and HGC-27 cells after 18β-GRA treatment ($P < 0.01$) (Figures B and 8C). This verified the results of miRNAs transcriptome.

MiR-345-5p could target TGM2 directly

We utilized TargetScan database to identify complementary binding sites between miR-345-5p and TGM2 (Figure 8D). According to dual-luciferase reporter analyses, overexpression of miR-345-5p reduced luciferase expression in the TGM2-wild-type reporter but not in the mutant reporter ($P < 0.05$) (Figure 8E). These results suggest that miR-345-5p can regulate the expression of TGM2.

Overexpression of miR-345-5p can inhibit TGM2

Lentivirus transfection technique caused miR-345-5p overexpression on AGS and HGC-27 cells, and the transfection rate reached about 90% after 72 h (Figure 9A). Then, qRT-PCR discovered that miR-345-5p expression in the LV-miR-345-5p group was higher compared to the LV-NC group on AGS and HGC-27 cells ($P < 0.001$) (Figure 9B). Meanwhile, overexpression of miR-345-5p inhibited the protein expression of TGM2 ($P < 0.01$) (Figures 9C and D).

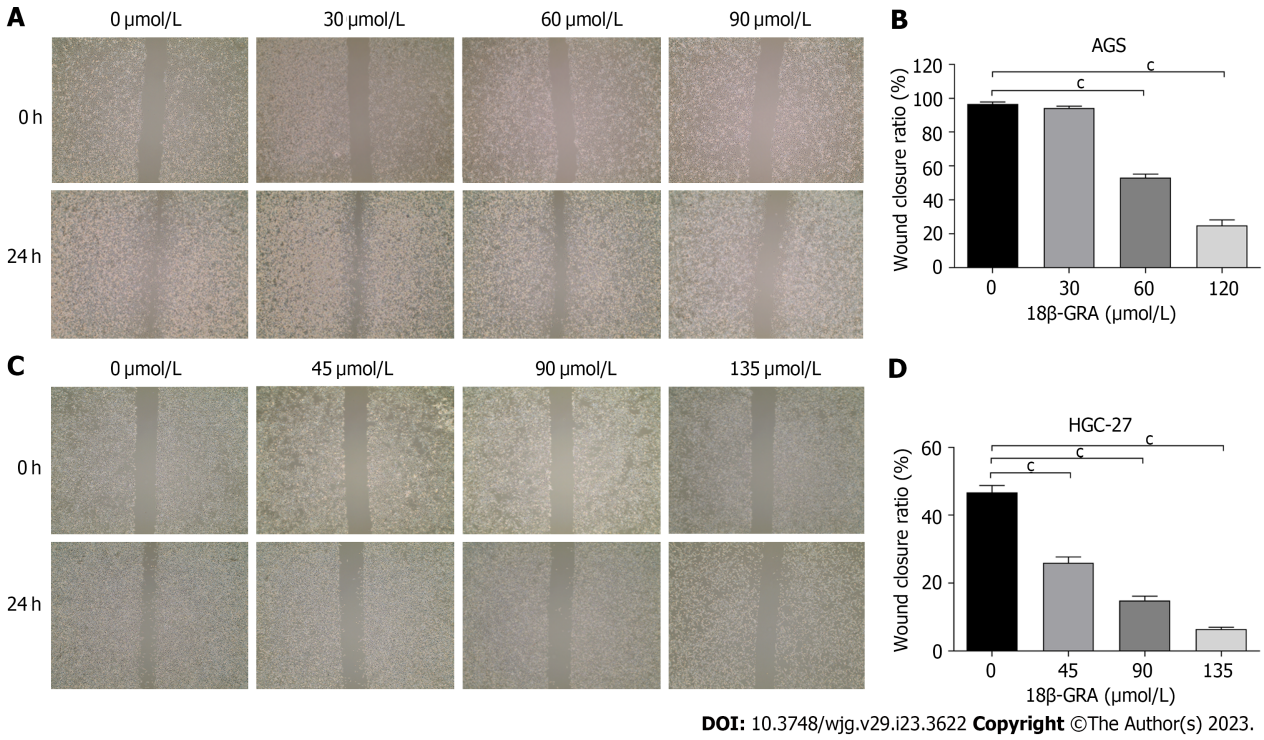

DOI: 10.3748/wjg.v29.i23.3622

Figure 4 Effect of 18β-glycyrrhetinic acid on cell wound healing of AGS and HGC-27 cells. A: Effect of 18β-glycyrrhetinic acid (18β-GRA) on the wound healing of AGS cells; B: Statistical results of the wound healing in AGS cells; C: Effect of 18β-GRA on wound healing of HGC-27 cells; D: Statistical results of the wound healing in HGC-27 cells. All data are from three independent samples. The data is represented as the mean ± SD. °P < 0.001. 18β-GRA: 18β-glycyrrhetinic acid.

Overexpression of miR-345-5p inhibit GC cells proliferation by promoting cell apoptosis and arresting cell cycle

Some researchers found that the expression of miR-345-5p in GC tissues was significantly lower than that in para-carcinoma tissue. which was correlated with aggressive stage and grade[27]. We evaluated the impact of miR-345-5p overexpression on cell viability in GC cells through CCK-8 assay. Our findings indicated that miR-345-5p overexpression resulted in a significant inhibition of the cell viability on AGS and HGC-27 cells (P < 0.01) (Figures 10A and B).

In order to further investigate the impart of miR-345-5p overexpression on GC cells, we conducted flow cytometry analysis to examine its effect on cell apoptosis and cell cycle. Our results showed the cell apoptosis rates in the miR-345-5p overexpression group were significantly higher than that in the LV-NC group on AGS and HGC-27 cells (P < 0.001) (Figures 10C and D). Moreover, the cell cycle experiment revealed that miR-345-5p overexpression caused cell cycle arrest in the G0/G1 phase on AGS and HGC-27 cells (P < 0.001) (Figures 10E and F). These results suggested that miR-345-5p overexpression could inhibit GC cells proliferation by promoting cell apoptosis and arresting cell cycle.

DISCUSSION

In this study, 18β-GRA treated GC cells phenotypic alterations were identified *in vitro*. The findings demonstrated that 18β-GRA had a minimal effect on the survival rate of normal gastric epithelial GES-1 cells, but dramatically reduced the AGS and HGC-27 cells viability. Next, we found that 18β-GRA could block the AGS and HGC-27 cells in G0/G1 phase and promote cell apoptosis. Both DNA replication and mitosis crucially depend on the G0/G1 phase. According to studies, after drug intervention, cells can either irreversibly end the cell cycle through senescence or apoptosis[28], or they can reversibly exit the cell cycle by beginning immobilization. We looked at how 18β-GRA affected the GC cells apoptosis and verified the results of cell cycle, which led us to conclude that 18β-GRA made GC cells exit the cell cycle selectively. It has been demonstrated that cells can exit the cell cycle reversibly by initiating immobilization, or irreversibly by senescence or apoptosis. Our findings confirmed the conclusion that 18β-GRA can induce GC cells to exit the cell cycle selectively.

18β-GRA decreased the migration ability of AGS and HGC-27 cells, according to a wound healing assay. At the same time, we also performed cell invasion experiments, but the results were not statistically significant. Studies have shown that TGM2 could promote GC cells' proliferation, migration and invasion by activating extracellular signal-regulated kinase 1/2[29]. In addition, TGM2 was thought to

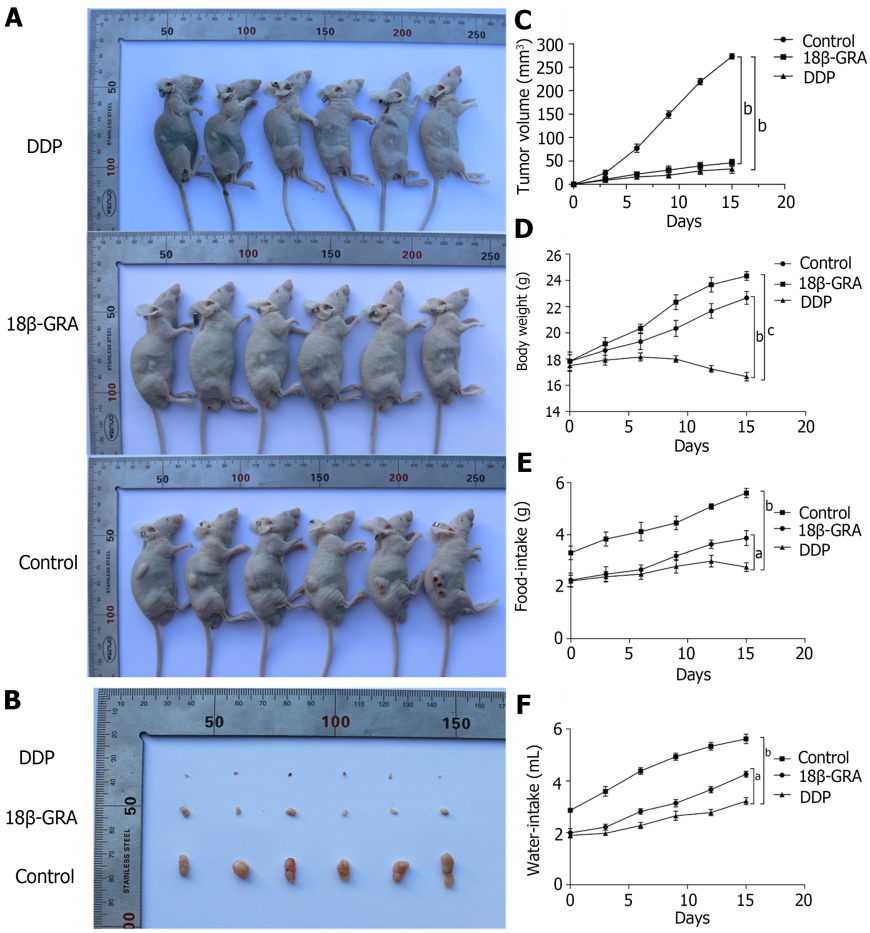

DOI: 10.3748/wjg.v29.i23.3622 **Copyright** ©The Author(s) 2023.

Figure 5 Effect of 18β-glycyrrhetinic acid on subcutaneous tumor growth in BALB/c nude mice. A: Comparison of back tumor in the cisplatin (DDP), 18β-glycyrrhetinic acid (18β-GRA) and control groups; B: Comparison of back tumor volume in the DDP, 18β-GRA and control groups; C: Effect of tumor volume growth in the DDP, 18β-GRA and control groups; D: Effect of body weight in the DDP, 18β-GRA and control groups; E: Effect of water-intake in the DDP, 18β-GRA and control groups; F: Effect of food-intake in the DDP, 18β-GRA and control groups. The data is represented as the mean ± SD. $^{a}P < 0.05$, $^{b}P < 0.01$, $^{c}P < 0.001$. 18β-GRA: 18β-glycyrrhetinic acid; DDP: Cisplatin.

be involved in EMT processes in breast cancer[30], colorectal cancer[31], and hepatocellular carcinoma [32], which are highly correlated with invasion phenotypes. These findings imply that TGM2 is involved in cancer cell invasion. In contrast, 18β-GRA had no impact on AGS and HGC-27 cells invasion during our studies.

In vivo tumorigenesis experiment was performed on immunodeficient nude mice. The results showed that 18β-GRA and DDP significantly inhibited the subcutaneous tumor volume in nude mice. At the same time, we monitored the body weight, diet and water intake of nude mice during the experiment. It was found that the body weight of nude mice in the DDP group was lighter than that in 18β-GRA and control groups, showing obvious adverse reactions. On the contrary, the body weight of nude mice in 18 β-GRA group was slightly higher than that in the control group and the nude mice were in good health during the experiment. In terms of diet and water intake, nude mice administered with 18β-GRA and DDP had reduced diet and water intake. Overall, the experimental results demonstrated 18β-GRA had fewer side effects.

We further investigated the mechanism of GC treatment with 18β-GRA. MDC staining results showed that 18β-GRA can promote autophagy of AGS and HGC-27 cells. TMT proteomic analysis and miRNAs transcriptome analysis revealed that TGM2 was the target of miR-345-5p, which was verified by a dual-luciferase reporter assay. The STRING database was used to build the PPI network, and it was found that TGM2 was closely related to autophagy marker proteins ULK1, p62, LC3I/II and AMPK. TGM2 induces autophagy, differentiation and inhibition of angiogenesis, and its role in cancer is very complex. In fact, it has been proven that TGM2 participates in all aspects of cancer progression by activating mTOR[33]. At the beginning phase of autophagy, AMPK promotes autophagy occurrence by directly activating ULK1 or by negatively regulating mTOR to block its inhibition of ULK1[34,35]. After the formation of pre-autophage, it enters the second stage, which is the stage of autophagy extending into nucleus. ULK1 activates p62 and promotes the binding of p62 mediated substrate proteins to autophagic bodies[36]. At the same time, the substrate protein passes through the LC3 domain of p62

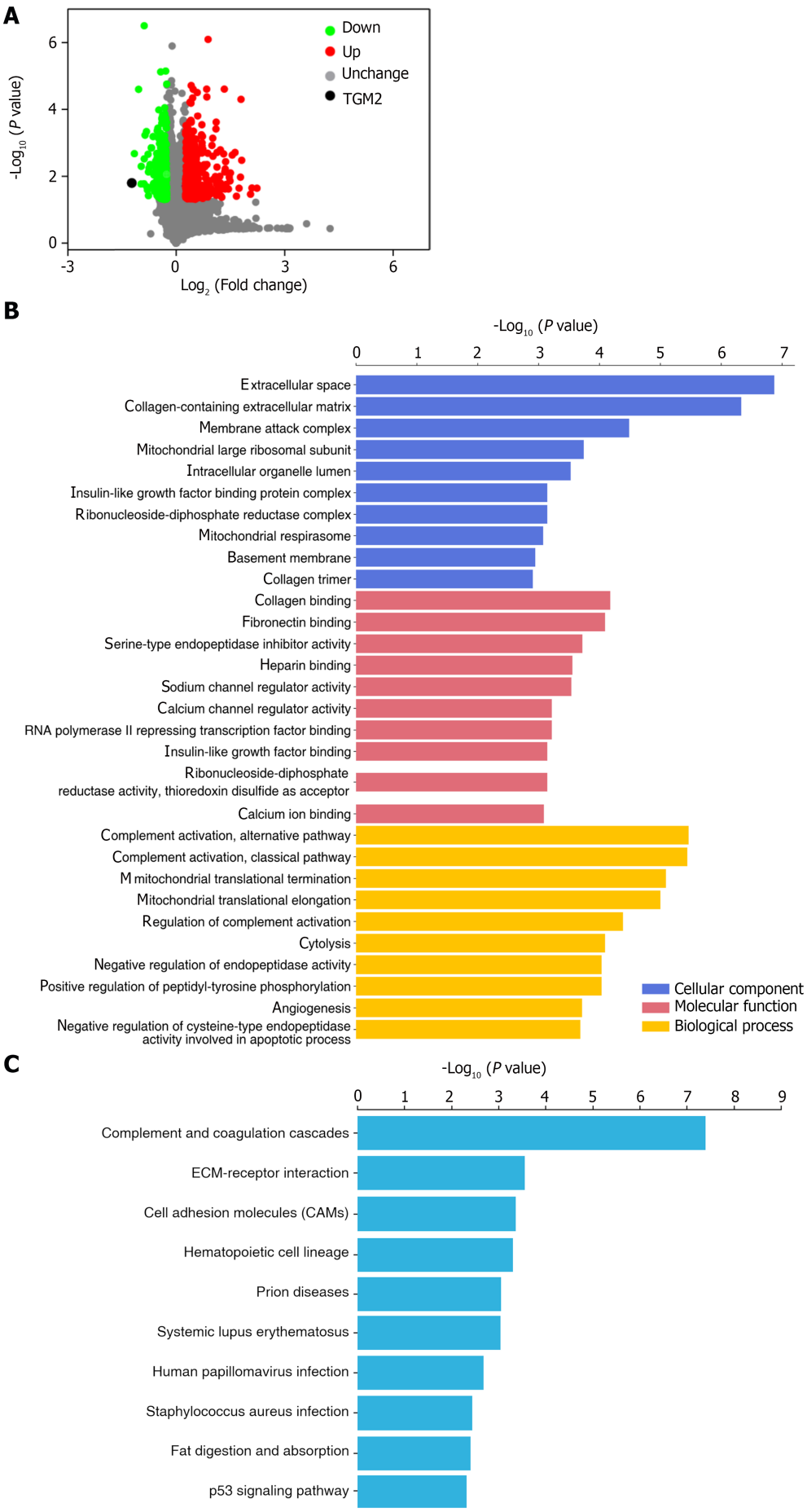
A
Down
Up
Unchange
TGM2
-Log10 (P value)
Log2 (Fold change)
B
-Log10 (P value)
Extracellular space
Collagen-containing extracellular matrix
Membrane attack complex
Mitochondrial large ribosomal subunit
Intracellular organelle lumen
Insulin-like growth factor binding protein complex
Ribonucleoside-diphosphate reductase complex
Mitochondrial respirasome
Basement membrane
Collagen trimer
Collagen binding
Fibronectin binding
Serine-type endopeptidase inhibitor activity
Heparin binding
Sodium channel regulator activity
Calcium channel regulator activity
RNA polymerase II repressing transcription factor binding
Insulin-like growth factor binding
Ribonucleoside-diphosphate reductase activity, thioredoxin disulfide as acceptor
Calcium ion binding
Complement activation, alternative pathway
Complement activation, classical pathway
M mitochondrial translational termination
Mitochondrial translational elongation
Regulation of complement activation
Cytolysis
Negative regulation of endopeptidase activity
Positive regulation of peptidyl-tyrosine phosphorylation
Angiogenesis
Negative regulation of cysteine-type endopeptidase activity involved in apoptotic process
Cellular component
Molecular function
Biological process
C
-Log10 (P value)
Complement and coagulation cascades
ECM-receptor interaction
Cell adhesion molecules (CAMs)
Hematopoietic cell lineage
Prion diseases
Systemic lupus erythematosus
Human papillomavirus infection
Staphylococcus aureus infection
Fat digestion and absorption
p53 signaling pathway

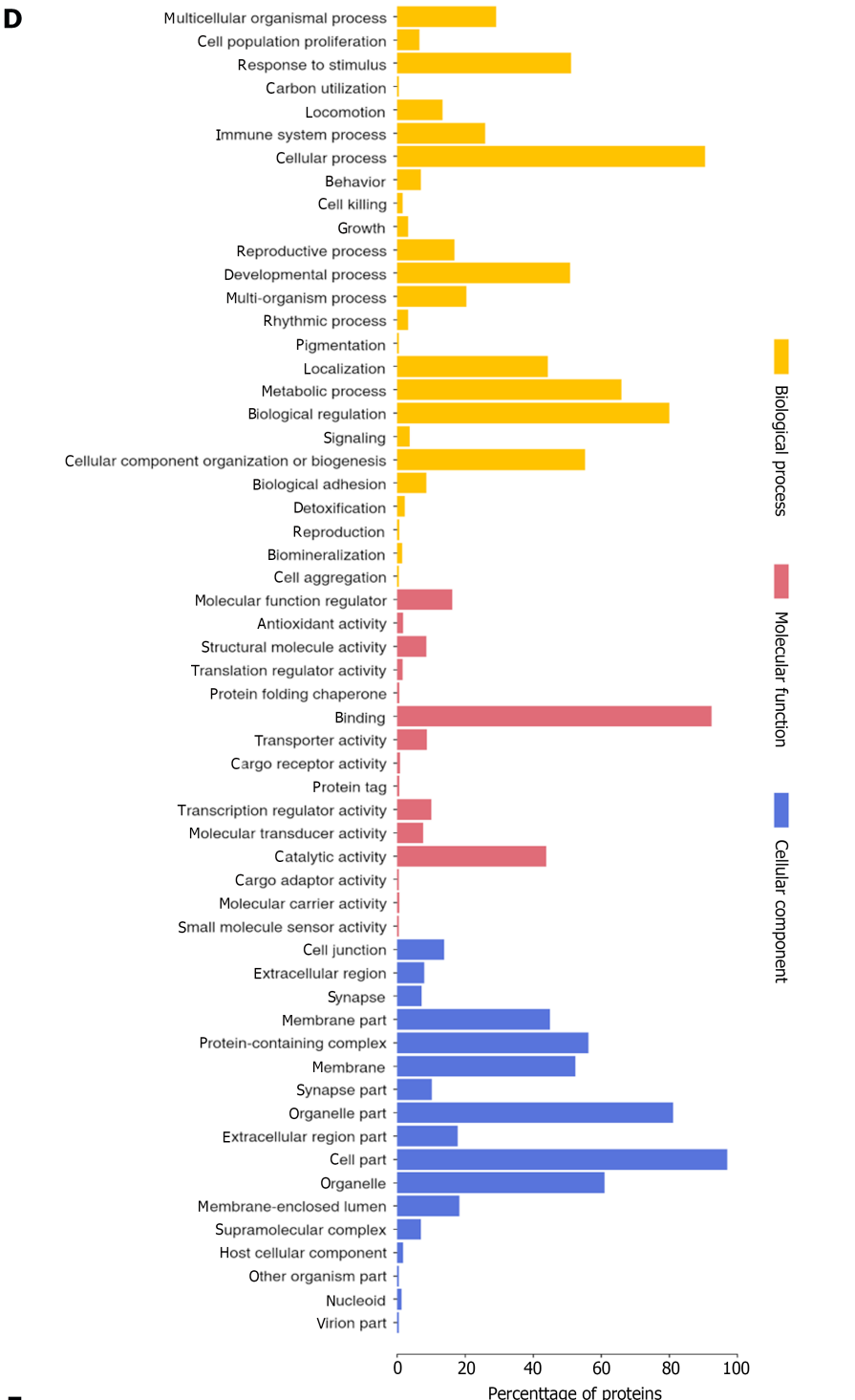
D
Multicellular organismal process
Cell population proliferation
Response to stimulus
Carbon utilization
Locomotion
Immune system process
Cellular process
Behavior
Cell killing
Growth
Reproductive process
Developmental process
Multi-organism process
Rhythmic process
Pigmentation
Localization
Metabolic process
Biological regulation
Signaling
Cellular component organization or biogenesis
Biological adhesion
Detoxification
Reproduction
Biomineralization
Cell aggregation
Molecular function regulator
Antioxidant activity
Structural molecule activity
Translation regulator activity
Protein folding chaperone
Binding
Transporter activity
Cargo receptor activity
Protein tag
Transcription regulator activity
Molecular transducer activity
Catalytic activity
Cargo adaptor activity
Molecular carrier activity
Small molecule sensor activity
Cell junction
Extracellular region
Synapse
Membrane part
Protein-containing complex
Membrane
Synapse part
Organelle part
Extracellular region part
Cell part
Organelle
Membrane-enclosed lumen
Supramolecular complex
Host cellular component
Other organism part
Nucleoid
Virion part
Biological process
Molecular function
Cellular component
0
20
40
60
80
100
Percenttage of proteins

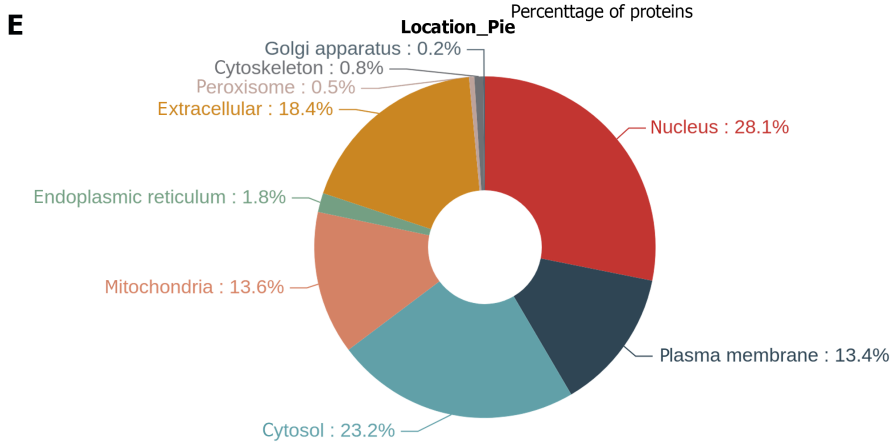
E
Location_Pie
Golgi apparatus : 0.2%
Cytoskeleton : 0.8%
Peroxisome : 0.5%
Extracellular : 18.4%
Nucleus : 28.1%
Endoplasmic reticulum : 1.8%
Mitochondria : 13.6%
Plasma membrane : 13.4%
Cytosol : 23.2%

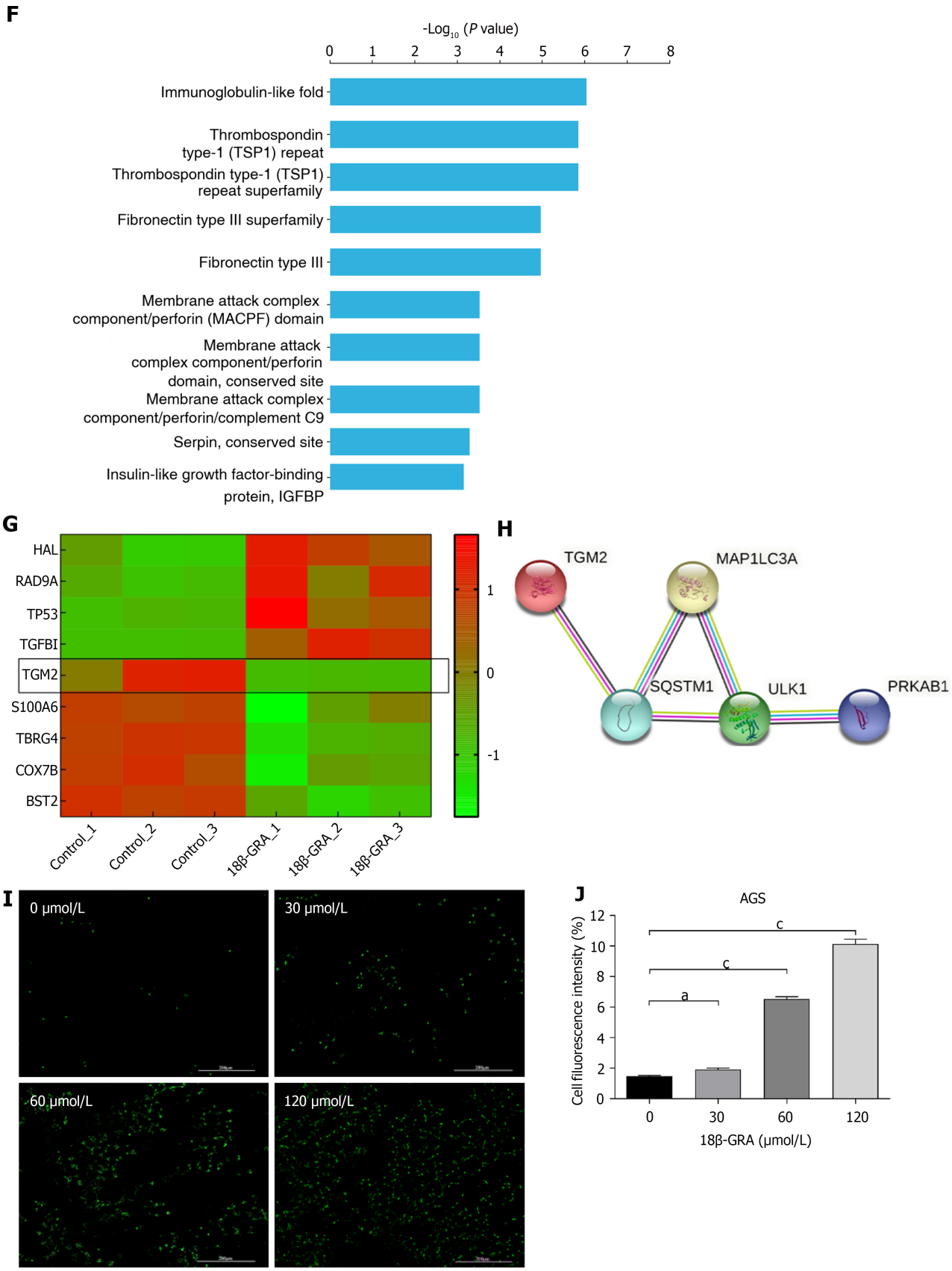
F
-Log10 (P value)
0 1 2 3 4 5 6 7 8
Immunoglobulin-like fold
Thrombospondin type-1 (TSP1) repeat
Thrombospondin type-1 (TSP1) repeat superfamily
Fibronectin type III superfamily
Fibronectin type III
Membrane attack complex component/perforin (MACPF) domain
Membrane attack complex component/perforin domain, conserved site
Membrane attack complex component/perforin/complement C9
Serpin, conserved site
Insulin-like growth factor-binding protein, IGFBP
G
HAL
RAD9A
TP53
TGFBI
TGM2
S100A6
TBRG4
COX7B
BST2
1
0
-1
Control_1
Control_2
Control_3
18β-GRA_1
18β-GRA_2
18β-GRA_3
H
TGM2
MAP1LC3A
SQSTM1
ULK1
PRKAB1
I
0 μmol/L
30 μmol/L
60 μmol/L
120 μmol/L
J
AGS
Cell filuorescence intensity (%)
0 2 4 6 8 10 12
a
c
c
0 30 60 120
18β-GRA (μmol/L)

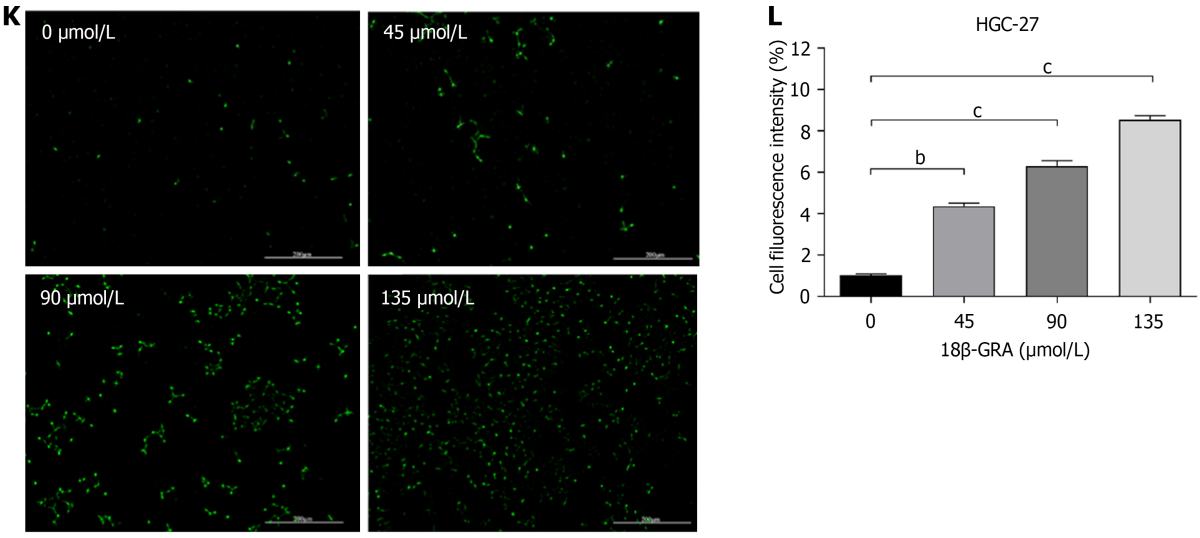

DOI: 10.3748/wjg.v29.i23.3622

Figure 6 The results of TMT proteomic analysis and MDC staining assay. A: TMT proteomic analysis of differentially expressed proteins (DEPs) volcano map; B: Gene Ontology (GO) enrichment analysis of DEPs. The Y axis denotes the GO functional classification enriched of DEPs, and the X axis denotes the -Log10 of the *P* value of Fisher's exact test of the significance of the enrichment; C: Kyoto Encyclopedia of Genes and Genomes (KEGG) pathway enrichment analysis. The Y axis denotes the categories of KEGG pathways. The X axis is the -Log_{10} of the p value of Fisher's exact test of the significance of enrichment; D: GO annotation analysis of DEPs; E: Subcellular localization analysis; F: Protein domain enrichment analysis; G: Proteins cluster analysis; H: Protein-protein interaction network diagram of TGM2 and autophagy marker proteins; I: The MDC staining results of AGS cells treated with different concentrations of 18β-glycyrrhetinic acid (18β-GRA); J: Statistical results of the MDC staining in AGS cells; K: The MDC staining results of HGC-27 cells treated with different concentrations of 18β-GRA; L: Statistical results of the MDC staining in HGC-27 cells. All data are from three independent samples. The data is represented as the mean ± SD. $^{a}P < 0.05$, $^{b}P < 0.01$, $^{c}P < 0.001$. DEPs: Differentially expressed proteins; GO: Gene Ontology; KEGG: Kyoto Encyclopedia of Genes and Genomes; 18β-GRA: 18β-glycyrrhetinic acid.

into the degradation phase of the autophagic vesicle, where it interacts with LC3, which is the third stage of autophagy. Thus, when the p62 content decreases, it indicates that autophagic lysosomal degradation is inhibited[37,38]. Therefore, when the content of p62 decreases, it indicates that autophagic lysosome degradation is inhibited. LC3I/II, one of the homologues of ATG8, is located in the cytoplasm. LC3I is formed after exposure to glycine at the carboxyl terminal, which is catalyzed to combine with phosphatidyl ethanolamine to form LC3II. The increased amount of LC3II can reflect the increased number of autophagosomes caused by enhanced autophagy activity[39] (Figure 11). Western blot results proved that TGM2 and p62 were reduced, while AMPK, ULK1, and LC3II were increased in AGS and HGC-27 cells treated with 18β-GRA. Additionally, we employed a lentiviral vector to miR-345-5p overexpress in GC cells and observed the expression of TGM2. Our findings indicate that miR-345-5p overexpression significantly reduced the protein expression of TGM2. At the same time, we also found that miR-345-5p overexpression could inhibit GC cells proliferation by promoting cell apoptosis and arresting cell cycle. Based on the aforementioned findings, we draw the conclusion that 18β-GRA may play a role in the occurrence and progression of GC *via* the miR-345-5p/TGM2 signaling pathway.

CONCLUSION

To sum up, this study proved that 18β-GRA can inhibit GC cells viability, induce cells apoptosis, block cell cycle, inhibit cell wound healing ability, and induce cell autophagy by regulating the miR-345-5p/TGM2 signaling pathway, thereby inhibiting the GC cells proliferation, which could provide theoretical basis for the research of 18β-GRA in GC treatment. However, our study has some limitations and more experiments are needed to support our future research. Hence, we will carry on exploring the relationship between 18β-GRA and GC in the future. First, GC cells were infected with RFP-GFP-LC3 double-labeled adenoviruses to research 18β-GRA's effect on the autophagic. Secondly, 18β-GRA's effect when combined with chemotherapeutic drugs on chemotherapeutic drug sensitivity will be investigated. Thirdly, the molecular mechanism of 18β-GRA treatment for GC was further studied by gene overexpression, CO-IP and other methods.

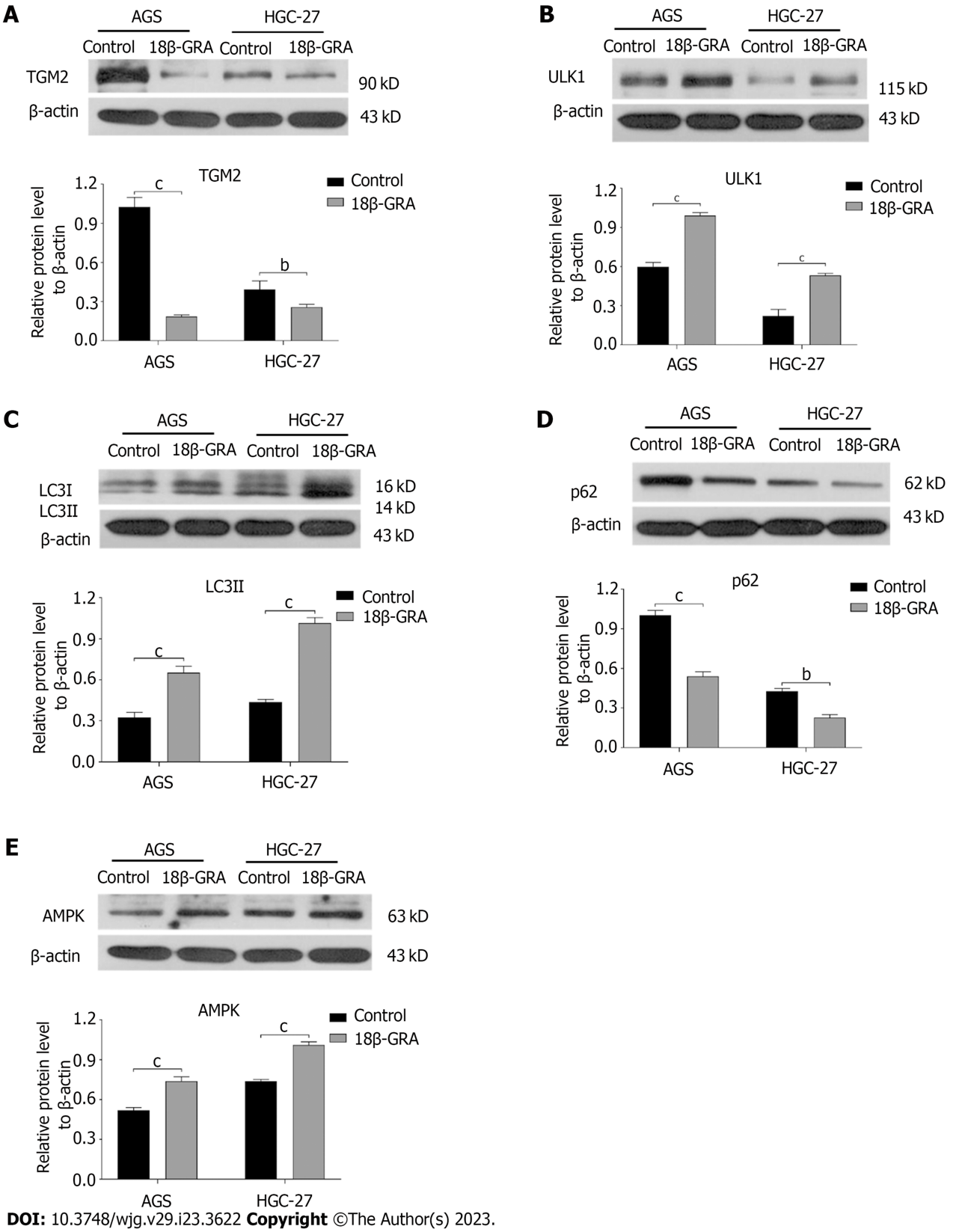

DOI: 10.3748/wjg.v29.i23.3622

Figure 7 Effect of 18β-glycyrrhetinic acid on the protein expression levels of TGM2, p62, LC3II, ULK1 and AMPK in AGS and HGC-27 cells. All data are from three independent samples. The data is represented as the mean ± SD. $^{b}P < 0.01$ $^{c}P < 0.001$. 18β-GRA: 18β-glycyrrhetinic acid.

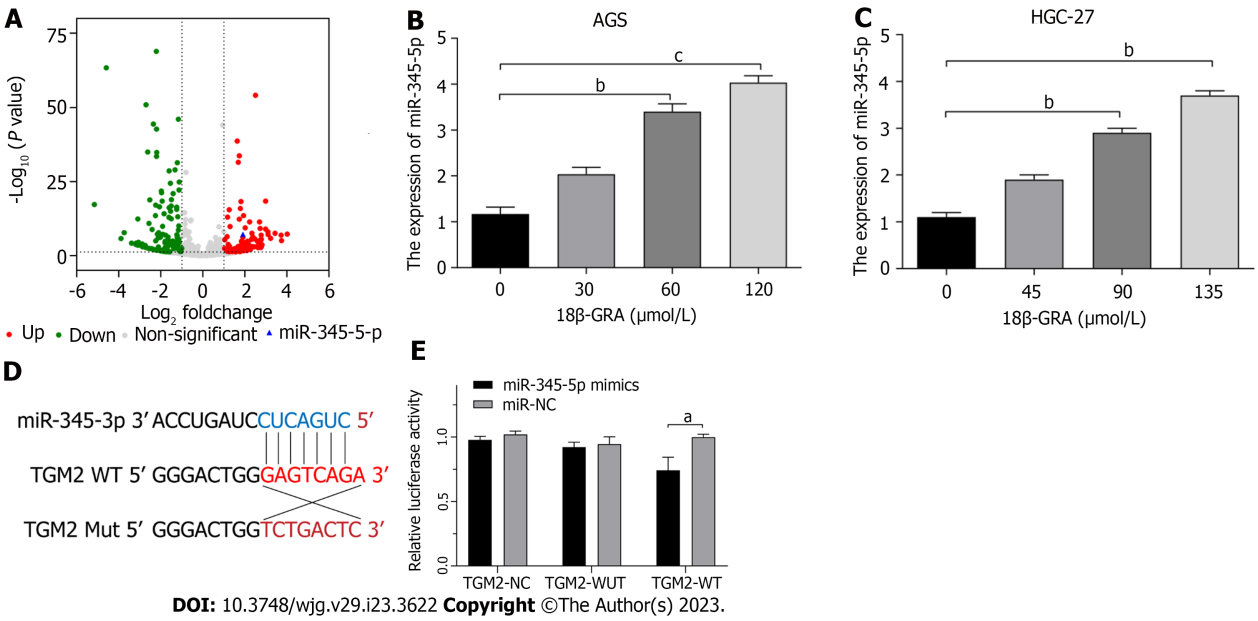

DOI: 10.3748/wjg.v29.i23.3622 **Copyright** ©The Author(s) 2023.

Figure 8 MicroRNAs transcriptomic analysis and dual-luciferase reporter assay. A: MicroRNAs (miRNAs) transcriptomics analysis of differentially expressed miRNAs; B: Effect of 18β-glycyrrhetinic acid (18β-GRA) with different concentrations of miR-345-5p expression level in AGS cells; C: Effect of 18β-GRA with different concentrations of miR-345-5p expression level in HGC-27 cells; D: Complementary binding sites of miR-345-5p and TGM2; E: Elevated expression of miR-345-5p suppressed the luciferase value of the TGM2-wild-type reporter but not that under the mutant reporter. All data are from three independent samples. The data is represented as the mean ± SD. $^{a}P < 0.05$, $^{b}P < 0.01$, $^{c}P < 0.001$. 18β-GRA: 18β-glycyrrhetinic acid; WUT: Mutant; WT: Wild type; NC: Empty lentiviral vector.

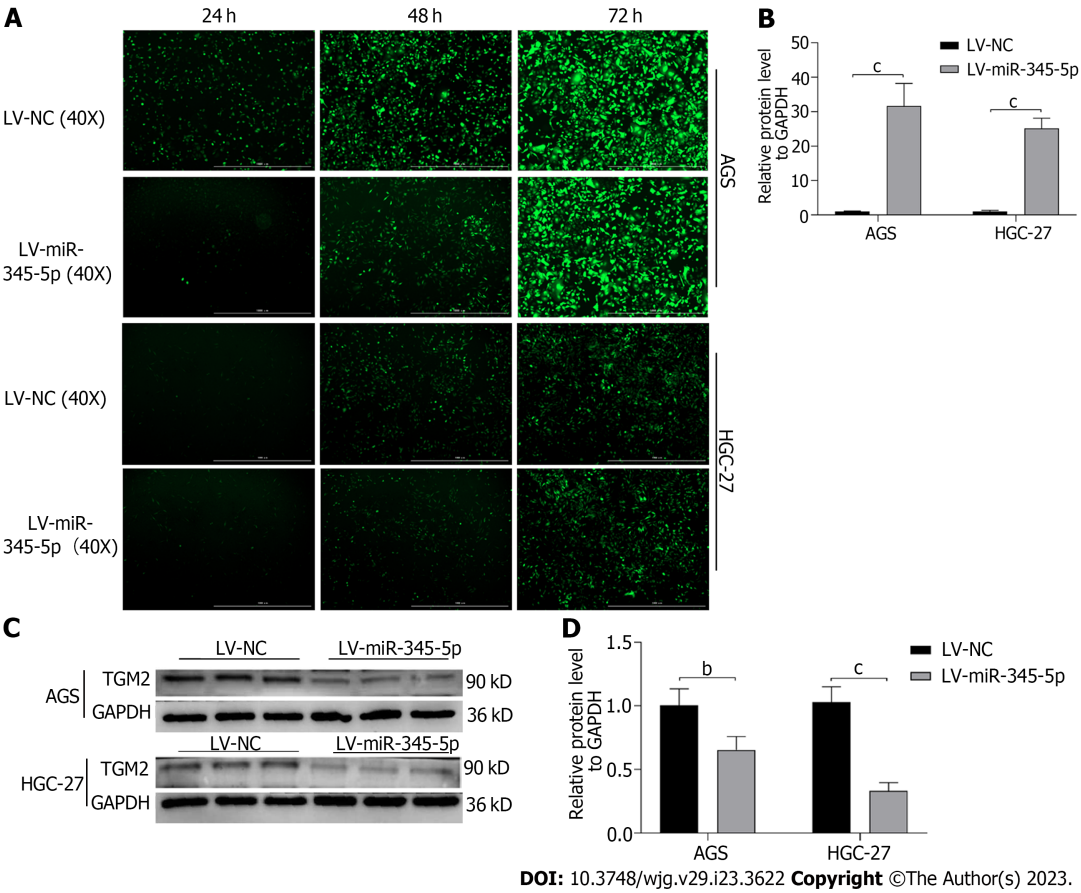

DOI: 10.3748/wjg.v29.i23.3622 **Copyright** ©The Author(s) 2023.

Figure 9 Overexpression of miR-345-5p can inhibit TGM2. A: Transfection efficiency of lentiviral vector; B: The expression level of miR-345-5p in lentivirus transfected AGS and HGC-27 cells; C: Effect of miR-345-5p overexpression on TGM2; D: Statistical results of the effect of miR-345-5p overexpression on TGM2. All data are from three independent samples. The data is represented as the mean ± SD. $^{b}P < 0.01$, $^{c}P < 0.001$. LV-NC: Empty lentiviral vector.

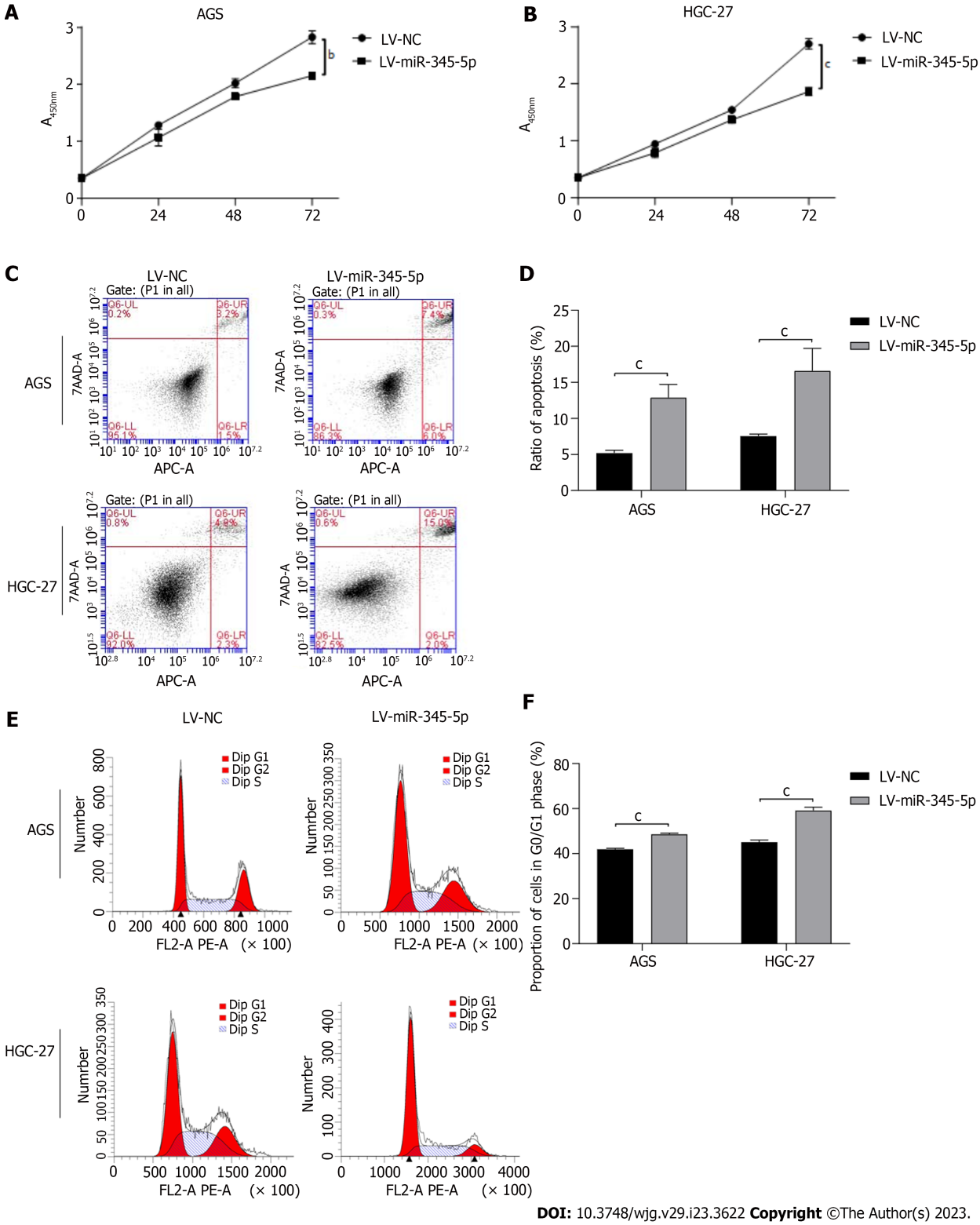

DOI: 10.3748/wjg.v29.i23.3622

Figure 10 Effect of miR-345-5p overexpression on AGS and HGC-27 cells. A: Effect of miR-345-5p overexpression on AGS cells viability; B: Effect of miR-345-5p overexpression on HGC-27 cells viability; C: Effect of miR-345-5p overexpression on cell apoptosis in AGS and HGC-27 cells; D: Statistical results of cell apoptosis; E: Effect of miR-345-5p overexpression on cell cycle in AGS and HGC-27 cells; F: Statistical results of cell cycle. All data are from three independent samples. The data is represented as the mean ± SD. $^{a}P < 0.05$, $^{b}P < 0.01$, $^{c}P < 0.001$. LV-NC: Empty lentiviral vector.

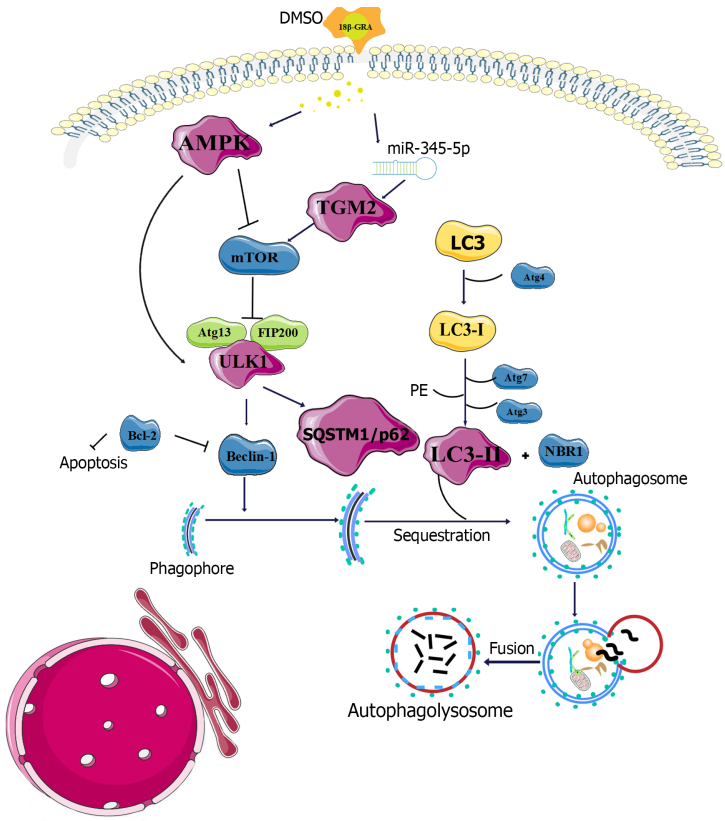

DOI: 10.3748/wjg.v29.i23.3622

Figure 11 Diagram of the mechanism of 18β-glycyrrhetinic acid therapy for gastric cancer cells. 18β-GRA: 18β-glycyrrhetinic acid; mTOR: Mammalian target of rapamycin; Bcl-2: B-cell lymphoma 2; NBR1: Neighbor of BRCA1 gene 1; PE: Phosphatidylethanolamine.

ARTICLE HIGHLIGHTS

Research background

Gastric cancer (GC) is a common gastrointestinal malignancy worldwide. Based on the cancer-related mortality, the current prevention and treatment strategies for GC still show poor clinical results. Therefore, it is important to find effective drug treatment targets.

Research motivation

At present, the treatment of GC is mainly surgery, chemotherapy and radiotherapy, and the first-line treatment drugs are harmful to side effects.

Research objectives

The purpose of this study was to explore the molecular mechanism of 18β-glycyrrhetinic acid (18β-GRA) regulating the miR-345-5p/TGM2 signaling pathway to inhibit the proliferation of GC cells.

Research methods

The effects of 18β-GRA on GC cell phenotype and tumor growth *in vivo* were studied. TMT proteomic analysis and microRNAs (miRNAs) transcriptome analysis were used to screen for targets, and targeted connections were validated using a dual-luciferase report assay. Finally, the prediction was confirmed by experiment *in vitro*.

Research results

Our experiment confirmed that 18β-GRA inhibited GC cells growth both *in vitro* and *in vivo*, and MDC staining showed that 18β-GRA promoted GC cell autophagy. By TMT proteomic analysis and miRNAs transcriptomic analysis, we found that 18β-GRA down-regulates TGM2 expression and up-regulates miR-345-5p expression in GC cells. Subsequently, TGM2 was verified as the target of miR-345-5p by a dual-luciferase report assay. In 18β-GRA treated GC cells, the expressions of autophagy-related proteins TGM2 and p62 were significantly decreased, while the expressions of LC3II, ULK1 and AMPK were significantly increased. In addition, overexpression of miR-345-5p not only inhibited TGM2 expression, but also inhibited GC cell proliferation by promoting apoptosis and blocking cell cycle.

Research conclusions

These observations indicate that 18β-GRA can promote autophagy and inhibit GC cells proliferation *via* regulating the miR-345-5p/TGM2 signaling pathway.

Research perspectives

MiR-345-5p can be used for targeted therapy of GC, and can also be used as a new biomarker for GC.

ACKNOWLEDGEMENTS

The authors would like to acknowledge Li-Qun Wang for statistical analysis assistance. Thanks to Joanna Tibenda for revising the article.

FOOTNOTES

Author contributions: Li X carried out most of the studies, and analyzed the data; Li X, Ma XL, and Du YH wrote the manuscript; Ma XL and Du YH carried out the chart-making work; Yang Y, Lu DD, and Zhang JF were responsible for network pharmacology analysis; Chen Y and Niu Y designed the study and revised the manuscript; Yuan L provided the conceptual and technical guidance as well as revised the manuscript critically for important intellectual content; and all authors have read and approved the manuscript.

Supported by the Ningxia Natural Science Foundation, No. 2022AAC03144.

Institutional review board statement: The study was reviewed and approved by the Institutional Review Board of Ningxia Medical University (No.2021-N0063).

Institutional animal care and use committee statement: The animal protocol was approved by the Institutional Animal Care and Use Committee of Ningxia Medical University (IACUC-NYLAC-2022-108).

Conflict-of-interest statement: All the authors report no relevant conflicts of interest for this article.

Data sharing statement: All data generated or analyzed during this study are included in this paper, and further inquiries can be directed to the corresponding author (20080017@nxmu.edu.cn).

ARRIVE guidelines statement: The authors have read the ARRIVE guidelines, and the manuscript was prepared and revised according to the ARRIVE guidelines.

Country/Territory of origin: China

ORCID number: Xia Li 0000-0002-4981-9768; Yi Nan 0000-0002-5511-9266; Yu-Hua Du 0000-0002-9669-8065; Yi Yang 0000-0002-8466-5717; Yan Chen 0000-0002-8673-398X; Ling Yuan 0000-0003-2838-0976.

S-Editor: Wang JJ
L-Editor: A
P-Editor: Cai YX

REFERENCES

1 **Sung H**, Ferlay J, Siegel RL, Laversanne M, Soerjomataram I, Jemal A, Bray F. Global Cancer Statistics 2020: GLOBOCAN Estimates of Incidence and Mortality Worldwide for 36 Cancers in 185 Countries. *CA Cancer J Clin* 2021; **71**: 209-249 [PMID: 33538338 DOI: 10.3322/caac.21660]

2 **Abbas M**, Habib M, Naveed M, Karthik K, Dhama K, Shi M, Dingding C. The relevance of gastric cancer biomarkers in prognosis and pre- and post- chemotherapy in clinical practice. *Biomed Pharmacother* 2017; **95**: 1082-1090 [PMID: 28922727 DOI: 10.1016/j.biopha.2017.09.032]

3 **Duan R**, Li X, Zeng D, Chen X, Shen B, Zhu D, Zhu L, Yu Y, Wang D. Tumor Microenvironment Status Predicts the Efficacy of Postoperative Chemotherapy or Radiochemotherapy in Resected Gastric Cancer. *Front Immunol* 2020; **11**: 609337 [PMID: 33569057 DOI: 10.3389/fimmu.2020.609337]

4 **Yang T**, Zhou J, Fang L, Wang M, Dilinuer M, Ainiwaer A. Protection function of 18β-glycyrrhetinic acid on rats with high-altitude pulmonary hypertension based on (1)H NMR metabonomics technology. *Anal Biochem* 2021; **631**: 114342 [PMID: 34419454 DOI: 10.1016/j.ab.2021.114342]

5 **Yang Y**, Zhu Q, Zhong Y, Cui X, Jiang Z, Wu P, Zheng X, Zhang K, Zhao S. Synthesis, anti-microbial and anti-inflammatory activities of 18β-glycyrrhetinic acid derivatives. *Bioorg Chem* 2020; **101**: 103985 [PMID: 32544739 DOI: 10.1016/j.bioorg.2020.103985]

6 **Wang LJ**, Geng CA, Ma YB, Huang XY, Luo J, Chen H, Zhang XM, Chen JJ. Synthesis, biological evaluation and structure-activity relationships of glycyrrhetinic acid derivatives as novel anti-hepatitis B virus agents. *Bioorg Med Chem Lett* 2012; **22**: 3473-3479 [PMID: 22520261 DOI: 10.1016/j.bmcl.2012.03.081]

7 **Stecanella LA**, Bitencourt APR, Vaz GR, Quarta E, Silva Júnior JOC, Rossi A. Glycyrrhizic Acid and Its Hydrolyzed Metabolite 18β-Glycyrrhetinic Acid as Specific Ligands for Targeting Nanosystems in the Treatment of Liver Cancer. *Pharmaceutics* 2021; **13** [PMID: 34834206 DOI: 10.3390/pharmaceutics13111792]

8 **Wang Z**, Ma J, He Y, Miu KK, Yao S, Tang C, Ye Y, Lin G. Nrf2-mediated liver protection by 18β-glycyrrhetinic acid against pyrrolizidine alkaloid-induced toxicity through PI3K/Akt/GSK3β pathway. *Phytomedicine* 2022; **102**: 154162 [PMID: 35598524 DOI: 10.1016/j.phymed.2022.154162]

9 **Liu J**, Xu Y, Yan M, Yu Y, Guo Y. 18β-Glycyrrhetinic acid suppresses allergic airway inflammation through NF-κB and Nrf2/HO-1 signaling pathways in asthma mice. *Sci Rep* 2022; **12**: 3121 [PMID: 35210449 DOI: 10.1038/s41598-022-06455-6]

10 **Yadav DK**, Kalani K, Singh AK, Khan F, Srivastava SK, Pant AB. Design, synthesis and *in vitro* evaluation of 18β-glycyrrhetinic acid derivatives for anticancer activity against human breast cancer cell line MCF-7. *Curr Med Chem* 2014; **21**: 1160-1170 [PMID: 24180274 DOI: 10.2174/09298673113206660330]

11 **Li X**, Liu Y, Wang N, Wang S, Wang H, Li A, Ren S. Synthesis and discovery of 18β-glycyrrhetinic acid derivatives inhibiting cancer stem cell properties in ovarian cancer cells. *RSC Adv* 2019; **9**: 27294-27304 [PMID: 35529208 DOI: 10.1039/c9ra04961d]

12 **Sun Y**, Jiang M, Park PH, Song K. Transcriptional suppression of androgen receptor by 18β-glycyrrhetinic acid in LNCaP human prostate cancer cells. *Arch Pharm Res* 2020; **43**: 433-448 [PMID: 32219716 DOI: 10.1007/s12272-020-01228-z]

13 **Cao D**, Wu Y, Jia Z, Zhao D, Zhang Y, Zhou T, Wu M, Zhang H, Tsukamoto T, Oshima M, Jiang J, Cao X. 18β-glycyrrhetinic acid inhibited mitochondrial energy metabolism and gastric carcinogenesis through methylation-regulated TLR2 signaling pathway. *Carcinogenesis* 2019; **40**: 234-245 [PMID: 30364936 DOI: 10.1093/carcin/bgy150]

14 **Cai H**, Chen X, Zhang J, Wang J. 18β-glycyrrhetinic acid inhibits migration and invasion of human gastric cancer cells *via* the ROS/PKC-α/ERK pathway. *J Nat Med* 2018; **72**: 252-259 [PMID: 29098529 DOI: 10.1007/s11418-017-1145-y]

15 **Yuan L**, Yang Y, Li X, Zhou X, Du YH, Liu WJ, Zhang L, Yu L, Ma TT, Li JX, Chen Y, Nan Y. 18β-glycyrrhetinic acid regulates mitochondrial ribosomal protein L35-associated apoptosis signaling pathways to inhibit proliferation of gastric carcinoma cells. *World J Gastroenterol* 2022; **28**: 2437-2456 [PMID: 35979263 DOI: 10.3748/wjg.v28.i22.2437]

16 **Peng Y**, Croce CM. The role of MicroRNAs in human cancer. *Signal Transduct Target Ther* 2016; **1**: 15004 [PMID: 29263891 DOI: 10.1038/sigtrans.2015.4]

17 **Coradduzza D**, Cruciani S, Arru C, Garroni G, Pashchenko A, Jedea M, Zappavigna S, Caraglia M, Amler E, Carru C, Maioli M. Role of miRNA-145, 148, and 185 and Stem Cells in Prostate Cancer. *Int J Mol Sci* 2022; **23** [PMID: 35163550 DOI: 10.3390/ijms23031626]

18 **Vo JN**, Cieslik M, Zhang Y, Shukla S, Xiao L, Wu YM, Dhanasekaran SM, Engelke CG, Cao X, Robinson DR, Nesvizhskii AI, Chinnaiyan AM. The Landscape of Circular RNA in Cancer. *Cell* 2019; **176**: 869-881.e13 [PMID: 30735636 DOI: 10.1016/j.cell.2018.12.021]

19 **Di Leva G**, Croce CM. miRNA profiling of cancer. *Curr Opin Genet Dev* 2013; **23**: 3-11 [PMID: 23465882 DOI: 10.1016/j.gde.2013.01.004]

20 **Komatsu S**, Imamura T, Kiuchi J, Takashima Y, Kamiya H, Ohashi T, Konishi H, Shiozaki A, Kubota T, Okamoto K, Otsuji E. Depletion of tumor suppressor miRNA-148a in plasma relates to tumor progression and poor outcomes in gastric cancer. *Am J Cancer Res* 2021; **11**: 6133-6146 [PMID: 35018247]

21 **Li X**, Zhu M, Zhao G, Zhou A, Min L, Liu S, Zhang N, Zhu S, Guo Q, Zhang S, Li P. MiR-1298-5p level downregulation induced by Helicobacter pylori infection inhibits autophagy and promotes gastric cancer development by targeting MAP2K6. *Cell Signal* 2022; **93**: 110286 [PMID: 35192930 DOI: 10.1016/j.cellsig.2022.110286]

22 **Itakura E**, Mizushima N. Characterization of autophagosome formation site by a hierarchical analysis of mammalian Atg proteins. *Autophagy* 2010; **6**: 764-776 [PMID: 20639694 DOI: 10.4161/auto.6.6.12709]

23 **Wen X**, Klionsky DJ. At a glance: A history of autophagy and cancer. *Semin Cancer Biol* 2020; **66**: 3-11 [PMID: 31707087 DOI: 10.1016/j.semcancer.2019.11.005]

24 **Wei Y**, Hong D, Zang A, Wang Z, Yang H, Zhang P, Wang Y. miR-183 Enhances Autophagy of GC Cells by Targeted Inhibition of mTOR. *Ann Clin Lab Sci* 2021; **51**: 837-843 [PMID: 34921037]

25 **Lin D**, Zhong W, Li J, Zhang B, Song G, Hu T. Involvement of BID translocation in glycyrrhetinic acid and 11-deoxy glycyrrhetinic acid-induced attenuation of gastric cancer growth. *Nutr Cancer* 2014; **66**: 463-473 [PMID: 24547973 DOI: 10.1080/01635581.2013.877498]

26 **Zhu Y**, Zhou B, Hu X, Ying S, Zhou Q, Xu W, Feng L, Hou T, Wang X, Zhu L, Jin H. LncRNA LINC00942 promotes chemoresistance in gastric cancer by suppressing MSI2 degradation to enhance c-Myc mRNA stability. *Clin Transl Med* 2022; **12**: e703 [PMID: 35073459 DOI: 10.1002/ctm2.703]

27 **Zhang J**, Wang C, Yan S, Yang Y, Zhang X, Guo W. miR-345 inhibits migration and stem-like cell phenotype in gastric cancer *via* inactivation of Rac1 by targeting EPS8. *Acta Biochim Biophys Sin (Shanghai)* 2020; **52**: 259-267 [PMID: 32147678 DOI: 10.1093/abbs/gmz166]

28 **Xiang SS**, Wang XA, Li HF, Shu YJ, Bao RF, Zhang F, Cao Y, Ye YY, Weng H, Wu WG, Mu JS, Wu XS, Li ML, Hu YP, Jiang L, Tan ZJ, Lu W, Liu F, Liu YB. Schisandrin B induces apoptosis and cell cycle arrest of gallbladder cancer cells. *Molecules* 2014; **19**: 13235-13250 [PMID: 25165862 DOI: 10.3390/molecules190913235]

29 **Wang X**, Yu Z, Zhou Q, Wu X, Chen X, Li J, Zhu Z, Liu B, Su L. Tissue transglutaminase-2 promotes gastric cancer

progression *via* the ERK1/2 pathway. *Oncotarget* 2016; **7**: 7066-7079 [PMID: 26771235 DOI: 10.18632/oncotarget.6883]

30 **He W**, Sun Z, Liu Z. Silencing of TGM2 reverses epithelial to mesenchymal transition and modulates the chemosensitivity of breast cancer to docetaxel. *Exp Ther Med* 2015; **10**: 1413-1418 [PMID: 26622499 DOI: 10.3892/etm.2015.2679]

31 **Shan H**, Zhou X, Chen C. MicroRNA214 suppresses the viability, migration and invasion of human colorectal carcinoma cells *via* targeting transglutaminase 2. *Mol Med Rep* 2019; **20**: 1459-1467 [PMID: 31173203 DOI: 10.3892/mmr.2019.10325]

32 **Ma H**, Xie L, Zhang L, Yin X, Jiang H, Xie X, Chen R, Lu H, Ren Z. Activated hepatic stellate cells promote epithelial-to-mesenchymal transition in hepatocellular carcinoma through transglutaminase 2-induced pseudohypoxia. *Commun Biol* 2018; **1**: 168 [PMID: 30393774 DOI: 10.1038/s42003-018-0177-5]

33 **Wang F**, Wang L, Qu C, Chen L, Geng Y, Cheng C, Yu S, Wang D, Yang L, Meng Z, Chen Z. Kaempferol induces ROS-dependent apoptosis in pancreatic cancer cells *via* TGM2-mediated Akt/mTOR signaling. *BMC Cancer* 2021; **21**: 396 [PMID: 33845796 DOI: 10.1186/s12885-021-08158-z]

34 **Mack HI**, Zheng B, Asara JM, Thomas SM. AMPK-dependent phosphorylation of ULK1 regulates ATG9 localization. *Autophagy* 2012; **8**: 1197-1214 [PMID: 22932492 DOI: 10.4161/auto.20586]

35 **Zibrova D**, Vandermoere F, Göransson O, Peggie M, Mariño KV, Knierim A, Spengler K, Weigert C, Viollet B, Morrice NA, Sakamoto K, Heller R. GFAT1 phosphorylation by AMPK promotes VEGF-induced angiogenesis. *Biochem J* 2017; **474**: 983-1001 [PMID: 28008135 DOI: 10.1042/BCJ20160980]

36 **Lim J**, Lachenmayer ML, Wu S, Liu W, Kundu M, Wang R, Komatsu M, Oh YJ, Zhao Y, Yue Z. Proteotoxic stress induces phosphorylation of p62/SQSTM1 by ULK1 to regulate selective autophagic clearance of protein aggregates. *PLoS Genet* 2015; **11**: e1004987 [PMID: 25723488 DOI: 10.1371/journal.pgen.1004987]

37 **Bjørkøy G**, Lamark T, Pankiv S, Øvervatn A, Brech A, Johansen T. Monitoring autophagic degradation of p62/SQSTM1. *Methods Enzymol* 2009; **452**: 181-197 [PMID: 19200883 DOI: 10.1016/S0076-6879(08)03612-4]

38 **Zhang H**, Zhang Y, Zhu X, Chen C, Zhang C, Xia Y, Zhao Y, Andrisani O, Kong L. DEAD Box Protein 5 Inhibits Liver Tumorigenesis by Stimulating Autophagy *via* Interaction with p62/SQSTM1. *Hepatology* 2019; **69**: 1046-1063 [PMID: 30281815 DOI: 10.1002/hep.30300]

39 **Yoshii SR**, Mizushima N. Monitoring and Measuring Autophagy. *Int J Mol Sci* 2017; **18** [PMID: 28846632 DOI: 10.3390/ijms18091865]

World Journal of Gastroenterology

Submit a Manuscript: https://www.f6publishing.com

World J Gastroenterol 2023 June 21; 29(23): 3645-3657

DOI: 10.3748/wjg.v29.i23.3645

ISSN 1007-9327 (print) ISSN 2219-2840 (online)

ORIGINAL ARTICLE

Retrospective Study

High expression of the circadian clock gene NPAS2 is associated with progression and poor prognosis of gastric cancer: A single-center study

Xiao-Meng Cao, Wen-Di Kang, Tian-Hong Xia, Shao-Bin Yuan, Chang-An Guo, Wen-Jie Wang, Hong-Bin Liu

Specialty type: Gastroenterology and hepatology

Provenance and peer review: Unsolicited article; Externally peer reviewed.

Peer-review model: Single blind

Peer-review report's scientific quality classification

Grade A (Excellent): 0
Grade B (Very good): 0
Grade C (Good): C, C, C, C
Grade D (Fair): D
Grade E (Poor): 0

P-Reviewer: Benna C, Italy; Papadia C, United Kingdom; Qin SS, China

Received: February 9, 2023
Peer-review started: February 9, 2023
First decision: March 9, 2023
Revised: March 16, 2023
Accepted: May 4, 2023
Article in press: May 4, 2023
Published online: June 21, 2023

Xiao-Meng Cao, Department of General Surgery, Gansu Provincial Hospital of TCM, Lanzhou 730050, Gansu Province, China

Xiao-Meng Cao, Shao-Bin Yuan, The First Clinical Medical College, Gansu University of Chinese Medicine, Lanzhou 730030, Gansu Province, China

Wen-Di Kang, Department of Interventional Therapy, National Cancer Center/National Clinical Research Center for Cancer/Cancer Hospital, Chinese Academy of Medical Sciences and Peking Union Medical College, Beijing 100021, China

Tian-Hong Xia, Clinical Medicine College, Ningxia Medical University, Clinical Medicine college, Ningxia Medical University, Yinchuan 750004, Ningxia Hui Autonomous Region, China

Chang-An Guo, Department of Emergency, Lanzhou University Second Hospital, Lanzhou 730030, Gansu Province, China

Wen-Jie Wang, Department of General Surgery, Lanzhou University Second Hospital, Lanzhou 730030, Gansu Province, China

Hong-Bin Liu, Department of General Surgery, The 940th Hospital of Joint Logistics Support Force of Chinese People's Liberation Army, Lanzhou 730050, Gansu Province, China. 1554153823@qq.com

Corresponding author: Hong-Bin Liu, MD, Professor, Department of General Surgery, The 940th Hospital of Joint Logistics Support Force of Chinese People's Liberation Army, No. 333 Nanbinhe Road, Qilihe District, Lanzhou 730050, Gansu Province, China. 1554153823@qq.com

Abstract

BACKGROUND

The prognostic assessment of patients after surgical resection of gastric cancer (GC) patients is critical. However, the role of the circadian clock gene NPAS2 expression in GC remains unknown.

AIM

To explore the relationship between NPAS2 and the survival prognosis of GC

patients and clarify its role in evaluating GC prognosis.

METHODS

The tumor tissues and clinical data of 101 patients with GC were collected retrospectively. Immunohistochemical staining (IHC) was used to detect the expression of NPAS2 protein in GC and adjacent tissues. Univariate and multivariate Cox regression analysis was used to determine the independent prognostic factors of GC, and a nomogram prediction model was established. The receiver operating characteristic (ROC) curve, the ROC area under the curve, the calibration curve, and C-index were used to evaluate the predictive effectiveness of the model. Kaplan Meier analysis was used to compare the risk stratification of subgroups according to the median score in the nomogram model of each patient.

RESULTS

Microarray IHC analysis showed that the positive rate of NPAS2 protein expression in GC tissues was 65.35%, which was significantly higher than 30.69% in adjacent tissues. The high expression of NPAS2 was correlated with tumor-node-metastasis (TNM) stage ($P < 0.05$), pN stage ($P < 0.05$), metastasis ($P < 0.05$), venous invasion ($P < 0.05$), lymphatic invasion ($P < 0.05$), and lymph node positive ($P < 0.05$) of GC. Kaplan Meier survival analysis showed that the 3-year overall survival (OS) of patients with high NPAS2 expression was significantly shortened ($P < 0.0001$). Univariate and multivariate COX regression analysis showed that TNM stage ($P = 0.009$), metastasis ($P = 0.009$), and NPAS2 expression ($P = 0.020$) were independent prognostic factors of OS in GC patients for 3 years. The nomogram prediction model based on independent prognostic factors has a C-Index of 0.740 (95%CI: 0.713-0.767). Furthermore, subgroup analysis showed that the 3-year OS time of the high-risk group was significantly lower than that of the low-risk group ($P < 0.0001$).

CONCLUSION

NPAS2 is highly expressed in GC tissues and is closely related to worse OS in patients. Therefore, the evaluation of NPAS2 expression may be a potential marker for GC prognosis evaluation. Notably, the nomogram model based on NPAS2 can improve the accuracy of GC prognosis prediction and assist clinicians in postoperative patient management and decision-making.

Key Words: NPAS2; Gastric cancer; Tissue microarray; Survival analysis; Prediction model; Nomogram

Core Tip: The prognostic assessment of patients after surgical resection of gastric cancer (GC) is critical. However, the role of NPAS2 expression in GC remains unknown. Our study identified for the first time that high NPAS2 protein expression was associated with poor overall survival prognosis in GC patients and was an independent risk factor for patients after radical resection of GC. We constructed a nomogram prediction model by combining NPAS2 and other clinically independent risk factors, thus improving the predictive accuracy of GC prognosis.

Citation: Cao XM, Kang WD, Xia TH, Yuan SB, Guo CA, Wang WJ, Liu HB. High expression of the circadian clock gene NPAS2 is associated with progression and poor prognosis of gastric cancer: A single-center study. *World J Gastroenterol* 2023; 29(23): 3645-3657

URL: https://www.wjgnet.com/1007-9327/full/v29/i23/3645.htm

DOI: https://dx.doi.org/10.3748/wjg.v29.i23.3645

INTRODUCTION

Gastric cancer (GC) ranks fifth and fourth in the incidence and mortality of global cancer, respectively, and is more likely to occur in men[1,2]. The etiology of GC remains unclear, involving multiple cell types and complex molecular mechanisms[3]. Despite recent improvements in the diagnosis and treatment of GC, the overall treatment outcome remains poor[4]. Notably, radical gastrectomy is the primary treatment method for GC. However, postoperative recurrence rates and mortality remain high, and their mortality rates are closely associated with peritoneal, hematologic, and lymph node metastases in GC[5]. Therefore, there is an urgent need to identify new markers to predict the malignant biological behavior and prognosis of GC to guide the treatment strategy and improve the clinical outcome of GC.

Biological rhythm is a regulatory system in almost all living things. It produces 24-h periodic rhythm changes in many essential behaviors and physiological processes[6], including the sleep-wake cycle, body temperature cycle, hormone secretion, heart rate, blood pressure, excretion, *etc.*[7,8]. The destruction of normal biological rhythm adversely affects mammalian physiology[9]. The role and mechanism of biological rhythm-related genes in tumors, and the design of tumor treatment methods targeting biological rhythm genes, are one of the hot spots in the current cancer research field[10]. NPAS2, also known as MOP4, is the largest core circadian gene found so far, with a length of about 176.68Kb, located on human chromosome 2 (2q11.2), encoding proteins belonging to the basic helix loop helix PAS domain of transcription factors[11]. NPAS2 is mainly present in the forebrain of mammals and is also expressed in some peripheral organs such as the liver and skin[12]. Additionally, it is an important part of the positive circadian rhythm feedback circuit[8]. Furthermore, Studies have confirmed that NPAS2 is associated with various rhythm-related diseases, such as cancer, diabetes, depression, sleep disorders, obesity, *etc.*[13].

Recent studies have shown that low expression of NPAS2 accelerates cell growth and tumor cell cycle progression and plays a unique and critical role in cancer progression[14]. The low expression of NPAS2 promotes the proliferation and invasion of colorectal cancer cells. Additionally, it increases the wound-healing ability of colorectal cancer cells, indicating that NPAS2 has a key tumor inhibitory effect. Additionally, its high expression is positively correlated with overall survival (OS)[15]. However, some studies have found that NPAS2, as an oncogene, promotes the proliferation of hepatocellular carcinoma (HCC) cells and participates in the critical process of hepatocellular carcinogenesis. Its high expression is related to the invasive clinical characteristics and low OS of HCC patients[16]. It promotes the survival of HCC cells by up-regulating the expression of mitotic cycle 25A and inhibiting mitochondrial-dependent intrinsic apoptosis[16]. These results have also been observed in acute myeloid leukemia [17]. In contrast, there are few studies on the expression and role of NPAS2 in GC at home and abroad, and there is a significant lack of experimental research. Therefore, the expression level of NPAS2 in GC and its role in the occurrence and development of GC in different signal pathways are controversial and need to be further studied.

This study intends to detect the expression level of NPAS2 in GC and paraneoplastic tissues by using tissue microarray immunohistochemical staining to establish a nomogram prediction model based on NPAS2 and other clinicopathologically independent risk factors. Furthermore, we aim to investigate the effect of NPAS2 on the prognosis of GC and its value in the prognosis prediction of GC patients.

MATERIALS AND METHODS

This study was approved by the Medical Ethics Committee of the Second Hospital of Lanzhou University. Informed consent was obtained from all patients, and all specimens were pseudonymous. The tumor tissues, precancerous tissues, and clinical data of 101 patients with primary GC resected by surgery from July to October 2019 in the second Hospital of Lanzhou University were collected and followed up by standard outpatient clinic and telephone. The inclusion criteria of the study were as follows: (1) Histopathological diagnosis of gastric adenocarcinoma; (2) age ≥ 18 years old; (3) patients with primary GC underwent surgical resection; (4) complete pathological, treatment, surgical and follow-up data; and (5) the patient gave written informed consent. Exclusion criteria: (1) Death before discharge; (2) preoperative radiotherapy and chemotherapy or neoadjuvant chemotherapy; (3) multiple cancers; and (4) gastric stump cancer. 10% neutral formalin fixation and routine paraffin-embedded GC and paraffin-embedded tissues were confirmed by pathology, and all pathology was independently reviewed by two pathologists. The patients were followed up every 3 mo in the first 2 years and every 6 mo in the third year. Follow-up included laboratory examination, chest X-ray examination, and abdominal computed tomography (CT) examination. The follow-up period was 36 mo, and OS was defined as from the date of the first operation to the end of follow-up or the time of death.

Construction of tissue microarray and immunohistochemical staining

One hundred one paraffin-embedded primary GC tissues and adjacent tissues were fixed with formalin and then serially sectioned on a microtome with a thickness of 4 μm. After drying, hematoxylin and eosin staining (HE) were performed. A professional pathologist selected and marked the representative positions of HE-stained pathological sections and corresponding wax blocks according to the view under the light microscope. The tissue chip wax blocks were made by a drilling mechanism and sliced with a thickness of 4μm. After being dewaxed in xylene and washed in gradient ethanol, the slices were immersed in a pressure tank containing 800 mL of 0.1% sodium citrate buffer solution (pH 6.0) and boiled for 3 min, followed by cooling. Following the manufacturer's instructions, we then conducted a streptavidin-Biotin Complex assay (Fuzhou Maxin Biotechnology Development Company). The slides were then incubated overnight with the primary antibody against NPAS2 at 4 ℃ (diluted, 1:200, rabbit anti-human NPAS2 polyclonal antibody, Biossantibodies, China). Color development, hematoxylin re-staining, differentiation, blueing, and dehydration were performed prior to sealing.

Evaluation of immunostaining

The complete immunohistochemical sections of 101 cases were observed under the microscope. NPAS2 was mainly expressed in the cytoplasm and nucleus, and the positive cells were yellow and brown granular. Two professional pathologists scored the section staining and did not know the clinicopathological factors and clinical outcome of the patient. The positive results were judged by the semi-quantitative integration method. Five high-power visual fields (400 ×) were selected for each chip on each slide under the microscope, and cells' positive rate and staining intensity were observed. (1) The score of cell positive rate: 0 indicates that the proportion of positive cells is less than 5%. The score of 5%-25% is 1, 26%-50% is 2, 51%-75% is 3, and more than 75% is 4; and (2) Staining intensity score: 0 = no coloring, 1 = light yellow, 2 = brown, 3 = brown. The immunostaining score was obtained by multiplying the positive rate of cells with the result of staining intensity. 0 was negative, 1 to 4 was weakly positive, 5 to 8 was moderately positive, and 9 to 12 was strongly positive. In this study, negative and weak positive was defined as low expression of NPAS2, while medium positive and strong positive was defined as high expression.

Statistical analysis

All data were analyzed using R software (Version 4.1.1, http://www.r-project.org) and SPSS (Version 26). Classification variables are represented by percentage (%), chi-square test, and continuity correction. Pearson's chi-squared test was used to evaluate the correlation between NPAS2 expression and clinicopathological factors. Survival analysis was performed by Kaplan-Meier curve and log-rank test. Univariate and multivariate Cox analysis determined the independent prognostic factors of OS and established the Cox proportional hazards model, and the hazard ratios (HRs) and 95% confidence intervals (CIs) were subsequently calculated. "Survival" and "surminer" R package were used for survival and Cox analysis. The "rms" package drew a nomogram model based on independent risk factors to predict OS. Furthermore, the receiver operating characteristic (ROC) curve, aera under the curve (AUC), calibration curve, and C-index were used to evaluate its prediction performance. In this study, $P < 0.05$ was considered to be statistically significant.

RESULTS

High expression of NPAS2 in human GC tissues

To explore the prognostic value of NPAS2 in GC, we performed immunohistochemical staining on 101 GC tissues collected. Strong or moderate positive immunostaining of NPAS2 protein was observed in the nucleus and cytoplasm of tumor cells in GC tissues. In contrast, weak positive or negative immunostaining was mainly detected in adjacent tissues. Representative positive staining results of NPAS2 showed that the positive rate of NPAS2 expression in GC tissues was 65.35% (66/101) (Figure 1), while the positive rate in corresponding adjacent tissues was 30.69% (31/101).

High expression of NPAS2 correlates with clinicopathological factors in GC patients

Of the 101 patients with GC, 65 (64.36%) died during follow-up. Table 1 summarizes the correlation between clinicopathological characteristics and NPAS2, showing that high expression of NPAS2 is associated with clinical progression in GC patients. The high expression of NPAS2 was significantly correlated with tumor-node-metastasis (TNM) stage ($P = 0.001$), pN stage ($P = 0.009$), metastasis ($P = 0.032$), venous invasion ($P = 0.012$), lymphatic invasion ($P = 0.001$) and lymph node positivity ($P = 0.001$).

The high expression of NPAS2 is associated with the prognosis of GC patients

The prognostic value of NPAS2 expression in GC was further investigated by Kaplan-Meier analysis and log-rank test. The results demonstrated that GC patients with high NPAS2 expression were significantly associated with shorter OS ($P < 0.001$) (Figure 2). Univariate Cox regression analysis showed that the TNM stage of GC patients (HR = 7.07, 95%CI: 3.47-14.41, $P < 0.001$), pN stage (HR = 1.72, 95%CI: 1.38-2.15, $P < 0.001$), metastasis (HR = 4.85, 95%CI: 2.24-10.46, $P < 0.001$), venous invasion (HR = 5.01, 95%CI: 1.57-15.98, $P = 0.007$), neural invasion (HR = 1.73, 95%CI: 1.03-2.9, $P = 0.037$), lymphatic invasion (HR = 3.53, 95%CI: 1.88-6.64, $P < 0.001$), lymph node positivity (HR = 3.35, 95%CI: 1.82-6.18, $P < 0.001$), and high expression of NPAS2 (HR = 5.13, 95%CI: 2.6-10.13, $P < 0.001$) were significantly correlated with OS. Multivariate Cox regression analysis showed that the TNM stage (HR = 3.61, 95%CI: 1.37-9.49, $P = 0.009$), metastasis (HR = 3.07, 95%CI: 1.33-7.1, $P = 0.009$), and high expression of NPAS2 (HR = 2.43, 95%CI: 1.15-5.13, $P = 0.020$) were independent risk factors for predicting OS (Table 2). Therefore, these collective data suggest that the expression level of NPAS2 has a good predictive value in the prognosis of GC patients.

Construction and evaluation of the prediction model

To obtain the best prediction model, TNM stage and metastasis were determined as independent

Table 1 Correlation between clinicopathological characteristic and NPAS2 in gastric cancer

Characteristic	Low expression of NPAS2	High expression of NPAS2	*P* value
Number	35	66	
Age, *n* (%)			0.599
< 60	21 (60.0)	36 (54.5)	
≥ 60	14 (40.0)	30 (45.5)	
Sex, *n* (%)			0.626
Female	7 (20.0)	16 (24.2)	
Male	28 (80.0)	51 (75.8)	
TNM stage, *n* (%)			0.001
I-II	25 (71.4)	11 (16.7)	
III-IV	10 (28.6)	55 (83.3)	
pT stage, *n* (%)			0.351
T1-T2	6 (17.1)	29 (82.9)	
T3-T4	7 (10.6)	59 (89.4)	
pN stage, *n* (%)			0.009
N0	16 (45.7)	12 (18.2)	
N1-N3	19 (54.3)	54 (81.8)	
Metastasis, *n* (%)			0.032
M0	35 (100.0)	58 (87.9)	
M1	0 (0.0)	8 (12.1)	
Tumor size, *n* (%)			0.626
< 5	15 (42.9)	25 (37.9)	
≥ 5	20 (57.1)	41 (62.1)	
Tumor location, *n* (%)			0.611
Antrum	14 (40.0)	33 (50.0)	
Body	9 (25.7)	13 (19.7)	
Cardia	12 (34.3)	20 (30.3)	
Venous invasion, *n* (%)			0.012
Negative	9 (25.7)	5 (7.6)	
Positive	26 (74.3)	61 (92.4)	
Neural invasion, *n* (%)			0.736
Negative	15 (42.9)	26 (39.4)	
Positive	20 (57.1)	40 (60.6)	
Lymphatic invasion, *n* (%)			0.001
Negative	22 (62.9)	12 (18.2)	
Positive	13 (37.1)	54 (81.8)	
Positive lymph node, *n* (%)			0.001
Negative	22 (62.9)	14 (21.2)	
Positive	13 (37.1)	52 (78.8)	
Differentiated degree, *n* (%)			0.16
Poorly	27 (77.1)	58 (87.9)	
Moderately and highly	8 (22.9)	8 (12.1)	

Lauren's Classification, *n* (%)			0.569
Intestinal	23 (65.7)	47 (71.2)	
Diffuse	12 (34.3)	19 (28.8)	

pT stage: Pathological assessment of primary tumor; pN stage: Pathological assessment of regional lymph nodes; TNM: Tumor-node-metastasis.

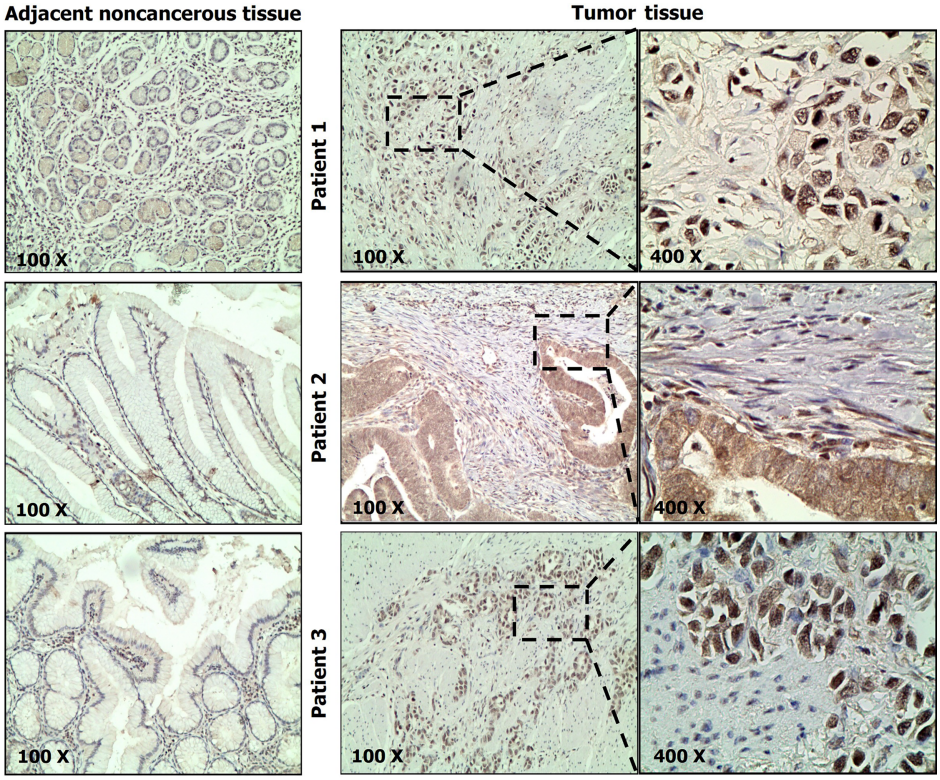

DOI: 10.3748/wjg.v29.i23.3645

Figure 1 Expression of NPAS2 in gastric cancer. The expression of NPAS2 in tumor tissues of gastric cancer was detected by immunohistochemical staining and compared with adjacent normal tissues. High expression of NPAS2 in gastric cancer and low expression in adjacent non-cancerous tissue.

prognostic factors for GC according to multivariate Cox regression analysis and combined with NAPS2 high expression. Together, these were used as a combined prediction model for predicting OS at 1, 2, and 3 years after GC resection was constructed. The prediction model was visualized by nomogram (Figure 3). The 1-year, 2-year, and 3-year ROC curves of the Nomogram prediction model and other independent factors (Figure 4A) and the Time-dependent ROC curve were used to show the model's prediction performance (Figure 4C). The AUC of the nomogram prediction model for 1, 2, and 3 years is 0.763, 0.800, and 0.848, respectively (Figure 4B). Additionally, the C-index of each model shows the prediction performance of different models (Figure 4D), and the nomogram has the best prediction performance with a C-index of 0.740 (95%CI: 0.713-0.767). Finally, the prediction accuracy of the nomogram was verified by calibration curves, and the results showed that the combined nomogram model's 1-year, 2-year, and 3-year survival rates based on NPAS2 were in good agreement with the actual survival probability (Figure 5).

Risk stratification of OS by the nomogram model

To evaluate the positive effect of the nomogram prediction model in different subgroups, we divided all patients into a low-risk subgroup (score < 158) and a high-risk subgroup (score ≥ 158) according to the median nomogram score. Our results showed that patients in the high-risk group had significantly lower OS than those in the low-risk group ($P < 0.0001$) (Figure 6).

DISCUSSION

Epidemiological studies have shown that the disruption of normal circadian rhythm may increase the

Table 2 Univariate and multivariate Cox analysis of clinicopathological factors associated with the overall survival of gastric cancers

Characteristics	Univariate analysis		Multivariate analysis	
	Hazard ratio (95%CI)	*P* value	Hazard ratio (95%CI)	*P* value
Age				
< 60	1			
≥ 60	1.33 (0.82-2.17)	0.25		
Gender				
Female	1			
Male	1.13 (0.63-2.05)	0.679		
TNM stage				
I-II	1			
III-IV	7.07 (3.47-14.41)	< 0.001	3.61 (1.37-9.49)	0.009
pT stage				
T1-T2	1			
T3-T4	1.87 (0.81-4.35)	0.143		
pN stage				
N0	1			
N1-N3	1.72 (1.38-2.15)	< 0.001	1.66 (0.68-4.07)	0.265
Metastasis				
M0	1			
M1	4.85 (2.24-10.46)	< 0.001	3.07 (1.33-7.1)	0.009
Tumor size				
< 5	1			
≥ 5	1.63 (0.97-2.72)	0.063		
Tumor location				
Antrum	1			
Body	0.92 (0.53-1.60)	0.76		
Cardia	1.13 (0.58-2.23)	0.72		
Venous invasion				
Negative	1			
Positive	5.01 (1.57-15.98)	0.007	1.69 (0.49-5.84)	0.409
Neural invasion				
Negative	1			
Positive	1.73 (1.03-2.9)	0.037	1.71 (0.98-3)	0.06
Lymphatic invasion				
Negative	1			
Positive	3.53 (1.88-6.64)	< 0.001	0.39 (0.09-1.77)	0.225
Positive lymph node				
Negative				
Positive	3.35 (1.82-6.18)	< 0.001	2.23 (0.58-8.49)	0.241
Differentiated degree				
Moderately and highly	1			
Poorly	0.62 (0.29-1.30)	0.203		

Lauren's Classification				
Diffuse type	1			
Intestinal type	0.97 (0.57-1.64)	0.908		
	0.97 (0.57-1.64)			
NPAS2 expression				
Low	1			
High	5.13 (2.6-10.13)	< 0.001	2.43 (1.15-5.13)	0.020

pT stage: Pathological assessment of primary tumor; pN stage: Pathological assessment of regional lymph nodes; TNM: Tumor-node-metastasis.

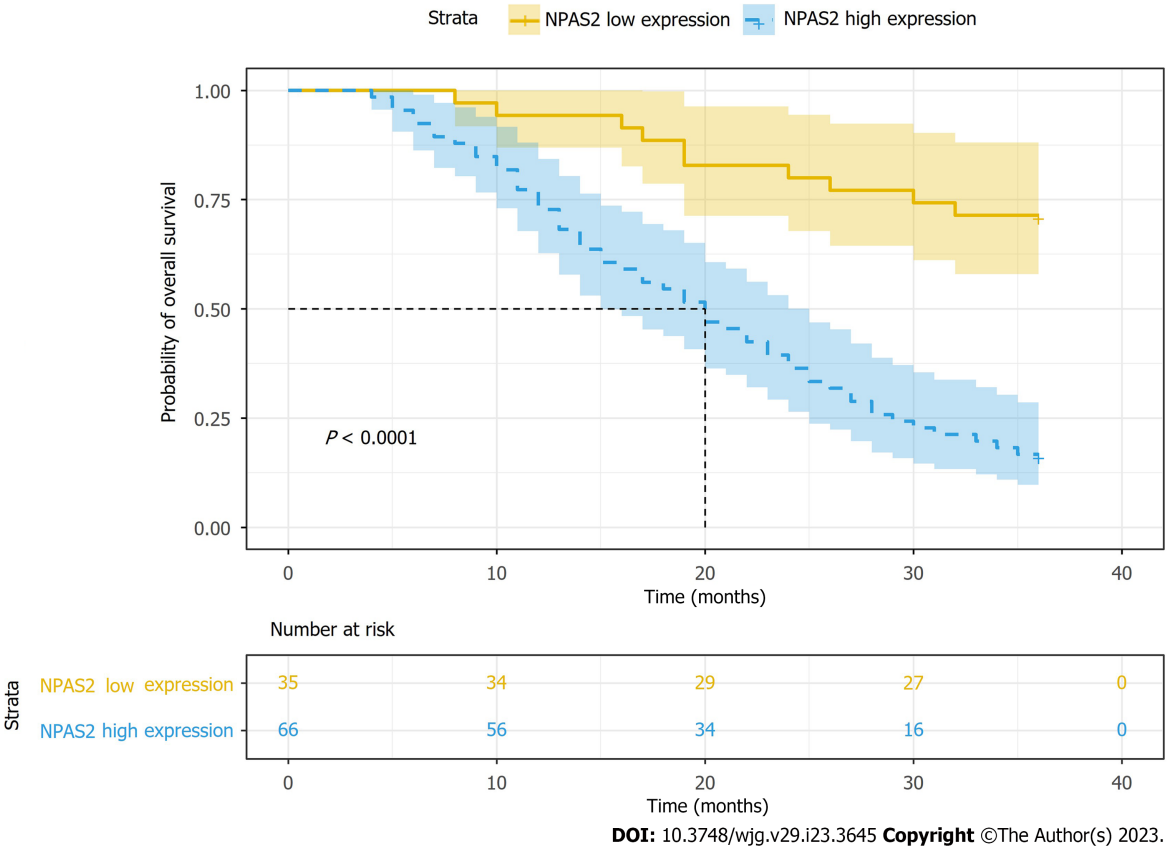

DOI: 10.3748/wjg.v29.i23.3645

Figure 2 Kaplan–Meier curves for NPAS2 expression in gastric cancer. Gastric cancer patients with high NPAS2 expression were significantly associated with shorter overall survival.

risk of a variety of cancers[18], such as breast cancer[19], lung cancer[20], bladder cancer[21], prostate cancer[22], and liver cancer[23]. Notably, women on night shifts have a higher risk of breast cancer[19]. Likewise, breast cancer patients with irregular circadian rhythms have a worse prognosis because of changes in the expression of NPAS2 in breast cancer tissues[19]. Additionally, the disruption of biorhythm can promote the occurrence of lung cancer, which is a promising diagnostic marker for patients with lung adenocarcinoma and an independent prognostic marker for non-small cell lung cancer[24]. Notably, NPAS2 regulates the expression of several genes as markers of bladder cancer and further reduces the migration ability of bladder cancer cells[21]. The development of prostate cancer depends on androgen levels, and NPAS2 may interact with dihydrotestosterone, thus affecting the androgen receptor-dependent signaling pathway leading to prostate cancer[25]. Importantly, NPAS2 plays a role in reprogramming glucose metabolism and the progression of liver cancer, suggesting that NPAS2 may be an important therapeutic target to normalize the abnormal glucose metabolism that leads to the advancement of HCC[23]. Furthermore, NPAS2 plays different roles in different tumors, which can be understood that the expression level and function of NPAS2 are tumor-specific. The exact molecular mechanism of the change of NPAS2 expression in GC remains unclear. Moreso, there are no reports on the correlation between NPAS2 expression and clinicopathological data of GC patients.

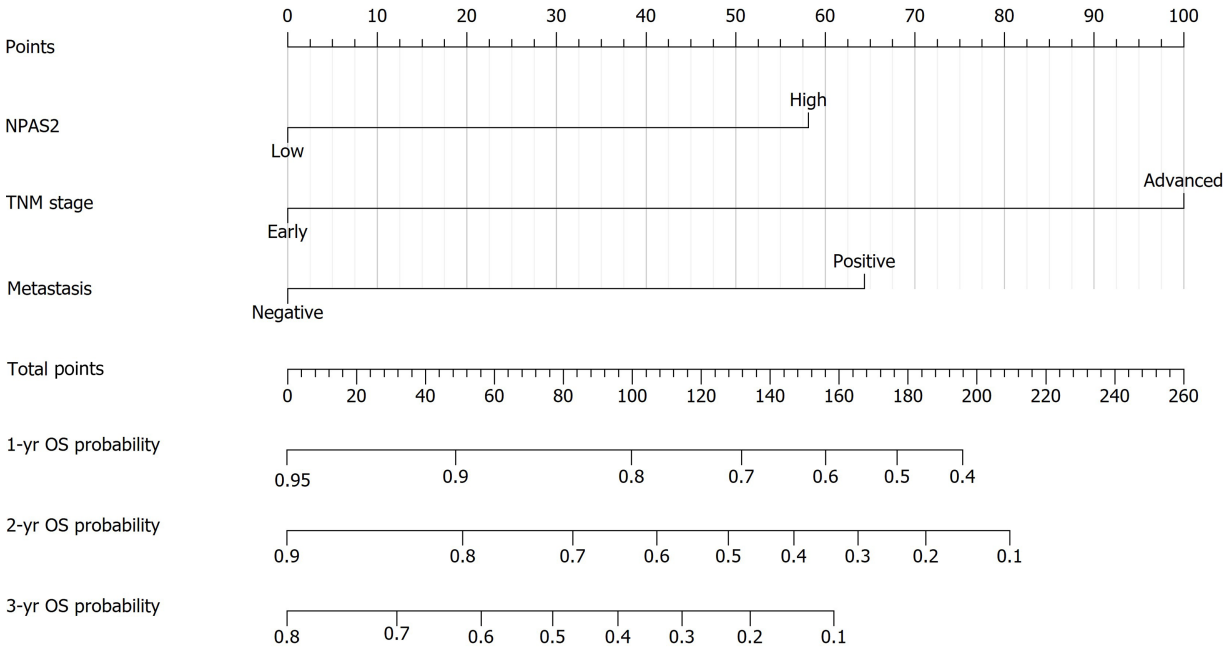

DOI: 10.3748/wjg.v29.i23.3645

Figure 3 Nomogram prediction of 1-, 2-and 3-year overall survival rate in patients with gastric cancer. The total points is calculated by adding up the points of each factor. The total points corresponds to the 1-year, 2-year and 3-year survival probability of the patients. OS: Overall survival; TNM: Tumor-node-metastasis.

The tissue microarray results in this study showed that NPAS2 was expressed in GC and precancerous tissues and was primarily located in the nucleus and cytoplasm. The results showed that the expression was high in 65.35% of GC tissues and low in 34.65% of GC tissues. To the best of our knowledge, our experimental data demonstrate the role of NPAS2 in the diagnosis and prognosis of GC for the first time. The survival analysis showed that the high expression of NPAS2 in GC was significantly correlated with the shorter OS ($P < 0.001$). Univariate and multivariate Cox analysis also showed that the high expression of NPAS2 was an independent risk factor for GC. Furthermore, the ROC curve shows that NPAS2 is valuable in predicting the prognosis of GC. Therefore, the expression level of NPAS2 in GC tissue directly affects the OS of GC patients and may be used as a tumor-promoting factor to affect the occurrence and development of GC, which is a new prognostic biomarker. Various animal and *in vitro* studies have found that NPAS2 can regulate the expression of oncogenes (such as c-myc), tumor suppressor genes (such as P53 and P21), and transcription factors[26], thereby regulating cell cycle, apoptosis, DNA damage and repair systems, invasion, metastasis, carcinogen metabolism, and detoxification[27]. Notably, DNA repair maintains genetic stability and protects DNA from internal and external stimuli. Once human biorhythm genes are mutated (due to spontaneous mutations, prolonged late nights, or other environmental factors), it may lead to irreversible disorders and loss of DNA repair capacity[27].

The American Joint Commission on the Cancer TNM staging system is widely used to monitor the prognosis of patients with GC[28]. Our study analyzed the clinicopathological factors affecting OS in patients with GC, and our results showed that TNM stage and metastasis were independent risk factors for poor survival outcomes. Although the TNM stage and metastasis of GC patients have been widely used in the formulation of the treatment plan and the evaluation of prognosis, with the increasing number of GC patients, more studies and related factors are needed to evaluate the survival and prognosis of these patients more accurately and individually. Our study combined three independent risk factors of NPAS2 and TNM stage and metastasis to establish a Cox regression model for predicting 3-year OS in patients with GC. Compared with the TNM stage alone, it has more predictive power and can be used as a more convenient and accurate tool to predict the prognosis of patients with GC following gastrectomy. Therefore, the accurate prognosis prediction by nomogram score is of great significance for postoperative management and diagnosis and treatment of patients.

However, we can not solve the causal relationship in this study. Therefore, further basic and clinical research is needed to explore these aspects. Our advantage is that this is the first study to show that the increased expression of NPAS2 may be related to the malignant biological behavior and poor prognosis of patients with GC. Of course, our research has the following noted limitations. First, the sample size of our study is small, and there may be selection bias. Secondly, this study is a single-center retrospective study, so it is necessary to conduct a multicenter prospective study to verify it further. Finally, we used immunohistochemical staining to detect the expression of NPAS2 in the center and periphery of each

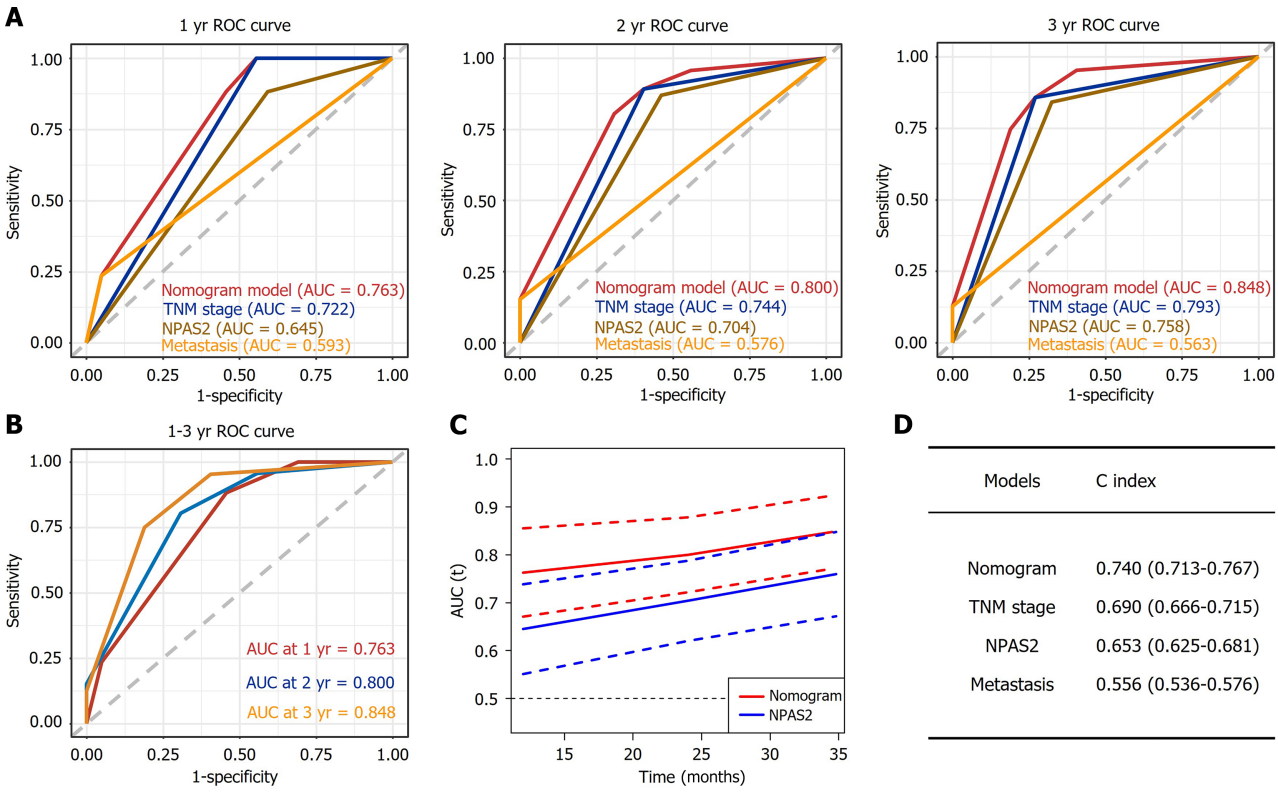

DOI: 10.3748/wjg.v29.i23.3645 **Copyright** ©The Author(s) 2023.

Figure 4 Construction of prognostic nomogram in gastric cancer. A: NPAS2, tumor-node-metastasis (TNM) stage, metastasis, and nomogram predict the receiver operating characteristic (ROC) curves of 1-year, 2-year and 3-year overall survival (OS) in gastric cancer patients; B: Nomogram predict the ROC curve of 1-year, 2-year and 3-year OS in gastric cancer patients; C: Comparison of time-dependent ROC curves between nomogram and NPAS2; D: C-index for nomogram, NPAS2, TNM stage, metastasis. ROC: Receiver operating characteristic; OS: Overall survival; TNM: Tumor-node-metastasis; AUC: Area under the curve.

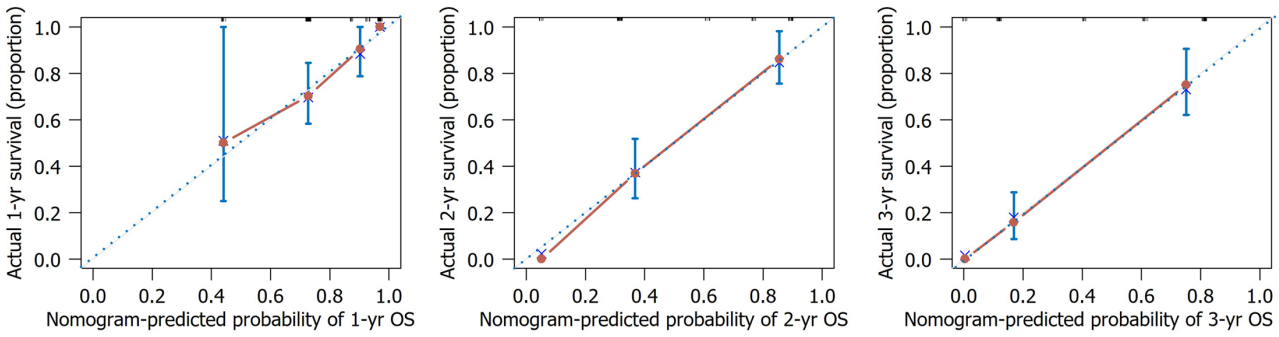

DOI: 10.3748/wjg.v29.i23.3645 **Copyright** ©The Author(s) 2023.

Figure 5 Nomogram calibration plots to predict 1-, 2-, and 3-year overall survival in gastric cancer patients. OS: Overall survival.

GC tissue. However, considering the heterogeneity, the expression level of NPAS2 in the sampling site may not represent whole tumor regions.

Based on these investigations, further exploration of the molecular mechanism and influence of NPAS2 in the occurrence and development of GC will help to promote its clinical application. The established nomogram prediction model provides a potential objective clinical prediction tool to assist clinicians in predicting the prognosis of GC patients and making postoperative management and clinical decisions.

CONCLUSION

In conclusion, our study found that high expression of NAPS2 is associated with poor prognosis of OS in patients with GC and is an independent risk factor for patients after radical resection of GC. We

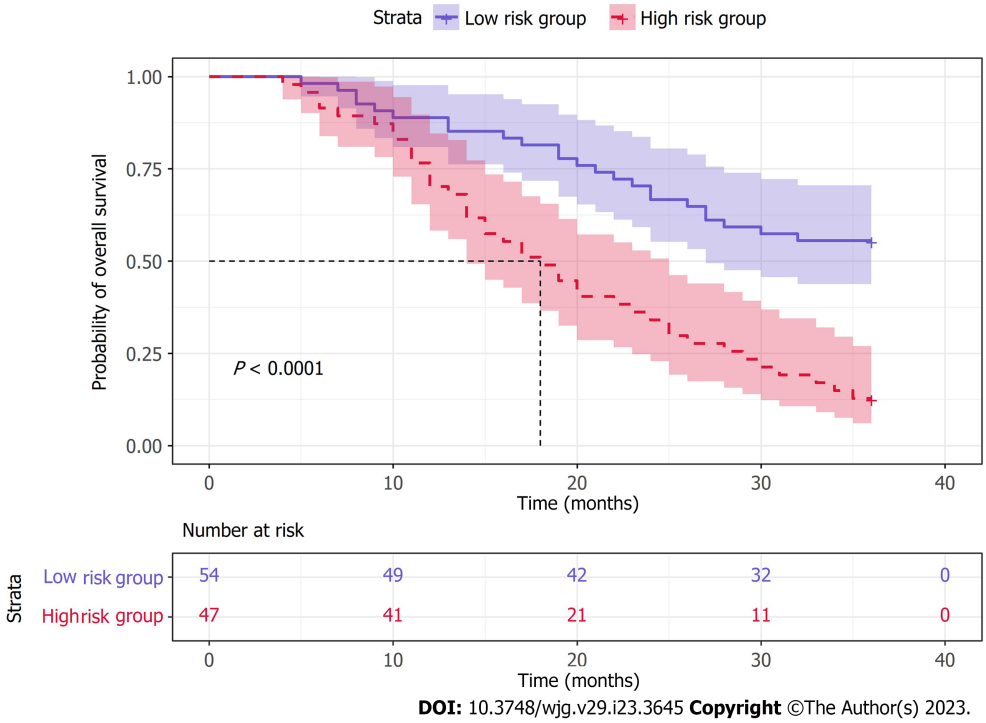

DOI: 10.3748/wjg.v29.i23.3645

Figure 6 Overall survival Kaplan-Meier curves for patients in the low- and high-risk groups.

further constructed a nomogram model by combining NAPS2 and other independent risk factors, thus improving the accuracy of predicting the prognosis of GC.

ARTICLE HIGHLIGHTS

Research background

The circadian clock gene NPAS2 expression is associated with multiple tumor prognosis, its role in gastric cancer (GC) is unknown.

Research motivation

NPAS2 can improve the accuracy of GC prognosis prediction and assist clinicians in postoperative patient management and decision-making.

Research objectives

This study aimed to explore the relationship between the circadian clock gene NPAS2 and the survival prognosis of GC patients and clarify its role in evaluating GC prognosis.

Research methods

Immunohistochemical staining was used to detect the expression of NPAS2 protein in GC and adjacent tissues. Univariate and multivariate Cox regression analysis was used to determine the independent prognostic factors of GC, and a nomogram prediction model was established. The receiver operating characteristic curve and area under the curve, the calibration curve, and C-index were used to evaluate the predictive effectiveness of the model.

Research results

The NPAS2 expression were independent prognostic factors of overall survival in GC patients for 3 years.

Research conclusions

NPAS2 is highly expressed in GC and is closely related to worse overall survival in patients. Therefore, the evaluation of NPAS2 expression may be a potential marker for GC prognosis evaluation.

Research perspectives

Based on NPAS2 expression, clinicians can predict patient prognosis and guide clinical decision making and follow up.

FOOTNOTES

Author contributions: Cao XM and Kang WD contributed equally to this work and share first authorship; Cao XM, Kang WD, and Liu HB designed the project and reviewed and edited the manuscript; Cao XM and Kang WD analyzed the data and wrote the main manuscripts; Xia TH and Yuan SB carried out research selection and data collection; Guo CA, Wang WJ and Liu HB participated in the discussion of classification criteria.

Institutional review board statement: The studies involving human participants were reviewed and approved by Medical Ethics Committee of the Second Hospital of Lanzhou University, approval No. 2021A-561. The patients/participants provided written informed consent to participate in this study.

Informed consent statement: The Medical Ethics Committee of the Second Hospital of Lanzhou University waived the need for informed consent due to the retrospective nature of the study.

Conflict-of-interest statement: The authors declare no conflict of interest.

Country/Territory of origin: China

ORCID number: Hong-Bin Liu 0000-0003-3668-6166.

S-Editor: Yan JP
L-Editor: A
P-Editor: Chen YX

REFERENCES

1 **Ferlay J**, Colombet M, Soerjomataram I, Parkin DM, Piñeros M, Znaor A, Bray F. Cancer statistics for the year 2020: An overview. *Int J Cancer* 2021 [PMID: 33818764 DOI: 10.1002/ijc.33588]
2 **Sung H**, Ferlay J, Siegel RL, Laversanne M, Soerjomataram I, Jemal A, Bray F. Global Cancer Statistics 2020: GLOBOCAN Estimates of Incidence and Mortality Worldwide for 36 Cancers in 185 Countries. *CA Cancer J Clin* 2021; **71**: 209-249 [PMID: 33538338 DOI: 10.3322/caac.21660]
3 **Lei ZN**, Teng QX, Tian Q, Chen W, Xie Y, Wu K, Zeng Q, Zeng L, Pan Y, Chen ZS, He Y. Signaling pathways and therapeutic interventions in gastric cancer. *Signal Transduct Target Ther* 2022; **7**: 358 [PMID: 36209270 DOI: 10.1038/s41392-022-01190-w]
4 **Ugai T**, Sasamoto N, Lee HY, Ando M, Song M, Tamimi RM, Kawachi I, Campbell PT, Giovannucci EL, Weiderpass E, Rebbeck TR, Ogino S. Is early-onset cancer an emerging global epidemic? Current evidence and future implications. *Nat Rev Clin Oncol* 2022; **19**: 656-673 [PMID: 36068272 DOI: 10.1038/s41571-022-00672-8]
5 **Gwee YX**, Chia DKA, So J, Ceelen W, Yong WP, Tan P, Ong CJ, Sundar R. Integration of Genomic Biology Into Therapeutic Strategies of Gastric Cancer Peritoneal Metastasis. *J Clin Oncol* 2022; **40**: 2830 [PMID: 35649219 DOI: 10.1200/JCO.21.02745]
6 **Shostak A**. Circadian Clock, Cell Division, and Cancer: From Molecules to Organism. *Int J Mol Sci* 2017; **18** [PMID: 28425940 DOI: 10.3390/ijms18040873]
7 **Milev NB**, Reddy AB. Circadian redox oscillations and metabolism. *Trends Endocrinol Metab* 2015; **26**: 430-437 [PMID: 26113283 DOI: 10.1016/j.tem.2015.05.012]
8 **Franzoni A**, Markova-Car E, Dević-Pavlić S, Jurišić D, Puppin C, Mio C, De Luca M, Petruz G, Damante G, Pavelić SK. A polymorphic GGC repeat in the NPAS2 gene and its association with melanoma. *Exp Biol Med (Maywood)* 2017; **242**: 1553-1558 [PMID: 28799406 DOI: 10.1177/1535370217724093]
9 **Liu H**, Gao Y, Hu S, Fan Z, Wang X, Li S. Bioinformatics Analysis of Differentially Expressed Rhythm Genes in Liver Hepatocellular Carcinoma. *Front Genet* 2021; **12**: 680528 [PMID: 34149816 DOI: 10.3389/fgene.2021.680528]
10 **Sancar A**, Van Gelder RN. Clocks, cancer, and chronochemotherapy. *Science* 2021; **371** [PMID: 33384351 DOI: 10.1126/science.abb0738]
11 **Chen W**, Zheng R, Baade PD, Zhang S, Zeng H, Bray F, Jemal A, Yu XQ, He J. Cancer statistics in China, 2015. *CA Cancer J Clin* 2016; **66**: 115-132 [PMID: 26808342 DOI: 10.3322/caac.21338]
12 **Renthlei Z**, Gurumayum T, Borah BK, Trivedi AK. Daily expression of clock genes in central and peripheral tissues of tree sparrow (Passer montanus). *Chronobiol Int* 2019; **36**: 110-121 [PMID: 30365349 DOI: 10.1080/07420528.2018.1523185]
13 **Roenneberg T**, Merrow M. The Circadian Clock and Human Health. *Curr Biol* 2016; **26**: R432-R443 [PMID: 27218855 DOI: 10.1016/j.cub.2016.04.011]
14 **Zhang J**, Lv H, Ji M, Wang Z, Wu W. Low circadian clock genes expression in cancers: A meta-analysis of its association with clinicopathological features and prognosis. *PLoS One* 2020; **15**: e0233508 [PMID: 32437452 DOI: 10.1371/journal.pone.0233508]

15 **Qiu MJ**, Liu LP, Jin S, Fang XF, He XX, Xiong ZF, Yang SL. Research on circadian clock genes in common abdominal malignant tumors. *Chronobiol Int* 2019; **36**: 906-918 [PMID: 31014126 DOI: 10.1080/07420528.2018.1477792]

16 **Yuan P**, Li J, Zhou F, Huang Q, Zhang J, Guo X, Lyu Z, Zhang H, Xing J. NPAS2 promotes cell survival of hepatocellular carcinoma by transactivating CDC25A. *Cell Death Dis* 2017; **8**: e2704 [PMID: 28333141 DOI: 10.1038/cddis.2017.131]

17 **Song B**, Chen Y, Liu Y, Wan C, Zhang L, Zhang W. NPAS2 regulates proliferation of acute myeloid leukemia cells *via* CDC25A-mediated cell cycle progression and apoptosis. *J Cell Biochem* 2019; **120**: 8731-8741 [PMID: 30536616 DOI: 10.1002/jcb.28160]

18 **Kiessling S**, Beaulieu-Laroche L, Blum ID, Landgraf D, Welsh DK, Storch KF, Labrecque N, Cermakian N. Enhancing circadian clock function in cancer cells inhibits tumor growth. *BMC Biol* 2017; **15**: 13 [PMID: 28196531 DOI: 10.1186/s12915-017-0349-7]

19 **Nagata C**, Tamura T, Wada K, Konishi K, Goto Y, Nagao Y, Ishihara K, Yamamoto S. Sleep duration, nightshift work, and the timing of meals and urinary levels of 8-isoprostane and 6-sulfatoxymelatonin in Japanese women. *Chronobiol Int* 2017; **34**: 1187-1196 [PMID: 28933565 DOI: 10.1080/07420528.2017.1355313]

20 **Gao LW**, Wang GL. Comprehensive bioinformatics analysis identifies several potential diagnostic markers and potential roles of cyclin family members in lung adenocarcinoma. *Onco Targets Ther* 2018; **11**: 7407-7415 [PMID: 30425528 DOI: 10.2147/OTT.S171705]

21 **Iyyanki T**, Zhang B, Wang Q, Hou Y, Jin Q, Xu J, Yang H, Liu T, Wang X, Song F, Luan Y, Yamashita H, Chien R, Lyu H, Zhang L, Wang L, Warrick J, Raman JD, Meeks JJ, DeGraff DJ, Yue F. Subtype-associated epigenomic landscape and 3D genome structure in bladder cancer. *Genome Biol* 2021; **22**: 105 [PMID: 33858483 DOI: 10.1186/s13059-021-02325-y]

22 **Yu CC**, Chen LC, Chiou CY, Chang YJ, Lin VC, Huang CY, Lin IL, Chang TY, Lu TL, Lee CH, Huang SP, Bao BY. Genetic variants in the circadian rhythm pathway as indicators of prostate cancer progression. *Cancer Cell Int* 2019; **19**: 87 [PMID: 30996687 DOI: 10.1186/s12935-019-0811-4]

23 **Yuan P**, Yang T, Mu J, Zhao J, Yang Y, Yan Z, Hou Y, Chen C, Xing J, Zhang H, Li J. Circadian clock gene NPAS2 promotes reprogramming of glucose metabolism in hepatocellular carcinoma cells. *Cancer Lett* 2020; **469**: 498-509 [PMID: 31765736 DOI: 10.1016/j.canlet.2019.11.024]

24 **He Y**, Wang G, Wang Q, Zhao Z, Gan L, Yang S, Wang Y, Guo S, An J, Zhang J, Zhang Z, Zhou F. Genetic variants in NPAS2 gene and clinical outcomes of resectable non-small-cell lung cancer. *Future Oncol* 2021; **17**: 795-805 [PMID: 33541123 DOI: 10.2217/fon-2020-0211]

25 **Mukhopadhyay NK**, Ferdinand AS, Mukhopadhyay L, Cinar B, Lutchman M, Richie JP, Freeman MR, Liu BC. Unraveling androgen receptor interactomes by an array-based method: discovery of proto-oncoprotein c-Rel as a negative regulator of androgen receptor. *Exp Cell Res* 2006; **312**: 3782-3795 [PMID: 17011549 DOI: 10.1016/j.yexcr.2006.07.017]

26 **Yang SL**, Ren QG, Wen L, Hu JL, Wang HY. Research progress on circadian clock genes in common abdominal malignant tumors. *Oncol Lett* 2017; **14**: 5091-5098 [PMID: 29113149 DOI: 10.3892/ol.2017.6856]

27 **LeVan TD**, Xiao P, Kumar G, Kupzyk K, Qiu F, Klinkebiel D, Eudy J, Cowan K, Berger AM. Genetic Variants in Circadian Rhythm Genes and Self-Reported Sleep Quality in Women with Breast Cancer. *J Circadian Rhythms* 2019; **17**: 6 [PMID: 31303884 DOI: 10.5334/jcr.184]

28 **Lu J**, Zheng ZF, Xie JW, Wang JB, Lin JX, Chen QY, Cao LL, Lin M, Tu RH, Huang CM, Zheng CH, Li P. Is the 8th Edition of the AJCC TNM Staging System Sufficiently Reasonable for All Patients with Noncardia Gastric Cancer? A 12,549-Patient International Database Study. *Ann Surg Oncol* 2018; **25**: 2002-2011 [PMID: 29725896 DOI: 10.1245/s10434-018-6447-0]

World Journal of Gastroenterology

Submit a Manuscript: https://www.f6publishing.com

World J Gastroenterol 2023 June 21; 29(23): 3658-3667

DOI: 10.3748/wjg.v29.i23.3658

ISSN 1007-9327 (print) ISSN 2219-2840 (online)

ORIGINAL ARTICLE

Retrospective Study

SGK3 overexpression correlates with a poor prognosis in endoscopically resected superficial esophageal squamous cell neoplasia: A long-term study

Ning Xu, Long-Song Li, Hui Li, Li-Hua Zhang, Nan Zhang, Peng-Ju Wang, Ya-Xuan Cheng, Jing-Yuan Xiang, En-Qiang Linghu, Ning-Li Chai

Specialty type: Gastroenterology and hepatology

Provenance and peer review: Unsolicited article; Externally peer reviewed.

Peer-review model: Single blind

Peer-review report's scientific quality classification

Grade A (Excellent): 0
Grade B (Very good): B, B
Grade C (Good): 0
Grade D (Fair): 0
Grade E (Poor): 0

P-Reviewer: Hwang GS, South Korea; Tsai NM, Taiwan

Received: February 24, 2023
Peer-review started: February 24, 2023
First decision: March 14, 2023
Revised: March 20, 2023
Accepted: May 23, 2023
Article in press: May 23, 2023
Published online: June 21, 2023

Ning Xu, Long-Song Li, Nan Zhang, Peng-Ju Wang, Ya-Xuan Cheng, Jing-Yuan Xiang, En-Qiang Linghu, Ning-Li Chai, Senior Department of Gastroenterology, The First Medical Center of PLA General Hospital, Beijing 100853, China

Hui Li, Department of Gastroenterology, Air Force Medical Center, Beijing 100142, China

Li-Hua Zhang, Department of Pathology, The Fourth Medical Center of PLA General Hospital, Beijing 100142, China

Corresponding author: Ning-Li Chai, MD, PhD, Chief Doctor, Senior Department of Gastroenterology, The First Medical Center of PLA General Hospital, No. 28 Fuxing Road, Haidian District, Beijing 100853, China. chainingli@vip.163.com

Abstract

BACKGROUND

The expression status of serum and glucocorticoid-induced protein kinase 3 (SGK3) in superficial esophageal squamous cell neoplasia (ESCN) remains unknown.

AIM

To evaluate the SGK3 overexpression rate in ESCN and its influence on the prognosis and outcomes of patients with endoscopic resection.

METHODS

A total of 92 patients who had undergone endoscopic resection for ESCN with more than 8 years of follow-up were enrolled. Immunohistochemistry was used to evaluate SGK3 expression.

RESULTS

SGK3 was overexpressed in 55 (59.8%) patients with ESCN. SGK3 overexpression showed a significant correlation with death (P = 0.031). Overall survival and disease-free survival rates were higher in the normal SGK3 expression group than in the SGK3 overexpression group (P = 0.013 and P = 0.004, respectively). Cox regression analysis models demonstrated that SGK3 overexpression was an independent predictor of poor prognosis in ESCN patients (hazard ratio 4.729;

95% confidence interval: 1.042-21.458).

CONCLUSION
SGK3 overexpression was detected in the majority of patients with endoscopically resected ESCN and was significantly associated with shortened survival. Thus, it might be a new prognostic factor for ESCN.

Key Words: Superficial esophageal squamous cell neoplasia; Serum and glucocorticoid-induced protein kinase; Endoscopic submucosal dissection; Immunohistochemistry; Overall survival

Core Tip: This study demonstrated that the expression status of serum and glucocorticoid-induced protein kinase 3 (SGK3) was high in the majority of patients with superficial esophageal squamous cell neoplasia (ESCN) and that high expression of SGK3 predicts a poor prognosis. These findings provide a new prognostic factor for ESCN.

Citation: Xu N, Li LS, Li H, Zhang LH, Zhang N, Wang PJ, Cheng YX, Xiang JY, Linghu EQ, Chai NL. SGK3 overexpression correlates with a poor prognosis in endoscopically resected superficial esophageal squamous cell neoplasia: A long-term study. *World J Gastroenterol* 2023; 29(23): 3658-3667
URL: https://www.wjgnet.com/1007-9327/full/v29/i23/3658.htm
DOI: https://dx.doi.org/10.3748/wjg.v29.i23.3658

INTRODUCTION

Esophageal cancer remains a leading cause of cancer-related death, and the incidence rates of esophageal cancer worldwide are increasing[1]. Esophageal squamous cell carcinoma (ESCC) accounts for the majority of esophageal cancer cases[2]. It is usually detected at an advanced stage after the symptoms of dysphagia appear[3]. Thus, its prognosis is the worst among digestive carcinomas[4]. Early detection of the malignant epithelium at an early stage followed by endoscopic resection has become the most effective way to improve clinical outcomes[5]. However, the prognosis of patients with superficial esophageal squamous cell neoplasia (ESCN) remains poor[6,7].

The serum and glucocorticoid-induced protein kinase (SGK) family consists of three isoforms (SGK1, SGK2 and SGK3), and they regulate a range of fundamental cellular processes, such as tumor growth, metastasis, autophagy and survival[8]. SGK is a ubiquitously expressed serine/threonine kinase and plays an active role in a multitude of pathophysiological conditions[9]. It is activated by insulin and growth factors *via* phosphatidylinositol 3-kinase (PI3K) and is frequently altered in human cancers, including breast cancer and hepatocellular carcinoma[10,11]. Although SGK1, SGK2 and SGK3 share a highly similar domain, the lack of a plasma membrane-targeting domain indicates nonoverlapping functions[12].

Previous studies have shown that SGK3 is expressed in all tissues tested thus far and is especially highly expressed in the heart and spleen[13]. Encoded by chromosome 8q12.2, SGK3 is known as a downstream factor of PI3K signaling and has been reported to play a pivotal role in the development and progression of diverse cancers[14]. Therefore, it has been regarded as a potential target for cancer intervention[15]. However, a minority of studies have evaluated the impact of SGK3 expression on clinical outcomes, and the expression of SGK3 in ESCN has not been investigated[16]. Whether SGK3 is associated with the prognosis of ESCN remains unknown. Herein, we assessed the SGK3 expression levels of patients with ESCN *via* immunohistochemistry (IHC) to investigate the possible role of SGK3 as a prognostic factor.

MATERIALS AND METHODS

Patients

Patients who underwent gastrointestinal endoscopy followed by endoscopic submucosal dissection (ESD) between November 2009 and July 2011 at the First Medical Center of PLA General Hospital were included. The inclusion criteria were as follows: (1) Patients were diagnosed with primary ESCN; (2) the histological type of tumor was ESCN; and (3) the tumor penetrated the submucosal layer < 200 μm or 200 μm from the muscularis mucosa. The exclusion criteria were as follows: (1) ESCN was previously

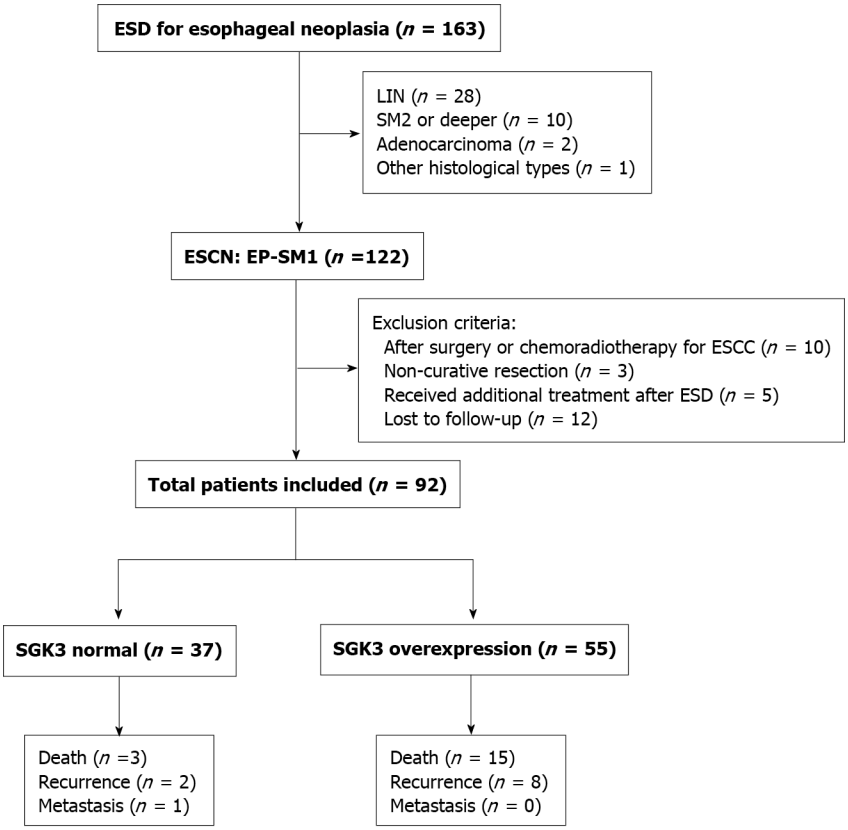

DOI: 10.3748/wjg.v29.i23.3658

Figure 1 Study flow chart. ESD: Endoscopic submucosal dissection; LIN: Low-grade intraepithelial neoplasia; SM2: Penetration of the submucosal layer > 200 μm from the muscularis mucosa; ESCN: Esophageal squamous cell neoplasia; ESCC: Esophageal squamous cell carcinoma; EP: Epithelium; SM1: Penetration of the submucosal layer < 200 μm or 200 μm from the muscularis mucosa; SGK3: Serum and glucocorticoid-induced protein kinase 3.

treated with surgery or chemoradiotherapy ESCN; (2) pathological evaluation post-ESD indicated noncurative resection; (3) patients received additional treatment immediately after ESD; and (4) incomplete follow-up. All follow-up data were obtained at least 8 years after the first detection of the tumor. Eventually, 92 patients with complete follow-up data were included in the analysis (Figure 1). This study was approved by the Ethics Board of the First Medical Center of PLA General Hospital (approval No. S2020-251-01).

ESD procedure

All procedures were performed under general anesthesia by experienced endoscopists. A single-channel upper gastrointestinal endoscope (GIF-Q230; Olympus, Tokyo, Japan) was used during the procedure. The standard ESD is described as follows: the lesions were detected on endoscopy under white light or narrow band imaging, lesion margins were shown by iodine staining, argon plasma coagulation (ERBE Elektromedizin GmbH) was used to mark 5 mm outside the boundary of the lesion, submucosal circumferential injection was performed to lift the lesions, and submucosal dissection followed by a circumferential mucosal incision was performed to remove the lesion.

Pathological examination

Tissue specimens were fixed in formalin. All samples were subjected to histological analysis of differentiation type, depth of invasion, and lymphovascular invasion. Lymphovascular invasion was recognized as any invasion using hematoxylin and eosin staining. Curative resection was defined as complete resection of a mucosal lesion with no lymphovascular invasion, and noncurative resection implied a pathologically positive margin or clinically incomplete resection.

IHC

For IHC, we used a rabbit anti-human SGK3 antibody (Roche Diagnostics Japan. Tokyo, Japan) and 4-μm-thick sections. All sections were deparaffinized in xylene 3 times and rehydrated in a graded series of ethanol with decreasing concentrations. Then, we used Tris-buffered saline (pH 7.4) for rinsing. Heat-induced epitope retrieval was conducted by immersing the slides in Coplin jars filled with 10 mmol/L citrate buffer (pH 6.0) and microwaving the buffer for 25 min. The jars were then cooled for 20 min. The reaction products were visualized with diaminobenzidine and counterstained with hematoxylin. Two

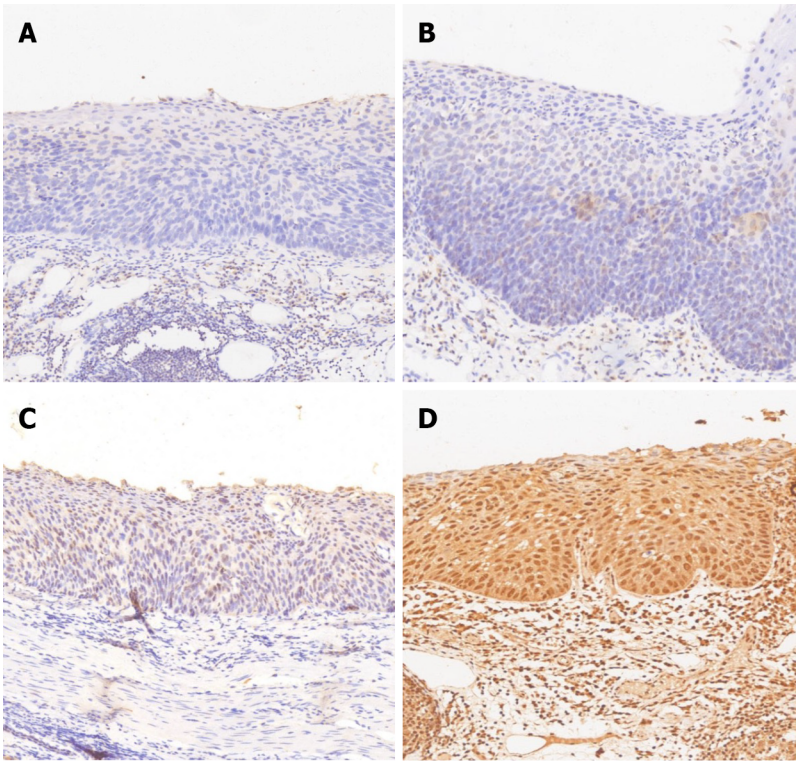

DOI: 10.3748/wjg.v29.i23.3658

Figure 2 Serum and glucocorticoid-induced protein kinase 3 protein expression in superficial esophageal squamous cell neoplasia (magnification: × 400). A: No serum and glucocorticoid-induced protein kinase 3 (SGK3) expression in esophageal squamous cell neoplasia (ESCN) samples (normal for SGK3 overexpression; 0); B: Weak SGK3 expression in ESCN samples (normal for SGK3 overexpression; 1+); C: Moderate SGK3 expression in ESCN samples (positive for SGK3 overexpression; 2+); D: Strong SGK3 expression in ESCN samples (positive for SGK3 overexpression; 3+).

experienced pathologists independently judged the immunostaining intensity. The staining intensity was graded based on the American Society of Clinical Oncology/College of American Pathology guidelines[17]. The criteria were as follows: 0 = no nuclear staining in tumor cells; 1+ = weak (staining in less than 10% of cells); 2+ = intense complete staining (up to 30% of tumor cells); and 3+ = uniform intense staining (more than 30% of tumor cells). The expression status of SGK3 was classified into 2 groups: normal (0 and 1+) and overexpression (2+ and 3+) (Figure 2).

Clinicopathologic parameters and definitions

In each case, clinicopathologic parameters were retrospectively obtained from the pathological results of our hospital. Basic clinical parameters included age, sex, smoking history and family history of cancer. The longest diameter of the lesion in the specimen was defined as the tumor size. Tumor location was categorized as upper thoracic, middle thoracic and lower thoracic. Based on the histological outcome, tumors were characterized into low-grade intraepithelial neoplasia, high-grade intraepithelial neoplasia, well-differentiated squamous cell carcinoma, intermediate differentiated squamous cell carcinoma, and poorly differentiated squamous cell carcinoma. The T stage of the tumor was categorized based on the 11th Japanese classification of esophageal cancer[18]. Tumors limited to the epithelium and tumors that invaded into the submucosa ≤ 200 or > 200 μm from the muscularis mucosae were classified as EP, submucosa 1 (SM1) or submucosa 2 (SM2), respectively. The two recurrence patterns, metachronous recurrence and metastatic recurrence, were both included in this study, and tumor recurrence was identified using endoscopy and histological biopsy. Tumor recurrence was defined as an ESCN or cancerous lesion detected on the esophagus during the follow-up period. Lymph node or distant metastasis was evaluated by contrast-enhanced computed tomography scan or magnetic resonance imaging and verified *via* histological examination of the biopsy.

Prognostic outcomes

The follow-up of patient survival status and cancer recurrence was completed in July 2022. Prognostic outcomes were obtained by calling patients themselves or asking the family members for the recorded death certificate of the patients. Two main variables were assessed: Overall survival (OS) and disease-free survival (DFS). OS was defined as the time that elapsed from the date of endoscopic treatment to the date of death from any cause. DFS was defined as the duration between the endoscopic treatment and any disease recurrence or any cause of death, whichever occurred first.

Statistical analysis

Continuous variables are expressed as the mean ± SD or median (interquartile range) and were compared using Student's *t* test. Categorical variables are expressed as percentages and were compared using the chi-square test or Fisher's exact test. Multivariate Cox regression was used to further analyze the relationship between SGK3 overexpression and clinical outcomes, and the covariates were screened using stepwise regression. The extended-model method was used to conduct covariate correction: Model 1 was corrected based on SGK3 expression status; Model 2 = model 1 + (age and gender); Model 3 = model 2 + (smoking history + family history of cancer); and Model 4 = model 3 + (tumor location + tumor size + T stage + differentiated types). Multicollinearity was tested using the variance inflation factor (VIF) method, and a VIF ≥ 10 was considered to indicate severe multicollinearity. Kaplan-Meier analysis was used to establish the survival curves based on each prognostic outcome. Survival curves were graphed using GraphPad Prism 8. A P value < 0.05 in the two-tailed tests was considered to indicate statistical significance. All statistical analyses were performed using SPSS 26.0 (SPSS, Inc., Chicago, IL, United States).

RESULTS

Baseline characteristics of patients with ESCN

A total of 92 patients aged 43 to 80 years were finally included in our study. Table 1 lists the baseline characteristics of the normal SGK3 expression group and the SGK3 overexpression group. The normal SGK3 expression group included 37 patients and consisted of 27 males and 10 females. There were 55 patients (36 males and 19 females) in the SGK3 overexpression group. No significant differences were observed in the baseline indicators (age, sex, tumor location, tumor size, T stage, differentiated types, smoking history, lymphovascular infiltration and family history of cancer) between the normal expression and overexpression groups.

Prognostic outcomes

Table 2 summarizes the prognostic outcomes in each group. Tumor recurrence occurred in 10 patients. Of these patients, 2 (5.4%) were in the normal SGK3 expression group, and 8 (14.5%) were in the SGK3 overexpression group. Metastasis was detected in only 1 patient in the normal SGK3 expression group during the follow-up period. No significant associations were observed between SGK3 expression and tumor recurrence and metastasis. Death occurred in 3 (8.1%) patients in the normal SGK3 expression group and 15 (27.3%) patients in the SGK3 overexpression group. A significant correlation was observed between SGK3 expression status and death (P = 0.031).

SGK3 expression is related to prognostic outcomes

To evaluate the association between SGK3 overexpression and OS, a multivariate Cox regression model was performed (Table 3): Model 1 [hazard ratio (HR) 4.243; 95% confidence interval (CI): 1.219-14.773], Model 2 (HR 3.648; 95%CI: 1.030-12.917), Model 3 (HR 3.637; 95%CI: 1.028-12.866), and Model 4 (HR 4.729; 95%CI: 1.042-21.458). The P value of all four models was less than 0.05. The results of the multicollinearity test showed an average VIF of 1.525 (all VIF < 10). Figure 3 show the Kaplan-Meier curves of the relationship between SGK3 expression status and OS and DFS, respectively. The OS and DFS rates of patients were higher in the normal SGK3 expression group than in the SGK3 overexpression group during the follow-up period (P = 0.013 and P = 0.004, respectively).

DISCUSSION

The SGK family is widely dysregulated in numerous human cancers and plays a vital role in tumor development and progression[19]. Among the three members of this family, SGK1 has been well researched, and its correlation with clinical outcomes has been reported in some cancers[20]. It has been suggested that low SGK1 expression in some tumors might induce feedback inhibition by activating the AKT pathway and might result in high SGK3 expression[21]. However, due to the later detection of SGK3, its relationship with tumors or other diseases has been revealed in only a few studies[22,23]. For instance, SGK3, as a novel regulator of renal phosphate transport, is associated with autosomal dominant hypophosphatemic rickets[24,25]. Its relationship with the clinical prognosis of tumors has rarely been reported thus far.

SGK3 exhibits structural and sequence similarity to the AKT family[26]. Its activation is mediated by the PI3K pathway and requires phosphorylation at two regulatory sites, Thr-320 and Ser-486[27]. Deletion of Thr-320 of SGK3 or disruption of the SGK3 protein tertiary structure yields nonfunctional proteins. To our knowledge, the SGK3 expression status of ESCN has not been illustrated. Our analysis of the expression of SGK3 in 92 ESCN tissues identified the expression status of SGK3 in ESCN tissues. Among the 92 tissue samples, the overexpression rate of SGK3 was close to 60%, confirming its high

Table 1 Basic characteristics according to serum and glucocorticoid-induced protein kinase 3 expression status

Characteristics	SGK3 normal, *n* = 37	SGK3 overexpression, *n* = 55	*P* value
Age (yr, mean ± SD)	58.73 ± 6.81	61.21 ± 8.05	0.118
Sex (male), *n* (%)	27 (73.0)	36 (65.5)	0.447
Tumor location, *n* (%)[1]			0.560
Upper esophagus	4 (10.8)	7 (12.7)	
Middle esophagus	14 (37.8)	26 (47.)	
Lower esophagus	19 (51.4)	22 (40.0)	
Tumor size (cm, mean ± SD)	3.16 ± 1.94	3.30 ± 1.89	0.742
Tumor stage, *n* (%)			0.720
Tis	25 (67.6)	38 (69.1)	
T1a	6 (16.2)	11 (20.0)	
T1b	6 (16.2)	6 (10.9)	
Differentiated types[1], *n* (%)			0.487
HIN	25 (67.6)	39 (70.9)	
Well-differentiation	7 (18.9)	13 (23.6)	
Intermediate differentiation	2 (5.4)	2 (3.6)	
Poor differentiation	3 (8.1)	1 (1.8)	
Smoking history, *n* (%)			0.313
Yes	10 (27.0)	10 (18.2)	
No	27 (73.0)	45 (81.8)	
Lymphovascular infiltration, *n* (%)[1]			0.402
Present	1 (2.7)	0 (0)	
Absent	36 (97.3)	55 (100)	
Family history of cancer[1], *n* (%)			0.698
Yes	2 (5.4)	5 (9.1)	
No	35 (94.6)	50 (90.9)	

[1]Tested by Fisher exact test.
SGK3: Serum and glucocorticoid-induced protein kinase 3; HIN: High-grade intraepithelial neoplasia.

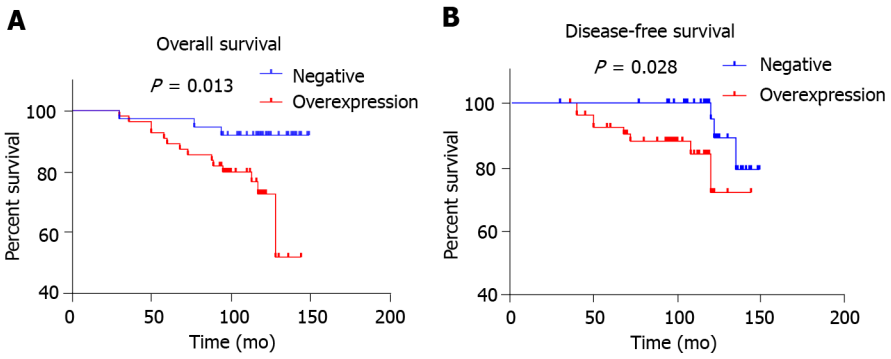

DOI: 10.3748/wjg.v29.i23.3668

Figure 3 Kaplan-Meier curves for overall survival and disease-free survival. A: Overall survival; B: Disease-free survival.

Table 2 Prognosis outcomes in the serum and glucocorticoid-induced protein kinase 3 normal and overexpression groups

Prognosis factors, *n* (%)	SGK3 normal, *n* = 37	SGK3 overexpression, *n* = 55	*P* value
Tumor recurrence[1], *n* (%)			0.306
Present	2 (5.4)	8 (14.5)	
Absent	35 (94.6)	47 (85.5)	
Metastasis[1], *n* (%)			0.402
Present	1 (2.7)	0 (0)	
Absent	36 (97.3)	55 (100)	
Death[1], *n* (%)			0.031
Yes	3 (8.1)	15 (27.3)	
No	34 (91.9)	40 (72.7)	

[1]Tested by Fisher exact test.
SGK3: Serum and glucocorticoid-induced protein kinase 3.

Table 3 Hazard ratio (95% confidence interval) for all-cause mortality between serum and glucocorticoid-induced protein kinase 3 normal and serum and glucocorticoid-induced protein kinase 3 overexpression

Model	HR (95%CI)	*P* value
Model 1	4.243 (1.219-14.773)	0.023
Model 2	3.648 (1.030-12.917)	0.045
Model 3	3.637 (1.028-12.866)	0.045
Model 4	4.729 (1.042-21.458)	0.044

Adjusted covariates: Model 1 = serum and glucocorticoid-induced protein kinase 3; Model 2 = model 1 + (age + sex); Model 3 = model 2 + (smoking history + family history of cancer); Model 4 = model 3 + (tumor location + tumor size + T stage + differentiated types). HR: Hazard ratio; CI: Confidence interval.

expression in esophageal neoplasia tissues. However, the defined functions of SGK3 in the growth or progression of ESCN have not been clarified.

ESCC is the most common pathological type of esophageal cancer and has a high incidence in some districts of China. It is difficult to detect at the early stage because its symptoms are insidious, and the majority of patients seek medical help when advanced symptoms of significant dysphagia occur. As a consequence, the traditional treatment of ESCN is mainly based on a combination of open surgery and chemotherapy/radiotherapy. Progress in imaging modalities and multidisciplinary comprehensive treatment has improved early diagnosis and clinical outcomes, respectively. However, the 5-year survival rate for ESCC is still lower than 30% because of its invasiveness and metastatic ability[28,29]. Recently, the development of endoscopy techniques has transformed the early diagnosis and treatment of diseases of the entire digestive system. In particular, the introduction of amplification techniques and narrow band imaging enables endoscopists to detect neoplasia at an early stage or in an asymptomatic period. In addition, the minimally invasive removal of lesions by ESD improves the clinical prognosis and even the quality of life. Although the 5-year survival rate of patients who undergo ESD is higher than that of patients who undergo open surgery, death caused by tumor recurrence or other reasons still occurs in some patients during the follow-up period[30]. This research focused on further exploration of ways to improve the survival rates of these patients.

The integration of small datasets in the present study demonstrated the high expression level of SGK3 in ESCN, as well as a significant relationship between its overexpression and OS. Furthermore, the 4 regression models showed that after adjusting for confounding factors, only the expression status of SGK3 was significantly associated with increased mortality. All these results indicate that the overexpression of SGK3 is correlated with the occurrence of death in ESCN patients. However, the influence of SGK3 on the occurrence and development of ESCN or cell cycle pathways has not yet been determined. Based on the results of our study, we speculate that SGK3 can be used as a prognostic indicator to assist in the outcome assessment of ESCN patients.

At present, follow-up of post-ESD patients with ESCN is generally performed *via* endoscopy as well as biopsy. The application of a standard follow-up method might aid endoscopists in identifying tumor recurrence in time, but this is only effective when endoscopists can detect the recurrence of cancerous

lesions followed by accurate biopsy sampling. Otherwise, no further action could be taken to intervene. As the overexpression of SGK3 is an independent factor in prognosis, IHC staining of SGK3 could be used to identify the population with a high mortality risk. Thus, active measures, including shortening the follow-up intervals and using moderate radiotherapy or chemotherapy, can be taken to improve survival.

However, our current study has several limitations. First, the sample size of our study was small, and all the included patients came from one hospital. Thus, these results need to be validated by expanding the sample size and performing a multicenter study. Second, this was a retrospective study. Therefore, we could not collect information without data bias. Thus, a prospective study, similar to this study, is needed in the future to verify the relationship between SGK3 overexpression and mortality.

CONCLUSION

In conclusion, SGK3 overexpression is significantly correlated with shortened survival in patients with endoscopic resection of superficial ESCN, and SGK3 might be a useful indicator for prognosis evaluation. Further studies are warranted to determine its mechanisms of action in the growth or progression of ESCN.

ARTICLE HIGHLIGHTS

Research background

Serum and glucocorticoid-induced protein kinase 3 (SGK3) regulate a range of fundamental cellular processes, such as tumor growth, metastasis, autophagy and survival, but SGK3 expression levels in patients with esophageal squamous cell neoplasia (ESCN) and their relationship with the prognosis of ESCN remain unknown.

Research motivation

SGK3 expression levels in patients with ESCN were assessed by immunohistochemistry to investigate the possible role of SGK3 as a prognostic factor.

Research objectives

Ninety-two patients who underwent gastrointestinal endoscopy followed by endoscopic submucosal dissection with complete follow-up data between November 2009 and July 2011 were included.

Research methods

A total of 92 patients who had undergone endoscopic resection for ESCN with more than 8 years of follow-up were enrolled. Immunohistochemistry was used to evaluate SGK3 expression.

Research results

Death occurred in 3 (8.1%) patients in the normal SGK3 expression group and 15 (27.3%) patients in the SGK3 overexpression group. A significant correlation was observed between SGK3 status and death (P = 0.031). The overall survival and disease-free survival rates of patients were higher in the normal SGK3 expression group than in the SGK3 overexpression group during the follow-up period.

Research conclusions

All these results indicate that the overexpression of SGK3 is correlated with the occurrence of death in ESCN patients and that SGK3 might be a useful indicator for prognosis evaluation.

Research perspectives

The sample size of this study was small, and the subjects both came from one hospital. Thus, the results need to be validated by expanding the sample size and performing a multicenter study. A prospective study, similar to this study, is needed in the future to verify the relationship between SGK3 overexpression and mortality.

FOOTNOTES

Author contributions: Xu N and Li LS contributed equally to this manuscript; Chai NL and Xu N contributed to manuscript drafting; Xu N and Li LS wrote the manuscript; Li H, Zhang LH collected the pathological data; Xiang JY, Zhang N, Wang PJ and Cheng YX were responsible for the revision of the manuscript for significant content; Chai NL and Linghu EQ reviewed the literature; all authors issued final approval for the version to be submitted.

Supported by National Natural Science Foundation of China, No. 82070682; and Beijing Municipal Science and Technology Commission, China, No. Z181100001718177.

Institutional review board statement: This study was approved by the Ethics Board of the First Medical Center of PLA General Hospital (approval No. S2020-251-01).

Informed consent statement: Patients were not required to give informed consent to the study because the analysis used anonymous clinical data that were obtained after each patient agreed to treatment by written consent.

Conflict-of-interest statement: There are no conflicts of interest to declare.

Data sharing statement: No additional data are available.

Country/Territory of origin: China

ORCID number: Ning Xu 0000-0002-7770-8731; Long-Song Li 0000-0002-4000-7501; Hui Li 0000-0002-2786-9844; Nan Zhang 0000-0001-9979-539X; Jing-Yuan Xiang 0000-0002-1755-7978; En-Qiang Linghu 0000-0003-4506-7877; Ning-Li Chai 0000-0002-6791-5817.

S-Editor: Yan JP
L-Editor: A
P-Editor: Yan JP

REFERENCES

1 **Wu Y**, Huang F, Zhou X, Yu S, Tang Q, Li S, Wang J, Chen L. Hypoxic Preconditioning Enhances Dental Pulp Stem Cell Therapy for Infection-Caused Bone Destruction. *Tissue Eng Part A* 2016; **22**: 1191-1203 [PMID: 27586636 DOI: 10.1089/ten.tea.2016.0086]
2 **Sánchez-Danés A**, Blanpain C. Deciphering the cells of origin of squamous cell carcinomas. *Nat Rev Cancer* 2018; **18**: 549-561 [PMID: 29849070 DOI: 10.1038/s41568-018-0024-5]
3 **van Rossum PSN**, Mohammad NH, Vleggaar FP, van Hillegersberg R. Treatment for unresectable or metastatic oesophageal cancer: current evidence and trends. *Nat Rev Gastroenterol Hepatol* 2018; **15**: 235-249 [PMID: 29235549 DOI: 10.1038/nrgastro.2017.162]
4 **Cui Y**, Chen H, Xi R, Cui H, Zhao Y, Xu E, Yan T, Lu X, Huang F, Kong P, Li Y, Zhu X, Wang J, Zhu W, Ma Y, Zhou Y, Guo S, Zhang L, Liu Y, Wang B, Xi Y, Sun R, Yu X, Zhai Y, Wang F, Yang J, Yang B, Cheng C, Liu J, Song B, Li H, Wang Y, Zhang Y, Cheng X, Zhan Q, Liu Z. Author Correction: Whole-genome sequencing of 508 patients identifies key molecular features associated with poor prognosis in esophageal squamous cell carcinoma. *Cell Res* 2022; **32**: 415-416 [PMID: 35177820 DOI: 10.1038/s41422-022-00625-x]
5 **Pimentel-Nunes P**, Libânio D, Bastiaansen BAJ, Bhandari P, Bisschops R, Bourke MJ, Esposito G, Lemmers A, Maselli R, Messmann H, Pech O, Pioche M, Vieth M, Weusten BLAM, van Hooft JE, Deprez PH, Dinis-Ribeiro M. Endoscopic submucosal dissection for superficial gastrointestinal lesions: European Society of Gastrointestinal Endoscopy (ESGE) Guideline - Update 2022. *Endoscopy* 2022; **54**: 591-622 [PMID: 35523224 DOI: 10.1055/a-1811-7025]
6 **Feng Y**, Wei W, Guo S, Li BQ. Associated risk factor analysis and the prognostic impact of positive resection margins after endoscopic resection in early esophageal squamous cell carcinoma. *Exp Ther Med* 2022; **24**: 457 [PMID: 35747151 DOI: 10.3892/etm.2022.11384]
7 **Yang X**, Men Y, Wang J, Kang J, Sun X, Zhao M, Sun S, Yuan M, Bao Y, Ma Z, Wang G, Hui Z. Additional Radiotherapy With or Without Chemotherapy Following Endoscopic Resection for Stage I Esophageal Carcinoma: A Pilot Study. *Technol Cancer Res Treat* 2021; **20**: 15330338211048051 [PMID: 34657505 DOI: 10.1177/15330338211048051]
8 **Kim J**, Kim D, Jung H, Lee J, Hong VS. Identification and Kinetic Characterization of Serum- and Glucocorticoid-Regulated Kinase Inhibitors Using a Fluorescence Polarization-Based Assay. *SLAS Discov* 2021; **26**: 655-662 [PMID: 33783250 DOI: 10.1177/24725552211002465]
9 **Lang F**, Böhmer C, Palmada M, Seebohm G, Strutz-Seebohm N, Vallon V. (Patho)physiological significance of the serum- and glucocorticoid-inducible kinase isoforms. *Physiol Rev* 2006; **86**: 1151-1178 [PMID: 17015487 DOI: 10.1152/physrev.00050.2005]
10 **Cao H**, Xu Z, Wang J, Cigliano A, Pilo MG, Ribback S, Zhang S, Qiao Y, Che L, Pascale RM, Calvisi DF, Chen X. Functional role of SGK3 in PI3K/Pten driven liver tumor development. *BMC Cancer* 2019; **19**: 343 [PMID: 30975125 DOI: 10.1186/s12885-019-5551-2]
11 **Xu J**, Wan M, He Q, Bassett RL Jr, Fu X, Chen AC, Shi F, Creighton CJ, Schiff R, Huo L, Liu D. SGK3 is associated with estrogen receptor expression in breast cancer. *Breast Cancer Res Treat* 2012; **134**: 531-541 [PMID: 22576469 DOI: 10.1007/s10549-012-2081-x]

12 **Alonso L**, Okada H, Pasolli HA, Wakeham A, You-Ten AI, Mak TW, Fuchs E. Sgk3 links growth factor signaling to maintenance of progenitor cells in the hair follicle. *J Cell Biol* 2005; **170**: 559-570 [PMID: 16103225 DOI: 10.1083/jcb.200504131]

13 **Kobayashi T**, Deak M, Morrice N, Cohen P. Characterization of the structure and regulation of two novel isoforms of serum- and glucocorticoid-induced protein kinase. *Biochem J* 1999; **344** Pt 1: 189-197 [PMID: 10548550 DOI: 10.1042/bj3440189]

14 **Hou M**, Lai Y, He S, He W, Shen H, Ke Z. SGK3 (CISK) may induce tumor angiogenesis (Hypothesis). *Oncol Lett* 2015; **10**: 23-26 [PMID: 26170971 DOI: 10.3892/ol.2015.3182]

15 **Basnet R**, Gong GQ, Li C, Wang MW. Serum and glucocorticoid inducible protein kinases (SGKs): a potential target for cancer intervention. *Acta Pharm Sin B* 2018; **8**: 767-771 [PMID: 30245963 DOI: 10.1016/j.apsb.2018.07.001]

16 **Wang Y**, Zhou D, Phung S, Warden C, Rashid R, Chan N, Chen S. SGK3 sustains ERα signaling and drives acquired aromatase inhibitor resistance through maintaining endoplasmic reticulum homeostasis. *Proc Natl Acad Sci U S A* 2017; **114**: E1500-E1508 [PMID: 28174265 DOI: 10.1073/pnas.1612991114]

17 **Vergara-Lluri ME**, Moatamed NA, Hong E, Apple SK. High concordance between HercepTest immunohistochemistry and ERBB2 fluorescence in situ hybridization before and after implementation of American Society of Clinical Oncology/ College of American Pathology 2007 guidelines. *Mod Pathol* 2012; **25**: 1326-1332 [PMID: 22699517 DOI: 10.1038/modpathol.2012.93]

18 **Japan Esophageal Society**. Japanese Classification of Esophageal Cancer, 11th Edition: part II and III. *Esophagus* 2017; **14**: 37-65 [PMID: 28111536 DOI: 10.1007/s10388-016-0556-2]

19 **Shanmugam I**, Cheng G, Terranova PF, Thrasher JB, Thomas CP, Li B. Serum/glucocorticoid-induced protein kinase-1 facilitates androgen receptor-dependent cell survival. *Cell Death Differ* 2007; **14**: 2085-2094 [PMID: 17932503 DOI: 10.1038/sj.cdd.4402227]

20 **Talarico C**, Dattilo V, D'Antona L, Menniti M, Bianco C, Ortuso F, Alcaro S, Schenone S, Perrotti N, Amato R. SGK1, the New Player in the Game of Resistance: Chemo-Radio Molecular Target and Strategy for Inhibition. *Cell Physiol Biochem* 2016; **39**: 1863-1876 [PMID: 27771704 DOI: 10.1159/000447885]

21 **Lang F**, Perrotti N, Stournaras C. Colorectal carcinoma cells--regulation of survival and growth by SGK1. *Int J Biochem Cell Biol* 2010; **42**: 1571-1575 [PMID: 20541034 DOI: 10.1016/j.biocel.2010.05.016]

22 **Gasser JA**, Inuzuka H, Lau AW, Wei W, Beroukhim R, Toker A. SGK3 mediates INPP4B-dependent PI3K signaling in breast cancer. *Mol Cell* 2014; **56**: 595-607 [PMID: 25458846 DOI: 10.1016/j.molcel.2014.09.023]

23 **Vasudevan KM**, Barbie DA, Davies MA, Rabinovsky R, McNear CJ, Kim JJ, Hennessy BT, Tseng H, Pochanard P, Kim SY, Dunn IF, Schinzel AC, Sandy P, Hoersch S, Sheng Q, Gupta PB, Boehm JS, Reiling JH, Silver S, Lu Y, Stemke-Hale K, Dutta B, Joy C, Sahin AA, Gonzalez-Angulo AM, Lluch A, Rameh LE, Jacks T, Root DE, Lander ES, Mills GB, Hahn WC, Sellers WR, Garraway LA. AKT-independent signaling downstream of oncogenic PIK3CA mutations in human cancer. *Cancer Cell* 2009; **16**: 21-32 [PMID: 19573809 DOI: 10.1016/j.ccr.2009.04.012]

24 **Cebeci AN**, Zou M, BinEssa HA, Alzahrani AS, Al-Rijjal RA, Al-Enezi AF, Al-Mohanna FA, Cavalier E, Meyer BF, Shi Y. Mutation of SGK3, a Novel Regulator of Renal Phosphate Transport, Causes Autosomal Dominant Hypophosphatemic Rickets. *J Clin Endocrinol Metab* 2020; **105** [PMID: 31821448 DOI: 10.1530/ey.18.5.3]

25 **Trepiccione F**, Capasso G. SGK3: a novel regulator of renal phosphate transport? *Kidney Int* 2011; **80**: 13-15 [PMID: 21673735 DOI: 10.1038/ki.2011.60]

26 **Gong GQ**, Wang K, Dai XC, Zhou Y, Basnet R, Chen Y, Yang DH, Lee WJ, Buchanan CM, Flanagan JU, Shepherd PR, Wang MW. Identification, structure modification, and characterization of potential small-molecule SGK3 inhibitors with novel scaffolds. *Acta Pharmacol Sin* 2018; **39**: 1902-1912 [PMID: 30038340 DOI: 10.1038/s41401-018-0087-6]

27 **Pearce LR**, Komander D, Alessi DR. The nuts and bolts of AGC protein kinases. *Nat Rev Mol Cell Biol* 2010; **11**: 9-22 [PMID: 20027184 DOI: 10.1038/nrm2822]

28 **Ohashi S**, Miyamoto S, Kikuchi O, Goto T, Amanuma Y, Muto M. Recent Advances From Basic and Clinical Studies of Esophageal Squamous Cell Carcinoma. *Gastroenterology* 2015; **149**: 1700-1715 [PMID: 26376349 DOI: 10.1053/j.gastro.2015.08.054]

29 **Liang H**, Fan JH, Qiao YL. Epidemiology, etiology, and prevention of esophageal squamous cell carcinoma in China. *Cancer Biol Med* 2017; **14**: 33-41 [PMID: 28443201 DOI: 10.20892/j.issn.2095-3941.2016.0093]

30 **Hirano S**, Nagami Y, Yamamura M, Tanoue K, Sakai T, Maruyama H, Ominami M, Nadatani Y, Fukunaga S, Otani K, Hosomi S, Tanaka F, Kamata N, Taira K, Shiba M, Watanabe T, Fujiwara Y. Evaluation of long-term survival in patients with severe comorbidities after endoscopic submucosal dissection for esophageal squamous cell carcinoma. *Surg Endosc* 2022; **36**: 5011-5022 [PMID: 34748088 DOI: 10.1007/s00464-021-08859-3]

World Journal of Gastroenterology

Submit a Manuscript: https://www.f6publishing.com

World J Gastroenterol 2023 June 21; 29(23): 3668-3677

DOI: 10.3748/wjg.v29.i23.3668

ISSN 1007-9327 (print) ISSN 2219-2840 (online)

ORIGINAL ARTICLE

Retrospective Study

Hot snare polypectomy *vs* endoscopic mucosal resection using bipolar snare for intermediate size colorectal lesions: Propensity score matching

Nobuhisa Minakata, Tatsuro Murano, Masashi Wakabayashi, Maasa Sasabe, Takashi Watanabe, Tomohiro Mitsui, Hiroki Yamashita, Atsushi Inaba, Hironori Sunakawa, Keiichiro Nakajo, Tomohiro Kadota, Kensuke Shinmura, Hiroaki Ikematsu, Tomonori Yano

Specialty type: Gastroenterology and hepatology

Provenance and peer review: Unsolicited article; Externally peer reviewed.

Peer-review model: Single blind

Peer-review report's scientific quality classification

Grade A (Excellent): 0
Grade B (Very good): B, B
Grade C (Good): C
Grade D (Fair): 0
Grade E (Poor): 0

P-Reviewer: Martino A, Italy; Nagami Y, Japan

Received: March 2, 2023
Peer-review started: March 2, 2023
First decision: April 8, 2023
Revised: April 21, 2023
Accepted: May 23, 2023
Article in press: May 23, 2023
Published online: June 21, 2023

Nobuhisa Minakata, Tatsuro Murano, Maasa Sasabe, Takashi Watanabe, Tomohiro Mitsui, Hiroki Yamashita, Atsushi Inaba, Hironori Sunakawa, Keiichiro Nakajo, Tomohiro Kadota, Kensuke Shinmura, Hiroaki Ikematsu, Tomonori Yano, Department of Gastroenterology and Endoscopy, National Cancer Center Hospital East, Kashiwa 2778577, Chiba, Japan

Masashi Wakabayashi, Department of Biostatistics Division, Center for Research Administration and Support, National Cancer Center, Kashiwa 2778577, Chiba, Japan

Corresponding author: Tatsuro Murano, MD, PhD, Doctor, Department of Gastroenterology and Endoscopy, National Cancer Center Hospital East, 6-5-1, Kashiwanoha, Kashiwa 2778577, Chiba, Japan. tatmuran@east.ncc.go.jp

Abstract

BACKGROUND

Endoscopic resection (ER) with bipolar snare, in which the electric current only passes through the tissue between the device's two electrodes, is a prominent method used to prevent perforation due to electricity potentially. ER using bipolar snare with or without submucosal injection enabled safe resection of colorectal lesions measuring 10–15 mm in an *ex vivo* porcine model. ER with bipolar snare is expected to have good treatment outcomes in 10–15 mm colorectal lesions, with high safety even without submucosal injection. However, no clinical reports have compared treatment outcomes with and without submucosal injection.

AIM

To compare the treatment outcomes of bipolar polypectomy with hot snare polypectomy (HSP) to those with endoscopic mucosal resection (EMR).

METHODS

In this single-centre retrospective study, we enrolled 10–15 mm nonpedunculated colorectal lesions (565 Lesions in 463 patients) diagnosed as type 2A based on the Japan Narrow-band Imaging Expert Team classification, resected by either HSP or EMR between January 2018 and June 2021 at the National Cancer Center Hospital East. Lesions were divided into HSP and EMR groups, and propensity score

matching was performed. In the matched cohort, *en bloc* and R0 resection rates and adverse events were compared between the two groups.

RESULTS

Of the 565 lesions in 463 patients, 117 lesions each in the HSP and EMR groups were selected after propensity score matching. In the original cohort, there was a significant difference in antithrombotic drug use ($P < 0.05$), lesion size ($P < 0.01$), location ($P < 0.01$), and macroscopic type ($P < 0.05$) between the HSP and EMR groups. In the matched cohort, the *en bloc* resection rates were comparable between both groups [93.2% (109/117) *vs* 92.3% (108/117), $P = 0.81$], and there was no significant difference in the R0 resection rate [77.8% (91/117) *vs* 80.3% (94/117), $P = 0.64$]. The incidence of delayed bleeding was similar in both groups [1.7% (2/117)]. Perforation occurred in the EMR group [0.9% (1/117)] but not in the HSP group.

CONCLUSION

Using bipolar snare, ER of nonpedunculated 10–15 mm colorectal lesions may be performed safely and effectively, even without submucosal injection.

Key Words: Adenoma; Cohort studies; Colonoscopy; Colorectal cancer; Endoscopic mucosal resection; Treatment outcome

Core Tip: This study is the first to compare treatment outcomes between hot snare polypectomy (HSP) and endoscopic mucosal resection (EMR) using a bipolar snare for nonpedunculated colorectal lesions measuring 10–15 mm. First, there was no significant difference in *en bloc* and R0 resection rates between the HSP and EMR groups. Second, the incidence of adverse events was similar in both groups, but perforation occurred only in the EMR group. These results suggest that comparable treatment efficiency and safety may be obtained even without submucosal injection when resecting nonpedunculated colorectal lesions measuring 10–15 mm using a bipolar snare.

Citation: Minakata N, Murano T, Wakabayashi M, Sasabe M, Watanabe T, Mitsui T, Yamashita H, Inaba A, Sunakawa H, Nakajo K, Kadota T, Shinmura K, Ikematsu H, Yano T. Hot snare polypectomy *vs* endoscopic mucosal resection using bipolar snare for intermediate size colorectal lesions: Propensity score matching. *World J Gastroenterol* 2023; 29(23): 3668-3677

URL: https://www.wjgnet.com/1007-9327/full/v29/i23/3668.htm

DOI: https://dx.doi.org/10.3748/wjg.v29.i23.3668

INTRODUCTION

Colorectal cancer (CRC) is the leading cause of morbidity and mortality worldwide[1]. Detection and resection of colorectal lesions *via* colonoscopy reduce CRC-related mortality[2,3]. However, complications associated with endoscopic resection (ER), such as post-procedural bleeding and perforation, are concerning[4,5]. Perforation, although infrequent, is the most serious complication that may result in hospitalization, stoma formation, and mortality[6]. Various devices and techniques related to ER have been developed to reduce the risk of complications.

ER using a bipolar snare, wherein the electric current only passes through the tissue between the two electrodes of the device, may potentially prevent perforation due to electricity. Apart from reducing electric damage to tissues, using a bipolar snare does not require a counter electrode, carries a lower risk of burns, and can be used even when a metal, such as a pacemaker, is present inside the patient's body [7]. In an *ex vivo* porcine model, using a bipolar snare for intramucosal lesions measuring 10–15 mm did not cause thermal damage to the muscularis propria. However, perforation occurred with a monopolar snare. Furthermore, thermal damage to the muscularis propria was not observed in bipolar polypectomy, regardless of whether a submucosal injection was performed before resection[8].

An ER with a bipolar snare for 10–15 mm colorectal lesions could result in favourable outcomes even without submucosal injection. However, no reports have compared bipolar polypectomy with and without submucosal injection in clinical practice. Hence, using a bipolar snare for colorectal lesions measuring 10–15 mm, this study aimed to compare the safety and efficiency of hot snare polypectomy (HSP), which involves resection without submucosal injection, to those of endoscopic mucosal resection (EMR), which involves resection with submucosal injection.

MATERIALS AND METHODS

Patients

We retrospectively enrolled 10–15-mm nonpedunculated colorectal lesions diagnosed as type 2A based on the Japan Narrow-band Imaging Expert Team (JNET) classification, resected by either HSP or EMR using a bipolar snare between January 2018 and June 2021 at the National Cancer Center Hospital East. The exclusion criteria were: (1) History of inflammatory bowel disease and familial adenomatous polyposis; (2) Pedunculated type lesions; (3) Residual lesions after previous ER; and (4) Lesions pathologically diagnosed as inflammatory or hyperplastic polyps.

HSP and EMR

Before the colonoscopy, a polyethylene glycol electrolyte solution with ascorbic acid (MobiPrep, EA Pharma, Tokyo, Japan) or magnesium citrate (Magcorol P, Horii Pharmaceutical Industries, Osaka, Japan) was administered to all patients according to the manufacturer's instructions. The examinations were performed using a magnifying endoscope (PCF-H290ZI, CF-HQ290, CF-H290ECI, CF-EZ1500DI, CF-XZ1200I colonoscope, Olympus, Tokyo, Japan; EC-L590ZP, EC-L600ZP, Fujifilm Co., Tokyo, Japan), light source, and video processor (EVIS LUCERAELITE, EVIS X1, Olympus; LASEREO, Fujifilm Co.).

All procedures were performed by either four experts (≥ 2000 colonoscopies performed) or 18 nonexperts (< 2000 colonoscopies performed) endoscopists. The treatment choice (HSP or EMR) was at the endoscopist's discretion. For EMR, a submucosal injection was performed using saline solution alone or combined with sodium hyaluronate acid. A bipolar snare (Dragonare® Xemex Co. Ltd., Tokyo, Japan) was used in both HSP and EMR. An electrosurgery generator unit (ICC200, VIO300D, VIO3; ERBE Elektromedizin GmbH Co. Ltd., Tubingen, Germany; ESG100, Olympus) was used for all ERs. The cutting mode in the forced coagulation mode was used for resection. Subsequently, resection margins were evaluated endoscopically to confirm the absence of remnants. Prophylactic clipping after resection was performed at the endoscopist's discretion. Resected lesions were retrieved by suctioning through the endoscope into a trap, using pentapod-type grasping forceps or a retrieval net. The endocopists recorded the size, location, and macroscopic type of the lesions, diagnosis according to the JNET classification, and *en bloc* or piecemeal resection. The location was recorded as right colon if the lesion was in the caecum, ascending, or transverse colon, and as left colon if it was in the descending or sigmoid colon. Once removed, the lesions were fixed in formalin, embedded in paraffin, sectioned into 2–3 mm slices, stained with hematoxylin-eosin, and evaluated by two experienced pathologists blinded to the patient's clinical information. Pathological results were described according to World Health Organization criteria[9].

Outcomes

Study outcomes were *en bloc* and R0 resection rates, and adverse events, including delayed bleeding and perforation. *En bloc* resection was defined as ER with the entire lesion resected in a single piece. Upon histological evaluation of the horizontal and vertical margins of specimens, R0 resection was defined as negative margins both horizontally and vertically; RX resection, as unclear resection margins either horizontally or vertically; and R1 resection, as positive resection margins either horizontally or vertically [10]. Delayed bleeding was defined as haemorrhage requiring endoscopic intervention within 2 wk after polypectomy. Perforation was defined as any organ or fat outside the muscularis layer visualized on endoscopy during the procedure or free air observed on computed tomography after the procedure. For subgroup analysis, the R0 resection rate according to each clinical characteristic related to lesions was assessed.

Ethical considerations

This was a single-centre retrospective study, and the protocol was approved by the Institutional Review Board of the National Cancer Center (2017-434). All data were collected from the medical records. All procedures were performed after written informed consent was obtained.

Statistical analysis

Propensity score matching was applied at a 1:1 HSP-to-EMR ratio using greedy matching with a calliper width of 0.20 of the standard deviation of the logit transformation for the estimated propensity score[11, 12]. The propensity score was estimated using the multivariate logistic regression model, which included the following: age (continuous), sex (male/female), antithrombotic drug use (no/yes), size (continuous), location (right-sided colon/Left-sided colon/rectum), macroscopic type (0-Is/0-Isp/0-IIa), and endoscopist experience (expert/nonexpert) as explanatory variables without considering outcome variables. To evaluate the balance of patient characteristics between the HSP and EMR groups, we calculated standardized differences and created histograms and box plots. The chi-square and Mann–Whitney U tests were used to compare patient characteristics between groups. For treatment outcomes, univariable analyses were performed using the χ^2 test in all enrolled lesions and the McNemar test in pair-matched lesions. All *P* values were two-sided with a significance level of 0.05. All statistical analyses were performed using EZR (Saitama Medical Center, Jichi Medical University,

Saitama, Japan) and SAS (version 9.4) graphical user interface for R 4.1.0 (R Foundation for Statistical Computing, Vienna, Austria). EZR is a modified version of R commander (version 2.7-0), designed to add statistical functions frequently used in biostatistics[13]. The statistical methods of this study were reviewed by Masashi Wakabayashi from the Biostatistics Division of Center for Research Administration and Support at National Cancer Center.

RESULTS

Background characteristics of patients

Of the 711 consecutive lesions in 602 patients, 463 patients were enrolled, and 565 Lesions in them were analysed in the present study. Of the 565 Lesions, 440 in 346 patients were resected *via* HSP; 125 in 117 patients were resected *via* EMR. A flowchart of patient enrolment is shown in Figure 1. Patient characteristics before and after propensity score matching are shown in Table 1. There was a significant difference in antithrombotic drug use ($P < 0.05$), lesion size ($P < 0.01$), location ($P < 0.01$), and macroscopic type ($P < 0.05$) between the HSP and EMR groups in the original cohort. After propensity score matching, 117/440 Lesions in the HSP group and 117/125 in the EMR group were selected. Nearly all baseline characteristics were balanced (Table 1; standardized differences < 0.1 between HSP and EMR).

En bloc and R0 resection rates

In the original cohort, the *en bloc* and R0 resection rates between the HSP and EMR groups were similar [94.8% (417/440) *vs* 92.8% (116/125), $P = 0.40$; 81.6% (359/440) *vs* 80.8% (101/125), $P = 0.84$, respectively] (Table 2). In the propensity score-matched cohort, the *en bloc* resection rate remained similar between the HSP and EMR groups [93.2% (109/117) *vs* 92.3% (108/117), $P = 0.81$]. Furthermore, there was no significant difference between the HSP and EMR groups in the R0 resection rate [77.8% (91/117) *vs* 80.3% (94/117), $P = 0.64$] (Table 2). All patients who underwent RX/R1 resection were classified as HMX/HM1, and there were no patients with VMX/VM1. There was no significant difference in the R0 resection rate between the HSP and EMR groups according to size, macroscopic type, and endoscopist experience. However, in terms of rectal location, the R0 resection rate was significantly higher in the EMR group than in the HSP group [75.0% (18/24) *vs* 100% (22/22), $P = 0.022$] (Table 3).

Adverse events

In the original cohort, there was no significant difference in the incidence of delayed bleeding between the HSP and EMR groups [1.1% (5/440) *vs* 1.7% (2/125), $P = 0.68$]. Perforation occurred in the EMR group [0.9% (1/125); $P = 0.060$] but not in the HSP group (Table 2). In the propensity score-matched cohort, the incidence of delayed bleeding was similar in both groups [1.7% (2/117)]. Perforation occurred in the EMR group [0.9% (1/117)] but not in the HSP group. One case of perforation in the EMR group occurred intraoperatively.

DISCUSSION

This study is the first to compare treatment outcomes between HSP and EMR using a bipolar snare for nonpedunculated colorectal lesions measuring 10–15 mm in clinical practice. Two important results were obtained in this study. First, there was no significant difference in *en bloc* and R0 resection rates between the HSP and EMR groups. Second, the incidence of adverse events was similar in both groups; however, perforation occurred only in the EMR group. These results suggest that comparable treatment efficiency and safety may be obtained when resecting nonpedunculated colorectal lesions measuring 10–15 mm using a bipolar snare and even without submucosal injection.

Several ER methods have been widely adopted for colorectal lesions, including cold snare polypectomy (CSP), HSP, and EMR. The European Society of Gastrointestinal Endoscopy clinical guidelines proposed selecting ER methods according to the size and macroscopic type of lesions. For nonpedunculated lesions, CSP is recommended for lesions ≤ 9 mm, HSP or EMR for lesions 10–19 mm, and EMR or piecemeal EMR for lesions ≥ 20 mm[14,15]. For HSP and EMR, electrosurgical resection with a monopolar snare is generally performed. However, there is a risk of thermal damage because high-frequency current derived from the monopolar snare flows to the patient's plate through the deep part of the patient's living tissue[7]. In fact, in treatment outcomes of ER using a monopolar snare, perforation occurs in approximately 1.3%–2.8% of cases[16,17]. Therefore, when using a monopolar snare during ER for 10–19 mm colorectal lesions, EMR is recommended instead of HSP as it can reduce the risk of deep thermal damage[14].

We recently reported on endoscopic procedures using either a monopolar or bipolar snare in an *ex vivo* porcine model[8]. When 10–15-mm lesions were resected by HSP, the muscularis propria was thermally damaged when a monopolar snare was used but not when a bipolar snare was used.

Table 1 Patient and lesion characteristics

	Original cohort				Propensity score-matched cohort			
	HSP	EMR	*P* value	Standardized difference	HSP	EMR	*P* value	Standardized difference
No. of lesions	440	125			117	117		
Age (yr), mean ± SD (range)	69.7 ± 9.47 (36–90)	69.8 ± 8.36 (46–89)	0.53	0.013	69.5 ± 8.34 (43–85)	70.1 ± 8.78 (46–89)	0.67	0.072
Sex, *n* (%)			0.83	0.022			1.00	0
Male	328 (74.6)	92 (73.6)			87 (74.4)	87 (74.4)		
Female	112 (25.5)	33 (26.4)			30 (25.6)	30 (25.6)		
Antithrombotic drugs use, *n* (%)			0.031	0.21			0.87	0.021
Yes	66 (15.0)	29 (23.2)			25 (21.4)	26 (22.2)		
No	374 (85.0)	96 (76.8)			92 (78.6)	91 (77.8)		
Size (mm), mean ± SD (range)	11.2 ± 1.76 (10–15)	12.7 ± 2.02 (10–15)	< 0.01	0.77	12.4 ± 2.08 (10–15)	12.5 ± 2.01 (10–15)	0.72	0.054
Location, *n* (%)			< 0.01	0.38			0.94	0.054
Right-sided colon	240 (54.6)	63 (50.4)			61 (52.1)	63 (53.9)		
Left-sided colon	155 (35.2)	36 (28.8)			32 (27.4)	32 (27.4)		
Rectum	45 (10.2)	26 (20.8)			24 (20.5)	22 (18.8)		
Histological findings, *n* (%)			0.087	0.26			0.081	0.23
SSL	5 (1.1)	0 (0)			3 (2.6)	0 (0)		
LGD/HGD	434 (98.6)	123 (98.4)			114 (97.4)	117 (100)		
T1a/T1b	1 (0.2)	2 (1.6)			0 (0)	0 (0)		
Macroscopic type, *n* (%)			0.011	0.3			0.79	0.034
Type 0–Is, 0–Isp	176 (40.0)	66 (52.8)			62 (53.0)	60 (51.3)		
Type 0–IIa	264 (60.0)	59 (47.2)			55 (47.0)	57 (48.7)		
Endoscopist, *n* (%)			0.053	0.2			0.51	0.086
Expert	186 (42.3)	65 (52.0)			63 (53.9)	58 (49.6)		
Non-expert	254 (57.7)	60 (48.0)			54 (46.2)	59 (50.4)		

HSP: Hot snare polypectomy; EMR: Endoscopic mucosal resection; right-sided colon: Caecum to transverse colon; left-sided colon: Descending colon to sigmoid colon; SSL: Sessile serrated lesion; LGD: Low-grade dysplasia; HGD: High-grade dysplasia; T1a: Shallow submucosal invasive cancer; T1b: Deep submucosal invasive cancer; SD: Standard deviation.

Therefore, greater safety can be expected even without submucosal injection when a bipolar snare is used. However, no studies compared the safety and effectivity between HSP and EMR using a bipolar snare in clinical practice. This study revealed that HSP had a similar complication rate as EMR when a bipolar snare was used for 10–15-mm nonpedunculated colorectal lesions. Notably, perforation did not occur following HSP, suggesting a better safety profile when using a bipolar snare over a monopolar snare. The delayed bleeding rate was also reported to be 1.4%–3.1% for EMR[16,17] and 5.3% for HSP [18] when a monopolar snare was used. However, in this study, the delayed bleeding rate for both HSP and EMR when a bipolar snare was used was 1.7%, which is relatively lower than previously reported values. Saraya *et al*[19] also reported that HSP and EMR using a bipolar snare had a similar or lower risk of delayed bleeding and perforation than EMR using a monopolar snare[19]. Although the present study had a small number of cases, HSP did not cause perforation and resulted in less delayed bleeding, suggesting that HSP using a bipolar snare might be an option that results in fewer complications than EMR using a monopolar or bipolar snare.

For ER of medium-sized lesions ≥ 10 mm, determining whether *en bloc* or R0 resection is possible is important for ER method selection. Piecemeal ER and RX/R1 resection are known risk factors for local

Table 2 Comparison of outcomes between the hot snare polypectomy and endoscopic mucosal resection groups

	Original cohort			Propensity score-matched cohort		
	HSP	EMR	*P* value	HSP	EMR	*P* value
No. of lesions	440	125		117	117	
En bloc resection, *n*, % (95%CI)	417, 94.8 (92.3-96.7)	116, 92.8 (86.8-96.7)	0.4	109, 93.2 (87.0-97.0)	108, 92.3 (85.9-96.4)	0.81
Piecemeal resection, *n*, % (95%CI)	23, 5.2 (3.3-7.7)	9, 7.2 (3.3-13.2)		8, 6.8 (3.0-13.0)	9, 7.7 (3.6-14.1)	
R0 resection, *n*, % (95%CI)	359, 81.6 (77.6-85.1)	101, 80.8 (72.8-87.3)	0.84	91, 77.8 (69.2-84.9)	94, 80.3 (72.0-87.1)	0.64
RX/R1 resection, *n*, % (95%CI)	81, 18.4 (14.9-22.4)	24, 19.2 (12.7-27.2)		26, 22.2 (15.1-30.8)	23, 19.7 (12.9-28.0)	
Delayed bleeding, *n*, % (95%CI)	5, 1.1 (0.4-2.6)	2, 1.6 (0.2-5.7)	0.68	2, 1.7 (0.2-6.0)	2, 1.7 (0.2-6.0)	1.00
Perforation, *n*, % (95%CI)	0, 0 (0-0.8)	1, 0.8 (0.0-4.4)	0.06	0, 0 (0-3.1)	1, 0.9 (0-4.7)	N/A

HSP: Hot snare polypectomy; EMR: Endoscopic mucosal resection; R0: Negative margin both horizontally and vertically; RX: Unclear resection margin either horizontally or vertically; R1: Positive resection margin either horizontally or vertically; CI: Confidence interval; N/A: Not applicable.

Table 3 Comparison of negative margin both horizontally and vertically resection rates between the hot snare polypectomy group and endoscopic mucosal resection groups

	R0 resection rate, %, *n/n* (95%CI)		
	HSP	EMR	*P* value
Total	77.8, 91/117 (69.2-84.9)	80.3, 94/117 (72.0-87.1)	
Size			
10–12 mm	77.9, 53/68 (66.2-87.1)	82.9, 58/70 (72.0-90.8)	0.52
13–15 mm	77.6, 38/49 (63.4-88.2)	76.6, 36/47 (62.0-87.7)	1.00
Macroscopic type			
Type 0-Is, 0-Isp	77.4, 48/62 (65.0-87.1)	86.7, 52/60 (75.4-94.1)	0.24
Type 0-IIa	78.2, 43/55 (65.0-88.2)	73.7, 42/57 (60.3-84.5)	0.66
Location			
Right-sided colon	75.4, 46/61 (62.7-85.5)	74.6, 47/63 (62.1-84.7)	1.00
Left-sided colon	84.4, 27/32 (67.2-94.7)	78.1, 25/32 (60.0-90.7)	0.75
Rectum	75.0, 18/24 (53.3-90.2)	100, 22/22 (84.6-100)	0.022
Endoscopist			
Expert	81.0, 51/63 (69.1-89.8)	82.8, 48/58 (70.6-91.4)	0.82
Non-expert	74.1, 40/54 (60.3-85.0)	78.0, 46/59 (65.3-87.7)	0.66

HSP: Hot snare polypectomy; EMR: Endoscopic mucosal resection; R0: Negative margin both horizontally and vertically.

recurrence after ER[20,21]. As the lesion grows, piecemeal endoscopic and RX/R1 resection rates increase, leading to an increased risk of local recurrence. However, the R0 resection rate is equivalent between HSP and EMR using a monopolar snare for colorectal lesions measuring 10–14 mm[22]. Therefore, the *en bloc* and R0 resection rates are equivalent between HSP and EMR with a bipolar snare, although no studies have been conducted to confirm this. In this study, for nonpedunculated colorectal lesions measuring 10–15 mm, HSP resulted in *en bloc* and R0 resection rates equivalent to those of EMR with a bipolar snare. Meanwhile, the *en bloc* resection rate was as high as ≥ 90% in both groups, and the R0 resection rate was approximately 80%, lower than previously reported values[22]. This could be because resection at our hospital is performed under the coagulation mode. Also, given the characteristics of ER using a bipolar snare, it is difficult to horizontally evaluate the pathological specimen due to crushing by cauterization in lesions where the resection margin is close to the lesion edge. However,

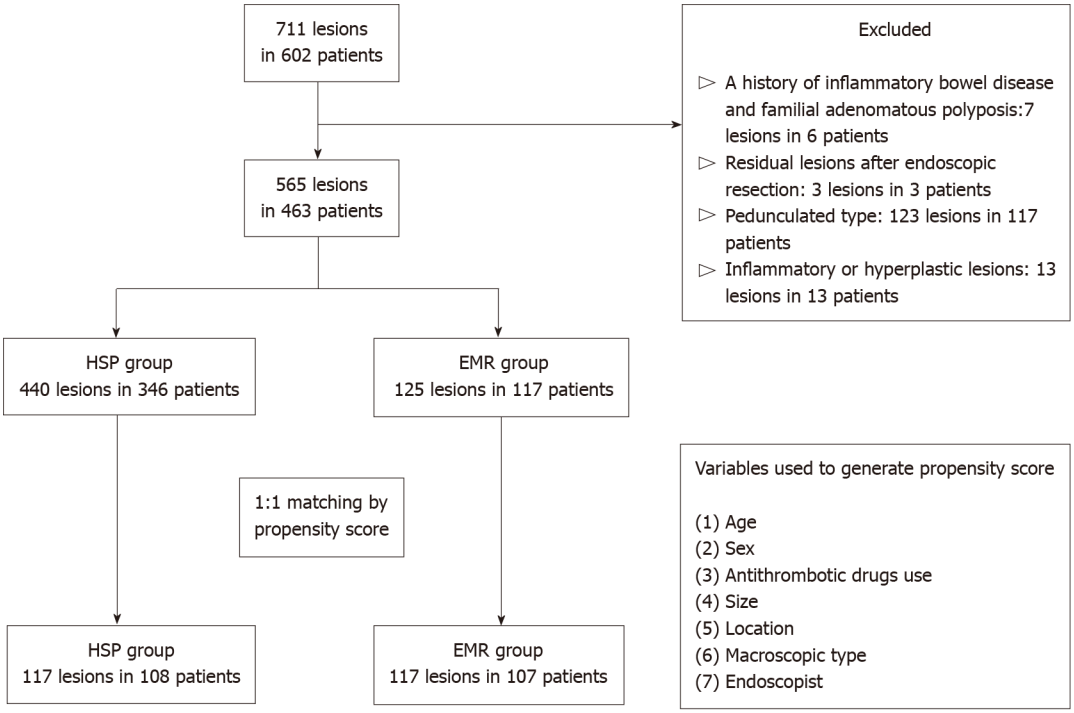

DOI: 10.3748/wjg.v29.i23.3668

Figure 1 Flowchart of patient enrollment. Of the 711 consecutive lesions in 602 patients, 565 lesions in 463 patients were enrolled for the analysis. Of the 565 lesions, 440 in 346 patients were resected *via* hot snare polypectomy (HSP); 125 in 117 patients were resected *via* endoscopic mucosal resection (EMR). After propensity score matching, 117 lesions in the HSP group and 117 lesions in the EMR group were selected. HSP: Hot snare polypectomy; EMR: Endoscopic mucosal resection.

resection in coagulation mode may have contributed to a lower rate of delayed bleeding than previously reported because of the ability to coagulate the vessel[16-18].

The following points contributed to this innovative study design. First, patient and lesion backgrounds were matched using property score matching. The size, location, and macroscopic type of the lesions and endoscopic experience are known factors related to *en bloc* and R0 resection, and oral intake of antithrombotic agents is related to delayed bleeding[23-26]. This is the only study to balance the many confounding factors that may affect the estimation of results by property score matching and to compare treatment outcomes between HSP and EMR with a bipolar snare.

Second, only lesions diagnosed as JNET type 2A using magnifying observation combined with narrow-band imaging were included. In the qualitative diagnosis of colorectal lesions, those diagnosed as JNET type 2A can be diagnosed as adenomas or intramucosal cancers with high accuracy[27]. On the other hand, lesions diagnosed as JNET type 2B or 3 are generally known to develop into T1 cancer more frequently, resulting in bias wherein endoscopists who perform therapeutic endoscopy more carefully select ER methods that secure lesion margins. In this study, only JNET type 2A lesions potentially avoided bias due to differences in ER methods based on the preoperative diagnosis. Therefore, although the results of this study can be applied to adenomas and intramucosal cancers, it is unclear whether ER for T1 cancers will provide similar results. Third, we analysed the R0 resection rate as a factor between HSP and EMR. There was no difference in the R0 resection rate between HSP and EMR for most of the factors. However, the R0 resection rate for lesions in the rectum was better for EMR. No study has reported a change in the R0 resection rate with or without submucosal injection for rectal lesions. However, the R0 resection rate was reportedly significantly better in EMR than in HSP for the left colon [22]. Additionally, it can be difficult to diagnose a range of lesions due to factors such as 'skirt' in the rectum compared to the colon[28]. In rectal lesions of a difficult-to-identify extent with 'skirt', EMR provides wider margins, which may lead to fewer leftovers and improved R0 resection rates.

This study had some limitations. First, this was a single-centre retrospective study. In particular, the sample size was not large enough to prove the non-inferiority of HSP to EMR for any of the outcomes. Furthermore, since the treatment choices for HSP and EMR were left to the discretion of each endoscopist, the present results may be strongly influenced by the skill of a specific endoscopist. They may have been affected by imbalanced confounding factors that were not included in the analysis between the two groups. Second, there was no clear standard for measuring lesion size. Each endoscopist judged the size of the lesion by comparing it with the size of the snare, suggesting inaccurate lesion measurements. Third, the size of the bipolar snare used for resection was not specified, and the effects on the results cannot be denied. To eliminate these biases, conducting a large-cohort, multicentre, prospective, randomized controlled trial after clarifying ER methods, size of the snare, and

lesion measurement methods is desirable.

CONCLUSION

When using a bipolar snare, HSP has comparable treatment outcomes to EMR for nonpedunculated colorectal lesions measuring 10–15 mm. This suggests that the use of a bipolar snare may replace submucosal injection and may enable a more accessible ER while maintaining efficiency and safety.

ARTICLE HIGHLIGHTS

Research background

In endoscopic resection (ER) of colorectal lesions, it is important to develop resection methods that enable efficient and safe resection. Most recently, we have reported in *ex vivo* porcine model that endoscopic resection using bipolar snare for intermediate size lesions didn't lead to thermal injury for the intrinsic muscle layer even without submucosal injection. Therefore, the bipolar ER for intermediate size colorectal lesions of 10-15 mm has the potential to provide prominent outcomes in an efficient and highly safe manner even without submucosal injection.

Research motivation

We would like to assess the treatment outcomes of the bipolar resection with and without submucosal injection.

Research objectives

The present study aims to compare the resection results of endoscopic mucosal resection (EMR), which refers to the resection following submucosal injection, and hot snare polypectomy (HSP), which refers to the resection with no submucosal injection, to evaluate the efficacy and safety of HSP with bipolar snare for 10-15 mm lesions.

Research methods

We conducted the single-centre retrospective analysis of all 10-15 mm size colorectal lesions with a diagnosis of JNET Type 2A and resected by either EMR or HSP from January 2018 to June 2021. The target lesions were divided into two groups, HSP group and EMR group, and treatment outcomes and the adverse events were compared by conducting propensity score matching analysis.

Research results

Of the 565 lesions in 463 patients, 117 lesions each in the HSP and EMR groups were selected after propensity score matching. In the original cohort, there was a significant difference in antithrombotic drug use ($P < 0.05$), lesion size ($P < 0.01$), location ($P < 0.01$), and macroscopic type ($P < 0.05$) between the HSP and EMR groups. In the matched cohort, the *en bloc* resection rates were 93.2% (109/117) in the HSP group and 92.3% (108/117) in the EMR group, in which there was no significant difference ($P = 0.81$). Moreover, no significant difference was observed in the R0 resection rate [77.8% (91/117) *vs* 80.3% (94/117), $P = 0.64$]. The rates of delayed bleeding were comparable between the groups [1.7% (2/117)]. Perforation occurred in the EMR group [0.9% (1/117)] but not in the HSP group.

Research conclusions

Using bipolar snare, ER of nonpedunculated 10–15 mm colorectal lesions may be performed safely and effectively, even without submucosal injection.

Research perspectives

A large-cohort, multicentre, prospective, randomized controlled trial is warranted to prove the non-inferiority of bipolar HSP to bipolar EMR in treatment outcomes with ER of nonpedunculated 10–15 mm colorectal lesions.

FOOTNOTES

Author contributions: Minakata N, Murano T and Ikematsu H contributed to conceptualization; Minakata N and Murano T contributed to methodology; Minakata N and Wakabayashi M contributed to statistical analysis; Minakata N and Murano T contributed to writing - original draft preparation; Wakabayashi M, Sasabe M, Watanabe T, Mitsui T, Yamashita H, Inaba A, Sunakawa H, Nakajo K, Kadota T, Shinmura K, Ikematsu H, and Yano T contributed to writing - review and editing.

Institutional review board statement: The study protocol was approved by the Institutional Review Board of our hospital, No. 2017-434.

Informed consent statement: Patients were not required to provide informed consent for the study because the analysis used anonymous clinical data obtained after each patient agreed to treatment by written consent.

Conflict-of-interest statement: All the authors report no relevant conflicts of interest for this article.

Data sharing statement: The data supporting this study's findings are available from the corresponding author, Murano T, upon reasonable request at tatmuran@east.ncc.go.jp.

Country/Territory of origin: Japan

ORCID number: Nobuhisa Minakata 0000-0003-4540-4036; Tatsuro Murano 0000-0003-0423-2151; Masashi Wakabayashi 0009-0001-6368-5671; Maasa Sasabe 0000-0001-5219-4706; Takashi Watanabe 0009-0003-0294-3889; Tomohiro Mitsui 0000-0003-3518-1350; Hiroki Yamashita 0000-0002-6190-7904; Atsushi Inaba 0000-0001-7036-9485; Hironori Sunakawa 0000-0003-0792-9560; Keiichiro Nakajo 0000-0002-7138-9848; Tomohiro Kadota 0000-0002-0408-3494; Kensuke Shinmura 0000-0001-8786-4634; Hiroaki Ikematsu 0000-0001-9840-4588; Tomonori Yano 0000-0002-8030-1449.

S-Editor: Li L
L-Editor: A
P-Editor: Li L

REFERENCES

1 **Siegel RL**, Miller KD, Jemal A. Cancer statistics, 2016. *CA Cancer J Clin* 2016; **66**: 7-30 [PMID: 26742998 DOI: 10.3322/caac.21332]
2 **Winawer SJ**, Zauber AG, Ho MN, O'Brien MJ, Gottlieb LS, Sternberg SS, Waye JD, Schapiro M, Bond JH, Panish JF. Prevention of colorectal cancer by colonoscopic polypectomy. The National Polyp Study Workgroup. *N Engl J Med* 1993; **329**: 1977-1981 [PMID: 8247072 DOI: 10.1056/NEJM199312303292701]
3 **Zauber AG**, Winawer SJ, O'Brien MJ, Lansdorp-Vogelaar I, van Ballegooijen M, Hankey BF, Shi W, Bond JH, Schapiro M, Panish JF, Stewart ET, Waye JD. Colonoscopic polypectomy and long-term prevention of colorectal-cancer deaths. *N Engl J Med* 2012; **366**: 687-696 [PMID: 22356322 DOI: 10.1056/NEJMoa1100370]
4 **Kim SY**, Kim HS, Park HJ. Adverse events related to colonoscopy: Global trends and future challenges. *World J Gastroenterol* 2019; **25**: 190-204 [PMID: 30670909 DOI: 10.3748/wjg.v25.i2.190]
5 **Paszat LF**, Sutradhar R, Luo J, Rabeneck L, Tinmouth J. Perforation and post-polypectomy bleeding complicating colonoscopy in a population-based screening program. *Endosc Int Open* 2021; **9**: E637-E645 [PMID: 33880399 DOI: 10.1055/a-1381-7149]
6 **Derbyshire E**, Hungin P, Nickerson C, Rutter MD. Colonoscopic perforations in the English National Health Service Bowel Cancer Screening Programme. *Endoscopy* 2018; **50**: 861-870 [PMID: 29590669 DOI: 10.1055/a-0584-7138]
7 **Rey JF**, Beilenhoff U, Neumann CS, Dumonceau JM; European Society of Gastrointestinal Endoscopy (ESGE). European Society of Gastrointestinal Endoscopy (ESGE) guideline: the use of electrosurgical units. *Endoscopy* 2010; **42**: 764-772 [PMID: 20635311 DOI: 10.1055/s-0030-1255594]
8 **Shinmura K**, Ikematsu H, Kojima M, Nakamura H, Osera S, Yoda Y, Hori K, Oono Y, Ochiai A, Yano T. Safety of endoscopic procedures with monopolar *vs* bipolar instruments in an *ex vivo* porcine model. *BMC Gastroenterol* 2020; **20**: 27 [PMID: 32005163 DOI: 10.1186/s12876-020-1176-9]
9 **WHO Classification of Tumours Editorial Board**. WHO Classification of Tumors: Digestive System Tumours. 5th ed. Lyon, France: International Agency for Research on Cancer; 2019
10 **Japanese Society for Cancer of the Colon and Rectum**. Japanese Classification of Colorectal, Appendiceal, and Anal Carcinoma: the 3d English Edition [Secondary Publication]. *J Anus Rectum Colon* 2019; **3**: 175-195 [PMID: 31768468 DOI: 10.23922/jarc.2019-018]
11 **Austin PC**. Some methods of propensity-score matching had superior performance to others: results of an empirical investigation and Monte Carlo simulations. *Biom J* 2009; **51**: 171-184 [PMID: 19197955 DOI: 10.1002/bimj.200810488]
12 **Austin PC**. An Introduction to Propensity Score Methods for Reducing the Effects of Confounding in Observational Studies. *Multivariate Behav Res* 2011; **46**: 399-424 [PMID: 21818162 DOI: 10.1080/00273171.2011.568786]
13 **Kanda Y**. Investigation of the freely available easy-to-use software 'EZR' for medical statistics. *Bone Marrow Transplant* 2013; **48**: 452-458 [PMID: 23208313 DOI: 10.1038/bmt.2012.244]
14 **Ferlitsch M**, Moss A, Hassan C, Bhandari P, Dumonceau JM, Paspatis G, Jover R, Langner C, Bronzwaer M, Nalankilli K, Fockens P, Hazzan R, Gralnek IM, Gschwantler M, Waldmann E, Jeschek P, Penz D, Heresbach D, Moons L, Lemmers

A, Paraskeva K, Pohl J, Ponchon T, Regula J, Repici A, Rutter MD, Burgess NG, Bourke MJ. Colorectal polypectomy and endoscopic mucosal resection (EMR): European Society of Gastrointestinal Endoscopy (ESGE) Clinical Guideline. *Endoscopy* 2017; **49**: 270-297 [PMID: 28212588 DOI: 10.1055/s-0043-102569]

15 **Kawamura T**, Takeuchi Y, Asai S, Yokota I, Akamine E, Kato M, Akamatsu T, Tada K, Komeda Y, Iwatate M, Kawakami K, Nishikawa M, Watanabe D, Yamauchi A, Fukata N, Shimatani M, Ooi M, Fujita K, Sano Y, Kashida H, Hirose S, Iwagami H, Uedo N, Teramukai S, Tanaka K. A comparison of the resection rate for cold and hot snare polypectomy for 4-9 mm colorectal polyps: a multicentre randomised controlled trial (CRESCENT study). *Gut* 2018; **67**: 1950-1957 [PMID: 28970290 DOI: 10.1136/gutjnl-2017-314215]

16 **van Hattem WA**, Shahidi N, Vosko S, Hartley I, Britto K, Sidhu M, Bar-Yishay I, Schoeman S, Tate DJ, Byth K, Hewett DG, Pellisé M, Hourigan LF, Moss A, Tutticci N, Bourke MJ. Piecemeal cold snare polypectomy *vs* conventional endoscopic mucosal resection for large sessile serrated lesions: a retrospective comparison across two successive periods. *Gut* 2021; **70**: 1691-1697 [PMID: 33172927 DOI: 10.1136/gutjnl-2020-321753]

17 **Saito Y**, Fukuzawa M, Matsuda T, Fukunaga S, Sakamoto T, Uraoka T, Nakajima T, Ikehara H, Fu KI, Itoi T, Fujii T. Clinical outcome of endoscopic submucosal dissection *vs* endoscopic mucosal resection of large colorectal tumors as determined by curative resection. *Surg Endosc* 2010; **24**: 343-352 [PMID: 19517168 DOI: 10.1007/s00464-009-0562-8]

18 **Ket SN**, Mangira D, Ng A, Tjandra D, Koo JH, La Nauze R, Metz A, Moss A, Brown G. Complications of cold *vs* hot snare polypectomy of 10-20 mm polyps: A retrospective cohort study. *JGH Open* 2020; **4**: 172-177 [PMID: 32280761 DOI: 10.1002/jgh3.12243]

19 **Saraya T**, Ikematsu H, Fu KI, Tsunoda C, Yoda Y, Oono Y, Kojima T, Yano T, Horimatsu T, Sano Y, Kaneko K. Evaluation of complications related to therapeutic colonoscopy using the bipolar snare. *Surg Endosc* 2012; **26**: 533-540 [PMID: 21938574 DOI: 10.1007/s00464-011-1914-8]

20 **Buchner AM**, Guarner-Argente C, Ginsberg GG. Outcomes of EMR of defiant colorectal lesions directed to an endoscopy referral center. *Gastrointest Endosc* 2012; **76**: 255-263 [PMID: 22657404 DOI: 10.1016/j.gie.2012.02.060]

21 **Yoshida N**, Fukumoto K, Hasegawa D, Inagaki Y, Inoue K, Hirose R, Dohi O, Ogiso K, Murakami T, Tomie A, Okuda K, Inada Y, Okuda T, Rani RA, Morinaga Y, Kishimoto M, Itoh Y. Recurrence rate and lesions characteristics after cold snare polypectomy of high-grade dysplasia and T1 Lesions: A multicenter analysis. *J Gastroenterol Hepatol* 2021; **36**: 3337-3344 [PMID: 34260116 DOI: 10.1111/jgh.15625]

22 **Horiuchi A**, Makino T, Kajiyama M, Tanaka N, Sano K, Graham DY. Comparison between endoscopic mucosal resection and hot snare resection of large nonpedunculated colorectal polyps: a randomized trial. *Endoscopy* 2016; **48**: 646-651 [PMID: 27100717 DOI: 10.1055/s-0042-105557]

23 **Ito A**, Suga T, Ota H, Tateiwa N, Matsumoto A, Tanaka E. Resection depth and layer of cold snare polypectomy *vs* endoscopic mucosal resection. *J Gastroenterol* 2018; **53**: 1171-1178 [PMID: 29516270 DOI: 10.1007/s00535-018-1446-2]

24 **Pohl H**, Srivastava A, Bensen SP, Anderson P, Rothstein RI, Gordon SR, Levy LC, Toor A, Mackenzie TA, Rosch T, Robertson DJ. Incomplete polyp resection during colonoscopy-results of the complete adenoma resection (CARE) study. *Gastroenterology* 2013; **144**: 74-80.e1 [PMID: 23022496 DOI: 10.1053/j.gastro.2012.09.043]

25 **Tavakkoli A**, Law RJ, Bedi AO, Prabhu A, Hiatt T, Anderson MA, Wamsteker EJ, Elmunzer BJ, Piraka CR, Scheiman JM, Elta GH, Kwon RS. Specialist Endoscopists Are Associated with a Decreased Risk of Incomplete Polyp Resection During Endoscopic Mucosal Resection in the Colon. *Dig Dis Sci* 2017; **62**: 2464-2471 [PMID: 28600656 DOI: 10.1007/s10620-017-4643-6]

26 **Kishida Y**, Hotta K, Imai K, Ito S, Yoshida M, Kawata N, Tanaka M, Kakushima N, Takizawa K, Ishiwatari H, Matsubayashi H, Ono H. Risk Analysis of Colorectal Post-Polypectomy Bleeding Due to Antithrombotic Agent. *Digestion* 2019; **99**: 148-156 [PMID: 30179871 DOI: 10.1159/000490791]

27 **Hirata D**, Kashida H, Iwatate M, Tochio T, Teramoto A, Sano Y, Kudo M. Effective use of the Japan Narrow Band Imaging Expert Team classification based on diagnostic performance and confidence level. *World J Clin Cases* 2019; **7**: 2658-2665 [PMID: 31616682 DOI: 10.12998/wjcc.v7.i18.2658]

28 **Miyamoto H**, Ikematsu H, Fujii S, Osera S, Odagaki T, Oono Y, Yano T, Ochiai A, Sasaki Y, Kaneko K. Clinicopathological differences of laterally spreading tumors arising in the colon and rectum. *Int J Colorectal Dis* 2014; **29**: 1069-1075 [PMID: 24986136 DOI: 10.1007/s00384-014-1931-x]

World Journal of Gastroenterology

Submit a Manuscript: https://www.f6publishing.com

World J Gastroenterol 2023 June 21; 29(23): 3678-3687

DOI: 10.3748/wjg.v29.i23.3678

ISSN 1007-9327 (print) ISSN 2219-2840 (online)

ORIGINAL ARTICLE

Retrospective Study

Lymphocyte-to-white blood cell ratio is associated with outcome in patients with hepatitis B virus-related acute-on-chronic liver failure

Yue Zhang, Peng Chen, Xuan Zhu

Specialty type: Gastroenterology and hepatology

Provenance and peer review: Unsolicited article; Externally peer reviewed.

Peer-review model: Single blind

Peer-review report's scientific quality classification

Grade A (Excellent): 0
Grade B (Very good): B, B, B
Grade C (Good): 0
Grade D (Fair): 0
Grade E (Poor): 0

P-Reviewer: Desai GS, India; Kao JT, Taiwan; Papazafiropoulou A, Greece

Received: March 22, 2023
Peer-review started: March 22, 2023
First decision: April 14, 2023
Revised: April 28, 2023
Accepted: May 22, 2023
Article in press: June 21, 2023
Published online: June 21, 2023

Yue Zhang, Peng Chen, Xuan Zhu, Department of Gastroenterology, Jiangxi Clinical Research Center for Gastroenterology, The First Affiliated Hospital of Nanchang University, Nanchang 330006, Jiangxi Province, China

Corresponding author: Xuan Zhu, PhD, Professor, Department of Gastroenterology, Jiangxi Clinical Research Center for Gastroenterology, The First Affiliated Hospital of Nanchang University, Yongwaizhengjie Road, Donghu District, Nanchang 330006, Jiangxi Province, China. waiyongtg@163.com

Abstract

BACKGROUND

The lymphocyte-to-white blood cell ratio (LWR) is a blood marker of the systemic inflammatory response. The prognostic value of LWR in patients with hepatitis B virus-associated acute-on-chronic liver failure (HBV-ACLF) remains unclear.

AIM

To explore whether LWR could stratify the risk of poor outcomes in HBV-ACLF patients.

METHODS

This study was conducted by recruiting 330 patients with HBV-ACLF at the Department of Gastroenterology in a large tertiary hospital. Patients were divided into survivor and non-survivor groups according to their 28-d prognosis. The independent risk factors for 28-d mortality were calculated by univariate and multivariate Cox regression analyses. Patients were divided into low- and high-LWR groups according to the cutoff values. Kaplan-Meier analysis was performed according to the level of LWR.

RESULTS

During the 28-d follow-up time, 135 patients died, and the mortality rate was 40.90%. The LWR level in non-surviving patients was significantly decreased compared to that in surviving patients. A lower LWR level was an independent risk factor for poor 28-d outcomes (hazard ratio = 0.052, 95% confidence interval: 0.005-0.535). The LWR level was significantly negatively correlated with the Child-Turcotte-Pugh, model for end-stage liver disease, and Chinese Group on the Study of Severe Hepatitis B-ACLF II scores. In addition, the 28-d mortality was higher for patients with LWR < 0.11 than for those with LWR ≥ 0.11.

CONCLUSION
LWR may serve as a simple and useful tool for stratifying the risk of poor 28-d outcomes in HBV-ACLF patients.

Key Words: Lymphocyte-to-white blood cell ratio; Hepatitis B virus; Acute-on-chronic liver failure; Child-Turcotte-Pugh score; Model for end-stage liver disease score; Chinese Group on the Study of Severe Hepatitis B-Acute-on-chronic liver failure II score

Core Tip: This manuscript introduced a simple and effective inflammatory marker, the lymphocyte-to-white blood cell ratio (LWR). Our study found that a lower LWR level was associated with poor 28-d outcomes in hepatitis B virus-associated acute-on-chronic liver failure (HBV-ACLF) patients. It may serve as a simple and useful tool for stratifying the risk of poor 28-d outcomes in HBV-ACLF patients, and it may be helpful in guiding a clinician to treatment allocation and assist in the prediction of prognosis.

Citation: Zhang Y, Chen P, Zhu X. Lymphocyte-to-white blood cell ratio is associated with outcome in patients with hepatitis B virus-related acute-on-chronic liver failure. *World J Gastroenterol* 2023; 29(23): 3678-3687
URL: https://www.wjgnet.com/1007-9327/full/v29/i23/3678.htm
DOI: https://dx.doi.org/10.3748/wjg.v29.i23.3678

INTRODUCTION

Acute-on-chronic liver failure (ACLF) is a life-threatening clinically complex syndrome characterized by high short-term mortality due to different combinations of multiorgan failures[1-3]. The main etiology of ACLF is hepatitis B virus (HBV) infection, with HBV-associated ACLF (HBV-ACLF) accounting for more than 70% of ACLF cases in most Asian countries[4]. The clinical characteristics of HBV-ACLF patients differ from those of alcoholic-related ACLF patients in Western countries, wherein coagulation and liver failure are the most common types of organ failure[5]. Early prediction of the prognosis of HBV-ACLF is important for clinical management and diminishing mortality. However, current score models are based on complicated assessments of organ failure. Therefore, it is necessary to identify an accurate and simple indicator to detect high-risk patients.

A growing body of research evidence suggests that HBV-ACLF is associated with systemic inflammation and immune paralysis[6,7]. In many recent studies, inflammation-related markers such as the platelet (PLT) to white blood cell ratio, neutrophil-to-lymphocyte ratio, and monocyte-to-lymphocyte ratio have received increasing attention in clinical settings and are used in predicting the prognosis of HBV-ACLF[8-10]. The lymphocyte-to-white blood cell ratio (LWR) is a blood marker of the systemic inflammatory response. Studies have suggested that LWR has good prognostic value for patients with cancer, infective endocarditis and COVID-19[11-13]. However, the prognostic role of LWR in HBV-ACLF patients remains unclear. Therefore, our study aims to reveal whether LWR can risk-stratify poor prognosis in HBV-ACLF patients.

MATERIALS AND METHODS

Subjects

A total of 330 patients diagnosed with HBV-ACLF were retrospectively included from May 2014 to February 2021 at the Department of Gastroenterology, the First Affiliated Hospital of Nanchang University. The inclusion criteria were as follows: (1) Age ≥ 18 years; (2) Chronic liver disease due to HBV infection; and (3) HBV-ACLF diagnosed based on the diagnostic guidelines for liver failure established in 2019[14]. The exclusion criteria were as follows: (1) Coinfection with hepatitis A/C/D/E virus; (2) Other etiologies such as drugs, autoimmunity, alcohol, or toxins that may contribute to HBV-ACLF; (3) Complicated with hepatocellular carcinoma; (4) Human immunodeficiency virus infection; and (5) Loss to follow-up. The study was approved by the Institutional Review Board of the First Affiliated Hospital of Nanchang University.

Data collection

Demographic information and clinical data were comprehensively collected by searching medical

records. Laboratory blood tests were measured in the first 24-h period on admission. LWR was computed as the lymphocyte count (× 10^9/L) divided by the white blood cell count (× 10^9/L)[12]. The Child-Turcotte-Pugh (CTP), model for end-stage liver disease (MELD) and Chinese Group on the Study of Severe Hepatitis B-ACLF II (COSSHACLFII) scores were calculated as previously described[15-17]. All patients were followed from their diagnosis until either their death or the end of the 28-d follow-up period. The survival rates at 28 d were obtained from patients' medical records or by telephone calls with the patients or their kinsfolks.

Definitions

Chronic HBV infection was defined by the presence of hepatitis B surface antigen for > 6 mo[18]. HBV-ACLF was defined according to the Asian Pacific Association for the Study of the Liver criteria in 2019: (1) Serum bilirubin ≥ 5 mg/dL; (2) International normalized ratio (INR) ≥ 1.5 or prothrombin activity < 40%; (3) Complicated within 4 wk by clinical ascites and/or encephalopathy in patients with pre-existing chronic liver diseases (diagnosed or undiagnosed); and (4) High 28-d mortality[14].

Statistical analysis

Statistical analysis was performed using the SPSS 24.0 statistical package (SPSS Inc., Chicago, IL), R software version 4.1.0 (http://www.r-project.org/), and X-tile software (Version 3.6.1, Yale University, New Haven, CT, United States). Continuous variables were compared using the *t* test or the Mann-Whitney *U* test, whereas categorical variables were compared using the chi-square test or Fisher's exact test. Univariate analysis and multivariate Cox proportional hazards models were performed to identify whether LWR was related to poor outcomes. The optimal cutoff value of LWR was determined by using X-tile. The Kaplan-Meier survival curve was generated by the "survival" and "survminer" packages in R software. All statistical tests were two-sided with a statistical significance level set at *P* values < 0.05.

RESULTS

Baseline characteristics

The baseline characteristics of the patients are summarized in Table 1. A total of 330 patients with HBV-ACLF were recruited. In the cohort, the average age of patients was 49.68 ± 12.39 years, and approximately 83.9% of patients were male. The HBV-ACLF patients were divided into survivor and non-survivor groups according to the prognosis at 28 d. At follow-up, the age, prothrombin time (PT), INR, bilirubin, CTP score (CTPs), MELD score (MELDs), and COSSHACLFII score (COSSHACLFIIs) of the non-survivors were significantly higher than those of the survivors (*P* < 0.05). However, the PLT count and LWR level of the non-survivors were significantly lower than those of the survivors (*P* < 0.05). In addition, there were no significant differences in sex, costs, hemoglobin, albumin, creatinine, blood urea nitrogen (BUN), or serum Na between the non-survivor group and survivor group (*P* > 0.05).

Low LWR as an independent risk factor for mortality in patients with HBV-ACLF

The association between the LWR level and 28-d mortality is shown in Table 2. In univariate analysis, age, PLT, PT, hemoglobin, bilirubin, BUN, and LWR were significant factors for 28-d mortality (all *P* < 0.05). In multivariable analysis, the results showed that age, PT, bilirubin, and LWR were associated with short-term mortality [hazard ratio (HR) = 1.015, 95% confidence interval (CI): 1.001-1.030; HR = 1.028, 95%CI: 1.015-1.042; HR = 1.001, 95%CI: 1.000-1.003; HR = 0.052, 95%CI: 0.005-0.535, respectively].

Correlation between LWR levels and other score models

Next, we investigated the correlation between LWR levels and other score models, including CTPs, MELDs and COSSHACLFIIs. As shown in Figures 1A-C, LWR levels were significantly correlated with the CTPs, MELDs and COSSHACLFIIs (*r* = -0.29, *P* < 0.001; *r* = -0.31, *P* < 0.001; *r* = -0.49, *P* < 0.001, respectively).

Comparison of clinical data with different LWR levels

The median LMR of HBV-ACLF patients was 0.17 (0.11-0.23), and X-tile software was used to determine the optimal cutoff values for LWR for 28-d mortality. Consequently, the threshold of 0.11 enabled us to distinguish favorable and poor outcomes that were most significant in HBV-ACLF patients (Figure 2). HBV-ACLF patients were stratified into low LWR (LWR < 0.11) and high LWR (LWR ≥ 0.11) groups according to the cutoff values. As shown in Table 3, the patients in the group with LWR < 0.11 had an older age, lower PLT count, higher PT, higher INR, lower hemoglobin, lower albumin, higher creatinine, higher BUN, higher CTPs, higher MELDs, higher COSSHACLFIIs, and significantly shorter survival rate than those in the group with LWR ≥ 0.11.

Impact of LWR on the mortality of HBV-ACLF patients

As shown above, the patients with LWR < 0.11 had higher 28-d mortality than the high LWR group (*P* <

Table 1 Baseline characteristics of hepatitis B virus-acute on chronic liver failure patients

	All patients (*n* = 330)	Survivor patients (*n* = 195)	Non-survivor patients (*n* = 135)	*P* value
Age (yr)	49.68 ± 12.39	47.91 ± 12.12	52.23 ± 12.39	0.002
Male, *n* (%)	277 (83.9)	162 (83.1)	115 (85.2)	0.068
Costs (dollars)	10133.88 (5886.57-15955.07)	10734.72 (5958.59-16913.77)	9107.89 (5727.32-14945.14)	0.065
Ascites, *n* (%)				0.016
Mild	158 (47.9)	104 (53.3)	54 (40.0)	
Medium	102 (30.9)	59 (30.3)	43 (31.9)	
Severe	70 (21.2)	32 (16.4)	38 (28.1)	
PLT (10^9/L)	108.00 (72.75-144.25)	115.00 (82.00-148.00)	89.00 (57.00-138.00)	0.004
PT (s)	22.70 (19.30-29.25)	21.10 (18.90-25.20)	25.40 (21.80-32.80)	< 0.001
INR	2.01 (1.74-2.64)	1.88 (1.69-2.30)	2.4 (1.94-3.07)	< 0.001
Hemoglobin (g/L)	122.00 (102.00-136.00)	123.00 (107.00-137.00)	121.00 (94.00-135.00)	0.166
Bilirubin (μmol/L)	312.91 ± 135.85	299.15 ± 126.15	332.79 ± 146.96	0.027
Albumin (g/L)	31.40 (28.20-34.25)	31.50 (28.20-34.60)	31.10 (28.20-33.30)	0.151
Creatinine (μmol/L)	66.60 (57.08-84.73)	65.60 (57.00-81.00)	68.30 (57.50-91.90)	0.294
BUN (mmol/L)	4.00 (2.80-6.10)	4.00 (2.80-5.50)	4.10 (3.00-7.60)	0.074
Serum Na (mmol/L)	137.00 (133.30-139.10)	137.00 (133.20-139.00)	136.90 (133.30-139.10)	0.882
LWR	0.17 (0.11-0.23)	0.19 (0.12-0.25)	0.13 (0.08-0.20)	< 0.001
CTPs	11.00 (10.00-12.00)	11.00 (10.00-12.00)	12.00 (11.00-13.00)	< 0.001
MELDs	23.17 (20.03-27.27)	21.59 (18.86-25.46)	25.04 (21.78-29.10)	< 0.001
COSSHACLFIIs	7.18 (6.54-8.12)	6.80 (6.30-7.37)	7.95 (7.20-8.70)	< 0.001

PLT: Platelet; PT: Prothrombin time; INR: International normalized ratio; BUN: Blood urea nitrogen; LWR: Lymphocyte-to-white blood cell ratio; CTPs: Child-Turcotte-Pugh score; MELDs: Model for end-stage liver disease score; COSSHACLFIIs: Chinese group on the study of severe Hepatitis B-Acute-on-chronic liver failure II score.

0.05). To confirm the association of the LWR level and 28-d outcomes in detail, Kaplan-Meier analysis was performed to assess LWR in HBV-ACLF patients, and patients with low LWR levels had a worse outcome than those with high LWR levels (Figure 3).

DISCUSSION

In our study, we found that a low LWR level was an independent prognostic factor related to poor 28-d outcomes in patients with HBV-ACLF. Patients with LWR < 0.11 had higher 28-d mortality than those with high LWR levels.

Systemic inflammation plays an important role in the development of HBV-ACLF[19]. The activation of inflammatory cytokines causes organ hypoperfusion and systemic circulatory dysfunction, which increase the activation of coagulation, tissue microthrombosis, and the development of organ failure [20]. Many studies have indicated that the inflammatory response can be reflected by inflammatory markers such as lymphocytes, white blood cells, PLTs, and neutrophils[21,22]. The combination of these inflammatory markers, such as the neutrophil-lymphocyte ratio (NLR), platelet-to-white blood cell ratio (PWR), and LWR, has been confirmed as a prognostic marker in a variety of liver diseases. Bernsmeier *et al*[23] reported that the NLR was an independent risk factor in patients with acute decompensation (AD) cirrhosis. Kim *et al*[22] included 1670 AD patients from a prospective cohort and found that patients with a PWR ≤ 12.1 had a higher 28-d mortality than those with a PWR > 12.1, and a lower PWR level was a prognostic factor for 28-d adverse outcomes. Overall, these inflammation-based markers could be useful for stratifying the severity of liver disease.

Our study found that LWR levels were significantly decreased in non-survivor HBV-ACLF patients, and low LWR levels were an independent risk factor for 28-d mortality in HBV-ACLF patients. The decreased LWR levels may reflect an enhanced inflammatory response and/or impaired immune

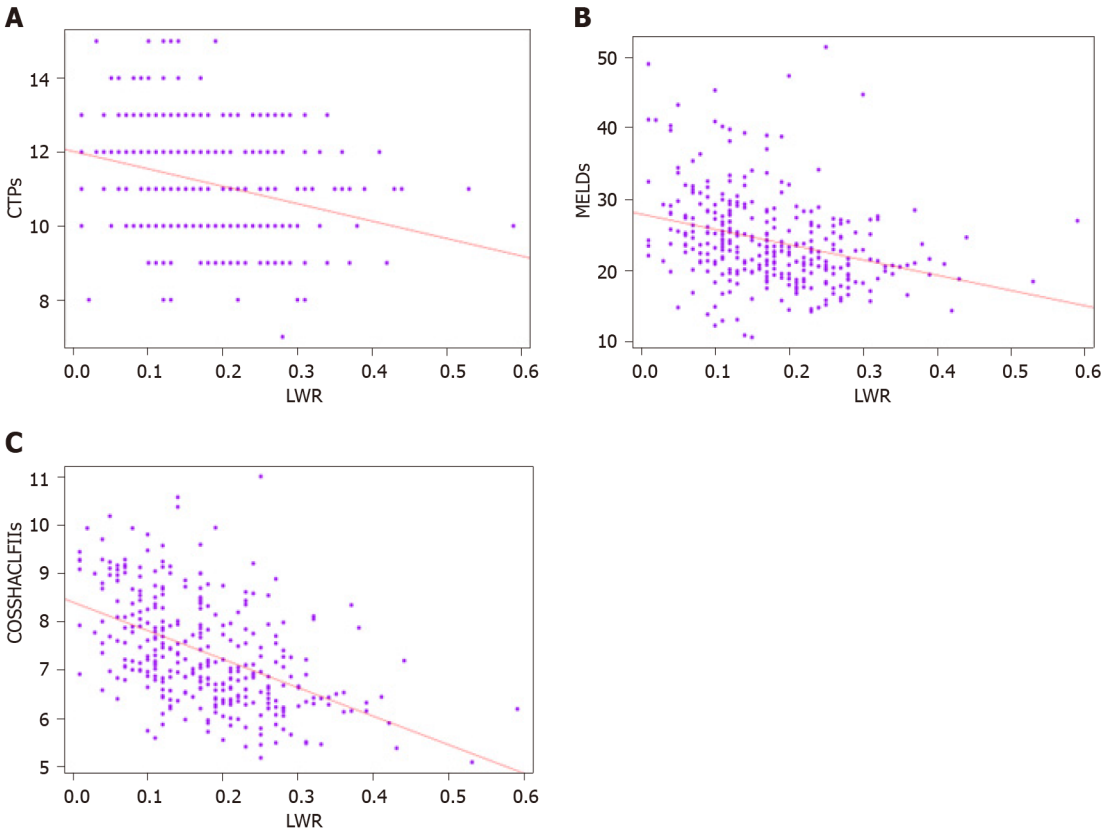

DOI: 10.3748/wjg.v29.i23.3678 **Copyright** ©The Author(s) 2023.

Figure 1 Scatter plot illustrating the correlation. A: Scatter plot illustrating the correlation between lymphocyte-to-white blood cell ratio (LWR) and Child-Turcotte-Pugh scores; B: Scatter plot illustrating the correlation between LWR and model for end-stage liver disease scores; C: Scatter plot illustrating the correlation between LWR and Chinese group on the study of severe Hepatitis B-Acute-on-chronic liver failure II scores. CTPs: Child-Turcotte-Pugh score; MELDs: Model for end-stage liver disease score; COSSHACLFIIs: Chinese group on the study of severe Hepatitis B-Acute-on-chronic liver failure II score; LWR: Lymphocyte-to-white blood cell ratio.

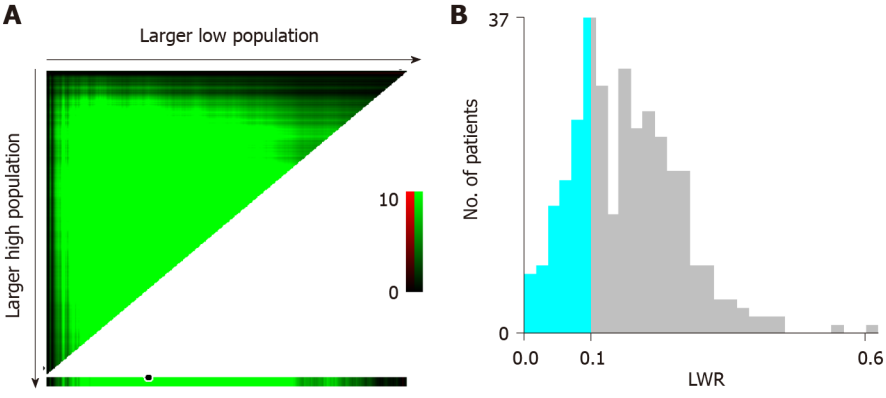

DOI: 10.3748/wjg.v29.i23.3678 **Copyright** ©The Author(s) 2023.

Figure 2 Analysis of lymphocyte-to-white blood cell ratio by using X-tile. A: The data on the horizontal ordinate increase from the left to the right, defined as the larger low population. The data on the vertical ordinate decrease from the top to the bottom, defined as the larger high population; B: The prognostic significance of lymphocyte-to-white blood cell ratio for hepatitis B virus-acute on chronic liver failure patients was determined by using a statistical algorithm in X-tile to calculate the most efficient cutoff point. LWR: Lymphocyte-to-white blood cell ratio.

response, which may explain the results. A previous study confirmed that lymphocytes play a critical role in the body's immune defense functions, immune response, and immune surveillance[12]. The elevated white blood cell count showed severe systemic inflammation, which was related to the prognosis of HBV-ACLF patients[24]. In addition, a recent study indicated that a low LWR level was an independent factor for poor outcomes in patients with decompensated liver cirrhosis, and the cut off value of LWR for 1 mo was 0.163. Patients with LWR < 0.163 had higher mortality than patients with LWR > 0.163[25]. Similar to this study, our research found that the cutoff value of LWR was 0.11, and

Table 2 Univariate and multivariate Cox regression analyses in hepatitis B virus-acute on chronic liver failure patients (*n* = 330)

	Univariate analysis		Multivariate analysis	
	HR (95%CI)	*P* value	HR (95%CI)	*P* value
Age	1.021 (1.007-1.035)	0.002	1.015 (1.001-1.030)	0.037
Male sex	1.202 (0.747-1.932)	0.448		
PLT (10^9/L)	0.997 (0.994-0.999)	0.046		
PT (s)	1.020 (1.011-1.030)	< 0.001	1.028 (1.015-1.042)	< 0.001
INR	1.042 (0.993-1.094)	0.093		
Hemoglobin (g/L)	0.993 (0.987-0.999)	0.027		
Bilirubin (μmol/L)	1.001 (1.000-1.003)	0.025	1.001 (1.000-1.003)	0.041
Albumin (g/L)	0.968 (0.933-1.005)	0.091		
Creatinine (μmol/L)	1.001 (1.000-1.001)	0.179		
BUN (mmol/L)	1.036 (1.014-1.058)	0.001		
Serum Na (mmol/L)	1.001 (0.999-1.003)	0.249		
LWR	0.011 (0.001-0.088)	< 0.001	0.052 (0.005-0.535)	0.013

In univariate analysis, $P < 0.1$ were subjected to multivariate analysis and was indicated in bold; in multivariate analysis, $P < 0.05$ was considered significant and was indicated in bold. CI: Confidence interval; HR: Hazard ratio; PLT: Platelet; PT: Prothrombin time; INR: International normalized ratio; BUN: Blood urea nitrogen; LWR: Lymphocyte-to-white blood cell ratio.

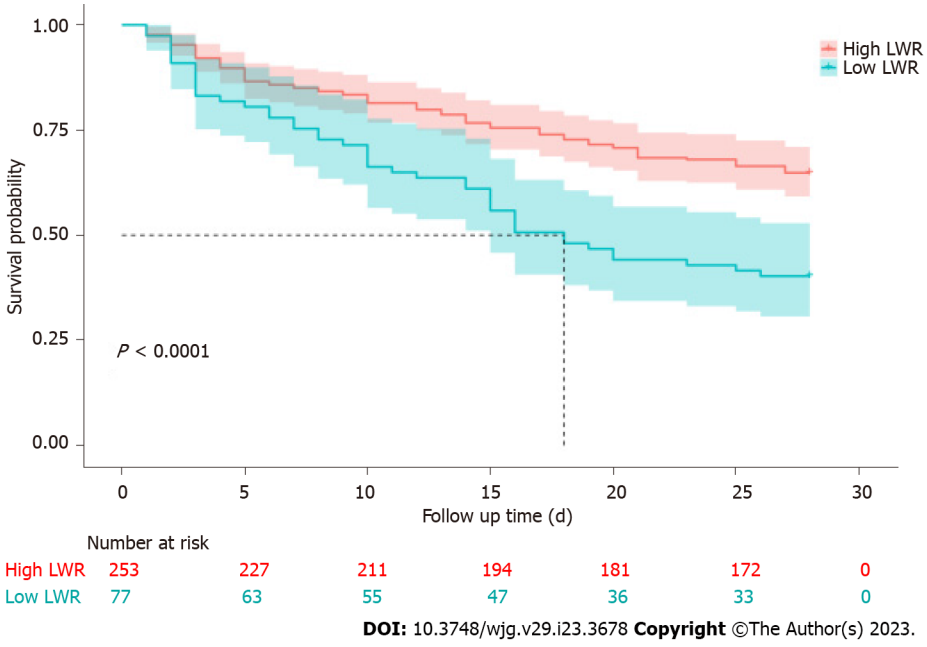

DOI: 10.3748/wjg.v29.i23.3678

Figure 3 Kaplan-Meier analysis of 28-d overall survival. The mortality rate was higher in patients with lymphocyte-to-white blood cell ratio (LWR) < 0.11 than in patients with LWR ≥ 0.11. LWR: Lymphocyte-to-white blood cell ratio.

patients with LWR < 0.11 had higher mortality than patients with LWR ≥ 0.11, and the results showed a significant negative correlation between LWR and CTPs, MELDs and COSSHACLFIIs. There are several limitations in our study. First, this is a single-center and retrospective study, which may cause selection biases. Second, lymphocytes and white blood cells were not tested dynamically during follow-up.

CONCLUSION

In conclusion, LWR is easily accessible and conveniently calculated, and it might be a good marker for

Table 3 Clinical characteristics between low and high lymphocyte-to-white blood cell ratio groups in hepatitis B virus-acute on chronic liver failure patients

	Low LWR level (*n* = 77)	High LWR level (*n* = 253)	*P* value
Age (yr)	52.99 ± 12.57	48.67 ± 12.19	0.007
Male, *n* (%)	59 (76.6)	218 (86.2)	0.046
Costs (dollars)	7625.18 (3899.37-12070.55)	10984.59 (6639.92-16693.10)	< 0.001
Ascites, *n* (%)			0.007
Mild	25 (32.5)	133 (52.6)	
Medium	29 (37.7)	73 (28.9)	
Severe	23 (29.9)	47 (18.6)	
PLT (10^9/L)	86.00 (55.50-138.50)	110.00 (79.50-145.50)	0.039
PT (s)	23.20 (19.70-33.50)	22.40 (19.20-28.00)	0.016
INR	2.13 (1.76-3.11)	1.99 (1.73-2.54)	0.018
Hemoglobin (g/L)	109.00 (89.50-125.50)	125.00 (108.00-139.00)	< 0.001
Bilirubin (μmol/L)	331.52 ± 153.46	307.25 ± 129.82	0.170
Albumin (g/L)	30.10 (26.30-32.50)	31.80 (28.85-34.55)	< 0.001
Creatinine (μmol/L)	82.40 (58.40-126.10)	64.80 (56.85-77.95)	< 0.001
BUN (mmol/L)	7.00 (4.00-11.10)	3.70 (2.70-5.20)	< 0.001
Serum Na (mmol/L)	135.30 (131.50-139.05)	137.20 (133.90-139.10)	0.086
CTPs	12.00 (11.00-13.00)	11.00 (10.00-12.00)	< 0.001
MELDs	25.79 (22.52-30.91)	22.44 (19.55-26.13)	< 0.001
COSSHACLFIIs	8.11 (7.26-9.06)	6.94 (6.40-7.79)	< 0.001
28-d mortality, *n* (%)	46 (59.7)	89 (35.2)	< 0.001

PLT: Platelet; PT: Prothrombin time; INR: International normalized ratio; BUN: Blood urea nitrogen; LWR: Lymphocyte-to-white blood cell ratio; CTPs: Child-Turcotte-Pugh score; MELDs: Model for end-stage liver disease score; COSSHACLFIIs: Chinese group on the study of severe Hepatitis B-Acute-on-chronic liver failure II score.

identifying the risk of poor outcomes in HBV-ACLF patients. Therefore, our findings can help clinicians intervene in high-risk patients as early as possible.

ARTICLE HIGHLIGHTS

Research background

The lymphocyte-to-white blood cell ratio (LWR) is a blood marker that reflects the systemic inflammatory response. The prognostic value of the LWR remains unclear in hepatitis B virus-associated acute-on-chronic liver failure (HBV-ACLF) patients.

Research motivation

It is necessary to find an easy and effective marker that can reflect the prognosis in HBV-ACLF patients, so we explored whether LWR can risk-stratify poor prognosis in HBV-ACLF patients.

Research objectives

This study aimed to investigate whether LWR could be an easy and useful marker that can identify the risk of poor outcomes in HBV-ACLF patients.

Research methods

A total of 330 HBV-ACLF patients were included in this study, and patients were divided into survivor and non-survivor groups according to 28-d outcome. Univariate and multivariate Cox regression analyses were performed to select independent risk factors for 28-d mortality. The correlation test was

performed to evaluate the correlation between LWR and Child-Turcotte-Pugh score (CTPs), model for end-stage liver disease score (MELDs), and Chinese Group on the Study of Severe Hepatitis B-ACLF II score (COSSHACLFIIs). The cutoff value of LWR was calculated by X-tile software, and Kaplan-Meier analysis was performed to assess the association of the LWR level and 28-d outcomes in HBV-ACLF patients.

Research results

Low LWR was an independent risk factor for 28-d mortality in patients with HBV-ACLF (hazard ratio = 0.052, 95% confidence interval: 0.005-0.535), and LWR levels were significantly negatively correlated with CTPs, MELDs and COSSHACLFIIs. Moreover, the patients with low LWR levels had a higher 28-d mortality than those with high LWR levels.

Research conclusions

LWR is a simple, useful, and effective marker that could stratify the risk of 28-d adverse outcomes in HBV-ACLF patients.

Research perspectives

Further large-sample and multicenter prospective studies should be conducted to verify and confirm the prognostic value of the LWR.

FOOTNOTES

Author contributions: Zhang Y and Chen P contributed equally to this study, and they wrote the original draft; Zhang Y designed this study; Chen P analyzed the data; Zhu X critically revised the manuscript; and all authors have read and approved the final manuscript.

Supported by the National Natural Science Foundation of China, No. 81960120 and 81660110; the Postgraduate Innovation Special Foundation of Jiangxi Province, No. YC2022-B052; and "Gan-Po Talent 555" Project of Jiangxi Province, No. GCZ (2012)-1.

Institutional review board statement: The study was reviewed and approved by the First Affiliated Hospital of Nanchang University Institutional Review Board (Approval No. IIT2021009).

Informed consent statement: All study participants, or their legal guardian, provided informed written consent prior to study enrollment.

Conflict-of-interest statement: All the authors report no relevant conflicts of interest for this article.

Data sharing statement: Data can be acquired from the corresponding author.

Country/Territory of origin: China

ORCID number: Yue Zhang 0000-0003-1514-2303; Peng Chen 0000-0002-2215-214X; Xuan Zhu 0000-0002-1240-0947.

S-Editor: Wang JJ
L-Editor: A
P-Editor: Wang JJ

REFERENCES

1 **Zaccherini G**, Weiss E, Moreau R. Acute-on-chronic liver failure: Definitions, pathophysiology and principles of treatment. *JHEP Rep* 2021; **3**: 100176 [PMID: 33205036 DOI: 10.1016/j.jhepr.2020.100176]

2 **Moreau R**, Jalan R, Gines P, Pavesi M, Angeli P, Cordoba J, Durand F, Gustot T, Saliba F, Domenicali M, Gerbes A, Wendon J, Alessandria C, Laleman W, Zeuzem S, Trebicka J, Bernardi M, Arroyo V; CANONIC Study Investigators of the EASL–CLIF Consortium. Acute-on-chronic liver failure is a distinct syndrome that develops in patients with acute decompensation of cirrhosis. *Gastroenterology* 2013; **144**: 1426-1437, 1437.e1 [PMID: 23474284 DOI: 10.1053/j.gastro.2013.02.042]

3 **Trebicka J**, Fernandez J, Papp M, Caraceni P, Laleman W, Gambino C, Giovo I, Uschner FE, Jimenez C, Mookerjee R, Gustot T, Albillos A, Bañares R, Janicko M, Steib C, Reiberger T, Acevedo J, Gatti P, Bernal W, Zeuzem S, Zipprich A, Piano S, Berg T, Bruns T, Bendtsen F, Coenraad M, Merli M, Stauber R, Zoller H, Ramos JP, Solè C, Soriano G, de Gottardi A, Gronbaek H, Saliba F, Trautwein C, Özdogan OC, Francque S, Ryder S, Nahon P, Romero-Gomez M, Van Vlierberghe H, Francoz C, Manns M, Garcia E, Tufoni M, Amoros A, Pavesi M, Sanchez C, Curto A, Pitarch C, Putignano A, Moreno E, Shawcross D, Aguilar F, Clària J, Ponzo P, Jansen C, Vitalis Z, Zaccherini G, Balogh B, Vargas V, Montagnese S, Alessandria C, Bernardi M, Ginès P, Jalan R, Moreau R, Angeli P, Arroyo V; PREDICT STUDY group of the EASL-CLIF Consortium. The PREDICT study uncovers three clinical courses of acutely decompensated cirrhosis that have distinct pathophysiology. *J Hepatol* 2020; **73**: 842-854 [PMID: 32673741 DOI: 10.1016/j.jhep.2020.06.013]

4 **Zheng MH**, Shi KQ, Fan YC, Li H, Ye C, Chen QQ, Chen YP. A model to determine 3-month mortality risk in patients with acute-on-chronic hepatitis B liver failure. *Clin Gastroenterol Hepatol* 2011; **9**: 351-356.e3 [PMID: 21195790 DOI: 10.1016/j.cgh.2010.12.027]

5 **Wu T**, Li J, Shao L, Xin J, Jiang L, Zhou Q, Shi D, Jiang J, Sun S, Jin L, Ye P, Yang L, Lu Y, Li T, Huang J, Xu X, Chen J, Hao S, Chen Y, Xin S, Gao Z, Duan Z, Han T, Wang Y, Gan J, Feng T, Pan C, Li H, Huang Y, Xie Q, Lin S, Li L; Chinese Group on the Study of Severe Hepatitis B (COSSH). Development of diagnostic criteria and a prognostic score for hepatitis B virus-related acute-on-chronic liver failure. *Gut* 2018; **67**: 2181-2191 [PMID: 28928275 DOI: 10.1136/gutjnl-2017-314641]

6 **Clària J**, Stauber RE, Coenraad MJ, Moreau R, Jalan R, Pavesi M, Amorós À, Titos E, Alcaraz-Quiles J, Oettl K, Morales-Ruiz M, Angeli P, Domenicali M, Alessandria C, Gerbes A, Wendon J, Nevens F, Trebicka J, Laleman W, Saliba F, Welzel TM, Albillos A, Gustot T, Benten D, Durand F, Ginès P, Bernardi M, Arroyo V; CANONIC Study Investigators of the EASL-CLIF Consortium and the European Foundation for the Study of Chronic Liver Failure (EF-CLIF). Systemic inflammation in decompensated cirrhosis: Characterization and role in acute-on-chronic liver failure. *Hepatology* 2016; **64**: 1249-1264 [PMID: 27483394 DOI: 10.1002/hep.28740]

7 **Bernsmeier C**, van der Merwe S, Périanin A. Innate immune cells in cirrhosis. *J Hepatol* 2020; **73**: 186-201 [PMID: 32240716 DOI: 10.1016/j.jhep.2020.03.027]

8 **Jie Y**, Gong J, Xiao C, Zhu S, Zhou W, Luo J, Chong Y, Hu B. Low Platelet to White Blood Cell Ratio Indicates Poor Prognosis for Acute-On-Chronic Liver Failure. *Biomed Res Int* 2018; **2018**: 7394904 [PMID: 29854786 DOI: 10.1155/2018/7394904]

9 **Sun J**, Guo H, Yu X, Zhu H, Zhang X, Yang J, Wang J, Qian Z, Shen Z, Mao R, Zhang J. A neutrophil-to-lymphocyte ratio-based prognostic model to predict mortality in patients with HBV-related acute-on-chronic liver failure. *BMC Gastroenterol* 2021; **21**: 422 [PMID: 34758747 DOI: 10.1186/s12876-021-02007-w]

10 **Liu XY**, He X, Cai M, Peng SQ. Prognostic Value of Complete Blood Cell Count-Derived Inflammatory Markers in Hepatitis B Virus-Related Acute-on-Chronic Liver Failure. *Clin Lab* 2021; **67** [PMID: 34655197 DOI: 10.7754/Clin.Lab.2021.210217]

11 **Zhao W**, Wang P, Jia H, Chen M, Gu X, Liu M, Zhang Z, Cheng W, Wu Z. Lymphocyte count or percentage: which can better predict the prognosis of advanced cancer patients following palliative care? *BMC Cancer* 2017; **17**: 514 [PMID: 28768490 DOI: 10.1186/s12885-017-3498-8]

12 **Pitre T**, Jones A, Su J, Helmeczi W, Xu G, Lee C, Shamsuddin A, Mir A, MacGregor S, Duong M, Ho T, Beauchamp MK, Costa AP, Kruisselbrink R; COREG Investigators. Inflammatory biomarkers as independent prognosticators of 28-day mortality for COVID-19 patients admitted to general medicine or ICU wards: a retrospective cohort study. *Intern Emerg Med* 2021; **16**: 1573-1582 [PMID: 33496923 DOI: 10.1007/s11739-021-02637-8]

13 **Zhang M**, Ge Q, Qiao T, Wang Y, Xia X, Zhang X, Zhou J. Prognostic Value of Lymphocyte-to-White Blood Cell Ratio for In-Hospital Mortality in Infective Endocarditis Patients. *Int J Clin Pract* 2022; **2022**: 8667054 [PMID: 35685545 DOI: 10.1155/2022/8667054]

14 **Sarin SK**, Choudhury A, Sharma MK, Maiwall R, Al Mahtab M, Rahman S, Saigal S, Saraf N, Soin AS, Devarbhavi H, Kim DJ, Dhiman RK, Duseja A, Taneja S, Eapen CE, Goel A, Ning Q, Chen T, Ma K, Duan Z, Yu C, Treeprasertsuk S, Hamid SS, Butt AS, Jafri W, Shukla A, Saraswat V, Tan SS, Sood A, Midha V, Goyal O, Ghazinyan H, Arora A, Hu J, Sahu M, Rao PN, Lee GH, Lim SG, Lesmana LA, Lesmana CR, Shah S, Prasad VGM, Payawal DA, Abbas Z, Dokmeci AK, Sollano JD, Carpio G, Shresta A, Lau GK, Fazal Karim M, Shiha G, Gani R, Kalista KF, Yuen MF, Alam S, Khanna R, Sood V, Lal BB, Pamecha V, Jindal A, Rajan V, Arora V, Yokosuka O, Niriella MA, Li H, Qi X, Tanaka A, Mochida S, Chaudhuri DR, Gane E, Win KM, Chen WT, Rela M, Kapoor D, Rastogi A, Kale P, Sharma CB, Bajpai M, Singh V, Premkumar M, Maharashi S, Olithselvan A, Philips CA, Srivastava A, Yachha SK, Wani ZA, Thapa BR, Saraya A, Shalimar, Kumar A, Wadhawan M, Gupta S, Madan K, Sakhuja P, Vij V, Sharma BC, Garg H, Garg V, Kalal C, Anand L, Vyas T, Mathur RP, Kumar G, Jain P, Pasupuleti SSR, Chawla YK, Chowdhury A, Song DS, Yang JM, Yoon EL; APASL ACLF Research Consortium (AARC) for APASL ACLF working Party. Acute-on-chronic liver failure: consensus recommendations of the Asian Pacific association for the study of the liver (APASL): an update. *Hepatol Int* 2019; **13**: 353-390 [PMID: 31172417 DOI: 10.1007/s12072-019-09946-3]

15 **Pugh RN**, Murray-Lyon IM, Dawson JL, Pietroni MC, Williams R. Transection of the oesophagus for bleeding oesophageal varices. *Br J Surg* 1973; **60**: 646-649 [PMID: 4541913 DOI: 10.1002/bjs.1800600817]

16 **Li J**, Liang X, You S, Feng T, Zhou X, Zhu B, Luo J, Xin J, Jiang J, Shi D, Lu Y, Ren K, Wu T, Yang L, Li J, Li T, Cai Q, Sun S, Guo B, Chen J, He L, Li P, Yang H, Hu W, An Z, Jin X, Tian J, Wang B, Chen X, Xin S; Chinese Group on the Study of Severe Hepatitis B (COSSH). Development and validation of a new prognostic score for hepatitis B virus-related acute-on-chronic liver failure. *J Hepatol* 2021; **75**: 1104-1115 [PMID: 34090929 DOI: 10.1016/j.jhep.2021.05.026]

17 **Kamath PS**, Wiesner RH, Malinchoc M, Kremers W, Therneau TM, Kosberg CL, D'Amico G, Dickson ER, Kim WR. A model to predict survival in patients with end-stage liver disease. *Hepatology* 2001; **33**: 464-470 [PMID: 11172350 DOI: 10.1053/jhep.2001.22172]

18 **Liaw YF**, Kao JH, Piratvisuth T, Chan HL, Chien RN, Liu CJ, Gane E, Locarnini S, Lim SG, Han KH, Amarapurkar D, Cooksley G, Jafri W, Mohamed R, Hou JL, Chuang WL, Lesmana LA, Sollano JD, Suh DJ, Omata M. Asian-Pacific consensus statement on the management of chronic hepatitis B: a 2012 update. *Hepatol Int* 2012; **6**: 531-561 [PMID:

26201469 DOI: 10.1007/s12072-012-9365-4]

19 **Premkumar M**, Saxena P, Rangegowda D, Baweja S, Mirza R, Jain P, Bhatia P, Kumar G, Bihari C, Kalal C, Vyas T, Choudhury A, Sarin SK. Coagulation failure is associated with bleeding events and clinical outcome during systemic inflammatory response and sepsis in acute-on-chronic liver failure: An observational cohort study. *Liver Int* 2019; **39**: 694-704 [PMID: 30589495 DOI: 10.1111/liv.14034]

20 **Lisman T**, Luyendyk JP. Systemic inflammation and disorders of hemostasis in the AD-ACLF syndrome. *J Hepatol* 2021; **74**: 1264-1265 [PMID: 33347950 DOI: 10.1016/j.jhep.2020.12.017]

21 **Cai YJ**, Dong JJ, Dong JZ, Chen Y, Lin Z, Song M, Wang YQ, Chen YP, Shi KQ, Zhou MT. A nomogram for predicting prognostic value of inflammatory response biomarkers in decompensated cirrhotic patients without acute-on-chronic liver failure. *Aliment Pharmacol Ther* 2017; **45**: 1413-1426 [PMID: 28345155 DOI: 10.1111/apt.14046]

22 **Kim JH**, Kim SE, Song DS, Kim HY, Yoon EL, Kim TH, Jung YK, Suk KT, Jun BG, Yim HJ, Kwon JH, Lee SW, Kang SH, Kim MY, Jeong SW, Jang JY, Yoo JJ, Kim SG, Jin YJ, Cheon GJ, Kim BS, Seo YS, Kim HS, Sinn DH, Chung WJ, Lee HA, Nam SW, Kim IH, Suh JI, Kim JH, Chae HB, Sohn JH, Cho JY, Kim YJ, Yang JM, Park JG, Kim W, Cho HC, Kim DJ. Platelet-to-White Blood Cell Ratio Is Associated with Adverse Outcomes in Cirrhotic Patients with Acute Deterioration. *J Clin Med* 2022; **11** [PMID: 35566588 DOI: 10.3390/jcm11092463]

23 **Bernsmeier C**, Cavazza A, Fatourou EM, Theocharidou E, Akintimehin A, Baumgartner B, Dhar A, Auzinger G, Thursz M, Bernal W, Wendon JA, Karvellas CJ, Antoniades CG, McPhail MJW. Leucocyte ratios are biomarkers of mortality in patients with acute decompensation of cirrhosis and acute-on-chronic liver failure. *Aliment Pharmacol Ther* 2020; **52**: 855-865 [PMID: 32683724 DOI: 10.1111/apt.15932]

24 **Chen L**, Zhang J, Lu T, Cai J, Zheng J, Yao J, Yi S, Li H, Chen G, Zhao H, Zhang Y, Yang Y. A nomogram to predict survival in patients with acute-on-chronic hepatitis B liver failure after liver transplantation. *Ann Transl Med* 2021; **9**: 555 [PMID: 33987253 DOI: 10.21037/atm-20-6180]

25 **Xie Y**, He C, Wang W. A potential novel inflammation biomarker for predicting the prognosis of decompensated liver cirrhosis. *Ann Med* 2022; **54**: 3201-3210 [PMID: 36369931 DOI: 10.1080/07853890.2022.2142277]

World Journal of Gastroenterology

Submit a Manuscript: https://www.f6publishing.com

World J Gastroenterol 2023 June 21; 29(23): 3688-3702

DOI: 10.3748/wjg.v29.i23.3688

ISSN 1007-9327 (print) ISSN 2219-2840 (online)

ORIGINAL ARTICLE

Observational Study

Spatial cluster mapping and environmental modeling in pediatric inflammatory bowel disease

Mielle Michaux, Justin M Chan, Luke Bergmann, Luis F Chaves, Brian Klinkenberg, Kevan Jacobson

Specialty type: Gastroenterology and hepatology

Provenance and peer review: Unsolicited article; Externally peer reviewed.

Peer-review model: Single blind

Peer-review report's scientific quality classification

Grade A (Excellent): 0
Grade B (Very good): 0
Grade C (Good): C, C
Grade D (Fair): 0
Grade E (Poor): 0

P-Reviewer: Maric I, Croatia; Wang LH, China

Received: February 7, 2023
Peer-review started: February 7, 2023
First decision: March 20, 2023
Revised: March 31, 2023
Accepted: April 23, 2023
Article in press: April 23, 2023
Published online: June 21, 2023

Mielle Michaux, Justin M Chan, Kevan Jacobson, Department of Pediatrics, Division of Gastroenterology, Hepatology and Nutrition, Faculty of Medicine, British Columbia Children's Hospital, University of British Columbia, Vancouver V6H 3V4, British Columbia, Canada

Mielle Michaux, Justin M Chan, Kevan Jacobson, British Columbia Children's Hospital Research Institute, British Columbia Children's Hospital, Vancouver V5Z 4H4, British Columbia, Canada

Luke Bergmann, Brian Klinkenberg, Department of Geography, University of British Columbia, Vancouver V6T 1Z2, British Columbia, Canada

Luis F Chaves, Department of Environmental and Occupational Health, School of Public Health, Indiana University, Bloomington, IN 47405, United States

Kevan Jacobson, Department of Cellular and Physiological Sciences, University of British Columbia, Vancouver V6T 1Z3, British Columbia, Canada

Corresponding author: Kevan Jacobson, AGAF, FRCPC, MBChB, Professor, Senior Scientist, Department of Pediatrics, Division of Gastroenterology, Hepatology and Nutrition, Faculty of Medicine, British Columbia Children's Hospital, University of British Columbia, 4480 Oak Street, Room K4-184, Vancouver V6H 3V4, British Columbia, Canada. kjacobson@cw.bc.ca

Abstract

BACKGROUND

Geographical (geospatial) clusters have been observed in inflammatory bowel disease (IBD) incidence and linked to environmental determinants of disease, but pediatric spatial patterns in North America are unknown. We hypothesized that we would identify geospatial clusters in the pediatric IBD (PIBD) population of British Columbia (BC), Canada and associate incidence with ethnicity and environmental exposures.

AIM

To identify PIBD clusters and model how spatial patterns are associated with population ethnicity and environmental exposures.

METHODS

One thousand one hundred eighty-three patients were included from a BC Children's Hospital clinical registry who met the criteria of diagnosis with IBD ≤

age 16.9 from 2001–2016 with a valid postal code on file. A spatial cluster detection routine was used to identify areas with similar incidence. An ecological analysis employed Poisson rate models of IBD, Crohn's disease (CD), and ulcerative colitis (UC) cases as functions of areal population ethnicity, rurality, average family size and income, average population exposure to green space, air pollution, and vitamin-D weighted ultraviolet light from the Canadian Environmental Health Research Consortium, and pesticide applications.

RESULTS

Hot spots (high incidence) were identified in Metro Vancouver (IBD, CD, UC), southern Okanagan regions (IBD, CD), and Vancouver Island (CD). Cold spots (low incidence) were identified in Southeastern BC (IBD, CD, UC), Northern BC (IBD, CD), and on BC's coast (UC). No high incidence hot spots were detected in the densest urban areas. Modeling results were represented as incidence rate ratios (IRR) with 95%CI. Novel risk factors for PIBD included fine particulate matter ($PM_{2.5}$) pollution (IRR = 1.294, CI = 1.113-1.507, $P < 0.001$) and agricultural application of petroleum oil to orchards and grapes (IRR = 1.135, CI = 1.007-1.270, $P = 0.033$). South Asian population (IRR = 1.020, CI = 1.011-1.028, $P < 0.001$) was a risk factor and Indigenous population (IRR = 0.956, CI = 0.941-0.971, $P < 0.001$), family size (IRR = 0.467, CI = 0.268-0.816, $P = 0.007$), and summer ultraviolet (IBD = 0.9993, CI = 0.9990–0.9996, $P < 0.001$) were protective factors as previously established. Novel risk factors for CD, as for PIBD, included: $PM_{2.5}$ air pollution (IRR = 1.230, CI = 1 .056-1.435, $P = 0.008$) and agricultural petroleum oil (IRR = 1.159, CI = 1.002-1.326, $P = 0.038$). Indigenous population (IRR = 0.923, CI = 0.895–0.951, $P < 0.001$), as previously established, was a protective factor. For UC, rural population (UC IRR = 0.990, CI = 0.983-0.996, $P = 0.004$) was a protective factor and South Asian population (IRR = 1.054, CI = 1.030–1.079, $P < 0.001$) a risk factor as previously established.

CONCLUSION

PIBD spatial clusters were identified and associated with known and novel environmental determinants. The identification of agricultural pesticides and $PM_{2.5}$ air pollution needs further study to validate these observations.

Key Words: Inflammatory bowel diseases; Crohn disease; Ulcerative colitis; Pesticides; Air pollution; South Asian people

Core Tip: Utilizing spatial mapping methodology, high and low incidence clusters of pediatric inflammatory bowel disease (IBD) were identified in British Columbia, Canada. Associating geographical location with IBD, rurality was negatively associated with ulcerative colitis. Notably, no high incidence hot spots were detected in the densest urban areas, suggesting unexplored urban protective factors. Novel risk factors for PIBD and specifically Crohn's disease included fine particulate matter pollution and agricultural applications of petroleum oil to orchards and grapes. Spatial distribution was partially explained by rurality, population ethnicity, family size, pesticide applications, air pollution, ultraviolet exposure, and residential greenness.

Citation: Michaux M, Chan JM, Bergmann L, Chaves LF, Klinkenberg B, Jacobson K. Spatial cluster mapping and environmental modeling in pediatric inflammatory bowel disease. *World J Gastroenterol* 2023; 29(23): 3688-3702
URL: https://www.wjgnet.com/1007-9327/full/v29/i23/3688.htm
DOI: https://dx.doi.org/10.3748/wjg.v29.i23.3688

INTRODUCTION

Canada has one of the world's highest rates of pediatric inflammatory bowel disease (IBD), which includes Crohn's disease (CD) and ulcerative colitis (UC)[1]. Incidence within countries can be quite varied, but local patterns of IBD incidence are unknown for most countries[1]. Results from studies in Finland, Norway, Northern France, and Manitoba, Canada suggest that IBD may have a clustered spatial distribution, but more research is necessary for understanding local spatial patterns[2-5]. To date, no study has focused on empirically detecting and evaluating disease clusters in Canadian or North American pediatric IBD (PIBD) populations. Notably, detecting local spatial clusters of IBD would allow for a better understanding of clinical populations and identify areas where services are needed.

Moreover, spatial epidemiology can be used to identify novel environmental risk and protective factors. Although it is evident that environmental factors are important determinants for disease development, additional study is necessary.

A variety of population and environmental factors are thought to influence IBD risk. High incidence has been observed in Canadian populations of Jewish ethnicity and South Asian pediatric populations in British Columbia (BC), and low incidence has been reported in Canadian Indigenous communities[4,6,7]. Higher socioeconomic status has been associated with IBD[4,8]. A variety of environmental exposures, including rural residence, green space, ultraviolet (UV) radiation, and air pollution have also been studied[9-13]. No study known to us has examined pesticides as a potential determinant of PIBD. Pesticides can be present in food and the environment, and a variety of pesticides have been linked with changes to the gut microbiota which could have implications for IBD development[14]. Based on Canadian immigration and rural residence studies of IBD, exposures during early life appear to be important[9,15].

The aims of this exploratory study were (1) To determine spatial patterning of PIBD and identify location of disease hot and cold spots in the Canadian province of BC; and (2) to model the association between IBD case counts and population-level ethnicity, average income, rural residence, and known as well as novel environmental determinants. We hypothesized that we would identify IBD clusters that would be associated with ethnicity and environmental exposures. Modeling potential population risk factors provided context to the spatial analysis and helped identify areas where additional novel environmental risk or protective factors might have meaningfully affected disease incidence.

MATERIALS AND METHODS

Study area

BC is Canada's westernmost province. It is divided into five Regional Health Authorities, which can be further subdivided into 89 Local Health Areas (LHAs) (see Figure 1 and Supplementary Figure 1). The majority of BC's population live in urban areas located in the Vancouver Coastal and Fraser Health Authorities near the United States border[16]. Northern, Interior, and Vancouver Island Health serve largely more rural populations.

Participants

Patients for this study were selected from a clinical registry of IBD patients maintained by the BC Children's Hospital (BCCH) Division of Gastroenterology, Hepatology and Nutrition who were diagnosed with or received care for IBD at BCCH in Vancouver[17]. Author Jacobson K is data steward for this registry. As BCCH is the only tertiary care pediatric institution with academic pediatric gastroenterologists in the province, it is where most children with IBD are diagnosed. Our recent study comparing PIBD incidence derived from the BCCH registry with incidence derived from population-wide provincial health administrative data between 1996 and 2008 found similar overall rates, particularly from 2001 onwards, reaffirming the validity of the registry as a reflection of population-based cases[18]. Notably, a small number of cases are diagnosed in the community, use health services from a different province or, in the case of older patients (> 16.9 years), are diagnosed by adult gastroenterology physicians. Registry patients were excluded from the study if they were diagnosed outside the study period (2001 to 2016) or over age 16.9 years, did not have a valid postal code on file, or had a postal code associated with BCCH as this was likely not their permanent address. Postal codes were cleaned to provide consistent formatting. See Table 1 for BC pediatric incidence, and Supplementary Table 1 for incidence by patient age. Patient six-digit postal code point location at diagnosis was associated with latitude and longitude coordinates from DMTI Spatial Inc. obtained from the Canadian Urban Environmental Health Research Consortium (CANUE)[19]. Incidence was pooled for the full study period to maximize the number of cases in each analysis.

This study was approved by the University of British Columbia Children's and Women's Research Ethics Board, No. H19-00739.

Methods

Guidelines from the REporting of studies Conducted using Observational Routinely-collected health Data statement were adapted for this ecological study. The statistical methods of this study were reviewed by biostatistician Jeffrey Bone from the BCCH Research Institute. Data is summarized in Table 2, with additional details on environmental exposures presented in the Supplementary materials. Ethnicity and family size (married or common-law spouses, single parents, and at least one child) data from the Canadian census were obtained at the Dissemination Area level and resampled to LHAs by population-weighted overlay[16,20,21]. Average family income for 2005 and 2015 was available for LHAs[22]. To approximate average environmental exposures for each LHA, census population age 0-19 was used to population-weight postal code exposure data in a process that captured 92.6% of BC's youth population (excluded population resided in areas not covered by single link postal codes). Environmental data provided by CANUE for six digit postal codes included Normalized Difference

Table 1 British Columbia average pediatric incidence for inflammatory bowel disease, Crohn's disease, ulcerative colitis, and inflammatory bowel disease-unclassified from 2001–2016

Diagnosis	Health authority	Cases	Incidence per 100000	95%CI for incidence	
All IBD	All British Columbia	1183	9.22	8.7	9.76
	Fraser	558	10.95	10.06	11.9
	Interior	143	7.15	6.03	8.43
	Northern	64	6.17	4.75	7.88
	Vancouver Coastal	254	9.28	8.17	10.49
	Vancouver Island	164	8.36	7.13	9.74
CD	All British Columbia	780	6.08	5.66	6.52
	Fraser	356	6.99	6.28	7.74
	Interior	96	4.8	3.89	5.85
	Northern	40	3.86	2.76	5.24
	Vancouver Coastal	166	6.06	5.18	7.06
	Vancouver Island	122	6.22	5.17	7.43
UC	All British Columbia	288	2.24	1.99	2.52
	Fraser	151	2.96	2.51	3.48
	Interior	32	1.6	1.09	2.26
	Northern	16	1.54	0.88	2.51
	Vancouver Coastal	62	2.27	1.74	2.9
	Vancouver Island	27	1.38	0.91	2
IBD-U	All British Columbia	115	0.9	0.74	1.08
	Fraser	51	1	0.75	1.32
	Interior	15	0.75	0.42	1.24
	Northern	8	0.77	0.33	1.52
	Vancouver Coastal	26	0.95	0.62	1.39
	Vancouver Island	15	0.76	0.43	1.26

IBD: Inflammatory bowel disease; CD: Crohn's disease, UC: Ulcerative colitis; IBD-U: Inflammatory bowel disease-unclassified.

Vegetation Index (NDVI)[19,23-26] greenness[27,28], vitamin D UV[19,29,30], nitrogen dioxide (NO_2)[19,31,32], ozone (O_3)[33-37], and fine particulate matter ($PM_{2.5}$)[19,38]. Data on metam, petroleum oil, and glyphosate pesticides was resampled from Global Pesticide Grids[39,40]. The least populous LHA was excluded from regression modeling due to missing data.

Spatial cluster analysis

Standardized incidence ratios (SIRs) for each of BC's LHAs were calculated from incident registry cases using BC incidence as the reference rate[41]. DataBC provided geographic data[42]. To reduce the instability in disease rates caused by low case counts and populations, rates were averaged for the study period. In addition, spatial linear empirical Bayes estimation was used to smooth SIRs in areas with average pediatric populations under 10000[43]. The smoothing process calculated averages between a LHA's SIR and the average SIR value of adjacent LHAs. Spatial relationships for smoothing and clustering were defined by direct adjacency (queen contiguity) to approximately model geographic connectivity.

Two forms of spatial analysis were used to identify spatial patterns in PIBD. The Global Moran's I statistic measured the degree to which spatial patterning of IBD, CD, and UC in BC was clustered, dispersed, or had no detectable spatial pattern. The Local Moran's I statistic was used as a Local Indicator of Spatial Association (LISA) to identify the location of hot spots (clusters of comparatively high SIRs) and cold spots (clusters of comparatively low SIRs) among LHAs[44]. To approximate the likelihood that a cluster would arise by chance, we used 999 Monte Carlo simulations to compute a pseudo-*P* value[44], which was then adjusted with a Holm correction for multiple comparisons. We

Table 2 Data used in environmental exposure modeling

Variable	Description	Data source and database
Income	Mean of 2005 (adjusted to 2015 dollars) and 2015 census average family income for Local Health Areas	Statistics Canada, BC Community Health Atlas
Ethnicity	Census percent of the population of South Asian, Indigenous, Chinese, Jewish, and Non-Jewish European ethnic origin	Statistics Canada, University of Toronto Computing in the Humanities and Social Sciences Data Centre
Family size	Census average family size	Statistics Canada, University of Toronto Computing in the Humanities and Social Sciences Data Centre
Rurality	Percent of residents in each Local Health Area who lived outside a census metropolitan area or census agglomeration	Statistics Canada
NDVI greenness	Green vegetation cover calculated from land satellite imagery of surface reflection. Maximum and average growing season (May – August) NDVI within 250 m from postal code location. Multiplied by 100 so changes could be assessed as percentages	United States Geological Survey, Canadian Urban Environmental Health Research Consortium
UV vitamin D	Long-term stable monthly mean daily vitamin D dose from solar UV radiation adjusted for postal code elevation (J/m^{-2}) which was averaged for winter (December through February) and summer (June through August)	Environment Canada and Cancer Care Ontario, Canadian Urban Environmental Health Research Consortium
NO_2 air pollution	Annual average NO_2 concentration in parts per billion	Canadian Urban Environmental Health Research Consortium
O_3 air pollution	Average of O_3 taken from the highest rolling 8-hour daily average concentration (parts per billion)	Environment and Climate Change Canada, Canadian Urban Environmental Health Research Consortium
$PM_{2.5}$ air pollution	Annual average surface $PM_{2.5}$ ($\mu g/m^3$) concentration	Atmospheric Composition Analysis Group, Canadian Urban Environmental Health Research Consortium
Metam pesticide	2015 metam pesticide applied to fruits and vegetables (kg/ha/yr)	Global Pesticide Grids, Version 1.01, based on the United States Geological Survey's Pesticide National Synthesis Project and the Food and Agriculture Organization Corporate Statistical Database pesticide databases
Petroleum oil pesticide	2015 petroleum oil employed for grapes and orchards (kg/ha/yr)	Global Pesticide Grids, Version 1.01, based on the United States Geological Survey's Pesticide National Synthesis Project and the Food and Agriculture Organization Corporate Statistical Database pesticide databases
Glyphosate pesticide	2015 total glyphosate employed in major crops (wheat, corn, alfalfa, and others) in (kg/ha/yr)	Global Pesticide Grids, Version 1.01, based on the United States Geological Survey's Pesticide National Synthesis Project and the Food and Agriculture Organization Corporate Statistical Database pesticide databases
Population age 0-16.9	Yearly estimates of population age 0-16.9 for Local Health Areas averaged for 2001–2016	Statistics Canada, BC Stats

BC: British Columbia; NDVI: Normalized difference vegetation index; NO_2: Nitrogen dioxide; O_3: Ozone; $PM_{2.5}$: Fine particulate matter; UV: Ultraviolet.

chose LISA statistics over spatial and spatiotemporal SCAN methods given the irregular nature of the spatial areal units under analysis and the relative rarity of the disease, conditions under which LISA statistics have offered high sensitivity and specificity in cluster detection[45,46]. Data was aggregated over time (*i.e.* no spatio-temporal cluster analyses) given the aforementioned relative rarity of PIBD cases in BC.

Count regression modeling

Poisson Rate generalized linear models (PR-GLM) were used in an ecological analysis of LHAs to quantify the impact of population ethnicity, income, family size, rurality, air pollution, greenness, UV, and pesticide exposure on raw (unsmoothed) IBD, CD, and UC case counts. These models adjust for the population of each LHA and have an equal mean and variance. Model selection was based on the minimization of the Akaike Information Criterion using a stepwise algorithm combining backward elimination and forward addition[47]. PR-GLMs performed better than Negative Binomial, zero-inflated Poisson, and hurdle Poisson models. Considerations for reducing collinearity, conducting model selection, testing spatial independence of residuals, examining best model diagnostics, and considerations around the mapping of Incidence Rate Ratios (IRRs) are presented in the Supplementary materials. Multivariate models and high-quality Canadian census and exposure data were used to minimize sources of potential bias.

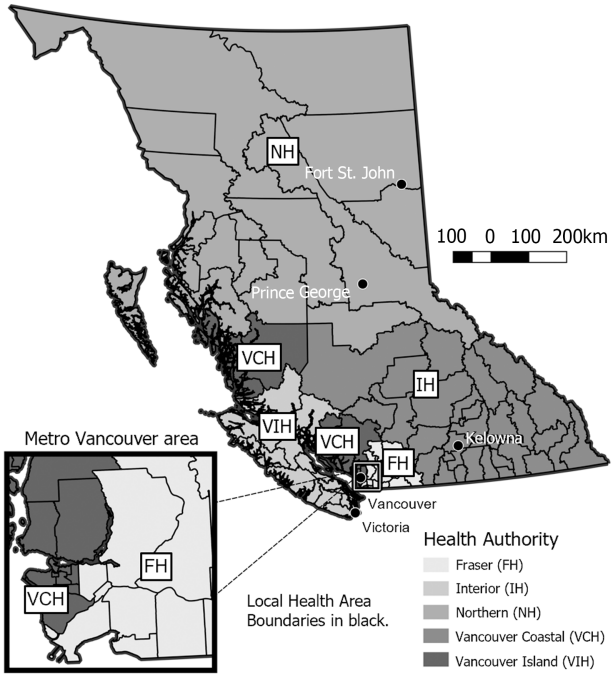

DOI: 10.3748/wjg.v29.i23.3688

Figure 1 British Columbia's five Health Authorities and 89 Local Health Areas (black boundaries).

RESULTS

Spatial clustering results

The registry consisted of 1232 eligible patients diagnosed at or before age 16.9. Of these, 49 were associated with invalid or BCCH postal codes. In the spatial cluster modeling of the remaining 1183 PIBD patients, we observed a statistically significant (pseudo-$P < 0.05$) clustered distribution with a Moran's I statistic of 0.65 ($P = 0.001$). For the 780 CD patients we observed a Moran's I of 0.56 ($P = 0.001$) and for the 288 UC patients a Moran's I of 0.28 ($P = 0.001$). See Figure 2 for local cluster locations. Hot spots were observed in the lower mainland, the main urban centre of BC, for IBD ($P \leq 0.031$), CD ($P \leq 0.031$), and UC ($P \leq 0.007$), in the Okanagan region for IBD ($P \leq 0.029$) and CD ($P = 0.030$), and on Vancouver Island for CD ($P = 0.034$). A cold spot cluster was detected in southeastern BC for IBD (P values < 0.001), CD ($P \leq 0.0499$), and UC ($P \leq 0.040$), in Northern BC for IBD ($P = 0.026$) and CD ($P = 0.038$), and on BC's coast for UC ($P = 0.036$). We observed no LHA which had a significantly different trend in incidence than neighboring LHAs (spatial outliers) for IBD, CD, or UC.

Environmental modeling results

Summary statistics for variables are presented in Table 3 for BC and Supplementary Table 2 by Health Authority (see Figure 1 for reference and Table 1 for incidence). Variables (Table 3) were modeled individually and combined in a multivariate model. Lack of spatial clustering observed in the residuals indicates that the model assumption of spatial independence was met, and suggests that within the parameters of the analysis there were either no important missing variables with spatial patterning or that the existing predictors capture similar spatial variability of important unmeasured variables. The final models included variables shown in Table 4 and logged average population as an offset variable.

For the whole PIBD population, Indigenous ethnic origin, average family size, summer UV radiation, and metam pesticide application were identified as significant protective factors. In contrast, South Asian origin, greenness, $PM_{2.5}$, and petroleum oil application were significant risk factors. When broken down by disease subtype, Indigenous ethnic origin, NO_2, and O_3 were statistically significantly negatively correlated with CD, while maximum growing season greenness, $PM_{2.5}$, and petroleum oil application were significant risk factors. Rurality, and alfalfa and corn glyphosate were statistically significant protective factors for UC, while significant risk factors included South Asian origin, mean growing season greenness, O_3 pollution, and wheat glyphosate.

A 1% increase in the Indigenous population of a LHA was associated with a 4.4% decrease in the number of IBD cases (IRR = 0.956, $P < 0.001$) and a 7.7% decrease in CD (IRR = 0.923, $P < 0.001$), while a 20% increase in Indigenous population was associated with a 59% decrease in IBD. Each additional family member added to family size was associated with a 53.3% decrease in IBD cases (IRR = 0.467, $P = 0.007$). An increase of 1 J/m^{-2} in summer UV was associated with 0.001% decrease in IBD cases (IRR = 0.999, $P < 0.001$) while an increase of 500 J/m^{-2} was associated with a 29.4% decrease. A 1% increase in

Table 3 Summary statistics for variables of interest for the 88 local health areas used for modeling

Explanatory variable	Minimum LHA value	Maximum LHA value	Mean of LHA values
Chinese ethnic origin (%)	0.00	47.21	4.35
Indigenous ethnic origin (%)	1.07	93.22	14.38
Jewish ethnic origin (%)	0.00	2.82	0.45
Non-Jewish European ethnic origin (%)	10.67	90.98	70.91
South Asian ethnic origin (%)	0.00	31.19	2.71
Average family income ($)	60265.01	216769.60	91884.26
Family size	2.25	3.13	2.76
Population density (per square km)	0.01	9443.44	553.95
Rural population (%)	0.00	100.00	53.05
NDVI maximum	0.59	0.80	0.70
NDVI mean	0.23	0.62	0.45
NO_2 (ppb)	0.10	23.61	7.71
O_3 (ppb)	17.49	39.54	30.14
$PM_{2.5}$ (μg m^3)	2.73	8.32	6.02
UV vitamin D summer (J/m^{-2})	4488.80	7272.52	6053.15
UV vitamin D winter (J/m^{-2})	102.02	449.6	274.98
Glyphosate used in common crops (kg/ha/yr)	0.00	6.71	0.61
Glyphosate used in alfalfa crops (kg/ha/yr)	0.00	0.17	0.02
Glyphosate used in corn crops (kg/ha/yr)	0.00	6.06	0.49
Glyphosate used in wheat crops (kg/ha/yr)	0.00	0.21	0.02
Metam used in fruits and vegetables (kg/ha/yr)	0.00	8.82	0.60
Petroleum oil used in orchards and grapes (kg/ha/yr)	0.00	4.75	0.28

LHA: Local Health Area; NDVI: Normalized difference vegetation index; UV: Ultraviolet; NO_2: Nitrogen dioxide; O_3: Ozone; $PM_{2.5}$: Fine particulate matter.

rural population was associated with a 1% decrease in UC (IRR = 0.990, P = 0.004). Each unit increase of metam pesticide was associated with a 6.9% decrease in IBD cases (IRR = 0.931, P = 0.001 for 1 kg/ha). Each ppb increase in O_3 was associated with a 9.5% increase in UC (IRR = 1.095, P = 0.001) and a 5.3% decrease in CD (IRR = 9.47, P = 0.010). Each ppb increase in NO_2 was associated with a 4.8% decrease in CD cases (IRR = 0.952, P = 0.006). Each unit increase of glyphosate applied to wheat was associated with an increase in UC (IRR = 121.196, P = 0.019 for 1 kg/ha), while the same pesticide applied to corn (IRR = 0.828, P = 0.021 for 1 kg/ha) and alfalfa (IRR = 0.001, P = 0.024 for 1 kg/ha) was a significant protective factor. It is important to note that glyphosate applications to corn (range 0.00–6.06, mean 0.49 kg/ha) were much higher than those to alfalfa (range 0.00–0.17, mean 0.02 kg/ha) and wheat (range 0.00–0.21, mean 0.02 kg/ha), and the extremely high and low IRRs for glyphosate are more reflective of the small data values than actual effect size.

A 1% increase in the percent of South Asian residents was associated with a 2% increase in IBD (IRR = 1.020, P < 0.001) and a 5.4% increase in UC (IRR = 1.054, P < 0.001), while a 20% increase in South Asian residents was associated with a 47.5% increase in IBD. A 1% increase in maximum growing season greenness was associated with a 6% increase in IBD and a 3.8% increase in CD (IRR = 1.060, P < 0.001, and IRR = 1.038, P = 0.002, respectively). A 1% increase in mean growing season greenness was associated with a 4.3% increase in UC (IRR = 1.043, P = 0.006). Each 1 μg/m^3 concentration increase in $PM_{2.5}$ air pollution was associated with a 29.4% increase in IBD cases (IRR = 1.294, P = 0.001) and a 23% increase in CD cases (IRR = 1.230, P = 0.008). Finally, a 1 kg/ha increase in the application of petroleum oil in grapes and orchards was associated with a 13.5% increase in IBD (IRR = 1.135, P = 0.033) and a 15.9% increase in CD (IRR = 1.159, P = 0.038).

Table 4 Incidence rate ratios and 95%CIs for the best model explaining inflammatory bowel disease, Crohn's disease, and ulcerative colitis rates in local health areas of British Columbia, Canada (*n* = 88)

Variable	Inflammatory bowel disease		Crohn's disease		Ulcerative colitis	
	IRR and 95%CI	*P* value	IRR and 95%CI	*P* value	IRR and 95%CI	*P* value
Average family size	0.467 (0.268–0.816)	0.007[b]				
Average family income			0.912 (0.827–1.006)	0.064		
Glyphosate used in alfalfa crops					0.001 (0.000–0.253)	0.024[a]
Glyphosate used in corn crops					0.828 (0.707–0.974)	0.021[a]
Glyphosate used in wheat crops					121.196 (2.252–6671.461)	0.019[a]
Indigenous ethnic origin	0.956 (0.941–0.971)	< 0.001[c]	0.923 (0.895–0.951)	< 0.001[c]		
Metam used in fruits and vegetables	0.931 (0.892–0.970)	0.001[b]				
NDVI Maximum at 250 m (× 100)	1.060 (1.040–1.082)	< 0.001[c]	1.038 (1.014–1.062)	0.002[b]		
NDVI Mean at 250 m (× 100)					1.043 (1.013–1.075)	0.006[b]
NO_2			0.952 (0.919–0.986)	0.006[b]		
O_3			0.947 (0.909–0.987)	0.010[a]	1.095 (1.039–1.154)	0.001[b]
Petroleum oil used in orchards and grapes	1.135 (1.007–1.270)	0.033[a]	1.159 (1.002–1.326)	0.038[a]		
$PM_{2.5}$	1.294 (1.113–1.507)	0.001[b]	1.230 (1.056–1.435)	0.008[b]		
Rural population					0.990 (0.983–0.996)	0.004[b]
South Asian ethnic origin	1.020 (1.011–1.028)	< 0.001[c]			1.054 (1.030–1.079)	< 0.001[c]
UV Summer	0.9993 (0.9990–0.9996)	< 0.001[c]	0.9997 (0.9993–1.0001)	0.091		
UV Winter					0.996 (0.992–1.000)	0.067

[a]$P < 0.05$.
[b]$P < 0.01$.
[c]$P < 0.001$.
IRR: Incidence rate ratio; NDVI: Normalized difference vegetation index; NO_2: Nitrogen dioxide; O_3: Ozone; $PM_{2.5}$: Fine particulate matter; UV: Ultraviolet.

DISCUSSION

Based on our exploratory analysis describing spatial patterning of PIBD in BC, incidence varied substantially across the province in both rural and urban areas, likely reflective of BC's diverse population and environments. The spatial distribution of IBD, CD, and UC was significantly clustered during the period of 2001 to 2016, with substantial overlap between cluster locations for each of the three. The lower mainland hotspot and southeastern BC cold spot were consistent across the study period in the IBD population. As previously reported in PIBD, UC represented a lower percentage of IBD cases than CD and in addition, displayed a less clustered distribution with fewer shared clusters. It is unlikely that these observed clusters resulted from chance. Notably, patients living near the eastern border (Alberta) may receive care in that province, potentially explaining the cold spot in southeastern BC.

In our modeling of the association between IBD case counts and population and environment variables, higher proportions of South Asians tended to be associated with higher IBD and UC case counts. In Ontario, Canada, similar incidence of IBD has been observed for children of immigrants of South Asian origin born in Canada and children of non-immigrants[15]. However, higher rates of IBD have been documented in South Asian populations in BC, the United States, the United Kingdom, New Zealand, and Singapore and Malaysia[7,48-51]. Our observation of lower IBD and CD cases associated with higher proportions of Indigenous residents is consistent with previous Canadian studies[4,52]. When interpreting modeling results, locations where IBD rates were well predicted by population ethnicity should still be considered places where environmental risk or protective factors were also present. Larger family size has been associated with a protective effect on CD, which is consistent with our results for IBD but not CD[6]. Higher socioeconomic status is an established risk factor[4,8], but average income quantile was not a significant predictor in any model (though it improved CD model

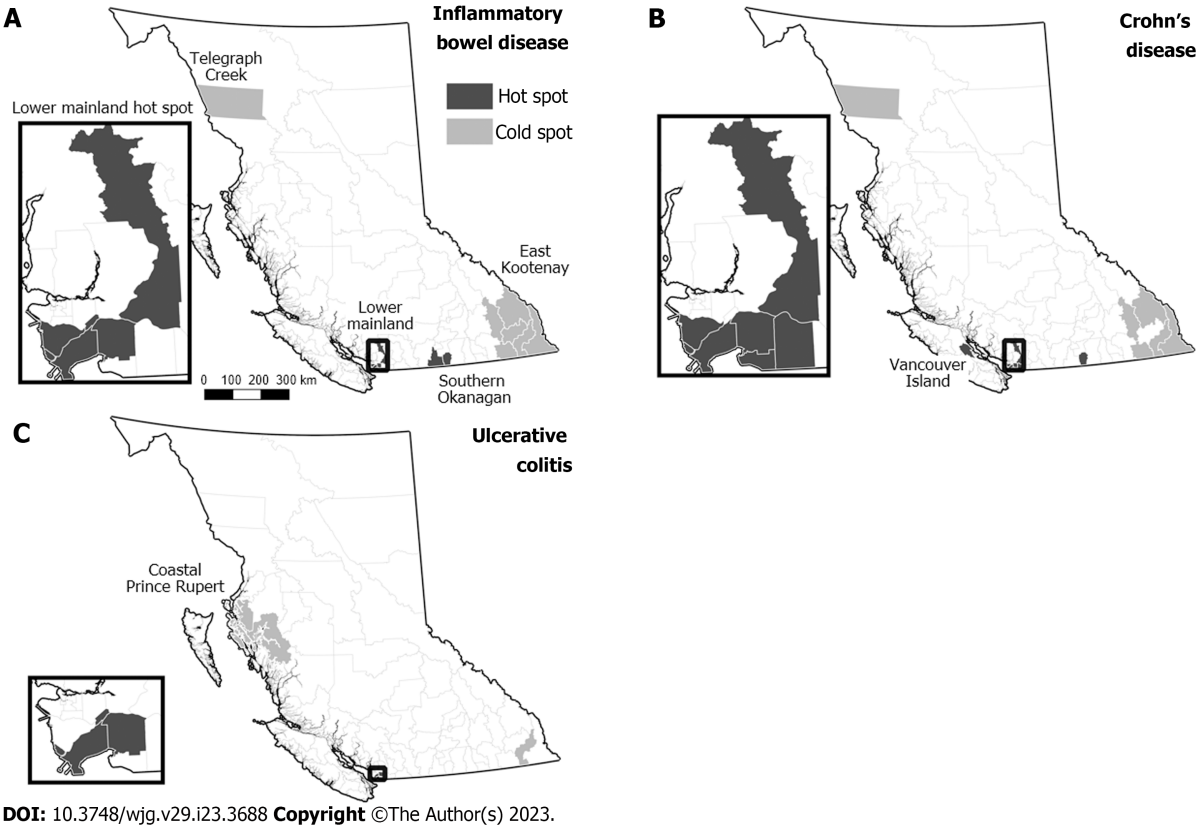

DOI: 10.3748/wjg.v29.i23.3688

Figure 2 Statistically significant standardized incidence ratio spatial clusters, 2001–2016. A: Inflammatory bowel disease; B: Crohn's disease; C: Ulcerative colitis.

fit). While several identified hot spots were located in the highest income areas of BC and cold spots in the lowest income areas, there were also hot spots with low income and cold spots with high income. It may be that average household income is less relevant than other socioeconomic indicators in BC, or that an effect was not observable for aggregated populations.

Our results suggest that at the LHA level, residential environmental exposures at diagnosis may also be significant potential determinants. Links with vitamin D and sunlight have been inconsistent, due in part to variability in study design and exposure assessment[12]. Our findings indicate that summer vitamin D UV radiation may confer a protective effect on IBD development. An individual unit of UV (1 J/m^{-2}) is quite small which resulted in a low measured IRR. Mean UV in BC is significantly higher in summer (6053.15 J/m^{-2}) than winter (274.98 J/m^{-2}) and varies within the province (summer maximum of 7272.52 and minimum of 4488.80 J/m^{-2}). An increase in UV of 500 J/m^{-2}, which is more representative of actual geographic and seasonal UV variation, was associated with a 29.4% decrease in IBD cases. In the analysis stratified by disease type, summer and winter UV vitamin D were nonsignificant protective factors that improved model fit for CD and UC, respectively. Smaller sample size in stratified analysis may have contributed to nonsignificant results. Low winter UV across BC could be particularly relevant for people of South Asian descent who have a higher level of skin melanin and require substantially more UV exposure to synthesize sufficient vitamin D[30]. $PM_{2.5}$ air pollution was a significant risk factor for PIBD and CD. Italian (IBD) and Chinese (UC but not CD) studies of middle and older aged adults have identified $PM_{2.5}$ as a risk factor for incident cases as well as IBD and UC hospitalizations in China [53-55]. In contrast, an Ontario pediatric study found no association and a European adult study found a negative association with $PM_{2.5}$[13,56]. Though population exposure for most LHAs met 2020 national and provincial air quality objectives, BC experiences seasonal wildfire events which can cause short-term high $PM_{2.5}$ concentrations that would be obscured in the yearly average values used in this study [57]. Regular high exposure events should be investigated further, especially as climate change is projected to increase wildfire potential[58]. O_3 air pollution was a significant risk factor for UC which is consistent with a Chinese study which measured an association between O_3 and IBD and UC hospital visits[54]. We observed statistically significant negative associations with CD for NO_2 and O_3. This is in contrast to the lack of association observed for IBD in Ontario and Europe, a United Kingdom study which found a positive association between NO_2 pollution and CD onset before age 23, and a Chinese study which found a positive association between NO_2 and UC incidence in middle and older aged adults[13,55,56,59]. Differential effects on CD and UC have been observed for environmental exposures such as smoking and appendectomy[60].

BC had few areas of low residential greenness and high incidence (Supplementary Figures 3–5), and we observed statistically significant positive associations between IBD, CD, UC, and greenness. Our findings contrast with a pediatric cohort study in Ontario, which found a protective effect for maximum growing season NDVI at 250 m[11]. This inconsistency could be due to methodological differences between the two studies. NDVI is a measure of vegetation greenness only and may not capture other elements of green spaces, such as vegetation composition, environmental microbiome, or pesticide and herbicide applications, which may differ in BC. Measures of greenness in BC are highly dependent on specific indicators, as a Metro Vancouver study comparing green space metrics found that NDVI at 250 m from postal codes diverged significantly from other measures such as street tree density, total percentage of green space, and park quality[61].

A previous Canadian study found a protective effect of rurality on pediatric CD and UC, while our study only observed an effect for UC[9]. BC may have more diverse environments than other provinces; for example, the largely rural Interior Health Authority had many of the highest average $PM_{2.5}$ and O_3 exposures while the majority-urban lower mainland region included significant sections of Agricultural Land Reserve. A hot spot near Vancouver included mostly suburban LHAs rather than the main urban center, which is similar to results observed in Oslo, Norway[62]. Perhaps some suburban and rural areas lack protective effects conferred by other rural regions while also missing potential health-promoting features of dense urban areas (*e.g.* public transportation, public parks, and access to amenities). Some rural and peri-urban areas can also be associated with potential risk factors such as petroleum pesticides.

A novel result in this study is the measured associations between pesticides and PIBD. Petroleum oil applied to grapes and orchards was a significant risk factor for IBD and CD. Indeed, exposure to agricultural petroleum oil has been previously associated with systemic autoimmunity (measured with antinuclear antibodies) and rhinitis in a prospective cohort of pesticide applicators in the United States, suggesting that petroleum pesticide products may have inflammatory properties[63,64]. As numerous other pesticides have been linked with dysbiosis, and petroleum is used as a fungicide, agricultural applications of petroleum oil should be investigated for potential impacts on the gut microbiome which could induce CD[14,39]. Interestingly, glyphosate application appeared to have a different effect on UC depending on which crop it was applied to. Wheat crop glyphosate was a significant risk factor, while alfalfa and corn crop glyphosate were significant protective factors. Differences in agricultural practices between alfalfa, corn, and wheat may be responsible for the negative or both associations observed for UC. The unexpected negative association between IBD and metam pesticide also warrants further investigation. This association could have resulted from an unmeasured confounder such as diet. For example, proximity to fruit and vegetable crops where metam is applied could be correlated with access to these food groups which are known to lower IBD risk[65].

A key strength of this study is the use of high resolution national environmental exposure metrics which increased the quality of the study and will facilitate comparisons between our results and future research. In addition, the clinical registry only contained patients with a confirmed IBD diagnosis, confirmed diagnosis of CD or UC, and accurate date of diagnosis which minimizes risk of misclassification. Moreover, we have demonstrated that our registry data is representative of the BC IBD population[18]. The use of aggregate case counts and reliable population data in both analyses and areal geographic analysis combined with spatial smoothing in the cluster analysis reduced the instability of disease rates caused by low cases numbers. The use of Monte Carlo simulation and a multiple comparison correction for statistical significance increased confidence in the spatial results. Finally, future healthcare service planning in BC would be implemented for health administrative units such as LHAs, so our scale of analysis would allow this research to be directly integrated into planning and intervention efforts.

Despite these strengths, there are several limitations which warrant discussion. Some patients were excluded due to missing data and it is possible that cases were missing from our clinical registry, either of which may have altered spatial clustering or biased modeling results. However, the registry likely included the vast majority of PIBD patients diagnosed in BC during the study period[18]. Patient data was not initially collected for research purposes, which may have affected available variables and may have contributed to missing data. Small numbers of cases could have produced large variation in incidence in sparsely populated areas. In addition, missing early environmental exposure data for several LHAs may have impacted the results, though all but one of the modeled LHAs included environment data from the majority of the study period. An important unmeasured variable in this analysis is diet, and missing potential confounding variables may have biased the results. This was not a birth cohort study, so there is uncertainty about exposures at gestation or early life. However, specific critical periods for many environmental exposures have not been established; consequently, further prospective studies are required. Previous environmental studies have used average childhood exposure[11,13] or did not have a standardized lookback period dating from diagnosis[56,59]. Accordingly, we used broad metrics of average population-level exposure during the study period. This was an ecological analysis and our findings should not be used to make claims about individual risk.

CONCLUSION

To our knowledge, this is the first spatial hot spot analysis focused on PIBD in North America and the first study identifying an association with pesticides. Spatial cluster detection was a valuable method for exploring patterns of IBD, and we identified $PM_{2.5}$ air pollution, petroleum oil, glyphosate, and metam pesticides as novel determinants of PIBD. Given the inconsistency of IBD incidence in urban areas and relatively high incidence in some suburban and rural areas, future research should move beyond binary urban-rural classifications and use specific characteristics such as built environment and pollutant exposures to characterize environments. Expanded regional and global studies are needed to validate these results and to determine the relationship between timing of exposure and clinical onset of disease. Furthermore, the inclusion of other immune-mediated inflammatory diseases will likely uncover potential shared disease clusters and environmental determinants.

ARTICLE HIGHLIGHTS

Research background

Geospatial patterning has been observed in inflammatory bowel disease (IBD) incidence and linked to environmental determinants of disease. However, knowledge of North American IBD spatial patterns is limited, and unknown in pediatric IBD (PIBD). A further understanding of geospatial patterns of IBD will help guide distribution of healthcare services and aid in identifying potential environmental risk and protective factors and populations at risk.

Research motivation

There is a lack of knowledge of the spatial distribution and environmental exposures relevant to PIBD in Canada and specifically in the Canadian province of British Columbia (BC).

Research objectives

The main objectives of this study were (1) To determine spatial patterning of PIBD and identify location of disease hot and cold spots in the Canadian province of BC during the period of 2001–2016; and (2) to model the association between IBD case counts and population-level ethnicity, average income, rural residence, and known as well as novel environmental determinants. Both objectives were addressed using the methods described below.

Research methods

The Moran's I statistic was used as a Local Indicator of Spatial Association to measure the degree, location, and type of geographic clustering of PIBD incidence, a method which improves on visual analysis of mapped incidence by empirically quantifying clustering. Statistical significance of observed clusters was approximated using Monte Carlo simulation. Case counts of IBD, Crohn's disease (CD), and ulcerative colitis (UC) were modeled in Poisson rate models as a function of average population characteristics and average population environmental exposures to assess associations between IBD and rurality, ethnicity, income, family size, and air pollution, green space, ultraviolet (UV) light, and pesticide exposures. Data sources included a BCCH clinical registry of patients diagnosed with IBD ≤ age 16.9, high-quality national environmental exposure datasets developed for health research, and Canadian census data.

Research results

No high incidence hot spots were detected in the densest urban areas, suggesting unexplored urban protective factors. Rurality was negatively associated with UC. Novel risk factors for PIBD and specifically CD included fine particulate matter ($PM_{2.5}$) pollution and agricultural applications of petroleum oil to orchards and grapes. Spatial distribution was partially explained by rurality, population ethnicity, family size, pesticide applications, air pollution, UV exposure, and residential greenness.

Research conclusions

Pesticide and $PM_{2.5}$ exposure are linked to the development of PIBD. Suburban and low-density urban areas of BC appear to lack protective exposures conferred by rural and dense urban areas.

Research perspectives

Exploring geographic patterns of PIBD facilitated the identification of novel environmental determinants, which has prompted followup studies of environmental exposures and IBD onset.

ACKNOWLEDGEMENTS

Mielle Michaux was supported as a MSc student by the University of British Columbia Graduate Support Initiative and International Tuition Award and is currently a research assistant supported by the Moffat Foundation. Justin M Chan is a PhD candidate supported by the BCCH Research Institute Studentship and the Lutsky Foundation. Luke Bergmann acknowledges support by the Canada Research Chairs Program and the Canada Foundation for Innovation. Luis F Chaves acknowledges funding from Indiana University. Kevan Jacobson is a Senior Clinician Scientist supported by the Children with Intestinal and Liver Disorders (CHILD) Foundation and the BCCH Research Institute Clinician Scientists Award Program, University of British Columbia. NDVI metrics, nitrogen dioxide data, calculated ozone metrics, and $PM_{2.5}$ metrics were indexed to DMTI Spatial Inc. postal codes and provided by CANUE (Canadian Urban Environmental Health Research Consortium). Long-term monthly UV data were accessed *via* the CANUE data portal (https://canuedata.ca). Portions of this methodology were developed for Mielle Michaux's MSc thesis.

FOOTNOTES

Author contributions: Michaux M participated in designing the study, acquisition, analysis, and interpretation of the data, and drafted the initial manuscript; Chan JM participated in designing the study, acquisition, analysis, and interpretation of the data, and revised the article critically for important intellectual content; Bergmann L and Chaves LF participated in the acquisition, analysis, and interpretation of the data, and revised the article critically for important intellectual content; Klinkenberg B participated in designing the study and revised the article critically for important intellectual content; Jacobson K was the guarantor and participated in designing the study, analysis, and interpretation of the data, and revised the article critically for important intellectual content.

Institutional review board statement: The study was reviewed and approved by the University of British Columbia Children's and Women's Research Ethics Board (Vancouver), No. H19-00739.

Conflict-of-interest statement: Dr. Jacobson reports other from BC Children's Hospital Research Institute Clinician Scientist Awards Program Award, grants from Janssen, non-financial support from adMare Bioinnovations, other from Engene, outside the submitted work; and has served on the advisory boards of Janssen, AbbVie, Merck, Amgen, Mylan Inc, and McKesson.

Data sharing statement: Data is available upon reasonable request to the corresponding author subject to research ethics board approval, at kjacobson@cw.bc.ca.

STROBE statement: The authors have read the STROBE Statement—checklist of items, and the manuscript was prepared and revised according to the STROBE Statement—checklist of items.

Country/Territory of origin: Canada

ORCID number: Mielle Michaux 0000-0003-4742-3126; Justin M Chan 0000-0002-8298-3594; Luis F Chaves 0000-0002-5301-2764; Brian Klinkenberg 0000-0002-3357-1446; Kevan Jacobson 0000-0001-7269-8557.

Corresponding Author's Membership in Professional Societies: Canadian Association of Gastroenterology.

S-Editor: Li L
L-Editor: A
P-Editor: Cai YX

REFERENCES

1 **Benchimol EI**, Fortinsky KJ, Gozdyra P, Van den Heuvel M, Van Limbergen J, Griffiths AM. Epidemiology of pediatric inflammatory bowel disease: a systematic review of international trends. *Inflamm Bowel Dis* 2011; **17**: 423-439 [PMID: 20564651 DOI: 10.1002/ibd.21349]

2 **Aamodt G**, Jahnsen J, Bengtson MB, Moum B, Vatn MH; IBSEN Study Group. Geographic distribution and ecological studies of inflammatory bowel disease in southeastern Norway in 1990-1993. *Inflamm Bowel Dis* 2008; **14**: 984-991 [PMID: 18338775 DOI: 10.1002/ibd.20417]

3 **Declercq C**, Gower-Rousseau C, Vernier-Massouille G, Salleron J, Baldé M, Poirier G, Lerebours E, Dupas JL, Merle V, Marti R, Duhamel A, Cortot A, Salomez JL, Colombel JF. Mapping of inflammatory bowel disease in northern France: spatial variations and relation to affluence. *Inflamm Bowel Dis* 2010; **16**: 807-812 [PMID: 19774647 DOI: 10.1002/ibd.21111]

4 **Green C**, Elliott L, Beaudoin C, Bernstein CN. A population-based ecologic study of inflammatory bowel disease: searching for etiologic clues. *Am J Epidemiol* 2006; **164**: 615-23; discussion 624 [PMID: 16920784 DOI: 10.1093/aje/kwj260]

5 **Nikkilä A**, Auvinen A, Kolho KL. Clustering of pediatric onset inflammatory bowel disease in Finland: a nationwide register-based study. *BMC Gastroenterol* 2022; **22**: 512 [PMID: 36503475 DOI: 10.1186/s12876-022-02579-1]

6 **Bernstein CN**, Rawsthorne P, Cheang M, Blanchard JF. A population-based case control study of potential risk factors for IBD. *Am J Gastroenterol* 2006; **101**: 993-1002 [PMID: 16696783 DOI: 10.1111/j.1572-0241.2006.00381.x]

7 **Pinsk V**, Lemberg DA, Grewal K, Barker CC, Schreiber RA, Jacobson K. Inflammatory bowel disease in the South Asian pediatric population of British Columbia. *Am J Gastroenterol* 2007; **102**: 1077-1083 [PMID: 17378907 DOI: 10.1111/j.1572-0241.2007.01124.x]

8 **Bernstein CN**, Burchill C, Targownik LE, Singh H, Roos LL. Events Within the First Year of Life, but Not the Neonatal Period, Affect Risk for Later Development of Inflammatory Bowel Diseases. *Gastroenterology* 2019; **156**: 2190-2197.e10 [PMID: 30772341 DOI: 10.1053/j.gastro.2019.02.004]

9 **Benchimol EI**, Kaplan GG, Otley AR, Nguyen GC, Underwood FE, Guttmann A, Jones JL, Potter BK, Catley CA, Nugent ZJ, Cui Y, Tanyingoh D, Mojaverian N, Bitton A, Carroll MW, deBruyn J, Dummer TJB, El-Matary W, Griffiths AM, Jacobson K, Kuenzig ME, Leddin D, Lix LM, Mack DR, Murthy SK, Sánchez JNP, Singh H, Targownik LE, Vutcovici M, Bernstein CN. Rural and Urban Residence During Early Life is Associated with Risk of Inflammatory Bowel Disease: A Population-Based Inception and Birth Cohort Study. *Am J Gastroenterol* 2017; **112**: 1412-1422 [PMID: 28741616 DOI: 10.1038/ajg.2017.208]

10 **Soon IS**, Molodecky NA, Rabi DM, Ghali WA, Barkema HW, Kaplan GG. The relationship between urban environment and the inflammatory bowel diseases: a systematic review and meta-analysis. *BMC Gastroenterol* 2012; **12**: 51 [PMID: 22624994 DOI: 10.1186/1471-230X-12-51]

11 **Elten M**, Benchimol EI, Fell DB, Kuenzig ME, Smith G, Kaplan GG, Chen H, Crouse D, Lavigne E. Residential Greenspace in Childhood Reduces Risk of Pediatric Inflammatory Bowel Disease: A Population-Based Cohort Study. *Am J Gastroenterol* 2021; **116**: 347-353 [PMID: 33038129 DOI: 10.14309/ajg.0000000000000990]

12 **Holmes EA**, Rodney Harris RM, Lucas RM. Low Sun Exposure and Vitamin D Deficiency as Risk Factors for Inflammatory Bowel Disease, With a Focus on Childhood Onset. *Photochem Photobiol* 2019; **95**: 105-118 [PMID: 30155900 DOI: 10.1111/php.13007]

13 **Elten M**, Benchimol EI, Fell DB, Kuenzig ME, Smith G, Chen H, Kaplan GG, Lavigne E. Ambient air pollution and the risk of pediatric-onset inflammatory bowel disease: A population-based cohort study. *Environ Int* 2020; **138**: 105676 [PMID: 32217428 DOI: 10.1016/j.envint.2020.105676]

14 **Jin Y**, Wu S, Zeng Z, Fu Z. Effects of environmental pollutants on gut microbiota. *Environ Pollut* 2017; **222**: 1-9 [PMID: 28086130 DOI: 10.1016/j.envpol.2016.11.045]

15 **Benchimol EI**, Mack DR, Guttmann A, Nguyen GC, To T, Mojaverian N, Quach P, Manuel DG. Inflammatory bowel disease in immigrants to Canada and their children: a population-based cohort study. *Am J Gastroenterol* 2015; **110**: 553-563 [PMID: 25756238 DOI: 10.1038/ajg.2015.52]

16 **Statistics Canada**. 2011 census profiles files / 2016 census profiles files / Profile of census dissemination areas; n.d. Database: Canadian Census Analyser. 2011. [cited 1 December 2020]. Available from: http://dc1.chass.utoronto.ca/cgi-bin/census/2011/displayCensus.cgi?year=2011&geo=da

17 **Michaux M**. Exploring spatio-temporal patterns and environmental determinants of pediatric inflammatory bowel disease in British Columbia. M.Sc. Thesis, University of British Columbia. 2020. Available from: https://open.library.ubc.ca/collections/ubctheses/24/items/1.0394067

18 **Chan JM**, Carroll MW, Smyth M, Hamilton Z, Evans D, McGrail K, Benchimol EI, Jacobson K. Comparing Health Administrative and Clinical Registry Data: Trends in Incidence and Prevalence of Pediatric Inflammatory Bowel Disease in British Columbia. *Clin Epidemiol* 2021; **13**: 81-90 [PMID: 33603489 DOI: 10.2147/CLEP.S292546]

19 DMTI Spatial Inc. CanMap postal code suite; n.d. [cited 24 March 2021]. Available from: https://canue.ca/wp-content/uploads/2019/09/CANUE-Browser-Metadata-PostalCodes.pdf

20 **Statistics Canada**. 2011 National Household Survey (NHS) profiles files / Profile of census dissemination areas; n.d. Database: Canadian Census Analyser. 2011. [cited 1 December 2020]. Available from: http://dc1.chass.utoronto.ca/cgi-bin/census/2011nhs/displayCensus.cgi?year=2011&geo=da

21 **Statistics Canada**. Profile of dissemination areas: 2001 census / 2006 census / Cumulative profiles; n.d. 2011. [cited 1 December 2020]. Available from: Database: Canadian Census Analyser. Available from: http://dc1.chass.utoronto.ca/cgi-bin/census/2001/displayCensusDA.cgi

22 **Statistics Canada**. Average family income (dollars), 2005, 2015 n.d. Database: BC Community Health Atlas. [cited 1 December 2020]. Available from: http://maps.gov.bc.ca/ess/hm/cha/

23 **Google Earth Engine**. Landsat 5 TM annual greenest-pixel TOA reflectance composite, 1984 to 2012; n.d. Database: Google Earth Engine. [cited 20 July 2017]. Available from: https://explorer.earthengine.google.com/#detail/LANDSAT%2FLT5_L1T_ANNUAL_GREENEST_TOA

24 **Google Earth Engine**. Landsat 8 annual greenest-pixel TOA reflectance composite, 2013 to 2015; n.d. Database: Google Earth Engine. [cited 20 July 2017]. Available from: https://explorer.earthengine.google.com/#detail/LANDSAT%2FLC8_L1T_ANNUAL_GREENEST_TOA

25 **Google Earth Engine**. USGS Landsat 5 TM TOA reflectance (orthorectified), 1984 to 2011; n.d. Database: Google Earth Engine. [cited 20 July 2007]. Available from: https://explorer.earthengine.google.com/#detail/LANDSAT%2FLT5_L1T_TOA

26 **Google Earth Engine**. USGS Landsat 8 TOA reflectance (orthorectified), 2013 to 2017; n.d. Database: Google Earth

Engine. [cited 20 July 2007]. Available from: https://explorer.earthengine.google.com/#detail/LANDSAT%2FLC8_L1T_TOA

27 **Gorelick N**, Hancher M, Dixon M, Ilyushchenko S, Thau D, Moore R. Google Earth Engine: Planetary-scale geospatial analysis for everyone. *Remote Sens Environ* 2017; **202**: 18-27 [DOI: 10.1016/j.rse.2017.06.031]

28 **Robinson N**, Allred B, Jones M, Moreno A, Kimball J, Naugle D, Erickson T, Richardson A. A dynamic landsat derived normalized difference vegetation index (NDVI) product for the conterminous United States. *Remote Sens* 2017; **9**: 863 [DOI: 10.3390/rs9080863]

29 **Fioletov VE**, Kimlin MG, Krotkov N, McArthur LJB, Kerr JB, Wardle DI, Herman JR, Meltzer R, Mathews TW, Kaurola J. UV index climatology over the United States and Canada from ground-based and satellite estimates. *J Geophys Res Atmospheres* 2004; **109**: 1-13 [DOI: 10.1029/2004JD004820]

30 **Fioletov VE**, McArthur LJ, Mathews TW, Marrett L. Estimated ultraviolet exposure levels for a sufficient vitamin D status in North America. *J Photochem Photobiol B* 2010; **100**: 57-66 [PMID: 20554218 DOI: 10.1016/j.jphotobiol.2010.05.002]

31 **Hystad P**, Setton E, Cervantes A, Poplawski K, Deschenes S, Brauer M, van Donkelaar A, Lamsal L, Martin R, Jerrett M, Demers P. Creating national air pollution models for population exposure assessment in Canada. *Environ Health Perspect* 2011; **119**: 1123-1129 [PMID: 21454147 DOI: 10.1289/ehp.1002976]

32 **Weichenthal S**, Pinault LL, Burnett RT. Impact of Oxidant Gases on the Relationship between Outdoor Fine Particulate Air Pollution and Nonaccidental, Cardiovascular, and Respiratory Mortality. *Sci Rep* 2017; **7**: 16401 [PMID: 29180643 DOI: 10.1038/s41598-017-16770-y]

33 **Environment and Climate Change Canada**. CHRONOS_Ground-Level_O3_NA_2002.nc to CHRONOS_Ground-Level_O3_NA_2009.nc inclusive, generated. July 2017. [cited 18 April 2023]. Available from: https://www.canuedata.ca/tmp/CANUE_METADATA_O3CHG_A_YY.pdf

34 **Environment and Climate Change Canada**. GEMMACH_Ground Level_O3_NA_2010.nc to GEMMACH_Ground-Level_O3_NA_2015.nc inclusive, generated. Jul 2017. [cited 18 April 2023]. Available from: https://www.canuedata.ca/tmp/CANUE_METADATA_O3CHG_A_YY.pdf

35 **Robichaud A**, Ménard R, Zaïtseva Y, Anselmo D. Multi-pollutant surface objective analyses and mapping of air quality health index over North America. *Air Qual Atmos Health* 2016; **9**: 743-759 [PMID: 27785157 DOI: 10.1007/s11869-015-0385-9]

36 **Robichaud A**, Ménard R. Multi-year objective analyses of warm season ground-level ozone and PM 2.5 over North America using real-time observations and Canadian operational air quality models. *Atmospheric Chem Phys* 2014; **14**: 1769-800 [DOI: 10.5194/acp-14-1769-2014]

37 **Canadian Urban Environmental Health Research Consortium**. Canue Metadata - Air Quality Ozone (O3). 2021. [cited 18 April 2023]. Available from: https://www.canuedata.ca/tmp/CANUE_METADATA_O3CHG_A_YY.pdf

38 **Hammer MS**, van Donkelaar A, Li C, Lyapustin A, Sayer AM, Hsu NC, Levy RC, Garay MJ, Kalashnikova OV, Kahn RA, Brauer M, Apte JS, Henze DK, Zhang L, Zhang Q, Ford B, Pierce JR, Martin RV. Global Estimates and Long-Term Trends of Fine Particulate Matter Concentrations (1998-2018). *Environ Sci Technol* 2020; **54**: 7879-7890 [PMID: 32491847 DOI: 10.1021/acs.est.0c01764]

39 **Maggi F**, Tang FHM, la Cecilia D, McBratney A. PEST-CHEMGRIDS, global gridded maps of the top 20 crop-specific pesticide application rates from 2015 to 2025. *Sci Data* 2019; **6**: 170 [PMID: 31515508 DOI: 10.1038/s41597-019-0169-4]

40 **Maggi F**, Tang FHM, la Cecilia D, McBratney A. Global Pesticide Grids (PEST-CHEMGRIDS); Database: NASA Socioeconomic Data and Applications Center (SEDAC) 2020 [DOI: 10.7927/weq9-pv30]

41 **BC Stats**. British Columbia - Population estimates; 2020. [cited 1 December2020]. Available from: https://bcstats.shinyapps.io/popApp/

42 **Ministry of Health**. Local health area boundaries; Database: BC Data Catalogue. 2019. [cited 26 May 2020]. Available from: https://catalogue.data.gov.bc.ca/dataset/Local-health-area-boundaries

43 **Marshall RJ**. Mapping disease and mortality rates using empirical Bayes estimators. *J R Stat Soc Ser C Appl Stat* 1991; **40**: 283-294 [DOI: 10.2307/2347593]

44 **Anselin L**. Local indicators of spatial association-LISA. *Geogr Anal* 1995; **27**: 93-115 [DOI: 10.1111/j.1538-4632.1995.tb00338.x]

45 **Kulldorff M**, Nagarwalla N. Spatial disease clusters: detection and inference. *Stat Med* 1995; **14**: 799-810 [PMID: 7644860 DOI: 10.1002/sim.4780140809]

46 **Moraga P**, Montes F. Detection of spatial disease clusters with LISA functions. *Stat Med* 2011; **30**: 1057-1071 [PMID: 21484847 DOI: 10.1002/sim.4160]

47 **Venables WN**, Ripley BD. Modern Applied Statistics with S. 4th ed. New York: Springer, 2002: 1-498 [DOI: 10.1007/978-0-387-21706-2_1]

48 **Malhotra R**, Turner K, Sonnenberg A, Genta RM. High prevalence of inflammatory bowel disease in United States residents of Indian ancestry. *Clin Gastroenterol Hepatol* 2015; **13**: 683-689 [PMID: 25083563 DOI: 10.1016/j.cgh.2014.06.035]

49 **Misra R**, Faiz O, Munkholm P, Burisch J, Arebi N. Epidemiology of inflammatory bowel disease in racial and ethnic migrant groups. *World J Gastroenterol* 2018; **24**: 424-437 [PMID: 29391765 DOI: 10.3748/wjg.v24.i3.424]

50 **Rajasekaran V**, Evans HM, Andrews A, Bishop JR, Lopez RN, Mouat S, Han DY, Alsweiler J, Roberts AJ. Rising Incidence of Inflammatory Bowel Disease in South Asian children in New Zealand - A Retrospective Population-Based Study. *J Pediatr Gastroenterol Nutr* 2023 [PMID: 36800276 DOI: 10.1097/MPG.0000000000003735]

51 **Huang JG**, Wong YKY, Chew KS, Tanpowpong P, Calixto Mercado KS, Reodica A, Rajindrajith S, Chang KC, Ni YH, Treepongkaruna S, Lee WS, Aw MM. Epidemiological characteristics of Asian children with inflammatory bowel disease at diagnosis: Insights from an Asian-Pacific multi-centre registry network. *World J Gastroenterol* 2022; **28**: 1830-1844 [PMID: 35633913 DOI: 10.3748/wjg.v28.i17.1830]

52 **Torabi M**, Bernstein CN, Yu BN, Wickramasinghe L, Blanchard JF, Singh H. Geographical Variation and Factors Associated With Inflammatory Bowel Disease in a Central Canadian Province. *Inflamm Bowel Dis* 2020; **26**: 581-590

[PMID: 31504519 DOI: 10.1093/ibd/izz168]

53 **Adami G**, Pontalti M, Cattani G, Rossini M, Viapiana O, Orsolini G, Benini C, Bertoldo E, Fracassi E, Gatti D, Fassio A. Association between long-term exposure to air pollution and immune-mediated diseases: a population-based cohort study. *RMD Open* 2022; **8** [PMID: 35292563 DOI: 10.1136/rmdopen-2021-002055]

54 **Ding S**, Sun S, Ding R, Song S, Cao Y, Zhang L. Association between exposure to air pollutants and the risk of inflammatory bowel diseases visits. *Environ Sci Pollut Res Int* 2022; **29**: 17645-17654 [PMID: 34669131 DOI: 10.1007/s11356-021-17009-0]

55 **Li FR**, Wu KY, Fan WD, Chen GC, Tian H, Wu XB. Long-term exposure to air pollution and risk of incident inflammatory bowel disease among middle and old aged adults. *Ecotoxicol Environ Saf* 2022; **242**: 113835 [PMID: 35816845 DOI: 10.1016/j.ecoenv.2022.113835]

56 **Opstelten JL**, Beelen RMJ, Leenders M, Hoek G, Brunekreef B, van Schaik FDM, Siersema PD, Eriksen KT, Raaschou-Nielsen O, Tjønneland A, Overvad K, Boutron-Ruault MC, Carbonnel F, de Hoogh K, Key TJ, Luben R, Chan SSM, Hart AR, Bueno-de-Mesquita HB, Oldenburg B. Exposure to Ambient Air Pollution and the Risk of Inflammatory Bowel Disease: A European Nested Case-Control Study. *Dig Dis Sci* 2016; **61**: 2963-2971 [PMID: 27461060 DOI: 10.1007/s10620-016-4249-4]

57 **Matz CJ**, Egyed M, Xi G, Racine J, Pavlovic R, Rittmaster R, Henderson SB, Stieb DM. Health impact analysis of PM(2.5) from wildfire smoke in Canada (2013-2015, 2017-2018). *Sci Total Environ* 2020; **725**: 138506 [PMID: 32302851 DOI: 10.1016/j.scitotenv.2020.138506]

58 **Wang X**, Thompson DK, Marshall GA, Tymstra C, Carr R, Flannigan MD. Increasing frequency of extreme fire weather in Canada with climate change. Clim Change 2015; 130: 573-586 [DOI: 10.1007/s10584-015-1375-5]

59 **Kaplan GG**, Hubbard J, Korzenik J, Sands BE, Panaccione R, Ghosh S, Wheeler AJ, Villeneuve PJ. The inflammatory bowel diseases and ambient air pollution: a novel association. *Am J Gastroenterol* 2010; **105**: 2412-2419 [PMID: 20588264 DOI: 10.1038/ajg.2010.252]

60 **Piovani D**, Danese S, Peyrin-Biroulet L, Nikolopoulos GK, Lytras T, Bonovas S. Environmental Risk Factors for Inflammatory Bowel Diseases: An Umbrella Review of Meta-analyses. *Gastroenterology* 2019; **157**: 647-659.e4 [PMID: 31014995 DOI: 10.1053/j.gastro.2019.04.016]

61 **Rugel EJ**, Henderson SB, Carpiano RM, Brauer M. Beyond the Normalized Difference Vegetation Index (NDVI): Developing a Natural Space Index for population-level health research. *Environ Res* 2017; **159**: 474-483 [PMID: 28863302 DOI: 10.1016/j.envres.2017.08.033]

62 **Moum B**, Vatn MH, Ekbom A, Aadland E, Fausa O, Lygren I, Stray N, Sauar J, Schulz T. Incidence of Crohn's disease in four counties in southeastern Norway, 1990-93. A prospective population-based study. The Inflammatory Bowel South-Eastern Norway (IBSEN) Study Group of Gastroenterologists. *Scand J Gastroenterol* 1996; **31**: 355-361 [PMID: 8726303 DOI: 10.3109/00365529609006410]

63 **Slager RE**, Poole JA, LeVan TD, Sandler DP, Alavanja MC, Hoppin JA. Rhinitis associated with pesticide exposure among commercial pesticide applicators in the Agricultural Health Study. *Occup Environ Med* 2009; **66**: 718-724 [PMID: 19289390 DOI: 10.1136/oem.2008.041798]

64 **Parks CG**, Santos ASE, Lerro CC, DellaValle CT, Ward MH, Alavanja MC, Berndt SI, Beane Freeman LE, Sandler DP, Hofmann JN. Lifetime Pesticide Use and Antinuclear Antibodies in Male Farmers From the Agricultural Health Study. *Front Immunol* 2019; **10**: 1476 [PMID: 31354699 DOI: 10.3389/fimmu.2019.01476]

65 **Milajerdi A**, Ebrahimi-Daryani N, Dieleman LA, Larijani B, Esmaillzadeh A. Association of Dietary Fiber, Fruit, and Vegetable Consumption with Risk of Inflammatory Bowel Disease: A Systematic Review and Meta-Analysis. *Adv Nutr* 2021; **12**: 735-743 [PMID: 33186988 DOI: 10.1093/advances/nmaa145]

World Journal of Gastroenterology

Submit a Manuscript: https://www.f6publishing.com

World J Gastroenterol 2023 June 21; 29(23): 3703-3714

DOI: 10.3748/wjg.v29.i23.3703

ISSN 1007-9327 (print) ISSN 2219-2840 (online)

ORIGINAL ARTICLE

Prospective Study

Novel multi-parametric diagnosis of non-alcoholic fatty liver disease using ultrasonography, body mass index, and Fib-4 index

Kei Funada, Yumi Kusano, Yoshinori Gyotoku, Ryosaku Shirahashi, Toshikuni Suda, Masaya Tamano

Specialty type: Gastroenterology and hepatology

Provenance and peer review: Unsolicited article; Externally peer reviewed.

Peer-review model: Single blind

Peer-review report's scientific quality classification

Grade A (Excellent): 0
Grade B (Very good): B
Grade C (Good): C
Grade D (Fair): 0
Grade E (Poor): 0

P-Reviewer: Pécsi D, Hungary; Sempokuya T, United States

Received: February 8, 2023
Peer-review started: February 8, 2023
First decision: March 7, 2023
Revised: March 14, 2023
Accepted: May 22, 2023
Article in press: May 22, 2023
Published online: June 21, 2023

Kei Funada, Yumi Kusano, Yoshinori Gyotoku, Ryosaku Shirahashi, Toshikuni Suda, Masaya Tamano, Department of Gastroenterology, Dokkyo Medical University Saitama Medical Center, Koshigaya-shi 343-8555, Saitama, Japan

Corresponding author: Masaya Tamano, PhD, Professor, Department of Gastroenterology, Dokkyo Medical University Saitama Medical Center, 2-1-50 Minami-Koshigaya, Koshigaya-shi 343-8555, Saitama, Japan. mstamano@dokkyomed.ac.jp

Abstract

BACKGROUND

Shear wave speed (SWS), shear wave dispersion (SWD), and attenuation imaging (ATI) are new diagnostic parameters for non-alcoholic fatty liver disease. To differentiate between non-alcoholic steatohepatitis (NASH) and non-alcoholic fatty liver (NAFL), we developed a clinical index we refer to as the "NASH pentagon" consisting of the 3 abovementioned parameters, body mass index (BMI), and Fib-4 index.

AIM

To investigate whether the area of the NASH pentagon we propose is useful in discriminating between NASH and NAFL.

METHODS

This non-invasive, prospective, observational study included patients diagnosed with fatty liver by abdominal ultrasound between September 2021 and August 2022 in whom shear wave elastography, SWD, and ATI were measured. Histological diagnosis based on liver biopsy was performed in 31 patients. The large pentagon group (LP group) and the small pentagon group (SP group), using an area of 100 as the cutoff, were compared; the NASH diagnosis rate was also investigated. In patients with a histologically confirmed diagnosis, receiver-operating characteristic (ROC) curve analyses were performed.

RESULTS

One hundred-seven patients (61 men, 46 women; mean age 55.1 years; mean BMI 26.8 kg/m^2) were assessed. The LP group was significantly older (mean age: 60.8 ± 15.2 years *vs* 46.4 ± 13.2 years; $P < 0.0001$). Twenty-five patients who underwent liver biopsies were diagnosed with NASH, and 6 were diagnosed with NAFL. On ROC curve analyses, the areas under the ROC curves for SWS, dispersion slope, ATI value, BMI, Fib-4 index, and the area of the NASH pentagon were 0.88000,

0.82000, 0.58730, 0.63000, 0.59333, and 0.93651, respectively; the largest was that for the area of the NASH pentagon.

CONCLUSION

The NASH pentagon area appears useful for discriminating between patients with NASH and those with NAFL.

Key Words: Non-alcoholic fatty liver disease; Non-alcoholic steatohepatitis; Attenuation imaging; Shear wave elastography; Shear wave dispersion; Diagnosis

Core Tip: The non-alcoholic steatohepatitis (NASH) pentagon is a novel clinical index consisting of the five parameters of shear wave speed, dispersion slope, attenuation imaging value, Fib-4 index, and body mass index. It is simple and the calculation of its area is easy. The area of the NASH pentagon is useful for discriminating between patients with NASH and those with non-alcoholic fatty liver.

Citation: Funada K, Kusano Y, Gyotoku Y, Shirahashi R, Suda T, Tamano M. Novel multi-parametric diagnosis of non-alcoholic fatty liver disease using ultrasonography, body mass index, and Fib-4 index. *World J Gastroenterol* 2023; 29(23): 3703-3714

URL: https://www.wjgnet.com/1007-9327/full/v29/i23/3703.htm

DOI: https://dx.doi.org/10.3748/wjg.v29.i23.3703

INTRODUCTION

Non-alcoholic fatty liver disease (NAFLD) is a global public health problem[1,2]. It is a grouping of diseases consisting of either non-alcoholic fatty liver (NAFL) or non-alcoholic steatohepatitis (NASH) [3]. If NASH progresses, it can lead to liver cirrhosis and hepatocellular carcinoma; thus, a clinical index needs to be developed that can efficiently discriminate NASH patients from NAFL patients[4,5]. Assessments based on multiple parameters using ultrasound, including shear wave elastography (SWE), are reported to be useful in stratifying the risk of advanced NASH[6].

SWE measures the speed of shear waves (shear wave speed; SWS) generated by push pulses. SWS is slow in soft objects and fast in hard objects. Measurements of SWS by SWE are considered useful in assessing liver fibrosis in viral hepatitis and NAFLD[7-11].

The shear wave dispersion (SWD) developed in recent years obtains the "frequency dependence" (dispersion slope; DS), which is the extent of the changes in the speed of shear waves, from changes in their frequency. Some preliminary evidence has been reported that DS measurements with SWD are an index of necroinflammation of the liver[12,13].

Attenuation imaging (ATI) was developed as a new testing method for evaluation of hepatic steatosis with ultrasound technology. ATI is a technique that uses the principle of attenuation due to phenomena such as absorption and diffusion of ultrasonic pulses emitted within the body when they pass through body tissue, and it produces a value referred to as the attenuation coefficient. Magnetic resonance imaging (MRI)-determined proton density fat fraction (PDFF) values have been reportedly used for assessing histological hepatic steatosis grades[14], and Tada *et al*[15] reported a good correlation between ATI values and MRI-determined PDFF values.

On the other hand, it is important to have parameters that do not require special equipment to measure. The prevalence of NAFLD in Japanese non-obese patients is 15%[16]. In other words, 85% of NAFLD patients are obese. Therefore, the body mass index (BMI), which can be easily used to determine obesity, is one such parameter of importance.

Similarly, the scoring system for liver fibrosis by the biochemical examination of blood is also relevant. The Fib-4 index, calculated by aspartate aminotransferase (AST), alanine aminotransferase (ALT), platelets (Plts), and age, is simple and easy to use[17].

In this study, a pentagon consisting of five parameters was prepared with the addition of the BMI and the Fib-4 index to the three parameters of SWS, SWD, and ATI. Whether the area of this pentagon is useful in discriminating NASH from NAFL was then investigated.

MATERIALS AND METHODS

Patients

This was a non-invasive, prospective, observational study that conformed with the ethical guidelines of the Declaration of Helsinki in its 2008 revision and was approved by the ethics review board of the hospital with which the authors are affiliated (No. 21057). The study was conducted after complete information disclosure on the website of the authors' hospital.

Of the patients diagnosed with fatty liver by abdominal ultrasound between September 2021 and August 2022, the subjects were patients in whom SWE, SWD, and ATI were measured. Patients with a history of alcohol intake of ethanol ≥ 20 g/d, who had hepatitis B, hepatitis C, or autoimmune liver disease, and patients with concurrent drug-induced liver injury or cholangitis were excluded.

Diagnosis of fatty liver with ultrasonography

The ultrasound scanner used was an Aplio i800 from Canon Medical Systems Corp. (Otawara, Tochigi, Japan). Fatty liver was diagnosed if the following were seen on B-mode ultrasound examination: (1) Bright liver[18]; (2) Positive hepatorenal echo contrast[19]; (3) Deep ultrasound attenuation in the liver [20]; and (4) Vascular blurring in the liver[21]. Specialists with ten or more years of ultrasonographic experience (Suda T and Tamano M) performed the B-mode ultrasound examination and measured SWE, SWD, and ATI.

Measurements of shear wave elastography and SWD

All SWE measurements were done following B-mode scans, using the same diagnostic equipment and transducers. The measurement results are shown as SWS (m/s). A 1-cm-diameter, circular region of interest was placed on the sample box.

SWD was measured at the same time as SWE. Simultaneous measurements could be taken by switching to quad view mode including a SWS map and a SWD slope map. This test was also performed using five or more measurement values, and the measurement results are shown as DS [(m/s)/KHz].

Measurements of attenuation imaging

After SWE and SWD were measured, the same physician performed the ATI test. The measurement result is shown as the ATI value [(dB/cm)/MHz]. A sample box with the default settings was used to acquire the data, set at least 1.5 cm below the liver capsule to avoid reverberation artifacts. The reliability of the results is displayed with R^2 values, categorized as poor ($R^2 < 0.80$), good ($R^2 = 0.81$-0.89), or excellent ($R^2 > 0.90$). According to information provided by the manufacturer, measurements are considered to be valid when $R^2 \geq 0.80$. Attenuation imaging examinations were performed until five valid measurements were obtained, and the mean value of the five measurements was used in the analysis.

Structure of the NASH pentagon

AST, ALT, and Plts were measured on the same day as the abdominal ultrasound. The Fib-4 index was calculated from these values and age. The BMI was calculated from height and weight on the day on which abdominal ultrasound was performed.

A pentagon consisting of these five parameters (SWS, DS, ATI value, BMI, and Fib-4 index) was created. This was defined as the NASH pentagon. The area of the NASH pentagon was calculated automatically by inputting a calculation formula into an Aplio i800 work station.

The standard value for each item was set according to previous studies as follows. The standard value of SWS was set as 1.33 m/s (cutoff value of fibrosis stage 1), that of DS was set to 8.5 (m/s)/KHz (cutoff value of lobular inflammation grade 1)[22]. Similarly, the standard value of ATI was set to 0.66 (dB/cm)/MHz, defining steatosis grade 1[16,22]. The standard value for BMI was set at 25.0 kg/m^2 based on the index of the Japanese Society for the Study of Obesity[1]. The standard value for the Fib-4 index was set to 1.30, which is the low cutoff value for advanced fibrosis (stage 3-4), based on a report by Shah *et al*[24] The investigation was done taking the area of this pentagon as 100 (Figure 1).

Diagnosis of NASH

Histological diagnosis based on liver biopsy was performed within three months from SWE measurement in those patients who provided consent. NASH diagnosis was made by an experienced pathologist certified by the Japanese Society of Pathology, based on comprehensive findings including macrovesicular steatosis, ballooning degeneration of hepatocytes, scattered inflammation and apoptotic bodies in the lobules, Mallory-Denk bodies, and fibrosis[25-27]. In this study, all patients without liver biopsy were judged to have NAFL, even if NASH was suspected clinically.

Comparison of two groups classified by the area of the NASH pentagon

Patient characteristics and individual parameters were compared between a large pentagon group (LP group), in which the area of the NASH pentagon was 100 or greater, and a small pentagon group (SP

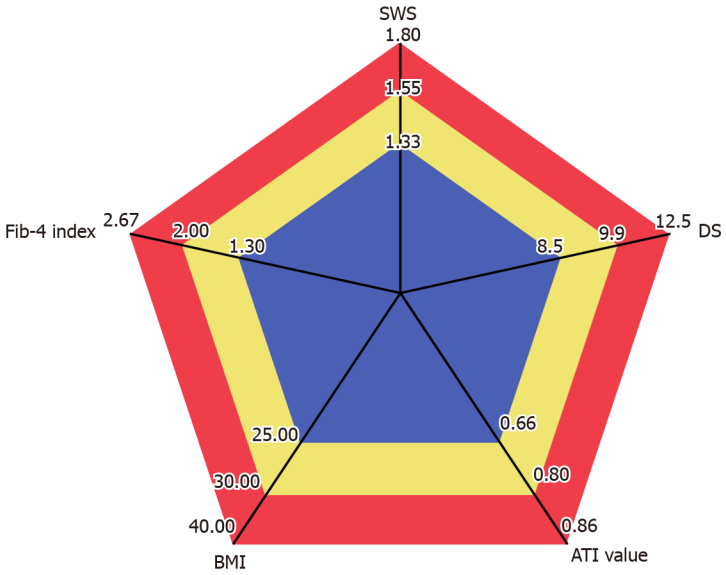

DOI: 10.3748/wjg.v29.i23.3703

Figure 1 Non-alcoholic steatohepatitis pentagon. The non-alcoholic steatohepatitis pentagon consists of the five parameters of shear wave speed (SWS), dispersion slope (DS), attenuation imaging value (ATI value), Fib-4 index, and the body mass index (BMI). Based on past reports, the reference values were set as SWS 1.33 m/s, DS 8.5 (m/s)/KHz, ATI value 0.66 (dB/cm)/MHz, BMI 25.0 kg/m^2, and Fib-4 index 1.3. SWS: Shear wave speed; DS: Dispersion slope; BMI: Body mass index; ATI: Attenuation imaging.

group), in which the area was less than 100. In addition, the NASH diagnosis rate was investigated when the NASH pentagon area of 100 was taken as the reference.

Diagnostic accuracy for NASH using the area of the NASH pentagon

In patients for whom liver biopsies were performed during the study period and a histologically confirm-ed diagnosis was made, a receiver-operating characteristic (ROC) curve was drawn for SWS, DS, ATI value, BMI, Fib-4 index, and area of the NASH pentagon.

Statistical analysis

Continuous data for SWS, DS, ATI value, and other clinical parameters are expressed as mean ± SD. A Spearman rank-order correlation coefficient test was used to test the independency of these clinical parameters. A non-paired Wilcoxon test was used in comparisons of each parameter between the two groups divided by NASH pentagon area, with $P < 0.05$ taken to indicate a significant difference.

The NASH diagnostic performance of SWS, DS, ATI value, BMI, Fib-4 index, and the area of the pentagon was investigated using the ROC curve. The area under the ROC curve (AUROC) was used to evaluate NASH diagnostic performance.

RESULTS

Patients' characteristics

The number of patients who were diagnosed with fatty liver based on abdominal ultrasound and in whom SWE, SWD, and ATI were measured was 126. After excluding 7 patients with an alcohol intake history of ≥ 20 g ethanol/d, 10 patients with concurrent hepatitis B, hepatitis C, or autoimmune liver injury, and 2 patients for other reasons, the investigation was conducted with the remaining 107 patients (Figure 2).

The characteristics for these 107 patients are shown in Table 1. There were 61 men and 46 women, with a mean age of 55.1 years. The mean BMI was 26.8 kg/m^2. Of the 107 patients, diabetes mellitus was seen in 25, dyslipidemia in 35, and hypertension in 37. Mean AST, ALT, and γ-glutamyltransferase concentrations were all mildly elevated at 44.9 U/L, 70.6 U/L, and 99.6 U/L, respectively. The mean Fib-4 index was 1.53. Twenty-five of the 107 patients were diagnosed with NASH, and the remaining 82 were diagnosed with NAFL.

The Spearman rank correlation coefficient between SWS and the Fib-4 index was 0.3486; no strong correlation was found. Similarly, the rank correlation coefficient between ATI and BMI was 0.1955, showing no correlation.

Table 1 Patients' characteristics

Patients' characteristics	*n* = 107
M/F	61/46
Age (yr)	55.1 ± 15.9
BMI (kg/m^2)	26.8 ± 4.1
Metabolic diseases	
Diabetes mellitus (yes/no)	25/82
Dyslipidemia (yes/no)	35/72
Hypertension (yes/no)	37/70
Concomitant drugs	
SGLT2 inhibitor	12
DPP-4 inhibitor	13
Thiazolidinedione	2
GLP-1 agonist	2
Statin	19
Bezafibrate	0
Pemafibrate	8
EPA and DHA preparation	1
AST (U/L)	44.9 ± 38.0
ALT (U/L)	70.6 ± 57.7
GGT (U/L)	99.6 ± 139.7
T-B (mg/dL)	0.9 ± 0.5
Alb (mg/dL)	4.5 ± 0.4
eGFR (mL/min)	73.0 ± 15.0
HbA1c (%)	6.5 ± 1.2
T-chol (mg/dL)	202.1 ± 52.6
TG (mg/dL)	180.0 ± 119.0
WBC (10^3/μL)	6731.8 ± 1882.5
Hb (g/dL)	14.7 ± 1.3
Plts (10^4/μL)	23.9 ± 7.6
Fib-4 index	1.53 ± 1.90

M: Male; F: Female; AST: Aspartate aminotransferase; ALT: Alanine aminotransferase; GGT: γ-glutamyltransferase; T-Bil: Total bilirubin; Alb: Albumin; eGFR: Estimated glomerular filtration rate; HbA1c: Glycated hemoglobin A1c; T-chol: Total cholesterol; TG: Triglycerides; WBC: White blood cells; Hb: Hemoglobin; Plts: Platelets.

Comparison of two groups classified by the area of the NASH pentagon

The LP group with a NASH pentagon area ≥ 100 had 64 patients, and the SP group with an area < 100 had 43 patients. A comparison of the two groups is shown in Table 2.

There was no difference in sex between the two groups, but mean age was 60.8 ± 15.2 years in the LP group and 46.4 ± 13.2 years in the SP group, with the LP group significantly older ($P < 0.0001$).

Concurrent diabetes mellitus was seen in 18/64 patients (28.1%) in the LP group and 6/43 patients (13.9%) in the SP group. While this represents a higher tendency in the LP group, no significant difference was seen ($P = 0.0849$). Concurrent dyslipidemia was seen in 27/64 patients (42.2%) in the LP group and 8/43 patients (18.6%) in the SP group, and concurrent hypertension was seen in 29/64 patients (45.3%) and 7/43 patients (16.3%), respectively; both were significantly higher in the LP group ($P = 0.0108$, $P = 0.0183$).

Table 2 Comparison of the two groups classified by area of non-alcoholic steatohepatitis pentagon

	Large pentagon group (*n* = 64)	Small pentagon group (*n* = 43)	*P* value
M/F	33/31	28/15	0.165
Age (yr)	60.8 ± 15.2	46.4 ± 13.2	< 0.0001
Metabolic diseases			
Diabetes mellitus (yes/no)	18/46	6/37	0.0849
Dyslipidemia (yes/no)	27/37	8/35	0.0108
Hypertension (yes/no)	29/35	7/36	0.0183
AST (U/L)	52.6 ± 44.2	40.3 ± 24.4	0.0521
ALT (U/L)	61.1 ± 45.2	83.0 ± 71.6	0.1699
GGT (U/L)	97.3 ± 123.2	102.9 ± 162.0	0.7238
T-B (mg/dL)	1.01 ± 0.6	0.77 ± 0.3	0.0044
Alb (mg/dL)	4.5 ± 0.4	4.6 ± 0.4	0.2843
eGFR (mL/min)	71.8 ± 16.4	74.7 ± 12.1	0.1639
HbA1c (%)	6.5 ± 1.1	6.3 ± 1.2	0.2847
T-chol (mg/dL)	188.5 ± 59.4	221.3 ± 33.8	0.008
TG (mg/dL)	172.9 ± 126.5	189.9 ± 108.8	0.1278
WBC (10^3/μL)	6225.0 ± 1586.9	7463.9 ± 2050.9	0.008
Hb (g/dL)	14.7 ± 1.3	14.7 ± 1.5	0.6836
Plts (10^4/μL)	21.0 ± 6.5	28.8 ± 6.6	< 0.0001
SWS (m/s)	1.78 ± 0.36	1.39 ± 0.14	< 0.0001
DS [(m/s)/kHz]	13.3 ± 3.7	10.8 ± 2.0	< 0.0001
ATI value [(dB/cm)/MHz]	0.78 ± 0.13	0.74 ± 0.13	0.1047
Fib-4 index	2.2 ± 2.3	0.7 ± 0.4	< 0.0001
BMI (kg/m^2)	27.8 ± 4.4	25.6 ± 3.2	0.0249
NASH/NAFL	22/42	3/40	0.0042

M: Male; F: Female; AST: Aspartate aminotransferase; ALT: Alanine aminotransferase; GGT: γ-glutamyltransferase; T-chol: Total cholesterol; TG: Triglycerides; WBC: White blood cells; Hb: Hemoglobin; Plts: Platelets; SWS: Shear wave speed; DS: Dispersion slope; ATI value: Attenuation imaging value; BMI: Body mass index; Alb: Albumin; eGFR: Estimated glomerular filtration rate; NASH: Non-alcoholic steatohepatitis; NAFL: Non-alcoholic fatty liver.

On blood biochemistry tests, total bilirubin was significantly higher in the LP group (P = 0.0044), whereas total cholesterol, white blood cells, and Plts were significantly lower in the LP group (P = 0.0080, P = 0.0080, P < 0.0001). There were no significant differences between the two groups in any of the other test results.

Comparisons of the five parameters that make up the NASH pentagon showed no significant difference between the groups in the ATI value (P = 0.1407), and significantly higher values in the LP group for SWS, DS, Fib-4 index, and BMI (P < 0.0001, P = 0.0004, P < 0.0001, P = 0.0249).

The number of patients diagnosed with NASH was 22 (34.3%) of 64 in the LP group and 3 (7.0%) of 43 in the SP group. The LP group had a significantly higher percentage of NASH patients (P = 0.0042).

Diagnostic accuracy of histological NAFLD using the area of the NASH pentagon

Liver biopsy was performed during the period of this study in 31 patients. Twenty-five of these 31 patients were diagnosed with NASH, and six were diagnosed with NAFL. The ROC curves indicating the NASH diagnostic performance in these 31 patients are shown in Figure 3. The AUROCs for SWS, DS, ATI value, BMI, Fib-4 index, and the area of the NASH pentagon were 0.88000, 0.82000, 0.58730, 0.63000, 0.59333, and 0.93651, respectively. Of these six items, the largest AUROC was that for the area of the NASH pentagon.

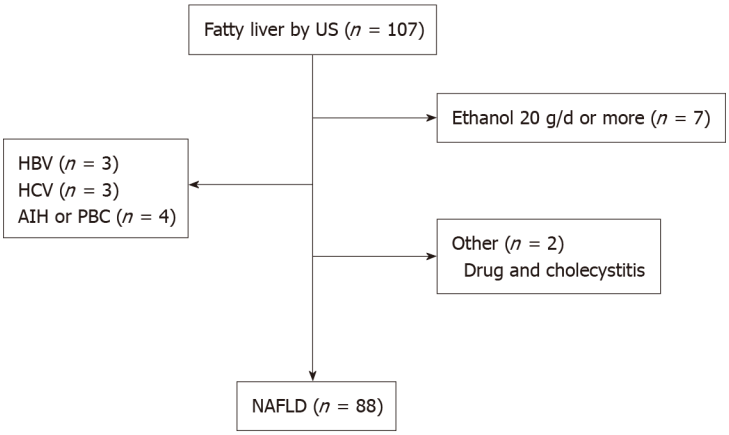

DOI: 10.3748/wjg.v29.i23.3703 **Copyright** ©The Author(s) 2023.

Figure 2 Flowchart of the study. A total of 126 patients who were diagnosed with fatty liver based on abdominal ultrasound and in whom shear wave elastography, shear wave dispersion, and attenuation imaging were measured during the period of this study were entered in the study. Of them, 7 patients with an alcohol intake history of 20 g ethanol/d or more, 3 with hepatitis B, 3 with hepatitis C, and 4 with autoimmune hepatitis or primary biliary cholangitis were excluded. In addition, 1 patient with drug-induced liver injury and 1 patient with cholangitis were excluded, bringing the final number of subjects in this investigation to 107. HBV: Hepatitis B virus; HCV: Hepatitis C virus; AIH: Autoimmune hepatitis; PBC: Primary biliary cholangitis; NAFLD: Non-alcoholic fatty liver disease.

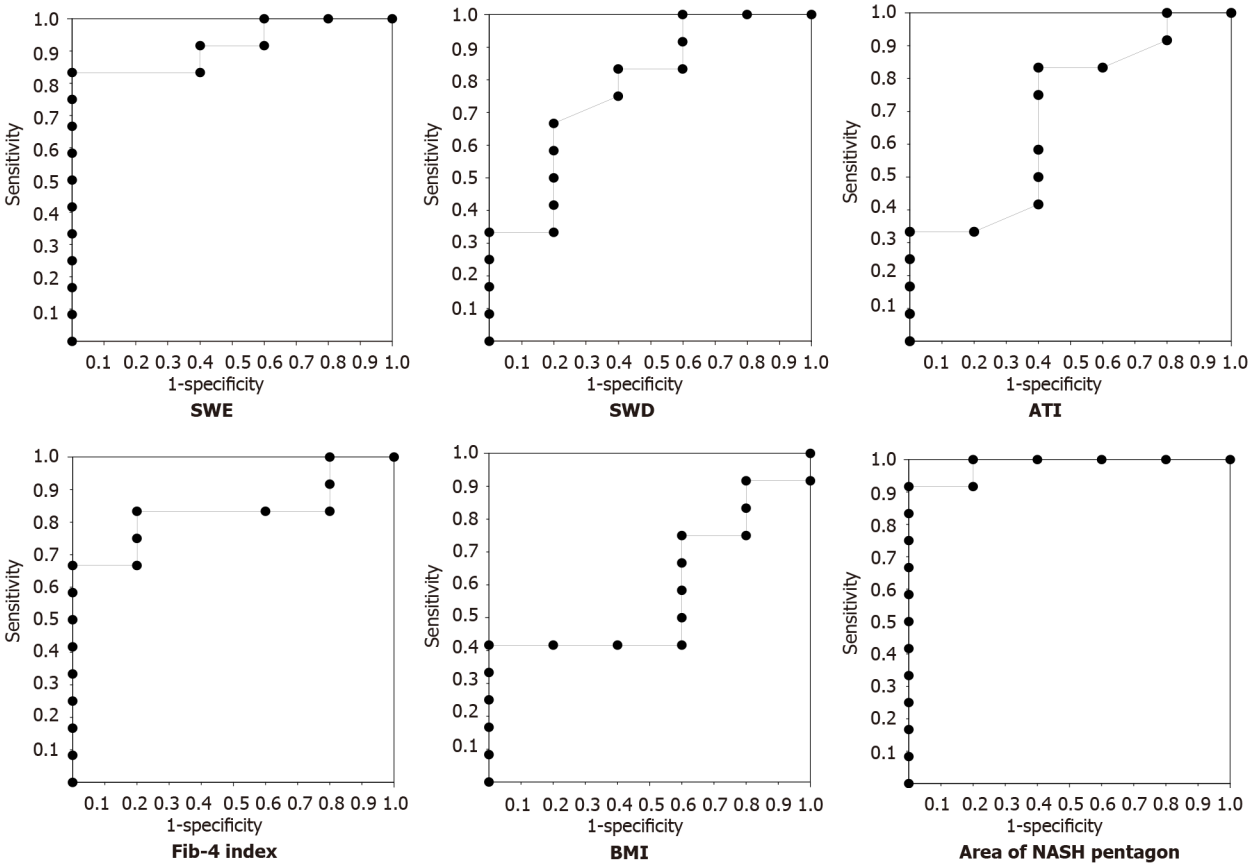

DOI: 10.3748/wjg.v29.i23.3703 **Copyright** ©The Author(s) 2023.

Figure 3 Receiver-operating characteristic curve for each parameter. This shows the receiver-operating characteristic (ROC) curve of the 17 patients who underwent liver biopsy during the period of this study. The areas under the ROC curves (AUROCs) of shear wave speed, dispersion slope, attenuation imaging value, body mass index, Fib-4 index, and the area of the non-alcoholic steatohepatitis (NASH) pentagon are 0.88000, 0.82000, 0.58730, 0.63000, 0.59333, and 0.93651, respectively. Of these six parameters, the largest AUROC is that for the area of the NASH pentagon. SWE: Shear wave elastography; SWD: Shear wave dispersion; ATI: Attenuation imaging; BMI: Body mass index; NASH: Non-alcoholic steatohepatitis.

DISCUSSION

Ultrasound elastography has been used to evaluate fibrosis noninvasively. SWE, one type of ultrasound

elastography, includes transient elastography, point SWE, and other techniques[28-30]. The Aplio i800 used in the present study can measure SWE, SWD, and ATI with the same transducer. This machine is also equipped with a function that automatically creates radar charts from these measured values. The radar charts are created using five parameters. The three parameters of SWS, DS, and ATI value are set in the initial settings, and the remaining two can be freely set by the user. In the present study, these two were set as BMI and Fib-4 index, and it was thought that the area of this pentagon (NASH pentagon) may be useful for the diagnosis of NASH.

There are various reports about the cutoff values of SWE and DS[31]. In the present study, the cutoff values of SWE and DS were set from the report of Sugimoto *et al*[22] based on 120 liver biopsies. The cutoff values for steatosis grade 1 of ATI are reported to be 0.62-0.79[32-34]. In the present study, it was set to 0.66 from the report of Tada *et al*[35] based on 148 liver biopsies.

Obesity is the most important factor in the development of NAFLD. In NASH patients, there is a positive correlation between visceral fat and the amount of fat in hepatocytes[36]. Thus, obesity can lead to a diagnosis of NASH. In the present study, the reference value for BMI was set at 25.0 kg/m^2 based on the index of the Japanese Society for the Study of Obesity and a WHO recommendation[23,37].

The Fib-4 index calculated from age, AST, ALT, and platelet count is regularly used as a noninvasive parameter of hepatic fibrosis[38]. In this study, a value of 1.30, which is the low cutoff value for advanced fibrosis (stage 3-4), based on a report by Shah *et al*[24], was set as the reference value.

SWE and the Fib-4 index are indices of liver fibrosis. However, SWE makes use of ultrasound technology and predicts fibrosis. The Fib-4 index is calculated from biochemical evaluation and age. The correlation of the factors was examined, and no strong correlation was found. ATI is an index of hepatic steatosis assessed using ultrasound technology. BMI is an index of obesity of patients calculated from height and weight. In the present statistical analysis, there was no correlation between these two factors. Due to the above-mentioned reasons, the Fib-4 index and BMI were adopted as constituent factors of the NASH pentagon.

In a comparison of the LP group with a NASH pentagon area of 100 or more and the SP group with an area of less than 100, the LP group was older and had a lower platelet count. This is thought to be a result of the strong involvement of the Fib-4 index among the constituent elements of the pentagon. In fact, a very large difference was seen in the Fib-4 index between the groups, which was 2.2 in the LP group and 0.7 in the SP group ($P < 0.0001$).

The mean BMI, on the other hand, was 27.8 kg/m^2 in the LP group and 25.6 kg/m^2 in the SP group, tending to be higher in the SP group. Obesity is an important element of NAFLD, but as NAFL progresses to NASH, there is a tendency for weight loss. Moreover, even in the SP group, the mean BMI of 25.6 kg/m^2 was only slightly above the reference of 25.0 kg/m^2. This result is also consistent with reports that nonobese NAFLD is more common in Asia than in western countries[39,40].

The onset and progression of NAFLD/NASH are related to metabolic syndrome, and they have an especially strong relationship with diabetes mellitus[41]. In the present study, no difference was seen in concurrent diabetes mellitus by differences in the NASH pentagon area, but concurrent dyslipidemia and hypertension were significantly higher in the LP group.

The NASH pentagon consists of five parameters: Fibrosis based on SWS, inflammation as assessed by DS, steatosis as assessed by ATI value, obesity assessed by BMI, and the level of serological and clinical progression based on the Fib-4 index. Once this pentagon is programmed in the ultrasound machine, it can be automatically created and its area subsequently calculated, making it very simple to use. We thus consider it to be a useful method for identifying NASH among NAFLD patients.

In fact, when ROC curves were made for the six parameters of SWS, DS, ATI value, BMI, Fib-4 index, and the area of the NASH pentagon in 31 patients who underwent liver biopsy during the study period, the largest AUROC was the one for the area of the NASH pentagon.

In the early stage of NASH, liver fibrosis is mild, and in these patients, SWS is expected to be either normal or only mildly elevated. In young patients, the Fib-4 index also tends to be low. Even in these patients, however, DS, ATI value, and BMI are expected to be high, so it may be possible to identify them using the NASH pentagon.

Conversely, BMI tends to decrease when NASH progresses to cirrhosis, and even histologically, a state is present in which reduced fat deposition is seen (so-called "burned-out NASH")[42,43]. Such patients are expected to have low BMI and ATI values in conjunction with high SWS and Fib-4 index values. DS may have different values depending on the individual case, but the NASH pentagon is thought to be useful even in these patients.

Limitations

This was a prospective study, but only 107 patients were included, and only 31 underwent liver biopsy during the study period. These numbers are too small to obtain sufficient results. Additional studies with a larger number of patients will be needed to confirm our results. It may also be necessary to conduct a more detailed pathological investigation and a review of the reference values for the five parameters.

CONCLUSION

The preparation of a NASH pentagon consisting of five parameters, SWS, DS, ATI value, Fib-4 index, and BMI, is simple and the calculation of its area is easy. The authors believe that this multi-parametric index will be useful for identifying NASH patients among NAFLD patients.

ARTICLE HIGHLIGHTS

Research background

Non-alcoholic fatty liver disease (NAFLD) is a major problem throughout the world. If non-alcoholic steatohepatitis (NASH) progresses, it can lead to hepatocellular carcinoma. Novel clinical index needs to be developed that can efficiently discriminate NASH patients from non-alcoholic fatty liver (NAFL) patients.

Research motivation

Shear wave speed (SWS), shear wave dispersion (SWD), and attenuation imaging (ATI) are new ultrasound diagnostic parameters for NAFLD. We developed a novel clinical index as the "NASH pentagon" consisting of the 3 abovementioned parameters, body mass index (BMI), and Fib-4 index.

Research objectives

Objective of this study is to prove the utility of NASH pentagon area in the differentiation of NASH and NAFL.

Research methods

Patients diagnosed with fatty liver by abdominal ultrasound between September 2021 and August 2022 were enrolled. Histological diagnosis based on liver biopsy was performed in 31 patients. The large pentagon group (LP group) and the small pentagon group (SP group), using an area of 100 as the cutoff, were compared; the NASH diagnosis rate was also investigated. In patients with a histologically confirmed diagnosis, receiver-operating characteristic curve analyses were performed.

Research results

The preparation of a NASH pentagon consisting of five parameters, SWS, DS, ATI value, Fib-4 index, and BMI, is simple and the calculation of its area is easy. The LP group with a NASH pentagon area ≥ 100 had 64 patients, and the SP group with an area < 100 had 43 patients. The number of patients diagnosed with NASH was 22 (34.3%) of 64 in the LP group and 3 (7.0%) of 43 in the SP group. The LP group had a significantly higher percentage of NASH patients (P = 0.0042).

Research conclusions

The NASH pentagon is a novel multi-parametric index, and will be useful for identifying NASH patients among NAFLD patients.

Research perspectives

NASH pentagon should be tried in more patients. Besides, the area of NASH pentagon and the details of the histologic diagnosis should be considered.

ACKNOWLEDGEMENTS

The authors would like to thank the institutions that participated in the working group and everyone who helped collect clinical data.

FOOTNOTES

Author contributions: Funada K, Kusano Y, Gyotoku Y and Shirahashi R conceptualized and designed the study, collected data, carried out the initial analysis, and drafted the initial manuscript; Suda T and Tamano M coordinated and supervised data collection and critically reviewed the manuscript for important intellectual content; and all authors approved the final manuscript as submitted and agree to be accountable for all aspects of the work.

Institutional review board statement: The study was reviewed and approved by the Dokkyo Medical University Saitama Medical Center Institutional Review Board (approval No. 21057).

Clinical trial registration statement: This study is registered at clinical research support office, Dokkyo Medical University Saitama Medical Center. The registration identification number is 21057.

Informed consent statement: Patients were not required to give informed consent for participation in the present study because the analysis used anonymous clinical data that were obtained after each patient gave informed consent to treatment. For full disclosure, the details of this prospective, observational study were published on the home page of the medical center.

Conflict-of-interest statement: All the authors report no relevant conflicts of interest for this article.

Data sharing statement: No additional data are available.

CONSORT 2010 statement: The authors have read the CONSORT 2010 statement, and the manuscript was prepared and revised according to the CONSORT 2010 statement.

Country/Territory of origin: Japan

ORCID number: Kei Funada 0000-0003-1190-5588; Yumi Kusano 0000-0001-8000-0884; Yoshinori Gyotoku 0000-0003-2395-3421; Ryosaku Shirahashi 0000-0001-7843-3138; Toshikuni Suda 0000-0003-1017-3725; Masaya Tamano 0000-0001-5595-2330.

S-Editor: Gao CC
L-Editor: A
P-Editor: Wang JJ

REFERENCES

1 **Sayiner M**, Koenig A, Henry L, Younossi ZM. Epidemiology of Nonalcoholic Fatty Liver Disease and Nonalcoholic Steatohepatitis in the United States and the Rest of the World. *Clin Liver Dis* 2016; **20**: 205-214 [PMID: 27063264 DOI: 10.1016/j.cld.2015.10.001]
2 **Asrani SK**, Devarbhavi H, Eaton J, Kamath PS. Burden of liver diseases in the world. *J Hepatol* 2019; **70**: 151-171 [PMID: 30266282 DOI: 10.1016/j.jhep.2018.09.014]
3 **Yeh MM**, Brunt EM. Pathological features of fatty liver disease. *Gastroenterology* 2014; **147**: 754-764 [PMID: 25109884 DOI: 10.1053/j.gastro.2014.07.056]
4 **Tsochatzis EA**, Newsome PN. Non-alcoholic fatty liver disease and the interface between primary and secondary care. *Lancet Gastroenterol Hepatol* 2018; **3**: 509-517 [PMID: 29893235 DOI: 10.1016/S2468-1253(18)30077-3]
5 **Younossi ZM**. Non-alcoholic fatty liver disease - A global public health perspective. *J Hepatol* 2019; **70**: 531-544 [PMID: 30414863 DOI: 10.1016/j.jhep.2018.10.033]
6 **Kuroda H**, Fujiwara Y, Abe T, Nagasawa T, Oguri T, Noguchi S, Kamiyama N, Takikawa Y. Two-dimensional shear wave elastography and ultrasound-guided attenuation parameter for progressive non-alcoholic steatohepatitis. *PLoS One* 2021; **16**: e0249493 [PMID: 33826669 DOI: 10.1371/journal.pone.0249493]
7 **Suda T**, Okawa O, Masaoka R, Gyotoku Y, Tokutomi N, Katayama Y, Tamano M. Shear wave elastography in hepatitis C patients before and after antiviral therapy. *World J Hepatol* 2017; **9**: 64-68 [PMID: 28105260 DOI: 10.4254/wjh.v9.i1.64]
8 **Tada T**, Kumada T, Toyoda H, Ito T, Sone Y, Okuda S, Tsuji N, Imayoshi Y, Yasuda E. Utility of real-time shear wave elastography for assessing liver fibrosis in patients with chronic hepatitis C infection without cirrhosis: Comparison of liver fibrosis indices. *Hepatol Res* 2015; **45**: E122-E129 [PMID: 25580959 DOI: 10.1111/hepr.12476]
9 **Meyer G**, Dauth N, Grimm M, Herrmann E, Bojunga J, Friedrich-Rust M. Shear Wave Elastography Reveals a High Prevalence of NAFLD-related Fibrosis even in Type 1 Diabetes. *Exp Clin Endocrinol Diabetes* 2022; **130**: 532-538 [PMID: 34784620 DOI: 10.1055/a-1666-0431]
10 **Bâldea V**, Bende F, Popescu A, Şirli R, Sporea I. Comparative study between two 2D-Shear Waves Elastography techniques for the non-invasive assessment of liver fibrosis in patients with chronic hepatitis C virus (HCV) infection. *Med Ultrason* 2021; **23**: 257-264 [PMID: 33657193 DOI: 10.11152/mu-2863]
11 **Podrug K**, Sporea I, Lupusoru R, Pastrovic F, Mustapic S, Bâldea V, Bozin T, Bokun T, Salkic N, Şirli R, Popescu A, Puljiz Z, Grgurevic I. Diagnostic Performance of 2-D Shear-Wave Elastography with Propagation Maps and Attenuation Imaging in Patients with Non-Alcoholic Fatty Liver Disease. *Ultrasound Med Biol* 2021; **47**: 2128-2137 [PMID: 33985827 DOI: 10.1016/j.ultrasmedbio.2021.03.025]
12 **Sugimoto K**, Moriyasu F, Oshiro H, Takeuchi H, Yoshimasu Y, Kasai Y, Furuichi Y, Itoi T. Viscoelasticity Measurement in Rat Livers Using Shear-Wave US Elastography. *Ultrasound Med Biol* 2018; **44**: 2018-2024 [PMID: 29936025 DOI: 10.1016/j.ultrasmedbio.2018.05.008]

13 **Lee DH**, Lee JY, Bae JS, Yi NJ, Lee KW, Suh KS, Kim H, Lee KB, Han JK. Shear-Wave Dispersion Slope from US Shear-Wave Elastography: Detection of Allograft Damage after Liver Transplantation. *Radiology* 2019; **293**: 327-333 [PMID: 31502939 DOI: 10.1148/radiol.2019190064]

14 **Jeon SK**, Lee JM, Joo I, Yoon JH, Lee DH, Lee JY, Han JK. Prospective Evaluation of Hepatic Steatosis Using Ultrasound Attenuation Imaging in Patients with Chronic Liver Disease with Magnetic Resonance Imaging Proton Density Fat Fraction as the Reference Standard. *Ultrasound Med Biol* 2019; **45**: 1407-1416 [PMID: 30975533 DOI: 10.1016/j.ultrasmedbio.2019.02.008]

15 **Tada T**, Kumada T, Toyoda H, Nakamura S, Shibata Y, Yasuda S, Watanuki Y, Tsujii K, Fukuda N, Fujioka M, Takeshima K, Niwa F, Ogawa S, Hashinokuchi S, Kataoka S, Ichikawa H, Iijima H. Attenuation imaging based on ultrasound technology for assessment of hepatic steatosis: A comparison with magnetic resonance imaging-determined proton density fat fraction. *Hepatol Res* 2020; **50**: 1319-1327 [PMID: 32876367 DOI: 10.1111/hepr.13563]

16 **Nishioji K**, Sumida Y, Kamaguchi M, Mochizuki N, Kobayashi M, Nishimura T, Yamaguchi K, Itoh Y. Prevalence of and risk factors for non-alcoholic fatty liver disease in a non-obese Japanese population, 2011-2012. *J Gastroenterol* 2015; **50**: 95-108 [PMID: 24619537 DOI: 10.1007/s00535-014-0948-9]

17 **Vilar-Gomez E**, Chalasani N. Non-invasive assessment of non-alcoholic fatty liver disease: Clinical prediction rules and blood-based biomarkers. *J Hepatol* 2018; **68**: 305-315 [PMID: 29154965 DOI: 10.1016/j.jhep.2017.11.013]

18 **Joseph AE**, Dewbury KC, McGuire PG. Ultrasound in the detection of chronic liver disease (the "bright liver"). *Br J Radiol* 1979; **52**: 184-188 [PMID: 435696 DOI: 10.1259/0007-1285-52-615-184]

19 **Yajima Y**, Ohta K, Narui T, Abe R, Suzuki H, Ohtsuki M. Ultrasonographical diagnosis of fatty liver: significance of the liver-kidney contrast. *Tohoku J Exp Med* 1983; **139**: 43-50 [PMID: 6220488 DOI: 10.1620/tjem.139.43]

20 **Hamaguchi M**, Kojima T, Itoh Y, Harano Y, Fujii K, Nakajima T, Kato T, Takeda N, Okuda J, Ida K, Kawahito Y, Yoshikawa T, Okanoue T. The severity of ultrasonographic findings in nonalcoholic fatty liver disease reflects the metabolic syndrome and visceral fat accumulation. *Am J Gastroenterol* 2007; **102**: 2708-2715 [PMID: 17894848 DOI: 10.1111/j.1572-0241.2007.01526.x]

21 **Saadeh S**, Younossi ZM, Remer EM, Gramlich T, Ong JP, Hurley M, Mullen KD, Cooper JN, Sheridan MJ. The utility of radiological imaging in nonalcoholic fatty liver disease. *Gastroenterology* 2002; **123**: 745-750 [PMID: 12198701 DOI: 10.1053/gast.2002.35354]

22 **Sugimoto K**, Moriyasu F, Oshiro H, Takeuchi H, Abe M, Yoshimasu Y, Kasai Y, Sakamaki K, Hara T, Itoi T. The Role of Multiparametric US of the Liver for the Evaluation of Nonalcoholic Steatohepatitis. *Radiology* 2020; **296**: 532-540 [PMID: 32573385 DOI: 10.1148/radiol.2020192665]

23 **Examination Committee of Criteria for 'Obesity Disease' in Japan**; Japan Society for the Study of Obesity. New criteria for 'obesity disease' in Japan. *Circ J* 2002; **66**: 987-992 [PMID: 12419927 DOI: 10.1253/circj.66.987]

24 **Shah AG**, Lydecker A, Murray K, Tetri BN, Contos MJ, Sanyal AJ; Nash Clinical Research Network. Comparison of noninvasive markers of fibrosis in patients with nonalcoholic fatty liver disease. *Clin Gastroenterol Hepatol* 2009; **7**: 1104-1112 [PMID: 19523535 DOI: 10.1016/j.cgh.2009.05.033]

25 **Angulo P**. Nonalcoholic fatty liver disease. *N Engl J Med* 2002; **346**: 1221-1231 [PMID: 11961152 DOI: 10.1056/NEJMra011775]

26 **Matteoni CA**, Younossi ZM, Gramlich T, Boparai N, Liu YC, McCullough AJ. Nonalcoholic fatty liver disease: a spectrum of clinical and pathological severity. *Gastroenterology* 1999; **116**: 1413-1419 [PMID: 10348825 DOI: 10.1016/s0016-5085(99)70506-8]

27 **Kleiner DE**, Brunt EM, Van Natta M, Behling C, Contos MJ, Cummings OW, Ferrell LD, Liu YC, Torbenson MS, Unalp-Arida A, Yeh M, McCullough AJ, Sanyal AJ; Nonalcoholic Steatohepatitis Clinical Research Network. Design and validation of a histological scoring system for nonalcoholic fatty liver disease. *Hepatology* 2005; **41**: 1313-1321 [PMID: 15915461 DOI: 10.1002/hep.20701]

28 **Tamano M**, Kojima K, Akima T, Murohisa T, Hashimoto T, Uetake C, Sugaya T, Nakano M, Hiraishi H, Yoneda M. The usefulness of measuring liver stiffness by transient elastography for assessing hepatic fibrosis in patients with various chronic liver diseases. *Hepatogastroenterology* 2012; **59**: 826-830 [PMID: 22469726 DOI: 10.5754/hge11255]

29 **Yoneda M**, Yoneda M, Fujita K, Inamori M, Tamano M, Hiriishi H, Nakajima A. Transient elastography in patients with non-alcoholic fatty liver disease (NAFLD). *Gut* 2007; **56**: 1330-1331 [PMID: 17470477 DOI: 10.1136/gut.2007.126417]

30 **Fang C**, Konstantatou E, Romanos O, Yusuf GT, Quinlan DJ, Sidhu PS. Reproducibility of 2-Dimensional Shear Wave Elastography Assessment of the Liver: A Direct Comparison With Point Shear Wave Elastography in Healthy Volunteers. *J Ultrasound Med* 2017; **36**: 1563-1569 [PMID: 28370146 DOI: 10.7863/ultra.16.07018]

31 **Suda T**, Kanefuji T, Abe A, Nagayama I, Hoshi T, Morita S, Yagi K, Hatakeyama S, Hayatsu M, Hasegawa N, Terai S. A cut-off value of shear wave speed to distinguish nonalcoholic steatohepatitis candidates. *Medicine (Baltimore)* 2019; **98**: e13958 [PMID: 30633176 DOI: 10.1097/MD.0000000000013958]

32 **Sporea I**, Bâldea V, Lupușoru R, Bende F, Mare R, Lazăr A, Popescu A, Șirli R. Quantification of Steatosis and Fibrosis using a new system implemented in an ultrasound machine. *Med Ultrason* 2020; **22**: 265-271 [PMID: 32399537 DOI: 10.11152/mu-2495]

33 **Hsu PK**, Wu LS, Yen HH, Huang HP, Chen YY, Su PY, Su WW. Attenuation Imaging with Ultrasound as a Novel Evaluation Method for Liver Steatosis. *J Clin Med* 2021; **10** [PMID: 33801163 DOI: 10.3390/jcm10050965]

34 **Jang JK**, Lee ES, Seo JW, Kim YR, Kim SY, Cho YY, Lee DH. Two-dimensional Shear-Wave Elastography and US Attenuation Imaging for Nonalcoholic Steatohepatitis Diagnosis: A Cross-sectional, Multicenter Study. *Radiology* 2022; **305**: 118-126 [PMID: 35727151 DOI: 10.1148/radiol.220220]

35 **Tada T**, Iijima H, Kobayashi N, Yoshida M, Nishimura T, Kumada T, Kondo R, Yano H, Kage M, Nakano C, Aoki T, Aizawa N, Ikeda N, Takashima T, Yuri Y, Ishii N, Hasegawa K, Takata R, Yoh K, Sakai Y, Nishikawa H, Iwata Y, Enomoto H, Hirota S, Fujimoto J, Nishiguchi S. Usefulness of Attenuation Imaging with an Ultrasound Scanner for the Evaluation of Hepatic Steatosis. *Ultrasound Med Biol* 2019; **45**: 2679-2687 [PMID: 31277922 DOI: 10.1016/j.ultrasmedbio.2019.05.033]

36 **Koda M**, Kawakami M, Murawaki Y, Senda M. The impact of visceral fat in nonalcoholic fatty liver disease: cross-

sectional and longitudinal studies. *J Gastroenterol* 2007; **42**: 897-903 [PMID: 18008034 DOI: 10.1007/s00535-007-2107-z]

37 **WHO Expert Consultation**. Appropriate body-mass index for Asian populations and its implications for policy and intervention strategies. *Lancet* 2004; **363**: 157-163 [PMID: 14726171 DOI: 10.1016/S0140-6736(03)15268-3]

38 **Sumida Y**, Yoneda M, Hyogo H, Itoh Y, Ono M, Fujii H, Eguchi Y, Suzuki Y, Aoki N, Kanemasa K, Fujita K, Chayama K, Saibara T, Kawada N, Fujimoto K, Kohgo Y, Yoshikawa T, Okanoue T; Japan Study Group of Nonalcoholic Fatty Liver Disease (JSG-NAFLD). Validation of the FIB4 index in a Japanese nonalcoholic fatty liver disease population. *BMC Gastroenterol* 2012; **12**: 2 [PMID: 22221544 DOI: 10.1186/1471-230X-12-2]

39 **Fan JG**, Kim SU, Wong VW. New trends on obesity and NAFLD in Asia. *J Hepatol* 2017; **67**: 862-873 [PMID: 28642059 DOI: 10.1016/j.jhep.2017.06.003]

40 **Wei JL**, Leung JC, Loong TC, Wong GL, Yeung DK, Chan RS, Chan HL, Chim AM, Woo J, Chu WC, Wong VW. Prevalence and Severity of Nonalcoholic Fatty Liver Disease in Non-Obese Patients: A Population Study Using Proton-Magnetic Resonance Spectroscopy. *Am J Gastroenterol* 2015; **110**: 1306-14; quiz 1315 [PMID: 26215532 DOI: 10.1038/ajg.2015.235]

41 **El-Serag HB**, Tran T, Everhart JE. Diabetes increases the risk of chronic liver disease and hepatocellular carcinoma. *Gastroenterology* 2004; **126**: 460-468 [PMID: 14762783 DOI: 10.1053/j.gastro.2003.10.065]

42 **Tokushige K**, Ikejima K, Ono M, Eguchi Y, Kamada Y, Itoh Y, Akuta N, Yoneda M, Iwasa M, Otsuka M, Tamaki N, Kogiso T, Miwa H, Chayama K, Enomoto N, Shimosegawa T, Takehara T, Koike K. Evidence-based clinical practice guidelines for nonalcoholic fatty liver disease/nonalcoholic steatohepatitis 2020. *J Gastroenterol* 2021; **56**: 951-963 [PMID: 34533632 DOI: 10.1007/s00535-021-01796-x]

43 **Tokushige K**, Ikejima K, Ono M, Eguchi Y, Kamada Y, Itoh Y, Akuta N, Yoneda M, Iwasa M, Otsuka M, Tamaki N, Kogiso T, Miwa H, Chayama K, Enomoto N, Shimosegawa T, Takehara T, Koike K. Evidence-based clinical practice guidelines for nonalcoholic fatty liver disease/nonalcoholic steatohepatitis 2020. *Hepatol Res* 2021; **51**: 1013-1025 [PMID: 34533266 DOI: 10.1111/hepr.13688]

World Journal of Gastroenterology

Submit a Manuscript: https://www.f6publishing.com

World J Gastroenterol 2023 June 21; 29(23): 3715-3732

DOI: 10.3748/wjg.v29.i23.3715

ISSN 1007-9327 (print) ISSN 2219-2840 (online)

ORIGINAL ARTICLE

Prospective Study

Robotic-assisted proctosigmoidectomy for Hirschsprung's disease: A multicenter prospective study

Meng-Xin Zhang, Xi Zhang, Xiao-Pan Chang, Ji-Xiao Zeng, Hong-Qiang Bian, Guo-Qing Cao, Shuai Li, Shui-Qing Chi, Ying Zhou, Li-Ying Rong, Li Wan, Shao-Tao Tang

Specialty type: Gastroenterology and hepatology

Provenance and peer review: Unsolicited article; Externally peer reviewed.

Peer-review model: Single blind

Peer-review report's scientific quality classification

Grade A (Excellent): 0
Grade B (Very good): B, B
Grade C (Good): 0
Grade D (Fair): 0
Grade E (Poor): 0

P-Reviewer: Grawish ME, Egypt; Trébol J, Spain

Received: March 16, 2023
Peer-review started: March 16, 2023
First decision: April 21, 2023
Revised: April 29, 2023
Accepted: May 22, 2023
Article in press: May 22, 2023
Published online: June 21, 2023

Meng-Xin Zhang, Xi Zhang, Guo-Qing Cao, Shuai Li, Shui-Qing Chi, Ying Zhou, Li-Ying Rong, Li Wan, Shao-Tao Tang, Department of Pediatric Surgery, Union Hospital, Tongji Medical College, Huazhong University of Science and Technology, Wuhan 430022, Hubei Province, China

Xiao-Pan Chang, Ji-Xiao Zeng, Department of Pediatric Surgery, Guangzhou Women and Children's Medical Center, Guangzhou Medical University, Guangzhou 510623, Guangdong Province, China

Hong-Qiang Bian, Department of General Surgery, Wuhan Children's Hospital, Tongji Medical College, Huazhong University of Science and Technology, Wuhan 430019, Hubei Province, China

Corresponding author: Shao-Tao Tang, Doctor, MD, PhD, Chief Doctor, Professor, Surgeon, Department of Pediatric Surgery, Union Hospital, Tongji Medical College, Huazhong University of Science and Technology, No. 1277 Jiefang Avenue, Wuhan 430022, Hubei Province, China. tshaotao83@hust.edu.cn

Abstract

BACKGROUND

Robotic surgery is a cutting-edge minimally invasive technique that overcomes many shortcomings of laparoscopic techniques, yet few studies have evaluated the use of robotic surgery to treat Hirschsprung's disease (HSCR).

AIM

To analyze the feasibility and medium-term outcomes of robotic-assisted proctosigmoidectomy (RAPS) with sphincter- and nerve-sparing surgery in HSCR patients.

METHODS

From July 2015 to January 2022, 156 rectosigmoid HSCR patients were enrolled in this multicenter prospective study. Their sphincters and nerves were spared by dissecting the rectum completely from the pelvic cavity outside the longitudinal muscle of the rectum and then performing transanal Soave pull-through procedures. Surgical outcomes and continence function were analyzed.

RESULTS

No conversions or intraoperative complications occurred. The median age at surgery was 9.50 months, and the length of the removed bowel was 15.50 ± 5.23 cm. The total operation time, console time, and anal traction time were 155.22 ± 16.77, 58.01 ± 7.71, and 45.28 ± 8.15 min. There were 25 complications within 30 d and 48 post-30-d complications. For children aged ≥ 4 years, the bowel function score (BFS) was 17.32 ± 2.63, and 90.91% of patients showed moderate-to-good bowel function. The postoperative fecal continence (POFC) score was 10.95 ± 1.04 at 4 years of age, 11.48 ± 0.72 at 5 years of age, and 11.94 ± 0.81 at 6 years of age, showing a promising annual trend. There were no significant differences in postoperative complications, BFS, and POFC scores related to age at surgery being ≤ 3 mo or > 3 mo.

CONCLUSION

RAPS is a safe and effective alternative for treating HSCR in children of all ages; it offers the advantage of further minimizing damage to sphincters and perirectal nerves and thus providing better continence function.

Key Words: Robotic-assisted; Hirschsprung's disease; Continence function; Sphincter; Nerve

Core Tip: We present the largest series of patients with Hirschsprung's disease treated with robotic-assisted proctosigmoidectomy (RAPS). RAPS is a safe and effective alternative for treating Hirschsprung's disease in children of all ages. It offers the advantage of further minimizing damage to sphincters and perirectal nerves and thus providing better fecal function.

Citation: Zhang MX, Zhang X, Chang XP, Zeng JX, Bian HQ, Cao GQ, Li S, Chi SQ, Zhou Y, Rong LY, Wan L, Tang ST. Robotic-assisted proctosigmoidectomy for Hirschsprung's disease: A multicenter prospective study. *World J Gastroenterol* 2023; 29(23): 3715-3732
URL: https://www.wjgnet.com/1007-9327/full/v29/i23/3715.htm
DOI: https://dx.doi.org/10.3748/wjg.v29.i23.3715

INTRODUCTION

Although beneficial for children with Hirschsprung's disease (HSCR), laparoscopic operation is more challenging than open operation, especially in newborns and infants. To address the drawbacks of laparoscopic surgery, a robotic system may be considered. Robotic-assisted surgery is utilized in various areas due to its numerous advantages, particularly in complex operations, such as anorectal malformations in children[1] and prostate and rectal cancer in adults[2,3].

Recently, laparoscopic techniques have developed into an effective treatment for HSCR. As previously shown, these minimally invasive surgical techniques result in better early postoperative outcomes than the open procedure[4,5], and the long-term results are similar between laparoscopic and open procedures[6]. Nevertheless, laparoscopic surgery for HSCR is still considered to be one of the most difficult operations in anorectal surgery. With the introduction and application of robotic surgical platforms, this technology is gradually being adopted for the treatment of HSCR. However, the safety and efficacy of the technology in treating pediatric HSCR patients have been evaluated in only a few studies.

In this paper, we present our initial experience with robotic-assisted proctosigmoidectomy (RAPS) with sphincter- and nerve-sparing surgery (SNS) for treating HSCR. To our knowledge, this represents the largest series of SNS-RAPS in children reported to date. The SNS-RAPS procedure is thoroughly detailed.

MATERIALS AND METHODS

Study design

From July 2015 to January 2022, a multicenter prospective study of consecutive children with rectosigmoid HSCR who underwent uniform SNS-RAPS was carried out at three centers (Union Hospital, Tongji Medical College, Huazhong University of Science and Technology; Guangzhou Women and Children's Medical Center, Guangzhou Medical University; Wuhan Children's Hospital, Tongji Medical College, Huazhong University of Science and Technology). A total of 156 patients were

enrolled, and all operations were performed by experienced surgical teams from three centers. Since the time the da Vinci Surgical System Si (Intuitive Surgical, Sunnyvale, CA) was introduced at the three centers to treat HSCR, all HSCR cases have been recorded in a prospectively designed database. Patient demographics, surgical parameters, and postoperative data were recorded.

This study was approved by the ethics committee at each participating center and registered in the Chinese Clinical Trial Registry (Registration ID: ChiCTR2000035220). Written informed consent was obtained from the legal guardians of each patient. The study has been reported in accordance with the Declaration of Helsinki.

Patients

Patients diagnosed with rectosigmoid HSCR preoperatively were candidates for SNS-RAPS. The diagnosis was based on clinical symptoms and signs, barium enema results, rectal aspiration biopsy, anorectal manometry, and intraoperative biopsy. Patients with trisomy 21, total colonic aganglionosis, long-segment HSCR, HSCR combined with preoperative enterostomy, and surgical contraindications were excluded. The patient selection process is detailed in Figure 1. All patients received a unified preoperative preparation and postoperative treatment plan at all centers.

Colonic irrigation with warm saline (100-200 mL/kg) was used to prepare the colon for 3-7 d. Metronidazole (25 mg/kg, bid) was given orally for 3 d (1-2 d for neonates) preoperatively, and one dose of cefoperazone was provided during anesthesia induction.

Operative procedure

Under general anesthesia, the patient was placed in the supine position, and three trocars were placed. The CO_2 insufflation pressure was set at 8-10 mmHg, and the flow rate at 2.5-4.5 L/min. The operation was performed using three ports, including a straight-cut umbilical trocar accommodating a 12 mm 30° telescope and two working trocars with 8 mm robotic devices on either side (Figure 2). The robotic arms were oriented from the caudal direction. The aganglionic segment range was assessed by seromuscular biopsy using robotic monopolar scissors and interrupted 5-0 sutures were placed in cases of bleeding or mucosal rupture. The needle and suction were alternately inserted for operation through the 8 mm port on one side, which required the process of removing and reinserting the operative instrument. A Maryland dissector and a robotic hook were used to perform the dissection. After creating a window on the sigmoid mesentery, we clipped and divided the sigmoid artery trunk and then mobilized the mesentery up to the level of the inferior mesenteric artery. SNS robotic endorectal dissection was performed circumferentially down to the pelvis, which was the most unique and crucial part of the operation. Dissection was begun circumferentially at 1.0 cm above the peritoneal reflection. The rectum was mobilized outside the longitudinal muscle layer (that is, under its serosa or proper rectal fascia extended serous layer below the peritoneal reflection), with the anatomical plane farther away from Denonvillier's fascia and the nerve plexus anterior or lateral to the rectum (Figure 3A). When we pulled the rectum cranially, intestinal wall muscle layers provided greater tensile strength than the mucosa, allowing the pelvis to be shallower (Figure 4) and avoiding intraoperative intestinal mucosal tearing with peritoneal contamination. Since the robotic platform allowed for dissection in a narrow field, we were able to dissect the rectum to a lower level, nearly up to the dentate line. The mobilization of the rectum reached 4-7 cm into the pelvis (Figure 3B).

After the robot was unlocked, a circular incision was made 0.5-1 cm from the dentate line (Figure 5A), dividing the mucosa upward by 0.2-0.4 cm, breaking through the muscular cuff, and exposing the robotic dissection plane in the pelvis. The diseased colon was then gently pulled out through the anus. The posterior wall was partially resected in a V-shape, and the pointed end of the "V" reached the level of the dentate line to release internal anal sphincter achalasia. To avoid residual dysfunctional bowel, we uniformly excised the dilated and thickened bowel; we then performed Soave's anastomosis with interrupted 5-0 or 4-0 absorbable sutures above the biopsy site. After the diseased bowel was removed, the specimen was measured for its overall length and the pelvic dissection length (Figure 5B).

Postoperative management

Intravenous antibiotics (cefoperazone, 50 mg/kg, bid) were given for the first 3 d, and a urinary catheter was left for 24-48 h after surgery. No nasogastric tube or drains were left in place, but a rectal tube was left for 5 d postoperatively to help the passage of intestinal contents and gas through the anus. Instead of sutures, we used butterfly shaped tape to fixate the tube and reduce postoperative discomfort. The patient was discharged after being confirmed to be clinically stable and tolerant of a full oral diet. A routine digital rectal examination was performed postoperatively at 2 wk, and an anal dilatation plan was formulated.

Postoperative variables and definitions

The bowel function score (BFS) was used to evaluate overall bowel function[7], while the postoperative fecal continence (POFC) score focused on SNS-related incontinence[8]. Children aged ≥ 4 years were assessed twice for each score as shown in Tables 1 and 2. A BFS ≥ 17 was represented as the lower limit of good/normal functional outcomes as more than 90% of people aged ≥ 4 years in the normal

Table 1 Scale for bowel function score

Evaluation on fecal continence	Score
Feels the urge to defecate	
Always	3
Most of the time	2
Uncertain	1
Absent	0
Ability to hold back defecation	
Always	3
Problems less than once a week	2
Weekly problems	1
No voluntary control	0
Frequency of defecation	
Every other day-twice a day	2
More often	1
Less often	1
Soiling	
Never	3
Staining less than once a week, no change of underwear required	2
Frequent staining/soiling, change of underwear required	1
Daily soiling, requires protective aids	0
Accidents	
Never	3
Less than once a week	2
Weekly accidents, often requires protective aids	1
Daily, protective aids required day and night	0
Constipation	
No constipation	3
Manageable with diet	2
Manageable with laxatives	1
Manageable with enemas	0
Social problems	
No social problems	3
Sometimes (fouls odors)	2
Problems causing restrictions in social life	1
Major social/psychosocial problems	0

population met this criterion[9]. Soiling referred to the actual presence of feces in the underwear without the patient's awareness, while fecal marks on the underwear were regarded as staining. We briefly defined the normal stool frequency as 1-3 times daily or once every 1-3 d. The diagnosis of HSCR-associated enterocolitis was based on the definitions by Teitelbaum and Coran[10]. Post-30-d complications were defined as complications occurring 30 d to 1 year after surgery.

Statistical analysis

Categorical variables are presented as counts and percentages, while continuous variables are presented as the mean ± SD or median (range). The Kolmogorov–Smirnov test was used to assess the normality

Table 2 Scale for postoperative fecal continence score

Evaluation on the POFC scores	0	1	2
Frequency of motions (/day)	≥ 6	3-5	1-2
Severity of staining/soiling	Soiling	Staining	None
Severity of perianal erosion	Often	Occasionally	Nil
Anal shape	Prolapse needing surgery	Mucosa visible	Normal
Requirement for medications	Antidiarrheals	Laxatives/enemas	Nil
Sensation of rectal fullness	Not at all[1]	Occasionally	Always[2]
Ability to distinguish flatus from stool	Not at all[1]	Occasionally	Always[2]

[1]Full awareness or ability to distinguish less than once a week.
[2]Full awareness or ability to distinguish at least 4 out of 5 times (more than 80%).
POFC: postoperative fecal continence.

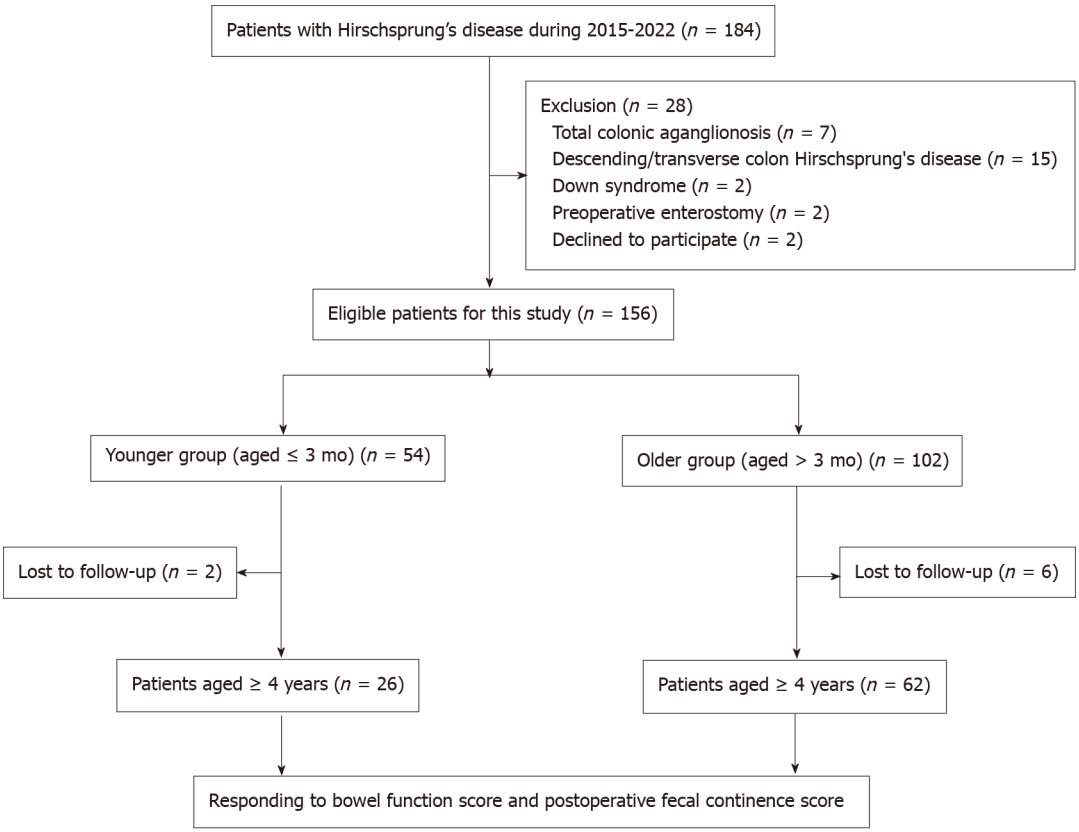

DOI: 10.3748/wjg.v29.i23.3715

Figure 1 Flowchart of patient selection.

distribution of the data. To evaluate the differences between groups, the chi-square test or Fisher exact test was used to analyze categorical variables, and the Mann-Whitney U test was used to compare continuous variables because the data did not meet the normal distribution criteria. IBM SPSS Statistics version 26.0 was used for statistical analysis. A P value of < 0.05 was considered indicative of statistical significance.

RESULTS

Patient demographics and operative data

A total of 184 participants were assessed for eligibility, and 156 patients were finally enrolled in this multicenter prospective study (Figure 1). The demographics and operative outcomes are shown in

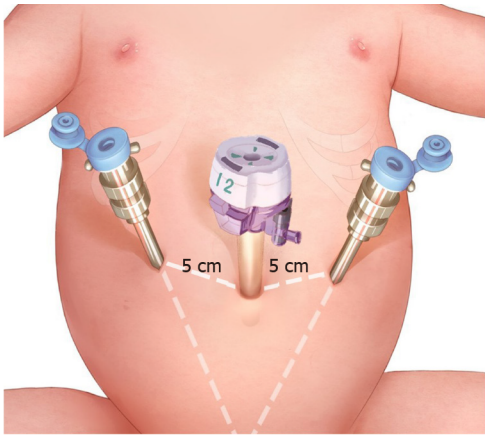

DOI: 10.3748/wjg.v29.i23.3715 **Copyright** ©The Author(s) 2023.

Figure 2 Trocar site in robotic-assisted proctosigmoidectomy. There are three trocar ports, including a straight-cut umbilical trocar and two 8 mm working trocars located 5 cm from the umbilical trocar on either side.

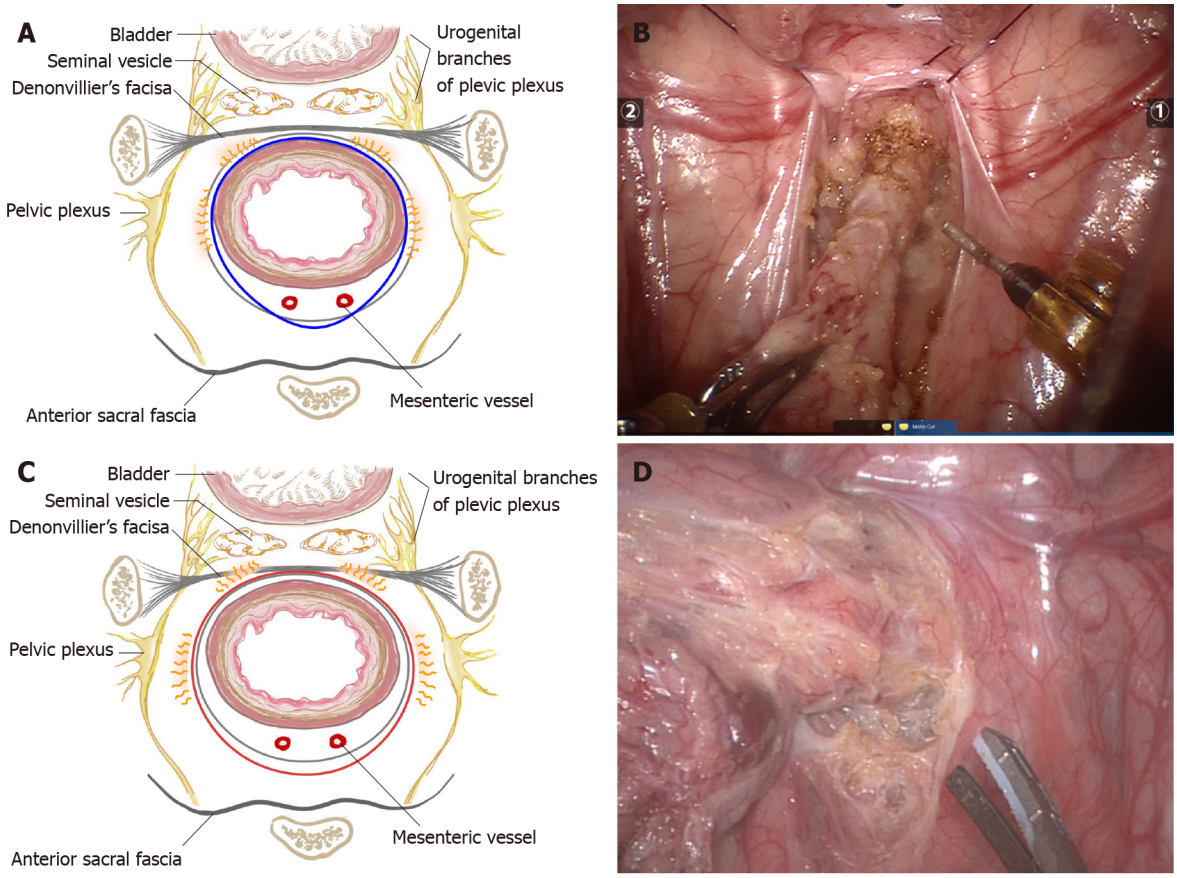

DOI: 10.3748/wjg.v29.i23.3715 **Copyright** ©The Author(s) 2023.

Figure 3 Diagram of pelvic dissection planes and intraoperative images of pelvic dissection. A: Pelvic dissection plane of robotic-assisted proctosigmoidectomy is under the serosa of the rectum or proper rectal fascia extended serous layer below the peritoneal reflection; B: Pelvic dissection under robotic endoscopy; C: Pelvic dissection plane of conventional laparoscopic Soave surgery is performed tightly around the rectal wall; D: Pelvic dissection under laparoscopy.

Table 3. No conversions or intraoperative complications occurred. The median age at surgery was 9.50 (range: 0.60-132.00) mo, and the weight was 9.09 ± 3.68 kg. The total operative time was 155.22 ± 16.77 min, and the robotic console time was 58.01 ± 7.71 min. The anal traction time was 45.28 ± 8.15 min, which included 15.21 ± 2.67 min for transanal dissection and 30.01 ± 5.82 min for anastomosis. The length of the removed bowel was 15.50 ± 5.23 cm, and the pelvic dissection depth under endoscopy was 4.50 ± 0.47 cm. The intraoperative estimated blood loss was 5.01 ± 1.81 mL.

Table 3 Operative parameters of patients

Parameter	*n* (%) or mean ± SD/median (range)
Age at surgery (month)	9.50 (0.60-132.00)
≤ 1 mo	4 (2.56%)
≤ 3 mo	50 (32.05%)
≤ 1 yr	77 (49.36%)
≤ 3 yr	16 (10.26%)
> 3 yr	9 (5.77%)
Level of aganglionosis	
Sigmoid colon	29 (32.95%)
Upper rectum	39 (44.32%)
Lower rectum	20 (22.73%)
Weight at surgery (kg)	9.09 ± 3.68
Operative time (min)	155.22 ± 16.77
Console time (min)	58.01 ± 7.71
Anal traction time (min)	45.28 ± 8.15
Transanal dissection time (min)	15.21 ± 2.67
Anastomosis time	30.01 ± 5.82
Estimated blood loss (mL)	5.01 ± 1.81
Pelvic dissection depth (cm)	4.50 ± 0.47
Length of the removed bowel (cm)	15.50 ± 5.23
Conversion	0 (0)
Intraoperative complications	0 (0)

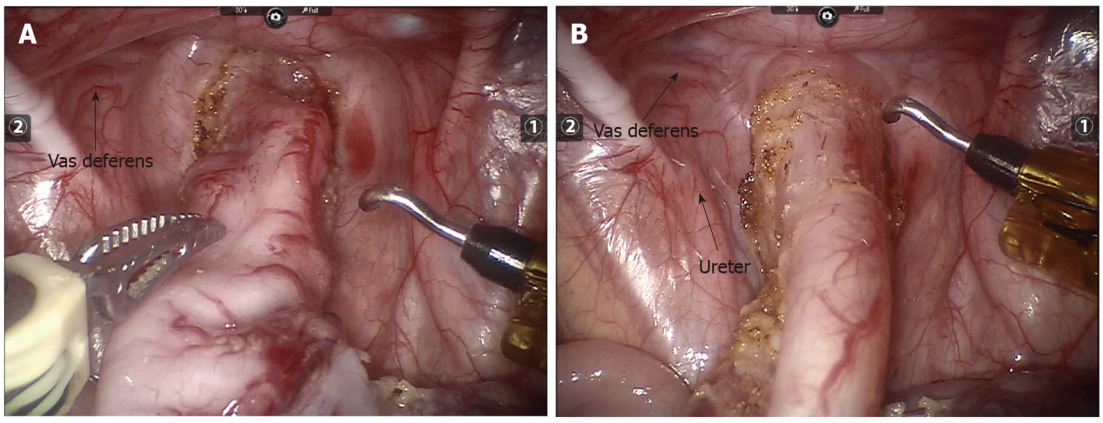

DOI: 10.3748/wjg.v29.i23.3715

Figure 4 The pelvic depth in robotic vision before and after pulling the rectum cranially; the depth becomes shallower after pulling. A: Before pulling; B: After pulling.

Postoperative outcomes

Postoperative outcomes are detailed in Table 4. The hospital stay was 7.25 ± 1.67 d, and the median follow-up duration was 44.00 (range: 6.00-78.00) mo. Eight patients were lost to follow-up one year after surgery. Postoperative complications were assessed in accordance with the Classification of Surgical Complications[11]. The postoperative 30-d complications included Clavien–Dindo grade II complications in two patients with wound infections, two patients with lung infections, six patients with enterocolitis, and thirteen patients with perianal dermatitis, all of whom were corrected by conservative treatment. One patient exhibited a Clavien–Dindo grade IIIa complication (anastomotic leakage treated

Table 4 Postoperative outcomes of patients

Parameter	*n* (%) or mean ± SD /median (range)
Hospital stay (day)	7.25 ± 1.67
Follow-up time (month)	44.00 (6.00-78.00)
Outcomes within postoperative 30 d	
Omental hernia	1 (0.64%)
Wound infections	2 (1.28%)
Lung infections	2 (1.28%)
Perianal dermatitis	13 (8.33%)
Uroschesis	0 (0)
Urinary incontinence	0 (0)
Anastomotic leakage	1 (0.64%)
Enterocolitis	6 (3.85%)
Cuff abscess	0 (0)
Post 30-d complications	
Perianal dermatitis	0 (0)
Anastomotic strictures	2 (1.28%)
Sphincter spasm	0 (0)
Enterocolitis	16 (10.26%)
Soiling	7 (4.49%)
Staining	18 (11.54%)
Constipation	4 (2.56%)
Perianal dermatitis	1 (0.64%)

by resuturing with presacral drainage[12]), and one patient had a Clavien–Dindo grade IIIb complication (omental hernia requiring surgical correction). There was no uroschesis, urinary incontinence, or cuff abscess. Post-30-d complications included Clavien–Dindo grade I complications, namely, seven soilings (received bowel habit training) and eighteen stainings (no change of underwear required) as well as Clavien–Dindo grade II complications, namely, two cases of anastomotic strictures (underwent anal dilation treatment without anesthesia), sixteen cases of enterocolitis (received rectal decompression, irrigation, and broad-spectrum antibiotics), four cases of constipation (received a laxative and enema) and one case of perianal dermatitis (received topical medication).

Normal stool frequency and enterocolitis at 1-6 years after surgery

As listed in Table 5, we divided follow-up into four phases: ≤ 1 year, 1 < years ≤ 2, 2 < years ≤ 4, and 4 < years ≤ 6, with further analysis of short- to medium-term stool frequency and enterocolitis. The incidence of normal stool frequency increased steadily while the enterocolitis rate decreased gradually over time; the overall normal stool frequency rate increased from 55.13% to 89.06% under diet control (younger group: 53.70% to 86.36%, older group: 55.88% to 90.48%) (Figure 6A) and the overall enterocolitis rate declined from 10.26% to 4.69% (younger group: 11.11% to 4.55%, older group: 9.8% to 4.76%) (Figure 6B).

BFS and POFC score in the assessment of medium-term functional outcomes

The BFS and POFC score are shown in Table 6. Eighty-eight patients aged ≥ 4 years were evaluated with two scoring systems during follow-up. The bowel functional result was good (BFS ≥ 17) in 66 patients (75.00%), moderate (12 ≤ BFS ≤ 16) in 14 patients (15.91%), and poor (BFS < 12) in 8 patients (9.09%). The total BFS was 17.32 ± 2.63, with satisfactory scores for each item. The POFC score at 4, 5 and 6 years of age postoperatively demonstrated a promising trend annually, with values of 10.95 ± 1.04, 11.48 ± 0.72, and 11.94 ± 0.81, respectively (Figure 6C).

Comparison of efficacy between patients aged ≤ 3 mo and aged > 3 mo at surgery

The outcomes comparing normal stool frequency and enterocolitis are shown in Table 5. The comparison results of postoperative complications are detailed in Table 7, while the comparison results

Table 5 Normal stool frequency and enterocolitis 1-6 years after surgery

	Younger group				Older group				*P* value	Total			
	≤ 1 yr	1 < yr ≤ 2	2 < yr ≤ 4	4 < yr ≤ 6	≤ 1 yr	1 < yr ≤ 2	2 < yr ≤ 4	4 < yr ≤ 6		≤ 1 yr	1 < yr ≤ 2	2 < yr ≤ 4	4 < yr ≤ 6
	n = 54	*n* = 48	*n* = 38	*n* = 22	*n* = 102	*n* = 91	*n* = 74	*n* = 42		*n* = 156	*n* = 139	*n* = 112	*n* = 64
Normal stool frequency, *n* (%)	29 (53.70%)	34 (70.83%)	30 (78.95%)	19 (86.36%)	57 (55.88%)	67 (73.63%)	61 (82.43%)	38 (90.48%)	0.80, 0.73, 0.66, 0.94	86 (55.13%)	101 (72.66%)	91 (81.25%)	57 (89.06%)
Enterocolitis, *n* (%)	6 (11.11%)	5 (10.42%)	3 (7.89%)	1 (4.55%)	10 (9.80%)	7 (7.69%)	4 (5.41%)	2 (4.76%)	0.80, 0.82, 0.92, 1.00	16 (10.26%)	12 (8.63%)	7 (6.25%)	3 (4.69%)

of BFS and POFC scores are shown in Table 8. Due to the small number of neonates in this series, we carried out a subgroup analysis to assess defecation function in younger infants, grouping the patients by age into ≤ 3 mo (younger group, n = 54) and > 3 mo (older group, n = 102). There was no significant difference in postoperative complication rates, BFSs (younger group: 17.19 ± 2.87, older group: 17.37 ± 2.54) or POFC scores at 4, 5 and 6 years of age postoperatively (younger group: 10.70 ± 0.99, 11.38 ± 0.62, 11.71 ± 0.76; older group: 11.07 ± 1.05, 11.52 ± 0.76, 12.00 ± 0.83) between the two groups (Figure 6C).

DISCUSSION

Robotic procedures are rapidly replacing open or laparoscopic procedures for the adult population in challenging procedures, such as operations for rectal and prostate cancer[2,3]. Nevertheless, the adoption of robots in pediatric surgery is low. Robotic surgery failed to show substantial benefits in studies comparing it to laparoscopic surgery because the procedures were initially used for less complex operations, such as the Nissen fundoplication[13]. In technically demanding situations, the application of robots for abdominal surgeries in children is relatively limited. Furthermore, only a few studies have revealed the feasibility of robotic-assisted surgery for HSCR, and the patient numbers were too small to generalize the application of robotic surgery in this field[14-17]. There is still a lack of studies involving large samples and long follow-up on functional outcomes. To our knowledge, 156 consecutive HSCR children who received RAPS represent the largest series in the literature. Long-segmental HSCR, total colonic aganglionosis, and trisomy 21 have been demonstrated to negatively affect the prognosis of HSCR patients[18-20]. Aiming to focus on the effect of surgical techniques on the postoperative outcomes of HSCR, we excluded these influencing factors and performed RAPS only on children with rectosigmoid HSCR.

The core of the original Soave procedure is pelvic endorectal dissection under the mucosa, but the mucosa is easily ruptured, resulting in pelvic contamination or mucosal residue. This explains the high rate of muscular sleeve infection following surgery in that era[4]. Pelvic endorectal dissection is a determining step in minimally invasive surgery for HSCR. Laparoscopic surgery facilitates tissue dissection in narrow spaces, and the technique still follows the concept of the original Soave procedure for nerve sparing. However, stiff laparoscopic instruments and unstable vision make submucosal rectal dissection more challenging, resulting in a higher mucosa rupture rate. Instead, extrarectal dissection is performed tightly around the rectal wall to 1-2 cm below the peritoneal reflection, and then a long-

Table 6 Bowel function scores and postoperative fecal continence scores among 88 patients aged 4 years or older

Parameter	Total (*n* = 88)
Bowel function score (Mean score ± SD)/*n* (%)	
Feels the urge to defecate	
Always	66 (75.00%)
Most of the time	19 (21.59%)
Uncertain	3 (3.41%)
Absent	0 (0)
Mean score ± SD	2.72 ± 0.52
Ability to hold back defecation	
Always	63 (71.59%)
Problems less than once a week	17 (19.32%)
Weekly problems	8 (9.09%)
No voluntary control	0 (0)
Mean score ± SD	2.63 ± 0.65
Normal defecation frequency	55 (62.50%)
Mean score ± SD	1.63 ± 0.49
Fecal soiling	
Never	32 (36.36%)
Staining < 1/wk	42 (47.73%)
Frequent soiling, change of underwear required	14 (15.91%)
Daily soiling, protective aids required	0 (0)
Mean score ± SD	2.23 ± 0.69
Fecal accidents	
Never	63 (71.59%)
Less than once a week	18 (20.45%)
Weekly accidents, protective aids often required	6 (6.82%)
Daily, aids required day and night	1 (1.14%)
Mean score ± SD	2.63 ± 0.67
Constipation	
No constipation	82 (93.18%)
Manageable with diet	0 (0)
Manageable with laxatives	4 (4.55%)
Manageable with enemas	2 (2.27%)
Mean score ± SD	2.84 ± 0.60
Social problems	
No social problems	61 (69.32%)
Sometimes (fouls odors)	18 (20.45%)
Problems causing restrictions in social life	9 (10.23%)
Major social/psychosocial problems	0 (0)
Mean score ± SD	2.59 ± 0.67
Total score	17.32 ± 2.63
Good bowel function (total score ≥ 17)	66 (75.00%)

Moderate bowel function (12 ≤ total score ≤ 16)	14 (15.91%)
Poor bowel function (total score < 12)	8 (9.09%)
Postoperative fecal incontinence scores (Mean score ± SD)	
Aged ≥ 4 years (n = 88)	10.95 ± 1.04
Aged ≥ 5 years (n = 60)	11.48 ± 0.72
Aged ≥ 6 years (n = 34)	11.94 ± 0.81

Table 7 Comparison of postoperative outcomes between the younger group and the older group

Parameter	Younger group (n = 54)	Older group (n = 102)	P value
Outcomes within postoperative 30 d, n (%)			
Omental hernia	1 (1.85%)	0 (0)	0.35
Wound infections	1 (1.85%)	1 (0.98%)	1.00
Lung infections	2 (3.70%)	0 (0)	0.24
Perianal dermatitis	5 (9.26%)	8 (7.84%)	1.00
Uroschesis	0 (0)	0 (0)	-
Urinary incontinence	0 (0)	0 (0)	-
Anastomotic leakage	1 (1.85%)	0 (0)	0.35
Enterocolitis	4 (7.41%)	2 (1.96%)	0.21
Cuff abscess	0 (0)	0 (0)	-
Post-30-d complications, n (%)			
Perianal dermatitis	0 (0)	0 (0)	-
Anastomotic strictures	1 (1.85%)	1 (0.98%)	1.00
Sphincter spasm	0 (0)	0 (0)	-
Enterocolitis	6 (11.11%)	10 (9.80%)	0.80
Soiling	3 (5.56%)	4 (3.92%)	0.95
Staining	7 (12.96%)	11 (10.78%)	0.69
Constipation	1 (1.85%)	3 (2.94%)	1.00
Perianal dermatitis	1 (1.85%)	0 (0)	0.35

distance submucosal dissection is conducted through the anus as in Georgeson's technique (Figure 3C and D) [21]. For selected patients, a totally transanal endorectal technique with submucosal dissection can even be performed as in Torre's technique[22]. These procedures have been demonstrated to provide better short-term outcomes than open surgery, with similar long-term outcomes[6,23,24]. Nonetheless, some studies have found that minimally invasive surgery, particularly totally transanal surgery that requires more anal dissection, results in poorer long-term defecation function than open surgery, especially in neonates[7,25,26]. This is probably a result of the technique's increased risk of anal sphincter traction/injury[27]. Therefore, we hypothesized that RAPS could reduce these risks to support better long-term bowel function for patients.

Herein, the primary strength of our robotic-assisted technique is that a new endorectal dissection layer (outside the longitudinal muscle) can be established. This potential gap between anatomical structures exists objectively[28]. The new layer is farther away from the urinal nerves on both sides of the rectum and the sexual nerves ahead of the Denonvillier's fascia[29]. A diagram of the pelvic dissection layer is shown in Figure 3A. The robotic system provides a magnified 3D image, stable maneuverability, and articulated movement in the narrow area *via* small incisions. Another major advantage is the image stability from robotic arm support as minor camera movements can cause image shifting. These merits facilitate ideal identification of the subserosa and precise rectum dissection, thus guaranteeing nerve-sparing. In addition, the rectum with intact longitudinal and circular muscles can be pulled strongly and is less prone to rupture; thus, the surgeon is able to pull the rectum cranially to make the pelvis shallower (Figure 4), allowing the dissection to nearly reach the dentate line (Figure 3B). Extensive intra-abdominal endorectal dissection would result in less need for transanal dissection and

Table 8 Bowel function scores and postoperative fecal incontinence scores among patients aged 4 years or older between the younger group and the older group

Parameters	Younger group (*n* = 26)	Older group (*n* = 62)	*P* value
Bowel function scores (Mean score ± SD)			
Feels the urge to defecate	2.65 ± 0.63	2.74 ± 0.48	0.68
Ability to hold back defecation	2.58 ± 0.70	2.65 ± 0.63	0.71
Normal defecation frequency	1.69 ± 0.47	1.60 ± 0.49	0.40
Fecal soiling	2.19 ± 0.63	2.24 ± 0.72	0.67
Fecal accidents	2.58 ± 0.81	2.65 ± 0.60	0.98
Constipation	2.81 ± 0.69	2.85 ± 0.57	0.82
Social problems	2.62 ± 0.64	2.58 ± 0.69	0.93
Total bowel function score	17.19 ± 2.87	17.37 ± 2.54	0.90
Postoperative fecal incontinence scores (Mean score ± SD)			
Aged ≥ 4 yr	10.70 ± 0.99	11.07 ± 1.05	0.16
Aged ≥ 5 yr	11.38 ± 0.62	11.52 ± 0.76	0.46
Aged ≥ 6 yr	11.71 ± 0.76	12.00 ± 0.83	0.35

simpler transanal procedures, thus permitting minor or no sphincter damage. Figure 5C and D show a comparison of the length of endorectal dissection and transanal dissection between two minimally invasive approaches. As our results show, the pelvic dissection could reach a depth of 4.50 ± 0.47 cm, so the length of the rectum dissected transanally was greatly shortened to 0.20-0.40 cm (Figure 5B). This reduces the time and intensity of sphincter traction. As reported, prolonged transanal dissection is prone to sphincter traction/injury[18,30]. Hence, robotic practice in pelvic rectal dissection may offer an excellent surgical tool.

Due to the additional docking and setting time of the robotic arms, the total operation time of robotic procedures is generally longer than that of open or laparoscopic procedures[15,31]. In our series, however, the operative time was 155.22 ± 16.77 min and was comparable to that of laparoscopic surgery, which varied from 94.00 to 294.00 min in previous large-sample studies[6,18,32-36]. Moreover, our results revealed that postoperative complication rates were similar or even lower than those of transanal or laparoscopic approaches[18,32-34]. There were no cuff abscesses in our series. This is related to precise and complete dissection of the rectum outside the longitudinal muscle up to the dentate line, preventing mucosal tube injury and ensuring no residual rectal mucosa. Previous studies have shown that the incidence of urinary incontinence in HSCR patients postoperatively ranges from 2.70%-22.00% [37-41], and urine retention ranges from 1.04%-6.67%[42-44]. Urinary complications following pelvic procedures may be caused by direct damage or indirect thermal radiation injury to the nerve endings controlling voiding. No uroschesis or urinary incontinence occurred after removal of the urinary catheter 24-48 h after surgery in any of the patients. This highlights the most obvious advantage of SNS-RAPS, which is the precise safeguarding of the urinal nerve around the rectum. Following this logic, good short-term bladder nerve protection after RAPS could indirectly predict better long-term defecation and sexual nerve function.

Postoperative bowel function and continence are the most important criteria for evaluating the effectiveness of SNS-RAPS. BFS was used for a comprehensive assessment of defecation, soiling, constipation, and social problems. Previous studies evaluating long-term outcomes (follow-up ranged from 9.5 to 28 years) after open, laparoscopic or transanal approaches have shown that 88.00% to 89.00% of HSCR patients obtained moderate-to-good bowel function (good: BFS ≥ 17, 52.00%-63.00%; moderate: 12 ≤ BFS ≤ 16, 26.00%-36.00%)[7,45], with an overall score of 15.00 to 17.10[7,9,18,45-47]. One clinical trial even found that neonates with HSCR achieved a BFS of 17.44 for long -segment HSCR and 19.06 for short-segment HSCR after a transanal procedure (follow-up for more than 8 years)[48]. Our medium-term findings showed an overall BFS of 17.32 ± 2.63 and that 90.91% of patients achieved moderate-to-good bowel function (good: 75.00%; moderate: 15.91%), which was comparable to or better than the long-term results of previous studies. As studies have shown, postoperative bowel function improves with age[8, 46], so we predict that our series of patients will have better long-term bowel function. Furthermore, we used the POFC score to analyze fecal incontinence, reflecting the role of SNS-RAPS in nerve and sphincter protection[8]. The total POFC score gradually improved and was satisfactory in patients at 4, 5 and 6 years of age following surgery (10.95 ± 1.04, 11.48 ± 0.72 and 11.94 ± 0.81), representing a result similar to or superior to that of laparoscopic operation (8.60-11.30)[8,49]. Postoperative functional results are strongly related to long-term quality of life (QoL)[9,46,47]. Satisfactory BFS and POFC scores in this

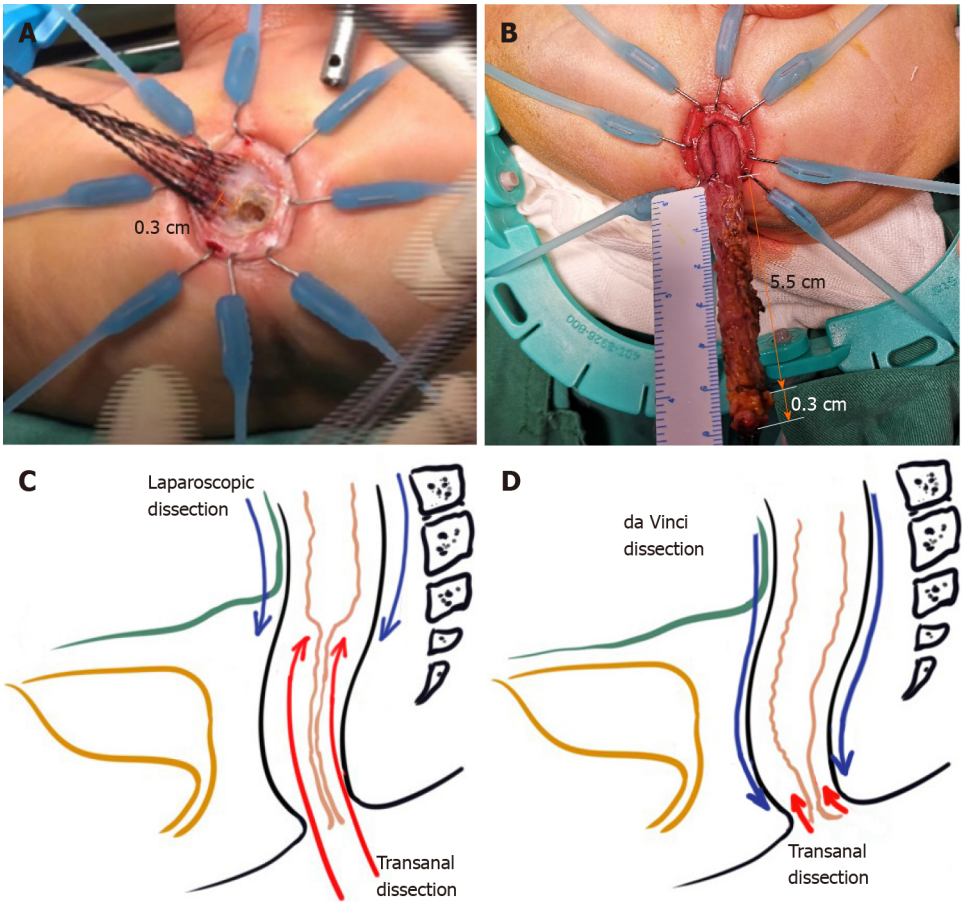

DOI: 10.3748/wjg.v29.i23.3715 **Copyright** ©The Author(s) 2023.

Figure 5 Comparison of two minimally invasive approaches and dissection length measurement of robotic-assisted proctosigmoidectomy. A: The transanal Soave anastomosis procedure is performed by making a circular incision 0.5-1 cm from the dentate line and dividing the mucosa upward by 0.2-0.4 cm; B: The length of pelvic dissection was 5.5 cm and the length of transanal dissection was 0.3 cm of robotic-assisted proctosigmoidectomy; C: The length of endorectal dissection and transanal dissection in the laparoscopic approach; D: The length of endorectal dissection and transanal dissection in the robotic approach.

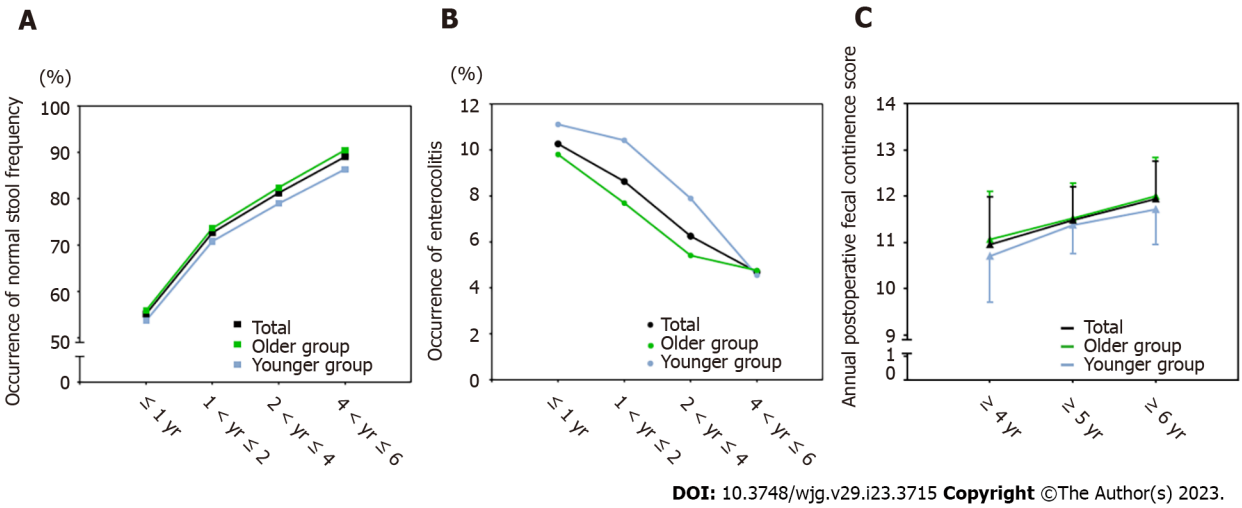

DOI: 10.3748/wjg.v29.i23.3715 **Copyright** ©The Author(s) 2023.

Figure 6 Short- to medium-term outcomes of robotic-assisted proctosigmoidectomy. A: Occurrence of normal stool frequency at 1-6 years after surgery; B: Occurrence of enterocolitis at 1-6 years after surgery; C: Annual postoperative fecal continence score analysis among patients aged 4 years or more.

series suggested that patients will achieve good long-term QoL.

Researchers in previous studies have mixed opinions on the efficacy in younger infants, especially neonates, compared with that in older children[49,50]. Although its appropriateness for younger infants with HSCR is debatable, robotic surgery could be successfully utilized for other diseases in the neonatal period[51]. We have gained experience in robotic surgery for these disorders and successfully applied

robotic surgery for neonates and infants with HSCR. As younger infants have a narrower pelvis and more compact structures than older children, the distance between the rectum and the surrounding structures is smaller. Moreover, younger age is associated with more fragile tissue that is vulnerable to operative injury[52]. These features increase the risk of injuring perirectal neurovascular tissues and sphincters during laparoscopic procedures, but the robotic system supplies a stable magnified 3D surgical field and precise rectal dissection to avoid the risk of disruption to the perirectal tissues. We found that HSCR patients in the younger group (aged ≤ 3 mo) and older group (aged > 3 mo) exhibited comparable complication rates, BFS and POFC scores. These data demonstrated that SNS-RAPS is feasible for HSCR patients aged ≤ 3 mo, and its efficacy was comparable to that in the older group. This also indicated that SNS-RAPS has better efficacy than previously reported open and laparoscopic procedures when considered from another perspective. Although totally transanal surgery was an option for 22.73% of patients with lower rectum HSCR in this study, our RAPS could reduce the time and intensity of sphincter traction and provide better outcomes. Taken together, our findings further support the view that the protection afforded by RAPS to the anal sphincter and perirectal nerves is no worse than other approaches and that RAPS is a preferred option for HSCR.

Although our study demonstrated favorable outcomes for RAPS, the limitations include only short- to medium-term outcomes and the absence of comparative data with other approaches. Therefore, a long-term follow-up and comparative trial should be performed to evaluate the effect of SNS-RAPS on HSCR. Currently, assessing long-term outcomes is not an option because SNS-RAPS has been used for less than 10 years. We intend to perform this clinical trial in the next several years. Moreover, the currently documented drawbacks of robotic surgery are longer operative time, expensive costs and oversized robotic devices for infants and neonates, creating economic and technical constraints. With the further advancement of pediatric robot devices, the reduction in surgical costs, and the improvement in surgeons' skills, the application of robots in pediatric surgery will mature. If surgery is to provide less pain and more effective therapy, then minimally invasive procedures achieved *via* robots that share the advantages of open or laparoscopic procedures may offer the answer.

CONCLUSION

SNS-RAPS is a safe and effective option for children of all ages with HSCR. The robotic platform can be utilized to further minimize surgical damage to the perirectal neurovascular tissue and anal sphincter, contributing to better bowel and urination function.

ARTICLE HIGHLIGHTS

Research background

Robotic-assisted surgery has been gradually introduced and applied to treat children with Hirschsprung's disease (HSCR). However, few studies have been conducted to evaluate its safety and efficacy for HSCR treatment.

Research motivation

We aimed to investigate the medium-term outcomes of robotic-assisted surgery for treating HSCR.

Research objectives

We aimed to analyze the feasibility and efficacy of robotic-assisted proctosigmoidectomy (RAPS) with sphincter- and nerve-sparing surgery (SNS) in the treatment of HSCR.

Research methods

We conducted a multicenter prospective study of 156 infants with rectosigmoid HSCR who underwent SNS-RAPS and divided them by age into a younger group (aged ≤ 3 mo) and an older group (aged > 3 mo) for comparison. Intraoperative data, postoperative complications, and medium-term outcomes were recorded and analyzed. In patients aged ≥ 4 years, the bowel function score (BFS) was used to assess overall bowel function, and the postoperative fecal continence (POFC) score was used to evaluate SNS-related incontinence.

Research results

A total of 156 patients underwent successful SNS-RAPS, with 25 complications within 30 d and 48 post-30-d complications after surgery. For children aged ≥ 4 years, the overall BFS was 17.32 ± 2.63 and 90.91% of patients showed moderate-to-good bowel function, while the POFC score increased annually from 4 to 6 years old (4 years old: 10.95 ± 1.04, 5 years old: 11.48 ± 0.72, 6 years old: 11.94 ± 0.81). There were no significant differences between the younger and older groups in postoperative complications

and POFC score.

Research conclusions

SNS-RAPS is a safe and effective alternative treatment for children of all ages with HSCR. It provides the advantage of further minimizing damage to sphincters and perirectal nerves, thus providing better continence function.

Research perspectives

Robotic-assisted surgery is beneficial for treating HSCR in infants and young children.

ACKNOWLEDGEMENTS

We are grateful to Professor Ping Yin for the statistical evaluation.

FOOTNOTES

Author contributions: Zhang MX, Zhang X, Chang XP, and Tang ST contributed to conceptualization and design; Zhang MX, Zhang X, Chang XP, Cao GQ, Li S, Chi SQ, Wan L, Zeng JX, and Bian HQ contributed to material preparation, data acquisition, and analysis; Zhang MX, Zhang X, and Chang XP contributed equally to this study; All authors contributed to writing-draft manuscript and writing-revision and approved to submit the final version.

Supported by the National Health and Family Planning of China, No. 201402007; and the National Natural Science Foundation of China, No. 81873848 and No. 82170528.

Institutional review board statement: This study was approved by the Ethics Committee at three centers: Union Hospital, Tongji Medical College, Huazhong University of Science and Technology; Guangzhou Women and Children's Medical Center, Guangzhou Medical University; and Wuhan Children's Hospital, Tongji Medical College, Huazhong University of Science and Technology.

Clinical trial registration statement: The clinical trial is registered in the Chinese Clinical Trial Registry (Registration ID: ChiCTR2000035220). Details are available at https://www.chictr.org.cn/showproj.aspx?proj=41379.

Informed consent statement: All study participants, or their legal guardians, provided written consent prior to study enrollment.

Conflict-of-interest statement: All the authors report no relevant conflicts of interest for this article.

Data sharing statement: There is no additional data available.

CONSORT 2010 statement: The authors have read the CONSORT 2010 Statement, and the manuscript was prepared and revised according to the CONSORT 2010 Statement.

Country/Territory of origin: China

ORCID number: Meng-Xin Zhang 0000-0001-9622-4882; Xi Zhang 0000-0001-8159-0855; Xiao-Pan Chang 0000-0002-6901-5716; Ji-Xiao Zeng 0000-0003-4854-4966; Hong-Qiang Bian 0000-0003-2417-1560; Guo-Qing Cao 0000-0002-1267-9714; Shuai Li 0000 -0001-7585-018X; Shui-Qing Chi 0000-0002-7537-0255; Ying Zhou 0000-0002-9257-0523; Li-Ying Rong 0000-0001-6670-050X; Li Wan 0000-0003-2839-2475; Shao-Tao Tang 0000-0002-1851-0610.

S-Editor: Li L
L-Editor: A
P-Editor: Li Li

REFERENCES

1 **Ahmad H**, Shaul DB. Pediatric colorectal robotic surgery. Semin Pediatr Surg 2023; 32:151259 [PMID: 36739693 DOI:

10.1016/j.sempedsurg.2023.151259]
2 **Crippa J**, Grass F, Dozois EJ, Mathis KL, Merchea A, Colibaseanu DT, Kelley SR, Larson DW. Robotic Surgery for Rectal Cancer Provides Advantageous Outcomes Over Laparoscopic Approach: Results From a Large Retrospective Cohort. *Ann Surg* 2021; **274**: e1218-e1222 [PMID: 32068552 DOI: 10.1097/SLA.0000000000003805]
3 **Stolzenburg JU**, Holze S, Arthanareeswaran VK, Neuhaus P, Do HM, Haney CM, Dietel A, Truss MC, Stützel KD, Teber D, Hohenfellner M, Rabenalt R, Albers P, Mende M. Robotic-assisted Versus Laparoscopic Radical Prostatectomy: 12-month Outcomes of the Multicentre Randomised Controlled LAP-01 Trial. *Eur Urol Focus* 2022; **8**: 1583-1590 [PMID: 35216946 DOI: 10.1016/j.euf.2022.02.002]
4 **Langer JC**, Seifert M, Minkes RK. One-stage Soave pull-through for Hirschsprung's disease: a comparison of the transanal and open approaches. *J Pediatr Surg* 2000; **35**: 820-822 [PMID: 10873018 DOI: 10.1053/jpsu.2000.6849]
5 **Tian Y**, Shi T, Wang F, Wu Y. Difference of efficacy between Laparoscopic Modified Soave operation and Open Radical Resection in the treatment of Hirschsprung's disease. *Pak J Med Sci* 2017; **33**: 1385-1389 [PMID: 29492064 DOI: 10.12669/pjms.336.13220]
6 **Kubota A**, Kawahara H, Okuyama H, Oue T, Tazuke Y, Okada A. Clinical outcome of laparoscopically assisted endorectal pull-through in Hirschsprung's disease: comparison of abdominal and perineal approaches. *J Pediatr Surg* 2004; **39**: 1835-1837 [PMID: 15616944 DOI: 10.1016/j.jpedsurg.2004.08.015]
7 **Neuvonen MI**, Kyrklund K, Rintala RJ, Pakarinen MP. Bowel Function and Quality of Life After Transanal Endorectal Pull-through for Hirschsprung Disease: Controlled Outcomes up to Adulthood. *Ann Surg* 2017; **265**: 622-629 [PMID: 28169931 DOI: 10.1097/SLA.0000000000001695]
8 **Miyano G**, Koga H, Okawada M, Doi T, Sueyoshi R, Nakamura H, Seo S, Ochi T, Yamada S, Imaizumi T, Lane GJ, Okazaki T, Urao M, Yamataka A. Rectal mucosal dissection commencing directly on the anorectal line *vs* commencing above the dentate line in laparoscopy-assisted transanal pull-through for Hirschsprung's disease: Prospective medium-term follow-up. *J Pediatr Surg* 2015; **50**: 2041-2043 [PMID: 26386879 DOI: 10.1016/j.jpedsurg.2015.08.022]
9 **Jarvi K**, Laitakari EM, Koivusalo A, Rintala RJ, Pakarinen MP. Bowel function and gastrointestinal quality of life among adults operated for Hirschsprung disease during childhood: a population-based study. *Ann Surg* 2010; **252**: 977-981 [PMID: 21107107 DOI: 10.1097/SLA.0b013e3182018542]
10 **Teitelbaum DH**, Coran AG. Enterocolitis. *Semin Pediatr Surg* 1998; **7**: 162-169 [PMID: 9718654 DOI: 10.1016/S1055-8586(98)70012-5]
11 **Dindo D**, Demartines N, Clavien PA. Classification of surgical complications: a new proposal with evaluation in a cohort of 6336 patients and results of a survey. *Ann Surg* 2004; **240**: 205-213 [PMID: 15273542 DOI: 10.1097/01.sla.0000133083.54934.ae]
12 **Chi S**, Guo J, Zhang X, Li K, Xu P, Cao G, Li S, Tang ST. Resuturing Without Enterostomy for the Treatment of Early-Stage Anastomotic Leaks After Laparoscopic Soave Procedure in Hirschsprung's Disease. *J Laparoendosc Adv Surg Tech A* 2020; **30**: 1295-1300 [PMID: 33181061 DOI: 10.1089/lap.2020.0640]
13 **Markar SR**, Karthikesalingam AP, Hagen ME, Talamini M, Horgan S, Wagner OJ. Robotic vs. laparoscopic Nissen fundoplication for gastro-oesophageal reflux disease: systematic review and meta-analysis. *Int J Med Robot* 2010; **6**: 125-131 [PMID: 20506440 DOI: 10.1002/rcs.309]
14 **Quynh TA**, Hien PD, Du LQ, Long LH, Tran NTN, Hung T. The follow-up of the robotic-assisted Soave procedure for Hirschsprung's disease in children. *J Robot Surg* 2022; **16**: 301-305 [PMID: 33843006 DOI: 10.1007/s11701-021-01238-z]
15 **Pini Prato A**, Arnoldi R, Dusio MP, Cimorelli A, Barbetta V, Felici E, Barbieri P, Barbero S, Carlini C, Petralia P, Mattioli G, Roveta A, Maconi A. Totally robotic soave pull-through procedure for Hirschsprung's disease: lessons learned from 11 consecutive pediatric patients. *Pediatr Surg Int* 2020; **36**: 209-218 [PMID: 31659436 DOI: 10.1007/s00383-019-04593-z]
16 **Delgado-Miguel C**, Camps JI. Robotic Soave pull-through procedure for Hirschsprung's disease in children under 12-months: long-term outcomes. *Pediatr Surg Int* 2022; **38**: 51-57 [PMID: 34557957 DOI: 10.1007/s00383-021-05018-6]
17 **Li W**, Lin M, Hu H, Sun Q, Su C, Wang C, Li Y, Chen J, Luo Y. Surgical Management of Hirschsprung's Disease: A Comparative Study Between Conventional Laparoscopic Surgery, Transumbilical Single-Site Laparoscopic Surgery, and Robotic Surgery. *Front Surg* 2022; **9**: 924850 [PMID: 35860198 DOI: 10.3389/fsurg.2022.924850]
18 **Bjørnland K**, Pakarinen MP, Stenstrøm P, Stensrud KJ, Neuvonen M, Granström AL, Graneli C, Pripp AH, Arnbjörnsson E, Emblem R, Wester T, Rintala RJ; Nordic Pediatric Surgery Study Consortium. A Nordic multicenter survey of long-term bowel function after transanal endorectal pull-through in 200 patients with rectosigmoid Hirschsprung disease. *J Pediatr Surg* 2017; **52**: 1458-1464 [PMID: 28094015 DOI: 10.1016/j.jpedsurg.2017.01.001]
19 **Sakurai T**, Tanaka H, Endo N. Predictive factors for the development of postoperative Hirschsprung-associated enterocolitis in children operated during infancy. *Pediatr Surg Int* 2021; **37**: 275-280 [PMID: 33245447 DOI: 10.1007/s00383-020-04784-z]
20 **Morabito A**, Lall A, Gull S, Mohee A, Bianchi A. The impact of Down's syndrome on the immediate and long-term outcomes of children with Hirschsprung's disease. *Pediatr Surg Int* 2006; **22**: 179-181 [PMID: 16362310 DOI: 10.1007/s00383-005-1617-0]
21 **Georgeson KE**, Fuenfer MM, Hardin WD. Primary laparoscopic pull-through for Hirschsprung's disease in infants and children. *J Pediatr Surg* 1995; **30**: 1017-21; discussion 1021 [PMID: 7472924 DOI: 10.1016/0022-3468(95)90333-X]
22 **De la Torre-Mondragón L**, Ortega-Salgado JA. Transanal endorectal pull-through for Hirschsprung's disease. *J Pediatr Surg* 1998; **33**: 1283-1286 [PMID: 9722005 DOI: 10.1016/S0022-3468(98)90169-5]
23 **Chen Y**, Nah SA, Laksmi NK, Ong CC, Chua JH, Jacobsen A, Low Y. Transanal endorectal pull-through *vs* transabdominal approach for Hirschsprung's disease: a systematic review and meta-analysis. *J Pediatr Surg* 2013; **48**: 642-651 [PMID: 23480925 DOI: 10.1016/j.jpedsurg.2012.12.036]
24 **Zhang S**, Li J, Wu Y, Hu Y, Duan C, Wang M, Gai Z. Comparison of Laparoscopic-Assisted Operations and Laparotomy Operations for the Treatment of Hirschsprung Disease: Evidence From a Meta-Analysis. *Medicine (Baltimore)* 2015; **94**: e1632 [PMID: 26426651 DOI: 10.1097/MD.0000000000001632]

25 **El-Sawaf MI**, Drongowski RA, Chamberlain JN, Coran AG, Teitelbaum DH. Are the long-term results of the transanal pull-through equal to those of the transabdominal pull-through? A comparison of the 2 approaches for Hirschsprung disease. *J Pediatr Surg* 2007; **42**: 41-7; discussion 47 [PMID: 17208539 DOI: 10.1016/j.jpedsurg.2006.09.007]

26 **Stensrud KJ**, Emblem R, Bjørnland K. Anal endosonography and bowel function in patients undergoing different types of endorectal pull-through procedures for Hirschsprung disease. *J Pediatr Surg* 2015; **50**: 1341-1346 [PMID: 25783406 DOI: 10.1016/j.jpedsurg.2014.12.024]

27 **Stensrud KJ**, Emblem R, Bjørnland K. Functional outcome after operation for Hirschsprung disease--transanal *vs* transabdominal approach. *J Pediatr Surg* 2010; **45**: 1640-1644 [PMID: 20713213 DOI: 10.1016/j.jpedsurg.2010.02.065]

28 **Zhang C**, Ding ZH, Li GX, Yu J, Wang YN, Hu YF. Perirectal fascia and spaces: annular distribution pattern around the mesorectum. *Dis Colon Rectum* 2010; **53**: 1315-1322 [PMID: 20706076 DOI: 10.1007/DCR.0b013e3181e74525]

29 **He M**, Muro S, Akita K. Positional relationship between the lateral border of Denonvilliers' fascia and pelvic plexus. *Anat Sci Int* 2022; **97**: 101-109 [PMID: 34529236 DOI: 10.1007/s12565-021-00629-4]

30 **Pratap A**, Gupta DK, Shakya VC, Adhikary S, Tiwari A, Shrestha P, Pandey SR, Yadav RK. Analysis of problems, complications, avoidance and management with transanal pull-through for Hirschsprung disease. *J Pediatr Surg* 2007; **42**: 1869-1876 [PMID: 18022438 DOI: 10.1016/j.jpedsurg.2007.07.017]

31 **D'Annibale A**, Morpurgo E, Fiscon V, Trevisan P, Sovernigo G, Orsini C, Guidolin D. Robotic and laparoscopic surgery for treatment of colorectal diseases. *Dis Colon Rectum* 2004; **47**: 2162-2168 [PMID: 15657669 DOI: 10.1007/s10350-004-0711-z]

32 **Karlsen RA**, Hoel AT, Fosby MV, Ertresvåg K, Austrheim AI, Stensrud KJ, Bjørnland K. Comparison of clinical outcomes after total transanal and laparoscopic assisted endorectal pull-through in patients with rectosigmoid Hirschsprung disease. *J Pediatr Surg* 2022; **57**: 69-74 [PMID: 35123788 DOI: 10.1016/j.jpedsurg.2022.01.011]

33 **van de Ven TJ**, Sloots CE, Wijnen MH, Rassouli R, van Rooij I, Wijnen RM, de Blaauw I. Transanal endorectal pull-through for classic segment Hirschsprung's disease: with or without laparoscopic mobilization of the rectosigmoid? *J Pediatr Surg* 2013; **48**: 1914-1918 [PMID: 24074667 DOI: 10.1016/j.jpedsurg.2013.04.025]

34 **Aubdoollah TH**, Li K, Zhang X, Li S, Yang L, Lei HY, Dolo PR, Xiang XC, Cao GQ, Wang GB, Tang ST. Clinical outcomes and ergonomics analysis of three laparoscopic techniques for Hirschsprung's disease. *World J Gastroenterol* 2015; **21**: 8903-8911 [PMID: 26269680 DOI: 10.3748/wjg.v21.i29.8903]

35 **Tang ST**, Wang GB, Cao GQ, Wang Y, Mao YZ, Li SW, Li S, Yang Y, Yang J, Yang L. 10 years of experience with laparoscopic-assisted endorectal Soave pull-through procedure for Hirschsprung's disease in China. *J Laparoendosc Adv Surg Tech A* 2012; **22**: 280-284 [PMID: 22449115 DOI: 10.1089/lap.2011.0081]

36 **Wang YJ**, He YB, Chen L, Lin Y, Liu MK, Zhou CM. Laparoscopic-assisted Soave procedure for Hirschsprung disease: 10-year experience with 106 cases. *BMC Surg* 2022; **22**: 72 [PMID: 35219304 DOI: 10.1186/s12893-022-01528-9]

37 **Boemers TM**. Urinary incontinence and vesicourethral dysfunction in pediatric surgical conditions. *Semin Pediatr Surg* 2002; **11**: 91-99 [PMID: 11973761 DOI: 10.1053/spsu.2002.31807]

38 **Ieiri S**, Nakatsuji T, Akiyoshi J, Higashi M, Hashizume M, Suita S, Taguchi T. Long-term outcomes and the quality of life of Hirschsprung disease in adolescents who have reached 18 years or older--a 47-year single-institute experience. *J Pediatr Surg* 2010; **45**: 2398-2402 [PMID: 21129554 DOI: 10.1016/j.jpedsurg.2010.08.040]

39 **Granström AL**, Danielson J, Husberg B, Nordenskjöld A, Wester T. Adult outcomes after surgery for Hirschsprung's disease: Evaluation of bowel function and quality of life. *J Pediatr Surg* 2015; **50**: 1865-1869 [PMID: 26164226 DOI: 10.1016/j.jpedsurg.2015.06.014]

40 **Allin BSR**, Opondo C, Bradnock TJ, Kenny SE, Kurinczuk JJ, Walker GM, Knight M; NETS2HD collaboration. Outcomes at five to eight years of age for children with Hirschsprung's disease. *Arch Dis Child* 2020; **106**: 484-490 [PMID: 33139346 DOI: 10.1136/archdischild-2020-320310]

41 **Fuchs O**, Booss D. Rehbein's procedure for Hirschsprung's disease. An appraisal of 45 years. *Eur J Pediatr Surg* 1999; **9**: 389-391 [PMID: 10661849 DOI: 10.1055/s-2008-1072289]

42 **Wang G**, Sun XY, Wei MF, Weng YZ. Heart-shaped anastomosis for Hirschsprung's disease: Operative technique and long-term follow-up. *World J Gastroenterol* 2005; **11**: 296-298 [PMID: 15633236 DOI: 10.3748/wjg.v11.i2.296]

43 **Wang M**, Pang W, Zhou L, Ma J, Xie S. Effect of Transumbilical Single-Port Laparoscopic-Assisted Duhamel Operation on Serum CRP and IL-6 Levels in Children with Hirschsprung's Disease. *J Healthc Eng* 2022; **2022**: 8349851 [PMID: 35281524 DOI: 10.1155/2022/8349851]

44 **Ateş O**, Hakgüder G, Kart Y, Olguner M, Akgür FM. The effect of dilated ganglionic segment on anorectal and urinary functions during 1-stage transanal endorectal pull through for Hirschsprung's disease. *J Pediatr Surg* 2007; **42**: 1271-1275 [PMID: 17618894 DOI: 10.1016/j.jpedsurg.2007.02.020]

45 **Davidson JR**, Kyrklund K, Eaton S, Pakarinen MP, Thompson DS, Cross K, Blackburn SC, De Coppi P, Curry J. Long-term surgical and patient-reported outcomes of Hirschsprung Disease. *J Pediatr Surg* 2021; **56**: 1502-1511 [PMID: 33706942 DOI: 10.1016/j.jpedsurg.2021.01.043]

46 **Stenström P**, Brautigam M, Borg H, Graneli C, Lilja HE, Wester T. Patient-reported Swedish nationwide outcomes of children and adolescents with total colonic aganglionosis. *J Pediatr Surg* 2017; **52**: 1302-1307 [PMID: 27912975 DOI: 10.1016/j.jpedsurg.2016.11.033]

47 **Xiong X**, Chen X, Wang G, Feng J. Long term quality of life in patients with Hirschsprung's disease who underwent heart-shaped anastomosis during childhood: A twenty-year follow-up in China. *J Pediatr Surg* 2015; **50**: 2044-2047 [PMID: 26423683 DOI: 10.1016/j.jpedsurg.2015.08.027]

48 **Zhang Y**, Liu Z, Li S, Yang S, Zhao J, Yang T, Chen Y, Guo W, Hou D, Li Y, Huang J. One-stage transanal endorectal pull-through for Hirschsprung disease: experience with 229 neonates. *Pediatr Surg Int* 2022; **38**: 1533-1540 [PMID: 36030350 DOI: 10.1007/s00383-022-05198-9]

49 **Yamataka A**, Kaneyama K, Fujiwara N, Hayashi Y, Lane GJ, Kawashima K, Okazaki T. Rectal mucosal dissection during transanal pull-through for Hirschsprung disease: the anorectal or the dentate line? *J Pediatr Surg* 2009; **44**: 266-9; discussion 270 [PMID: 19159754 DOI: 10.1016/j.jpedsurg.2008.10.054]

50 **Lu C**, Hou G, Liu C, Geng Q, Xu X, Zhang J, Chen H, Tang W. Single-stage transanal endorectal pull-through procedure

for correction of Hirschsprung disease in neonates and nonneonates: A multicenter study. *J Pediatr Surg* 2017; **52**: 1102-1107 [PMID: 28185631 DOI: 10.1016/j.jpedsurg.2017.01.061]

51 **Meehan JJ**, Sandler A. Robotic repair of a Bochdalek congenital diaphragmatic hernia in a small neonate: robotic advantages and limitations. *J Pediatr Surg* 2007; **42**: 1757-1760 [PMID: 17923210 DOI: 10.1016/j.jpedsurg.2007.06.013]

52 **Onishi S**, Kaji T, Nakame K, Yamada K, Murakami M, Sugita K, Yano K, Matsui M, Nagano A, Harumatsu T, Yamada W, Matsukubo M, Muto M, Ieiri S. Optimal timing of definitive surgery for Hirschsprung's disease to achieve better long-term bowel function. *Surg Today* 2022; **52**: 92-97 [PMID: 34383138 DOI: 10.1007/s00595-021-02356-9]

World Journal of Gastroenterology

Submit a Manuscript: https://www.f6publishing.com

World J Gastroenterol 2023 June 21; 29(23): 3733-3747

DOI: 10.3748/wjg.v29.i23.3733

ISSN 1007-9327 (print) ISSN 2219-2840 (online)

SYSTEMATIC REVIEWS

Paradoxical association between dyspepsia and autoimmune chronic atrophic gastritis: Insights into mechanisms, pathophysiology, and treatment options

Roberta Elisa Rossi, Alessandra Elvevi, Valentina Sciola, Francesco Vito Mandarino, Silvio Danese, Pietro Invernizzi, Sara Massironi

Specialty type: Gastroenterology and hepatology

Provenance and peer review: Invited article; Externally peer reviewed.

Peer-review model: Single blind

Peer-review report's scientific quality classification

Grade A (Excellent): 0
Grade B (Very good): B, B
Grade C (Good): C, C
Grade D (Fair): 0
Grade E (Poor): 0

P-Reviewer: Baryshnikova NV, Russia; Cheng H, China; Huang YQ, China; Jia J, China

Received: March 21, 2023
Peer-review started: March 21, 2023
First decision: April 12, 2023
Revised: April 23, 2023
Accepted: May 6, 2023
Article in press: May 6, 2023
Published online: June 21, 2023

Roberta Elisa Rossi, Gastroenterology and Endoscopy Unit, IRCCS Humanitas Research Hospital, Rozzano 20089, Milan, Italy

Alessandra Elvevi, Pietro Invernizzi, Sara Massironi, Gastroenterology Unit, Fondazione IRCCS San Gerardo dei Tintori, Monza 20900, Italy and Department of Medicine and Surgery, University of Milano-Bicocca, Monza 20900, Italy

Valentina Sciola, Gastroenterology and Endoscopy Unit, Fondazione IRCCS Ca' Granda Ospedale Maggiore Policlinico, Milano 20100, Italy

Francesco Vito Mandarino, Silvio Danese, Department of Gastroenterology and Endoscopy, IRCCS Ospedale San Raffaele, Milan 20132, Italy

Silvio Danese, School of Medicine, Vita-Salute San Raffaele University, Milan 20132, Italy

Corresponding author: Sara Massironi, MD, PhD, Chief Physician, Doctor, Medical Assistant, Research Scientist, Division of Gastroenterology, Fondazione IRCCS San Gerardo dei Tintori, Via Pergolesi, 33, Monza 20900, Italy. sara.massironi@libero.it

Abstract

BACKGROUND

Autoimmune gastritis (AIG) is a progressive, chronic, immune-mediated inflammatory disease characterized by the destruction of gastric parietal cells leading to hypo/anacidity and loss of intrinsic factor. Gastrointestinal symptoms such as dyspepsia and early satiety are very common, being second in terms of frequency only to anemia, which is the most typical feature of AIG.

AIM

To address both well-established and more innovative information and knowledge about this challenging disorder.

METHODS

An extensive bibliographical search was performed in PubMed to identify guidelines and primary literature (retrospective and prospective studies, systematic reviews, case series) published in the last 10 years.

RESULTS
A total of 125 records were reviewed and 80 were defined as fulfilling the criteria.

CONCLUSION
AIG can cause a range of clinical manifestations, including dyspepsia. The pathophysiology of dyspepsia in AIG is complex and involves changes in acid secretion, gastric motility, hormone signaling, and gut microbiota, among other factors. Managing dyspeptic symptoms of AIG is challenging and there are no specific therapies targeting dyspepsia in AIG. While proton pump inhibitors are commonly used to treat dyspepsia and gastroesophageal reflux disease, they may not be appropriate for AIG. Prokinetic agents, antidepressant drugs, and non-pharmacological treatments may be of help, even if not adequately evidence-based supported. A multidisciplinary approach for the management of dyspepsia in AIG is recommended, and further research is needed to develop and validate more effective therapies for dyspepsia.

Key Words: Dyspepsia; Dyspeptic symptoms; Gastro-intestinal symptoms; Autoimmune gastritis; Chronic autoimmune atrophic gastritis; Treatment

Core Tip: The management of dyspepsia in patients with autoimmune gastritis (AIG), a chronic, immune-mediated disease, remains a challenge, as it can overlap with functional dyspepsia and gastroesophageal reflux disease. Currently, there are no specific therapies. A tailored treatment approach based on a better understanding of putative pathogenic mechanisms underlying symptoms is needed. Prokinetic agents, antidepressant drugs, and non-pharmacological treatments may be helpful, although not adequately evidence-based supported. As a future perspective, targeting dyspepsia in AIG based on changes in the microbiota and advanced endoscopic techniques to treat severe dyspeptic symptoms might be an area of ongoing research.

Citation: Rossi RE, Elvevi A, Sciola V, Mandarino FV, Danese S, Invernizzi P, Massironi S. Paradoxical association between dyspepsia and autoimmune chronic atrophic gastritis: Insights into mechanisms, pathophysiology, and treatment options. *World J Gastroenterol* 2023; 29(23): 3733-3747
URL: https://www.wjgnet.com/1007-9327/full/v29/i23/3733.htm
DOI: https://dx.doi.org/10.3748/wjg.v29.i23.3733

INTRODUCTION

Autoimmune gastritis (AIG) is an immune-mediated disease targeting the H+/K+ ATPase proton pump in the parietal cells, which are responsible for the secretion of gastric acid and intrinsic factor[1]. The pathogenesis of AIG involves the activation of both T and B lymphocytes, which infiltrate the gastric mucosa and destroy the parietal cells[1-5], leading to hypochloridria and vitamin B12 deficiency.

Symptoms of AIG can be nonspecific, with patients presenting with no or vague symptoms, including postprandial fullness, early satiation, abdominal pain, bloating[6], as well as epigastric pain. Therefore, the diagnosis of AIG can be challenging, as many of these symptoms overlap with other digestive disorders, mainly functional dyspepsia (FD) and gastroesophageal reflux disease (GERD). This overlap in clinical symptoms and characteristics can pose diagnostic challenges between AIG and FD, which share some common characteristics, including clinical symptoms, as well as a higher prevalence among women. Moreover, some patients may present with atypical symptoms, such as fatigue, joint pain, or skin rashes, which can further overlap with functional symptoms. Distinguishing between AIG and GERD can be even more challenging. While the pathophysiological mechanisms underlying GERD and AIG are different, they can present with similar abdominal symptoms, such as epigastric pain, heartburn, and nausea, which may pose diagnostic challenges, particularly in patients with atypical symptoms.

The pathophysiological mechanisms underlying clinical symptoms in AIG are poorly understood.

Appropriate evaluation, including endoscopy, is therefore required to differentiate these entities; indeed, based on the Rome Global Epidemiology Study, the diagnosis of FD requires the absence of organic, systemic, or metabolic disease upon routine investigation, including endoscopy[7,8].

It is therefore important to understand the different pathogenesis of symptoms in AIG, GERD, and FD, as the management of these conditions can be very different. This is particularly important when prescribing empirically proton pump inhibitors (PPIs) based therapies, which are often considered to be

the first-line therapy for GERD and are often used to manage symptoms of FD. Conversely, in AIG, a condition of hypochlorhydria, PPI therapy could further reduce acid secretion, stimulate gastrin hypersecretion, and further induce enterochromaffin-like (ECL) cell hyperplasia. As a result, the use of PPIs in patients with AIG is generally not indicated.

Therefore, accurate diagnosis and differentiation between these conditions are crucial to avoid inappropriate or potentially harmful management strategies. Understanding the pathophysiology of each condition can also guide the choice of appropriate treatments, including lifestyle modifications, dietary changes, and medication management.

In this review, we will discuss the putative pathogenic mechanisms underlying symptom generation in AIG, their clinical implications, and the current management strategies for this complex and multifaceted disease.

MATERIALS AND METHODS

An extensive bibliographical search was performed in PubMed to identify guidelines and primary literature (retrospective and prospective studies, systematic reviews, case series) published in the last 10 years, using both medical subject heading terms and free-language keywords: Dyspepsia; dyspeptic symptoms; gastro-intestinal symptoms; chronic autoimmune atrophic gastritis; diagnosis; treatment. The reference lists from the studies returned by the electronic search were manually searched to identify further relevant reports. The reference lists from all available review articles, primary studies, and proceedings of major meetings were also considered. Articles published as abstracts were included, whereas non-English language papers were excluded.

RESULTS

A total of 125 records were reviewed and 80 were defined as fulfilling the criteria for final consideration. Figure 1 presents the flow chart showing the process of study selection.

DISCUSSION

Dyspepsia in autoimmune gastritis: clinical manifestations and pathophysiological mechanisms

The spectrum of clinical manifestations in AIG is wide but often nonspecific[9,10]. Classical manifestations of AIG include pernicious anemia due to vitamin B12 deficiency, which can cause fatigue, weakness, and shortness of breath. Other hematological anomalies comprise micro/normocytic anemia due to the coexistence of iron deficiency anemia[9,11]. Neurological symptoms such as tingling, numbness, or weakness in the limbs, are due to vitamin B12 deficiency and are characterized by neuronal damage with peripheral neuropathy, myelopathy, and autonomic dysfunction[12,13]. Furthermore, psychiatric alterations have been reported such as depression, cognitive impairment, and psychosis[14,15]. As AIG is often associated with other autoimmune conditions, patients may also present with symptoms related to those conditions, such as joint pain, skin rashes, or thyroid dysfunction[16]. Also, the impaired absorption of other vitamins, such as 25-OH-vitamin D, or micronutrients, such as calcium, due to gastric hypo- or achlorhydria, has been hypothesized to be a predisposing factor also for the development of osteoporosis which can be a possible further extra gastrointestinal (GI) manifestation in AIG patients[17-19].

However, these manifestations usually characterize severe or long-standing disease.

In the early stages of AIG, patients may not present with these specific symptoms, and the patients may begin to experience non-specific GI symptoms such as upper abdominal discomfort, bloating, and nausea[11]. Focusing on GI symptoms, even if AIG is generally regarded as a silent disease, some recent studies highlight a not negligible percentage of patients who report upper GI discomfort mainly characterized by dyspeptic and/or GERD symptoms[20] and as in FD, dyspeptic symptoms may manifest as postprandial distress syndrome (PDS) with early satiation and/or postprandial fullness or as epigastric pain syndrome (EPS).

Indeed, according to both data from literature and real-life clinical practice, dyspepsia is frequently reported by AIG patients, which represents a challenge for their proper management.

In the cross-sectional study by Carabotti *et al*[21], more than half of the patients affected by AIG (56.7%, 215 out of 397) reported GI symptoms with a prevalence of upper GI symptoms (69.8%) including dyspepsia (71.2%), described as postprandial fullness, early satiety and/or epigastric pain, GERD related symptoms (7.2%) such as heartburn and/or regurgitation, overlap dyspepsia-GERD symptoms (17.2%) and nausea and vomiting (3.8%). Moreover, 15.8% of the patients enrolled in this study also reported lower irritable bowel syndrome (IBS) -like GI symptoms with overlapping of upper and lower GI symptoms in 14.4% of the patients (Figure 2).

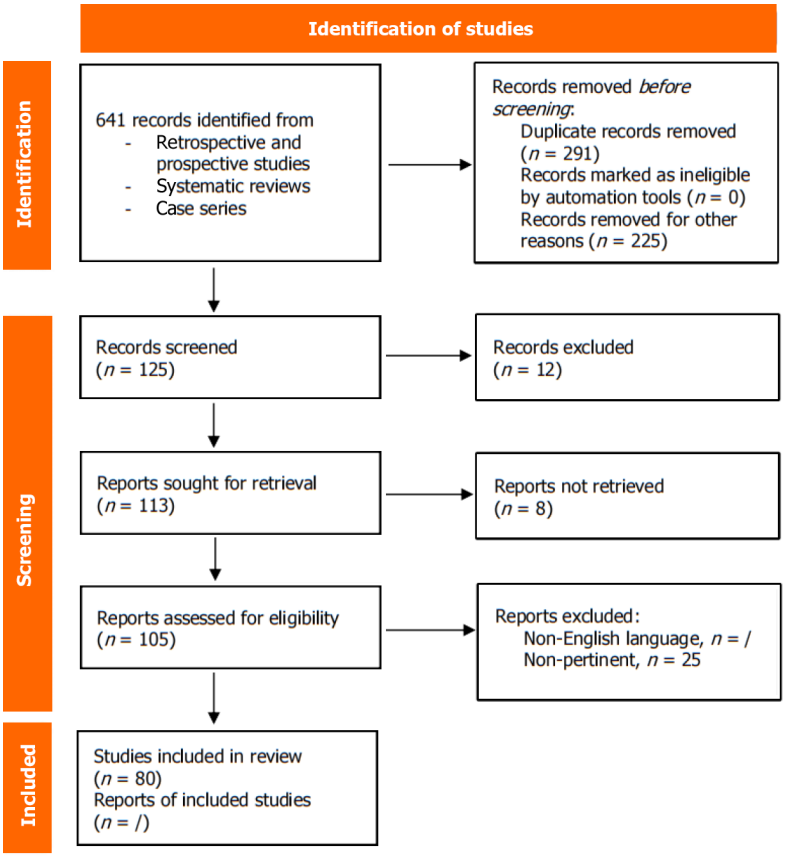

Figure 1 Flow chart showing the process of study selection.

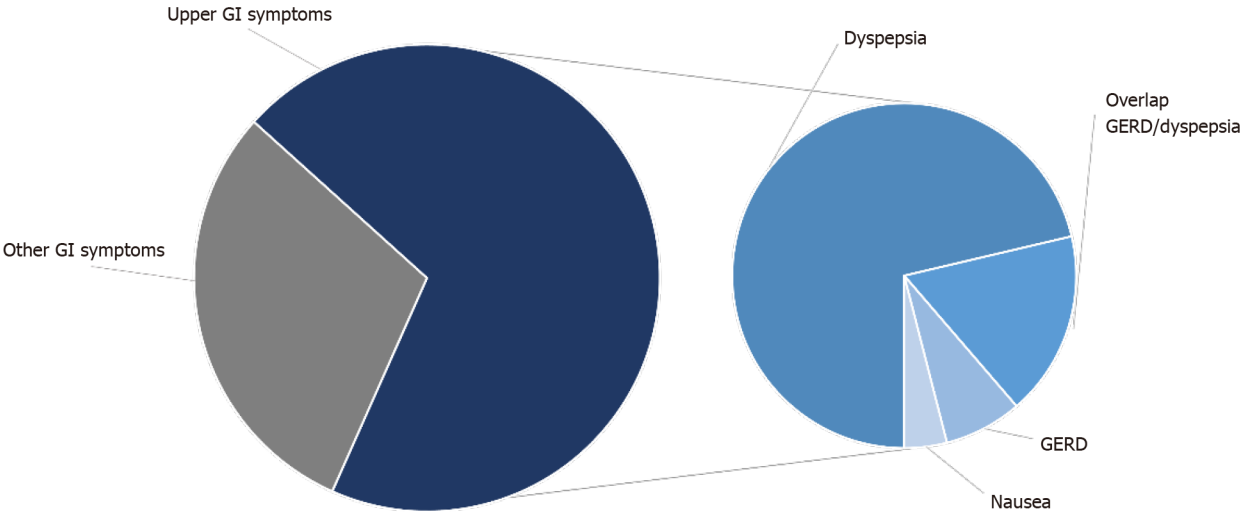

Figure 2 More common gastrointestinal symptoms seen in patients with autoimmune gastritis. GERD: Gastroesophageal reflux disease; GI: Gastrointestinal.

Dyspepsia, meant either as EPS or PDS, together with GERD symptoms such as acid regurgitation and heartburn, are reported as the most frequent symptoms also in the paper by Miceli *et al*[22] with a prevalence of 52.4% and 36.3%, respectively in the study population of 99 AIG patients. Contextually, weight loss and nausea are referred to approximately a quarter of patients (28.3% and 22.2%, respectively), while vomiting and dysphagia are in a lower percentage (9.1% and 3%, respectively).

According to another study[23], including a cohort of 54 patients with AIG, 70% were symptomatic for one or more upper GI symptoms, particularly a quarter of patients referred at least one typical GERD symptom such as regurgitation (18.5%) or heartburn (9%), while a major percentage complained

of atypical GERD symptoms including cough (29.6%), non-cardiac chest pain (22.2%) and dysphagia (14.8%).

As far as GERD symptom is concerned, in the prospective observational study published by Tenca *et al*[24], the prevalence of GERD has been investigated in a cohort of 41 AIG patients, 28 of whom with upper GI symptoms (53% GERD-related, 47% dyspepsia-like). The authors found that 24% of patients had GERD at multichannel intraluminal impedance-pH (MII-pH) monitoring mostly defined as non-acidic reflux, hypothesizing that non-acidic reflux could play a key role in the pathogenesis of the upper GI clinical manifestations. Consistent with the data above, those from the observational prospective study by Pilotto *et al*[25] confirm that among the group of AIG patients complaining of reflux symptoms (38/172, 22%) only 2 patients had documented GERD while 9 patients (24.7%) had reflux hypersensitivity predominantly related to non-acid-reflux (6/9 patients). The remaining 27 patients didn't have alterations at MII-pH but six of them had a major motility disorder. Therefore, the presence of upper GI symptoms appears to be paradoxical as AIG is typically characterized by gastric mucosal atrophy with resulting hypochlorhydria and alkaline gastric pH.

The pathophysiological mechanisms underlying GI symptoms in AIG are poorly understood. Several mechanisms have been hypothesized. The hypochlorhydria resulting from gastric oxyntic atrophy may contribute to dyspeptic symptoms[5], even if other mechanisms may be responsible, such as delayed gastric emptying[26,27], visceral hypersensitivity, and hormonal effects. Delayed gastric emptying may occur due to reduced acid secretion, which can lead to incomplete homogenization of gastric contents with macroscopic residues of undigested food and altered peristalsis, giving feelings of fullness, bloating, and discomfort after eating.

However, in patients with AIG, delayed gastric emptying has been described with elevated circulating gastrin levels and increase in parallel with the degree of the atrophy of the gastric mucosa, affecting gastric emptying T ½ time[27]. Visceral hypersensitivity is an important candidate pathogenic mechanism for several disorders characterized by dyspepsia, even if only a few studies are available for AIG patients[26]. Moreover, some gut hormones such as motilin and ghrelin levels were significantly decreased in AIG subjects with delayed gastric emptying and deranged autonomic function[26], suggesting their potential role in the delayed gastric emptying observed in these subjects. Additionally, the loss of intrinsic factor may result in impaired absorption of nutrients such as iron and vitamin B12, which can contribute to fatigue and other symptoms. Also, low-grade chronic inflammation associated with AIG could contribute to the development of dyspepsia, in parallel to what is described for low-grade bowel inflammation with increased numbers of submucosal mast cells and lymphocytes reported in IBS[28]. Finally, chronic inflammation associated with AIG together with impaired gastric acid secretion may cause changes in the gut microbiota, and this may contribute to the development of dyspeptic symptoms; however, further research is needed to better understand the pathophysiological mechanisms underlying dyspeptic symptoms in AIG and to develop more effective treatments for this condition. It is also important to remember that abnormal thyroid function, which is quite commonly associated with AIG, has been blamed for gastric dysmotility and dyspeptic symptoms[29], which is another possible cause of dyspepsia in AIG patients. However, it is difficult to understand whether the dyspepsia observed in AIG patients is the direct result of abnormal thyroid function or is caused by AIG itself or by a combination of these two autoimmune diseases. Table 1 summarizes the most frequent upper GI symptoms reported by AIG patients together with the underlying pathophysiological mechanisms.

Diagnostic work-up of dyspepsia in AIG

According to recent guidelines on the management of dyspepsia[30-32], upper GI endoscopy [esophagogastroduodenoscopy (EGDs)] is a key test to identify any organic disease of the upper digestive tract (*i.e.*, peptic ulcer, neoplasm), which may explain dyspeptic symptoms. Since EGDs is an invasive and expensive test and most patients with dyspepsia have FD[32], the American and British guidelines suggest limiting the use of EGDs to patients with suspected organic disease. Both the American and the British guidelines[30,32] as well as a recent evidence-based revision of the existing guidelines[31] suggest screening patients for past medical history and family history, medications, previous examinations, presence of *Helicobacter pylori* (*H. pylori*) infection, age, alarm symptoms and signs (*i.e.* anemia or bleeding, weight loss, age > 55 years, recurrent vomiting, dysphagia or odynophagia, fever). When one of the aforementioned alarm symptoms or signs is present, EGDs is mandatory to exclude or confirm an organic disease. If EGDs is negative for esophago-gastric diseases, an abdominal computed tomography -scan is suggested in order to exclude pancreatic, liver, or biliary tract cancers[32]. Distinguishing between AIG and FD in patients with dyspeptic symptoms may result difficult, as the two conditions can produce similar symptoms[20,21]. However, certain factors such as a medical history of autoimmune disease, anemia (including microcytic and macrocytic), vitamin B12 deficiency, and positivity for anti-parietal cells antibodies should raise clinical suspicion of AIG. In such cases, it is important to perform an EGDs to confirm the diagnosis, stage the disease, and evaluate for possible pre-cancerous lesions[33]. According to international guidelines[33], gastric biopsies should be picked up according to Sidney protocol. The protocol requires 5 gastric biopsies, which should be placed in separately labeled jars: 2 from the antrum along the lesser and greater curvature, within 2-3 cm of the pylorus; 2 from the gastric corpus (including 1 from the lesser curvature at 4 cm proximal to the incisura angularis and the

Table 1 Reported upper gastrointestinal symptoms and the underlying pathophysiological mechanisms in patients with autoimmune atrophic gastritis

Clinical manifestation	Pathophysiological mechanisms
Dyspeptic symptoms	
Postprandial fullness; Early satiety; Epigastric pain	Hypochlorhydria. Delayed gastric emptying due to: Hormonal effects (ghrelin, motilin); Reduced acid secretion. Visceral hypersensitivity. Low-grade chronic inflammation. Changes in the gut microbiota
Typical GER like symptoms	
Heartburn; Regurgitation	Non-acid reflux; Delayed gastric emptying; Visceral hypersensitivity; Changes in the gut microbiota
Atypical GERD-like symptoms	
Cough; Non-cardiac chest pain; Dysphagia	Delayed gastric emptying; Visceral hypersensitivity
Overlap dyspepsia-GER like symptoms	As above
Vomiting	Delayed gastric emptying; Visceral hypersensitivity
Nausea	Delayed gastric emptying
Fatigue	Impaired absorption of iron and vitamin B12

GER: Gastro-esophageal reflux; GERD: Gastroesophageal reflux disease.

other from the middle portion of the greater curvature of the gastric body at 8 cm from the cardia), and 1 from the incisura angularis[34]. Severity and topographic distribution of atrophic lesions should be reported according to Operative Link for Gastritis Assessment (OLGA)[35] and Operative Link for Gastric Intestinal Metaplasia Assessment (OLGIM)[36]. By following this protocol, it is less likely to miss the diagnosis of AIG. Moreover, OLGA e OLGIM scores are then used to determine whether endoscopic surveillance is needed and its frequency. Conversely, if there is no suspicion of organic disease, FD could be diagnosed. However, even in these cases, both the American and British guidelines[30,32] suggest testing dyspeptic patients for *H. pylori* with non-invasive tests (*i.e.* fecal antigen or carbon-urea breath testing) and treating the infected ones accordingly, as *H. pylori* infection is considered to be an etiologic factor of dyspepsia in 5% of dyspeptic patients[37].

In case of PDS, with dyspeptic symptoms that recall altered gastric emptying, gastric emptying scintigraphy (GES) is a useful tool to explore impaired (rapid or delayed) gastric dysmotility. Briefly, the test consists of a standard meal, which is marked with Technetium (Tc)-99m; after food ingestion, imaging is performed in the anterior and posterior projections at only four-time points (0, 1, 2, and 4 h). Delayed gastric emptying is determined to be > 90% at 1 h, > 60% at 2 h, and > 10% gastric retention at 4 h. Conversely, rapid gastric emptying is determined to be < 30% at 1 h[38]. While GES performs well in diagnosing gastroparesis[39], it is not reliable for the diagnosis of FD, which is supposed to be a lighter spectrum of the same gastric disorders[40], and no specific studies exist for AIG, therefore further studies are needed to clarify this item[39]. However, this technique can be time-consuming, as the test requires imaging at set intervals over several hours, it involves radiation exposure from the radioactive material in the meal and, as for FD, also in the case of AIG, it may not be reliable, as there is only a milder form of a gastric motility disorder. Moreover, it appears to have limited therapeutic implications, as it may suggest treating the patient with prokinetic drugs at most, which can also be done ex adjuvantibus**.** Recently, the wireless motility capsule (WMC) has been introduced, in order to simultaneously assess both regional and whole gut transit[41,42]. Ingestion of this non-digestible capsule that simultaneously measures luminal temperature, pH, and pressure facilitates the measurement of the gastric, small bowel, and colonic transit times. Approved by the United States Food and Drug Administration for the evaluation of gastroparesis and slow colonic transit, WMC should be considered in suspected GI motility disorders as it provides a single study capable of simultaneously assessing for regional, multi-regional, or generalized motility disorders[43]. Triadafilopoulos *et al*[43] suggested a potential WMC role in AIG diagnosis since it is able to register intragastric pH (usually > 6) and eventually associated dysmotility[43]. However, as for GES, even for WMC at present, considering the limited availability of prokinetic drugs, therapeutic implications are limited. Finally, a recent physiologic tool has been proposed to assess the functionality of the pyloric sphincter. The functional luminal imaging probe known as EndoFlip® is a 240-cm catheter with impedance electrodes at its distal end[44,45], that is used to assess the functionality of the pyloric sphincter. The device is placed in the pylorus either through the endoscope, under endoscopic visualization[45], or either by fluoroscopy guidance[46]. After positioning the device, the balloon is filled to set volumes of 10, 20, 30, 40, and 50 mL using a stepwise protocol, and the cross-sectional area (CSA), bag pressure, and distensibility index are recorded. The pyloric distensibility index (P-DI) is calculated in the zone with the narrowest CSA

with the corresponding intra-bag pressure[46]. A decreased P-DI has been observed in patients with gastroparesis[47], and also in patients with chronic nausea and vomiting without delayed gastric emptying, suggesting that pyloric dysfunction could explain "gastroparesis-like" symptoms in this group of patients[48]. However, normal and pathological values still need to be confirmed.

As mentioned above, GERD symptoms are frequently reported by AIG patients[24,25]. According to recent guidelines[49] and Lyon consensus[50], GERD is usually a clinical diagnosis, based on patients' symptoms (typical GERD symptoms, pyrosis, and acidic regurgitation) and empiric proton pump inhibitors (PPIs) treatment response (*i.e.* single dose for 4-8 wk).

Since AIG patients are supposed to have a higher intragastric pH (registered in one study, being median intragastric pH of 6.2 (4.6-7.0)[24], due to parietal cells atrophy, it may be surprising that AIG patients complain of GERD symptoms. A previous paper by Tenca *et al*[24] registered that 15 out of 41 AIG patients had GERD symptoms. Among them, acidic reflux, recorded by MII-pH monitoring, had a minor role, being present in one patient only. This could be explained by the residual production of acid from partially atrophic mucosa. Non-acidic reflux was instead more frequent, being present in 22% of the AIG population studied. It is common knowledge that non-acidic reflux can give rise to typical or atypical GERD symptoms[51-53].

Moreover, it could be useful to study these patients with MII-pH-monitoring, which is able to identify acidic, weakly acidic, and non-acidic reflux events. The observation of a role of GERD in these patients' symptoms independently of acid is clinically relevant because it can guide their management. These patients may benefit from drugs that lower their visceral sensitivity (*i.e.*, tricyclic antidepressants and selective serotonin reuptake inhibitors)[7,54]. Furthermore, for those with severe drug-unresponsive symptoms anti-reflux surgery is an option[55,56]. Another study by Pilotto *et al*[25] characterizes AIG patients according to their GERD symptoms and MII-pH-monitoring results. Similarly, Tenca *et al*[24] found pathologic esophageal acid exposure in two out of 38 patients reporting GERD symptoms. On the contrary, a great part of them (30 out of 38 patients) had an increased number of non-acidic reflux episodes. Combining symptoms and MII-pH-monitoring results, the Authors classified AIG patients as having GERD (5%), functional heartburn (50%), and reflux hypersensitivity (24%). Interestingly, the Authors studied AIG patients with high-resolution esophageal manometry (HRM) and found that 37% of AIG patients had various motility disorders, including 8 minor disorders (n = 7 weak peristalsis and n = 1 hypertensive peristalsis), and 6 major disorders (n = 6 EGJ outflow obstruction) according to Chicago classification v 3.0[57]. Whether these manometric findings correlate with AIG is still debated. Similarly, the role of HRM in the diagnostic work-up of these patients remains unclear. MII-pH-monitoring could also have a role in the diagnosis of dyspepsia. It is known from the literature that epigastric pain is often more frequent in patients with pathologic MII-pH-monitoring[58]. In the population studied by Tenca *et al*[24], two dyspeptic patients showed a positive correlation between epigastric pain and non-acidic reflux. A possible diagnostic algorithm is represented in Figure 3.

In summary, dyspeptic symptoms and GERD are common in AIG patients; the diagnostic algorithm provides an EGDs study as the first diagnostic test to exclude organic disease and to confirm AIG diagnosis. If GERD symptoms are present, MII-pH-monitoring is useful to measure the entity of reflux and to classify patients (GERD, functional heartburn, hypersensitive esophagus) and treat them accordingly. Moreover, it could be useful in dyspepsia diagnosis. Esophageal motility tests, as well as gastric emptying tests, could have a role in AIG patients but further studies are needed to clarify these items.

Treatment

Dyspepsia is a common symptom in AIG and its management can be challenging, as the pathophysiology underlying dyspeptic symptoms in AIG is multifactorial. However, this issue is still understudied, and more research is needed to better understand the mechanisms of dyspepsia in AIG and to develop effective treatments tailored to the individual patient's symptoms and underlying pathophysiology. Indeed, although the primary goal of AIG treatment is to address vitamin deficiencies and prevent and monitor for gastric neoplasms, effectively managing common and difficult-to-treat symptoms like dyspepsia is crucial for improving patients' quality of life.

As a matter of fact, according to available guidelines[10], there is poor evidence regarding the best treatment options for dyspeptic symptoms in patients with AIG, also considering that PPIs are not indicated in this subset of patients who are typically hypochlorhydric. Despite this, several AIG patients referring dyspeptic symptoms are often prescribed PPIs by General Practitioners or gastroenterologists with no or low knowledge of this disease. The use of PPIs in this subgroup of patients should be discouraged for two main reasons. Firstly, AIG is characterized by a suppressed gastric acid secretion and consequent hypochlorhydria, thus treatment with antisecretory drugs is generally ineffective as already reported[24,59] taking into account that these patients refer reflux-like symptoms whose nature is non-acid. Secondly, and far more important, the long-term use of PPIs has been reported to be associated with the development or progression of gastric pre-malignant lesions. Of note, as already reported[60], the long-term treatment with PPIs which is responsible for increased levels of serum gastrin seems to be linked to a higher risk of progression of ECL-cell hyperplasia which precedes the development of gastric type 1 neuroendocrine neoplasm[61]; however, no clear-cut evidence was found between PPI therapy and increased progression of AIG or intestinal metaplasia[60].

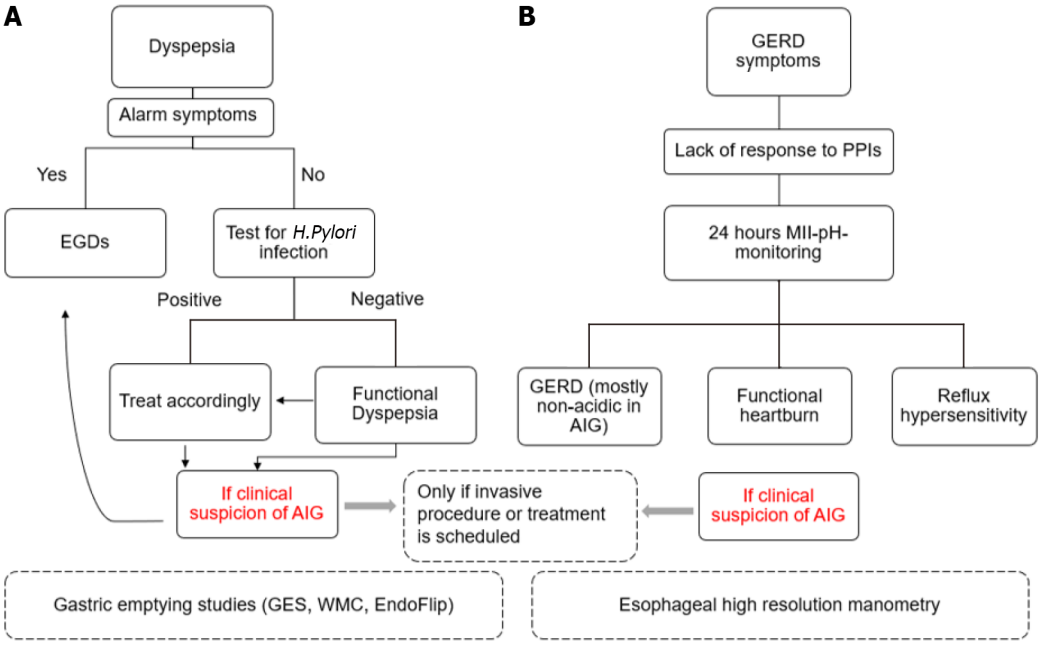

DOI: 10.3748/wjg.v29.i23.3733 **Copyright** ©The Author(s) 2023.

Figure 3 Possible diagnostic algorithm for dyspepsia or gastroesophageal reflux disease -like symptoms in autoimmune atrophic gastritis. A: Dyspeptic symptoms; B: Gastroesophageal reflux disease symptoms. AIG: Autoimmune gastritis; EGDs: Esophagogastroduodenoscopy; GERD: Gastroesophageal reflux disease; GI: Gastrointestinal; *H. pylori*: *Helicobacter pylori*; PPIs: Proton pump inhibitors.

Initial management of dyspepsia in AIG may involve dietary modifications, such as avoiding trigger foods or eating smaller, more frequent meals. Patients may also benefit from lifestyle modifications, such as weight loss or stress reduction techniques, even if these procedures are not evidence-supported.

It is important to highlight that patients with AIG often have evidence of current or prior *H. pylori* infection[62]. Therefore, it is important to test these patients for *H. pylori* and, if positive, to eradicate it according to guidelines that suggested the "Test and treat" strategy[63]. Of note, *H. pylori* eradication appears to reduce the risk of gastric cancer[64]. In the specific setting of AIG, according to a randomized double-blinded placebo-controlled trial[65], that compared triple eradication therapy for *H. pylori* with placebo in histologically diagnosed AIG patients, at 3-years follow-up dyspeptic symptoms scores improved significantly in the patients in whom *H. pylori* had been eradicated. Similar findings were reported by another recent study[66], which showed that the beneficial effect of *H. pylori* eradication treatment on dyspeptic symptoms lasted until one year after treatment, being associated with a higher pretreatment symptom score and age inferior to 70 years old. Obviously, the benefit of *H. pylori* eradication in AIG patients is further increased by the fact that *H. pylori* more that autoimmunity per se, is linked to the risk of evolution towards dysplasia and gastric cancer in AIG, as recently described[1].

In addition to *H. pylori* eradication, several treatment options[67] have been investigated for their efficacy in managing dyspeptic symptoms in AIG. These treatments include prokinetic agents, neuromodulators, and herbal agents, as well as non-pharmacological treatments such as acupuncture, cognitive-behavioral therapy, and hypnotherapy. However, the evidence regarding their effectiveness is conflicting also taken into account the lack of dedicated prospective studies exploring the efficacy of prokinetics and neuromodulators in this specific setting of patients, making the management of AIG patients experiencing dyspeptic symptoms very challenging. Medications such as prokinetic agents including metoclopramide or domperidone may be used to improve gastric motility and reduce symptoms of bloating and nausea in patients with predominantly PDS symptoms. For patients presenting with EPS symptoms, a rational approach could therefore be to guide therapy based on the altered pathophysiological mechanism. As mentioned before, 24-h MII-pH-monitoring may be a useful tool to classify AIG patients having GERD symptoms. If MII-pH-monitoring found true acidic GERD, PPIs treatment could have a role. Being this an extremely rare condition, there are no clear-cut recommendations on treatment dosage and duration. Conversely, if MII-pH-impedance diagnoses a non-acidic reflux disease, as well as functional heartburn and reflux hypersensitivity, these patients may benefit from drugs that lower their visceral sensitivity (*i.e.* tricyclic antidepressants and selective serotonin reuptake inhibitors)[7,54]. Moreover, patients who did not respond to medical treatment as well as patients with a high burden of non-acidic reflux, may benefit from anti-reflux surgery[55,56].

In cases where dyspepsia is associated with underlying anxiety or depression, treatment with antidepressants or anxiolytics may be warranted[7,54]. However, future research is needed to identify more effective treatments for dyspepsia in AIG and to better understand the underlying mechanisms that drive dyspeptic symptoms in this condition.

Furthermore, a known consequence of atrophic gastritis-related hypochlorhydria and/or achlorhydria is a change in the gastric microbiome composition. However, there are currently no specific therapies targeting dyspepsia in AIG based on changes in the microbiota, even if an abnormally elevated presence of endoluminal bacteria which produce acetaldehyde from glucose metabolism has been described[68]. Again, according to some authors[69,70], L-cysteine, a non-essential amino acid, can modify the microenvironment of the achlorhydric stomach by both inactivating acetaldehyde and promoting recovery of gastric function[71,72]; furthermore, there is some anecdotal evidence that L-cysteine might improve functional symptoms often associated with atrophic gastritis. Based on these observations, Di Mario *et al*[73] recently conducted a study including a total of 330 patients with atrophic gastritis (both autoimmune or *H. pylori*-related), who were divided into two groups, treated with long-term L-cysteine and no specific treatment, respectively, and reported a significant improvement in the symptom scores of patients treated with L-cysteine when compared to the non-treated group. Of note, symptom improvement lasted all the two years of the follow-up. One limitation of this study is the inclusion of different etiologies from atrophic gastritis, which might be responsible for a certain grade of heterogeneity. While research into the gut microbiota and its role in AIG is ongoing[74,75], some studies suggest that probiotics and prebiotics may have a role in modulating the gut microbiota and reducing symptoms in patients with dyspepsia, including those with AIG[76,77]. Overall, while the potential for microbiota-based therapies in managing dyspepsia in AIG is promising, further research is needed to develop and validate such approaches.

Finally, further treatment may be available in the near future. Gastric per-oral endoscopic myotomy (G POEM) is a novel endoscopic procedure that has shown promising results in the management of refractory gastroparesis[78]. This technique has received increasing attention and emerged as a promising treatment for refractory gastroparesis, targeting the pylorus[79], as a result of the use of new tools to identify pyloric dysfunction in routine care, including functional luminal impedance planimetry (FLIP). The procedure involves creating a myotomy or an incision in the inner lining of the stomach, thereby allowing for better gastric emptying. Since AIG patients with PDS may have the same functional dysfunction of patients affected by gastroparesis, both from a pathophysiological and clinical point of view, G POEM may represent a feasible treatment for AIG patients with severe dyspeptic symptoms, which did not respond to medical treatment. Even if it is considered a safe procedure, a potential concern associated with G POEM is the risk of complications, such as bleeding, perforation, and infection[80]. Additionally, the long-term outcomes of G POEM are still unclear, and more studies are needed to assess its durability and impact on patient quality of life. Recently, Mandarino *et al*[81] found that a lower Intragastric Meal Distribution at pre-intervention gastric emptying study, which indicates antral food retention, could be associated with post-procedural functional success, defined as a decrease of more than 30% 2-h retention. However, further data are needed to establish long-term efficacy of endoscopic pyloromyotomy, especially in the management of dyspeptic AIG patients.

CONCLUSION

AIG can cause a range of clinical manifestations, including dyspepsia. Accurate diagnosis and appropriate management of dyspepsia in AIG are important to improve the patient's quality of life, as well as to prevent and monitor for potential complications such as vitamin deficiencies and gastric neoplasms. The pathophysiology of dyspepsia in AIG is complex and involves changes in acid secretion, gastric motility, hormone signaling, and gut microbiota, among other factors. Specifically, investigating the role of visceral hypersensitivity, impaired gastric accommodation, and impaired gastric motility in AIG-related dyspepsia may help to identify new targets for treatment.

Managing dyspeptic symptoms of AIG is challenging and there are no specific therapies targeting dyspepsia in AIG. While PPIs are commonly used to treat dyspepsia and GERD, they may not be appropriate for AIG, as the condition is already characterized by hypochlorhydria. Instead, prokinetic agents, antidepressant drugs, and non-pharmacological treatments may be of help, even if not adequately evidence-based supported.

Targeting dyspepsia in AIG based on changes in the microbiota is an area of ongoing research and some studies suggest that probiotics and prebiotics may have a role in reducing symptoms. G POEM may represent a feasible treatment for AIG patients with severe dyspeptic symptoms, even if more research is needed to establish its safety and efficacy in this specific setting of patients. Figure 4 summarizes the possible therapeutic approaches for dyspeptic or with GERD-like symptoms in patients with AIG.

Overall, a multidisciplinary approach for the management of dyspepsia in AIG is recommended, and further research is needed to develop and validate more effective therapies for dyspepsia in AIG, as well as to better understand the underlying pathophysiology of the disease; GERD: Gastroesophageal reflux disease.

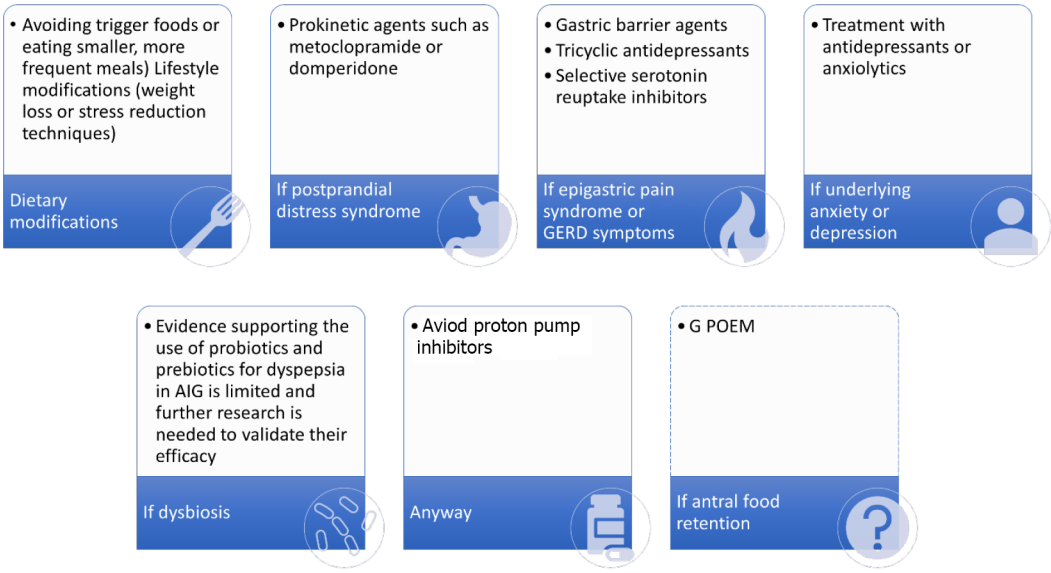

DOI: 10.3748/wjg.v29.i23.3733

Figure 4 Therapeutic approaches for dyspeptic or with gastroesophageal reflux disease -like symptoms in patients with autoimmune gastritis. AIG: Autoimmune gastritis; G POEM: Gastric per-oral endoscopic myotomy; GERD: Gastroesophageal reflux disease.

ARTICLE HIGHLIGHTS

Research background

Gastrointestinal symptoms such as dyspepsia and early satiety are very common in autoimmune gastritis (AIG), being second in terms of frequency only to anemia, which is the most typical feature of AIG. Understanding the pathophysiology of each condition can also guide the choice of appropriate treatments, including lifestyle modifications, dietary changes, and medication management.

Research motivation

The management of dyspepsia in patients with AIG, a chronic, immune-mediated disease, remains a challenge, as it can overlap with functional dyspepsia and gastroesophageal reflux disease. Currently, there are no specific therapies. A tailored treatment approach based on a better understanding of putative pathogenic mechanisms underlying symptoms is needed.

Research objectives

In this review, we will discuss the putative pathogenic mechanisms underlying symptom generation in AIG, their clinical implications, and the current management strategies for this complex and multi-faceted disease.

Research methods

An extensive bibliographical search was performed in PubMed to identify guidelines and primary literature (retrospective and prospective studies, systematic reviews, case series) published in the last 10 years, using both medical subject heading terms and free-language keywords: Dyspepsia; dyspeptic symptoms; gastro-intestinal symptoms; chronic autoimmune atrophic gastritis; diagnosis; treatment.

Research results

A total of 125 records were reviewed and 80 were defined as fulfilling the criteria.

Research conclusions

AIG can cause a range of clinical manifestations, including dyspepsia. The pathophysiology of dyspepsia in AIG is complex and involves changes in acid secretion, gastric motility, hormone signaling, and gut microbiota, among other factors. Managing dyspeptic symptoms of AIG is challenging and currently, there are no specific therapies. A tailored treatment approach based on a better understanding of putative pathogenic mechanisms underlying symptoms is needed. While proton pump inhibitors are commonly used to treat dyspepsia and GERD, they may not be appropriate for AIG. Prokinetic agents, antidepressant drugs, and non-pharmacological treatments may be of help, even if not adequately evidence-based supported. A multidisciplinary approach for the management of dyspepsia in AIG is recommended, and further research is needed to develop and validate more effective therapies for dyspepsia.

Research perspectives

As a future perspective, targeting dyspepsia in AIG based on changes in the microbiota and advanced endoscopic techniques to treat severe dyspeptic symptoms might be an area of ongoing research.

FOOTNOTES

Author contributions: Massironi S conceived the idea for the review; Rossi RE, Elvevi A, Sciola V, and Mandarino FV conducted the literature search; Rossi RE, Elvevi A, and Sciola V screened the articles for inclusion and exclusion criteria; Rossi RE, Sciola V, and Elvevi A wrote the initial draft of the manuscript; Massironi S, Mandarino FV, Danese S, and Invernizzi P contributed to revising the manuscript critically for important intellectual content and finally all authors approved the final version for submission.

Conflict-of-interest statement: All the authors declare no conflict of interests for this article.

PRISMA 2009 Checklist statement: The authors have read the PRISMA 2009 Checklist, and the manuscript was prepared and revised according to the PRISMA 2009 Checklist.

Country/Territory of origin: Italy

ORCID number: Roberta Elisa Rossi 0000-0003-4208-4372; Alessandra Elvevi 0000-0001-9841-2051; Francesco Vito Mandarino 0000-0002-9931-7221; Silvio Danese 0000-0001-7341-1351; Pietro Invernizzi 0000-0003-3262-1998; Sara Massironi 0000-0003-3214-8192.

S-Editor: Liu JH
L-Editor: A
P-Editor: Yuan YY

REFERENCES

1 **Rugge M**, Bricca L, Guzzinati S, Sacchi D, Pizzi M, Savarino E, Farinati F, Zorzi M, Fassan M, Dei Tos AP, Malfertheiner P, Genta RM, Graham DY. Autoimmune gastritis: long-term natural history in naïve Helicobacter pylori-negative patients. *Gut* 2023; **72**: 30-38 [PMID: 35772926 DOI: 10.1136/gutjnl-2022-327827]
2 Autoimmune gastritis. *Nat Rev Dis Primers* 2020; **6**: 57 [PMID: 32647157 DOI: 10.1038/s41572-020-0198-5]
3 **Massironi S**, Zilli A, Elvevi A, Invernizzi P. The changing face of chronic autoimmune atrophic gastritis: an updated comprehensive perspective. *Autoimmun Rev* 2019; **18**: 215-222 [PMID: 30639639 DOI: 10.1016/j.autrev.2018.08.011]
4 **Lenti MV**, Annibale B, Di Sabatino A, Lahner E. Editorial: Dissecting the immunological, pathological, and clinical aspects of autoimmune gastritis and its neoplastic complications. *Front Immunol* 2022; **13**: 1070250 [PMID: 36389672 DOI: 10.3389/fimmu.2022.1070250]
5 **Neumann WL**, Coss E, Rugge M, Genta RM. Autoimmune atrophic gastritis--pathogenesis, pathology and management. *Nat Rev Gastroenterol Hepatol* 2013; **10**: 529-541 [PMID: 23774773 DOI: 10.1038/nrgastro.2013.101]
6 **Hall SN**, Appelman HD. Autoimmune Gastritis. *Arch Pathol Lab Med* 2019; **143**: 1327-1331 [PMID: 31661309 DOI: 10.5858/arpa.2019-0345-RA]
7 **Broeders BWLCM**, Carbone F, Balsiger LM, Schol J, Raymenants K, Huang I, Verheyden A, Vanuytsel T, Tack J. Review article: Functional dyspepsia-a gastric disorder, a duodenal disorder or a combination of both? *Aliment Pharmacol Ther* 2023; **57**: 851-860 [PMID: 36859629 DOI: 10.1111/apt.17414]
8 **Wauters L**, Dickman R, Drug V, Mulak A, Serra J, Enck P, Tack J; ESNM FD Consensus Group, Accarino A, Barbara G, Bor S, Coffin B, Corsetti M, De Schepper H, Dumitrascu D, Farmer A, Gourcerol G, Hauser G, Hausken T, Karamanolis G, Keszthelyi D, Malagelada C, Milosavljevic T, Muris J, O'Morain C, Papathanasopoulos A, Pohl D, Rumyantseva D, Sarnelli G, Savarino E, Schol J, Sheptulin A, Smet A, Stengel A, Storonova O, Storr M, Törnblom H, Vanuytsel T, Velosa M, Waluga M, Zarate N, Zerbib F. United European Gastroenterology (UEG) and European Society for Neurogastroenterology and Motility (ESNM) consensus on functional dyspepsia. *United European Gastroenterol J* 2021; **9**: 307-331 [PMID: 33939891 DOI: 10.1002/ueg2.12061]
9 **Rustgi SD**, Bijlani P, Shah SC. Autoimmune gastritis, with or without pernicious anemia: epidemiology, risk factors, and clinical management. *Therap Adv Gastroenterol* 2021; **14**: 17562848211038771 [PMID: 34484423 DOI: 10.1177/17562848211038771]
10 **Lahner E**, Zagari RM, Zullo A, Di Sabatino A, Meggio A, Cesaro P, Lenti MV, Annibale B, Corazza GR. Chronic atrophic gastritis: Natural history, diagnosis and therapeutic management. A position paper by the Italian Society of Hospital Gastroenterologists and Digestive Endoscopists [AIGO], the Italian Society of Digestive Endoscopy [SIED], the

Italian Society of Gastroenterology [SIGE], and the Italian Society of Internal Medicine [SIMI]. *Dig Liver Dis* 2019; **51**: 1621-1632 [PMID: 31635944 DOI: 10.1016/j.dld.2019.09.016]

11 **Rodriguez-Castro KI**, Franceschi M, Noto A, Miraglia C, Nouvenne A, Leandro G, Meschi T, De' Angelis GL, Di Mario F. Clinical manifestations of chronic atrophic gastritis. *Acta Biomed* 2018; **89**: 88-92 [PMID: 30561424 DOI: 10.23750/abm.v89i8-S.7921]

12 **Yang GT**, Zhao HY, Kong Y, Sun NN, Dong AQ. Correlation between serum vitamin B12 level and peripheral neuropathy in atrophic gastritis. *World J Gastroenterol* 2018; **24**: 1343-1352 [PMID: 29599609 DOI: 10.3748/wjg.v24.i12.1343]

13 **O'Leary F**, Samman S. Vitamin B12 in health and disease. *Nutrients* 2010; **2**: 299-316 [PMID: 22254022 DOI: 10.3390/nu2030299]

14 **Wu H**, Liang G, Kong M, Zhang Y, Zhou Y, Han J, Hu X, Li Y, Zhan Q, Chen S, Du Y, Chen W. The status and risk factors for anxiety/depression in patients with atrophic chronic gastritis: a cross-sectional study. *Ann Palliat Med* 2022; **11**: 3147-3159 [PMID: 36096741 DOI: 10.21037/apm-22-730]

15 **Miceli E**, Brondino N, Lenti MV, Di Stefano M, Staiani M, Zugnoni F, Pisati M, Caccia Dominioni C, Corazza GR, Politi P, Di Sabatino A. Impaired Quality of Life in Patients with Autoimmune Atrophic Gastritis. *Dig Dis Sci* 2021; **66**: 3322-3329 [PMID: 33098024 DOI: 10.1007/s10620-020-06656-x]

16 **Utiyama SRR**, De Bem RS, Skare TL, De Carvalho GA, Teixeira LM, Bertolazo M, Ioshii SO, Nisihara R. Anti-parietal cell antibodies in patients with autoimmune thyroid diseases. *J Endocrinol Invest* 2018; **41**: 523-529 [PMID: 28929353 DOI: 10.1007/s40618-017-0755-2]

17 **Kim HW**, Kim YH, Han K, Nam GE, Kim GS, Han BD, Lee A, Ahn JY, Ko BJ. Atrophic gastritis: a related factor for osteoporosis in elderly women. *PLoS One* 2014; **9**: e101852 [PMID: 25003598 DOI: 10.1371/journal.pone.0101852]

18 **Goerss JB**, Kim CH, Atkinson EJ, Eastell R, O'Fallon WM, Melton LJ 3rd. Risk of fractures in patients with pernicious anemia. *J Bone Miner Res* 1992; **7**: 573-579 [PMID: 1615763 DOI: 10.1002/jbmr.5650070514]

19 **Massironi S**, Cavalcoli F, Zilli A, Del Gobbo A, Ciafardini C, Bernasconi S, Felicetta I, Conte D, Peracchi M. Relevance of vitamin D deficiency in patients with chronic autoimmune atrophic gastritis: a prospective study. *BMC Gastroenterol* 2018; **18**: 172 [PMID: 30409113 DOI: 10.1186/s12876-018-0901-0]

20 **Lenti MV**, Rugge M, Lahner E, Miceli E, Toh BH, Genta RM, De Block C, Hershko C, Di Sabatino A. Autoimmune gastritis. *Nat Rev Dis Primers* 2020; **6**: 56 [PMID: 32647173 DOI: 10.1038/s41572-020-0187-8]

21 **Carabotti M**, Lahner E, Esposito G, Sacchi MC, Severi C, Annibale B. Upper gastrointestinal symptoms in autoimmune gastritis: A cross-sectional study. *Medicine (Baltimore)* 2017; **96**: e5784 [PMID: 28072728 DOI: 10.1097/MD.0000000000005784]

22 **Miceli E**, Lenti MV, Padula D, Luinetti O, Vattiato C, Monti CM, Di Stefano M, Corazza GR. Common features of patients with autoimmune atrophic gastritis. *Clin Gastroenterol Hepatol* 2012; **10**: 812-814 [PMID: 22387252 DOI: 10.1016/j.cgh.2012.02.018]

23 **Carabotti M**, Esposito G, Lahner E, Pilozzi E, Conti L, Ranazzi G, Severi C, Bellini M, Annibale B. Gastroesophageal reflux symptoms and microscopic esophagitis in a cohort of consecutive patients affected by atrophic body gastritis: a pilot study. *Scand J Gastroenterol* 2019; **54**: 35-40 [PMID: 30638085 DOI: 10.1080/00365521.2018.1553062]

24 **Tenca A**, Massironi S, Pugliese D, Consonni D, Mauro A, Cavalcoli F, Franchina M, Spampatti M, Conte D, Penagini R. Gastro-esophageal reflux and antisecretory drugs use among patients with chronic autoimmune atrophic gastritis: a study with pH-impedance monitoring. *Neurogastroenterol Motil* 2016; **28**: 274-280 [PMID: 26568317 DOI: 10.1111/nmo.12723]

25 **Pilotto V**, Maddalo G, Orlando C, Fassan M, Rugge M, Farinati F, Savarino EV. Objective Evidence of Gastro-Esophageal Reflux Disease is Rare in Patients with Autoimmune Gastritis. *J Gastrointestin Liver Dis* 2021; **30**: 30-36 [PMID: 33723550 DOI: 10.15403/jgld-3033]

26 **Kalkan Ç**, Soykan I. The Relations Among Serum Ghrelin, Motilin and Gastric Emptying and Autonomic Function in Autoimmune Gastritis. *Am J Med Sci* 2018; **355**: 428-433 [PMID: 29753372 DOI: 10.1016/j.amjms.2017.12.021]

27 **Kalkan Ç**, Soykan I, Soydal Ç, Özkan E, Kalkan E. Assessment of Gastric Emptying in Patients with Autoimmune Gastritis. *Dig Dis Sci* 2016; **61**: 1597-1602 [PMID: 26725066 DOI: 10.1007/s10620-015-4021-1]

28 **Bashashati M**, Moossavi S, Cremon C, Barbaro MR, Moraveji S, Talmon G, Rezaei N, Hughes PA, Bian ZX, Choi CH, Lee OY, Coëffier M, Chang L, Ohman L, Schmulson MJ, McCallum RW, Simren M, Sharkey KA, Barbara G. Colonic immune cells in irritable bowel syndrome: A systematic review and meta-analysis. *Neurogastroenterol Motil* 2018; **30** [PMID: 28851005 DOI: 10.1111/nmo.13192]

29 **Daher R**, Yazbeck T, Jaoude JB, Abboud B. Consequences of dysthyroidism on the digestive tract and viscera. *World J Gastroenterol* 2009; **15**: 2834-2838 [PMID: 19533804 DOI: 10.3748/wjg.15.2834]

30 **Moayyedi P**, Lacy BE, Andrews CN, Enns RA, Howden CW, Vakil N. ACG and CAG Clinical Guideline: Management of Dyspepsia. *Am J Gastroenterol* 2017; **112**: 988-1013 [PMID: 28631728 DOI: 10.1038/ajg.2017.154]

31 **Miwa H**, Nagahara A, Asakawa A, Arai M, Oshima T, Kasugai K, Kamada K, Suzuki H, Tanaka F, Tominaga K, Futagami S, Hojo M, Mihara H, Higuchi K, Kusano M, Arisawa T, Kato M, Joh T, Mochida S, Enomoto N, Shimosegawa T, Koike K. Evidence-based clinical practice guidelines for functional dyspepsia 2021. *J Gastroenterol* 2022; **57**: 47-61 [PMID: 35061057 DOI: 10.1007/s00535-021-01843-7]

32 **Black CJ**, Paine PA, Agrawal A, Aziz I, Eugenicos MP, Houghton LA, Hungin P, Overshott R, Vasant DH, Rudd S, Winning RC, Corsetti M, Ford AC. British Society of Gastroenterology guidelines on the management of functional dyspepsia. *Gut* 2022; **71**: 1697-1723 [PMID: 35798375 DOI: 10.1136/gutjnl-2022-327737]

33 **Shah SC**, Piazuelo MB, Kuipers EJ, Li D. AGA Clinical Practice Update on the Diagnosis and Management of Atrophic Gastritis: Expert Review. *Gastroenterology* 2021; **161**: 1325-1332.e7 [PMID: 34454714 DOI: 10.1053/j.gastro.2021.06.078]

34 **Dixon MF**, Genta RM, Yardley JH, Correa P. Classification and grading of gastritis. The updated Sydney System. International Workshop on the Histopathology of Gastritis, Houston 1994. *Am J Surg Pathol* 1996; **20**: 1161-1181 [PMID: 8827022 DOI: 10.1097/00000478-199610000-00001]

35 **Rugge M**, Meggio A, Pennelli G, Piscioli F, Giacomelli L, De Pretis G, Graham DY. Gastritis staging in clinical practice: the OLGA staging system. *Gut* 2007; **56**: 631-636 [PMID: 17142647 DOI: 10.1136/gut.2006.106666]

36 **Capelle LG**, de Vries AC, Haringsma J, Ter Borg F, de Vries RA, Bruno MJ, van Dekken H, Meijer J, van Grieken NC, Kuipers EJ. The staging of gastritis with the OLGA system by using intestinal metaplasia as an accurate alternative for atrophic gastritis. *Gastrointest Endosc* 2010; **71**: 1150-1158 [PMID: 20381801 DOI: 10.1016/j.gie.2009.12.029]

37 **Moayyedi P**, Forman D, Braunholtz D, Feltbower R, Crocombe W, Liptrott M, Axon A. The proportion of upper gastrointestinal symptoms in the community associated with Helicobacter pylori, lifestyle factors, and nonsteroidal anti-inflammatory drugs. Leeds HELP Study Group. *Am J Gastroenterol* 2000; **95**: 1448-1455 [PMID: 10894577 DOI: 10.1111/j.1572-0241.2000.2126_1.x]

38 **Abell TL**, Camilleri M, Donohoe K, Hasler WL, Lin HC, Maurer AH, McCallum RW, Nowak T, Nusynowitz ML, Parkman HP, Shreve P, Szarka LA, Snape WJ Jr, Ziessman HA; American Neurogastroenterology and Motility Society and the Society of Nuclear Medicine. Consensus recommendations for gastric emptying scintigraphy: a joint report of the American Neurogastroenterology and Motility Society and the Society of Nuclear Medicine. *J Nucl Med Technol* 2008; **36**: 44-54 [PMID: 18287197 DOI: 10.2967/jnmt.107.048116]

39 **Camilleri M**, Kuo B, Nguyen L, Vaughn VM, Petrey J, Greer K, Yadlapati R, Abell TL. ACG Clinical Guideline: Gastroparesis. *Am J Gastroenterol* 2022; **117**: 1197-1220 [PMID: 35926490 DOI: 10.14309/ajg.0000000000001874]

40 **Pasricha PJ**, Grover M, Yates KP, Abell TL, Bernard CE, Koch KL, McCallum RW, Sarosiek I, Kuo B, Bulat R, Chen J, Shulman RJ, Lee L, Tonascia J, Miriel LA, Hamilton F, Farrugia G, Parkman HP; National Institute of Diabetes and Digestive and Kidney Diseases/National Institutes of Health Gastroparesis Clinical Research Consortium. Functional Dyspepsia and Gastroparesis in Tertiary Care are Interchangeable Syndromes With Common Clinical and Pathologic Features. *Gastroenterology* 2021; **160**: 2006-2017 [PMID: 33548234 DOI: 10.1053/j.gastro.2021.01.230]

41 **Lee YY**, Erdogan A, Rao SS. How to assess regional and whole gut transit time with wireless motility capsule. *J Neurogastroenterol Motil* 2014; **20**: 265-270 [PMID: 24840380 DOI: 10.5056/jnm.2014.20.2.265]

42 **Saad RJ**. The Wireless Motility Capsule: a One-Stop Shop for the Evaluation of GI Motility Disorders. *Curr Gastroenterol Rep* 2016; **18**: 14 [PMID: 26908282 DOI: 10.1007/s11894-016-0489-x]

43 **Triadafilopoulos G**, Lombard C. Use of the Wireless Motility Capsule in the Diagnosis of Gastric Hypochlorhydria: pHinding Extra Value. *Dig Dis Sci* 2021; **66**: 1442-1445 [PMID: 32974808 DOI: 10.1007/s10620-020-06605-8]

44 **Gourcerol G**, Tissier F, Melchior C, Touchais JY, Huet E, Prevost G, Leroi AM, Ducrotte P. Impaired fasting pyloric compliance in gastroparesis and the therapeutic response to pyloric dilatation. *Aliment Pharmacol Ther* 2015; **41**: 360-367 [PMID: 25523288 DOI: 10.1111/apt.13053]

45 **Malik Z**, Sankineni A, Parkman HP. Assessing pyloric sphincter pathophysiology using EndoFLIP in patients with gastroparesis. *Neurogastroenterol Motil* 2015; **27**: 524-531 [PMID: 25712043 DOI: 10.1111/nmo.12522]

46 **Wuestenberghs F**, Gourcerol G. Pyloric distensibility in health and disease. *Am J Physiol Gastrointest Liver Physiol* 2021; **321**: G133-G138 [PMID: 34160292 DOI: 10.1152/ajpgi.00460.2020]

47 **Desprez C**, Chambaz M, Melchior C, Basile P, Prevost G, Jacques J, Leroi AM, Gourcerol G. Assessment of pyloric sphincter distensibility and pressure in patients with diabetic gastroparesis. *Neurogastroenterol Motil* 2021; **33**: e14064 [PMID: 33314491 DOI: 10.1111/nmo.14064]

48 **Snape WJ**, Lin MS, Agarwal N, Shaw RE. Evaluation of the pylorus with concurrent intraluminal pressure and EndoFLIP in patients with nausea and vomiting. *Neurogastroenterol Motil* 2016; **28**: 758-764 [PMID: 26813266 DOI: 10.1111/nmo.12772]

49 **Yadlapati R**, Gyawali CP, Pandolfino JE; CGIT GERD Consensus Conference Participants. AGA Clinical Practice Update on the Personalized Approach to the Evaluation and Management of GERD: Expert Review. *Clin Gastroenterol Hepatol* 2022; **20**: 984-994.e1 [PMID: 35123084 DOI: 10.1016/j.cgh.2022.01.025]

50 **Gyawali CP**, Kahrilas PJ, Savarino E, Zerbib F, Mion F, Smout AJPM, Vaezi M, Sifrim D, Fox MR, Vela MF, Tutuian R, Tack J, Bredenoord AJ, Pandolfino J, Roman S. Modern diagnosis of GERD: the Lyon Consensus. *Gut* 2018; **67**: 1351-1362 [PMID: 29437910 DOI: 10.1136/gutjnl-2017-314722]

51 **Vela MF**, Camacho-Lobato L, Srinivasan R, Tutuian R, Katz PO, Castell DO. Simultaneous intraesophageal impedance and pH measurement of acid and nonacid gastroesophageal reflux: effect of omeprazole. *Gastroenterology* 2001; **120**: 1599-1606 [PMID: 11375942 DOI: 10.1053/gast.2001.24840]

52 **Sifrim D**, Dupont L, Blondeau K, Zhang X, Tack J, Janssens J. Weakly acidic reflux in patients with chronic unexplained cough during 24 hour pressure, pH, and impedance monitoring. *Gut* 2005; **54**: 449-454 [PMID: 15753524 DOI: 10.1136/gut.2004.055418]

53 **de Bortoli N**, Martinucci I, Savarino E, Franchi R, Bertani L, Russo S, Ceccarelli L, Costa F, Bellini M, Blandizzi C, Savarino V, Marchi S. Lower pH values of weakly acidic refluxes as determinants of heartburn perception in gastroesophageal reflux disease patients with normal esophageal acid exposure. *Dis Esophagus* 2016; **29**: 3-9 [PMID: 25212408 DOI: 10.1111/dote.12284]

54 **Viazis N**, Karamanolis G, Vienna E, Karamanolis DG. Selective-serotonin reuptake inhibitors for the treatment of hypersensitive esophagus. *Therap Adv Gastroenterol* 2011; **4**: 295-300 [PMID: 21922028 DOI: 10.1177/1756283X11409279]

55 **Mainie I**, Tutuian R, Shay S, Vela M, Zhang X, Sifrim D, Castell DO. Acid and non-acid reflux in patients with persistent symptoms despite acid suppressive therapy: a multicentre study using combined ambulatory impedance-pH monitoring. *Gut* 2006; **55**: 1398-1402 [PMID: 16556669 DOI: 10.1136/gut.2005.087668]

56 **del Genio G**, Tolone S, del Genio F, Aggarwal R, d'Alessandro A, Allaria A, Rossetti G, Brusciano L, del Genio A. Prospective assessment of patient selection for antireflux surgery by combined multichannel intraluminal impedance pH monitoring. *J Gastrointest Surg* 2008; **12**: 1491-1496 [PMID: 18612705 DOI: 10.1007/s11605-008-0583-y]

57 **Kahrilas PJ**, Bredenoord AJ, Fox M, Gyawali CP, Roman S, Smout AJ, Pandolfino JE; International High Resolution Manometry Working Group. The Chicago Classification of esophageal motility disorders, v3.0. *Neurogastroenterol Motil* 2015; **27**: 160-174 [PMID: 25469569 DOI: 10.1111/nmo.12477]

58 **Tack J**, Caenepeel P, Arts J, Lee KJ, Sifrim D, Janssens J. Prevalence of acid reflux in functional dyspepsia and its

association with symptom profile. *Gut* 2005; **54**: 1370-1376 [PMID: 15972301 DOI: 10.1136/gut.2004.053355]

59 **Lahner E**, Carabotti M, Annibale B. Treatment of Helicobacter pylori infection in atrophic gastritis. *World J Gastroenterol* 2018; **24**: 2373-2380 [PMID: 29904244 DOI: 10.3748/wjg.v24.i22.2373]

60 **Song H**, Zhu J, Lu D. Long-term proton pump inhibitor (PPI) use and the development of gastric pre-malignant lesions. *Cochrane Database Syst Rev* 2014; CD010623 [PMID: 25464111 DOI: 10.1002/14651858.CD010623.pub2]

61 **Cavalcoli F**, Zilli A, Conte D, Ciafardini C, Massironi S. Gastric neuroendocrine neoplasms and proton pump inhibitors: fact or coincidence? *Scand J Gastroenterol* 2015; **50**: 1397-1403 [PMID: 26059834 DOI: 10.3109/00365521.2015.1054426]

62 **Annibale B**, Lahner E, Santucci A, Vaira D, Pasquali A, Severi C, Mini R, Figura N, Delle Fave G. CagA and VacA are immunoblot markers of past Helicobacter pylori infection in atrophic body gastritis. *Helicobacter* 2007; **12**: 23-30 [PMID: 17241297 DOI: 10.1111/j.1523-5378.2007.00467.x]

63 **Collin A**, Mion F, Kefleyesus A, Beets C, Jaafari N, Boussageon R. Critical appraisal of international guidelines for the management of Helicobacter pylori infection in case of dyspepsia. *Helicobacter* 2023; **28**: e12952 [PMID: 36897573 DOI: 10.1111/hel.12952]

64 **Kato M**, Hayashi Y, Nishida T, Oshita M, Nakanishi F, Yamaguchi S, Kitamura S, Nishihara A, Akasaka T, Ogiyama H, Nakahara M, Yamada T, Kishida O, Yamamoto M, Shimayoshi A, Tsujii Y, Kato M, Shinzaki S, Iijima H, Takehara T. Helicobacter pylori eradication prevents secondary gastric cancer in patients with mild-to-moderate atrophic gastritis. *J Gastroenterol Hepatol* 2021; **36**: 2083-2090 [PMID: 33403702 DOI: 10.1111/jgh.15396]

65 **Kamada T**, Haruma K, Hata J, Kusunoki H, Sasaki A, Ito M, Tanaka S, Yoshihara M. The long-term effect of Helicobacter pylori eradication therapy on symptoms in dyspeptic patients with fundic atrophic gastritis. *Aliment Pharmacol Ther* 2003; **18**: 245-252 [PMID: 12869086 DOI: 10.1046/j.1365-2036.2003.01669.x]

66 **Yamada S**, Tomatsuri N, Kawakami T, Nakatsugawa Y, Nishimura T, Fujii H, Sato H, Okuyama Y, Kimura H, Yoshida N. Helicobacter pylori Eradication Therapy Ameliorates Latent Digestive Symptoms in Chronic Atrophic Gastritis. *Digestion* 2018; **97**: 333-339 [PMID: 29587295 DOI: 10.1159/000486618]

67 **Masuy I**, Van Oudenhove L, Tack J. Review article: treatment options for functional dyspepsia. *Aliment Pharmacol Ther* 2019; **49**: 1134-1172 [PMID: 30924176 DOI: 10.1111/apt.15191]

68 **Jokelainen K**, Siitonen A, Jousimies-Somer H, Nosova T, Heine R, Salaspuro M. In vitro alcohol dehydrogenase-mediated acetaldehyde production by aerobic bacteria representing the normal colonic flora in man. *Alcohol Clin Exp Res* 1996; **20**: 967-972 [PMID: 8892513 DOI: 10.1111/j.1530-0277.1996.tb01932.x]

69 **Linderborg K**, Marvola T, Marvola M, Salaspuro M, Färkkilä M, Väkeväinen S. Reducing carcinogenic acetaldehyde exposure in the achlorhydric stomach with cysteine. *Alcohol Clin Exp Res* 2011; **35**: 516-522 [PMID: 21143248 DOI: 10.1111/j.1530-0277.2010.01368.x]

70 **Maejima R**, Iijima K, Kaihovaara P, Hatta W, Koike T, Imatani A, Shimosegawa T, Salaspuro M. Effects of ALDH2 genotype, PPI treatment and L-cysteine on carcinogenic acetaldehyde in gastric juice and saliva after intragastric alcohol administration. *PLoS One* 2015; **10**: e0120397 [PMID: 25831092 DOI: 10.1371/journal.pone.0120397]

71 **Hellström PM**, Hendolin P, Kaihovaara P, Kronberg L, Meierjohann A, Millerhovf A, Paloheimo L, Sundelin H, Syrjänen K, Webb DL, Salaspuro M. Slow-release L-cysteine capsule prevents gastric mucosa exposure to carcinogenic acetaldehyde: results of a randomised single-blinded, cross-over study of Helicobacter-associated atrophic gastritis. *Scand J Gastroenterol* 2017; **52**: 230-237 [PMID: 27806647 DOI: 10.1080/00365521.2016.1249403]

72 **Crafa P**, Di Mario F, Grillo S, Landi S, Franceschi M, Rodriguez-Castro K, Tursi A, Brandimarte G, Franzoni L. Recovery of gastric function in patients affected by chronic atrophic gastritis using l-cysteine (Acetium®): one year survey in comparison with a control group. *Acta Biomed* 2022; **93**: e2022184 [PMID: 35775759 DOI: 10.23750/abm.v93i3.12812]

73 **Di Mario F**, Rodriguez-Castro KI, Franceschi M, Landi S, Grillo S, Franzoni L, Russo M, Brandimarte G, Tursi A, Crafa P. Improvement of Symptoms in Patients Affected by Chronic Atrophic Gastritis Using L-Cysteine (Acetium®). *Dig Dis* 2023; **41**: 198-205 [PMID: 36423587 DOI: 10.1159/000528168]

74 **Conti L**, Borro M, Milani C, Simmaco M, Esposito G, Canali G, Pilozzi E, Ventura M, Annibale B, Lahner E. Gastric microbiota composition in patients with corpus atrophic gastritis. *Dig Liver Dis* 2021; **53**: 1580-1587 [PMID: 34116969 DOI: 10.1016/j.dld.2021.05.005]

75 **Parsons BN**, Ijaz UZ, D'Amore R, Burkitt MD, Eccles R, Lenzi L, Duckworth CA, Moore AR, Tiszlavicz L, Varro A, Hall N, Pritchard DM. Comparison of the human gastric microbiota in hypochlorhydric states arising as a result of Helicobacter pylori-induced atrophic gastritis, autoimmune atrophic gastritis and proton pump inhibitor use. *PLoS Pathog* 2017; **13**: e1006653 [PMID: 29095917 DOI: 10.1371/journal.ppat.1006653]

76 **Rajilic-Stojanovic M**, Figueiredo C, Smet A, Hansen R, Kupcinskas J, Rokkas T, Andersen L, Machado JC, Ianiro G, Gasbarrini A, Leja M, Gisbert JP, Hold GL. Systematic review: gastric microbiota in health and disease. *Aliment Pharmacol Ther* 2020; **51**: 582-602 [PMID: 32056247 DOI: 10.1111/apt.15650]

77 **Lahner E**, Conti L, Annibale B, Corleto VD. Current Perspectives in Atrophic Gastritis. *Curr Gastroenterol Rep* 2020; **22**: 38 [PMID: 32542467 DOI: 10.1007/s11894-020-00775-1]

78 **Gregor L**, Wo J, DeWitt J, Yim B, Siwiec R, Nowak T, Mendez M, Gupta A, Dickason D, Stainko S, Al-Haddad M. Gastric peroral endoscopic myotomy for the treatment of refractory gastroparesis: a prospective single-center experience with mid-term follow-up (with video). *Gastrointest Endosc* 2021; **94**: 35-44 [PMID: 33373646 DOI: 10.1016/j.gie.2020.12.030]

79 **Soliman H**, Gourcerol G. Targeting the pylorus in gastroparesis: From physiology to endoscopic pyloromyotomy. *Neurogastroenterol Motil* 2023; **35**: e14529 [PMID: 36594414 DOI: 10.1111/nmo.14529]

80 **Ichkhanian Y**, Vosoughi K, Aghaie Meybodi M, Jacques J, Sethi A, Patel AA, Aadam AA, Triggs JR, Bapaye A, Dorwat S, Benias P, Chaves DM, Barret M, Law RJ, Browers N, Pioche M, Draganov PV, Kotzev A, Estremera F, Albeniz E, Ujiki MB, Callahan ZM, Itani MI, Brewer OG, Khashab MA. Comprehensive Analysis of Adverse Events Associated with Gastric Peroral Endoscopic Myotomy: An International Multicenter Study. *Surg Endosc* 2021; **35**: 1755-1764 [PMID: 32328824 DOI: 10.1007/s00464-020-07570-z]

81 **Mandarino FV**, Testoni SGG, Barchi A, Pepe G, Esposito D, Fanti L, Viale E, Biamonte P, Azzolini F, Danese S. Gastric emptying study before gastric peroral endoscopic myotomy (G-POEM): can intragastric meal distribution be a predictor of success? *Gut* 2023; **72**: 1019-1020 [PMID: 35697421 DOI: 10.1136/gutjnl-2022-327701]

Published by **Baishideng Publishing Group Inc**
7041 Koll Center Parkway, Suite 160, Pleasanton, CA 94566, USA
Telephone: +1-925-3991568
E-mail: bpgoffice@wjgnet.com
Help Desk: https://www.f6publishing.com/helpdesk
https://www.wjgnet.com